
# Functional Analysis of Mutations in Isocitrate Dehydrogenase Involved in Gliomagenesis

---

Daniel Krell

**Nuffield Department of Clinical Medicine and Green Templeton College**

**University of Oxford**

**Trinity Term 2014**

A thesis submitted for the Degree of Doctor of Philosophy

# Functional Mutations in Isocitrate Dehydrogenase Involved in Gliomagenesis

Daniel Krell, Green Templeton College, Oxford

D.Phil, Hilary Term, 2014

## Abstract

The main subject of my thesis is the investigation of mechanisms of glioma tumorigenesis associated with the recently identified mutations in isocitrate dehydrogenase. Gliomas account for 80% of primary brain cancers. They represent a diverse group of tumours, and are graded from I-IV based on histopathological features. Whilst grade I tumours may be curable with surgery alone, grade II and III gliomas inevitably progress to glioblastoma multiforme (GBM), which is highly resistant to current therapies and carries a very poor prognosis. Despite an improved understanding of the pathways and mechanisms involved in the development of glioma and its progression to grade IV disease, current and novel treatments have so far failed to significantly improve outcome.

Isocitrate dehydrogenase (IDH) enzymes catalyse the oxidative decarboxylation of isocitrate to α-ketoglutarate (α-KG). Somatic mutations in genes encoding IDH1 and IDH2 were first identified in glioma and subsequently in acute myeloid leukemia and other solid tumours. These heterozygous point mutations occur at the arginine residue of the enzymes active site and cause both loss of normal enzyme function and gain-of-function, causing the reduction of α-KG to D-2-hydroxyglutarate (D-2HG), which accumulates. D-2HG may act as an oncometabolite through the inhibition of various α-KG dependent enzymes, stimulating angiogenesis, histone modifications and aberrant DNA methylation. Possibly, IDH1/2 mutations may also cause oncogenic effects through dysregulation of the tricarboxylic acid (TCA) cycle, or by increasing susceptibility to oxidative stress. The exact role of mutant IDH1/2 in tumorigenesis however remains unclear.

In the work outlined in this thesis, I have demonstrated that the expression of mutant IDH1/2 in glioma cell lines leads to 2-HG accumultation and a reduction in α-KG production and results in HIF1α accumulation and a reduction in 5hmC production. Furthermore, the brain-specific expression of mutant Idh1 in mice also results in 2-HG accumulation and reduced α-KG production, whilst a reduction in 5hmC levels are also seen. This data appears to support the theory that IDH1/2 mutant activity results in the inhibition of α-KG dependent enzymes, either through the accumulation of 2-HG or due to a reduction in α-KG levels. The brain-

specific expression of mutant Idh1 in mice also results in increased cellular proliferation and an increase in the expression of the neural stem cell marker, nestin. However gliomas do not develop, perhaps suggesting that additional mutations are required in conjunction with those occuring in *IDH1/2* in order to initiate tumourigenesis.

Clinically, IDH1/2 mutations may represent a novel therapeutic target in glioma and may also serve as useful diagnostic, prognostic and predictive biomarkers. However, a better understanding of the pathogenesis of mutant IDH is required, to enable effective IDH1/2 directed therapies to be developed in the future.

## Statement of originality

All work in this thesis is my own unless otherwise stated. The idea for the theme of this thesis was my own and was made following discussion with Dr C. Bardella and Prof. I Tomlinson. The first draft of all published manuscripts were written by me and then critically appraised by senior co-authors. All publications were peer reviewed.

The idea for the laboratory study outlined in Chapter 3, its execution and analysis was entirely my own, and all laboratory tests were performed by me. The idea for the laboratory studies outlined in Chapters 4 and 5 was made by myself and Dr C. Bardella in collaboration, but the laboratory work was my own unless otherwise stated. I acknowledge the work of Dr J. Mccullagh and K. Al-Qahtani in undertaking UPLC-MS analysis of cell line and tissue samples, and of S. Kriaucionis and P. Brazauskas HPLC analysis the same samples as outlined in Chapters 4 and 5.

## Funding

I would like to thank Hospital Corporation of America (HCA) for funding me for four years as a research fellow. I have been extremely lucky to have received a full salary during this time and this post would not have been available without their support.

**Word Count**

**67,324**

# List of publications arising from this thesis

Several sections of this thesis have been published in peer reviewed journals as a combination of original articles and review articles. I am the first author of these publications. In keeping with copyright laws, copyright transfer agreements have been obtained from the publishers. These allow reproduction of part or all of the published material, provided it is clearly acknowledged. In keeping with these agreements, for each publication below, I have indicated which chapter of this thesis it is included in.

## Publications

1 ***Krell D***, Assoku M, Galloway M, Mulholland P, Tomlinson I, Bardella C. Screen for *IDH1*, *IDH2*, *IDH3*, *D2HGDH* and *L2HGDH* Mutations in Glioblastoma. PLoS One. 2011; 6(5): e19868

**Original article - Reproduced in part in Chapter 3 with permission from PLos One**

2 ***Krell D***, Mulholland P, Frampton AE, Krell J, Stebbing J, Bardella C. IDH mutations in tumorigenesis and their potential role as novel therapeutic targets. Future Oncol. 2013 Dec; 9(12): 1923-35

**Review- Reproduced in part in Chapter 1 with permission from Future Science Publishing Group Ltd.**

# Abbreviations used in this thesis

| | |
|---|---|
| **5mC** | 5-methylcytosine |
| **5hmC** | 5-hydroxymethycytosine |
| **αKG** | alpha-ketoglutarate |
| **AITL** | angioimmunoblastic T-cell lymphoma |
| **AtrA** | all-trans retinoic acid |
| **AQP4** | aquaporin-4 |
| **CDK** | cyclin-dependent kinase |
| **Cdk5** | cyclin-dependent kinase 5 |
| **CNP** | 2′,3′-cyclic nucleotide 3′-phosphodiesterase |
| **$CoCl_2$** | cobalt chloride |
| **C-P4H** | collagen prolyl 4-hydroxlase |
| **Cre** | cyclization recombination |
| **CSPG4** | chondroitin sulfate proteoglycan 4 |
| **$CO_2$** | carbon dioxide |
| **DAB** | 3,3'-diaminobenzidinetetrahydrochloride |
| **cDNA** | complementary DNA |
| **D-2HG** | D-2-Hydroxyglutarate |
| **D-2-HGA** | D-2-Hydroxyglutaric aciduria |
| **D-2HGDH** | D-2-Hydroxyglutarate Dehydrogenase |
| **DNMT** | de novo methyltransferase |
| **DEPC** | Diethylpyrocarbonate |
| **DMEM** | Dulbecco's Modified Eagle Medium |
| **DMSO** | Dimethyl sulfoxide |
| **DTT** | dithiothreitol |
| **EDTA** | Ethylenediaminetetraacetic acid |
| **EGF** | epidermal growth factor |
| **EGFR** | epidermal growth factor receptor |
| **EGLN** | EGL nine homolog |
| **EYFP** | Enhanced Yellow Fluorescent Protein |
| **FBS** | fetal bovine serum |
| **FFPE** | formalin fixed paraffin embedded |
| **FGF** | fibroblast growth factor |
| **FGFR** | fibroblast growth factor receptor |
| **FOXA3** | forkhead box protein A3 |
| **GBM** | glioblastoma multiforme |
| **GLUT1** | glucose transporter type 1 |
| **GHB** | γ-hydroxybutyrate |
| **GICs** | glioblastoma initiating cells |
| **GR** | glucocorticoid receptor |
| **GSIS** | glucose stimulated insulin secretion |
| **$H_20_2$** | hydrogen peroxide |
| **$H_20$** | water |
| **H3** | Histone 3 |
| **H3K4** | Histone 3 lysine 4 |
| **H3K4me3** | trimethylated histone 3 lysine 4 |
| **H3K9** | Histone 3 lysine 9 |
| **H3K9me2** | Dimethylated histone 3 lysine 9 |

| | |
|---|---|
| **H3K9me3** | Trimethylated histone 3 lysine 9 |
| **H3K27** | Histone 3 lysine 27 |
| **H3K36** | Histone 3 lysine 36 |
| **H3K79** | Histone 3 lysine 79 |
| **H4K20** | Histone 4 lysine 20 |
| **HEK** | human derived embryonic kidney |
| **Hepes** | hydroxyethyl piperazineethanesulfonic acid |
| **HIF** | hypoxia-inducible factor |
| **HIF-PHD** | HIF prolyl hydroxylase |
| **HOT** | hydroxyacid-oxoacid transhydrogenase |
| **HPLC** | high performance liquid chromatography |
| **IDH** | isocitrate dehydrogenase |
| **IHC** | immunohistochemistry |
| **IMDM** | Iscove's Modified Dulbecco's Medium |
| **JHDMs** | Jumonji-C domain containing histone demethylases |
| **$K_{cat}$** | catalytic rate |
| **KCl** | potassium chloride |
| **KLF5** | Krueppel-like factor 5 |
| **KPS** | Karnofsky Performance Score |
| **KSP** | Kidney specific |
| **L-2HG** | L-2-Hydroxyglutarate |
| **L-2-HGA** | L-2-Hydroxyglutaric aciduria |
| **L-2HGDH** | L-2-Hydroxyglutarate Dehydrogenase |
| **LOH** | loss of heterozygosity |
| **LoxP** | locus of crossing (X-ing) over in P1 |
| **LTR** | long terminal repeat |
| **LV** | lentiviral vector |
| **MBP** | myelin basic protein |
| **mTOR** | mammalian target of rapamycin |
| **MeOH** | methanol |
| **MGMT** | O-6-methylguanine-DNA methyltransferase |
| **NaCl** | sodium chloride |
| **$NADP^+$** | nicotinamide adenine dinucleotide phosphate (oxidised form) |
| **NADPH** | nicotinamide adenine dinucleotide phosphate (reduced form) |
| **NaOH** | sodium hydroxide |
| **NEAA** | non-essential amino acid |
| **NP40** | nonyl phenoxypolyethoxylethanol-40 |
| **NSCs** | neural stem cells |
| **OB** | Olfactory bulb |
| **OF** | open field |
| **OFT** | open field test |
| **OS** | overall survival |
| **PAC** | puromycin N-acetyltransferase |
| **PBS** | phosphate buffered saline |
| **PCR** | polymerise chain reaction |
| **PDGF** | platelet derived growth factor |
| **PDGFR** | platelet derived growth factor recetor |
| **PFS** | progression free survival |
| **PGK1** | phosphoglycerate kinase 1 |
| **PHH3** | Phospho-histone H3 |

| | |
|---|---|
| **PI3K** | phosphosphatidylinositol-3-OH kinase |
| **Plod1–3** | procollagen-lysine 2-oxoglutarate 5-dioxygenases 1, 2, and 3 |
| **PMSF** | phenylmethyl sulfonyl fluoride |
| **PS** | Penicillin and streptomycin |
| **PTK** | proteinase K |
| **RAR** | retinoic acid receptor |
| **RBP1** | retinol Binding Protein 1 |
| **RMS** | rostral migratory stream |
| **RT-PCR** | reverse transcription polymerase chain reaction |
| **qRT-PCR** | quantitative real time polymerase chain reaction |
| **ROS** | reactive oxygen species |
| **SDS** | sodium dodecyl sulphate |
| **SGZ** | subgranular zone |
| **siRNA** | small interfering RNA |
| **shRNA** | short hairpin RNA |
| **SNP** | single nucleotide polymorphism |
| **SSA** | succinic semialdehyde |
| **SSADHD** | succinic semialdehyde dehydrogenase deficiency |
| **SVZ** | subventricular zone |
| **TCA** | Tricarboxylic acid cycle |
| **TET** | Ten-Eleven Translocation |
| **UPLC-MS** | Ultra performance liquid chromatography–mass spectrometry |
| **VEGF** | vascular endothelial growth factor |
| **VEGFR** | vascular endothelial growth factor receptor |
| **VHL** | von Hippel-Lindau |
| **WT** | wild-type |

# Table of Contents

**Abstract** ..... **i**

**Statement of originality** ..... **iii**

**List of publications arising from this thesis** ..... **iv**

**Abbreviations used in this thesis** ..... **v**

**Table of Contents** ..... **viii**

**List of Tables** ..... **xiii**

**List of Figures** ..... **xiv**

**1. Chapter One** ..... **1**

**Introduction, literature review and aims of thesis** ..... **1**

**1.1 Glioma** ..... **1**

**1.2 Glioblastoma Multiforme** ..... **4**

1.2.1 Incidence and Aetiology ..... 4

1.2.2 The Natural History of GBM ..... 6

1.2.3 GBM cell of origin ..... 11

1.2.4 Symptoms and Presentation in GBM ..... 16

1.2.5 Diagnosis of GBM ..... 16

1.2.6 Treatment of newly diagnosed GBM ..... 17

1.2.7 Treatment of recurrent GBM ..... 19

1.2.8 Novel targeted therapy in GBM ..... 20

1.2.9 Prognosis ..... 29

**1.3 The role of IDH mutations in gliomagenesis** ..... **31**

1.3.1 IDH function ..... 31

1.3.2 Frequency of IDH mutations in GBM and other tumours ..... 34

1.3.3 IDH mutation spectrum ..... 37

1.3.4 Cellular effects of mutations in IDH ..... 38

1.3.5 Effects of D-2HG on the activity of α-KG-dependent enzymes ..... 42

1.3.6 IDH Mutation effects on TCA cycle Function and Glucose Sensing ..... 53

1.3.7 Mutations in IDH1/2 and Cellular Response to Oxidative Stress ..... 57

**1.4 IDH1/2 mutant mouse models of cancer** ..... **58**

**1.5 The clinical relevance of IDH1/2 mutations** ..... **59**

**1.6 Aims and outline of this thesis** ..... **62**

1.6.1 Aims of thesis ..... 62

1.6.2 Outline of thesis ..... 63

**2. Chapter Two** ..... **64**

**Materials and Methods** ..... **64**

**2.1 DNA extraction** ..... **64**

2.1.1 DNA extraction from formalin fixed paraffin embedded tissue ..... 64
2.1.2 DNA extraction from ES cells ..... 64
2.1.3 DNA extraction from mouse ear snips for genotyping ..... 65
2.1.4 DNA extraction from mouse tissue ..... 66
**2.2 RNA extraction ..... 66**
2.2.1 RNA extraction from cell lines ..... 66
2.2.2 RNA extraction from mouse tissue ..... 67
**2.3 Spectrophotometry ..... 68**
**2.4 Polymerase Chain Reaction ..... 68**
2.4.1 Purification of PCR products ..... 70
**2.5 Agarose Gel Electrophoresis ..... 70**
**2.6 Fluorescence sequencing of PCR products ..... 71**
**2.7 Reverse transcription PCR (RT-PCR) ..... 73**
**2.8 Quantitative Real Time-PCR (qRT-PCR) ..... 74**
**2.9 Immunohistochemistry ..... 75**
**2.10 Protein ..... 77**
2.10.1 Total protein extraction from cells ..... 77
2.10.2 Nuclear and cytosolic protein extraction from cells ..... 77
2.10.3 Protein extraction from mouse tissue ..... 78
2.10.4 Western Blot ..... 79
**2.11 Cell Culture ..... 80**
2.11.1 Cell culture conditions ..... 80
2.11.2 Freezing down and resuspending cells to replace stocks ..... 81
2.11.3 Generation of knockdown cell lines with shRNA ..... 81
2.11.4 Generation of IDH1 and IDH2 knockdown cells with siRNA ..... 82
2.11.5 Generation of IDH1/2 mutant cell LN18 cells ..... 84
2.11.6 Generation of conditional Idh1 R132H and Idh2 R172K mutant ES cells ..... 85
2.11.7 Assessment of cellular proliferation rate ..... 86
**2.12 Assessment of $NADP^+$/NADPH ..... 87**
**2.13 Assessment of ROS ..... 89**
**2.14 UPLC-MS ..... 90**
2.14.1 Cell extraction protocol for UPLC-MS ..... 90
2.14.2 Tissue extraction protocol for UPLC-MS ..... 91
2.14.3 UPLC-MS protocol ..... 91
**2.15 Assessment of 5hmc and 5mC ..... 93**
**2.16 Mouse Husbandry ..... 95**
2.16.1 Tamoxifen induced expression of inducible-Cre in mice ..... 95
2.16.2 Formalin fixation and paraffin embedding of mouse tissue ..... 96
2.16.3 Hematoxylin and eosin (H&E) stain ..... 96
2.16.4 Histological assessment ..... 97
2.16.5 Assessment of mouse behaviour using an open field test ..... 97

2.16.6 MRI imaging of mouse brains ..... 98
**2.17 Ethical Approval ..... 99**
**2.18 Solutions ..... 99**
**3. Chapter Three ..... 102**
**Screen for mutations in IDH, D2HGDH, L2HGDH, and HOT in GBM ..... 102**
**3.1 Introduction ..... 102**
**3.2 Aims ..... 105**
**3.3 Methods ..... 106**
**3.4 Results ..... 107**
**3.5 Discussion and Conclusions ..... 112**
**4. Chapter Four ..... 116**
**Generation of cell models of mutant IDH ..... 116**
**4.1 Introduction ..... 116**
**4.2 Aims ..... 120**
**4.3 Methods ..... 121**
4.3.1 Cell lines ..... 121
4.3.2 Generation of knockdown cell lines using shRNA ..... 121
4.3.3 Generation of IDH1/2 U87MG knockdown cell lines using siRNA ..... 122
4.3.4 Generation of IDH1/2 mutant LN18 cell lines ..... 123
4.3.5 Generation of Idh1 R132H and Idh2 R172K mutant ES cell lines ..... 123
4.3.6 Analysis of cellular 2-HG and $\alpha$-KG and other TCA cycle metabolites ..... 123
4.3.7 Analysis of HIF expression ..... 124
4.3.8 Assessment of TET function ..... 125
4.3.9 Assessment of markers of histone methylation ..... 125
4.3.10 Assessment of oxidation state and oxidative stress ..... 126
4.3.11 Assessment of cellular proliferation rate ..... 126
**4.4 Results ..... 127**
4.4.1 Knockdown of IDH1 and IDH2 expression using siRNA ..... 127
4.4.2 Knockdown of IDH and 2HGDH expression using shRNA ..... 128
4.4.3 Overexpression of wildtype and mutant IDH1 and IDH2 in LN18 cells ..... 137
4.4.4 Mutant expression of IDH1/2 in ES cells ..... 140
4.4.5 Analysis of changes in cellular 2-HG and $\alpha$-KG and other TCA cycle metabolites ..... 141
4.4.6 Analysis of HIF1α expression ..... 147
4.4.7 Assessment of TET function in IDH mutant ES cells ..... 153
4.4.8 Assessment of markers of histone methylation in IDH mutant ES cells ..... 154
4.4.9 Assessment of oxidation state and oxidative stress ..... 155
4.4.10 Assessment of cellular proliferation rate ..... 160
**4.5 Discussion ..... 163**
4.5.1 shRNA knockdown of a single IDH enzyme does not reduce cellular α-KG levels in vitro ..... 163

4.5.2 shRNA knockdown of D2HGDH does not lead to an accumulation of 2-HG ..... 166
4.5.3 Expression of mutant IDH1 and IDH2 in LN18 cells results in an accumulation of 2-HG and a reduction in α-KG ..... 168
4.5.4 Expression of mutant IDH1 and IDH2 in ES cells does not result in a significant accumulation of 2-HG or a reduction in α-KG production ..... 169
4.5.5 Levels of TCA cycle metabolites are not altered by shRNA knockdown of IDH1/2 function or expression of mutant IDH1/2 ..... 170
4.5.6 HIF1α expression is increased in association with siRNA knockdown of IDH1 and IDH2 and shRNA knockdown of IDH1 ..... 172
4.5.7 HIF1α expression is increased in association mutant IDH1/2 expression in LN18 and ES cell lines ..... 173
4.5.8 Mutant IDH1/2 expression in ES cells reduces 5hmC production suggesting an inhibition of TET function ..... 174
4.5.9 Mutant IDH1/2 expression in ES cells does not increase markers of histone methylation . 175
4.5.10 Mutant IDH expression and down-modulation of wild-type IDH expression reduces NADPH levels but does not consistently increase ROS levels ..... 175
4.5.11 Cellular proliferation rate is reduced by shRNA knockdown of IDH function and IDH mutant expression ..... 176

**4.6 Conclusions ..... 177**

**5. Chapter Five ..... 179**

**Development of an Idh1 mutant mouse model of glioma ..... 179**

**5.1 Introduction ..... 179**

**5.2 Aims ..... 185**

**5.3 Methods ..... 186**

5.3.1 Mouse breeding ..... 186
5.3.2 Genotyping ..... 188
5.3.3 Analysis of embryos ..... 190
5.3.4 Analysis of nesER$^{T2}$-KI mice ..... 190
5.3.5 Analysis of D2hgdh KO mice ..... 193
5.3.6 Histological assessment ..... 194

**5.4 Results ..... 195**

5.4.1 Removal of the Neo R cassette of Idh1-KI mice ..... 195
5.4.2 Analysis of the constitutive expression of mutant Idh1 ..... 196
5.4.3 Analysis of non-inducible brain-specific expression of mutant Idh1in mice ..... 197
5.4.4 Analysis of inducible brain-specific expression of mutant Idh1 in mice ..... 201
5.4.5 Analysis of D2hgdh KO mice ..... 229
5.4.6 Analysis of Ksp-KI and Vil-KI mice ..... 235

**5.5 Discussion ..... 237**

5.5.1 No live-born Neo-KI mice were generated from Idh1-KI x Flp crosses ..... 238
5.5.2 No live-born Sox-KI mice were generated from Idh1-KI x Sox-Cre crosses ..... 239
5.5.3 Expression of Idh1 R132H in the murine brain in utero results in 2-HG accumulation, reduced α-KG production and embryonic lethality ..... 239
5.5.4 NesER$^{T2}$-KI mice do not demonstrate behaviour associated with stress or anxiety during an open field test ..... 240

5.5.5 2-HG accumulates and α-KG levels are reduced in NesER$^{T2}$-KI mice ..... 241
5.5.6 Hunching and weight loss are observed in NesER$^{T2}$-KI, Ksp-KI, Vil-KI and NeoR mice ..... 242
5.5.7 Hydrocephalus and ventriculomegaly are observed in NesER$^{T2}$-KI and NeoR mice ..... 243
5.5.8 Leaky expression of Idh1 R132H occurred in Idh1-KI mice ..... 245
5.5.9 2-HG accumulates in D2hgdh KO mice but there is no gross phenotype or brain related defect and α-KG levels are unchanged ..... 247
5.5.10 Brain-specific expression of Idh1 R132H results in an upregulation of nestin ..... 247
5.5.11 Markers of oligodendrocytic differentiation are reduced in the brain of NesER$^{T2}$-KI mice . 251
5.5.12 Idh1 R132H reduces 5hmC production in the brain of NesER$^{T2}$-KI mice suggesting an inhibition of Tet function ..... 252
5.5.13 Idh1 R132H reduces Rbp1 expression in the brain of NesER$^{T2}$-KI mice ..... 253
5.5.14 Idh1 R132H does not increase the methylation of H3K9 in the brain of NesER$^{T2}$-KI mice .. 254
5.5.15 Idh1 R132H expression in utero results in reduced levels of TCA cycle metabolites and reduced glutamine and glutamate concentrations in the brain ..... 255
5.5.16 Stabilisation of HIF1α does not occur in NesER$^{T2}$-KI or D2hgdh KO mice ..... 256
5.5.17 NesER$^{T2}$-KI mice do not develop glioma ..... 258

**5.6 Conclusions ..... 260**

**6. Chapter Six ..... 262**

**Summary, Implication of Findings and Future Perspectives ..... 262**

**6.1 Summary and implication of findings ..... 262**

**6.2 Future Perspectives ..... 271**

**7. Chapter Seven ..... 273**

**Future Work ..... 273**

**References. ..... 276**

**Appendix ..... 329**

# List of Tables

Table 1-1: The WHO classification of glioma based on histopathological feature ..... 1

Table 1-2: Classification of glioma based on cell type of origin and location ..... 2

Table 1-3: An overview of some of the targeted therapies that have been trialled in GBM ..... 21

Table 1-4: R132H mutation alters the enzymatic properties of IDH1 (taken from Dang 2009). ..... 40

Table 2-1: Primary antibodies used for immunohistochemistry ..... 76

Table 2-2: Primary antibodies used for western blots ..... 80

Table 2-3: Concentrations of TCA intermediates calibrators for LC-MS analysis after addition of mobile phase solution ..... 92

Table 3-1: Patient demographics and results of sequencing analyses for the 47 GBMs studied ..... 109

Table 4-1: Changes in D-2HG and α-KG in mutant IDH1 and IDH2 expressing in vitro models. ..... 169

Table 5-1: Genotype, abbreviated name and intended purpose of mice developed in this study ..... 189

Table 5-2: Genotype of live-born mice from *Idh1-KI* x *Flp* crosses ..... 195

Table 5-3: Genotype of live-born mice from *Idh1-KI* x *Sox2-Cre* crosses ..... 196

Table 5-4: Genotype of live-born mice from *Idh1-KI*$^{+/fl}$;*Tp53*$^{+/fl}$ x *Nestin-Cre* crosses ..... 197

Table 5-5: Levels of fumarate, succinate, malate, glutamine and glutamate in *Nes-KI* embryos compared to *Idh1-WT* controls ..... 201

Table 5-6: Hunching and weight loss *nesER*$^{T2}$*-KI* and *Neo*$^{R}$ mice ..... 205

Table 5-7: Characteristics of mice that developed weight loss and hunching ..... 205

Table 5-8: Ventriculomegaly in *nesER*$^{T2}$*-KI* and NeoR mice ..... 207

Table 5-9: Characteristics of *nesER*$^{T2}$*-KI* and NeoR mice that developed ventriculomegaly ..... 211

Table 5-10: Unpaired t-test analysis of fumarate data ..... 216

Table 5-11: Hunching and weight loss in offspring from *Idh1-KI* x *Ksp-Cre* crosses ..... 236

Table 5-12: Hunching and weight loss in offspring from *Idh1-KI* x *Villin-Cre* crosses ..... 236

Table 5-13: Age at which mice developed hunching and weight loss ..... 242

Table 5-14: Commonly used mouse strains and corresponding percentage of mice culled at weaning age due to hydrocephalus ..... 245

Table 6-1: Summary of results from cell and mouse models discussed in this thesis ..... 265

# List of Figures

Figure 1-1: Histological specimens from a patient who presented with grade II glioma (left panel) and recurred with GBM 5 years later (right panel) (Taken from Maher EA, 2001) ..... 3

Figure 1-2: Major signalling pathways in the pathogenesis of GBM. (red represents primary GBM, blue secondary GBM, and green both primary and secondary GBM) (taken from Ohgaki H, 2007) ..... 7

Figure 1-3: Cell cycle arrest pathways (taken from Holland E, 2001) ..... 9

Figure 1-4: The hierarchical neural stem cell system demonstrating the gene expression pattern associated with each cell type ..... 13

Figure 1-5: The location of stem cells in the SVZ and Hippocampus and their migration to the Olfactory Bulb via the RMS in mice ..... 14

Figure 1-6: The reaction catalysed by wild-type IDH1 and IDH2 (A) and IDH3 (B). ..... 32

Figure 1-7: The function of the IDH enzymes in the TCA cycle. Shown are the cytoplasmic reaction involving IDH1 and the mitochondrial reactions involving IDH2/3 (taken from Losman JA 2013). ..... 32

Figure 1-8: Structure of the active site of IDH1 (Adapted from Parsons DW 2008). ..... 39

Figure 1-9: The functions of wild-type and mutant IDH1 and IDH2. ..... 40

Figure 2-1: Calibration curve of some TCA intermediates concentration vs. the peak area. ..... 93

Figure 3-1: Identification of the G395A mutation at codon 132 by sequencing analysis of the *IDH1* gene. ..... 110

Figure 3-2: D2HGDH and L2HGDH are expressed in wildtype *IDH1/2* and *IDH1* R132H glioblastomas. ..... 111

Figure 3-3: Exon 4 of the IDH2 gene and electropherogram showing the wild-type sequence at nucleotide position 515. ..... 113

Figure 4-1: qRT-PCR and western blots showing the effect of IDH1 and IDH2 siRNA on corresponding gene expression at RNA and protein levels ..... 127

Figure 4-2: qRT-PCR analysis showing the reduction in *IDH1* gene expression 72 hours after transient transfection with various shRNA clones directed against *IDH1* compared to an untransfected control (c). ..... 129

Figure 4-3: qRT-PCR and western blot analysis showing *IDH1* gene expression at RNA and protein level in LN18 cells transduced with 80ng of IDH1 TRCN0000027298 shRNA lentiviral vector ..... 130

Figure 4-4: qRT-PCR analysis showing the reduction in *IDH2* gene expression 72 hours after transient transfection with various shRNA clones directed against *IDH2* compared to untransfected control (c). ..... 131

Figure 4-5: qRT-PCR and western blot analysis showing *IDH2* gene expression at RNA and protein level in LN18 cells transduced with 40ng of IDH2 TRCN0000027296 shRNA lentiviral vector ..... 132

Figure 4-6: qRT-PCR analysis showing the effects on *IDH3A* gene expression 72 hours after transient transfection with various shRNA clones directed against *IDH3A* compared to untransfected control (c). ..... 133

Figure 4-7: qRT-PCR and western blot analysis showing *IDH3* gene expression at RNA and protein levels in LN18 cells transduced with 40ng of IDH3 TRCN0000027310 shRNA lentiviral vector ..... 133

Figure 4-8: Western blot analysis showing *IDH2* gene expression at a protein level in IDH and D2HGDH shRNA knockdown cell lines ..... 135

Figure 4-9: qRT-PCR analysis showing IDH2 gene expression in various shRNA knockdown cell lines ..... 136

Figure 4-10: Expression of D2HGDH and L2HGDH in D2HGDH knockdown cells transduced with either 20ng or 50ng of L2HGDH shRNA lentiviral vector ..... 137

Figure 4-11: Overexpression of wildtype and mutant IDH1 and IDH2 in LN18 cells by qRT-PCR and western blot. ..... 139

Figure 4-12: cDNA sequence results showing the substitution CGA to CAT at codon 132 of *IDH1* in IDH1 R132H mutant ES cells (A) and wild-type sequence in IDH1 R132H parental cells (B). ..... 140

Figure 4-13: cDNA sequence results showing the substitution AGG to AAG at codon 172 of *IDH2* in IDH2 R172K mutant ES cells (A) and wild-type sequence in IDH2 R172K parental cells (B). ..... 141

Figure 4-14: α-KG levels in shRNA knockdown LN18 cell lines ..... 142

Figure 4-15: 2-HG levels in shRNA knockdown LN18 cell lines ..... 142

Figure 4-16: Effects of IDH1, IDH2, and IDH3 shRNA knockdown on the expression of *IDH1*, *IDH2* and *IDH3*. ..... 143

Figure 4-17: α-KG levels in IDH1 and IDH2 mutant LN18 cell lines ..... 144

Figure 4-18: 2-HG levels in IDH1 and IDH2 mutant LN18 cell lines ..... 145

Figure 4-19: 2-HG levels in IDH1 and IDH2 mutant ES cell lines ..... 146

Figure 4-20: α-KG levels in IDH1 and IDH2 mutant ES cell lines ..... 146

Figure 4-21: HIF1α protein expression in U87MG cells 72 hours after transduction with siRNA targeting IDH1/IDH2 ..... 147

Figure 4-22: HIF target gene expression and HIF1α protein expression in LN18 cells transduced with shRNA. ..... 148

Figure 4-23: HIF1α protein expression in LN18 cells transduced with shRNA. Analysis of western blot using ImageJ to measure grey scale values. ..... 149

Figure 4-24: Expression of HIF target genes in mutant IDH1 expressing LN18 cells. ..... 150

Figure 4-25: Expression of HIF target genes in mutant IDH2 expressing LN18 cells. ..... 150

Figure 4-26: HIF1α protein expression in mutant IDH1 and mutant IDH2 expressing LN18 cells ..... 151

Figure 4-27: Expression of HIF target genes IDH1 and IDH2 mutant ES cells ..... 152

Figure 4-28: HIF1α protein expression in IDH1 and IDH2 mutant ES cell clones ..... 152

Figure 4-29: 5hmC content in IDH1 R132H mutant ES cell clones ..... 153

Figure 4-30: 5hmC content in IDH2 R172K mutant ES cell clones ..... 154

Figure 4-31: H3K4me3 and H3K9me2 levels in IDH2 R172K mutant ES cells ..... 154

Figure 4-32: NADPH quantification in IDH shRNA knockdown LN18 cells ..... 155

Figure 4-33: NADPH quantification in IDH mutant LN18 cells ..... 156

Figure 4-34: $NADP^+$/NADPH ratio in IDH mutant ES cells ..... 156

Figure 4-35: Percentage of ROS positive cells in IDH siRNA knockdown U87MG cell lines ..... 157

Figure 4-36: Percentage of ROS positive cells in IDH shRNA knockdown LN18 cell lines ..... 158

Figure 4-37: Percentage of ROS positive cells in IDH1 mutant LN18 cell lines ..... 159

Figure 4-38: Percentage of ROS positive cells in IDH1 and IDH2 mutant ES cells ..... 160

Figure 4-39: Cellular proliferation in IDH knockdown LN18 cells ..... 161

Figure 4-40: Cell proliferation in IDH1 mutant LN18 cells ..... 161

Figure 4-41: Cell proliferation in IDH2 mutant LN18 cells ..... 162

Figure 5-1: Construct design used to develop the *Idh1-KI* mice (16897 bp) ..... 186

Figure 5-2: Construct design used to develop the *D2hgdh* KO mice (22314 bp) ..... 188

Figure 5-3: Top: Haemorrhagic area compared in the brain of a *Nes-KI* embryo (E14.5) (A) versus *Idh1-WT* control (B) ..... 198

Figure 5-4: α-KG and 2-HG levels in the brains of *Nes-KI* embryos by UPLC-MS ..... 199

Figure 5-5: Ratio of α-KG and 2-HG levels in the brains of *Nes-KI* embryos compared to *Idh1-WT* controls ..... 199

Figure 5-6: Levels of fumarate, succinate and malate in brains of *Nes-KI* embryos ..... 200

Figure 5-7: Levels of glutamine and glutamate in brains of Nes-KI embryos ..... 201

Figure 5-8: Expression of mutant Idh1 compared in the brains of 4 month old *Idh1*-WT and *nesER$^{T2}$-KI* mice (cDNA) ..... 202

Figure 5-9: Expression of mutant Idh1 in the frontal (A) temporal (B) and occipital (C) lobes of 9 month old *nesER$^{T2}$-KI* mice (cDNA) ..... 202

Figure 5-10: Open field test results showing the average number of events observed in *NesER$^{T2}$-KI* mice compared to *Idh1*-WT controls ..... 204

Figure 5-11: Average weight of *NesER$^{T2}$-KI* and *Idh1*-WT mice ..... 206

Figure 5-12: Abnormal appearance of the brain in *nesER$^{T2}$-KI* mice ..... 208

Figure 5-13: Weight of *nesER$^{T2}$-KI* brain compared to *Idh1*-WT brain ..... 209

Figure 5-14: MRI brain image showing ventriculomegaly in a *nesER$^{T2}$-KI* mouse (bottom left) compared to age matched *Idh1*-WT control (top right) ..... 209

Figure 5-15: Sequencing analysis showing expression of Idh1 R132H in DNA and cDNA extracted from brains of *NeoR* (left) and *NesER$^{T2}$-KI* mice (right) ..... 212

Figure 5-16: Images of the spleen, heart and kidney from *NesER$^{T2}$-KI* mice (left) compared to *Idh1*-WT control (right) ..... 213

Figure 5-17: α-KG and 2-HG levels in 4 and 8 month old *NesER$^{T2}$-KI* mice compared to Idh1-WT controls ..... 214

Figure 5-18: Relative levels of 2-HG and α-KG in the brains of non-inducible *Nes-KI* and inducible *NesER$^{T2}$-KI* mice ..... 215

Figure 5-19: Fumarate levels in the brains of 4 and 8 month old *NesER$^{T2}$-KI* mice compared to *Idh1*-WT controls ..... 216

Figure 5-20: 2-HG and α-KG levels in the brain of *NeoR* mice compared to *Idh1*-WT controls ..... 217

Figure 5-21: Fold change in mRNA expression of Hif1α target genes in the brain of *NesER$^{T2}$-KI* mice by qRT-PCR ..... 218

Figure 5- 22: Western blot showing Hif1α protein expression in the brain of *NesER$^{T2}$-KI* mice ..... 218

Figure 5-23: Western blot showing Phd2 protein expression in the brain of *NesER$^{T2}$-KI* mice ..... 218

Figure 5- 24: Fold change in mRNA expression of stem cell markers in the brain of *NesER$^{T2}$-KI* mice by qRT-PCR ..... 219

Figure 5-25: Fold change in mRNA expression of *Nes* in the frontal, temporal and occipital lobes of NesERT2-KI mice brains compared to *Idh1*-WT controls by qRT-PCR ..... 220

Figure 5-26: Relative mRNA expression level of *Nes* in *nes-creER$^{T2}$;Idh1$^{+/+}$*, *Idh1$^{+/+}$ NesER$^{T2}$-KI* mice by qRT-PCR ..... 220

Figure 5-27: IHC analysis showing an increase in nestin expression in the SVZ of *NesERT2-KI* mice compared to *Idh1*-WT controls ..... 222

Figure 5-28: IHC showing an increase in PHH3 expression in the SVZ of *NesERT2-KI* mice compared to *Idh1*-WT controls.....224

Figure 5-29: Fold change in mRNA expression of markers of neural differentiation in the brain of 8 month old *NesER$^{T2}$-KI* mice compared to *Idh1*-WT controls.....225

Figure 5-30: Fold change in mRNA expression of markers of oligodendrocytic differentiation in the brains of 4 month old *NesER$^{T2}$-KI* mice compared to Idh1-WT controls .....226

Figure 5-31: Relative levels of 5-hmC and 5-mC levels in *NesER$^{T2}$-KI* mice .....227

Figure 5-32: qRT-PCR analysis of mRNA expression levels of *Rbp1* in the brain of *NesER$^{T2}$-KI* mice compared to *Idh1*-WT controls.....228

Figure 5-33: Western blot showing H3K9me3 and total H3 levels in the brain of *NesER$^{T2}$-KI* mice compared to *Idh1*-WT controls.....229

Figure 5-34: PCR analysis of *D2hgdh* expression in the brains of *D2hgdh* KO mice.....230

Figure 5-35: qRT-PCR analysis of *D2hgdh* expression in the brains of *D2hgdh* KO mice.....230

Figure 5-36: Relative levels of 2-HG and α-KG levels in the brain, liver, kidney and spleen of 10 week old *D2hgdh* KO mice compared to *D2hgdh* WT controls.....231

Figure 5-37: Relative levels of 5mC and 5hmC in the brain of *D2hgdh* KO mice compared to D2hgdh WT controls.....232

Figure 5-38: Relative mRNA expression level of *Nes* in the brain of *D2hgdh* KO mice compared to *D2hgdh* WT controls .....232

Figure 5-39: Hif1α target gene expression in the brain of *D2hgdh* KO mice.....233

Figure 5-40: Western blot showing Phd2 protein expression in the brain of *D2hgdh* KO mice and *D2hgdh* WT controls .....233

Figure 5-41: Hif1α target gene expression in the liver of *D2hgdh* KO mice compared to *D2hgdh* WT controls .....234

Figure 5-42: Hif1α target gene expression in the kidney of *D2hgdh* KO mice compared to *D2hgdh* WT controls .....234

Figure 5-43: *Idh2* expression in the brain of *D2hgdh* KO mice compared to *D2hgdh* WT controls ...235

# 1. Chapter One

## Introduction, literature review and aims of thesis

### 1.1 Glioma

Brain tumours comprise a wide range of histological and pathological entities, each with a distinct natural history, and are classified as gliomas or non-gliomas. Gliomas affect the glial portion of brain parenchyma and are the most common primary brain tumour, making up approximately 30% of all brain and central nervous system tumours and 80% of all primary malignant brain tumours (Goodenberger ML 2012). They show wide diversity with respect to location, morphology, genetic status, and response to therapy. The World Health Organisation (WHO) classifies gliomas based on histopathological features such as nuclear atypia, mitosis, endothelial proliferation and necrosis using a grading system I-IV ***(Table 1-1)***. Gliomas can also be classified based on the specific type of cell they share histological features with, or based on their location ***(Table 1-2).***

**Table 1-1: The WHO classification of glioma based on histopathological feature**

| Grade | Tumour |
|---|---|
| I | Pilocytic astrocytoma |
| II | Diffuse astrocytoma; oligodendroglioma; oligoastrocytoma |
| III | Anaplastric astrocytoma; anaplastic oligodendroglioma; anaplastic oligoastrocytoma |
| IV | Glioblastoma multiforme |

**Table 1-2: Classification of glioma based on cell type of origin and location**

| Classification based on cell type | Classification based on location |
|---|---|
| Ependymoma | Supratentorial- in the cerebrum |
| Astrocytoma | Infratentorial- in the cerebellum |
| Oligodendroglioma | Pontine- in the pons of the brainstem |
| Brain stem glioma | |
| Optic nerve glioma | |
| Mixed glioma e.g. oligoastrocytoma | |

Grade I gliomas are often considered to be benign, are generally curable with complete surgical resection and rarely evolve into higher-grade lesions.

Grade II tumours are low grade malignancies that may follow a long clinical course. They are divided into 3 histological variants: astrocytomas which express the astrocyte specific marker GFAP, oligodendrogliomas which do not express GFAP, and oligoastrocytomas which contain mixtures of both cell types. Median overall survival (OS) in grade II glioma is between 5 and 7 years, and although some patients may live for up to 10 years or longer, the condition is not curable (Stupp R 2007). Treatment consists of maximal surgical resection. The role and appropriate timing of radiotherapy remain undefined because although trials have shown radiotherapy to improve progression free survival (PFS) and symptom control, no OS benefit has yet been demonstrated (Bent MJ 2005). Adjuvant PCV [procarbazine, lomustine (CCNU)] chemotherapy after radiation in patients with high-risk, low-grade glioma did not improve outcome in a randomized RTOG trial (Shaw E 2006). The potential benefit of temozolomide (TMZ) chemotherapy in combination with radiotherapy is currently under investigation in a Radiation Therapy Oncology Group phase 2 clinical trial (RTOG0424) and in an Eastern Cooperative Oncology Group phase 3 clinical trial (ECOGE3F05), results from which have not yet been published. 70% of grade II gliomas

transform into grade III and IV tumours within 5-10 years of diagnosis, likely as a result of the acquisition of further mutations, and subsequently behave clinically like higher grade lesions (Maher EA 2001) ***(Figure 1-1)***.

**Figure 1-1: Histological specimens from a patient who presented with grade II glioma (left panel) and recurred with GBM 5 years later (right panel) (Taken from Maher EA, 2001)**

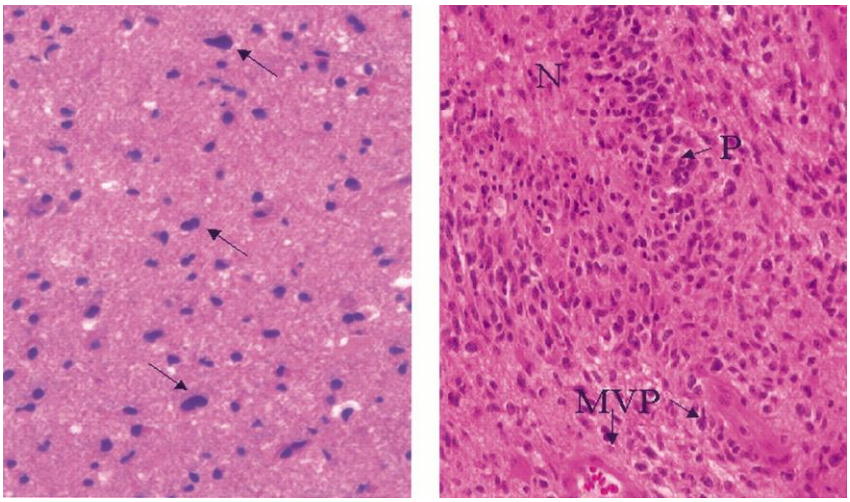


Grade III gliomas are invasive, progress to grade IV lesions, and lead to death within a few years of diagnosis (Maher EA 2001). Anaplastic oligodendrogliomas have a relatively better prognosis and demonstrate a higher response rate to both chemotherapy and radiation, whilst the prognosis of mixed anaplastic oligoastrocytomas and anaplastic astrocytomas is intermediate between glioblastoma multiforme (GBM) and pure anaplastic oligodendrogliomas (Stupp R 2010). Standard treatment consists of surgery followed by adjuvant radiotherapy up to 60 Gy (Stupp R 2010). The value of concomitant or maintenance chemotherapy with TMZ is not yet supported by available data (Stupp R 2007). Furthermore randomized clinical trials did not demonstrate prolonged OS with adjuvant PCV chemotherapy in newly diagnosed anaplastic oligoastrocytomas and oligodendrogliomas, even in the subgroup of the patients with the most chemo responsive tumours exhibiting chromosomal loss of 1p and 19q, although progression-free survival was prolonged (Cairncross G 2006, van den Bent M 2006).

Glioblastoma multiforme (GBM) is the most common and most malignant glioma. It is characterised by widespread intratumoural heterogeneity, and may develop rapidly without evidence of a less malignant precursor lesion (primary glioblastoma), or less commonly through progression from a lower grade tumour (secondary glioblastoma). Histopathological features of GBM include nuclear atypia, high mitotic activity, cellular pleomorphism, microvascular proliferation and necrosis (Furnari FB 2007), and it is associated with a very poor prognosis.

## 1.2 Glioblastoma Multiforme

### 1.2.1 Incidence and Aetiology

GBM accounts for 12-15% of all brain tumours with an incidence of 4 new cases per 100,000 population per year (Kleiheus P 2007) and a slight predominance in males (Surawicz TS 1999). Primary GBMs represent the majority (more than 90%) of diagnosed cases and develop in older patients (mean age, 62 years) with a peak incidence between 45-75 years, whilst secondary GBM which represent about 5% of cases develop in younger patients (mean age 45 years) (Ohgaki H 2005a)

The incidence of glioma in population-based studies is fairly constant in Europe and the United States (Ohgaki H 2005a, Kleiheus P 2007), leading some observers to conclude that environmental factors probably play less of a role in gliomagenesis than genetic factors. Furthermore due to the relative rarity of the disease and short survival after diagnosis, specific causal factors contributing to GBM remain largely unclear. High dose ionising radiation to the head is the only known environmental risk factor for GBM (Gurney JG 2001, Schwartzbaum JA 2006, Fisher JL 2007). Other established risk factors include the hereditary genetic syndromes Li-Fraumeni syndrome, Neurofibromatosis 1, Turcots syndrome and

Cowdens syndrome which are associated with mutations in p53, NF1, APC and MMR genes, and PTEN respectively. Apart from these syndromes, information on the familial aggregation of glioma is poorly understood, and although there appears to be an increased incidence of glioma in first degree relatives of patients with the disease, an exact mode of inheritance is not evident (Osborne RH 2001), and whilst various segregation analyses of GBM prone families suggest an autosomal recessive mode of inheritance, others support a polygenic model (Malmer B 2001). Additionally, recent genome-wide association studies have identified common susceptibility variants at 5p15.33 *(TERT)*, 8q24.21 *(CCDC26)*, 9p21.3 *(CDKN2A-CDKN2B)*, 20q13.33 *(RTEL1)*, 11q23.3 *(PHLDB1)*, and two independent signals at 7p11.2 *(EGFR)* (Shete S 2009, Wrensch M 2009, Sanson M 2011).

Studies examining non-inherited risk factors have suggested a possible viral aetiology in gliomagenesis. Viral antigens from both JC virus and human herpes virus 6 have been detected in glioma samples (Chi J 2012, Noch E 2012), although their perceived aetiological role is not clear. Furthermore nucleic acids and proteins from cytomegalovirus (CMV) have also been demonstrated in gliomas, and it has been proposed that CMV may predispose to glioma formation due to interactions with the STAT-3 signalling pathway (Price RL 2013). Interestingly there is an inverse association between glioma and allergic conditions such as asthma (Linos E 2007), and it has been observed that immunoglobulin E concentrations are reduced in glioma patients, further suggesting that immunological factors may play a role in gliomagenesis (Il'yasova D 2009).

The role of radiofrequency electromagnetic fields (RF-EMF) in gliomagenesis, such as those emitted from mobile phones, remains controversial, with some early studies suggesting no link (Gurney J 1999, Wrensch M 1999). However more recent meta-analysis studies suggested that mobile phone use may increase the risk of glioma (Khurana VG 2009, Myung SK 2009), and a case control study carried out between 2007 and 2009 concluded that RF-

EMFs play a role in both the initiation and promotion stages of carcinogenesis (Hardell L 2013). As a result of such data, in 2011 The International Agency for Research on Cancer classified RF-EMF as a group 2B, i.e. a 'possible' human carcinogen.

The link between alcohol consumption and glioma remains unclear, with some studies, including a recent meta-analysis suggesting no association (Wrensch M 1993, Galeone C 2013). However a retrospective study carried out in Australia has demonstrated that alcohol consumption may increase the risk of glioblastoma in a dose-dependent manner (Baglietto L 2011). Brain tumours may also be caused by known carcinogens such as vinyl chloride, polycyclic aromatic hydrocarbons and N-nitroso compounds (Schwartzbaum JA 2006), although again reports are conflicting (Wrensch M 2002). Studies of other environmental factors such as smoking, diet and vitamin intake do not convincingly demonstrate a causal relationship in gliomagenesis (Hurley SF 1996, Holick CN 2007a, Holick CN 2007b, Dubrow R 2012).

### 1.2.2 The Natural History of GBM

Gliomas arise from glial cells which are divided into astrocytes and oligodendrocytes. Glial cells are responsible for isolating neuronal processes and controlling the environment of neurons and are fundamental in the development of the nervous system by providing surfaces and building blocks for migrating neurons and outgrowing axons. Gliomas largely resemble undifferentiated astrocytes or oligodendrocytes in their gene expression and phenotypic characteristics, and malignant transformation is thought to occur as a result of a stepwise accumulation of multiple genetic alterations at chromosomal and gene expression levels (Sehgal 1998) affecting growth factor signalling and cell cycle control pathways, with resultant affects on cellular differentiation and proliferation ***(Figure 1-2)***. The degree of genetic and chromosomal aberrations tends to correlate with increasing clinical grade. A

concerted effort to more clearly characterise the GBM cancer genome was undertaken by the Cancer Genome Atlas project (TCGA), which through genome-wide analysis of DNA copy number, gene expression, and DNA methylation screening highlighted several genes involved in these pathways that were be significantly mutated in GBM (McLendon R 2008).

**Figure 1-2: Major signalling pathways in the pathogenesis of GBM. (red represents primary GBM, blue secondary GBM, and green both primary and secondary GBM) (taken from Ohgaki H, 2007)**

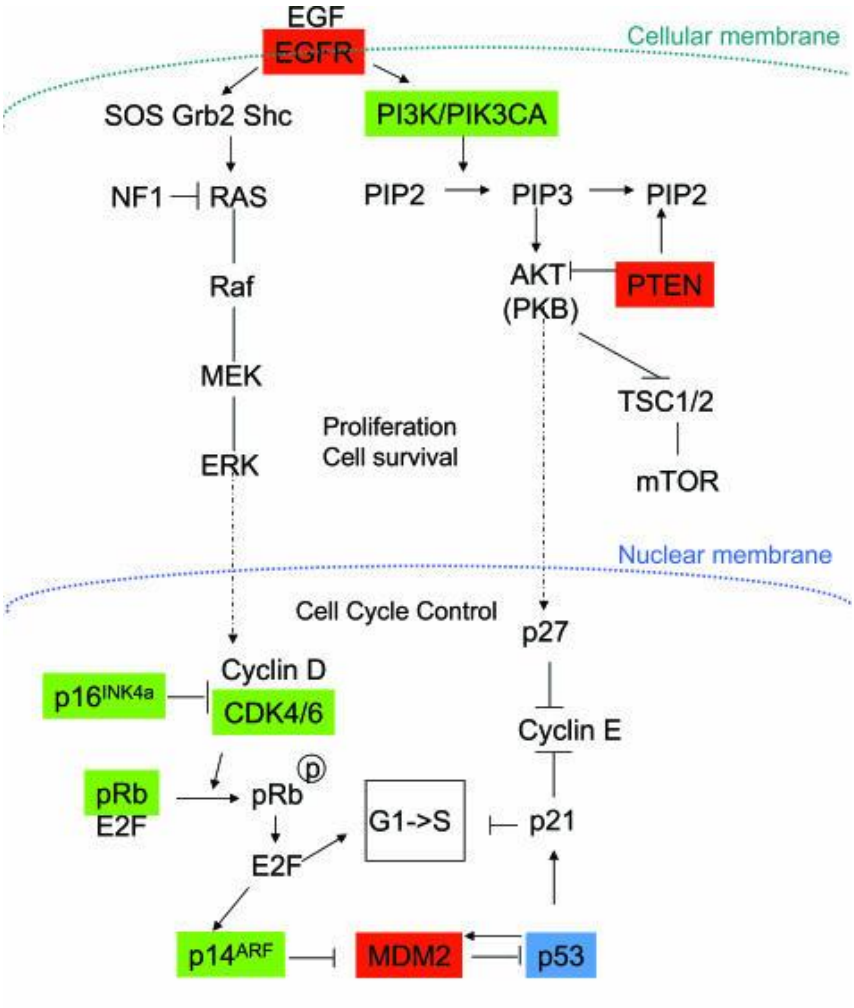

#### 1.2.2.1 Altered Growth Factor signaling

Genes encoding growth factors and their receptors that control glial cell differentiation and proliferation are commonly overexpressed in glioma (Holland E 2001). Common alterations observed are the overproduction of: fibroblast growth factor and its receptor (FGF,FGFR), platelet derived growth factor and its receptor (PDGF,PDGFR), vascular endothelial growth factor (VEGF) (Loilome W 2009), and epidermal growth factor (EGF) (Parsons DW 2008). Activating mutations in the *EGFR* gene are also common in GBM (Verhaak RG 2010), and result in a constitutively active receptor in the absence of EGF ligand (Hatanpaa KJ 2010). Variant III (EGFRvIII) deletion of the extracellular domain (Humphrey PA 1990) is most commonly observed, as are extracellular domain point mutations and cytoplasmic domain deletions (Lee JC 2006). The RAS pathway, whose activation by tyrosine kinase receptors such as EFGR leads to increased proliferation and inhibition of apoptosis (McCubrey JA 2007) through downstream effects on RAF, MEK and mitogen activated protein kinsases (MAPK) has also been implicated in gliomagenesis (Guha A 1997). The AKT pathway has also been shown to be activated in about 70% of GBMs (Holland E 2000). AKT is activated through Phosphoinositide 3-kinase (PI3K), whose activity is itself commonly altered in GBM (Ohgaki H 2011), and is negatively regulated by the tumour suppressor gene PTEN (Stiles BL 2009). Increased activation of AKT results in various pro-tumourigenic effects such as: enhanced metabolism; altered translation through activation of mTOR; increased proliferation; and inhibition of apoptosis (Holland E 2001). Mutation or complete loss of *PTEN* itself, a tumour suppressor gene which normally functions to inhibit proliferation, are also commonly seen (Sano T 1999).

### 1.2.2.2 Altered Cell cycle control

Mutations in genes encoding proteins involved in cell cycle arrest pathways have been shown to occur commonly in GBM (Ohgaki H 2007), in particular those involved in the TP53/MDM2/$p14^{ARF}$ pathway and the $p16^{INK4a}$/RB1 pathway ***(Figure 1-3)***

**Figure 1-3: Cell cycle arrest pathways (taken from Holland E, 2001)**

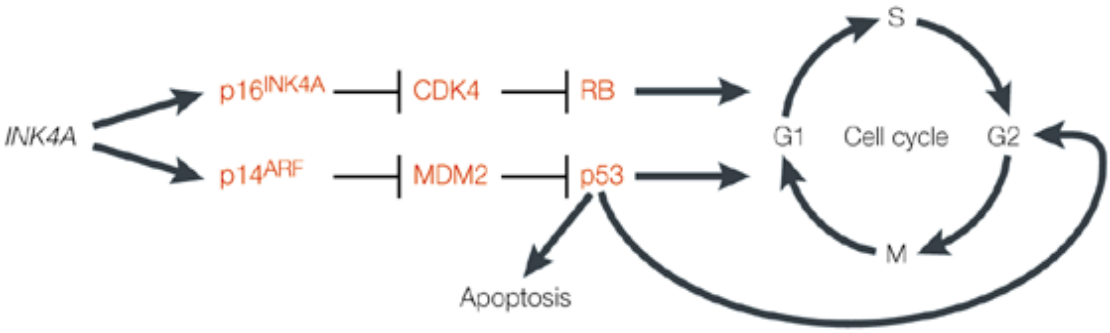


p53 controls the cell cycle by arresting cells in G1 and G2, and by inducing apoptosis (Fulci G 2000) in response to events such as DNA damage. Loss of normal TP53 function, and therefore cell cycle regulation, can result from altered expression of *TP53*, *MDM2*, or $p14^{ARF}$ genes. Mutations in *TP53* occur in about 30% of primary GBM and more commonly in secondary GBM (Ohgaki H 2004). Amplification of *MDM2*, whose gene product degrades p53, is present in <10% of cases and is exclusively found in primary GBM that lack *TP53* mutations (Reifenberger G 1993). $p14^{ARF}$ binds to MDM2 and inhibits its degradation of p53. Loss of $p14^{ARF}$ expression is observed in around three quarters of GBMs, typically resulting from homozygous deletion or promoter methylation of the $p14^{ARF}$ gene (also known as *CDKN2A*) (Nakamura M 2001a).

RB1 protein promotes cell cycle arrest in G1 and regulates progression from the G1 to S phase of the cell cycle (Holland E 2001). CDK4/cyclin D1 complex phosphorylates RB1, thereby inactivating it and inducing the release of transcription factors that activate genes involved in G1 to S transition (Sherr CJ 1999). $p16^{INK4a}$ binds to CDK4, and inhibits the

CDK4/cyclin D1 complex, thus inhibiting this transition (Sherr CJ 1999). Consequently, loss of normal RB1 function may result from reduced expression of *RB1* or $p16^{INK4a}$, and increased expression of *CDK4*. Homozygous $p16^{INK4a}$ deletions are found in both primary and secondary GBM, but are more common in the former (Nakamura M 2001a); loss of RB1 expression occurs in 14% of primary and 43% of secondary GBM, often in conjunction with promoter hypermethylation of the RB1 gene (Nakamura M 2001b); whilst amplification and overexpression of *CDK4* occurs in 15% of GBMs (Holland E 2001).

#### 1.2.2.3 Loss of Heterozygocity (LOH) associated with GBM

LOH of chromosome 10 is commonly seen in GBM. LOH 10q occurs in between 60-80% of both primary and secondary GBMs (Fujisawa H 2000, Ohgaki H 2004), whilst LOH 10p and complete loss of chromosome 10 are largely seen exclusively in primary GBM (Fujisawa H 2000). At least 3 commonly deleted loci have been identified on chromosome 10, namely 10p14-p15, 10q23-24 (PTEN), and 10q25-pter and it is probable that several tumour suppressor genes that play a role in gliomagenesis are located here (Rasheed BK 1995, Fults D 1998, Ichimura K 1998). LOH 10q25-qter is worth particular mention as it has been shown to occur during the transition between grade II or grade III glioma and GBM (Fujisawa H 1999). This locus contains several assumed tumour suppressor genes (Eagle LR 1995, Chernova OB 1998, Nakamura H 1998) and although mutations in these genes have rarely been detected in GBM, the fact that LOH 10q25-qter occurs commonly in both primary and secondary GBM (Rasheed BK 1995) implies that they may play a role.

LOH 22q also occurs frequently in GBM, a region that incorporates the tissue inhibitor of metalloproteinases-3 (*TIMP-3*) gene. Loss of TIMP-3 expression has also been reported, in association with *TIMP-3* promoter methylation (Nakamura M 2005). LOH 19q, 1p and 13q are also reported at varying frequency (Nakamura M 2000).

#### 1.2.2.4 Correlation between genetic changes and classification of GBM

In addition to providing insight in to the pathogenesis of glioma, genetic and chromosomal abnormalities can also be used to classify GBM into their primary and secondary forms, and into their recognised subtypes. Specifically primary GBM are typically associated with EGFR amplification, p16 deletion, and PTEN mutations as well as LOH on chromosome 10q (Ohgaki H 2005a); whilst secondary GBM frequently demonstrate mutations in TP53 and IDH1 (Ohgaki H 2005b, Yan H 2009), as well as combined loss of chromosome arms 1p and 19q (1p/19q deletion) (Schiff D 2007). Furthermore the 'classical', proneural and mesenchymal subtypes are associated with *EGFR* amplification, P53/PDGFRA/IDH1 mutations, and NF1 mutations respectively (Verhaak RG 2010).

### 1.2.3 GBM cell of origin

GBM cells most frequently resemble immature astrocytes, oligodendrocytes or a combination of the two. It was once thought that mature glia were the only cells in the brain capable of dividing, and hence GBM was proposed to occur as a result malignant transformation in these cells. However the discovery that new neurons and glia are produced throughout life from neural stem cells (NSCs) (Eriksson P 1998, Lie DC 2004) provided a new candidate cell of origin in GBM. The identity of GBM initiating cells (GICs) remains a source of debate, however tumours could feasibly arise from either dedifferentiated mature glial cells, glial precursors which have acquired oncogenic mutations, or indeed NSCs.

#### 1.2.3.1 The dedifferentiated cell theory

This theory proposes that mature oligodendrocytes or astrocytes undergo dedifferentiation and develop oncogenic capability through the acquisition of specific mutations, and is supported by the observation that activation of specific oncogenes in conjunction with the

loss of tumour suppressor genes in cortical astrocytes triggers cancer initiation with histological features similar to glioma in animal models (Stiles CD 2008). Indeed the combined loss of $p16^{INK4a}$ and $p19^{ARF}$ enabled astrocytes to dedifferentiate in response to EGFR activation, and in xenograph experiments Ink4a/Arf(−/−) astrocytes transduced with constitutively active EGFR induced a high grade glioma phenotype (Bachoo RM 2002). Similarly, loss of $p16^{INK4a}$ and $p19^{ARF}$ in conjunction with activation of K-Ras and Akt induced dedifferentiation of mature astrocytes and the formation of tumours with morphology closely resembling that of GBM (Uhrbom L 2002). Furthermore loss of p53 combined with the overexpression of Akt and c-Myc in mature astrocytes rendered them highly tumorigenic when transplanted into the brains of immunocompetent mice (Radke J 2013).

#### 1.2.3.2 The cancer stem cell theory

Neural stem-cells (NSCs) are highly undifferentiated clonogenic cells with an extensive proliferative potential and are capable of multipotent differentiation into the three main cell types of the CNS. They have extensive self-renewal capacity which they achieve by undergoing asymmetric divisions during which a copy of the mother cell together with a more mature progenitor cell are generated. Similarly they can undergo symmetrical division, yielding either two stem cells or two more mature progenitors.

NSCs are found in the human brain in two neurogenic niches: the subventricular zone (SVZ), which is located between the lateral ventricle and the parenchyma of the striatum (Silva-Vargas V 2013); and the subgranular zone (SGZ) located in the hippocampus (McKay R 1997). These areas function as a source of both NSCs and progenitor cells and retain the ability to produce neurons and glia throughout life (Luskin MB 1993).

Three cell types have been identified in the SVZ of the human brain: types A, B and C. Type B cells are the putative adult neural stem cell. They express the astroglial marker glial

fibrillary acidic protein (GFAP) and the neural stem cell marker nestin and are relatively quiescent (Doetsch F 1999). B cells give rise to highly proliferative transit-amplifying progenitor cells (type C cells) which retain multipotency and give rise to more mature transiently dividing lineage-committed progenitors (type A cells) (Alvarez-Buylla A 2004) ***(Figure 1-4)***.

**Figure 1-4: The hierarchical neural stem cell system demonstrating the gene expression pattern associated with each cell type**

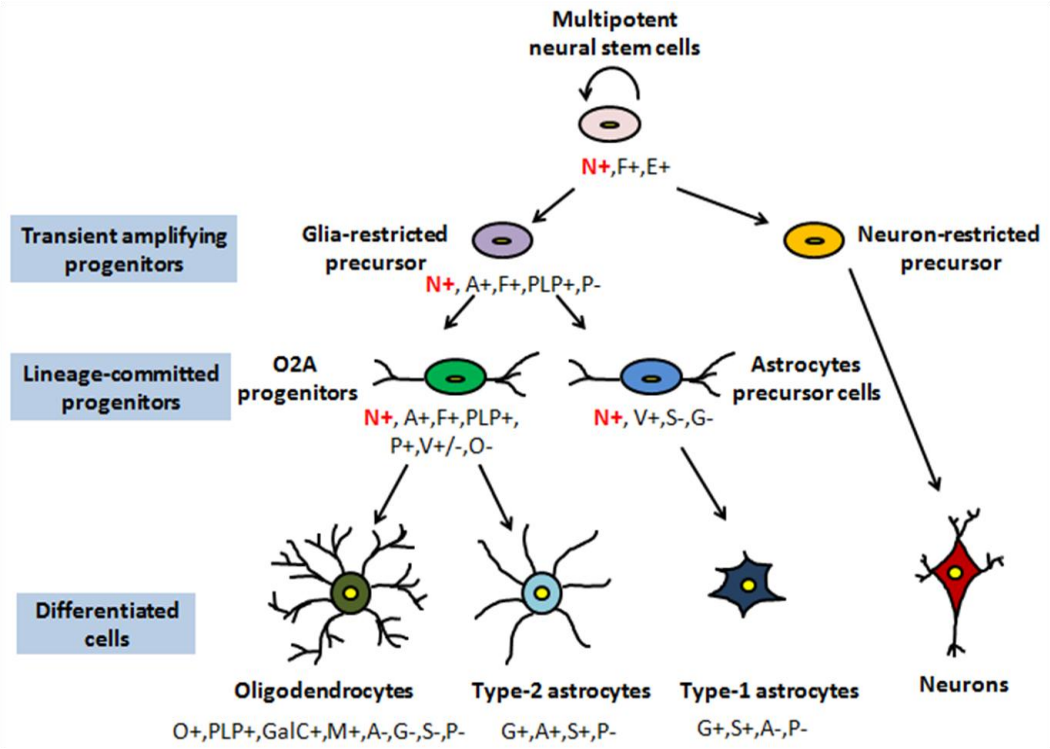


N:nestin; A: A2B5; E: EGFR; G: GFAP; P: PDGFR; V:Vimentin; F:FGFR; PLP: myelin proteolipid protein; O: 04; S: S100; GalC: galactocerebroside; M: myelin basic protein.

Type A cells, or neuroblasts, migrate in bundles to the olfactory bulb (OB) through the rostral migratory stream (RMS), a vestigial lumen that connects the lateral ventricle to the olfactory bulb, where they integrate as new interneurons in the cortical layers (Pincus DW 1997, Kukekov VG 1999, Curtis MA 2007). A similar hierarchical neural stem cell system and migratory pattern is also seen in the brains of mice (Seri B 2004, Quiñones-Hinojosa A 2006) ***(Figure 1-5)***.

**Figure 1-5: The location of stem cells in the SVZ and Hippocampus and their migration to the Olfactory Bulb via the RMS in mice.**

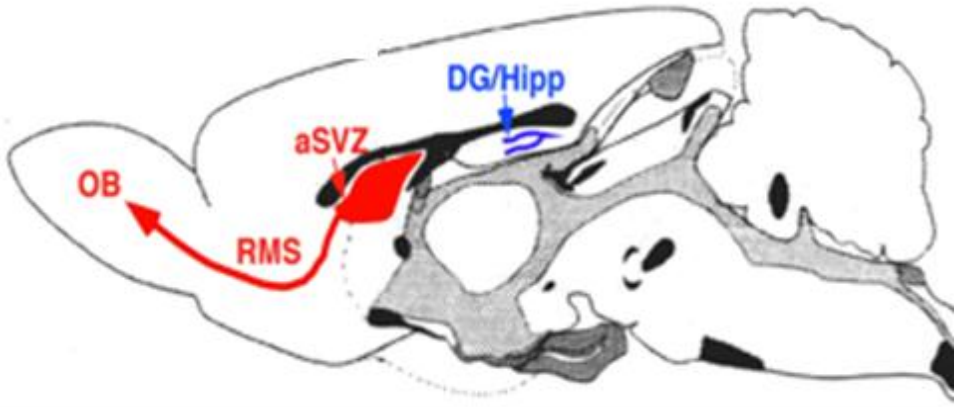


Type B and C cells can be defined by the expression of Nestin, a cytoplasmic intermediate filament protein (Hockfield S 1985). Nestin expression is lost *in vitro* with differentiation of NS cells, whilst *in vivo*, it is retained postnatally only in neurogenic zones. Indeed in mice, nestin is expressed from E7.75 in many proliferating CNS regions, at E10.5 it is expressed in cells of both the rostral and caudal neural tube, and at E15.5 and P0 expression is observed largely in the developing cerebellum, and in the subventricular areas of the developing telencephalon (Dahlstrand J 1995). Nestin expression is maintained in the SVZ of adult mice and has been detected in 26 month old adults in this regions, although its expression reduces in conjunction with a reduced level of neurogenesis in the brains of older mice (Maslov A 2004).

Human NS cells also express the cell surface marker prominin-1 (PROM1) (Uchida N 2000). PROM1, also known as CD133, is expressed in the SVZ of humans and mice on the apical membrane of cells lining the lateral ventricles, but with more restricted expression than Nestin.

A growing body of evidence suggests that GBMs originate from neural stem cells which accumulate genetic changes over a period of time, escape from the control of their environment, and give rise to tumour growth. Both NSCs or their progenitors could feasibly fulfil this role of tumour-initiating cell, and NSCs are particularly attractive candidates because they are tissue specific, can self-renew and are multipotent. Indeed the presence of a subpopulation of immature, undifferentiated cells with tumour initiating capacity, so called glioblastoma stem cells (GSCs) or glioblastoma initiating cells (GICs) have been demonstrated in tumours (Ignatova T 2002, Singh SK 2003, Tabatabai G 2011), and these cells are thought to be responsible for the high level of tumour recurrences and resistance to radiotherapy and chemotherapy observed in GBM (Bao S 2006, Liu G 2006, Salmaggi A 2006, Murat A 2008, Johannessen TC 2009). Furthermore, GSCs cells have also been shown to have the potential to initiate GBM formation when isolated and injected into the brains of nude mice (Galli R 2004), whilst the expression of the GSC specific marker CD133, and the embryonic stem cell marker signature Oct4, Sox2, and Nanog in human gliomas have been shown to correlate with poorer prognosis and increased clinical aggressiveness (Beier D 2008, Holmberg J 2011). Consequently, the potential to target GSCs both directly and indirectly is currently being investigated (Binello E 2011)

GSCs are thought to originate in the SVZ, and several studies using murine glioma models have supported this theory (Zhu Y 2005, Alcantara Llaguno S 2009). Indeed mutations in both type B and type C cells have been shown to lead to tumour initiation in the early stages of gliomagenesis in mouse models (Wang Y 2009). Furthermore, when human GBM cells are injected into the brains of nude mice they exhibit a tropism for the SVZ and are able to migrate from there towards the olfactory bulbs (Kroonen J 2011), and when these cells are re-isolated from the SVZ and olfactory bulbs and injected into new mice, they demonstrate high tumorigenicity.

In humans, a proportion of GBMs have been shown to develop near the region of the SVZ, whilst exposure to oncogenic viruses or carcinogens results in the preferential formation of tumours in this region (Sanai N 2005). GBMs that originate in close proximity to SVZ are more likely to be multifocal, and recur at a greater distance from the primary lesion (Lim DA 2007). Furthermore, SVZ involvement has been shown to be an independent predictive factor for shorter survival in newly diagnosed patient undergoing treatment for GBM (Young GS 2011) and it has been demonstrated that giving high dose radiotherapy (>43Gy) to the SVZ in patients with grade III glioma and GBM improves both PFS and OS (Lee P 2013).

### 1.2.4 Symptoms and Presentation in GBM

Symptoms and signs of GBM result from the tumour mass and its infiltration of adjacent tissues as well as adjacent oedema, and raised intracranial pressure (ICP). Headaches occurs in about 50% of patients, and are typically not severe, worse in the morning and improve throughout the day. They may be exacerbated by activities that increase ICP. Other symptoms of raised ICP such as nausea, vomiting and visual abnormalities can occur. Seizures occur as the presenting feature in about 35% of patients with GBM (Vecht C 2003) and can be focal or generalised. Other focal neurological manifestations include motor or sensory deficits, visual field defects, dysphasia, cognitive dysfunction and personality changes.

### 1.2.5 Diagnosis of GBM

Magnetic resonance imaging (MRI) with intravenous gadolinium contrast enhancement is the standard technique used to diagnose GBM. The tumour demonstrates low signal intensity with a hypodense necrotic central area surrounded by an enhanced rim on T1-weighted images, reflecting the presence of central necrosis surrounded by a highly cellular

vascularised wall. Conversely it appears as a high-signal intensity mass on T2-weighted images. Imaging of tumour blood flow using perfusion MRI and assessment of tumour metabolite concentration with MR spectroscopy may add diagnostic value to standard MRI (Cha S 2006, Sibtain NA 2007). Definitive diagnosis requires a stereotactic biopsy or craniotomy with tumour resection to allow pathologic confirmation. Because the tumour grade is based on the most malignant portion of the tumour, biopsy or subtotal tumour resection may lead to under grading of the lesion.

### 1.2.6 Treatment of newly diagnosed GBM

Conventional treatment of newly-diagnosed GBM comprises surgical resection of the tumour followed by radiotherapy (60Gy in 30 fractions) in combination with TMZ chemotherapy (75mg/$m^2$/day for 6 weeks), followed by 6 cycles of adjuvant TMZ (150-200mg/$m^2$/day) given for 5 days during each 28-day cycle. TMZ is an oral alkylating agent that delivers a methyl group to purine bases of DNA (O6-guanine; N7-guanine and N3-adenine), increasing the cellular levels of these methylated bases. The primary cytotoxic lesion is O6-methylguanine (O6-MeG) (Esteller M 1999), although N3-methyladenine (M3-MeA) also exhibits cytotoxic effects (Horton JK 2007). Direct repair of O6-MeG by methylguanine-DNA methyltransferase (MGMT) normally removes the methyl adduct, restoring guanine. However unrepaired O6-MeG mispairs with thymine (instead of cytosine) during DNA replication, alerting DNA mismatch repair (MMR) (Kyrtopoulos SA 1997, Margison GP 2002). MMR exclusively recognises the mispaired thymine on the daughter strand and excises it, but O6-MeG persists in the template strand. Consequently, futile cycles of thymine re-insertion and excision result in persistent DNA strand breaks, causing replication fork collapse (Mojas N 2007). G2/M cell cycle arrest is triggered (Roos W 2004), via ATR/CHK1-dependent signalling (Stojic L 2004) and apoptosis ensues (D'Atri S 1998). A

good response to TMZ therefore requires functional MMR and low levels of MGMT. The N3-MeA lesion is normally rapidly repaired by DNA base excision repair (BER), but these lesions are lethal if not intercepted (Horton JK 2007). Therefore, MGMT, MMR and BER are all important DNA repair processes impacting the mechanism of action and cytotoxicty of TMZ.

Evidence for the benefit of TMZ in GBM emerged in 2005 from a randomised, multicentre, phase III trial of 573 patients with newly diagnosed GBM (Stupp R 2005). Patients who were candidates for surgery underwent maximal resection followed by either radiotherapy alone, or radiotherapy with concurrent and adjuvant TMZ. Median survival was improved in the TMZ group compared to the radiotherapy only group (14.6 months vs 12.1 months), and 2 year and 5 year survival rates improved to 26.5% from 10.4% (Stupp R 2005), and to 9.8% from 1.9% respectively (Stupp R 2009). Methylation of the MGMT promoter was found to the strongest predictor for benefit from TMZ chemotherapy (Stupp R 2009), and this relationship has also been demonstrated in other studies (Minniti G 2008, Gilbert MR 2011, Kim YS 2012, Malmström A 2012, Wick W 2012, Park CK 2013). MGMT promoter methylation results in MGMT gene silencing, and it has previously been suggested that this can result in reduced DNA repair and an increased susceptibility to chemotherapy (Esteller M 2000). Indeed among TMZ treated patients with MGMT promoter methylation, median and 2-year survival were 21.7 months and 46% respectively, compared to 12.7 month and 13.8% in those patients who retained normal MGMT expression (Stupp R 2005). Combinations of other alkylating agents namely procarbazine, lomustine and vincristine (PCV) have also been trialled in newly diagnosed GBM however prospective randomised trials have failed to demonstrate a survival benefit (Medical Research Council Brain Tumor Working Party 2001) and the toxicity of such regimens is not negligible (Lonardi S 2005). Trials using Gliadel wafers, which contain the alkylating agent carmustine and a biodegradable polyanhydride copolymer and are

implanted in the tumour resection cavity intraoperatively, have demonstrated a modest median survival benefit when compared to placebo controls (13.9 vs 11.6 months) (Westphal M 2006), but may be associated with side effects such as seizure, cerebral oedema, and intracranial infection (Attenello FJ 2008), and their use is not considered to be standard practice in the UK.

### 1.2.7 Treatment of recurrent GBM

The median time to recurrence after standard therapy in GBM is 6.9 months (Stupp R 2005). Treatment options at this stage include repeat surgical resection, re-irradiation, further chemotherapy with standard agents, or novel therapies as part of a clinical trial. Patients with recurrent GBM have almost invariably already undergone a full course of external beam radiotherapy making re-irradiation difficult and potentially toxic, particularly with the risk of radiation necrosis. It is therefore only offered to a minority of patients although responses have been observed and quality of life may be improved without significant toxicities (Veninga T 2001). The lack of randomised trials evaluating the role of repeat surgical resection makes it difficult to assess the potential benefit of such intervention, however dependent on certain prognostic factors such as age and performance status, further surgery may be considered in locally recurrent disease and has been shown to relieves symptoms, improve performance status and quality of life, reduce the requirements for steroids, and in some cases, increase survival (Kreth FW 1999).

No standard chemotherapy treatment exists for patients with recurrent GBM and the prognosis associated with relapsed disease remains poor. Patients with relapsed disease are traditionally offered nitrosourea-based chemotherapy such as carmustine and PCV. Historically however, these therapies have been associated with objective tumour response rates of less than 10% (Wong ET 1999) and do not offer any significant OS benefit

(Grossman SA 2004). Alternative agents such as carboplatin, irinotecan, oxaliplatin and etoposide have also been trialled but they offer lower response rates and additional toxicity (Friedman HS 1999, Grossman SA 2004). Consequently the enrolment of patients into clinical trials evaluating novel investigational therapies is often a more appropriate option in this setting if available.

### 1.2.8 Novel targeted therapy in GBM

Various potential therapeutic targets have been suggested in GBM based on the improved understanding of the molecular mechanisms and signalling pathways involved in the gliomagenesis arising from genome-wide molecular characterisation and profiling analyses (McLendon R 2008). These include pathways activated by amplification of receptor tyrosine kinases (RTKs) such as EGFR, IGFR, VEGFR and PDGFR, and activation of downstream effectors such as PI3K, Akt, PTEN, mTOR, Ras, Raf, MEK and MAPK ***(Table 1-3)***. Research efforts have focused on developing molecularly targeted therapies directed against such aberrations with the hope of improving survival whilst also minimising toxicity (Collins VP 2007). Such therapies include monoclonal antibodies with an affinity for receptors or their ligands; and tyrosine kinase inhibitors (TKIs) that inhibit signalling by binding with ATP binding pockets on the intracellular catalytic kinase domain of RTKs, preventing auto-phosphorylation and activation of downstream signalling pathways (Seshacharyulu P 2012). Generally however single agent novel therapies have been disappointing, demonstrating poor response rates and no OS benefit (Chi AS 2007). This lack of efficacy is thought to be due to factors such as tumour heterogeneity, redundancy and parallel processing of intracellular signalling pathways, constitutive RTK activation, coactivation of multiple RTKs, and limited drug delivery through the blood brain barrier (BBB) (Stommel JM 2007). The development of multi-kinase inhibitors and the combination of targeted therapies may help to improve

efficacy, but a better understanding of the pathogenesis of GBM and the development of therapies targeting previously unknown mechanisms are required.

**Table 1-3: An overview of some of the targeted therapies that have been trialled in GBM**

| Signalling Pathway | Compound Name |
|---|---|
| VEGF - directed monoclonal antibodies | bevacizumab |
| | aflibercept |
| VEGFR - directed monoclonal antibodies | Icrucumab |
| | Ramucirumab |
| VEGFR small molecules kinase inhibitors | Sorafenib |
| | Sunitinib |
| | Vatalanib |
| | Vandetanib |
| | Cediranib |
| Integrin inhibitors | Cilengitide |
| PDGFR - small molecules kinase inhibitors | Imatinib |
| | Tandutinib |
| EGFR - directed monoclonal antibodies | Cetixumab |
| | Panitumumab |
| | Nimotuzumab |
| EGFR small molecule kinase inhibitors | Gefitinib |
| | Erlotinib |
| | Lapatinib |
| | Canertinib |
| PI-3K inhibitors | GSK615 |
| | D-87503 |
| | XL765 |
| | XL147 |

| | |
|---|---|
| Akt inhibitors | GSK690693 |
| | Akt VIII |
| | MK-2206 |
| mTOR inhibitors | Rapamycin |
| | Torin |
| | pp242 |
| dual PI-3K/mTOR inhibitors | PI-103 |
| | GDC-0941 |
| gamma-secretase/Notch signaling | RO4929097 |
| HDAC inhibitors | Vorinostat |
| | Valproic acid |
| PARP inhibitors | Olaparib |

#### 1.2.8.1 Vascular targeted therapies

GBMs are highly vascular tumours and rely upon angiogenesis for growth and progression. Consequently, antiangiogenic therapy is seen as an attractive target (Shirai K 2012).

VEGF is a key signaling pathway in glioma angiogenesis, and overexpression of VEGF receptors VEGFR-1 and VEGFR-2, and upregulation of VEGF-A are observed (Cea V 2012). Bevacizumab (Avastin), a humanised anti-VEGF monoclonal antibody is the most extensively tested antiangiogenic agent in GBM. However although several clinical trials of bevacizumab given as a single agent, or in combination with irinotecan, have demonstrated an improvement in progression-free survival in recurrent GBM, no OS benefit has been identified (Vredenburgh JJ 2007, Cloughesy TF 2008). Similarly bevacizumab did not demonstrate an OS benefit in two phase III randomised controlled trials of patients with newly diagnosed GBM (Chinot O 2012, Gilbert MR 2013).

Other VEGF-targeting agents such as cediranib, aflibercept, and vatalanib have also been shown to be relatively ineffective in recurrent GBM (Conrad C 2004, de Groot JF 2011, Batchelor TT 2013). Furthermore, continuous daily treatment with sunitinib, a multikinase inhibitor of VEGFR did not prolong progression-free survival in a phase II study of patients recurrent GBM (Kreisl TN 2013), however sorafenib, another multikinase inhibitor demonstrated some activity in this patient group (Zustovich F 2013), and phase III trials are required to assess if it will offer an OS benefit.

Cilengitide, an integrin inhibitor with antiangiogenic properties exhibited modest anti-tumour activity in a phase II trial of patients with recurrent GBM (Reardon DA 2008). However no OS benefit was demonstrated when cilengitide was combined with standard TMZ chemoradiotherapy in a phase III randomised controlled trial of patients with newly diagnosed GBM and MGMT promoter methylation (Stupp R 2013).

Angiogenesis in GBM is also induced by PDGF and FGF through different signalling pathways (Johannessen TC 2009). Imatinib is a tyrosine kinase inhibitor that blocks the activity of PDGFR. Studies of imatinib in unselected patients with GBM demonstrated only modest 6 month PFS benefit (PFS6) (~16%) (Wen PY 2006, Raymond E 2008), however PFS6 has been shown to be higher (32%) in patients who had expression of PDGFR detected by immunohistochemistry (IHC) (Marosi C 2006), indicating that patient stratification based upon tumour phenotype may be beneficial. Another PDGF inhibitor, Dasatinib, when given alone or in combination with bevacizumab did not exhibit activity in recurrent GBM and demonstrated low central nervous system penetration (Lu-Emerson C 2011). Thalidomide and its more potent analogue lenalidomide inhibit FGF, and both have demonstrated modest activity in GBM (Fine HA 2000, Drappatz J 2009), and a Phase II study of irinotecan plus lenalidomide in patients with recurrent GBM is currently underway (http://clinicaltrials.gov/ct2/show/NCT00671801).

#### 1.2.8.2 EGFR inhibitors

*EGFR* is commonly mutated in GBM either by gene amplification, exon deletion or point mutation (Frederick L 2000, Lee JC 2006, Toth J 2009). Ordinarily EGFR activation is receptor-mediated with activating ligands contacting two distinct sites within a single receptor. Mutations in *EGFR* result in constitutive activation of the mutant receptor, independent of ligand stimulation, which induces various oncogenic effects such as an increased proliferative potential. Both monoclonal antibodies and TKIs directed against EGFR have been studied in glioma.

Cetuximab, a monoclonal antibody directed against EGFR, blocks EGFR-mediated signal transduction by interfering with ligand binding and extracellular dimerisation. Cetuximab showed preclinical anti-tumour activity in GBM (Eller JL 2005), however limited efficacy was demonstrated in a phase II trial of cetuximab in combination with TMZ and bevacizumab in recurrent GBM (Hasselbalch B 2010), possibly as a result of poor BBB penetration (Thaker NG 2009). Interestingly patients with an EGFR amplification lacking EGFRvIII expression have been shown to have a significantly superior PFS and improved OS following treatment with cetuximab, suggesting that the specific type of EGFR mutation may determine outcome (Lv S 2012). Another EGFR monoclonal antibody, nimotuzumab, was tested in a randomised phase III trial in combination with TMZ and radiotherapy in newly diagnosed GBM. Interim analysis failed to demonstrate significant efficacy (Bach F 2011), however on final analysis, a clear trend towards efficacy was shown in the subgroup of patients with MGMT non-methylated tumours (Westphal M 2012). A survival benefit was also demonstrated in a smaller study of nimotuzumab in combination with radiotherapy alone, and it has been suggested that it may have a role as a radiosensitizer (Solomón MT 2013). A phase II trial of a third EGFR monoclonal antibody, panitumumab, is currently

underway in combination with irinotecan in recurrent GBM (http://clinicaltrials.gov/show/NCT01017653).

TKIs of EGFR used in clinical trials in GBM include gefitinib (Lieberman FS 2004, Rich JN 2004, Uhm JH 2004, Chakravarti A 2013), erlotinib (Vogelbaum MA 2004, van den Bent MJ 2009, Peereboom DM 2010, Reardon DA 2010, Peereboom DM 2013), lapatinib (Thiessen B 2010, Reardon DA 2013) and afatinib (Eisenstat DD 2011). Phase II clinical trials of gefitinib in recurrent GBM report disappointing efficacy (Lieberman FS 2004, Rich JN 2004). Furthermore no OS benefit was demonstrated in newly diagnosed GBM patients when gefitinib was given either concurrently with radiotherapy (Chakravarti A 2013) or adjuvantly (Uhm JH 2004), although an association with improved OS was noted in a subgroup of patients who experienced gefitinib-associated diarrhoea (Uhm JH 2004). Similarly clinical trials of erlotinib given as a single agent or in combination, have failed to demonstrate significant survival benefit in patients with newly diagnosed or recurrent GBM (Vogelbaum MA 2004, van den Bent MJ 2009, Peereboom DM 2010, Reardon DA 2010, Peereboom DM 2013). It should be noted however that more favourable responses were typically seen with erlotinib in patients with tumours that had amplification of EGFR combined with low levels of Akt, or with expression of the EGFRvIII variant and preservation of PTEN, providing a rationale for stratifying patients for treatment based on genomic tumour profiles (Haas-Kogan DA 2005, Mellinghoff IK 2005). Lapatinib is dual TKI of EGFR type 2 (HER2/neu) and EGFR. It has shown efficacy in the treatment of brain metastases in patients with breast cancer (Metro G 2011) and has also been shown to distribute into glioma tissue (Kuhn J 2008). However lapatinib has not demonstrated significant activity in phase I/II trials in GBM (Thiessen B 2010, Reardon DA 2013). Afatinib is an irreversible EGFR TKI that has been shown to be highly active in lung cancer cell lines that are resistant to reversible EGFR inhibitors such as erlotinib (Li D 2008). However a phase II study of afatinib, given alone or

in combination with TMZ in patients with recurrent GBM, showed it to have limited activity as a single agent or in combination, although preliminary biomarker data suggested afatinib could achieve durable disease control in EGFRvIII-positive patients (Eisenstat DD 2011).

#### 1.2.8.3 Inhibition of intracellular signaling pathways

Growth factor receptors transduce a signal through several common intracellular pathways, including the Ras/Raf/MAPK and PI3K/Akt pathways which in turn modulate cell growth, differentiation, angiogenesis and apoptosis. Inhibition of intermediate and downstream components of growth factor signaling pathways therefore a promising therapeutic strategy.

Ras mutations are uncommon in gliomas, but Ras is often constitutively activated through the action of upstream signaling pathways (Guha A 1997). Farnesyltransferase inhibitors (FTIs) inhibit Ras farnesylation and have been shown to inhibit growth in gliomas (Feldkamp MM 1999, Glass TL 2000). The FTIs tipifarnib and lonafarnib have been trialed in GBM. The former has demonstrated poor activity in both newly diagnosed and recurrent GBM (Cloughesy TF 2006, Lustig R 2008), whilst the latter has been shown to potentiate the activity of TMZ and radiation in orthotopic mouse models (Chaponis D 2011), and to be active in combination with TMZ in phase I trials of patients with recurrent or refractory disease (Yust-Katz S 2013). Phase II/III trials of lonafarnib are required to determine its efficacy in GBM.

Protein kinase C (PKC) forms part of the signaling cascade downstream of growth factors such as EGF and PDGF. PKC activation induces the phosphorylation of Raf and MAPK, and activates Ras, and it has been shown to contribute to the aggressive behaviour of glioma cells (do Carmo A 2013). Enzastaurin, a PKC inhibitor, achieved objective radiographic responses in 22% of patients with recurrent high grade glioma, however a phase III study was terminated early due to clinical inefficacy (Wick W 2010). Furthermore, in patients with

newly diagnosed GBM enzastaurin did not provide additional survival benefit when given in combination with TMZ and radiotherapy (Butowski N 2011).

Activation of receptor tyrosine kinases results in activation of the PI3K/Akt/mTOR pathway which in turn induces cell growth and proliferation. Alterations in PI3K activity are seen in GBM (Ohgaki H 2011), as is the upregulation of Akt which is extremely common (McDowell KA 2011), and the resultant dysregulation of mTOR signaling has been shown to be an important determinant of gliomagenesis (Zheng H 2008). PI3K inhibitors such as LY294002 and wortmannin have been developed, however their use has been limited to pre clinical studies due to their toxic effects, poor pharmaceutical properties, and a lack of selectivity (Cleary JM 2010, Ohka F 2012). SF1126, a derivative of LY294002, has a more favourable pharmacokinetic and tolerability profile and has demonstrated encouraging results in phase 1 trials (Mahadevan D 2012). Perifosine, an oral Akt inhibitor has been shown to induce cell death and decreased proliferation in PDGF driven GBM mouse models (Momota H 2005, Pitter KL 2011), and is currently undergoing phase II clinical trials in various human cancers (Ohka F 2012). The mTOR inhibitor temsirolimus has been shown to be active in glioma and improved time to progression in a phase II clinical trial in patients with recurrent disease (Galanis E 2005). However other trials using temsirolimus as a monotherapy (De Witt Hamer PC 2010), or in combination with bevacizumab (Lassen U 2013) have not demonstrated an OS benefit. Everolimus, another mTOR inhibitor, was shown to potentiate TMZ induced autophagic cell death in vitro (Josset E 2013), and was well tolerated in a phase I clinical trial in combination with TMZ and radiotherapy in patients with newly diagnosed GBM (Chinnaiyan P 2013). Furthermore a modest efficacy benefit was demonstrated in the first line setting in a phase II trial when given in combination with bevacizumab, TMZ and radiotherapy (Hainsworth JD 2012). Phase III trials of everolimus in GBM are ongoing. XL765 an oral dual PI3K/mTOR inhibitor demonstrated activity in combination with TMZ in

preclinical trials using human GBM xenographs (Prasad G 2011), and this combination is being investigated in early phase clinical trials (http://clinicaltrials.gov/show/NCT00704080).

#### 1.2.8.4 Combination targeted therapies

Given the relative failures of single agent targeted therapy the use of multi-targeting combination treatments has been suggested. Combined inhibition of a TKR and one of its downstream effectors is one potential method of overcoming resistance that arises from simultaneous coactivation of TKRs (Thaker NG 2009). However clinical trials combining either EGFR or VEGFR TKIs with mTOR or Ras inhibitors have failed to demonstrate sufficient activity (Doherty L 2006, Nguyen TD 2006, Reardon DA 2006, Chang SM 2009, Peereboom DM 2013). The combined inhibition of multiple TKRs, has also been investigated, in particular those targeting VEGFR and EGFR. The rationale for targeting these two pathways comes in part from the observation that EGFR expression leads to up-regulation of VEGF production (Pore N 2003), and that enhanced VEGF expression is the possible basis of acquired resistance to EGFR targeted therapy (Naumov GN 2009). However results from clinical trials using combinations targeting both EGFR and VEGFR have been disappointing (Prados M 2009, Sathornsumetee S 2010, Reardon DA 2012). Results from the DORIC study, investigating the efficacy of cediranib in combination with gefitinib in patients with recurrent or progressive GBM are awaited.

#### 1.2.8.5 Immune Checkpoint Inhibitors

Immune checkpoint proteins have emerged as increasingly important therapuetic targets in various cancers (Creelan B 2014), and has led to the development of drugs targeting the CTLA-4, PD-1, and PD-L1 inhibitory pathways. These drugs have shown early promise in GBM but have not yet emereged as standard therapeutic options (Dietrich P 2014).

### 1.2.9 Prognosis

The median survival of patients with GBM is generally less than one year after diagnosis, and even in the most favourable cases death usually occurs within 2 years (Curran WJ Jr 1993, Puzzilli F 1998, Scott JN 1998, Buckner JC 2003, Stark AM 2005). Even with optimal combination therapy incorporating surgery and TMZ chemoradiotherapy, median OS is only 14.6 months, and observed 2- and 5-year survival rates are 26.5% and 9.8% respectively (Stupp R 2005, Stupp R 2009). The aggressive nature of the disease is due in part to the high proliferation rate, diffuse infiltration, resistance to apoptosis and robust angiogenesis that is associated with GBM (Giese A 1996), as well as the relative chemo- and radio-resistance of these tumours (Murat A 2008). Disease relapse invariably occurs during or after first-line treatment, and results in death in the majority of patients within 6 months (Wong ET 1999). The addition of concurrent and adjuvant TMZ chemotherapy to standard first line therapy was the first treatment to improve prognosis in a population in whom outcomes had not improved for three decades (Stupp R 2005, Stupp R 2009). However subsequent therapies both in the first line and relapsed setting have failed to supersede this.

Age at presentation is a strong prognostic indicator, and a significant negative relationship is seen between advancing age and survival (Korshunov A 2005). Functional status (Krex D 2007), tumour size and location(Lamborn KR 2004), extent of tumour resection (Schiff D 2003), and the use of multimodal therapy (Stupp R 2005, Minniti G 2008) also have prognostic implications, and, using recursive partitioning analysis, were utilised to stratify patients into four risk groups (Lamborn KR 2004). The two lower risk groups included patients under 40 years old, with the lowest group being those young patients with frontal lobe tumours. An intermediate-risk group included patients aged between 40 and 65, with Karnofsky performance status (KPS) >70, who had undergone subtotal or total resection. The

highest risk group included patients aged between 40 and 65 who had either undergone biopsy only without further resection, or who had a KPS <80, as well as all patients over the age of 65. Subgroup analyses indicated that inclusion of adjuvant chemotherapy provided an increase in survival, although that improvement was minimal for all patients over the age of 65, and for patients aged over 40 with a KPS <80 (Lamborn KR 2004).

Several histological characteristics have been shown to have prognostic significance. For example elevated expression of the cellular proliferation marker Ki-67 is associated with increased histological grade and shorter PFS and OS (Montine TJ 1994, Jin Q 2011 ). Furthermore a correlation exists between the presence of tumour necrosis and poor outcome (Barker FG 2nd 1996, Homma T 2006, Noch E 2009). Conversely, the presence of microcystic change and calcification predict a relatively better outcome (Burger PC 1987, Schmidt MC 2002, Bähr O 2011). The presence of oligodendroglial components within a tumour has also been shown to be predictive of better survival in some studies(Kraus JA 2001, Hilton DA 2004), although others report no such correlation (He J 2001).

Molecular markers also demonstrate prognostic value. *MGMT* promoter methylation has been shown to be an independent positive prognostic factor in GBM irrespective of treatment (Hegi ME 2005). A glioma specific CpG Island Methylator Phenotype (G-CIMP) has recently been described to occur in a subgroup of patients with GBM (Noushmehr H 2010). This phenotype is also associated with a relatively improved prognosis and shows a strong correlation with MGMT methylation (Lai RK 2014). Consequently it is possible that the improved prognosis associated with tumours demonstrating MGMT methylation may in fact be explained by the epigenetic and biological effects of global hypermethylation in these tumours.

Improved survival is also seen in patients with either LOH 1p (Homma T 2006) or concurrent LOH 1p and 19q (Schmidt MC 2002, Homma T 2006) but not in patients with LOH 19q alone (Homma T 2006). Conversely LOH 10q is associated with shorter survival (Schmidt MC 2002, Terada K 2002, Ohgaki H 2004). The prognostic value of mutations in *TP53* is unclear, with some studies showing no association with outcome (Simmons ML 2001, Smith JS 2001), whilst others reporting it to be a favourable prognostic factor (Schmidt MC 2002, Ohgaki H 2004). Likewise conflicting data exists regarding the prognostic value of *EGFR* mutations, which have been shown to be a poor prognostic factor and in some studies (Feldkamp MM 1999, Shinojima N 2003, Hoelzinger DB 2005) but not in others (Huncharek M 2000, Viana-Pereira M 2008), whilst further studies demonstrate it to have prognostic significance only in certain patient age groups (Simmons ML 2001, Batchelor TT 2004). GBMs carrying alterations in both *EGFR* and *TP53* are associated with worse survival (Ruano Y 2009), whilst mutations in *PTEN* are not prognostically significant (Smith JS 2001, Schmidt MC 2002, Ohgaki H 2004). Mutations in IDH1 and IDH2, which were recently discovered to occur at high frequency in secondary GBM and to a lesser extent in primary GBM (Parsons DW 2008, Kloosterhof NK 2011), are also associated with a more favourable prognosis (Hartmann C 2009, Yan H 2009). Much interest has since arisen into the role played by IDH1/2 mutations in gliomagenesis, with the anticipation that therapies directed against mutant IDH1/2 could offer clinical benefit in the future.

## 1.3 The role of IDH mutations in gliomagenesis

### 1.3.1 IDH function

Eukaryotic cells express three different isoforms of IDH: IDH1, IDH2 and IDH3 (Dalziel K 1980), with each one demonstrating overlapping but nonredundant roles in cellular metabolism. IDH1 and IDH2 are homodimeric enzymes which catalyse the oxidative

decarboxylation of isocitrate to α-ketoglutarate (α-KG) and reduce nicotinamide adenine dinucleotide phosphate ($NADP^+$) to NADPH ***(Figure 1-6)***. They share considerable sequence similarity and an almost identical protein structure (Xu X 2004), but function in different subcellular locations ***(Figure 1-7)***. The reactions catalyzed by IDH1 and IDH2 are reversible, and their directionality depends mainly on the relative $K_m$ values of the forward and reverse reactions and the relative cellular levels of isocitrate and α-KG (Lemons JM 2010).

**Figure 1-6: The reaction catalysed by wild-type IDH1 and IDH2 (A) and IDH3 (B).**

A. Isocitrate + $NADP^+$ $Mg^{2+}$(metal ion) ⇒ alpha-ketoglutarate + NADPH + $H^+$ + $CO_2$

B. Isocitrate + $NAD^+$ $Mg^{2+}$(metal ion) ⇒ alpha-ketoglutarate + NADH + $H^+$ + $CO_2$

**Figure 1-7: The function of the IDH enzymes in the TCA cycle. Shown are the cytoplasmic reaction involving IDH1 and the mitochondrial reactions involving IDH2/3 (taken from Losman JA 2013).**

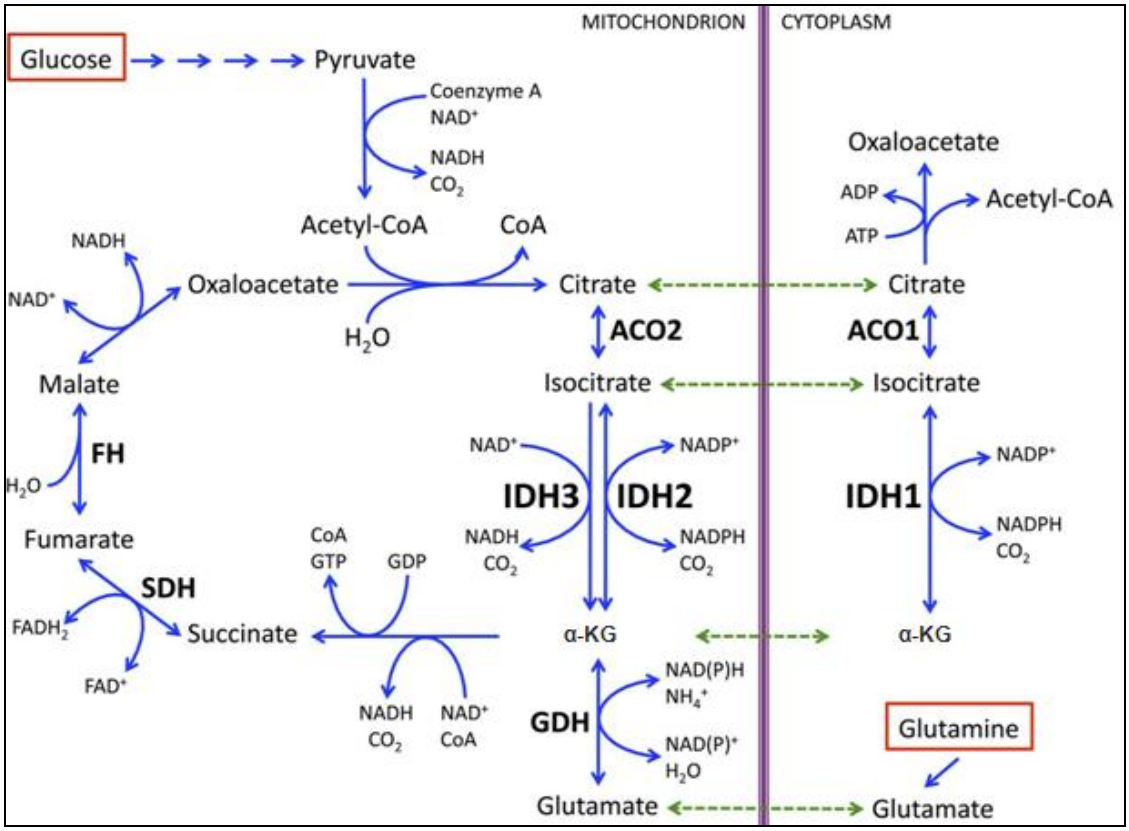

IDH1 is localised to the cytoplasm and peroxisome (Reitman ZJ 2010) where it serves as a major source of cytosolic NADPH. It plays an important role in cellular metabolic processes such as lipid and glucose metabolism (Haselback RJ 1993, Joseph JW 2006), and provides critical reducing equivalents required for cellular protection against reactive oxygen species (ROS) and radiation (Lee SH 2004, Kim SY 2007, Lee SM 2009, Reitman ZJ 2010). As the reaction catalyzed by IDH1 is reversible, it can reductively carboxylate α-KG to isocitrate, which is then further metabolized to acetyl-CoA and by this mechanism IDH1 can mediate de novo lipogenesis under hypoxic conditions (Filipp FV 2012, Metallo CM 2012). Furthermore IDH1 plays an important role in promoting the activity of the numerous cytoplasmic and nuclear enzymes that require α-KG as a cosubstrate (Hausinger RP 2004).

IDH2 is localised to the mitochondria (Reitman ZJ 2010). Its main function is to regulate energy metabolism within the tricarboxylic acid (TCA) cycle by modulating the relative levels of mitochondrial isocitrate and α-KG (DeBerardinis RJ 2008). IDH2 is also an important source of mitochondrial NADPH, and hence plays an important role in the protection of cells from mitochondrial-specific oxidative stress, such as those generated by the electron transport chain (Lee SH 2004, Kil IS 2007, Yang C 2009, Lee SM 2009). Furthermore, as a results of its ability to catalyse in a reverse direction, IDH2 plays an important role in maintaining cellular citrate levels and fatty acid biosynthesis, and in sustaining energy production during hypoxia (Wise DR 2011, Filipp FV 2012). In hypoxic conditions glutamate dehydrogenase (GDH) converts glutamate to α-KG (Comte B 2002) leading to an increase in the α-KG:isocitrate ratio. This balance favours the reverse IDH2 reaction and results in the conversion of α-KG to isocitrate which is then either fed into the TCA cycle and decarboxylated back to α-KG by IDH3, or is isomerised to citrate by aconitase.

IDH3 is an $NAD^+$-dependent enzyme also present in the mitochondrial matrix that similarly decarboxylates isocitrate, to produce α-KG and NADH. It is a tetrameric protein encoded by three separate genes: *IDH3A*, *IDH3B*, and *IDH3G* which encode it's α, β, and γ subunits, and whilst all three subunits appear to share substrate binding and enzyme activity, they cannot substitute for one another. IDH3 plays a key role in mitochondrial respiration by catalysing a rate limiting step in the TCA cycle. α-KG produced by IDH3 is metabolised further to succinate, whilst NADH is utilised by the electron transport chain to generate ATP (Barnes LD 1971). Unlike IDH1 and IDH2, the reaction catalyzed by IDH3 is irreversible and is principally regulated by substrate availability and by both positive allosteric effectors such as calcium, ADP, and citrate, and negative allosteric effectors such as ATP, NADH, and NADPH (Gabriel JL 1986, Reitman ZJ 2010).

### 1.3.2 Frequency of IDH mutations in GBM and other tumours

In 2008 a genome wide sequencing study of 22 adult primary and secondary GBM tumours identified recurrent mutations in *IDH1* in five out of six of the secondary GBMs included in the study (Parsons DW 2008). All 5 had the same heterozygous point mutation, a change of a guanine to an adenine at position 395 of the IDH1 transcript (G395A), leading to the replacement of an arginine with a histidine at amino acid residue 132 of the protein (R132H). Follow-up sequencing studies confirmed that mutations at R132 of *IDH1* occur in >70% of adult grade II and grade III gliomas, and in >80% of adult secondary GBMs, as well as in 5-10% of primary GBMs (Balss J 2008, Bleeker FE 2009, Yan H 2009, Kloosterhof NK 2011). Moreover, mutations at R172 of *IDH2* were found to occur in *IDH1* wild-type tumours, albeit at a lower frequency, with the two mutations being mutually exclusive of one another (Yan H 2009, (Hartmann C 2009). Mutations in IDH1/2 were shown to occur at higher frequencies in younger patients (Hartmann C 2009, Yan H 2009), and serial biopsy studies have

demonstrated that they are an early event in gliomagenesis (Watanabe T 2009). Furthermore IDH1/2 mutations occur in association with TP53 mutation, and with LOH 1p/19q (Reitman ZJ 2010), as well as with MGMT promoter methylation (McDonald KL 2010), and are inversely associated with genetic changes found commonly in primary GBM, such as EGFR amplification and cyclin-dependent kinase (CDKN) deletion (Yan H 2009).

To date no mutations in any of the genes encoding the IDH3 subunits have been identified in human glioma (TheCancerGenomeAtlasResearchNetwork 2008, Krell D 2011). Interestingly however, loss-of-function mutations in the subunit β of IDH3 have been found in affected members of families with retinitis pigmentosa (Hartong D 2008).

Mutations in *IDH1/2* have subsequently been reported in haematolological malignancies, and occur in 5%–30% of patients with cytogenetically normal primary AML, in 10%–20% of cases of secondary AML, and in up to 67% of cases of AML associated with cup-like nuclei (Mardis ER 2009, Kosmider O 2010, Pardanani A 2010, Rakheja D 2012), whilst mutations in *IDH2* have been found in 10%–40% of patients with angioimmunoblastic T-cell lymphoma(AITL) (Cairns RA 2012). Interestingly, unlike in GBM where *IDH1* and *IDH2* mutations do not occur in the same tumour, rare cases of *IDH1/2* double mutant AML have been reported, although this may be as a result of the presence of different leukaemic subclones within the same patient sample (Paschka P 2010).

IDH1/2 mutations also occur in over 50% of patients with central, periosteal, and dedifferentiated chondrosarcoma (Amary MF 2011a), in 40%–90% of cartilaginous tumours in patients with Ollier disease and Maffucci syndrome (Pansuriya TC 2011, Amary MF 2011b), and in 28% and 7% of intrahepatic and extrahepatic cholangiocarcinoma respectively (Borger DR 2012). They have also been reported in a few rare cases of paraganglioma (Gaal J 2010), nonepithelial melanoma (Shibata T 2011), lung cancer (Sequist LV 2011), colon

cancer, thyroid cancer (Ward PS 2012) and prostate cancer (Ghiam AF 2012). Most recently, a mutation in *IDH2* (an arginine to serine substitution at R172) has been reported to occur in 25% of patients with osteosarcoma (Liu X 2013).

Interestingly the prognostic significance of IDH1/2 mutations is inconsistent across some of these different tumour types. In GBM, IDH1/2 mutations have been shown to be an independent favourable prognostic marker (Nobusawa S 2009, Sanson M 2009, Wick W 2009, SongTao Q 2012). Indeed in one study the median OS of patients with IDH1/2 mutant GBM was shown to be 31 months, as compared to 15 months for patients with IDH wild-type disease (Yan H 2009). In AML, the prognostic significance of IDH1/2 mutation status is unclear, with several studies reporting no impact on prognosis, whereas others have found that IDH1/2 mutations are associated with an increased or decreased risk of disease relapse in different population groups (Abdel-Wahab O 2011, Rakheja D 2012, Zhou KG 2012.). Furthermore, in myelodysplastic syndrome and myeloproliferative disorders, IDH1/2 mutations have consistently been found to be markers of poor prognosis, and are thought to be involved in the transformation process from these conditions to secondary AML (Tefferi A 2010, Thol F 2010, Patnaik MM 2012).

Mutations in *IDH1* and to a lesser extent in *IDH2* have been shown to occur at a high frequency in tumours arising in patients with Ollier disease (OD) and Maffucci syndrome (MS) (Amary M 2011). These rare, nonfamilial conditions are characterized by multiple intramedullary cartilaginous tumours, and in the case of MS, with soft tissue hemangiomas. Both conditions generally present in childhood and can result in severe deformity of the affected tissues (Amary M 2011). Malignant transformation of chondromas and the development of secondary neoplasms, mainly gliomas and AML, have been reported in OD and MS, particularly in cases with severe phenotypes (Pansuriya F 2010). More interestingly, through sequencing analysis of multiple tumours from the same patient Amary *et al.*

demonstrated the same somatic mutations in *IDH* to occur in 1 or more tumours but wild-type sequences for *IDH* to occur in others. Given the frequency of somatic *IDH* mutations and wild-type sequences seen in tumours from patients with OD and MS in this study, the probability that a concordant pattern of sequences encoding an Arg132 substitution would occur by chance is statistically improbable (Amary M 2011). This finding raises the possibility that the *IDH* mutations described represent early post-zygotic events that result in a mosaic pattern of disease distribution, a theory that is supported by the presence of mutations in low-grade tumours and in tumours of two cell lineages and by the occurrence of *IDH1* mutations encoding the same Arg132 alteration in six tumours from a single individual (Amary M 2011). The detection of the same mutations in both nonlesional tissue and tumours from 2 of 12 individuals in Amary's study was taken as evidence that OD and MF represent somatic mosaic disorders (Amary M 2011).

### 1.3.3 IDH mutation spectrum

Mutations identified in *IDH1* and *IDH2* are mono-allelic, somatic, missense changes that occur at a single residue of the active site of the enzyme. In glioma, mutations in *IDH1* almost always affect arginine 132 (R132) (Parsons DW 2008), which has been found to be converted to histidine, serine, cysteine, glycine, and leucine, with histidine (R132H) being the most frequent change (Yan H 2009). Mutations affecting arginine 100 (R100) have also been identified (Pusch S 2011, Ward PS 2012). Recently two instances of an IDH1 R132S mutation caused by a previously undescribed dinucleotide deletion/insertion mutation, as well as a novel homozygous somatic IDH1 R132L mutation were also described (Gupta R 2013). In cholangiocarcinomas and chondrosarcomas IDH1 R132 mutations are also most common often resulting in an arginine-to-cysteine substitution (Amary MF 2011a, Borger DR 2012).

*IDH2* mutations in glioma exclusively affect arginine 172 (R172), which is analogous to IDH1 R132 (Yan H 2009), and substitutions of IDH2 R172 to lysine, glycine, serine, methionine and tryptophan have been reported (Dang L 2009). Mutations in *IDH2* affecting arginine 140 (R140), which is analogous to IDH1 R100 (Ward PS 2010, Pusch S 2011), occur as the most frequent mutation in AML and most commonly result in the replacement of arginine for glutamine, whilst mutations of R140 of *IDH2* to leucine have also been reported. However mutations at R140 have not been reported in glioma, chondrosarcoma or cholangiocarcinoma (Ward PS 2010, Losman JA 2013). In AITL, where all reported IDH mutations to date occur in IDH2, >90% are located at IDH2 R172 (Cairns RA 2012).

The reason for the variable frequency of the different amino acid substitutions associated with IDH1 and IDH2 in different tumours is not yet fully understood.

### 1.3.4 Cellular effects of mutations in IDH

The amino acids R132 and R100 of IDH1, and R172 and R140 of IDH2 perform a key function at the active site of their respective enzymes (Parsons DW 2008), where they form hydrogen bonds with the α-carboxyl and β-carboxyl groups of isocitrate and mediate isocitrate binding ***(Figure 1-8)***. Mutations affecting these arginine residues lead to a conformational change in the active site, and result in a decreased affinity for isocitrate, and an increased affinity for NADPH, which significantly alters the normal oxidative decarboxylation activity of these enzymes (Dang L 2009, Yang ES 2011).

Early studies demonstrated that mutant IDH1 had a reduced affinity for isocitrate (Zhao S 2009), and when expressed in cultured cells led to a reduction in the formation of α-KG and NADPH (Yan H 2009, Zhao S 2009). Thus IDH1/2 mutations were initially thought to promote tumour development through the loss of IDH1/2 enzyme function for the conversion of isocitrate to α-KG, the most plausible mechanism being a dominant negative effect due to

the formation of catalytically inactive heterodimers of mutant and wild-type proteins (Zhao S 2009).

**Figure 1-8: Structure of the active site of IDH1 (Adapted from Parsons DW 2008).**

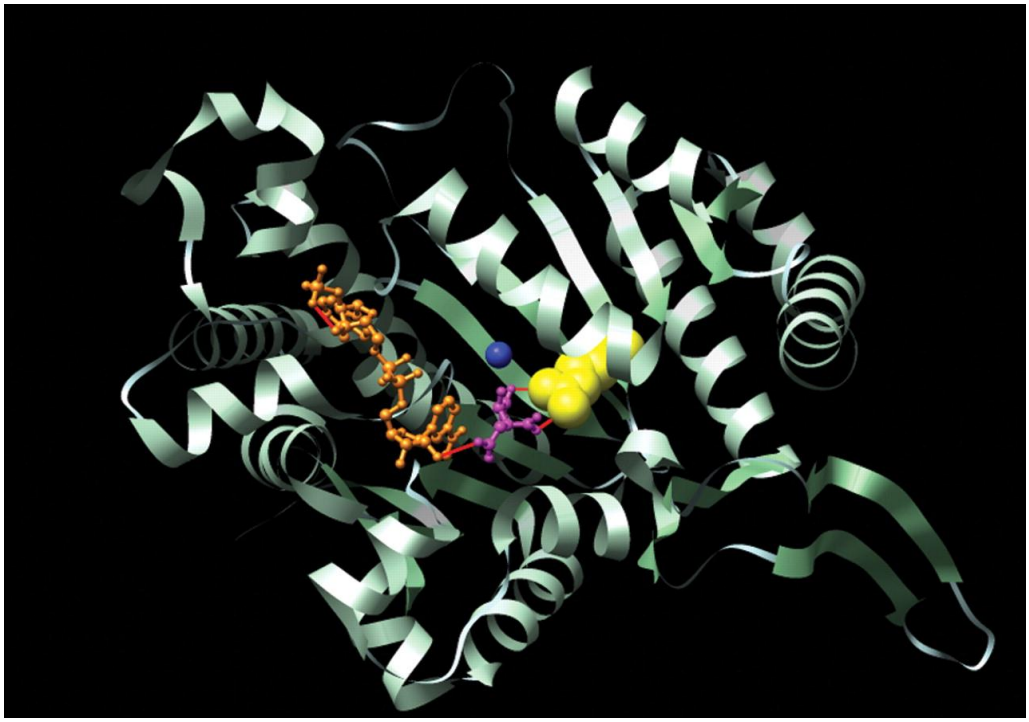

The crystal structure of the human cytosolic IDH1 in ribbon format. The active cleft of IDH1 consists of a NADP-binding site and the isocitrate-metal ion-binding site. The alpha-carboxylate oxygen and the hydroxyl group of isocitrate chelate the $Ca^{2+}$ ion. NADP is coloured in orange, isocitrate in purple, and $Ca^{2+}$ in blue. The R132 residue, displayed in yellow, forms hydrophilic interactions, shown in red with the alpha-carboxylate of isocitrate.

Subsequent studies however demonstrated that mutant IDH1/2 are not in fact inactive enzymes, but instead possess novel enzymatic activity resulting from their increased affinity for NADPH, and reduced affinity for isocitrate ***(Table 1-4)*** (Dang L 2009, Gross S 2010, Ward PS 2010, Jin G 2011).

This novel enzyme function results in the NADPH-dependent reduction of α-KG to D-2-Hydroxyglutarate (D-2HG) ***(Figure 1-9)***, which has been shown to accumulate at high levels in IDH1/2 mutant tumours (Dang L 2009, Ward PS 2010).

**Table 1-4: R132H mutation alters the enzymatic properties of IDH1 (taken from Dang 2009).**

| Oxidative → NADPH | Wild type | IDH1 R132H |
|---|---|---|
| $K_{M\ ,NADP+}$ (uM) | 49 | 84 |
| $K_{M,\ isocitrate}$ (uM) | 65 | 370 |
| $K_{i,\ \alpha KG}$ | 1871 | 24 |
| Reductive → $NADP^+$ | Wild type | IDH1 R132H |
| $K_{M,NADPH}$ (uM) | N/A | 0.44 |
| $K_{M,\ \alpha\text{-}KG}$ (uM) | N/A | 965 |

**Figure 1-9: The functions of wild-type and mutant IDH1 and IDH2.**

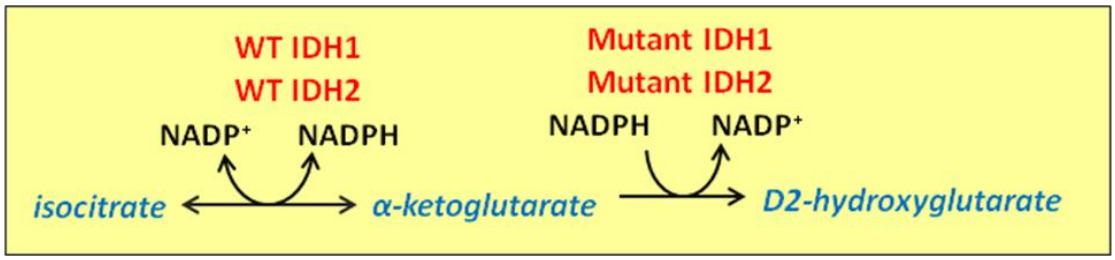


Shown are 1) the reaction catalysed by wild type (WT) IDH1/2 which converts isocitrate to α-KG and produces NADPH, and 2) the reaction catalysed by mutant IDH1/2 which convert α-KG to D-2HG and produces $NADP^+$.

Whilst both mutant IDH1 and mutant IDH2 produce D-2HG, their enzymatic properties differ somewhat and this may explain their differential prognosis and prevalence in different cancers (Ward PS 2013). Mutant IDH1 functions as a heterodimer consisting of one wild-type and one mutant protein. The activity of the wild-type protein is partially inhibited by the mutant protein, which itself exhibits novel enzymatic activity, resulting in a simultaneous decrease in α-KG production, and increase in D-2HG formation respectively (Pietrak B 2011). Studies of the IDH1 wild-type:mutant heterodimer demonstrate that both wild-type and mutant subunits contribute to the production of D-2HG from isocitrate and αKG respectively (Pietrak B 2011), and the genetic knock-down of wild-type IDH1 function in IDH1-mutant cell lines can significantly decrease D-2HG production (Jin G 2013). Indeed,

D-2HG levels were found to be 87-fold lower in an IDH1 mutant anaplastic astrocytoma cell line in which the *IDH1* wild-type allele had been knocked out using recombinant adeno-associated viruses ($IDH1^{R132H/-}$), when compared to parental cells harbouring both wild-type and mutant alleles ($IDH1^{R132H/WT}$), and this reduction was reversed by ectopic re-expression of wild-type IDH1 (Jin G 2013). Furthermore intratumoral D-2HG is significantly reduced in IDH1 mutant GBMs that have lost the wild-type IDH1 allele ($IDH1^{R132H/-}$), compared to GBMs with heterozygous IDH1 mutations ($IDH1^{R132H/WT}$), demonstrating the importance of wild-type as well as mutant IDH1 function in D-2HG production (Jin G 2013). It is possible that knocking out IDH1 wild-type function impairs the conversion of isocitrate to αKG, leading to intracellular αKG levels that are too low for efficient conversion to D-2HG. α-KG levels were not measured by Jin *et al.* in $IDH1^{R132H/-}$ GBMs and consequently it is unclear whether the lower levels of D-2HG seen in these tumours could have occurred as a result of reduced α-KG production. α-KG levels were however shown to be slightly reduced in $IDH1^{R132H/-}$ cell lines when compared to parental $IDH1^{R132H/WT}$ cells, but restoring cellular αKG to the levels seen in the parental cells using cell-permeable octyl-αKG did not rescue D-2HG production in $IDH1^{R132H/-}$ cells, which seems to refute the above theory. Nonetheless the wild-type:mutant IDH1 heterodimer does appear to be required in order for efficient D-2HG production to occur (Bralten LB 2011, Pietrak B 2011, Jin G 2013, Ward PS 2013).

Conversely, mutant IDH2 does not form heterodimers with wild-type IDH2, and mutant IDH2-expressing cells accumulate higher levels of D-2HG than do mutant IDH1-expressing cells, and they do so independently of wild-type IDH2 activity (Dang L 2009, Ward PS 2013). Indeed, whilst knockdown of wild-type IDH1 appears to hinder D-HG production, siRNA induced knockdown of wild-type IDH2 function in IDH2 mutant cell lines does not reduce the level of D-2HG accumulation (Ward PS 2013). The differences in enzymatic activity between IDH1 and IDH2 may be explained by the fact that cytoplasmic α-KG is

limited in cells, whereas mitochondrial α-KG, which is produced by both IDH2 and IDH3, is more abundant. Hence, whilst mutant IDH1 may require the presence of wild-type activity, and wild-type:mutant heterodimer formation, to provide it with a sufficient supply of α-KG, mutant IDH2 does not. This theory is strengthened by the finding that expression of a mutant IDH1 construct that is engineered to localize to the mitochondria rather than the cytosol results in an increase in D-2HG production (Ward PS 2013). The differences in the enzymatic function of mutant IDH1 and IDH2 and the fact that tumours resulting from mutations in IDH1and *IDH2* are associated with a differential prognosis and prevalence in different cancers (Ward PS 2013), suggests that IDH1 and IDH2 mutant tumours are in fact separate diseases, with subtle variations in their biology and development.

The excess production of D-2HG, and/or reduction in α-KG production via the mechanisms outlined above are thought to give IDH mutant cells their pro-tumourigenic potential, and although the exact importance of each of these factors is not yet fully defined, it is generally considered that D-2HG accumulation is the major contributing event.

### 1.3.5 Effects of D-2HG on the activity of α-KG-dependent enzymes

2-HG is a five-carbon dicarboxylic acid which has two enantiomers, D-2HG and L-2HG, both of which are by-products of normal mitochondrial metabolism (Kranendijk M 2012). Studies performed on rats demonstrated that D-2HG is produced from the activity of the enzyme hydroxyacid-oxoacid transhydrogenase (HOT) (Kaufman E 1988, Struys 2006). HOT converts γ-hydroxybutyrate (GHB) to succinic semialdehyde (SSA), with the concomitant reduction of α-KG to D-2HG. L-2HG on the other hand is generated as a by-product of the activity of the TCA cycle enzyme (*L*)-malate dehydrogenase during its conversion of oxaloacetate to (*L*)-malate (Rzem R 2007).

Our current understanding of the exact cellular roles of D- and L-2HG is limited (Yen KE 2010), and whilst both are thought to be unwanted by products of cellular metabolism, D-2HG may in fact function as an intermediate in the production of 5-aminolaevulinate and porphyrin in haem synthesis (Lindahl G 1967, Chalmers R 1980). The intracellular levels of both D- and L-2HG are normally maintained at <0.1 mM by the activity of D-2HG dehydrogenase (D-2HGDH) and L-2HG dehydrogenase (L-2HGDH) respectively, which convert them back to α-KG (Struys EA 2005, Steenweg M 2010).

IDH mutant-derived D-2HG accumulates in cells to levels ranging from 1 mM to as high as 30 mM (Dang L 2009, Gross S 2010, Choi C 2012), and it is thought that at this concentration D-2HG can act as an oncometabolite with numerous potential oncogenic effects. One of the rationales for the role of 2-HG in tumourigenesis is derived from the observation of patients with the rare inherited neurometabolic disorders, D-2- and L-2-hydroxyglutaric acidurias (2-HGA). These two distinct syndromes result from germline homozygous inactivating mutations in the genes that encode for D- and L-2HGDH (Struys EA 2005, Steenweg M 2010). Mutations in *D-* and *L2HGDH* result in the accumulation of D-2HG or L-2HG in patients' physiological fluids, and L-2HG aciduria (L-2HGA) affected individuals have an increased incidence of brain tumours (Moroni I 2004, Haliloglu G 2008, Aghili M 2009). Interestingly, D-2HG aciduria (D-2HGA) has also been found to be associated with germline mutations in *IDH2* at R140 in a cohort of patients who do not have alterations in *D2HGDH* (Kranendijk M 2010). Consequently D-2HGA has been distinguished into two different subtypes; type I which is associated with mutations in *D2HGDH*, and type II which is associated with mutations in *IDH2*. However, unlike in L-2HGA, patients with type I or type II D-2HGA do not have an increased risk of developing brain tumours (Kranendijk M 2012). Although this contrasts with the findings observed in *IDH1/2*-mutated tumours, where an accumulation of D-2HG (Dang L 2009, Ward PS 2010),

but not L-2HG is thought to promote tumorigenesis, it could be hypothesised that this discrepancy may be due to the fact that mutant IDH1/2 activity in glioma produces D-2HG at a significantly higher level than is seen in patients with D-2HGA, and that the levels produced in the latter disorder are simply insufficient to promote tumourigenesis. Alternatively it is possible that D-2HG accumulation alone is insufficient to promote tumourigenesis and that mutations in other genes such as p53, which are commonly observed in IDH1/2 mutant glioma (Ohgaki H 2005b, Yan H 2009) but not in type I/II D-2HGA, are required for this to occur. The association between brain tumours and L-2HGA, but not D-2HGA may be explained by the fact that L-2HG inhibits certain enzymes, whose activity have been implicated in tumourigenesis, more potently than D-2HG (Chowdhury R 2011, Xu W 2011). An alternative theory could be that because patients with D-2HGA have a more severe clinical course compared to L-2HGA patients (they often die in infancy or early adulthood) (Kranendijk M 2012), they simply do not live long enough for brain tumours to develop.

The difference in the phenotype observed in patients with 2-HGA (resulting from germ line mutations in D-/L-*2HGDHs* and *IDH2*) (Struys EA 2005, Steenweg M 2010), compared to that observed in patients with OD and MS (proposed to result from early post-zygotic mutations in *IDH* and associated with a mosaic pattern of disease distribution) (Amary M 2011), and in patients with *IDH* mutant glioma (resulting from somatic mutations in *IDH1*/2), illustrates the different biological effect consequent to mutant *IDH* expression and 2HG accumulation at different stages of development.

Interestingly, D-2HG concentrations are higher in fluids and lymphoblastic cells from patients with D-2HGA associated with *IDH2* mutations than from those with mutations in *D2HGDH*, with the mean serum levels being about 5 times higher in type II than in type I D-2HGA patients (e.g. 14,663-112,122 ng/mL range values, 54,210 ng/mL mean value vs.

3,851-18,218 ng/mL range values, 10,072 ng/mL mean value respectively) (Kranendijk M 2010, Kranendijk M 2012). Since the clinical outcome of patients affected by type II D-2HGA is more severe compared to that of patients affected by type I D-2HGA, it is plausible to establish a correlation between D-2HG concentration and the severity of the disorder. However, D-2HG levels present in the serum of patients affected by type II D-2HGA are also higher than those measured in IDH1 and IDH2 mutant AML patients, where pre-treatment D-2HG levels were measured to be between 30,000 ng/mL (median 3004 ng/ml) (Dinardo C 2013) and 66,207 ng/mL (median 1863 ng/mL) (Fathi AT 2012) compared to 61ng/ml (median) (Dinardo C 2013) and to 87ng/mL (median) (Fathi AT 2012) in IDH1/2 wild-type patients. These findings suggest that there may in fact be no direct correlation between the degree of D-2HG accumulation and the risk of tumour development, and perhaps provide further evidence that additional mutations are required in conjunction with mutations in *IDH1/2* in order for tumourigenesis to occur.

However, perhaps more compelling evidence to support the role of D-2HG in promoting tumourigenesis is illustrated by the findings observed in *IDH2*-mutant AML showing that patients with IDH2 R140 mutant AML produce lower levels of D-2HG and have a better prognosis than patients with IDH2 R172 mutant AML (Ward PS 2012). These findings suggests that a correlation does exist between the amount of D-2HG produced by mutant IDH1/2, and the characteristics of the resulting tumour. Moreover, the expression of IDH1 R132H in immortalised human astrocytes and in a human erythroleukaemic cell line, resulted in D-2HG accumulation and induced oncogenic transformation, whereas expression of the catalytically inactive R132H/3DN variant, which is unable to produce D-2HG, had no such effect (Koivunen P 2012, Losman J 2013). Furthermore treatment of the same human erythroleukaemic cells with a cell-permeable form of D-2HG was able to recapitulate the

effects of mutant IDH1 expression, whilst withdrawal of D-2HG reversed them (Losman J 2013).

More speculatively, the finding that patients with OD and MS can develop synchronous tumours, one carrying an *IDH1* mutation and accumulating 2HG and the other carrying a wild-type *IDH1* sequence (Amary M 2011) raises the possibility that circulating 2HG derived from a mutant tumour may be able to stimulate the growth of a second-site tumour in a paracrine manner.

It has been widely proposed that D-2HG transforms cells due to its ability to competitively inhibit α-KG dependent enzymes, which normally function as tumour suppressors (Chowdhury R 2011, Xu W 2011, Koivunen P 2012, Lu C 2012). This inhibition occurs due to the structural similarity between D-2HG and α-KG, which are identical except that a hydroxyl group in D-2HG replaces the C2 carbonyl group in α-KG (Figueroa ME 2010, Xu W 2011). Mammalian cells express over 60 α-KG dependent enzymes (Loenarz C 2008, McDonough M 2010), and the inhibition by D-2HG of several of these enzymes, such as Hypoxia inducible factor prolyl hydroxylase (HIF-PHD), the Jumonji-C domain containing histone demethylases (JHDMs), the Ten-Eleven Translocation (TET) family of 5-methylcytosine hydroxylases, and collagen prolyl 4-hydroxlase (C-P4H) could lead to IDH-mediated transformation by stimulating processes such as angiogenesis, histone modifications, aberrant DNA methylation, and abnormal collagen maturation.

#### 1.3.5.1 Inhibition of HIF-PHD

HIF-PHD1 (EGLN2), HIF-PHD2 (ELGN1) and HIF-PHD3 (EGLN3), are α-KG dependent enzymes that regulate the activity of HIF (Semenza GL 2012), a heterodimeric transcription factor which, when over expressed, is associated with malignant progression and a poor outcome in several cancers (Metellus P 2011). HIF has a wide range of target genes including

those that modulate angiogenesis, glycolysis, growth factor signalling, apoptosis, and metastasis (Gottlieb E 2005, Weljie AM 2011), some of which, in physiological conditions, function to promote adaptation of cells to hypoxia. In pathological conditions however their activation can be critical to tumour growth, by inducing a hypoxic response under normoxic conditions (pseudo-hypoxia). In normoxia, HIFα is labile, because the hydroxylation by HIF PHD of two proline residues in its oxygen-dependent degradation domain (ODDD) triggers its association with the von Hippel-Lindau (VHL) E3–ubiquitin ligase complex and subsequent degradation via the ubiquitin-proteasome pathway (MacKenzie ED 2007, Majmundar AJ 2010). HIF-PHD2 is believed to be the principal enzyme in this process, with HIF-PHD1 and HIF-PHD3 playing variable compensatory roles under specific cellular conditions. In physiologically hypoxic or pathologically pseudohypoxic conditions, the activity of HIF-PHD is inhibited, allowing HIFα to accumulate, heterodimerise with HIFβ, translocate to the nucleus, and activate a transcriptional response.

It has been demonstrated that D-2HG (Xu W 2011), and reduced levels of α-KG (Zhao S 2009) can inhibit HIF PHD, and HIF1α is in fact upregulated in cells that over express mutant *IDH1*, in cells treated with exogenous 2-HG, in tumours harbouring IDH1 R132H mutations and in the brains of brain-specific idh1 R132H knock-in (KI) mice (Zhao S 2009, Xu W 2011, Sasaki M 2012b). Furthermore the expression of HIF1α target genes glucose transporter type 1 (*GLUT1*), phosphoglycerate kinase 1 (*PGK1*), and vascular endothelial growth factor (*VEGF*) is increased in the brains of brain-specific idh1 R132H KI mice and in IDH1 knockdown cell lines (Zhao S 2009, Sasaki M 2012b).

However, D-2HG has been shown to be only a relatively weak inhibitor of HIF PHD (Chowdhury R 2011) and furthermore, studies by both Metellus *et al.* and Williams *et al.* found no correlation between IDH mutation status and the expression of HIF1α in patients with glioma (Metellus P 2011, Williams SC 2011). Additionally recent studies demonstrated

that in contrast to L-2HG which acts as an inhibitor of HIF PHD, D-2HG can actually stimulate rather than inhibit the activity of this enzyme, and in some cellular contexts such as human astrocyte, colorectal and erythroleukemia cell lines, the expression of IDH1 R132H reduced HIF levels (Koivunen P 2012, Losman J 2013). Furthermore, in human astrocytes, overexpression of HIF-PHD2 or depletion of HIF1α promoted malignant transformation of these cells (Koivunen P 2012). Moreover in erythroleukemic cells it has been shown that transformation is promoted specifically by D2-HG and not by L2-HG, which actually appeared to antagonise leukaemic transformation induced by TET2 loss through inhibition of HIF-PHD2 (Losman J 2013). More surprisingly, the loss of HIF PHD activity was able to block oncogenic transformation by mutant IDH in erythroleukemic cells (Losman J 2013), and in IDH-mutant astrocytes (Koivunen P 2012), suggesting that in these contexts HIF or other specific targets of hydroxylation by HIF PHD could in fact suppress the oncogenic potential of D-2HG. These findings are interesting given that they conflict with those of earlier studies and also because, although HIF is traditionally viewed as being oncogenic, it may also act as a tumour suppressor under certain conditions (Blouw B 2003, Acker T 2005). Consequently it remains unclear whether D-2HG has an agonistic or antagonistic effect on HIF-PHD, or whether HIF-PHD activity and HIF1α play a definitive role in promoting tumourigenesis in IDH-mutated tumours.

#### 1.3.5.2 Inhibition of JHDMs

Histone demethylases function as epigenetic regulators of gene expression (Klose RJ 2006). They bind to and remove methyl groups from specific histone lysine residues, and hence modulate chromatin structure and transcription factor binding (Frezza C 2011). Methylation of certain histone residues such as H3K4, H3K36, and H3K79 is associated with transcriptionally active euchromatin, where as methylation of others such as H3K9, H3K27 and H4K20 are associated with transcriptionally silent euchromatin. Alterations in histone

methylation can have significant effects on gene expression, and the activity of the JHDMs have been linked to the pathogenesis of a number of different tumours (Cloos PA 2008, Varier RA 2011).

Exogenous D-2HG and knockdown of wild-type IDH1 function, inhibit the activity of multiple JHDMs *in vitro*, and the levels of the histone methylation markers H3K4, H3K9, H3K27, H3K36, and H3K79 are elevated in mutant IDH1 and IDH2 expressing cells and in cell cultures treated with exogenous D-2HG (Chowdhury R 2011, Xu W 2011, Lu C 2012). Furthermore, a small increase in methylated H3K4 was seen in bone marrow stem cells extracted from haematopoietic-specific idh1 R132H KI mice although other histone methylation marks remained unchanged (Sasaki M 2012a), whilst no differences in global histone methylation were observed in the brains of brain-specific idh1 R132H KI mice (Sasaki M 2012b). H3K9 methylation was found to be increased commonly in IDH mutant gliomas (Duncan CG 2012), although H3K9 hypermethylation was also seen in IDH wild-type tumours (Venneti S 2013) suggesting that this may occur independent of IDH mutation status. Hence it remains unclear whether inhibition of histone demethylases by D-2HG contributes to malignant transformation in IDH mutant tumours.

#### 1.3.5.3 Inhibition of TET

TET1, TET2 and TET3, are α-KG-dependent DNA-modifying enzymes that hydroxylate 5-methylcytosine (5mC) to generate 5-hydroxymethylcytosine (5hmC) (Tahiliani M 2009). TET enzymes are thought to function as epigenetic regulators of gene expression by mediating the demethylation of DNA. 5hmC plays a role in passive DNA demethylation by preventing de novo methyltransferase (DNMT) maintenance of methylation, and induces active DNA demethylation by DNA repair mechanisms (Guo J 2011). 5hmC also controls transcriptional regulation by preventing the binding of methyl-cytosine-guanine (CpG)

binding proteins to methylated DNA (Guo J 2011). TET itself controls cellular differentiation and embryonic stem (ES) cell maintenance by regulating the expression of genes that maintain pluripotency (Figueroa ME 2010, Ito S 2010). *TET2* is proposed to act as a tumour suppressor gene and somatic mutations in *TET2*, but not *TET1/3*, are found in about 10% of patients with AML and are mutually exclusive with mutations in *IDH1/2* (Abdel-Wahab O 2009, Gaidzik VI 2012). Conversely, somatic mutations in *TET2* have not been found to occur in glioma, although promoter methylation was found in 14% of IDH1/2 wild- type tumours, but did not occur in those harbouring mutant *IDH1/2* (Kim YH 2011).

Expression of mutant IDH1/2 and administration of exogenous 2-HG inhibit TET *in vitro* and *in vivo,* resulting in reduced 5hmC production, in a process that is reversible by the addition of exogenous α-KG (Xu W 2011, Koivunen P 2012), whilst depletion of TET2 in immortalised human astrocytes results in transforming effects that mirror those seen with mutant IDH1/2 expression (Koivunen P 2012). Furthermore, IDH1 mutant gliomas accumulate significantly lower levels of 5hmC and higher levels of 5mC than IDH1 wild-type tumours (Xu W 2011), although it should be noted that 5hmc is also significantly depleted in several human cancers independent of IDH mutation status (Jin SG 2011).

The G-CIMP recently identified in a subgroup of gliomas has been shown to correlate strongly with mutations in *IDH1/2* (Noushmehr H 2010). Patients with tumours exhibiting G-CIMP present at a younger age and experience better survival, features that are also associated with IDH1/2 mutant glioma. Two subsequent studies also identified a distinct homogenous hypermethylation phenotype in IDH1/2 mutant gliomas that was similar to G-CIMP (Christensen BC 2011, Laffaire J 2011). These epigenetic changes remained stable from low to high grade gliomas, suggesting that they occur early in tumour development (Laffaire J 2011). Furthermore, the introduction of IDH1 R132H into primary human astrocytes induces significant DNA hypermethylation (Lu C 2012, Turcan S 2012), which

mirrors the changes seen in G-CIMP$^+$ glioma. Conversely, hypomethylation of DNA is observed at specific loci when wild-type IDH1 is overexpressed in the same cells, suggesting that alterations in α-KG levels may also impact on TET function (Turcan S 2012). It has been hypothesised, although not proven, that the extensive DNA methylation that occurs in G-CIMP$^+$ tumours maintains glioma cells in a dedifferentiated state, and that the aberrant gene expression profile resulting from mutant IDH confers a block to differentiation resulting in the malignant expansion of GICs with a capacity to self-renew (Duncan CG 2012, Turcan S 2012).

More compelling evidence that IDH1/2 mutations may affect TET activity comes from the discovery that both IDH1/2 mutant AML cells and TET mutant AML cells display a similar global hypermethylation and gene specific methylation profile (Figueroa ME 2010). Additionally, depletion of TET2 induces oncogenic changes such as growth factor independence and a cessation in cellular differentiation in a similar way to expression of mutant IDH1/2, and this transformation is enhanced by the addition of cell-permeable D-2HG (Losman J 2013). Global changes in DNA methylation were also observed in DNA analysed from haematopoietic-specific idh1 R132H KI mice, which paralleled those observed in human IDH1/2 mutant AML, and incorporated signalling pathways responsible for stem cell maintenance, haematopoietic cell proliferation and differentiation, and leukaemogenesis (Sasaki M 2012a). Consequently it appears that both IDH1/2 mutations and TET2 mutations exert effects on the same leukemogenic pathways, a theory which is supported by the fact that these mutations occur in a mutually exclusive manner in AML (Figueroa ME 2010, Gaidzik VI 2012).

More recently, a hypermethylation phenotype has also been reported in both IDH1/2 mutant chondrosarcoma (Guilhamon P 2013), and cholangiocarcinoma (Wang P 2013).

Taken together, these findings appear to suggest a common mechanism linking gain of function in IDH1/2 with reduced demethylation and subsequent oncogenic transformation. Consequently further correlation between methylation and gene expression profiles in IDH1/2 mutant tumours may help to identify the causative genes and pathways involved. However, to date, meta-analyses of methylation profiles of glioma, AML, cholagiocarcinoma and chondrosarcoma have not uncovered any genes that are hypermethylated in all 4 tumour types, although sixteen identical genes were found to be commonly affected in cholagiocarcinoma, chondrosarcoma and glioma (Guilhamon P 2013), and hypermethylation of various different genes involved in retinoic acid receptor (RAR) activation were found to be independently targeted in all four malignancies (Guilhamon P 2013). Given that aberrant RAR signalling commonly occurs as an early event in carcinogenesis (Tang 2011), it seems plausible that epigenetic changes in genes involved in RAR activation play a role in the development of IDH1/2 mutant tumours.

One gene of particular interest in the RAR pathway is retinol Binding Protein 1 (*RBP1*), which is located on 3q23 and functions in the synthesis of all-trans retinoic acid (AtrA) (Blomhoff R 2006). The promoter region of *RBP1* is hypermethylated in the vast majority of IDH1/2 mutant glioma, and results in decreased RBP1 expression (Chou A 2012). Furthermore, *RBP1* hypermethylation is associated with an improved prognosis in these patients (Chou A 2012). Given that AtrA functions as a regulator of transcription (Tang 2011), it is feasible that decreased RBP1 activity and consequent dysregulation of retinoic acid metabolism may lead to aberrant transcription and contribute to tumour formation in IDH1/2 mutant glioma.

#### 1.3.5.4 Inhibition of C-P4H

Prolyl hydroxylation is a post-translational modification that affects the structure, stability and function of proteins, and occurs through the activity of the α-KG-dependent collagen prolyl hydroxylases. One such enzyme, C-P4H mediates the hydroxylation of proline to hydroxyproline required for collagen synthesis, and also catalyses the production of endostatin (Xu W 2011). Its expression is down-regulated in many B-cell lymphomas suggesting that it may function as a tumour suppressor gene in some tissues (Hatzimichael E 2012). C-P4H activity is inhibited by D-2HG in vitro (Koivunen P 2012), and in the brains of brain-specific idh1 R132H KI mice, D-2HG inhibited collagen hydroxylation, causing defective collagen protein maturation and basement membrane abnormalities (Sasaki M 2012b). Furthermore, the expression of endostatin, a terminal fragment of collagen that inhibits angiogenesis and tumour growth (O'Reilly MS 1997), is reduced in IDH1 knock-down cells, in IDH1 mutant cell lines, and in IDH1 mutant glioma (Xu W 2011).

### 1.3.6 IDH Mutation effects on TCA cycle Function and Glucose Sensing

The TCA cycle is a central pathway in oxidative metabolism. It functions to generate NADH and FADH, which feed electrons into the respiratory chain, and is involved in the cellular metabolism of carbohydrates, lipids and amino acids (Raimundo N 2011). The 'Warburg effect' is a paradoxical phenomenon that describes a situation whereby malignant cells shift their energy production from oxidative phosphorylation towards glycolysis under aerobic conditions. It is considered to be one of the metabolic hallmarks of cancer (Hanahan D 2011), involving the diversion of the malignant cell's metabolism, so that survival, growth and division are favoured over cellular function (DeBerardinis RJ 2008). The identification of mutations in genes encoding the TCA cycle enzymes succinate dehydrogenase (SDH) and fumarate hydratase (FH) led to renewed interest in Warburg's hypothesis and the potential

link between metabolic dysregulation and cancer (Parsons DW 2008, Kaelin WG 2009). Furthermore, alterations in cancer metabolism and in particular metabolic signalling pathways such as the mTOR pathway are now recognised to be important in the pathogenesis of several cancers, and therapies such as the mTOR inhibitors everolimus have been developed to target these aberrations (Motzer R 2008). This has led to much interest in the link between mutant IDH and altered metabolism.

Different mechanisms have been proposed to explain the tumourigenic process associated with the loss of activity of SDH or FH enzymes. Indeed SDH and FH deficiencies support tumour formation by increasing the levels of their respective TCA cycle substrates, succinate or fumarate, which leads to oncogenic signalling in cells (Bardella C 2011, Frezza C 2011). Among the proposed mechanisms, different studies have shown that SDH and FH associated tumours are highly vascular and are characterised by a strong hypoxic signature, likely resulting from the inhibition of HIF-PHD by fumarate and succinate (Pollard P 2005, Pollard PJ 2005). FH, SDH and IDH1/2 are all enzymes with an essential role in cellular metabolism, and although the underlying mechanism of tumourigenesis in the associated tumours seems to be caused by the accumulation of the respective oncometabolites fumarate, succinate and D-2HG, the mechanisms of tumourigenesis and the pattern of tumour predisposition conferred by mutations in these genes look very different. This could be explained by the fact that the main feature of these oncometabolites is the inhibition of the α-KG-dependent enzyme family, with different specificities to different enzymes and thus with different biological consequences (Pollard P 2005).

Several studies have been performed to analyse the possibility that IDH1/2 mutations can cause changes in global cellular metabolism to favour tumour pathogenesis. Initial studies of the effect of mutations in *IDH1/2* on TCA cycle function failed to demonstrate significant alterations in TCA cycle metabolites (Dang L 2009, Ward PS 2010). However, a subsequent

study by Reitman *et al.* did demonstrate a depletion of the TCA cycle metabolites citrate, cis-aconitate, α-KG, malate and fumarate and an accumulation of biosynthetic precursors, in cell lines that expressed mutations in *IDH1/2* (Reitman ZJ 2011), suggesting that mutant IDH1/2 activity can result in TCA cycle down regulation. The fact that IDH1/2 mutant cells shared multiple metabolic changes with D-2HG treated cells, but not with cells in which wild-type IDH1/2 function was inhibited, suggests that D-2HG accumulation was responsible for the metabolic effects observed (Reitman ZJ 2011). Furthermore, the observation that patients with D2HGA have elevated levels of urinary lactate, also suggests that D-2HG accumulation may lead to some degree of mitochondrial dysfunction (Kranendijk M 2012).

Additionally, D-2HG may impair the electron transport chain through the inhibition cytochrome c oxidase and ATP synthase (Kolker S 2002, Latini A 2005). In fact inhibition of ATP synthase has been observed in some cancers and is thought to promote cellular transformation by causing the accumulation of excess electrons and increasing oxidative stress (Willers IM 2011).

Alterations in the cellular NADPH/$NADP^+$ ratio, may also affect TCA cycle function (Dang L 2009). Furthermore, alterations in cytoplasmic citrate levels could affect acetyl-CoA concentrations and hence lead to altered acetylation and activity of several potentially tumourigenic proteins (Wellen KE 2009, Reitman ZJ 2011).

The depletion of glutamate in IDH1/2 mutant cells observed in Reitman's study is also potentially relevant. Glutamate is a major excitatory neurotransmitter in the central nervous system, and the glutamatergic pathway is associated with tumour development, proliferation, survival, and metastasis in glioma as well as other tumours (Piao Y 2009, Luksch H 2011). Glioma cells actively secrete glutamate, by increasing cystine/glutamate exchange activity. This markedly elevates extracellular glutamate levels (Lyons S 2007) and stimulates

glutamate receptors on surrounding brain cells, promoting their cell death and encouraging glioma cell invasion and migration (Lyons S 2007). Interestingly, an elevated flux of glutamine to 2-HG via glutamate and α-KG is observed in IDH1 mutant cells (Dang L 2009). Furthermore, inhibition of glutaminase, which converts glutamine to glutamate, slows the growth of IDH1 mutant glioma cells (Seltzer MJ 2010). These findings suggest that IDH1/2 mutant tumours may rely on glutamine and glutamate to maintain cellular α-KG levels, or possibly as an alternative energy source to glycolysis, although it is also possible that these changes simply illustrate the importance of glutamate generally in glioma development and progression as described above.

Mutations in *IDH1/2* may also lead to aberrant glucose sensing. Abnormal glucose control has been linked to the development of colon, breast, prostate, liver and bladder cancers (McFarland MS 2010). Furthermore it has been suggested that the use of the anti-hyperglycaemic drug metformin decreases the risk of specific cancers in patients with type 2 diabetes (Evans JM 2005, Libby G 2009). IDH1 has been shown to play a role in glucose sensing by controlling glucose stimulated insulin secretion (GSIS) by pancreatic β-cells, and suppression of IDH1 activity impairs GSIS and pyruvate cycling flux (Ronnebaum SM 2006). The mechanism by which altered glucose sensing would lead to tumourigenesis is unclear, although it has been suggested that low cytosolic NADPH levels resulting from mutations in *IDH1* may play a role, by aberrantly signaling a low nutrient state to downstream effectors in the glucose-sensing pathway, leading to increased cellular nutrient consumption and providing a selective growth advantage (Reitman ZJ 2010).

More recently the expression of lactate dehydrogenase A (*LDHA*), whose gene product catalyses the conversion of lactate to pyruvate, has been shown to be down regulated as a result of promoter hypermethylation in IDH1 mutant glioma cell lines, and was also

underexpressed in IDH1/2 mutant tumours (Chesnelong C 2013). Furthermore low expression and hypermethylation of *LDHA* is also reported in The Cancer Genome Atlas to occur in IDH1/2 mutant GBM. Taken together, these findings suggest another mechanism by which mutant IDH1/2 activity may alter glycolytic function.

### 1.3.7 Mutations in *IDH1/2* and Cellular Response to Oxidative Stress

Dysregulation of cellular reduction-oxidation (redox) has been shown to contribute to malignant transformation in cancer (Valko M 2006). IDH1/2 act in a protective role against oxidative stresses and IDH1/2 activity increases in response to such insults (Lee SH 2004, Kil IS 2007, Lee SM 2009, Yang C 2009, Reitman ZJ 2010). Conversely, knockdown of wild-type *IDH1/2* gene expression has been shown to enhance cellular oxidative damage and exacerbate the induction of apoptosis by agents such as selenite and staurosporine (Lee SM 2009, Kil IS 2010, Yang ES 2011). NADPH, a product of IDH1 and IDH2 wild-type activity, is important in this protective process, and its synthesis may be reduced by the activity of mutant IDH1/2. NADPH is a carrier of reducing power in cells and is primarily involved in maintaining optimal redox metabolism by acting directly as a reducing agent and as a cofactor for enzymes that synthesize energy-rich molecules and provide reducing equivalents that protect cells from the toxicity of ROS. NADPH also interacts with the glutathione and thioredoxin systems which themselves regulate cellular redox states (Metellus P 2011, Block K 2012). α-KG is itself able to function as an anti-oxidant (Metellus P 2011), whilst conversely, D-2HG has been shown to induce oxidative stress in animal models (Metellus P 2011). Therefore it has been suggested that mutant IDH1/2 activity may result in increased oxidative stress through several mechanisms. However ROS production was not found to be significantly altered in IDH1 mutant cell lines (Koivunen P 2012), and ROS levels were actually reduced in the brains of brain-specific idh1 R132H KI mice, although the

intracellular $NADP^+$/NADPH ratio and glutathione levels were increased and decreased respectively (Sasaki M 2012b). Furthermore, in haematopoietic-specific idh1 R132H KI mice no alterations in the levels of either ROS, $NADP^+$ or NADPH were observed (Sasaki M 2012a). Consequently, although a depletion of cellular NADPH or α-KG, and the accumulation of D-2HG, may hypothetically lead to increased oxidative stress, resulting in oxidative DNA damage and tumourigenesis in IDH1/2 mutant tumours, current evidence from *in vitro* and *in vivo* studies is conflicting and does not entirely support this theory.

## 1.4 IDH1/2 mutant mouse models of cancer

The fact that abnormal histone and DNA methylation patterns are a common feature of IDH1/2 mutant tumours suggests that the inhibition of JHDMs and TET by 2-HG may be more likely to be responsible for tumourigenesis, rather than TCA cycle dysregulation per se. The development of a 'pseudohypoxic state' resulting from the stabilization of HIF1α is also likely to play a role, although activation of this pathway may not be the primary tumour initiating event. The absolute effects of these phenomena however remain unknown and further research, perhaps using genetically engineered mouse models, is required to characterize the 'downstream' genetic effects and pathways that give IDH1/2 mutant cells their pro-tumourigenic potential. The first such mouse model was developed using a human IDH1 R132H mutant glioma stem cell line in an orthotopic xenograph mouse. This model may be of use in the future to test IDH1 targeted therapies (Luchman HA 2012). Subsequently a haematopoietic-specific Idh1 R132H KI mouse was developed, in which a specific leukaemic methylation pattern was observed (Sasaki M 2012a). Most recently a brain-specific Idh1 R132H KI mouse was generated, which was associated with the development of intracerebral haemorrhage in utero and perinatal lethality (Sasaki M 2012b). Elevated D-2HG levels were observed in the embryonic brains of these mice, as well as

defective collagen protein maturation, suggesting that the inhibition of C-P4H was responsible for the resulting phenotype (Sasaki M 2012b). Moreover elevated levels of Hif1α, and upregulation of *Vegf, Glut1,* and *Pgk1* were observed, further demonstrating the potential of D-2HG to inhibit HIF-PHD (Sasaki M 2012b). To date however, no tumour-forming genetically engineered Idh1/2-mutant model has been established.

## 1.5 The clinical relevance of IDH1/2 mutations

IDH1/2 mutations may serve as prognostic biomarkers in several cancers. In patients with intrahepatic cholangiocarcinoma mutations in *IDH1/2* are associated with a longer time to tumour recurrence after surgical resection and a longer OS (Wang P 2013). In AML mutations in *IDH2* but not *IDH1* is associated with a better prognosis (Chou WC 2011), whilst in glioma, patients whose tumours carry mutations in *IDH1*/2 are reported to have a better prognosis than those with IDH1/2 wild-type disease (Sanson M 2009). Indeed in glioma, where prognosis has traditionally been based on WHO classification, the discovery of mutant IDH1/2 has important prognostic implications. Specifically, it is now considered that a patient diagnosed with an IDH mutant grade IV glioma has a better prognosis than a patient with an earlier grade IDH WT glioma. Hence the discovery of mutant IDH has changed the prognostic value of the WHO grading system.

IDH1/2 mutations may also act as predictive biomarkers in glioma. Patients with IDH1 mutant GBM have been shown to exhibit a better response to TMZ than patients with IDH1 wild-type disease (SongTao Q 2012); however, IDH1 mutation status does not predict response to PCV chemotherapy in patients with anaplastic oligodendroglioma (van den Bent MJ 2010).

IDH1 mutation testing is also a useful diagnostic tool in glioma and its use has become part of standard clinical practice (Agarwal S 2013). Mutations in *IDH1* can be detected in glioma through direct sequencing based techniques, or by IHC (IHC) (Takano S 2011) and can help to distinguish gliomas from benign CNS lesions (Horbinski C 2009), as well as astrocytoma and oligodendroglioma from other CNS tumours (Horbinski C 2009, Capper D 2011), and primary GBM from secondary GBM (Capper D 2010). Furthermore, identification of mutant IDH1 protein by IHC in pathological specimens, can enable the differentiation of tumour cells from reactive glial cells (Capper D 2010), which may help post operatively to determine the completeness of surgical resection, and aid in the analysis of post therapy biopsy samples (Capper D 2010). Direct sequencing based techniques used to detect IDH1 mutations may give false negative results if samples are insufficient or are contaminated with normal tissue (Agarwal S 2013). IHC is advantageous clinically as methods are time and cost efficient, and relatively simple to implement in hospital pathology laboratories (Preusser M 2011). Furthermore, antibodies have been developed that are specific to the most frequently occurring IDH1 mutation in glioma, IDH1 R132H (Capper D 2009, Kato Y 2009). These antibodies have been shown to be 100% sensitive and 100% specific (Capper D 2010, Loussouarn D 2012) in detecting IDH1 R132H, and this method appears to be more sensitive than direct sequencing, especially in cases of low-grade diffuse astrocytoma (Capper D 2010), and in diffuse glioma where biopsy samples are very small (Preusser M 2011). Moreover, IHC detection of IDH1 R132H has been shown to be reliable and consistent across different laboratories (Van den Bent M 2013). Indeed such is the degree of sensitivity and specificity of commercially available IDH1 R132H antibodies, they have been used to demonstrate intratumoural heterogeneity in *IDH1* mutant tumours in patients with OD and MS (Amary M 2011). Conversely however tumour heterogeneity has not been reported through IHC analysis of *IDH1* mutant gliomas (Capper D 2010) implying that mutant IDH1

is present in all tumour cells within an *IDH1* mutant glioma. This makes IHC analysis a reliable diagnostic tool in the delineation of tumour from non tumour in IDH1 mutant glioma.

Measurement of 2-HG levels can also be used for diagnostic purposes and may also be used in certain circumstances to monitor response to therapy. 2-HG can be detected non-invasively in patients with IDH1/2 mutant glioma using magnetic resonance spectroscopy (MRS) imaging of the brain (Choi C 2012, Pope WB 2012), and although the clinical relevance of this technology is not yet defined, it may in the future enable preoperative prediction of tumour histology, intraoperative visualisation of tumour margins, monitoring of treatment and early detection of disease recurrence. Serum measurements of 2-HG levels in glioma patients do not however appear to correlate with IDH1/2 mutation status or tumour size and therefore serum 2-HG assessment may not be useful in the diagnosis or monitoring of treatment in patients with glioma (Capper D 2012). However 2-HG can be detected in the serum and urine of patients with IDH1/2 mutant AML (Fathi AT 2012) and its levels decrease with response to treatment (Fathi AT 2012), suggesting that 2-HG may serve as a non-invasive biomarker of disease activity in this setting. Furthermore post treatment serum 2-HG levels <200ng/ml have been shown to correlate with longer OS in IDH1/2 mutant AML suggesting that serum 2-HG measurement may also provide prognostic information in these patients (Dinardo C 2013).

IDH1/2 mutations could also serve as therapeutic targets, and recently two compounds specifically targeting mutant IDH1 R132H (AGI 5198) (Popovici-Muller J 2012) and IDH2 R140Q (AGI 6780) (Wang F 2013) have been developed. Indeed, treatment of erythroleukemic cells expressing IDH1 R132H (Losman J 2013) or IDH2 R140Q (Wang F 2013) with the corresponding inhibitors blocked D-2HG production, reverting growth factor independent proliferation and restoring the ability of these cells to differentiate. Moreover, ex-vivo treatment of primary IDH2 R140 AML cells with AGI-6780, decreased the levels of

2-HG, relieving the block of differentiation consequent to the expression of mutant IDH2 (Wang F 2013). Other studies additionally demonstrated that the targeted inactivation of IDH1 R132H by the inhibitor AGI-5198 impaired growth of IDH1 mutant glioma cells and mouse xenografts, and promoted gliogenic differentiation (Rohle D 2013). The potential benefit of IDH1/2 inhibitors has to date only been assessed in pre-clinical trials and will require further evaluation in clinical trials in the future.

## 1.6 Aims and outline of this thesis

### 1.6.1 Aims of thesis

The tumourigenic mechanisms associated with IDH1/2 mutations remain unclear. There is however emerging data associating mutations in IDH1/2 with glioma, AML and other tumour types, and evidence demonstrating that such mutations result in both loss and gain of IDH1/2 enzyme function. Furthermore it has been proposed that 2-HG, which accumulates in cells as a result of mutant IDH1/2 activity, acts as an oncometabolite in IDH1/2 mutant tumours. The themes tackled in the ensuing chapters focus on investigating the role played by IDH1/2 mutations in tumourigenesis and the mechanisms responsible for tumour development, with particular relevance to GBM. Specifically I aim to:

1. Confirm the frequency of IDH1/2 mutations in a panel of human glioma samples and to establish whether mutations in other genes that could also potentially lead to 2-HG accumulation are present in these samples. This is discussed in Chapter 3.

2. Develop cell models of IDH1/2 gain and loss of function and to compare the effects of IDH1/2 knockdown and IDH1/2 mutant expression on potentially tumourigenic pathways, in order to understand if the tumourigenic properties of mutant IDH1/2 can result either solely from the loss of function of the wild-type enzyme or gain of function of the mutant enzyme, or if indeed both gain and loss of enzyme function are required. This is discussed in Chapter

4.

3. To generate a brain-specific Idh1 R132H transgenic mouse model of GBM in order to evaluate any brain-specific phenotype that arises, and investigate the mechanisms responsible for tumour development should tumours occur. A constitutive *D2hgdh*$^{-/-}$ knockout mouse (*D2hgdh* KO), predicted to accumulate 2-HG, will also be analysed in order to better evaluate the possible phenotypic effects given by 2-HG accumulation and to allow a comparison of these effects to be made with those seen in brain-specific Idh1 R132H mice, in which reduced levels of α-KG in addition to 2-HG accumulation are predicted to occur. This is discussed in Chapter 5.

### 1.6.2 Outline of thesis

1. Materials and methods are discussed in Chapter 2.

2. The primary analyses of the thesis are presented in Chapters 3 to 5. Within each chapter there is a brief introduction and where necessary some additional chapter specific methods, followed by results, discussion and conclusions.

3. A summary of the findings and implications of this thesis are presented in Chapter 6. This is followed in Chapter 7 by a description of further studies that are planned as a result of this programme of work.

4. References and appendices are presented at the end of the thesis.

# 2. Chapter Two

## Materials and Methods

## 2.1 DNA extraction

### 2.1.1 DNA extraction from formalin fixed paraffin embedded tissue

Paraffin embedded tumour samples were removed from slides by scraping with a 21 gauge needle. 220ul of ATL and 40ul of proteinase K (PTK) were added and samples were incubated overnight at 55ºC. A further 20ul of PTK was then added, and samples were mixed by vortexing, and incubated again for 8 hours at 55ºC. A further 20ul of PTK was then added, and samples were mixed by vortexing and incubated overnight at 55ºC. DNA was then extracted using DNeasy Blood and Tissue kit from Quiagen$^{R}$ (Alameda, CA) according to manufacturer's instructions. Typically an equal volume of buffer AL was added to each sample, which was then mixed by vortexing and incubated for 10 minutes at 70ºC. Samples were loaded on to a DNeasy spin column and centrifuged at 8000 rpm for 1 minute. The column was then washed with 500ul of buffer AW1 and centrifuged at 8000 rpm for 1 minute, and then washed with 500ul buffer AW2 and centrifuged at 13000 rpm for 3 minutes. Columns were centrifuged again at 13000 rpm for 3 minutes, following which DNA was eluted by adding 100ul of sterile $H_20$ directly to the spin column membrane, followed by centrifugation at 8000 rpm for 1 minute. DNA was then quantified with the NanoDrop-100 spectrophotometer (Thermo Scientific).

### 2.1.2 DNA extraction from ES cells

DNA was extracted from ES cells using lysis buffer made up of the following: 20 mM Tris HCl pH 8.0; 10 mM EDTA; 0.5% SDS; 100 mM NaCl; 100 ug/ml Proteinase K (5 ul 20 mg/ml stock per 1 ml buffer). Cells were cultured in a 6 well plate until they reached 90-

100% confluence. Media was aspirated off and cells were washed with PBS. 1 ml of lysis buffer containing proteinase K was added to each well. Plates were then covered with paraffin film and incubated for 1 hour at 55$^{o}$C (on a mechanical shaker). Cells were scraped using a scraper and lysates were then transferred using a wide bore pipette into an Eppendorf tube and incubated overnight at 55$^{o}$C. 300 ul of isopropanol was added to each tube (lysed volume) and invert several times. The Eppendorf tube was then centrifuged at maximum speed for 10 minutes and the supernatant was discarded. The pellet was then washed carefully with 70% ethanol. The sample was centrifuged again as above and the supernatant was again discarded. The pellet was then air dried and re-suspended in 40 ul 1X TE with RNase (10 ug/ml). DNA concentration was then quantified using the NanoDrop-100 spectrophotometer.

### 2.1.3 DNA extraction from mouse ear snips for genotyping

DNA was extracted from mouse ear snips using the HotSHOT method. This method uses hot sodium hydroxide (NaOH) to lyse cells and release nucleic acids from cell nuclei. NaOH also allows denaturation to take place by disrupting hydrogen bonds between nitrogen bases in double-stranded DNA (dsDNA), producing single stranded DNA (ssDNA). NaOH makes the solution very alkaline, and hence tris(hydroxymethyl)aminomethane hydrocholride (Tris-HCl) neutralization buffer is used to maintain the pH of the solution. This is an appropriate method for genotyping, but due to shearing, the quality and concentration of DNA yields are often not adequate for other applications such as sequencing.

Ear snips were incubated in 50ul of HotSHOT buffer, comprising of 25 mM NaOH and 0.2 mM disodium Ethylenediaminetetraacetic acid ($Na_2EDTA$), in an eppendorf at 95ºC for 30 minutes, following which 50ul of 40 mM Tris-HCl neutralisation buffer was then added.

### 2.1.4 DNA extraction from mouse tissue

Tissue samples were incubated in 220ul of ATL and 40ul of PTK overnight at 55ºC. A further 20ul of PTK was then added, and samples were mixed by vortexing, and incubated again for 8 hours at 55ºC. DNA was then extracted using DNeasy Blood and Tissue kit from Quiagen$^{R}$ (Alameda, CA) according to manufacturer's instructions. Typically an equal volume of buffer AL was added to each sample, which was then mixed by vortexing and incubated for 10 minutes at 70ºC. Samples were loaded on to a DNeasy spin column and centrifuged at 8000 rpm for 1 minute. The column was then washed with 500ul of buffer AW1 and centrifuged at 8000 rpm for 1 minute, and then washed with 500ul buffer AW2 and centrifuged at 13000 rpm for 3 minutes. Columns were centrifuged again at 13000 rpm for 3 minutes, following which DNA was eluted by adding 100ul of sterile $H_20$ directly to the spin column membrane, followed by centrifugation at 8000 rpm for 1 minute. DNA was then quantified with the NanoDrop-100 spectrophotometer.

## 2.2 RNA extraction

### 2.2.1 RNA extraction from cell lines

Total RNA was extracted and purified from cells with the RNeasy minikit (Qiagen), according to manufacturer's instructions. Typically media was aspirated from cell cultures and cells were washed twice with PBS. Cells were then lysed with 600ul of buffer RLT containing 6ul of β-mercaptoethanol and were detached using a Corning cell scraper(Sigma-Aldrich). Cell lysates were homogenised using the QIAshredder homogeniser. 600ul of 70% ethanol was added to the homogenised lysate and mixed by pipetting. 700ul of homogenised lysate was transferred to an RNeasy spin column and centrifuged for 15 seconds at 10,000 rpm. The spin column membrane was washed with 700ul of buffer RW1 by centrifugation at

10,000 rpm for 15 seconds, and was then washed twice with 500ul of buffer RPE for 15seconds and then 2 minutes at 10,000 rpm. 30ul of RNA free $H_20$ was added directly to the spin column membrane which was centrifuged at 10,000 rpm for 1 minute to elute the RNA. Purified RNA samples were treated with DNase I to degrade residual DNA, according to manufacturer's instructions. RNA samples were quantified with the NanoDrop-100 spectrophotometer.

### 2.2.2 RNA extraction from mouse tissue

RNA extraction from mouse tissue was undertaken using the Trizol (Invitron)/chloroform method. Trizol is a monophasic solution made up of phenol and guanidine isothiocyanate. Trizol maintains RNA integrity during RNA extraction, whilst disrupting the cell membrane and dissolving cellular components. Following the addition of chloroform, centrifugation separates the solution in to a colourless aqueous phase which contains the extracted RNA, a white interphase which contains DNA, and a red organic phenol-chloroform phase which contains proteins and lipids.

1ml of Trizol was added to frozen mouse tissue samples in an eppendorf. The sample was homogenised using a 1ml syringe and a 21 gauge needle. The homogenate was vortexed for 15 seconds and left to stand at room temperature for 5 minutes. 200µl of chloroform (Invitron, CA, USA) was added to each sample which was then vortexed for 15 seconds and left to stand at room temperature for 5 minutes. Samples were centrifuged at 14000 rpm for 15 minutes at 4 °C and the upper layer of the supernatant was then removed and transferred to a clean eppendorf. The RNA was then precipitated by adding 500 µl of isopropanol to each sample and left to stand for 10 minutes at room temperature and then centrifuged at 14000 rpm for 15 minutes at 4 °C. The supernatant was discarded and the pellet was centrifuged again for 3 minutes, with the remaining supernatant then being removed. 1ml of 75% ethanol

was added to the pellet and vortexed. Samples were centrifuged at 14000 rpm for 5 minutes at 4 °C. The supernatant was discarded and the above 2 steps repeated twice more. Ethanol was then removed and the samples left to air dry for 15 minutes. The samples were then re-suspended in 100 µl of DEPC treated water ($H_20$) and the RNA was quantified using the NanoDrop-100 spectrophotometer.

## 2.3 Spectrophotometry

DNA quantity and quality was measured with spectrophotometry at 260nm and 280nm using the NanoDrop-100 spectrophotometer. An optical density (OD) of 1 at 260nm equates to approximately 50µg/ml of double stranded DNA. Hence the concentration (µg/ml ) of DNA samples were calculated using the formula "dilution factor x 50 x $OD_{260}$". DNA quality was assessed by calculation of $OD_{260}$/ $OD_{280}$ ratios, with 1.8 being the ratio associated with a pure sample of DNA. Contamination of a sample with protein decreases the ratio towards 1.4 and contamination with RNA increases the ratio towards 2.0.

RNA samples (stored on wet ice) were assessed for quantity and quality using the Nanodrop spectrophotometer applying the same principles as those outlined above.

## 2.4 Polymerase Chain Reaction

The polymerase chain reaction (PCR) is an *in vitro* technique that is used to selectively amplify a specific DNA sequence. The DNA region of interest is amplified using two complimentary oligonucleotide primers which hybridise to the selected region of the DNA template on opposing strands.

A typical PCR reaction consists of thirty five cycles (although this can vary). Each cycle is made up of three steps: (i) denaturation of the DNA template through heating to 94°C, (ii)

annealing of the primers to the separated template strands through heating to 55-60°C (varies depending on the primer sets used) and (iii) extension of the primers by DNA polymerase at 72°C. This reaction requires the addition of the four deoxyribonucleotide triphosphates dATP, dTTP, dGTP, dCTP and a thermostable DNA polymerase.

The first cycle produces two new separate strands of DNA template which can then be a target for the primers in the second cycle. The third cycle results in the production of a double stranded DNA product incorporated in to which is the target region. The subsequent cycles produce an exponential doubling of the target sequence which becomes the predominant reaction product.

Primers for use in PCR were designed using the Primer3 programme designed by the Whitehead Institute of Biochemical Research (http://bioinfo.ut.ee/primer3-0.4.0/).

Typically a 25µl PCR reaction contains 30-50ng of template DNA, 0.4µM of each primer, 1 x PCR buffer (Bioline), 1mM $MgCl_2$ (Bioline), 200mM of each dNTP, and 1µl of Taq DNA polymerase (Qiagen). PCR reactions were undertaken in a 96 well plate (ABgene). DNA samples were aliquoted into the plate and the PCR master mix was then added. The plate was sealed with an adhesive PCR film seal (Thermo Scientific) and immediately run on a Tetrad PCR machine (MJ Research) using the appropriate programme. The PCR reaction programme typically consisted of initial denaturation at 94°C for 5 minutes followed by 35 cycles of 94°C for 1 minute, 55°C for 1 minute, 72°C for 1 minute with a final extension at 72°C for 10 minutes. Various parameters such as $Mg^{2+}$ concentration, annealing temperature and extension time or the addition of Q solution (Qiagen) were altered depending on which conditions suited the selected primer pairs and target DNA size.

Primer sequence details and required PCR conditions are listed in Appendix 1.

Resultant PCR products were analysed by agarose gel electrophoresis with ethidium bromide staining.

### 2.4.1 Purification of PCR products

PCR products were cleaned up prior to sequencing using ExoSAP-IT® (USB Corporation, Cleveland, Ohio), as per manufacturer's instructions. ExoSAP-IT utilises the action of recombinant exonuclease I and shrimp alkaline phosphatase (*Pandalus borealis*) in a buffered solution.

In brief, 5µl of PCR product was mixed with 2µl of ExoSAP-IT in a PCR plate (ABgene) and underwent the following programme on a PCR machine: Heating to 37°C for 15 minutes, followed by heating to 80°C for 15 minutes. The cleaned up PCR product was then diluted with 15µl of $H_20$.

## 2.5 Agarose Gel Electrophoresis

Agarose gel electrophoresis is a technique which separates DNA molecules by their size. When in solution, DNA molecules carry a negative charge and consequently migrate towards the anode of an electrical field. Agarose gel is a 3D matrix which enables DNA to migrate according to its size, with larger molecules migrating at a slower rate than smaller ones. Ethidium bromide dye staining can be used to visualise DNA. The ethidium bromide intercalates between DNA base pairs and fluoresces when exposed to UV light at a wavelength of 302nm.

Agarose gel electrophoresis was performed using 2% agarose. 20g of agarose powder (Invitrogen) was dissolved in 1x TBE buffer and boiled. The molten agarose was allowed to cool to 60°C and ethidium bromide was added at a final concentration of 0.25µg/ml. Molten

agarose was poured in to a gel casting tray (Bio-rad) with well combs in position and allowed to set at room temperature. Following removal of the comb, the gel was placed in a DC power pack (Bio-rad PowerPac 300) and covered with 1 x TBE buffer. 10µl of DNA was combined with 2µl of 5 x Orange G Loading Dye (Trevigen) and loaded in to a gel well. 10µl of 1 kB plus ladder (Invitrogen), prepared as per manufacturer's instructions, was added to the first well as a guide for the size of the DNA products being analysed. The gel was then run at 120V for 15-20 minutes. After removal from the tank, the DNA was visualised in UV light at 302nm in a ChemiDoc White/UV box transilluminator (Bio-Rad), and images were taken and saved using Image Lab™ image acquisition and analysis software (Bio-Rad).

## 2.6 Fluorescence sequencing of PCR products

DNA sequencing is the process of determining the exact order of nucleotides within a DNA molecule, and enables the detection of mutations in DNA target regions amplified by PCR.

Automated fluorescent sequencing using dye terminators is an automated method of DNA sequencing. This technique depends upon the ability of DNA polymerase to synthesise complementary copies of single stranded target DNA which are then labelled with a fluorescent dye corresponding to each base at the 3' end of a DNA fragment. Hence DNA synthesis is undertaken in the presence of one specific primer for the target sequence, the four deoxynucleotides (dNTPs), and a low concentration of their fluorescently labelled dideoxynucleotides (ddNTPs) analogues, DNA polymerase enzyme and buffer. The standard sequencing reaction involves 34 cycles of heat denaturation, primer annealing and extension. Due to the fact that the ddNTPs lack the 3'-hydroxyl group necessary for extension to take place, chain termination occurs during the extension phase whenever one of these nucleotides is incorporated into the DNA. As ddNTPs are present at a low concentration, chain

termination occurs at each nucleotide along the target DNA sequence. The resultant strands therefore have a common 5' end defined by the primers but vary in length depending on their base specific 3' ends. Each truncated fragment contains a fluorescently labelled ddNTP at its 3’ end (one for each base). These dye-labelled fragments are loaded onto a sequencing machine where they undergo capillary electrophoresis which separates them by size based on their total charge. This process involves a high voltage charge being applied that forces the negatively charged fragments into capillaries where they migrate through a liquid polymer and separate. Shortly before reaching the positive electrode, the fluorescently labelled DNA fragments pass through a 'read window' where a laser excites the fluorescent dyes and light is emitted at a wavelength specific for each dye. The resulting fluorescence can be detected by a charge-coupled device (CCD) camera and is translated into a chromatogram, allowing each discrete base to be identified in order.

PCR products selected for DNA sequencing were first purified, to remove unincorporated primers and nucleotides using ExoSAP-IT as outlined in section 2.4.1. The resultant purified PCR products were then sequenced in forward and reverse orientation using the same primer as in the original PCR reaction. Each 20µl reaction contained 8µl of Big Dye Terminator Ready Reaction mix (Applied Biosystems), 1µl of primer (forward or reverse), 4µl of the diluted purified PCR product and 7µl of sterile $H_20$. Sequencing cycle conditions for the Tetrad PCR machine (MJ Research) consisted of an initial denaturation step at 96°C for 5 minutes followed by 35 cycles of 96°C for 30 seconds, 50°C for 45 seconds, and 60°C for 4 minutes with a final extension at 72°C for 10 minutes. 20 µl of the resultant sequencing product was finally purified from excess dye-labelled ddNTPs using the DyeEx 96 kit (Qiagen) by centrifugation for 3 minutes at 3000 rpm. Samples were then concentrated to dryness in a SpeedVac.

Sequencing analysis was performed using the ABI3730xl sequencing machine (Applied Biosystems). The ABI3730xl sequencer is an automated, high-throughput, capillary electrophoresis systems used for analysing fluorescently labelled DNA fragments. All samples were run on 36cm capillaries containing POP-7 Polymer (Applied Biosystems) and BigDye sequencing buffer (10X) with EDTA (Applied Biosystems). Sequences were then analysed using the ApE plasmid editor programme. (http://biologylabs.utah.edu/jorgensen/wayned/ape/).

## 2.7 Reverse transcription PCR (RT-PCR)

RT-PCR is a sensitive method for the detection of mRNA expression levels. It involves two steps: (i) reverse transcription reaction where RNA is transcribed to cDNA using a reverse transcriptase and (ii) PCR amplification using primers specific for one or more genes. RT-PCR was achieved as using a one-step reaction. In this approach the entire reaction from cDNA synthesis to PCR amplification occurs in a single tube. cDNA was synthesised from 1µg of extracted RNA using the high capacity cDNA Reverse Transcription Kit (Applied Biosystems). In brief 1µg of extracted RNA (made up to 10µl volume with nuclease free $H_20$) was added to a master mix containing 2µl of 10x RT buffer, 0.8µl of 25x dNTP mix (100mM), 2.0µl 10x RT random primers, 1.0µl of MultiScribe reverse transcriptase, and 3.2µl of nuclease free $H_20$ in a 96 well plate (ABcam). The plate was then run on a Tetrad PCR machine (MJ Research) using the following conditions: 25°C for 10 minutes, 37°C for 120 minutes, and 85°C for 5 minutes. The resulting cDNA product was then diluted with 30µl of $H_20$ to make a total volume of 50 µl to be used for sequencing or quantitative real time PCR analysis.

## 2.8 Quantitative Real Time-PCR (qRT-PCR)

qRT-PCR is a technique that is used to quantitatively determine gene expression levels by analysing the amount of cDNA in a sample in real time using fluorescent DNA probes. SYBR green and Taqman probes were used.

**SYBR Green:** SYBR Green binds to the double-stranded DNA of the PCR product and emits light upon excitation. The intensity of the fluorescence increases as the PCR products accumulate. This technique negates the need to design probes given the lack of specificity of its binding. However, since the dye does not discriminate between dsDNA from the PCR product and dsDNA from the primer-dimers, overestimation of the target concentration can occur.

**TaqMan Probes:** TaqMan probes are oligonucleotides that have a fluorescent probe attached to the 5' end and a quencher at the 3' end. Generation of fluorescence depends on Förster Resonance Energy Transfer (FRET) coupling of the dye molecule and the quencher moiety to the oligonucleotide substrates. During PCR amplification, the probes hybridise to the target sequences and as polymerase replicates the template with TaqMan bound, it also cleaves the fluorescent probe. This results in an increase of intensity of fluorescence proportional to the number of the probe cleavage cycles and provides an accurate assessment of target sequence concentration.

Absolute quantification qRT-PCR was performed using the ABI 7900HT cycler (Applied Biosystems) for each sample (in triplicate for Syber green and duplicate for Taqman probe reactions), and with blank and control samples. For reactions using SYBR green, all quantitative PCR mixtures contained 1µl of retrotranscribed RNA, 25µl of SYBR Green PCR Master Mix (Applied Biosystems), and appropriate volumes of target specific primers. For

reactions using TaqMan probes, all quantitative PCR mixtures contained 2µl of retrotranscribed RNA, 5µl of 1x Taqman Universal master mix (Applied Biosystems), 2µl of $H_20$, and 1µl of the probe of interest. Reaction mixtures were loaded onto a 96 well plate (Applied Biosystems) which were then centrifuged for 1 minute at 1000 rpm. The expression of each target gene was evaluated using a standard relative quantification approach -$2^{\Delta\Delta CT}$ approach, with GAPDH or actin serving as an endogenous control.

## 2.9 Immunohistochemistry

1. Slide preparation

4µm sections of formalin-fixed, paraffin-embedded tissue (FFPE) sections were used. Human GBM tissue slides were already available from archival tissue. Slides made from mouse tissue were made from freshly cut paraffin blocks and were placed onto glass slides. Slides were de-waxed in xylene for 5 minutes and then rehydrated through graded alcohols to $H_20$ through incubation as follows: 100% ethanol for 5 minutes, 90% ethanol for 5 minutes, 70% ethanol for 5 minutes, $H_2O$ for 2 minutes. Endogenous peroxidase was blocked by incubating slides in 1.6% $H_2O_2$ (376ml methanol, 24ml peroxidase) for 20 minutes, before being rinsed with $H_2O$.

2. Antigen retrieval and applying primary antibody

For antigen retrieval, sections were pressure cooked in 10 mmol/L citrate buffer (pH6.0) at full pressure for 5 minutes. Slides were allowed to cool in the citrate buffer for 20 minutes and then rinsed in PBS. A PAP pen (Sigma-Aldrich) was used to draw around each section. Sections were then incubated in 100ul of 10% serum for 30 minutes to block non-specific binding, and serum was then carefully blotted off. Slides were then incubated with appropriate primary polyclonal antibody (antibodies summarised in Table 2-1), diluted to

appropriate concentration with PBS, for 1 hour. Positive and negative controls were included in each run.

3. Application of secondary antibody and counterstaining

Slides were rinsed in PBS for 5 minutes. Appropriate secondary antibody (5ul secondary antibody, 15ul serum, 980ul PBS was then applied for one hour at room temperature. Slides were the washed in PBS. Sections were then incubated in streptavidin-peroxidase conjugate (ABC solution-Vector labs) (1 drop solution A, 1 drop solution B, 2.5mls PBS for 30 minutes. 3,3'-diaminobenzidinetetrahydrochloride (DAB) solution (Sigma) was made by dissolving 1 silver and 1 gold tablet in 5ml $H_2O$, and peroxidase activity was demonstrated by incubating slides in DAB solution for 2–5 minutes. Development of the colour reaction was monitored microscopically. Slides were then washed with distilled $H_2O$ and counterstained with haematoxylin for 30 seconds, before being washed under tap $H_2O$ for 5 minutes. Finally slides were dehydrated through a series of 1 minute ethanol washes of 70%, 90% and 100%, then xylene, before being mounted using Pertex mountant (CellPath) cleared. Images were taken at various magnifications.

**Table 2-1: Primary antibodies used for immunohistochemistry**

| Primary Antibody | Dilution used |
|---|---|
| D2HGDH (rabbit) (ProteinTech Group, Chicago, IL) | 1:50 |
| L2HGDH (rabbit) (ProteinTech Group, Chicago, IL) | 1:100 |
| Nestin (rabbit) (Novus Biologicals, Littleton, CO) | 1:400 |
| Phospho-Histone H3 ($pSer^{10}$) (rabbit) (Sigmal-Aldrich, UK) | 1:800 |
| Active Caspase-3 (rabbit) (Abcam, UK) | 1:400 |

## 2.10 Protein

### 2.10.1 Total protein extraction from cells

Total protein extraction was performed using SDS containing tissue lysis buffer. Tissue culture media was aspirated off, and cells were washed twice with PBS. Typically 200ul SDS containing tissue lysis buffer was then added, and cells were detached using a Corning cell scraper (Sigma-Aldrich), transferred to an eppendorf and incubated in SDS at 95°C for 5 minutes. Extracts were then homogenised by ultrasound using an acoustic transducer, and centrifuged at 14,000 rpm for 10 minutes. The protein containing supernatant was removed and protein concentration was established using Pierce BCA Protein Assay Kit (Thermo Scientific).

### 2.10.2 Nuclear and cytosolic protein extraction from cells

3,000,000 cells were plated out for each cell line of interest onto a 10cm tissue culture plate in DMEM tissue culture media. Controls were plated out in duplicate and 300uM cobalt chloride ($CoCl_2$) was added. Cells were then incubated overnight at 37ºC in the tissue culture incubator. After 24 hours incubation, nuclear and cytosolic protein was extracted from cells.

Cytosolic protein extraction was carried out using buffer A. 10ml of 10x buffer A stock solution was made up of the following: 2ml hydroxyethyl piperazineethanesulfonic acid (Hepes) pH 7.9 (100mM), 2ml potassium chloride (KCl) (100mM), 2ml EDTA (100mM), 4ml $H_20$. 5ml of 1x buffer A solution was then made by diluting 500ul of 10x buffer A stock solution in 4500ul of $H_20$ and then 5ul Dithiothreitol (1mM) (DTT), 50ul phenylmethyl sulfonyl fluoride (100x) (PMSF), 250ul nonyl phenoxypolyethoxylethanol-40 (NP40) (10%), a cOmplete Mini Protease Inhibitor Tablet (Roche) and a PhosSTOP phosphatase inhibitor tablet (Roche) were added.

Nuclear protein extraction was carried out using buffer B. 5ml of 1x buffer B stock solution was made up of the following: 1ml Hepes Ph 7.9 (20mM), 400ul NaCl (400mM), 10ul EDTA (1mM), 500ul (10%) glycerol, 3.9ml $H_20$ and then 5ul (1mM) DTT, 50ul (100x) PMSF, half a cOmplete Mini Protease Inhibitor Tablet (Roche) and half a PhosSTOP phosphatase inhibitor tablet (Roche) were added. Buffers A and B were kept in ice.

Tissue culture plates were kept on ice. Media was aspirated from each plate and cells were washed twice with cold PBS. 250ul of 1x Buffer A was added to each plate. Cells were detached using a Corning cell scraper (Sigma-Aldrich). The lysate was transferred to an eppendorf and centrifuged at 4ºC for 3 minutes are 13000 rpm. The supernatant, containing cytosolic protein, was collected and transferred to a new eppendorf and stored in ice. The remaining pellet was resuspended in 50ul of x1 Buffer B, vortexed for 10 seconds, mixed on a mixing wheel for 2 hours at 4 ºC, and then centrifuged at 4 ºC for 5 minutes at 13000 rpm. The supernatant, containing nuclear protein was removed and transferred to a new eppendorf and stored on ice. Protein concentration was established using Pierce BCA Protein Assay Kit (Thermo Scientific).

### 2.10.3 Protein extraction from mouse tissue

Total protein extraction from mouse tissue was performed using urea tissue lysis buffer, made up of 7M urea, 10% glycerol, 10mM Tris-HCl (pH 6.8), 1% SDS, 5mM DTT, and a cOmplete Mini Protease Inhibitor Tablet (Roche). 200ul of buffer was added to tissue which was then homogenised through a 21 gauge needle. This homogenate was then sonicated for 10 seconds x3, and then mixed by rotation for 30 minutes at 4°C, before being centrifuged at 13000 rpm for 15 minutes at 4°C. The supernatant was removed and protein concentration was established using Pierce BCA Protein Assay Kit (Thermo Scientific).

### 2.10.4 Western Blot

Western blot was performed with the NuPAGE Gel system (Invitrogen) according to manufacturer's protocol. In brief, denatured lysates were loaded onto a gel to run at 150V for 2 hours. The gels were then transferred onto an Immobilon-P PVDF transfer membrane (Millipore) in a semi-dry tank (150mA for 2 hours), and the membrane was blocked by incubating for 1 hour at room temperature in 10% bovine serum albumin (BSA) or 10% milk.

The membranes were then incubated overnight in the appropriate primary antibody in 5% BSA, or 5% milk (antibodies summarised in Table 2-2). After washing, the membranes were incubated in the appropriate peroxidase-conjugated secondary antibody and the anti-Vinculin antibody or anti-actin antibody (as a loading control) for 1 hour at room temperature. After further washes, the blots were incubated in ECL reagents (GE healthcare) and bound antibodies were detected using enhanced chemiluminescence with developing chemiluminescence film (GE Healthcare) with a developer.

**Table 2-2: Primary antibodies used for western blots**

| Antibody | Dilution |
|---|---|
| IDH1 (rabbit)(Cell signaling technology, Boston, MA) | 1:800 |
| IDH2 (rabbit)(Protein Tech Group,Chicago,IL) | 1:800 |
| IDH3 (rabbit)(Abcam,Cambridge, MA) | 1:500 |
| D2HGDH (rabbit)(Protein Tech Group,Chicago,IL) | 1:800 |
| D2HGDH (rabbit)(Abcam, Cambridge, MA) | 1:1000 |
| Nestin (rabbit)(Novus Biologicals,Littleton, CO) | 1:1000 |
| HIF1 α (rabbit)(Cayman Chemical Company,Ann Arbor,MI) | 1:1000 |
| H3K9 (rabbit) (Abcam,Cambridge, MA) | 1:1000 |
| Total H3 (rabbit)(Abcam,Cambridge, MA) | 1:2000 |
| H3K4me3 (rabbit)(Abcam,Cambridge, MA) | 1:1000 |
| H3K9me2 (rabbit)(Sigmal-Aldrich, UK) | 1:1000 |
| PHD2 (rabbit)(Novus Biologicals,Littleton, CO) | 1:2000 |
| Actin (mouse)(Santa Cruz Biotechnology,Dallas,TX) | 1:1000 |
| Vinculin (mouse)(Sigmal-Aldrich, UK) | 1:1000 |
| Lamin (mouse)(Sigmal-Aldrich, UK) | 1:1000 |

## 2.11 Cell Culture

### 2.11.1 Cell culture conditions

LN18 cells were cultured in Dulbecco's Modified Eagle Medium (DMEM) (Gibco) with 4.5mg glucose, 1% penicillin/streptomycin (PS), and 5% fetal bovine serum (FBS).

U87MG cells were cultured in DMEM with 4.5mg glucose, 1% PS, 10% FBS and 1% non-essential amino acid (NEAA) cell culture supplement.

293T cells were cultured in Iscove's Modified Dulbecco's Medium (IMDM) (Gibco), with 1% PS and 10% FBS.

ES cells were cultured in iSTEM embryonic stem cell culture media (StemCells).

## 2.11.2 Freezing down and resuspending cells to replace stocks

To ensure permanent cell line resource aliquots of growing cells in culture were frozen down at an early passage and stored in liquid nitrogen. Media was removed and cells were washed twice with 5 ml of sterile PBS. 1ml of trypsin was used to detach the cells which were then removed and put into a falcon tube under sterile conditions and centrifuged at 2000 rpm for 5 minutes. The supernatant was removed and the pellet was re-suspended in 1ml of freeze mix (20% FBS/10% Dimethyl sulfoxide [DMSO]) and transferred to a cryotube (Corning) for long term storage. Tubes were stored at -80°C overnight and then in liquid nitrogen.

## 2.11.3 Generation of knockdown cell lines with shRNA

### 2.11.3.1 Cell lines

LN18 cells were purchased from the American Type Culture Collection (Manassas, VA) and grown as suggested by the provider.

### 2.11.3.2 Transduction with lentiviral vectors

*IDH1, IDH2, IDH3 D2HGDH and L2HGDH* gene knockdown was carried out using RNA interference with shRNA. Human shRNA target gene sets cloned in pLKO.1 lentiviral vectors were obtained for IDH1, IDH2, IDH3A, and D2HGDH from Open Biosystems, and for L2HGDH from Sigma Life Sciences.

shRNA clone IDs were as follows: IDH1- TRCN0000027284, TRCN0000027253, TRCN0000027249, TRCN0000027289, TRCN0000027298; IDH2- TRCN0000027307, TRCN0000027245, TRCN0000027296, TRCN0000027225, TRCN0000027262; IDH3A- TRCN0000027283, TRCN0000027270, TRCN0000027310, TRCN0000027252; D2HGDH- TRCN0000064034, TRCN0000064035, TRCN0000064036, TRCN0000064037,

TRCN0000064033; L2HGDH- TRCN0000064323, TRCN0000064324, TRCN0000064325.

The most efficient shRNA sequence was established for each gene by transient transfection of LN18 cells with the different shRNA clones using lipofectamine (Invitrogen). Protein and RNA were extracted from LN18 cells at 48 and 72 hours after the transfection. The knock down efficiency was then verified using western blot and quantitative real-time polymerase chain reaction (qRT-PCR). The most efficient shRNA clones were selected for lentiviral preparation.

The shRNA clones selected to be used for lentiviral preparation were the following: TRCN0000027289, TRCN0000027298 for IDH1; TRCN0000027296, TRCN0000027225 for IDH2; TRCN0000027310 for IDH3A; TRCN0000064037 for D2HGDH; TRCN0000064323 and TRCN0000064325 for L2HGDH. As a control, cells were also transduced with a scrambled shRNA sequence cloned in the pLKO.1 lentiviral vector.

Lentiviral Vector stocks were produced by transient transfection of 293T cells. Serial dilutions of freshly harvested conditioned medium were used to infect 4 x $10^5$ cells in a six-well plate in the presence of Polybrene (8 μg/ml). The viral p24 antigen concentration was measured by HIV-1 p24 Core profile ELISA (NEN Life Science Products) to determine the amount of infective particles before transduction, and to demonstrate that transduced cells did not produce viral particles after transduction.

### 2.11.4 Generation of IDH1 and IDH2 knockdown cells with siRNA

siRNA directed against *IDH1* and *IDH2* were obtained from Santa Cruz Biotechnology. 2 x $10^5$ U87MG cells were plated in each well of a 6-well tissue culture plate in a total of 2ml of

antibiotic-free tissue culture media. Cells were incubated at 37°C in an incubator until they reached 80% confluence. The following solutions were then prepared:

(1) Solution A: For each transfection, 4µl of siRNA duplex solution was diluted into 100µl of siRNA Transfection Medium (Santa Cruz Biotechnology).

(2) Solution B: For each transfection, 4µl of siRNA Transfection Reagent (Santa Cruz Biotechnology) was diluted into 100µl siRNA Transfection Medium (Santa Cruz Biotechnology).

The siRNA duplex solution (Solution A) was then added directly to the dilute Transfection Reagent (Solution B) using a pipette and the solution was mixed gently by pipetting up and down. The mixture was then incubated for 45 minutes at room temperature. The cells were then washed once with 2ml of siRNA Transfection Medium, which was then aspirated off. For each transfection, 0.8ml of siRNA Transfection Medium was then added to each tube containing the siRNA Transfection Reagent mixture (Solution A + Solution B) to make a volume of 1.008ml in total. This transfection mixture was mixed gently and then pipetted onto the washed cells. Cells were incubated in transfection mixture for 7 hours at 37° C in an incubator. 1ml of normal growth medium containing 2 times the normal serum and antibiotics concentration (2x normal growth medium) was then added without removing the transfection mixture, and cells were incubated for an additional 24 hours. The medium was then aspirated and replaced with fresh 1x normal growth medium. mRNA and protein were extracted and the degree of gene knockdown was assessed 48 hours after the addition of fresh growth media.

### 2.11.5 Generation of IDH1/2 mutant cell LN18 cells

The exogenous expression of either IDH1 or IDH2, and the corresponding mutant versions IDH1 R132H/R132C and IDH2 R172K/R172M was obtained by means of lentiviral transduction. Firstly wild-type *IDH1* or *IDH2* cDNA was amplified by PCR, using the following primers, which allowed the inclusion in the PCR amplicon of the ClaI and NheI enzyme restriction sites and the FLAG-tag sequence:

IDH1 FW: ctatatatcgatagtctgcaagactgggagga

IDH1 RV: ctatatgctagcttaCTTATCGTCGTCATCCTTGTAATCaagtttggcctgagctagtttg

IDH2 FW: ctatatatcgatCTCGTTCGCTCTCCAGCTT

IDH2RV: ctatatgctagcttaCTTATCGTCGTCATCCTTGTAATCCTGCCTGCCCAGGGCTCTGTC

Subsequently, the cDNA that was obtained was cloned as a ClaI-NheI fragment into the transfer vector #710.pCCL.sin36.PPT.Wpre.CMVtTA-s2.tet.gb, a TET-OFF system developed by Elisa Vigna (Vigna E 2005). Subsequently, IDH1 R132H/R132C and IDH2 R172K/R172M cDNA was obtained using a PCR-based technique described by Bardelli *et al.* (Bardelli A 1998), and cloned in the #710.pCCL.sin36.PPT.Wpre.CMVtTA-s2.tet.gb transfer vector by substituting the wild type *IDH1* or *IDH2* cassettes, for the ClaI-BmgBI fragment for *IDH1* and ClaI-NheI fragment for *IDH2*, respectively. The PCR primer set used to introduce the mutations into the IDH1 and IDH2 cDNA are listed below:

IDH1_R132H_a_fw: CGACGGTATCGGTTATCCAG

IDH1_R132H_b_fw: CTATCATCATAGGTcatCATGCTTAT

IDH1_R132H_b_rv: ATAAGCATGatgACCTATGATGATAG

IDH1_R132C_b_fw: CTATCATCATAGGTtgtCATGCTTAT

IDH1_R132C_b_rv: ATAAGCATGacaACCTATGATGATAG

IDH1_R132H_c_rv: TGGACGTCTCCTGTCCTTTC

IDH2_R172K_a_fw: CGACGGTATCGGTTATCCAG

IDH2_R172H_b_fw: AAGCCCATCACCATTGGCaagCACG

IDH2_R172H_b_rv: CGTCcttGCCAATGGTGATGGGCTT

IDH2_R172M_b_fw: AAGCCCATCACCATTGGCatgCACG

IDH2_R172M_b_rv: CGTGcatGCCAATGGTGATGGGCTT

IDH2_R172H_c_rv: TAAATCGATTGGCGCCTCCCCCTA

Vector stocks were produced by transient transfection of 293T cells. Serial dilutions of freshly harvested conditioned medium were used to infect $10^5$ cells in a six-well plate, in the presence of Polybrene (8g/ml). The viral p24 antigen concentration was measured by an HIV-1 p24 core profile enzyme-linked immunosorbent assay (ELISA; NEN Life Science Products) to determine the number of infective particles before transduction and to demonstrate that transduced cells did not produce viral particles after transduction.

### 2.11.6 Generation of conditional Idh1 R132H and Idh2 R172K mutant ES cells

Conditional Idh1 R132H and Idh2 R172K mutant transgenic murine ES cells were obtained from Caliper (Hopkinton, Ma) and cultured as outlined in Methods 2.11.1. Mutant gene expression was induced, by homologous recombination, using electroporation with a pCre-puromycin N-acetyltransferase (Pac) plasmid. ES cells were cultured in a 25cm tissue culture flask until they reached 70% confluence. Media was changed 3 hours prior to electroporation. Cells were trypsinised with 3ml of trypsin, and resuspended in 10ml of iSTEM media. A 200µl aliquot was removed and a manual cell count was made. The remaining cell suspension was centrifuged for 7 minutes at 1000 rpm. Cells were then resuspended in sterile PBS to a density of 7 x $10^6$ cells per 0.7ml of PBS. 0.7ml of this cell suspension was transferred to an electroporation cuvette. 40ug of the pCre-Pac plasmid was added to 100ul of sterile PBS and added to the electroporation cuvette containing the cell suspension, and mixed well by pipetting. The mixture was incubated on ice for 10 minutes. Electroporation was then carried out using a Biorad GenePulser set at 230V, 500 µF, and with a time constant of 6.0. The cuvette was then incubated on ice for 2 minutes and then transferred to a 15ml Falcon tube.

9.2ml of iSTEM media was added to make a total volume of 10ml. 50ul and 25ul of this mixture was then plated onto a 10cm tissue culture plate containing 10ml of iSTEM media each (to make a dilution of 1:200 and 1:400 respectively). After 6 hours, puromycin selection was started by adding puromycin (1ug/ml concentration) to each plate and continued for 48 hours. After 48 hours cells were grown in iSTEM media alone for a further 6 days prior to picking colonies.

Two 96-well plates were prepared with 50ul of feeder layer per well, for each electroporated sample, and each plate was incubated in an incubator. 30ul of trypsin was added to each well of a separate round bottom 96-well plate. Each 10cm tissue culture plate containing the electroporated ES cells was washed twice with 5ml of PBS. Cells were then overlayed with 5ml of PBS prior to picking colonies. Using a microscope, colonies were picked from each plate using a P-20 pipette set to a 10µl volume. Each colony was transferred to each well of the pre-prepared round bottom 96-well plate containing trysin (one colony per well). The presence of cells in each well was then confirmed under the microscope. The round bottom 96-well plate was then incubated in a $CO_2$ incubator for 3 minutes. Trypsin was inactivated by adding 150ul of iSTEM media to each well and mixing by pipetting with a multichannel pipette. The whole cell suspension was then transferred to the pre-prepared 96-well plate containing the feeder layer (total end volume of 230ul per well), and plates were incubated in the tissue culture incubator. The media was changed after 24 hours (200ul of media was used per well thereafter).

### 2.11.7 Assessment of cellular proliferation rate

100,000 cells were plated in duplicate in a 6 well plate for assessment of proliferation at 0, 24, 48, 72, and 96 hours. Cells were cultured in DMEM containing 5% FBS and 1% penicillin/streptomycin. On day 1, 2, 3, 4 and 5 the media was removed and the cells were

washed with sterile PBS. Cells were detached using trypsin and washed with DMEM. The media, PBS, and trypsin containing the detached cells were collected in a 15ml tube and centrifuged at 1000 rpm for 5 minutes. Cells were re-suspended in 500ul of media (1ml of media at 72 and 96 hours). 50ul of this suspension was added to 50ul of trypsin blue in an eppendorf tube, to allow for discrimination between viable and non viable cells. 9ul of this mix was placed in a cell counting slide and cells were counted using an automated cell counter. The number of viable cells were captured at 0, 24, 48, 96 and 72 hours for IDH1, IDH2, D2HGDH knockdown cells and LN18 wild-type cells. Cells transduced with scrambled shRNA were used as a control.

## 2.12 Assessment of $NADP^+$/NADPH

Total intracellular NADPH concentration and $NADP^+$:NADPH ratios were established using a $NADP^+$/NADPH Quantification Kit (BioVision). This kit allows an enzyme cycling reaction to take place, whereby NADP is converted to NADPH. Two samples are processed, one containing both NADPH and NADP i.e. total NADP (NADPt) and one containing only NADPH (as the NADP has been decomposed). By comparing the amount of NADPH in the NADPt sample to the NADPH only sample, the amount of NADP in the sample can be established, as can the NADP:NADPH ratio.

NADP Cycling Enzyme Mix, NADP Cycling Buffer, NADPH developer and NADPH standard were reconstituted as per manufacturer's instruction.

Cell samples were prepared as follows:

24 hours prior to the assay, 1 x $10^5$ cells were plated in a tissue culture dish with DMEM, and left in the tissue culture incubator overnight. The following day, cells were detached from tissue culture dishes using trypsin, washed with cold PBS, and placed in an eppendorf, before

being centrifuged at 2000 rpm for 5 minutes to form a pellet. NADP/NADPH was then extracted from cells by adding 200µl of NADP/NADPH Extraction Buffer to the pellet, and homogenising using a mechanical homogeniser. The extract was mixed by vortexing for 10 seconds, and then centrifuged at 14000 rpm for 5 min. The supernatant containing the extracted NADP/NADPH solution was then transferred to a new labelled eppendorf tube.

Tissue samples were prepared as follows

20mg of tissue was washed with cold PBS, and homogenised with 400µl of NADP/NADPH Extraction Buffer in an eppendorf. Samples were then centrifuged at 14000 rpm for 5 min. and the supernatant containing the extracted NADP/NADPH solution was transferred to a new eppendorf.

The NADP/NADPH assay was then performed as follows:

The standard curve mixes were generated by diluting 10µl of the 1nmol/µl NADPH standard with 990µl NADP/NADPH extraction buffer to generate 10pmol/µl standard NADPH. 0, 2, 4, 6, 8 and 10µl of the diluted NADPH standard was added to a labelled 96-well PCR plate to generate 0, 20, 40, 60, 80 and 100 pmol/well standards, and the final volume was made up to 50µl with NADP/NADPH extraction buffer.

In order to detect total NADP/NADPH, 50µl of extracted samples (from cell or tissues) were transferred into the labelled 96-well plate in duplicate.

In order to detect NADPH only, NADP was decomposed from the extract by heating the extract at 60°C for 30 minutes on a heat block , and then cooling them on ice. 50µl of this heated/cooled extract was then transferred to the labelled 96-well plate in duplicate.

100µl of NADP Cycling mix (comprising of 98µl of NADP Cycling Buffer Mix and 2µl of NADP Cycling Enzyme Mix) was added to each well of the 96-well plate containing the

standard curve, total NADP/NADPH, and NADPH mixes outlined above. The plate was incubated at room temperature to allow the conversion of NADP to NADPH in the samples. 10µl of NADPH developer was added to each well, and the reaction was left to develop at room temperature for 1 hour. The plate was then read on a plate reader OD450nm.

Values for NADP and NADPH concentration were then calculated by applying each samples OD450nm reading to the standard curve. NADP/NADPH ratio was calculated using the formula (NADPt - NADPH)÷NADPH.

## 2.13 Assessment of ROS

ROS assays were undertaken using the fluorogenic dye MitoSOX™ Red reagent (Molecular Probes, Invitron Detection Technologies) which functions as a mitochondrial superoxide indicator and detects ROS in the mitochondria of live cells. MitoSOX™ permeates into live cells and is selectively targeted to the mitochondria. Once in the mitochondria, MitoSOX™ is oxidized by superoxide and exhibits red fluorescence. MitoSOX™ Red is readily oxidized by superoxide but not by other ROS, and oxidation of the probe is prevented by superoxide dismutase. The oxidation product becomes highly fluorescent upon binding to nucleic acids.

Typically 300,000 cells were plated out with DMEM culture media for each cell line of interest in triplicate in a 6 well plate, and incubated overnight in the tissue culture incubator in order to reach a confluence of 50-60%. The following day appropriate cells were incubated with hydrogen peroxide ($H_20_2$) at a concentration of either 1mM or 2.5mM for 1 hour. Cells in the third well were not treated with $H_20_2$. The MitoSOX Red superoxide indictor was then prepared shielded from light. 100ug of MitoSOX was dissolved in 26ul of DMSO to make a 5mM stock solution. This was then diluted in 2.6ml of DMEM culture media in order to obtain a working solution of 5uM. This 5uM working solution was then further diluted in

450ul of DMEM to obtain a 0.5uM MitoSOX solution. After 1 hour of incubation with $H_20_2$ the media was removed from both $H_20_2$ treated and untreated cells, and 500ul of the 0.5uM MitoSOX solution was added to each well, and incubated for 20 minutes at 37ºC in the tissue culture incubator protected from light. Cells were then washed twice with 5ml of sterile PBS and detached using 1ml of trypsin and removed in to a falcon tube under sterile conditions and centrifuged at 2000 rpm for 5 minutes. The supernatant was removed and the pellet re-suspended in 500ul of sterile PBS and transferred to a flow cytometry tube. Fluorescence was measured using a DakoCytomation (Beckman Coulter) MoFlo flow cytometer, using an absorption wavelength of 510/580 nm. An appropriate sample, not treated with MitoSOX was used to assess normal cell morphology prior to measurement of fluorescence and the appropriate window used to ensure accurate assessments were made. Flow cytometeric data was then analysed using Summit V.4.3 software (Dako).

## 2.14 UPLC-MS

### 2.14.1 Cell extraction protocol for UPLC-MS

Cells were plated in a 10cm tissue culture dish and grown until 100% confluent. 80% methanol (MeOH) was prepared freshly and cooled on ice. Cell media was aspirated off (but not washed to avoid metabolite loss) and was extracted directly with 80% MeOH as follows: 1 ml of 80% MeOH was dispersed over the cells in the tissue culture dish. The cells were then scraped in the solution and transferred into an eppendorf, and mixed by vortexing for 30 seconds. Samples were then centrifuged at 14,800 rpm for 5 minutes at 4°C. The supernatant was transferred into a clean eppendorf tube and centrifugation repeated at 14,800 rpm for 5 minutes at 4°C. The supernatant was then transferred into a screw-cap total recovery vial (Waters) and transported on dry ice to The Chemistry Research Laboratory, Oxford where it was subjected to UPLC-MS analysis by Dr James Mccullagh and Khalid Al-Qahtani.

### 2.14.2 Tissue extraction protocol for UPLC-MS

Frozen mouse brain tissue samples were pulverised mechanically using a hammer and pestle. The samples were then weighed, and a 6-fold volume of ice-cold 80% MeOH was added to each sample. Each sample was then homogenised using an electric homogeniser. The homogenate was transferred to a pre-chilled eppendorf and centrifuged at 14,800 rpm for 10 minutes at 4 °C. The supernatant was then transferred to a fresh pre-chilled eppendorf and the centrifugation step repeated. The supernatant was transferred to a fresh eppendorf and was then concentrated to dryness in a SpeedVac before being transported on dry ice to The Chemistry Research Laboratory, Oxford, where it was subjected to UPLC-MS analysis by Dr James Mccullagh and Khalid Al-Qahtani.

### 2.14.3 UPLC-MS protocol

UPLC-MS analysis was performed by Dr James Mccullagh and Khalid Al-Qahtani at The Chemistry Research Laboratory, Oxford to study changes in TCA cycle intermediates and their associated metabolite concentrations. This method used a hybrid stationary phase with ACE C18-pentafluorophenyl (PFP) column (2.1 x 250mm) gradient. This provides a unique retention based on hydrophobic and hydrophilic interactions between the stationary phase and the analyte. Under the optimised chromatographic conditions, the two isomers were well separated with isocitrate eluting at ca. 10.20 min followed by the isomer citrate at ca. 9.35 min. Chromatographic separation was performed at 45ºC. The method was linear for TCA intermediates in the range of 1 – 1000µM with a correlation coefficient r2 >0.998.

Typically, a sample injection volume of 5µl was used with partial loop (loop size 20 µl) using needle overfill mode (PLNO). A cone voltage of 60V and a capillary voltage of 3.0kV were

used in negative ionization mode. The dissolving temperature was set to 190°C and the source temperature to 120°C.

Solutions were prepared in deionised $H_20$ purified using a *Millipore* Milli-Q system with a 0.22µm filter on the outlet. TCA cycle intermediates from Sigma-Aldrich (St. Louis, MO, USA) were used for calibration. Stock solutions of TCA cycle intermediates were prepared at 200mM concentration, stored at -20°C, and for calibration further diluted to the appropriate concentrations.

Once thawed, calibrator solutions were used immediately (freeze-thaw cycles were avoided). To 20 µl of calibrator solution in a (1.5mL total recovery auto sampler vials (Waters)), 20 µl of Mobile phase solution were added and mixed by vortex. The solutions with final concentrations as listed below were used to make a calibration curve (5µl injection volume) ***(Table 2-3)***.

**Table 2-3: Concentrations of TCA intermediates calibrators for LC-MS analysis after addition of mobile phase solution**

| **Calibrator ID** | **Concentration [µM]** |
|---|---|
| TCA-7 | 1000 |
| TCA-6 | 500 |
| TCA-5 | 100 |
| TCA-4 | 50 |
| TCA-3 | 10 |
| TCA-2 | 5 |
| TCA-1 | 1 |

Chromatographic data were collected with Waters MassLynx v4.1 software and analysed by Microsoft Excel. Quantification was achieved for each analyte using linear regression analysis of the peak area (Manually integrated from the beginning to the end of the peak) ***(Figure 2-1).***

**Figure 2-1: Calibration curve of some TCA intermediates concentration vs. the peak area.**

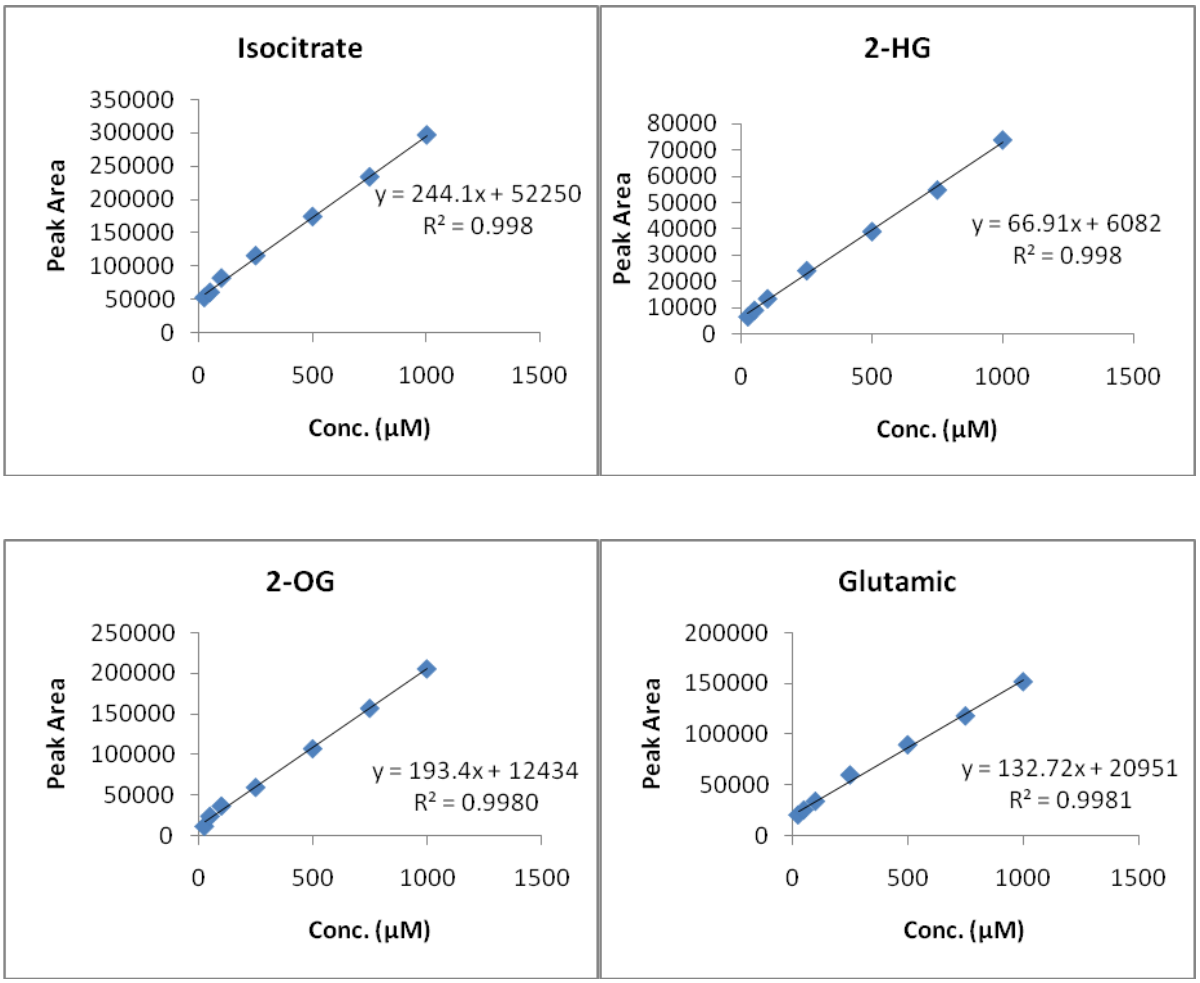


## 2.15 Assessment of 5hmc and 5mC

The levels of 5hmC in most cell lines is very low (Xu W 2011), and consequently it was not possible to measure 5hmC and 5mC levels in LN18 cells as the levels of these DNA bases were not high enough for the sensitivity of the methods used, and therefore could not be detected. 5hmC levels were however measured in Idh1 R132H and Idh2 R172K mutant

murine ES cells and in the brains of Idh1 R132H KI mice and the brains of D2HGDH KO mice.

Levels of 5hmC and 5mC were obtained from hydrolysed DNA using high performance liquid chromatography (HPLC) by Skirmantas Kriaucionis and Pijus Brazauskas at The Ludwig Institute for Cancer Research (LICR), Oxford, using a protocol taken from Quinlivan EP *et al*. (Quinlivan EP 2008).

DNA was extracted from ES cells as outlined in Methods 2.1.2, and from animal tissue as outlined in Methods 2.1.4. Purified DNA (10ug or less) was then incubated with 200U of RNase A/T1 Mix (Thermo Scientific) in 1x NEBuffer2 at 37°C for 2 hours. The DNA was extracted using Phenol:Chloroform:Isoamyl Alcohol 25:24:1 (Sigma) followed by ethanol precipitation according to manufacturer's instructions. In order to quantify the amount of modified bases in the DNA, DNA was then hydrolyzed to single nucleosides. This was achieved using the following mixture of enzymes: 1000 U/mL of Benzonase (Sigma) and 600 mU/ml Phosphodiesterase I (Sigma) to cleave phosphodiester bonds; 80 U/ml of Alkaline Phosphatase (Sigma) to remove residual phosphate groups from nucleotides; 36 μg/ml EHNA hydrochloride (adenosine deaminase inhibitor) to avoid unwanted deamination of the bases; and finally 2.7mM of deferoxamine, a potent iron chelating agent. Digestion was performed in DNA hydrolysis buffer (100mM NaCl, 20 mM MgCl2, 20 mM Tris pH7.9) overnight at 37C. Enzymes were then removed by centrifugation of the mixture through an Amicon ultra-0.5 (3kDa) column. The flow through was lyophilised and resuspended in 50uL of Buffer A (100mM Amonium acetate pH6) and 40uL was injected into an Agilent 1290 infinity series HPLC system. The flow rate was 0.400mL/min and nucleosides were resolved using an Eclipse Plus C18, 2.1x150mm, 1.8μm column (Agilent) at 40°C. Nucleosides were eluted using 1.8% to 30% linear gradient of 40% Acetonitrile. Acquired data was analysed using Agilent 1290 infinity series software.

## 2.16 Mouse Husbandry

Animals were bred in the animal unit at The Wellcome Trust Centre for Human Genetics, Oxford. Experiments were conducted in full accordance with the United Kingdom Animal Procedures Act 1986. All animals were sacrificed under schedule 1 regulations. Any sick animal was reviewed by the resident vet and either treated for its condition or sacrificed and post mortem examination undertaken.

The idh1 R132H KI mice were commercially developed by, and bought from Caliper (Hopkinton, Ma).

The D2HGDH knockout mice were a gift from Dr. Patrick Pollard (Cancer Biology and Metabolism Group, Edinburgh Cancer Research UK Centre, Edinburgh, UK).

Nestin-Cre mice used for crossing were obtained from C. Preece (Cancer Research UK, Clare Hall Laboratories, South Mimms, UK).

Nestin-Cre ERT2, PGK-Cre, GFAP-Cre, and villin-Cre mice were obtained from Wellcome Trust Centre stocks in the animal unit at The Wellcome Trust Centre for Human Genetics, Oxford.

### 2.16.1 Tamoxifen induced expression of inducible-Cre in mice

Working solutions of tamoxifen (10mg/ml) were prepared by dissolving 50mg of tamoxifen (Sigma-Aldrich) in 500ul of 70% ETOH and 4.5 ml of corn oil. This solution was mixed by pipetting, and then incubated at 37ºC for 30 minutes, or until all of the tamoxifen had dissolved. Once in solution the tamoxifen was stored in a light blocking vessel, at 4ºC for the duration of the injections. At 6 weeks post-partum, Cre-expression was induced by injecting

mice with 1mg of tamoxifen (100ul of 10mg/ml mix) intraperitoneally every 24 hours for 5 consecutive days using a 1ml syringe and a 26 gauge needle.

### 2.16.2 Formalin fixation and paraffin embedding of mouse tissue

Tissue was prepared for FFPE as follows:

Tissue was washed with PBS, placed in a plastic moulding cassette and incubated overnight in at least x10 volume of 10% neutral buffered formalin (NBF). The following day the tissue was rinsed with PBS and stored in 70% ETOH at 4ºC for 6 hours.

Prior to embedding, tissue samples were processed on the pre embedding machine overnight whereby they were dehydrated through graded ETOH (70-90-100%) and incubated in wax over a 7 hour period. The following day tissue samples were embedded in wax using an embedding machine. Samples were placed in molten wax, and molten wax was poured in to appropriate moulds. The tissue sample was placed into the mould in an appropriate orientation and the cassette was place over the top and filled with molten wax, without creating bubbles. The cassette and moulds were then place on the cold plate and left to solidify. FFPE samples were then stored at room temperature prior to use.

### 2.16.3 Haematoxylin and eosin (H&E) stain

4um sections mounted on slides were place in a slide rack. Slides were then incubated in xylene for 5 minutes, followed by 3 minutes in 100% ETOH, 90% ETOH and 70% ETOH sequentially. They were then washed in $H_20$.

Slides were then place in a glass trough and incubated in haematoxylin for 45 seconds, and then washed under running $H_20$ until the solution became clear. They were then dipped quickly into acid alcohol and rinsed again in $H_20$, before being incubated in eosin for 3

minutes. Slides were then washed with $H_20$ and dehydrated again through graded alcohols (3 minutes each-70%, 90%, 100%) followed by 2 minutes in xylene.

Cover slips were then mounted onto slides using DPX mounting media (Sigma-aldrich).

### 2.16.4 Histological assessment

H&E stained and unstained slides cut from FFPE brain tissue were examined by a pathologist (O. Ansorge) to determine if any microscopic abnormalities were present in the brain and to determine if any tumour foci were present.

### 2.16.5 Assessment of mouse behaviour using an open field test

The behaviour of *Idh1* mutant mice was assessed using the open field test (OFT). This test is used to measure the exploratory behaviour and response of a mouse to a new environment and allows both the quality and quantity of such activity to be measured. Movement is the most basic outcome of interest, which can be influenced by motor output, exploratory drive, sickness, and freezing or other fear-related behaviour. Distance moved, time spent moving, and rearing, are measures that can be tabulated and reported, whilst some outcomes, such as defaecation, centre time, and activity within the first 5 minutes, can gauge aspects of emotionality including anxiety. A new environment causes mice to move to explore the environment. However, anxiety and fear cause mice to crouch, and freeze. In general, mice that are inactive and defaecate more often in an OFT are assumed to have anxiety and fear, and mice that are active and defecate less are assumed to have less anxiety and fear. Other measures of anxiety used in an OFT include time to stay near walls (thigmotaxis) and stretching. Measures of decreased anxiety are an increased frequency of rearing and grooming.

The open field (OF) used in this study was a rectangular enclosure, marked out inside with 16 square areas, and with surrounding walls to prevent escape. *Idh1* mutant and *Idh1* wild-type mice of a similar age were placed individually into the OF for 5 minutes. The following measurements were made over this time period: number of squares crossed; number of rears made; time spent in the centre square (seconds); number of faecal boli produced; frequency of urination.

### 2.16.6 MRI imaging of mouse brains

To prepare mice for MRI imaging of the brain, they were culled using pentobarbitone and then fixed by intracardial perfusion with 4% paraformaldehyde (PFA). Gadoteridol (Bracco Diagnostics) contrast was added to 4% PFA prior to injection to allow imaging of the brain. Reagents were prepared as follows:

- Gadoteridol/PFA: 1ml of gadoteridol (279.3 mg/ml) was diluted in 9ml of 0.9% saline. 2ml of diluted gadoteridol was then added to 18ml of 4% PFA.
- Heparin/saline (hepsal): 125ul of heparin (25000 IU/ml) was diluted in 500ml of 0.9% saline
- Pentobarbitone: 1ml of pentobarbitone (50mg/ml) was diluted in 2ml of water.
- 1% agarose: 5g of agarose was dissolved in 500ml of 0.9% saline.

An *Idh1* mutant and *Idh1* wild-type mouse were selected of similar age. 300ul of diluted phenobarbitone was injected intraperitoneally in to each mouse. Anaesthesia was confirmed by applying pressure on the mouse's foot and assessing for signs of pain. Once anaesthesia was confirmed, the thorax was opened and the heart located. The right atrium was cut from the vena cava. A 21 gauge butterfly needle was inserted into the left ventricle and 10ml of hepsal was

injected through the butterfly to wash the blood out of the mouse. 20ml of the 4% PFA/contrast mix was then injected to fix the mouse tissues. The head of the mouse was then dissected from the body. The fur and skin were removed from the head and face. The jaw was then removed. The head was then incubated in 4% PFA on ice overnight. A 3cm layer of 1% agarose was added to a 20ml tube and allowed to set on ice. The mutant and wild-type mouse heads were then placed into the agarose face up and in opposite orientations. They were then entirely covered in 1% agarose and this was allowed to set. MRI scanning was then performed by S. Cerres at the CR-UK/MRC Gray Institute for Radiation Oncology and Biology, Department of Oncology, Oxford.

## 2.17 Ethical Approval

All samples and clinico-pathological data were obtained with informed consent and local ethical review board approval in accordance with the tenets of the Declaration of Helsinki. Anonymised patient samples were analysed under the REC reference number 05/Q1605/66.

## 2.18 Solutions

**Citrate buffer stock pH6.0**

210.14g citric acid in 1000ml $H_20$, adjusted to pH6.0 using NaOH pellets.

**Citrate buffer solution**

20ml citrate stock (pH6.0), 1980ml $H_20$

**DAB**

5mg DAB (Sigma), 10ml PBS, 20ul $H_2O_2$

**Ethanol**

70%- 700ml absolute ethanol and 300ml $H_20$

90%- 900ml absolute ethanol and 100ml $H_20$

100%- absolute ethanol

**EDTA 0.5M for 1L**

Na-EDTA 184.1g, pH8.0, autoclave

**Ethidium bromide (10mg/ml)**

0.1g Ethidium bromide dissolved in 10ml $H_20$. Store in dark

**Freeze mix (90% FBS/10% DMSO)**

9ml FBS mixed with 1ml DMSO

**$H_2O_2$ 0.1%**

600ml methanol, 1.8ml $H_2O_2$ (30%)

**$H_2O_2$ 3%**

600ml methanol, 54ml $H_2O_2$ (30%)

**Luria Broth (LB)**

10mg sodium chloride, 5g bacto yeast extract, 10mg bacto-trytone, 900ml $H_2O$, pH7.0 autoclaved

**LB agar plates**

LB media prepared as above, 15g bacto-agar added prior to autoclaving

**Phosphate buffered saline (1x), for 1L**

NaCl 8g (137mM), KCl 0.25g (2.7mM), $Na_2HPO_4$ 1.43g (10mM PO4), $KH_2PO_4$ (0.25g), pH7.4, autoclave

**PBS/2% Tween-20**

998ml PBS, 2ml Tween-20

**Proteinase K buffer**

2mg proteinase K in 1ml $H_20$

**Sodium chloride (5M)**

73.1g NaCl, made up to 250ml with $H_20$, autoclaved

**Sodium dodecyl sulphate (SDS)**

10% volume SDS in sterile $H_20$

**Sodium hydroxide 0.3M**

1.2g NaOH pellets, 100ml $H_20$

**Tail lysis buffer**

50mM Tris/HCL pH8.0, 100mM EDTA, 100mM NaCl, 1% SDS, store at room temperature

**TBE buffer (10x) for 1L**

Tris base 108g, boric acid 55g (0.89M), Na-EDTA 9.3g (0.02M), pH 8.3, autoclave

**Tris 1M for 1L**

Tris base 121.14g, pH as required using HCl, autoclave

# 3. Chapter Three

## Screen for mutations in *IDH*, *D2HGDH*, *L2HGDH*, and *HOT* in GBM

### 3.1 Introduction

Mutations in *IDH1* and *IDH2* have been shown to occur in about 5% of patients with primary glioblastoma, with mutations in *IDH1* occurring more frequently than *IDH2* (Kloosterhof NK 2011). A higher incidence is observed in earlier grade gliomas and secondary glioblastoma (Kloosterhof NK 2011). Whilst it was initially demonstrated that mutations in *IDH1/2* result in a loss of enzyme function, and a consequent reduction in the formation of α-KG (Yan H 2009, Zhao S 2009), subsequent studies offered a conflicting hypothesis by demonstrating that mutant IDH actually possessed novel enzyme function namely the ability to reduce α-KG to D-2HG (Dang L 2009, Gross S 2010, Ward PS 2010). In fact it is also thought that both loss and gain of enzyme function occur as a result of mutations in *IDH1/2* resulting in a simultaneous decrease in α-KG production, and increase in D-2HG formation respectively (Pietrak B 2011). No mutations in *IDH3* had been described in association with brain tumours (The Cancer Genome Atlas Research Network 2008), however if IDH loss-of-function alone is critical for tumourigenesis, one might expect mutations in *IDH3* to also occur in glioma, including those sub-types with relatively low frequencies of *IDH1/2* mutations, as well as in IDH1/2 wild-type tumours. Alternatively, if accumulation of D-2HG alone is critical for tumorigenesis, one might also expect loss of function mutations in *D2HGDH*, whose normal function is to convert D-2HG back to α-KG, to occur independently of mutations in *IDH1/2* in GBM. Additionally, given that one proposed mechanism by which mutant IDH1/2 leads to malignant transformation is by the inhibition of α-KG dependant enzymes by accumulated D-2HG, one might also expect loss of function

mutations in *L2HGDH*, and an accumulation of L-2HG, a more potent inhibitor of α-KG dependant enzymes (Chowdhury R 2011), to occur. A further and more speculative line of reasoning is that, if patients with mutations in *IDH1* and *IDH2* have normal D2HGDH and L2HGDH function, then excess D-2HG or L-2HG should simply be converted back to α-KG by D- or L-2HGDH respectively. The failure of this to occur might be due to saturation of the 2HGDH enzymes, but raises the possibility that patients with mutations in *IDH1/2* might also require inactivating mutations in *D2HGDH* and *L2HGDH* to be present in order for 2-HG to accumulate to a sufficient level.

HOT is another enzyme involved in the metabolism of D-2HG (Achouri Y 2004, Struys EA 2005). Its activity was first demonstrated in studies performed on mitochondrial fraction of rat kidney, liver and brain, which showed that HOT catalysed the conversion of GHB to SSA and resulted in the stoichiometric production of D-2HG from α-KG (Kaufman E 1988, Struys 2006). The existence of HOT activity in humans has since been demonstrated in homogenates of human liver, lymphoblasts and fibroblasts (Struys EA 2005, Struys EA 2005). Mass isotopomer studies, in patients with D-2HGA, have demonstrated that accumulated D-2HG derives from mitochondrial α-KG, and it has been suggested that in addition to inactivating mutations in *D2HGDH* associated with this condition, mutations affecting HOT activity may also be responsible for the excess D-2HG production observed (Kaufman E 1988, Gibson KM 1993, Craigen WJ 1994, Struys EA 2005). Conversely however, enzyme activity assays in fibroblast homogenates from patients with D-2HGA have in fact demonstrated normal HOT activity (Struys EA 2005).

Nevertheless, evidence for the potential ability of increased HOT activity to result in D-2HG accumulation comes from the observation of patients with two other hereditary metabolic disorders; succinic semialdehyde dehydrogenase deficiency (SSADHD) (Struys EA 2006),

and α-KG dehydrogenase deficiency (Kranendijk M 2010), which are associated with an accumulation of GHB and α-KG respectively. In addition to GHB, D-2HG also accumulates in body fluids of patients affected by SSADH deficiency, and it is thought that this secondary increase in D-2HG results from accumulated intracellular GHB driving HOT enzyme activity (Struys EA 2006). Interestingly D-2HG also accumulates in the brain, liver and kidney of SSADH deficient mice, demonstrating a consistent link between SSADH deficiency and increased D-2HG production (Struys EA and Picklo MJ 2006). Similarly, elevated levels of urinary 2-HG are seen in patients with α-KG dehydrogenase deficiency (Kohlschutter A 1982, Al Aqeel A 1994), possibly due to the ability of accumulated α-KG to alter the kinetic equilibrium of HOT (Kranendijk M 2010).

No mutations in *HOT* had been described in association with glioma, however since an increase in HOT enzyme activity could lead to an accumulation of D-2HG, with tumourigenic effects similar to those observed in tumours with mutant *IDH1/2,* and only a minority of GBMs carry mutations in *IDH1/2*, it is feasible that such mutations may occur.

## 3.2 Aims

The aim of this chapter is to screen a panel of human GBM samples for mutations in the following genes:

1: Gain of function mutations in *IDH1* and *IDH2*- in order to confirm the frequency of these mutations in GBM.

2: Gain or loss of function mutations in *IDH3*- in order to investigate if loss of IDH3 function may also play a role in gliomagenesis.

3: Inactivating mutations in *D2HGDH* and *L2HGDH*- in order to establish whether mutations in *D2HGDH* or *L2HGDH* are also responsible for 2-HG accumulation in GBM either independently of, or in conjunction with, mutations in *IDH1*/2.

4: Activating mutations in *HOT*- in order to establish whether mutations in *HOT* occur in GBM carrying WT *IDH1/2*.

## 3.3 Methods

A retrospective study of 47 patients with confirmed primary GBM from The Royal Free Hospital, London was undertaken to determine the frequency of mutations in *IDH1* and *IDH2* in this cohort of patients, and to compare these findings with those documented in the literature. Furthermore the study undertook to determine whether gain or loss of function mutations in *IDH3*, or inactivating mutations in *D2HGDH* and *L2HGDH* were also associated with GBM as no such association has yet been described. Patients who were found to have wild-type *IDH1/2* were then screened for activating mutations in *HOT*. The number of patients chosen for analysis was dictated by the availability of sufficient tissue. All patients were confirmed to have primary GBM by the supporting pathologist.

Formalin-fixed, paraffin-embedded tissue sections (4μm) were obtained from the neuropathology department at The Royal Free Hospital, and histopathology reports were also reviewed. DNA was extracted from paraffin embedded samples as outlined in Methods 2.1.1

Primer sequences were designed to encompass the coding region and splice sites of exon 4 of *IDH1* and *IDH2*, and all exons of *IDH3A* (RefSeq: NM_005530.2), *IDH3B* (RefSeq: NM_174855.1), *IDH3G* (RefSeq: NM_004135.2 for the transcript variant 1 and RefSeq: NM_174869.1 for the transcript variant 2), *L2HGDH* (RefSeq: NM_024884.2), *D2HGDH* (RefSeq: NM_024884.2), and *HOT* (RefGene:NM_144650). Primer sequences for each are illustrated in Appendix 1. A targeted approach was used to identify mutations in *IDH1/2* because mutations at specific locations in these genes have previously been described to occur in GBM. Conversely, all exons of *IDH3A/B/G, L2HGDH, D2HGDH and HOT* were sequenced because no mutations in these genes have yet been described in GBM.

PCR conditions for each primer were set up and tested using DNA extracted from paraffin embedded control samples, and once conditions were optimised, PCR was performed with appropriate primers using DNA extracted from the patient samples as outlined in Methods 2.4. The presence of a PCR product of a size corresponding to the appropriate region of DNA of interest was confirmed by agarose gel electrophoresis with ethidium bromide staining as outlined in Methods 2.5. Clean up of PCR products was then undertaken using ExoSAP-IT® as outlined in Methods 2.4.1, and fluorescent sequencing performed as outlined in Methods 2.6. Sequencing data were then analysed using the ApE plasmid editor programme.

IHC for D2HGDH and L2HGDH was performed on GBM samples from 2 patients carrying wild-type *IDH1/2* and 2 patients carrying mutated *IDH1*, as well as from 2 patients with normal brain tissue, as described in Methods 2.9. Slides were then examined using a conventional light microscope and the level of expression of D2HGDH and L2HGDH (1, 2 or 3) was recorded separately for the nucleus, and cytoplasm according to the intensity in five random high-powered fields per slide. The intensity of staining was compared between tissue from patients with GBM carrying wild-type *IDH1*/*2*, mutant *IDH1* and patients with normal brain tissue. IHC was scored by myself, and re-scored by another laboratory member (C. Bardella) to ensure consistency, all under the guidance of a specialist neurological histopathologist (M. Galloway); any differences were resolved by consensus.

## 3.4 Results

47 patients were screened for mutations in *IDH1*, *IDH2*, *IDH3*, *D2HGDH* and *L2HGDH* (***Table 3-1)***. Heterozygous mutations of *IDH1* were found in 6/47 tumours (12%). All 6 mutations were single base substitutions c.395G>A occurring at residue R132, resulting in an arginine to histidine (p.R132H) substitution ***(Figure 3-1)***. This frequency is consistent with previously described data (Parsons DW 2008, Yan H 2009). No mutations were found in

*IDH2*, in keeping with the lower frequency of such changes that have previously been observed, in comparison to mutations in *IDH1* (Yan H 2009). All of the exons of *IDH3A*, *IDH3B* and *IDH3G* which encode α, β, and γ subunits of the IDH3 heterotetramer were sequenced, and in all cases, no mutations were found. In addition, all of the exons of *D2HGDH* and *L2HGDH* were sequenced and no mutations were found, including the known inactivating mutations that have been described in individuals affected by D-2- or L-2-HGA (Kranendijk M 2010, Steenweg M 2010).

In order to investigate the hypothesis that *D2HGDH* or *L2HGDH* might be inactivated by other mechanisms such as promoter methylation or miRNA over-expression, the expression of the corresponding proteins were evaluated in the panel of GBM samples using IHC ***(Figure 3-2)***. Expression of these enzymes would have been expected to occur in the mitochondria (Achouri Y 2004, Rzem R 2005). Both D2HGDH and L2HGDH were detected in GBMs carrying wild-type *IDH1/2* genes, as well as in IDH1 mutant tumours, demonstrating that *D2HGDH* or *L2HGDH* function was not in fact affected by other mechanisms in these tumours. However this data must be considered as preliminary and would need to be repeated in other patients with GBM in order to increase the sample size, before it can be validated.

Samples from 41 patients with IDH1/2 wild-type tumours were then screened for mutations in the fourteen exons of *HOT*. No somatic mutations were identified in *HOT*, although one previously described missense SNP (GCC->GTC) was identified in exon 1.

**Table 3-1: Patient demographics and results of sequencing analyses for the 47 GBMs studied**

| Patient no. | Age at diagnosis | IDH1 R132 | IDH2 R172 | IDH3A | IDH3B | IDH3G | L2HGDH | D2HGDH | HOT |
|---|---|---|---|---|---|---|---|---|---|
| 1 | 60 | wt | wt | wt | wt | wt | wt | wt | wt |
| 2 | 57 | mutated | wt | wt | wt | wt | wt | wt | N/A |
| 3 | 54 | wt | wt | wt | wt | wt | wt | wt | wt |
| 4 | 49 | wt | wt | wt | wt | wt | wt | wt | wt |
| 5 | 58 | wt | wt | wt | wt | wt | wt | wt | wt |
| 6 | 62 | wt | wt | wt | wt | wt | wt | wt | wt |
| 7 | 55 | wt | wt | wt | wt | wt | wt | wt | wt |
| 8 | 54 | mutated | wt | wt | wt | wt | wt | wt | N/A |
| 9 | 47 | wt | wt | wt | wt | wt | wt | wt | wt |
| 10 | 60 | wt | wt | wt | wt | wt | wt | wt | wt |
| 11 | 51 | wt | wt | wt | wt | wt | wt | wt | wt |
| 12 | 45 | wt | wt | wt | wt | wt | wt | wt | wt |
| 13 | 54 | wt | wt | wt | wt | wt | wt | wt | wt |
| 14 | 50 | wt | wt | wt | wt | wt | wt | wt | wt |
| 15 | 64 | wt | wt | wt | wt | wt | wt | wt | wt |
| 16 | 42 | wt | wt | wt | wt | wt | wt | wt | wt |
| 17 | 45 | mutated | wt | wt | wt | wt | wt | wt | N/A |
| 18 | 59 | wt | wt | wt | wt | wt | wt | wt | wt |
| 20 | 44 | wt | wt | wt | wt | wt | wt | wt | wt |
| 21 | 42 | wt | wt | wt | wt | wt | wt | wt | wt |
| 22 | 62 | mutated | wt | wt | wt | wt | wt | wt | N/A |
| 23 | 47 | wt | wt | wt | wt | wt | wt | wt | wt |
| 24 | 57 | wt | wt | wt | wt | wt | wt | wt | wt |
| 25 | 53 | wt | wt | wt | wt | wt | wt | wt | wt |
| 26 | 56 | wt | wt | wt | wt | wt | wt | wt | wt |
| 27 | 61 | mutated | wt | wt | wt | wt | wt | wt | N/A |
| 28 | 63 | wt | wt | wt | wt | wt | wt | wt | wt |
| 29 | 49 | wt | wt | wt | wt | wt | wt | wt | wt |
| 30 | 52 | wt | wt | wt | wt | wt | wt | wt | wt |
| 31 | 56 | wt | wt | wt | wt | wt | wt | wt | wt |
| 32 | 53 | wt | wt | wt | wt | wt | wt | wt | wt |
| 33 | 60 | wt | wt | wt | wt | wt | wt | wt | wt |
| 34 | 46 | wt | wt | wt | wt | wt | wt | wt | wt |
| 35 | 54 | wt | wt | wt | wt | wt | wt | wt | wt |
| 36 | 60 | wt | wt | wt | wt | wt | wt | wt | wt |
| 37 | 52 | wt | wt | wt | wt | wt | wt | wt | wt |
| 38 | 54 | wt | wt | wt | wt | wt | wt | wt | wt |
| 39 | 66 | wt | wt | wt | wt | wt | wt | wt | wt |
| 40 | 51 | wt | wt | wt | wt | wt | wt | wt | wt |
| 41 | 64 | wt | wt | wt | wt | wt | wt | wt | wt |
| 42 | 44 | wt | wt | wt | wt | wt | wt | wt | wt |
| 43 | 61 | mutated | wt | wt | wt | wt | wt | wt | N/A |
| 44 | 62 | mutated | wt | wt | wt | wt | wt | wt | N/A |
| 45 | 49 | wt | wt | wt | wt | wt | wt | wt | wt |
| 46 | 55 | wt | wt | wt | wt | wt | wt | wt | wt |
| 47 | 68 | wt | wt | wt | wt | wt | wt | wt | wt |

**Figure 3-1: Identification of the G395A mutation at codon 132 by sequencing analysis of the *IDH1* gene.**

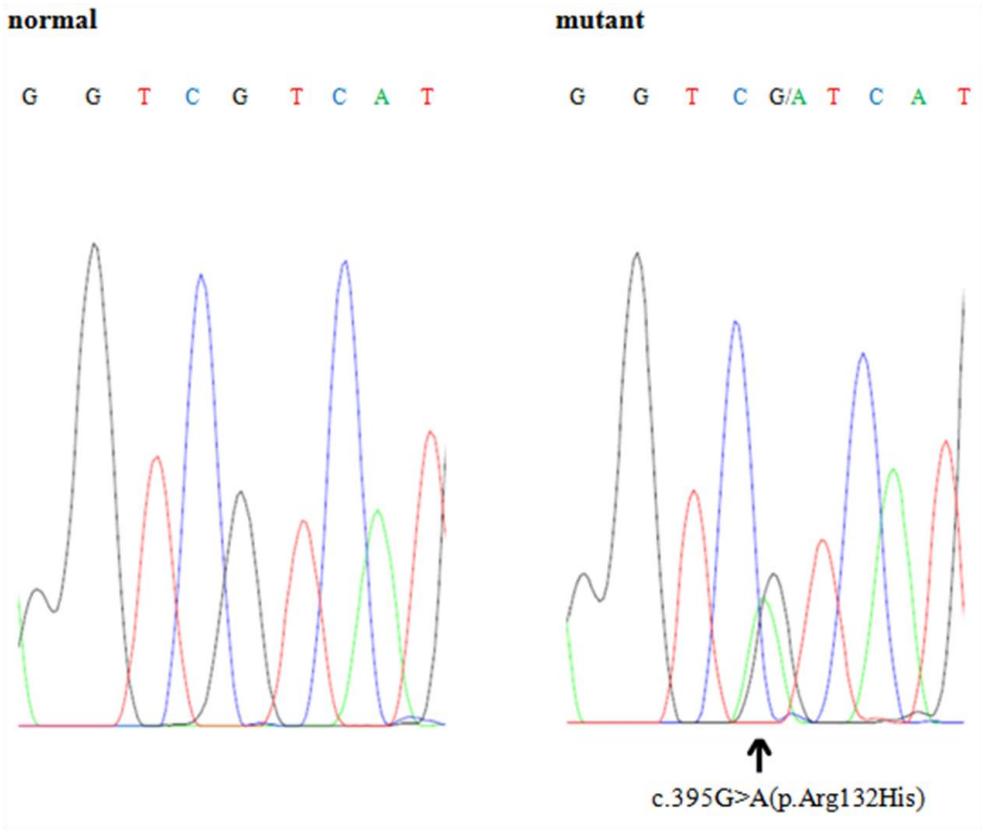


The electropherogram shows a representative example of the heterozygous, single base G-to-A substitution at nucleotide position 395 of the *IDH1* gene (right panel) and the corresponding wild-type sequence (left panel). The mutation was detected in 6 out of 47 GBMs analyzed.

**Figure 3-2: D2HGDH and L2HGDH are expressed in wildtype *IDH1/2* and *IDH1* R132H glioblastomas.**

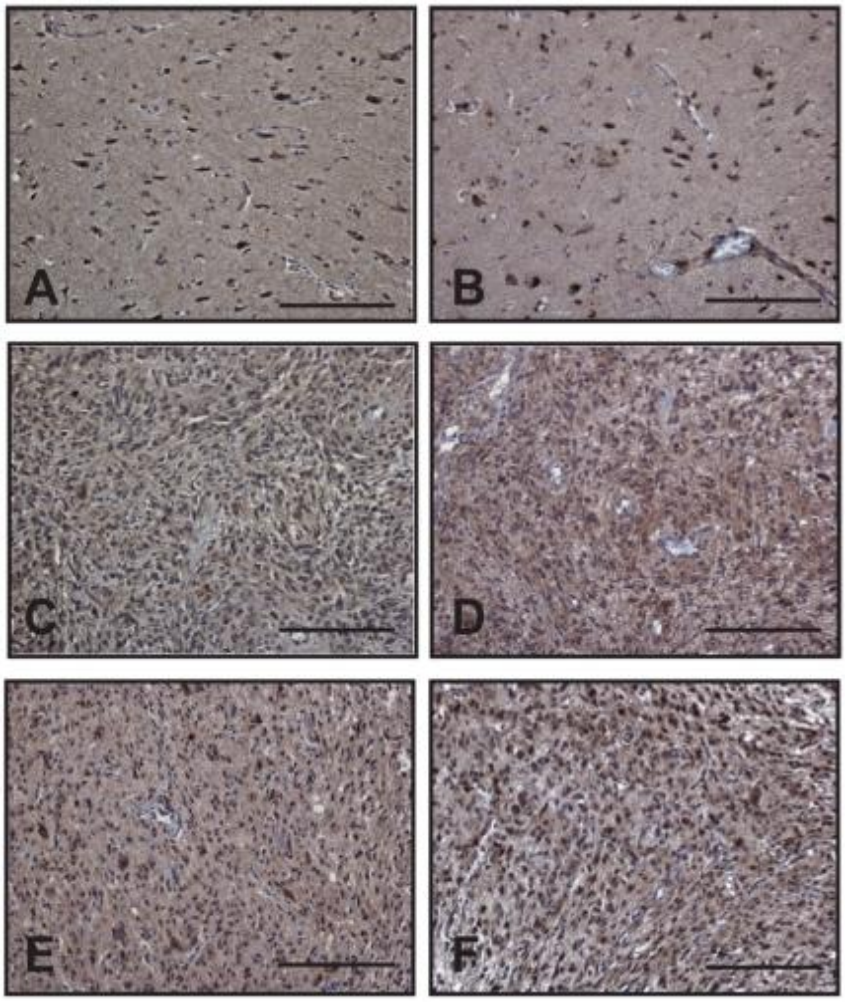


Expression of D2HGDH and L2HGDH in normal brain from 2 separate patients is shown respectively in panels A and B. D2HGDH and L2HGDH were detected in GBM samples from 2 separate patients carrying either wild-type *IDH1/IDH2* (C and D) or mutated *IDH1* allele (E and F) by IHC. Scale bar represents 50 µm in all panels. This data is preliminary and requires validation by repeating IHC analysis on a greater number of patients.

## 3.5 Discussion and Conclusions

The frequency of IDH1 mutations in 12% of primary GBMs observed in this sequencing analysis is consistent with that described in the literature, and confirms the association between mutant IDH1 and primary GBM. It also suggests that the sequencing techniques used to detect mutant IDH1 in this analysis were appropriate. Mutations in *IDH2* are known to occur frequently in AML (Mardis ER 2009), but are less commonly seen in glioma (Yan H 2009), and therefore the absence of mutations in *IDH2* observed in this analysis likely reflects this observation. Consequently, it is possible that mutations in *IDH2* may have been observed if a larger panel of GBM samples had been analysed. Technical errors in the IDH2 sequencing techniques were not responsible for these findings given that DNA bands of the appropriate size were detected on gel electrophoresis of PCR products using these primers, and that the appropriate region of Exon 4 of *IDH2* was seen on sequencing analysis ***(Figure 3-3)***. However if tissue from a GBM patient known to carry mutant IDH2 had been used as a positive control, this would have confirmed that the technique used was optimal.

Mutations in *IDH3, D2HGDH* and *L2HGDH*, or loss of expression of the 2HGDHs do not occur at an appreciable frequency in GBM. One explanation for this is simply that mono-allelic *IDH1* and *IDH2* mutations occur more frequently by chance than the bi-allelic mutations expected at *IDH3*, *D2HGDH* and *L2HGDH*. Alternatively, it is possible that both loss of IDH1/2 function and D-2HG accumulation are required for tumourigenesis, and that only mutations in *IDH1* and *IDH2*, but not *IDH3*, *D2HGDH* or *L2HGDH*, result in these dual effects. It is also possible that D-2HG accumulation is in fact an epiphenomenon, and it is a reduction in α-KG that truly promotes tumourigenesis, whilst IDH3 loss-of-function does not lead to a sufficient deficiency of the latter metabolite to achieve this.

**Figure 3-3: Exon 4 of the IDH2 gene and electropherogram showing the wild-type sequence at nucleotide position 515.**

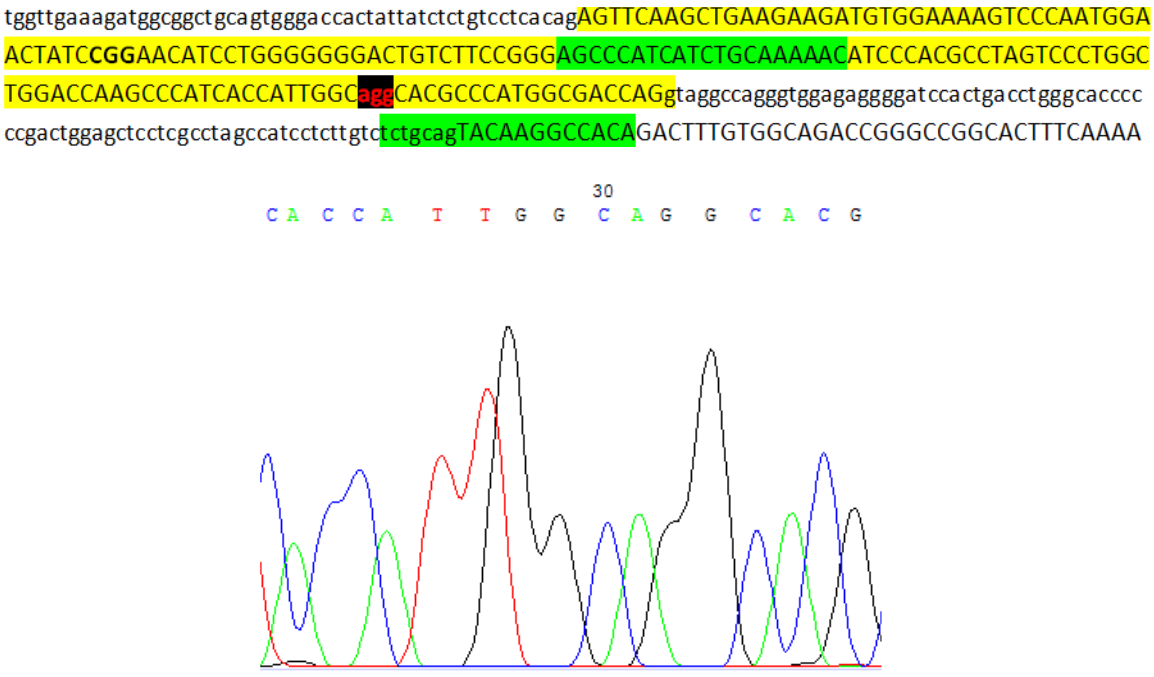


The top diagram shows exon 4 of IDH2 at the nucleotide level (yellow). The common site of mutation in *IDH2* at nucleotide position 515 (red), and the primer sequences used to sequence exon 4 are shown (green). The lower diagram shows an example of the electropherogram obtained by sequencing of exon 4 with these primers and includes nucleotide position 515 (AGG)

This theory is supported by the fact that the complete loss of IDH3 function, resulting from homozygous mutations in IDH3C, that is seen in patients with retinitis pigmentosa, causes detrimental effects limited only to the eye (Hartong D 2008), possibly because the TCA cycle is able to bypass IDH3, by using IDH2, and is a feasible explanation given the significant difference in structure and metabolic and biochemical function of IDH3 compared to IDH1 and IDH2. The theory that D-2HG accumulation is in fact an epiphenomenon would also explain why inactivating mutations in *D2HGDH* and *L2HGDH* are also not seen in glioma, and may explain why brain tumours are not observed in patients with hereditary D-2HGA (Kranendijk M 2012), despite the accumulation of D-2HG associated with this condition (Struys EA 2005), and may also explain why, despite the fact that D-2HG is a significantly

weaker inhibitor of α-KG-dependent enzymes than L-2HG (Chowdhury R 2011), there is only a relatively subtle link between brain tumours and L-2HGA (Struys 2006).

Alternatively, there might be another mechanism of tumourigenesis unrelated to D-2HG accumulation or α-KG deficiency, such as an alteration in glucose or glutamate metabolism, or an increased susceptibility to oxidative DNA damage, that is specific to defects in IDH1 or IDH2. Finally, in view of the fact that mutations in *IDH1* and *IDH2* do not occur in conjunction with mutations in *D2HGDH*, it is reasonable to conclude that the excess D-2HG produced by mutant IDH is not converted back to α-KG by D2HGDH due to the saturation of the latter enzyme, rather than as a result of its defective function. In fact, given that IDH1 R132H has an estimated catalytic rate ($K_{cat}$) of $1.0 \times 10^3$ $sec^{-1}$ (Dang L 2009), but D2HGDH has an estimated $K_{cat}$ of 0.8 $sec^{-1}$ (Engqvist M 2009) it seems likely that the activity of the former enzyme can simply overwhelm the capacity of the latter.

Mutations in *HOT* do not occur at an appreciable frequency in GBM carrying wild-type *IDH1/2*. The fact that mutations in *IDH1/2* occur more frequently in grade II and grade III glioma than in GBM raises the possibility that mutations in *HOT* may also be identified in earlier grade tumours than those included in this study. It is also possible that HOT activity may be increased by other mechanisms not investigated in this study such as increased *HOT* gene copy number. Alternatively this data may serve to support the hypothesis discussed above, that D-2HG accumulation alone is not sufficient to promote tumourigenesis, and illustrates the need for further analysis of the pathogenic role of D-2HG and indeed α-KG in IDH1/2 mutant tumours.

I recognise that this study has its limitations. Firstly a greater number of patients could have been analysed to give the results of the study more significance, but I was limited by the availability of tissue samples. Secondly, the Sanger sequencing technique used in this study is

known to be less sensitive in detecting mutations than novel "next-generation sequencing" techniques (Tsiatis A 2010, Querings S 2011). However at the start of this study such novel techniques were only recently emerging as a realistic tool in this setting, and would have proven too expensive to perform in the context of this study. A lack of sensitivity of the technique used could have resulted in both false positive and false negative results in regards to mutational analysis. In order to overcome this, I could have validated the mutations that I found by repeating the sequencing multiple times to assess if findings were reproducible, or alternatively by using recognised validation techniques. Furthermore, as discussed above I could have increased the study sample size.

It is also important to mention that in addition to testing for mutations in *D/LDHGDH* and *HOT* in GBM samples it would also have been important to assess other parameters of *D/LDHGDH* and *HOT* expression such as mRNA and protein levels, specifically in *IDH1/2* mutant GBM samples, using techniques such as qRT-PCR and western blotting. Hypothetically, one might expect to see an increase in the expression of *D/L2HGDH* in *IDH1/2* mutant glioma, in an attempt to counteract the increase in D2HG produced by mutant IDH. One might also expect to see an increase in the expression of *HOT* in *IDH1/2* mutant glioma, given that the HOT reaction is reversible and hence as well as producing 2HG in its forward reaction, HOT can also metabolise D2HG in its reverse reaction (Kaufman E 1988).

# 4. Chapter Four

## Generation of cell models of mutant IDH

### 4.1 Introduction

Point mutations occurring at the active site of IDH1 and IDH2 have been reported in glioma (Parsons DW 2008, Yan H 2009) and several other cancers (Mardis ER 2009, Amary MF 2011a, Borger DR 2012, Cairns RA 2012). These mutations cause both loss of normal enzyme function and gain-of-function, resulting in the accumulation of D-2HG (Dang L 2009). D-2HG is widely thought to act as an oncometabolite through the inhibition of α-KG dependent enzymes. However, the exact pathogenic role of mutant IDH1/2 remains uncertain and it is also feasible that a reduction in cellular α-KG levels, due to loss of enzyme function, may result in malignant transformation, perhaps through its own effects on α-KG dependent enzymes. In fact, it is possible that both D-2HG accumulation and reduced α-KG production can inhibit different specific α-KG dependent enzymes, and also that specific α-KG dependent enzymes are inhibited by different concentrations of these metabolites.

Indeed, although most tumour-associated mutations in *IDH1/2* result in D-2HG production, a few rare but recurring mutations in *IDH1/2*, namely: IDH1 A134D, IDH2 F394I, and IDH2 F394V, have been identified in lymphoma and thyroid tumours that do not result in D-2HG accumulation, but do display loss of IDH1/2 enzyme function (Ward PS 2012). It remains to be determined whether the loss-of-function mutations in *IDH1/2* seen in these lymphoid and thyroid tumours are driver mutations or simply passenger mutations, but these findings may support the theory that reduced catalytic activity of IDH1/2 in IDH1/2 mutant cells could be tumourigenic. Additionally, it is also possible that other mechanisms, unrelated to α-KG dependent enzymes, such as TCA cycle dysfunction and increased oxidative stress may also play a role.

The purpose of the work illustrated in this chapter is to investigate which tumourigenic mechanisms are responsible for the development of IDH1/2 mutant gliomas, and to further understand the roles played by D-2HG and α-KG in this process, through the use of cell models of IDH1/2 gain and loss of function.

A major challenge to the study of *IDH1/2* mutations *in vitro* has been the lack of human glioma cell lines that endogenously carry these mutant enzymes. In fact, several groups have reported the inability to propagate patient-derived glioma cell lines containing mutations in *IDH1/2* (Kelly JJ 2010, Piaskowski S 2011). To overcome these difficulties, the development of glioma cell lines which express exogenous mutant IDH1/2 is useful. This can be achieved through the delivery into cells of lentiviral vectors coding for mutant IDH1/2 and by other methods. Indeed, the human derived glioma cell lines U-87MG (Dang L 2009, Xu W 2011) and LN-18 (Dang L 2009), as well as HEK 293T cell lines (Zhao S 2009), have been stably transfected to express mutant IDH1/2 and have been successfully used to study the role of mutant IDH1/2 in gliomagenesis, albeit with some conflicting results (Dang L 2009, Zhao S 2009). Furthermore, human colon cancer derived cell lines (HCT116) (Koivunen P 2012), and mouse fibroblast derived cell lines (3T3-L1)(Lu C 2012) expressing ectopic IDH1/2 mutations have also been developed. Immortalised human astrocytes expressing exogenous mutant IDH1 have also been successfully developed, using lentiviral transfection techniques, to study the effects of mutant IDH1 in glioma (Chesnelong C 2013).

Transducing human GBM derived LN18 cells with a lentiviral vector coding for mutant IDH1/2 may provide a more accurate glioma specific model, because in contrast to U-87MG (Cerrato JA 2001), LN18 carries a p53 mutation and wild-type PTEN (Ishii N 1999), both of which are known to associate with IDH1/2 mutations in GBM (Reitman ZJ 2010). Furthermore, stable expression of R132H mutant IDH1 in LN18 cells has been shown to result in a greater accumulation of 2-HG than in IDH1 mutant expressing U87MG cells

(Dang L 2009). The LN18 cell line was developed over 30 years ago from the tumour of a patient with GBM (Diserens AC 1981), and in addition to mutant p53 and wild type PTEN, it exhibits homozygous deletions in p16 and $p14^{ARF}$ (Ishii N 1999). LN18 cells grow *in vitro* with a doubling time of 72 hours (Diserens AC 1981) and when injected into nude mice they induce tumour formation with morphology comparable to the tumour of origin (Diserens AC 1981). Consequently LN18 cells have been used in both *in vitro* (Combs SE 2007, Zhang R 2008, Dang L 2009, Roy Choudhury S 2011, Hossain M 2012) and *in vivo* studies of GBM (Hlavaty J 2011, Viel T 2013).

Given that mutations in *IDH1/2* are an early event in gliomagenesis, the introduction of mutant IDH1/2 to an established human glioma cell line may have some shortcomings. Hence, it would also be desirable to study the effect of mutant IDH1/2 in the more undifferentiated embryonic stem cells (ES cells). An alternative method would be to use human neural stem cell lines such as those developed by Monni *et al.* (Monni E 2014) which could be transfected with mutant IDH1/2 using lentiviral vectors or other methods. ES cells are pluripotent and can be derived from the inner cell mass of human or mouse blastocysts. They require special conditions to maintain their undifferentiated state in culture, and can be directed toward lineage-specific differentiation by the manipulation of culture conditions (Biswas A 2007). There is little published data on the use of IDH1/2 mutant ES cell models, but ES cells have been used to study the effects of TET inhibition on DNA methylation (Ito S 2010). ES cells provide an attractive model to study the effects of IDH1/2 mutations *in vitro* because mutant IDH1/2 is endogenously expressed in this model. Furthermore because IDH1/2 mutations can be introduced using homologous recombination in this model, only one allele of the *IDH1/2* gene is mutated, which more closely resembles the heterozygous mutations in *IDH1/2* that are observed in IDH1/2 mutant tumours (Parsons DW 2008, Yan H

2009), and this may therefore provide a more accurate model than cell lines in which mutant IDH1/2 is overexpressed.

The generation of IDH1/2 knockdown cell lines is also desirable in order to study the cellular effects of loss of wild-type IDH1/2 function, in case this is in fact a pathogenic mechanism in IDH1/2 mutant tumours. Furthermore, it is also desirable to study the effect of down-modulation of *IDH3* expression in order to better evaluate the biological effects of a reduction in α-KG production. Knockdown of gene expression can be achieved using RNA interference techniques by delivering small interfering RNAs (siRNAs) or short hairpin RNAs (shRNAs) into cells. siRNAs enable efficient gene knockdown and yield a high level of gene silencing with minimal cellular toxicity, however there is an increased probability of incurring off-target effects with this technique (Moore CB 2010). Furthermore siRNA concentrations become diluted as cells divide and hence the generation of long-term cell lines with target gene knockdown is unfeasible (Moore CB 2010). shRNA, on the other hand, can be used to generate stable knockdown cell lines, thereby greatly increasing reproducibility of results, although this technique is more time-consuming (Moore CB 2010). shRNA and siRNA have been previously used to knockdown wild-type IDH1/2 expression in U87MG cells (Zhao S 2009, Xu W 2011) and other glioma cell lines (Reitman ZJ 2011, Kim SY 2013), as well as in non glioma cell lines (Kil IS 2007, Lee SM 2009, Kil IS 2010), but to my knowledge, neither technique has been used to knockdown wild-type IDH1/2 expression in LN18 cells.

Several in vitro models were developed as part of this thesis. LN18 and ES cell lines carrying exogenous, mutant IDH1/2 were developed to study the cellular effects of IDH1/2 mutations, whilst LN18 cells with *IDH1, IDH2* and *IDH3* gene knockdown by shRNA and U87MG cells with *IDH1* and *IDH2* gene knockdown by siRNA were generated to study the effects of IDH1/2/3 loss of function. LN18 cells with D2HGDH and L2HGDH gene knockdown were

also developed as a positive control model, as it was hypothesised that knockdown of 2HGDHs would result in 2-HG accumulation, thus allowing a comparison with IDH1/2 mutant models. These different systems were developed in order to understand if the tumourigenic properties of mutant IDH1/2 can result either solely from the loss of function of the wild-type enzyme or gain of function of the mutant enzyme, or if indeed both gain and loss of enzyme function are required.

The generation and analysis of LN18 cells and ES cells harbouring mutations in *IDH1*/2 using lentiviral transduction or homologous recombination respectively, and the generation and analysis of IDH1 and IDH2 knockdown LN18 cells using siRNA, were already under development (by C.Bardella) as I joined the laboratory, and I became involved in experiments to analyse the cellular effects of these changes. The generation of IDH1, IDH2, IDH3, D2HGDH and L2HGDH knockdown cell lines using shRNA, and their subsequent analysis, was solely my own work.

## 4.2 Aims

To develop cell models of IDH1/2 gain and loss of function, in order to identify the pathogenic mechanisms responsible for the development and progression of IDH1/2 mutant glioma. More specifically the aim was to understand if the tumourigenic properties of mutant IDH1/2 can result either solely from the loss of function of the wild-type enzyme or gain of function of the mutant enzyme, or if indeed both gain and loss of enzyme function are required. I aimed to investigate the effects of IDH gain and loss of function on the following:

1. Cellular 2-HG and α-KG levels
2. TCA cycle function
3. HIF1α expression

4. TET function
5. JHDM function
6. Cellular NADPH and ROS levels
7. Cellular proliferation rate

The cell models developed were:

1. IDH1, IDH2 siRNA down-modulated U87MG cells
2. IDH1, IDH2, IDH3, D2HGDH, D2HGDH/L2HGDH shRNA down-modulated LN18 cells
3. Idh1 R132H and Idh2 R172K transgenic murine ES cells
4. IDH1 WT, IDH1 R132H, IDH1 R132C, IDH2 WT, IDH2 R172K, and IDH2 R172M overexpressing LN18 cells by means of tet off lentiviral transduction.

## 4.3 Methods

### 4.3.1 Cell lines

Wild-type LN18, U87MG and 293T cells were purchased from the American Type Culture Collection (Manassas, VA) and grown described in Methods 2.11.1.

Conditional Idh1 R132H and Idh2 R172K transgenic murine ES cells were obtained from Caliper (Hopkinton, Ma) and grown as outlined in Methods 2.11.1.

### 4.3.2 Generation of knockdown cell lines using shRNA

*IDH1, IDH2, IDH3, D2HGDH* and *L2HGDH* gene knockdown was carried out using RNA interference by means of shRNA as outlined in Methods 2.11.3.2. The most efficient shRNA sequence was established for each gene by transient transfection of LN18 cells with the different shRNA clones, and RNA and protein were extracted 48 and 72 hours after the transfection as outlined in Methods 2.2.1 and 2.10.1 respectively. The knock down efficiency was then verified using qRT-PCR and western blot as outlined in Methods 2.8 and 2.10.4

respectively. The most efficient shRNA clones were selected for lentiviral preparation. Lentiviral Vector stocks were produced by transient transfection of 293T cells, and vectors were used to transduce LN18 cells as outlined in Methods 2.11.3.2. Once generated, knockdown cell lines were passaged 4 times prior to being used for analysis, and aliquots of each cell line were frozen down to ensure stocks were replenished as outlined in Methods 2.11.2. It should be noted that I had not initially planned to establish L2HGDH knockdown cell lines, however following initial analysis of 2-HG levels in D2HGDH knockdown cells by UPLC-MS, which demonstrated no increase in 2-HG levels, I decided to establish cell lines with dual knockdown of *D2HGDH* and *L2HGDH* in an attempt to increase the accumulation of 2-HG. Hence D2HGDH knockdown cell lines were transduced with lentiviral vectors carrying shRNA targeting *L2HGDH*. Producing IDH1, IDH2 and IDH3 knockdown cell lines using LN18 proved difficult given that in order to obtain optimal knockdown of target gene expression, the required concentration of lentiviral vector often proved toxic and it was not possible to maintain cell viability. Consequently lentiviral transduction with shRNA was also attempted for *IDH1*, *IDH2* and *IDH3* gene knockdown using U87MG cells, with the same technique as described above.

### 4.3.3 Generation of IDH1/2 U87MG knockdown cell lines using siRNA

IDH1 and IDH2 U87MG knockdown cell lines were developed using siRNA as outlined in Methods 2.11.14.

RNA was extracted from transfected cells as outlined in Methods 2.2.1, and retrotranscribed as outlined in Methods 2.7. Total protein was extracted from transfected cells as outlined in Methods 2.10.1. Silencing of *IDH1/2* gene expression was confirmed by qRT-PCR and western blot as outlined in Methods 2.8 and 2.10.4 respectively.

### 4.3.4 Generation of IDH1/2 mutant LN18 cell lines

IDH1 and IDH2 mutant LN18 cell lines were generated as outlined in Methods 2.11.5. RNA and protein were extracted from transduced cells as outlined in Methods 2.2.1 and 2.10.1 respectively. RNA was retrotranscribed as outlined in Methods 2.7. The overexpression of wild-type and mutant IDH1 and IDH2 was then confirmed by qRT-PCR and western blot as outlined in Methods 2.8 and 2.10.4 respectively.

### 4.3.5 Generation of Idh1 R132H and Idh2 R172K mutant ES cell lines

Conditional Idh1 R132H and Idh2 R172K mutant murine ES cells were obtained from Caliper and mutant gene expression was induced by homologous recombination, using electroporation with a pCre-Pac plasmid as outlined in Methods 2.11.6. RNA was extracted from ES cells as outlined in Methods 2.2.1 and retrotranscribed as outlined in Methods 2.7. The presence of Idh1 R132H and Idh2 R172K mutant expression was confirmed in respective clones by direct sequencing of cDNA as outlined in Methods 2.6.

### 4.3.6 Analysis of cellular 2-HG and α-KG and other TCA cycle metabolites

Cellular extracts were obtained from IDH1 and IDH2 mutant LN18 and ES cells and from IDH1/2/3 and D2HGDH knockdown cells as outlined in Methods 2.14.1. UPLC-MS analysis was performed as outlined in Methods 2.14.3. Levels of 2-HG and α-KG were provided for each sample in addition to levels of other TCA cycle intermediates namely: citrate, cis-aconitate, isocitrate, succinate, fumarate and malate. Levels of glutamine and glutamate were also measured.

Untransduced LN18 cells and LN18 cells transduced with GFP were used as controls for IDH1/2 mutant LN18 cell experiments.

Parental ES cells were used as controls for IDH1/2 mutant ES cells. Untransduced LN18 cells and LN18 cells transduced with scramble shRNA were used as controls for shRNA knockdown cell lines.

Biological repeats were subsequently analysed to confirm findings.

### 4.3.7 Analysis of HIF expression

Effects of IDH gain and loss of function on HIF expression was established by analysing HIF target gene expression using qRT-PCR and by measuring nuclear and cytosolic HIF1α levels by western blot in IDH mutant and IDH knockdown cell lines.

#### 4.3.7.1 Analysis of HIF target gene expression using qRT-PCR

RNA was extracted from LN18 shRNA knockdown cell lines as outlined in Methods 2.2.1 and retrotranscribed to cDNA as outlined in Methods 2.7. The expression of the HIF target genes *GLUT1*, *VEGF*, and *PGK1* was quantified using qRT-PCR as outlined in Methods 2.8. These genes were chosen as other groups had previously shown their expression to be altered in association with mutant IDH1 (Zhao S 2009, Sasaki M 2012b). Biological repeats were analysed to confirm findings. Both untransduced LN18 cells and LN18 cells transduced with scramble shRNA were used as controls.

RNA was also extracted from IDH1/2 mutant LN18 and ES cells, and HIF target gene expression was established by qRT-PCR as above. Both untransduced LN18 cells and LN18 cells transduced with GFP were used as controls for IDH mutant LN18 cells. Parental ES cells were used as controls for IDH mutant ES cells. Biological repeat experiments were performed for IDH mutant LN18 and ES cells.

#### 4.3.7.2 Analysis of HIF1α expression using western blot

Nuclear and cytosolic protein was extracted from knockdown and mutant cell lines as outlined in Methods 2.10.2. and quantified. Western blot was performed as outlined in Methods 2.10.14 using HIF1α primary antibody, and either actin or lamin as loading controls. Untransduced LN18 cells were used as a control for LN18 knockdown and LN18 mutant cell lines, untransduced U87MG cells were used as a control for U87MG knockdown cells, and parental ES cells were used as a control for mutant ES cells. ImageJ was used to analyse the grey scale of the western blot obtained from LN18 shRNA knockdown cells in order to more accurately quantify the amount of HIF1α protein in each sample.

### 4.3.8 Assessment of TET function

The effect of mutant IDH1/2 on the activity of TET in IDH1/2 mutant ES cells was made through the measurement of 5hmC and 5mC levels as outlined in Methods 2.15. Parental ES cells were used as a control.

### 4.3.9 Assessment of markers of histone methylation

The effect of mutant IDH1/2 on the activity of the JHDMs in IDH1/2 mutant ES cells was made by measuring total and nuclear levels of the methylated histones H3K4me3 and H3K9me2 using western blotting. Total and nulcear protein extraction from ES cells was carried out as outlines in Methods 2.10.2. Western blotting was performed using H3K4me3 and H3K9me2 primary antibodies as outlined in Methods 2.10.14.

### 4.3.10 Assessment of oxidation state and oxidative stress

The effects exerted by mutant IDH1/2 and loss of IDH1/2/3 function on oxidative stress was made through the measurement of $NADP^+$/NADPH and ROS levels as outlined in Methods 2.12 and 2.13 respectively.

Assessment of ROS was made in U87MG siRNA IDH1 and IDH2 knockdown cells, in IDH1, IDH2, IDH3, and D2HGDH shRNA knockdown cells, in Idh1 and Idh2 mutant ES cells, and in IDH1 mutant LN18 cells. Tetracycline-controlled transcriptional activation was used in the latter model using a tet off system, and hence transcription of mutant IDH1 was inactivated by culturing IDH1 mutant LN18 cells in doxycycline.

Assessment of NADP/NADPH was made in IDH1 and IDH2 mutant LN18 and ES cells and in shRNA knockdown LN18 cells.

### 4.3.11 Assessment of cellular proliferation rate

The effects of IDH gain and loss of function on cellular proliferation rate was assessed in IDH1 and IDH2 mutant LN18 cell and in IDH1, IDH2, and IDH3 shRNA knockdown LN18 cells as outlined in Methods 2.11.7.

## 4.4 Results

### 4.4.1 Knockdown of IDH1 and IDH2 expression using siRNA

Transfection of U87MG cells with siRNA directed against IDH1 reduced *IDH1* gene expression by 73%. A small reduction was seen in the corresponding protein level although this reduction appeared less significant than that observed with shRNA knockdown. This may be expected given that siRNA transduction leads to a more transient effect on gene silencing than that of shRNA. Transduction of the same cell line with siRNA directed against IDH2 reduced *IDH2* gene expression by 69%. A moderate reduction was also seen in the corresponding protein level which again appeared less significant than that observed with shRNA knockdown. siRNA directed against IDH2 also resulted in a small reduction in IDH1 gene expression, and vice versa. This suggests a degree of off target effects occurred, however these effects were very small and did not impact on corresponding protein levels ***(Figure 4-1)***.

**Figure 4-1: qRT-PCR and western blots showing the effect of IDH1 and IDH2 siRNA on corresponding gene expression at RNA and protein levels**

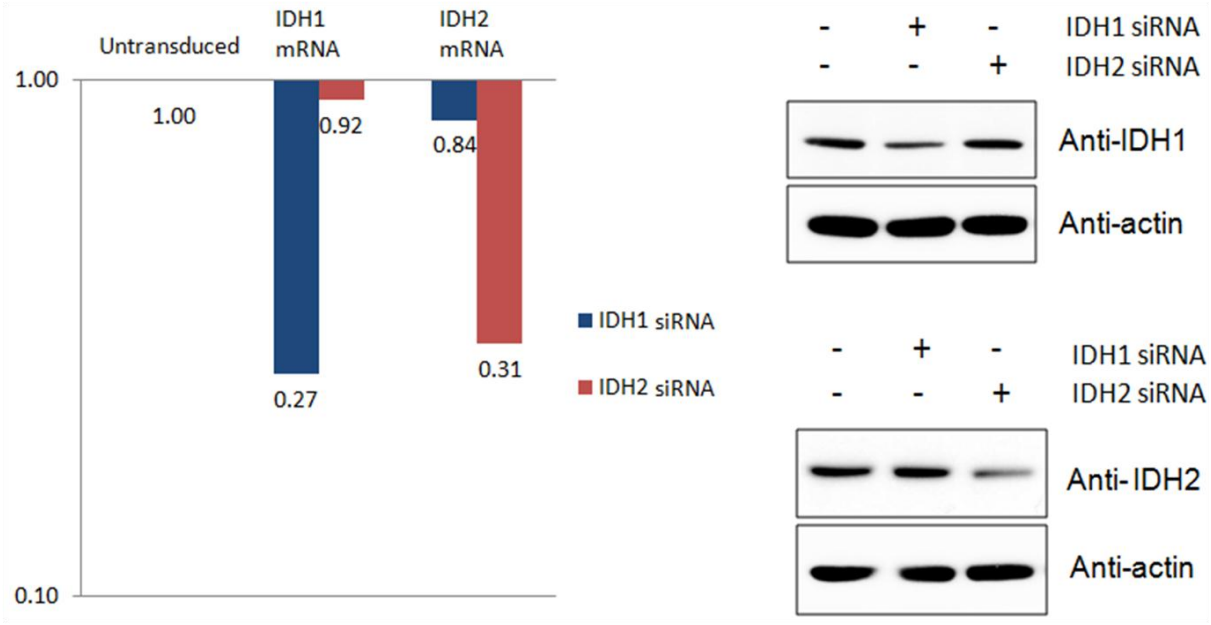

## 4.4.2 Knockdown of IDH and 2HGDH expression using shRNA

### 4.4.2.1 *IDH1* gene knockdown in LN18 cells using shRNA

To establish the most effective shRNA clones, I transiently transfected LN18 cells with 5 different shRNA constructs, and 72 hours after transfection I analysed the down-modulation of gene expression by qRT-PCR. I always applied this method to select the most effective shRNA sequence for each gene that was knocked-down in this study, namely *IDH1*, *IDH2*, *IDH3*, *D2HGDH,* and *L2HGDH*.

The 2 most efficient IDH1 shRNA clones were found to be TRCN0000027289, TRCN0000027298, which demonstrated a 61% and 53% reduction in IDH1 gene expression respectively ***(Figure 4-2)***. These 2 clones were therefore selected for lentiviral preparation. IDH1 shRNA lentiviral vector (LV) stocks were produced by transient transfection of 293T cells, and viral p24 antigen concentration was then measured to determine the concentration of infective viral particles. The titration of infective particles containing IDH1 TRCN0000027289 and TRCN0000027298 shRNA clones was 52.24 ng/ml and 147.6 ng/ml respectively. To achieve a stable transduction, I initially transduced LN18 cells (150,000 cells) with 100ng of LV containing IDH1 TRCN0000027289 shRNA. After 120 hours, no viable cells remained. I therefore repeated the transduction of LN18 cells using serial dilutions of 50ng, 20ng and 10ng of the same LV. Furthermore, I also transduced cells of a different glioma cell line, U87MG, with 100ng, 50ng and 20ng of the same LV. After 7 days, the LN18 cells transduced with 50ng of LV, and the U87MG cells transduced with 100ng, 50ng and 20ng of LV were not viable. Furthermore western blot analysis showed no reduction in IDH1 protein, in cellular protein extracts from LN18 cells transduced with 20ng or 10ng of LV. In an attempt to increase the concentration of LV used for transduction, whilst maintaining cell viability, 2 further serial stepwise transductions were performed, each of

them consisting of 40ng of LV. Using this method I was able to produce LN18 cells that were viable following transduction with a total of 80ng of LV. This was the maximum achievable concentration that did not lead to cell death. Western blot analysis showed a moderate reduction in IDH1 protein in cellular protein extracts from cells transduced with 80ng of this LV, and qRT-PCR analysis demonstrated a 53% reduction in IDH1 gene expression. I felt however that this reduction could be improved upon. I therefore repeated the transduction of LN18 cells using the second IDH1 TRCN0000027298 shRNA LV using serial dilutions of 20ng, 40ng and 80ng of vector. Cells transduced with 80ng of TRCN0000027298 shRNA LV remained viable and qRT-PCR analysis demonstrated an 87% reduction in *IDH1* gene expression ***(Figure 4-3)***. Furthermore, western blot analysis showed a significant reduction in IDH1 protein from cellular protein extracts. Consequently I used LN18 cells transduced with 80ng of IDH1 TRCN0000027298 shRNA LV for subsequent experiments.

**Figure 4-2: qRT-PCR analysis showing the reduction in *IDH1* gene expression 72 hours after transient transfection with various shRNA clones directed against *IDH1* compared to an untransfected control (c).**

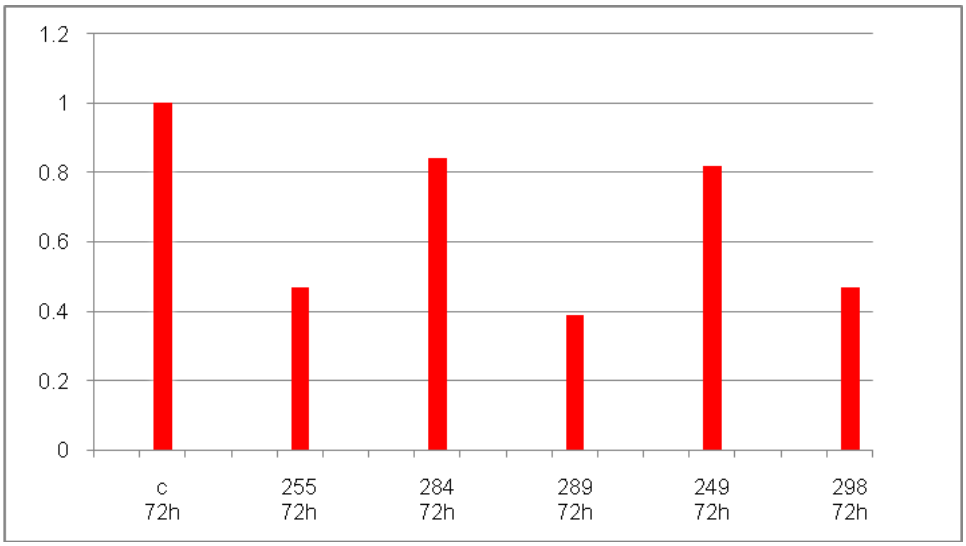

**Figure 4-3: qRT-PCR and western blot analysis showing *IDH1* gene expression at RNA and protein level in LN18 cells transduced with 80ng of IDH1 TRCN0000027298 shRNA lentiviral vector**

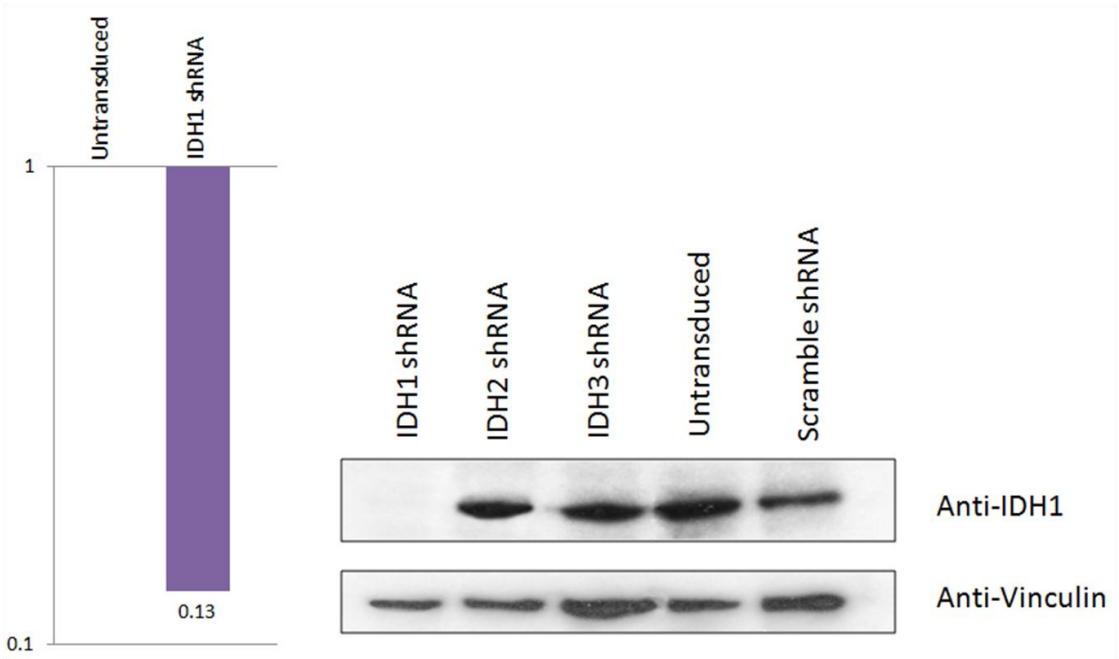


### 4.4.2.2 IDH2 gene knockdown in LN18 cells using shRNA

The 2 most efficient IDH2 shRNA clones were found to be TRCN0000027225 and TRCN0000027296, which demonstrated a 71% and 67% reduction in IDH2 gene expression respectively 72 hours post transfection ***(Figure 4-4)***. These 2 clones were selected for lentiviral preparation, IDH2 shRNA LV stocks were produced, and viral p24 antigen concentration was measured. The titration of infective particles containing IDH2 TRCN0000027225 and TRCN0000027296 shRNA clones was 89.2 ng/ml and 105.8 ng/ml respectively. To achieve a stable knockdown in *IDH2* expression, I initially transduced LN18 cells (150,000 cells) with 100ng of LV containing IDH2 TRCN0000027225 shRNA. However, after 120 hours, no viable cells remained. I repeated the transduction of LN18 cells using serial dilutions with 50ng, 20ng and 10ng of the same LV. Furthermore, I also transduced U87MG cells with 100ng, 50ng and 20ng of the same LV. After 7 days, the LN18 cells transduced with 50ng of LV, and the U87MG cells transduced with 100ng, 50ng and

20ng of LV were not viable. Additionally, western blot analysis failed to demonstrate a marked reduction in IDH2 protein in cellular protein extracts from LN18 cells transduced with 20ng or 10ng of LV. Three further serial stepwise transductions were performed but cells were not able to retain viability with transduction of more than 50ng of LV in total. qRT-PCR and western blot analysis following transduction with 50ng of LV again failed to demonstrate a reduction in *IDH2* gene expression at either protein (no reduction) or RNA (10% reduction) level. Transduction of LN18 cells was therefore repeated using the IDH2 TRCN0000027296 shRNA LV using serial dilutions of 20ng, 40ng and 80ng. Cells transduced with 80ng of this LV were not viable after 120 hours. Following a further stepwise transduction, the maximum concentration that I was able to transduce cells with, whilst still retaining viability, was 50ng. qRT-PCR analysis of cells transduced with 40ng of LV demonstrated a 77% reduction in *IDH2* gene expression ***(Figure 4-5)***, whilst western blot analysis showed a moderate reduction in IDH2 protein in cells, although this was not as marked as the reduction in IDH1 protein seen in IDH1 knockdown cells. Consequently LN18 cells transduced with 40ng of IDH2 TRCN0000027296 shRNA LV were used for subsequent experiments.

**Figure 4-4: qRT-PCR analysis showing the reduction in *IDH2* gene expression 72 hours after transient transfection with various shRNA clones directed against *IDH2* compared to untransfected control (c).**

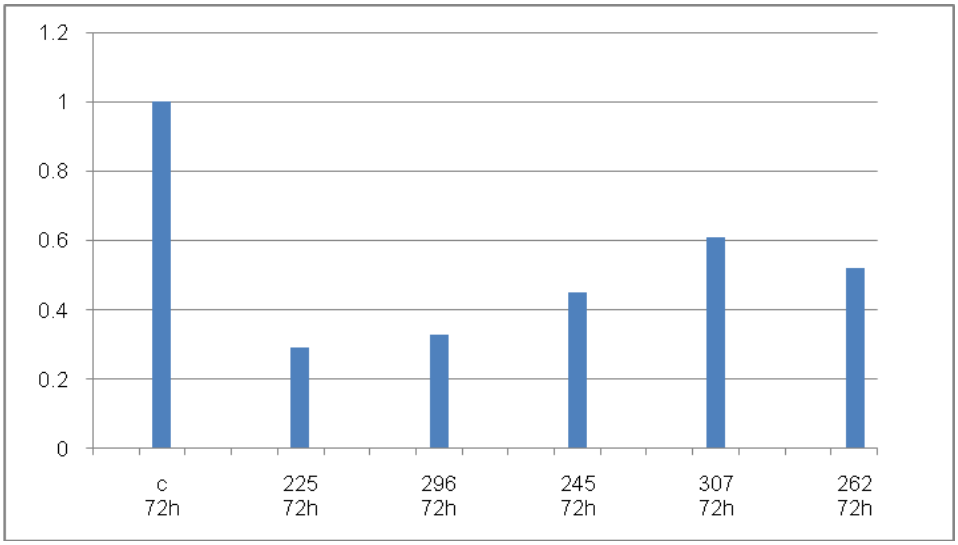

**Figure 4-5: qRT-PCR and western blot analysis showing *IDH2* gene expression at RNA and protein level in LN18 cells transduced with 40ng of IDH2 TRCN0000027296 shRNA lentiviral vector**

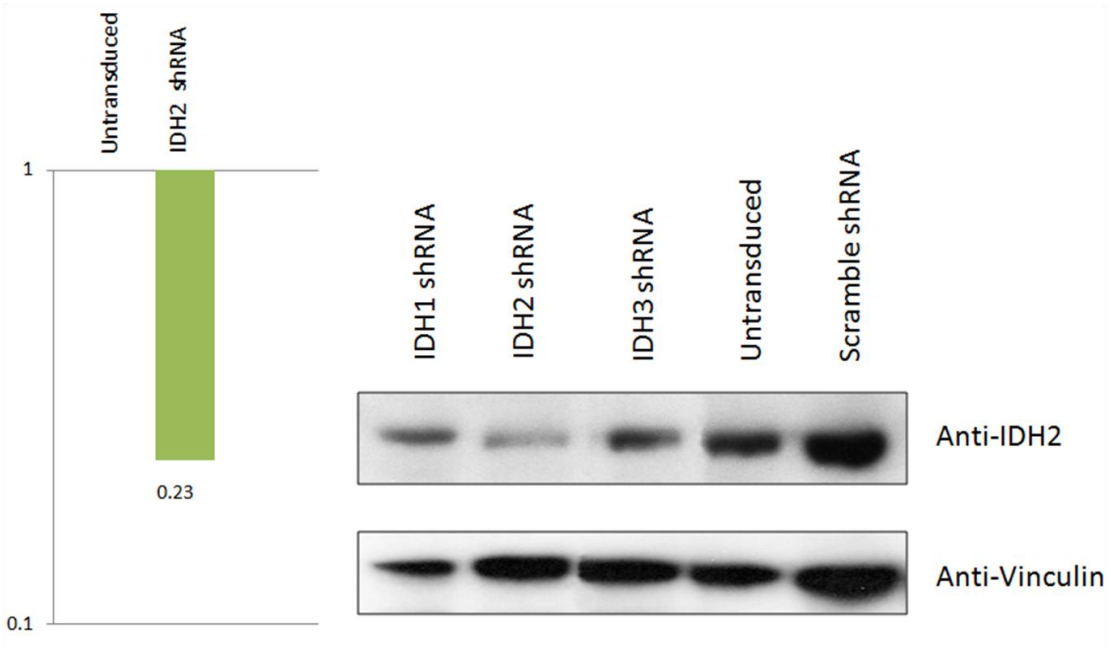


### 4.4.2.3 *IDH3A* gene knockdown in LN18 cells using shRNA

Only 1 of the 4 IDH3A shRNA clones, TRCN0000027310, demonstrated any reduction in *IDH3A* gene expression (21%) 72 hours post transfection, and this was therefore selected for LV preparation ***(Figure 4-6)***. The titration of infective particles containing the IDH3A TRCN0000027310 shRNA clone was 76.8 ng/ml. To achieve stable knockdown of *IDH3A* expression, I initially transduced LN18 cells (150,000 cells) with 100ng of LV containing IDH3A TRCN0000027310 shRNA. However after 120 hours, no viable cells remained. I therefore repeated the transduction with LN18 cells using 50ng of the same LV. Furthermore I also transduced U87MG cells with 100ng, 50ng and 20ng of the same LV. After 7 days, the LN18 cells transduced with 50ng of LV, and the U87MG cells transduced with 100ng, 50ng and 20ng of LV were not viable. I therefore performed 2 serial transduction with LN18 cells using 20ng of LV on each occasion. Cells transduced in this way with a total of 40ng of LV remained viable, and qRT-PCR analysis demonstrated a 68% reduction in *IDH3A* gene expression in these cells, whilst western blot analysis showed a marked and comparable

reduction in IDH3 protein expression ***(Figure 4-7)***. LN18 cell clones transduced with 40ng of IDH3A TRCN0000027310 shRNA LV were therefore used for subsequent experiments.

**Figure 4-6: qRT-PCR analysis showing the effects on *IDH3A* gene expression 72 hours after transient transfection with various shRNA clones directed against *IDH3A* compared to untransfected control (c).**

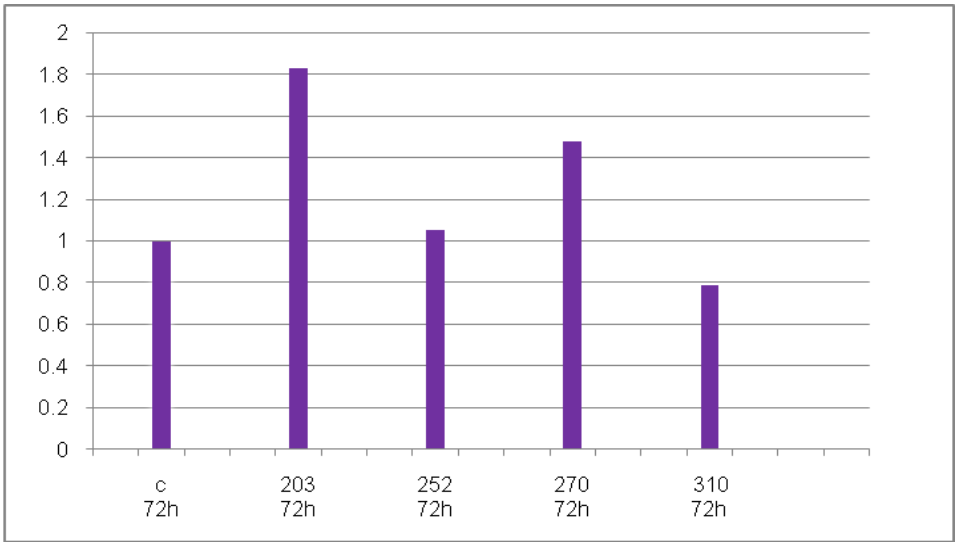


**Figure 4-7: qRT-PCR and western blot analysis showing *IDH3* gene expression at RNA and protein levels in LN18 cells transduced with 40ng of IDH3 TRCN0000027310 shRNA lentiviral vector**

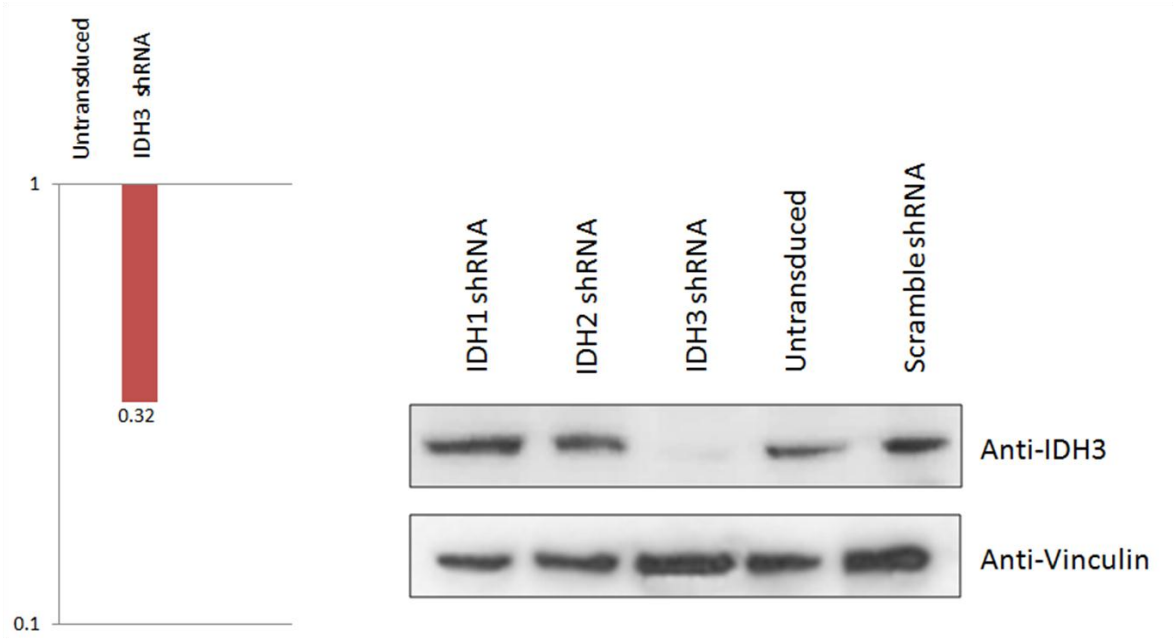

#### 4.4.2.4 *D2HGDH* gene knockdown in LN18 cells using shRNA

The most efficient D2HGDH shRNA clone was TRCN0000064037, which resulted in a 68% reduction in *D2HGDH* gene expression. This clone was therefore selected for lentiviral preparation. The titration of infective particles containing D2HGDH TRCN0000064037 shRNA clone was 134.3 ng/ml. LN18 cells remained viable following transduction with 100ng of this LV and qRT-PCR analysis demonstrated an 82% reduction in *D2HGDH* gene expression. Due to a lack of specificity of the D2HGDH antibody used (Protein Tech), and the presence of multiple non specific bands, I was unable to demonstrate a reduction in D2HGDH protein expression by western blot. I attempted to overcome this problem by loading a smaller amount of protein (30ug instead of 45ug) onto the western blot running gel, by reducing the concentration of the secondary antibody used, and by running the gel for a further 30 minutes in an attempt to separate the bands out further, but this did not result in an improvement. Finally a different primary D2HGDH antibody (Abcam) was used but this too demonstrated a lack of specificity, and the western blot was not interpretable. Again I attempted to improve this by using a lower amount of protein and by varying the concentration of secondary antibody used, but to no avail. Consequently, I was unable to convincingly demonstrate a reduction in *D2HGDH* expression at protein level, although *D2HGDH* expression was significantly reduced at RNA level.

Interestingly the level of IDH2 protein was also found to be reduced in D2HGDH knockdown cells ***(Figure 4-8)***. To verify this finding I analysed the level of *IDH2* gene expression at the RNA level in D2HGDH knockdown cells by qRT-PCR, and demonstrated a 77% reduction in *IDH2* gene expression, confirming the western blot findings. *IDH2* gene expression was however not found to be affected in IDH1 or IDH3 knockdown cell lines or in scramble shRNA controls ***(Figure 4-9)***. The degree of inhibition of *IDH2* gene expression appeared to be dependent on the efficiency of *D2HGDH* gene knockdown, with lower levels of *IDH2*

expression seen with increased efficiency of *D2HGDH* knockdown. Furthermore the reduction in *IDH2* expression was reproduced in cells transduced with a second D2HGDH shRNA clone (TRCN0000064035), whilst the expression of 2 non-IDH related genes, forkhead box protein A3 (*FOXA3)* and Krueppel-like factor 5 (*KLF5),* in these cells were unchanged. As will be discussed in Chapter 5 IDH2 expression was not reduced in D2hgdh knockout mice, suggesting that the tissue effects of D2HGDH knockdown may differ in different models.

**Figure 4-8: Western blot analysis showing *IDH2* gene expression at a protein level in IDH and D2HGDH shRNA knockdown cell lines**

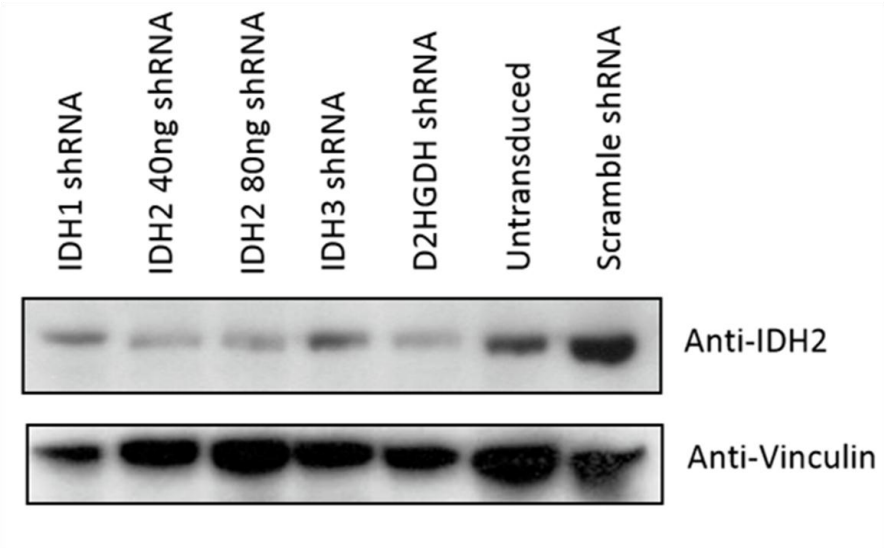

**Figure 4-9: qRT-PCR analysis showing IDH2 gene expression in various shRNA knockdown cell lines**

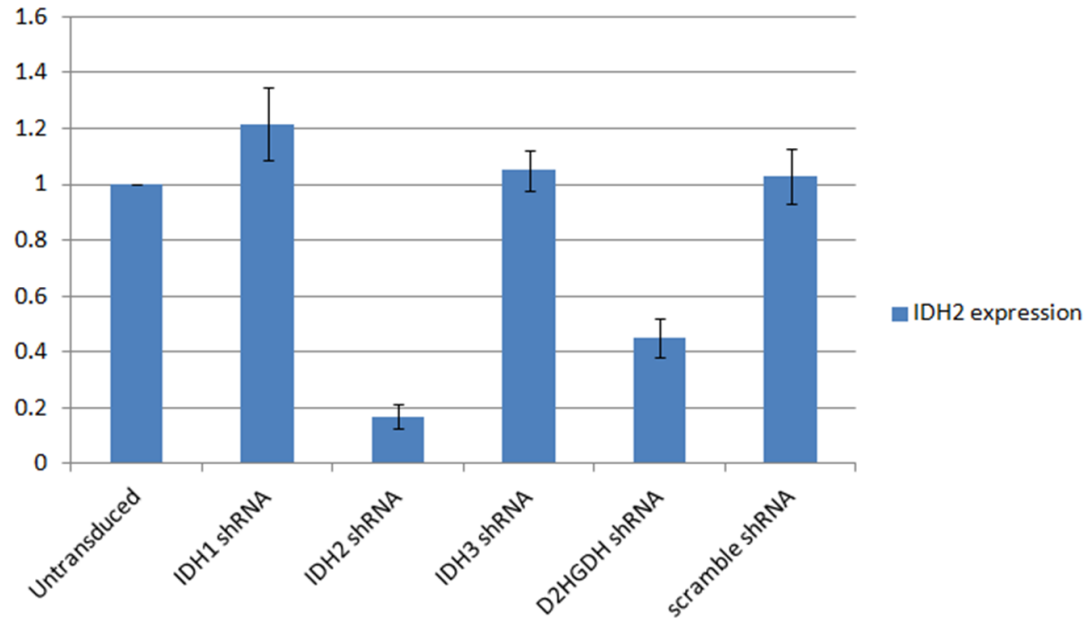


qRT-PCR analysis data from 3 separate experiments. GAPDH used as internal control.

### 4.4.2.5 Dual *D2HGDH*/*L2HGDH* gene knockdown in LN18 cells using shRNA

The most efficient L2HGDH shRNA clones were TRCN0000064323 and TRCN0000064325, and these clones were therefore selected for lentiviral preparation. The titration of infective particles containing the L2HGDH TRCN0000064323 and TRCN0000064325 shRNA clones were 299 ng/ml and 324 ng/ml respectively. Transduction of D2HGDH knockdown cells with 20ng and 50ng of L2HGDH shRNA LV, resulted in a 36% (p=0.0069) and 73% (p=0.0023) reduction in *L2HGDH* gene expression at an RNA level as assessed by qRT-PCR, and cells remained viable. In cells transduced with 20ng of L2HGDH shRNA LV, *D2HGDH* gene knockdown was maintained at a 37% (p=0.0044) reduction. However, interestingly, *D2HGDH* gene knockdown was lost (10% reduction; p=0.079) in cells transduced with 50ng of L2HGDH shRNA LV, in which *L2HGDH* expression was reduced by 73% (p=0.0023) ***(Figure 4-10)***. These findings suggest that cells do not remain viable when both L2HGDH and D2HGDH enzyme function are significantly inhibited, and that in this situation, cells

with reduced D2HGDH function are effectively selected out *in vitro*. However, when both *L2HGDH* and *D2HGDH* expression are inhibited to a lesser extent, enzyme function is maintained and cells remain viable. Consequently, D2HGDH knockdown cells transduced with 20ng of L2HGDH shRNA vector were used as a model of dual *D2HGDH/L2HGDH* knockdown for subsequent experiments, whilst those transduced with 50ng of vector were used as a model of *L2HGDH* knockdown alone.

**Figure 4-10: Expression of D2HGDH and L2HGDH in D2HGDH knockdown cells transduced with either 20ng or 50ng of L2HGDH shRNA lentiviral vector.**

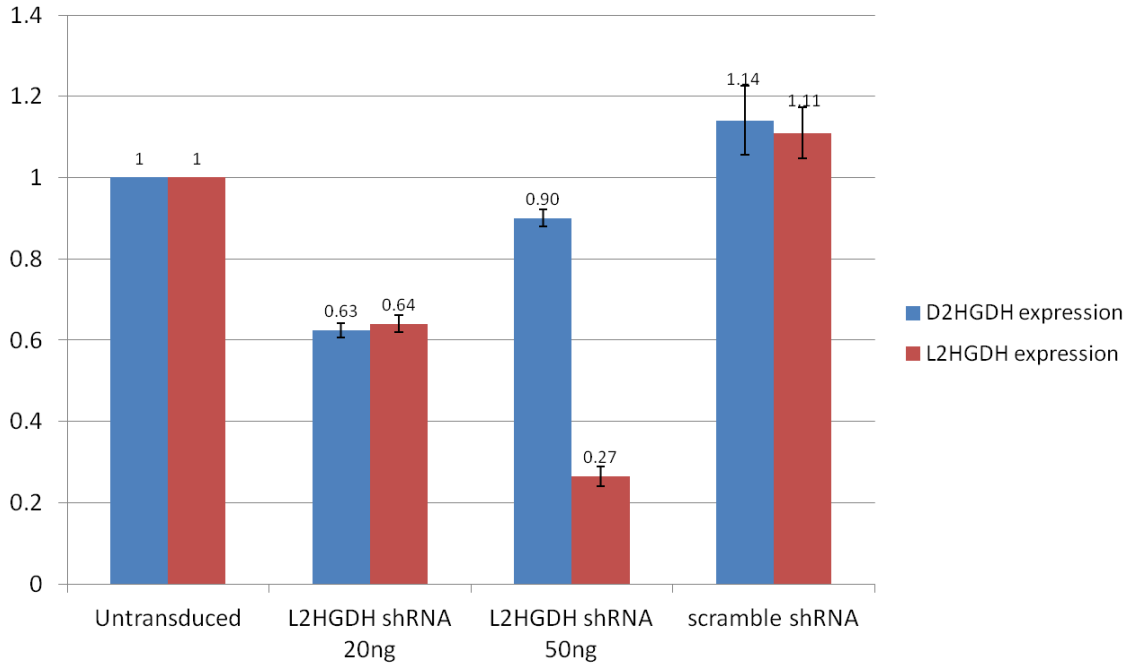


## 4.4.3 Overexpression of wildtype and mutant IDH1 and IDH2 in LN18 cells

The overexpression of wildtype and mutant IDH1 and IDH2 was confirmed by qRT-PCR and western blot in IDH1 and IDH2 mutant LN18 cells ***(Figure 4-11)***. Furthermore, expression was successfully inhibited by doxycycline, demonstrating the tet-off system to be effective. The expression of mutant IDH1 was higher than that of mutant IDH2, and there

was a degree of variation in the level of mutant expression between IDH1 R132H and IDH1 R132C vectors and between IDH2 R172K and IDH2 R172M vectors.

**Figure 4-11: Overexpression of wildtype and mutant IDH1 and IDH2 in LN18 cells by qRT-PCR and western blot.**

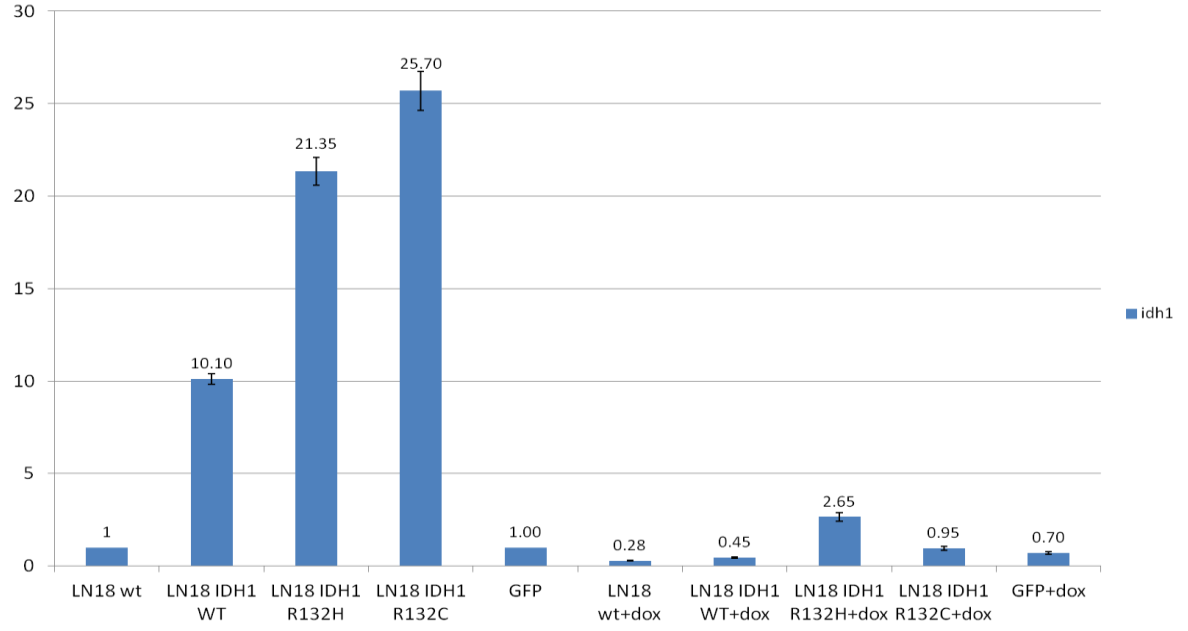


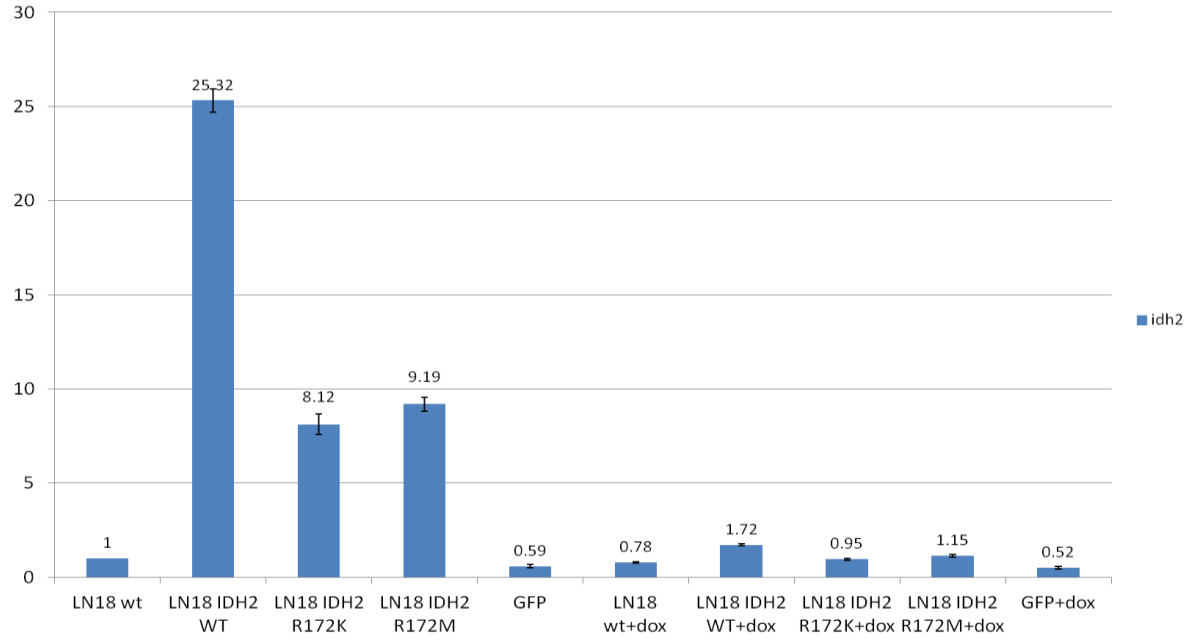


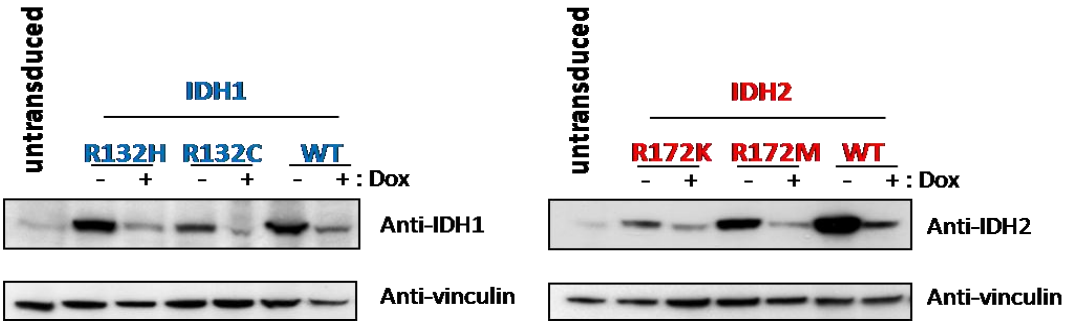

### 4.4.4 Mutant expression of Idh1/2 in ES cells

Mutant expression in Idh1 R132H mutant ES cell clones was confirmed by the detection of an arginine (wild-type) to histidine (mutant) substitution at codon 132 of *Idh1*, whilst wild-type Idh1 expression was observed in corresponding parental cells ***(Figure 4-12)***.

**Figure 4-12: cDNA sequence results showing the substitution CGA to CAT at codon 132 of *Idh1* in Idh1 R132H mutant ES cells (A) and wild-type sequence in Idh1 R132H parental cells (B).**

**(A)**

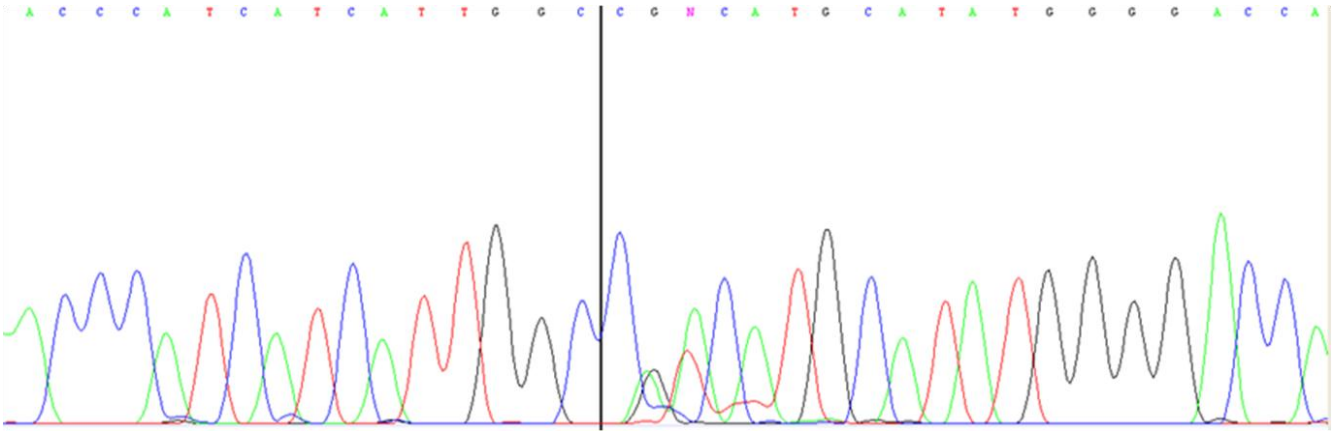

**(B)**

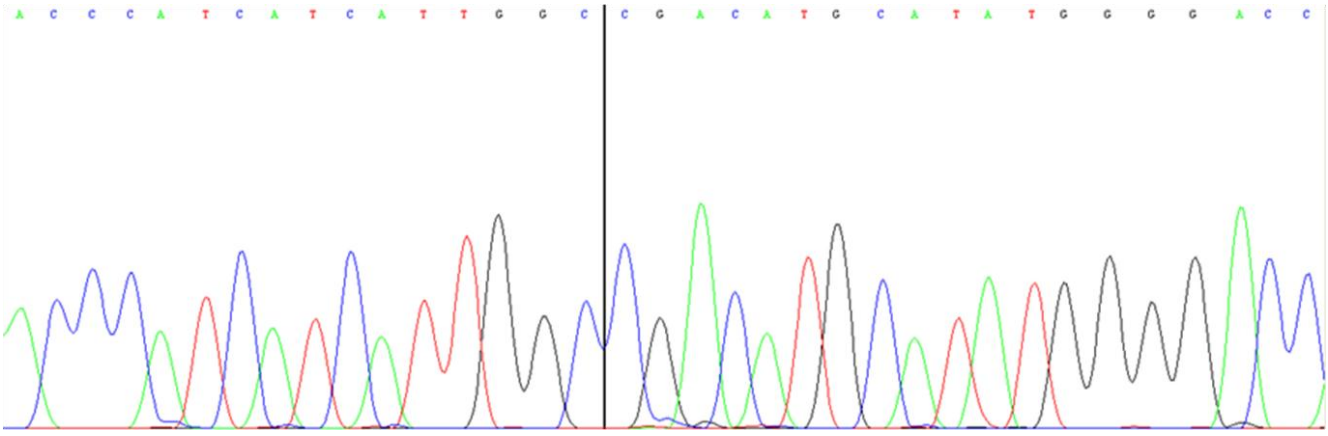

Mutant expression in Idh2 R172K mutant ES cell clones was confirmed by the detection of an arginine (wild-type) to lysine (mutant) substitution at codon 172 of *Idh2*, whilst wild-type Idh2 expression was observed in corresponding parental cells ***(Figure 4-13)***.

**Figure 4-13: cDNA sequence results showing the substitution AGG to AAG at codon 172 of *Idh2* in Idh2 R172K mutant ES cells (A) and wild-type sequence in Idh2 R172K parental cells (B).**

**(A)**

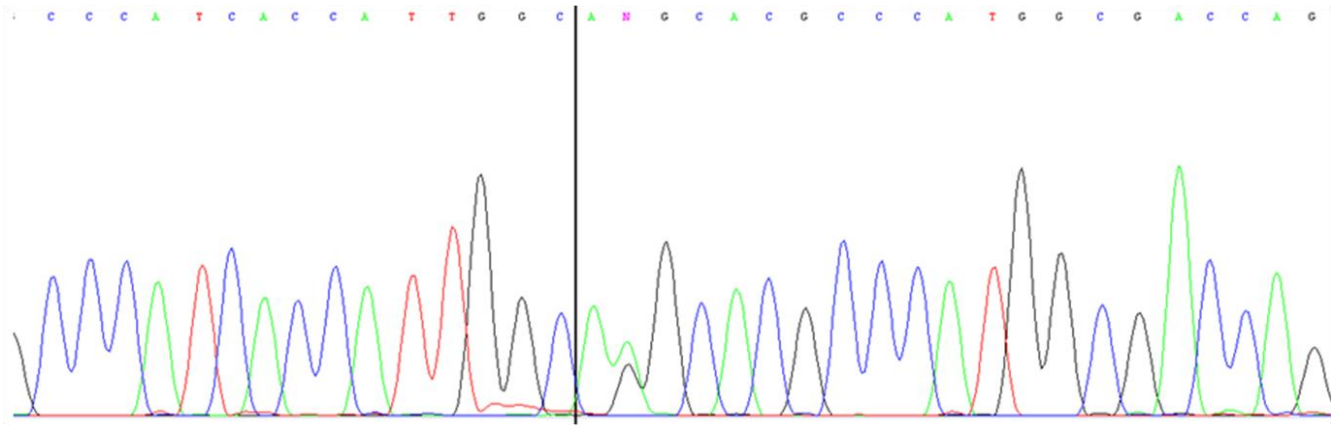

**(B)**

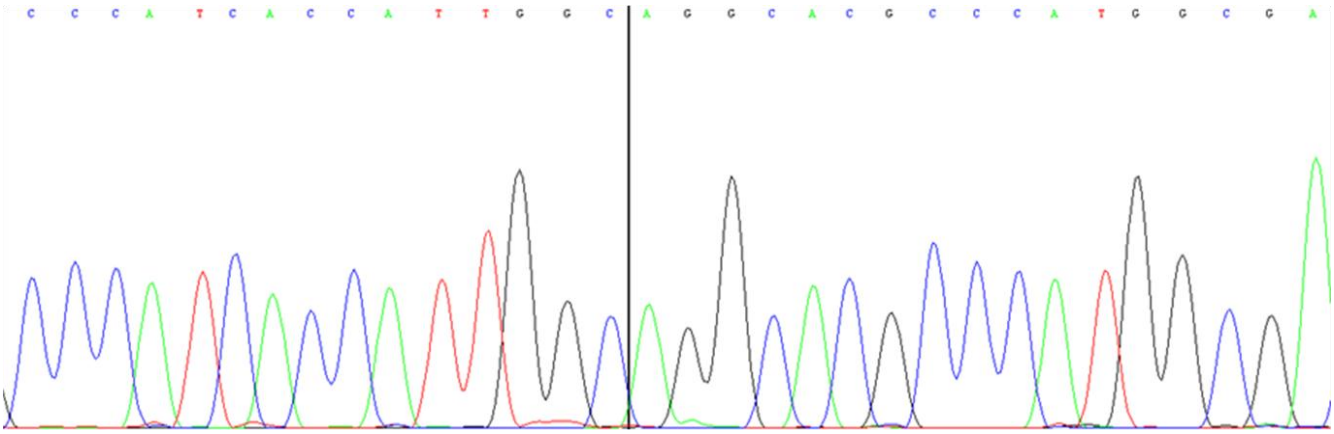

## 4.4.5 Analysis of changes in cellular 2-HG and α-KG and other TCA cycle metabolites

αKG levels were not reduced in IDH1, IDH2 or IDH3 knockdown LN18 cell lines ***(Figure 4-14)***, and levels of the other TCA cycle metabolites analysed were unchanged. Furthermore 2-HG levels were not increased in D2HGDH knockdown LN18 cell lines ***(Figure 4-15)***.

**Figure 4-14: α-KG levels in shRNA knockdown LN18 cell lines**

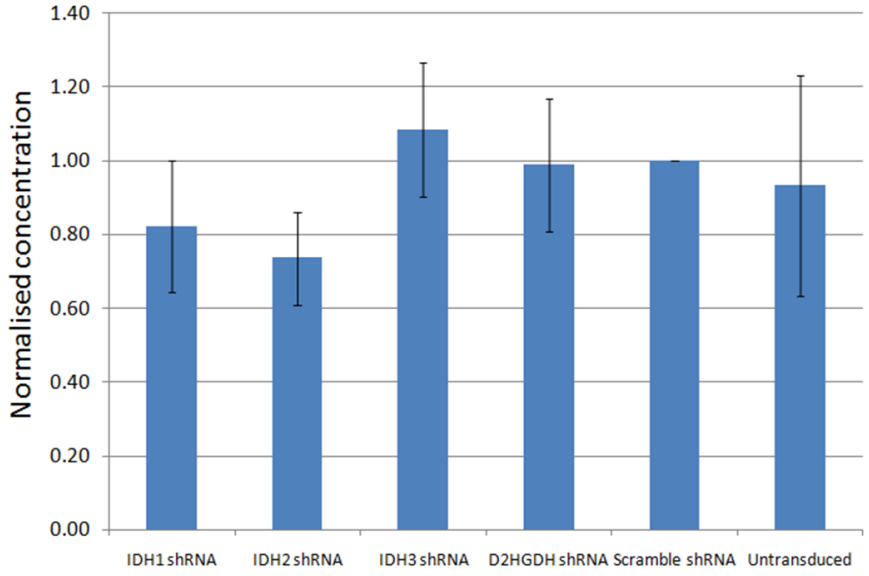


**Figure 4-15: 2-HG levels in shRNA knockdown LN18 cell lines**

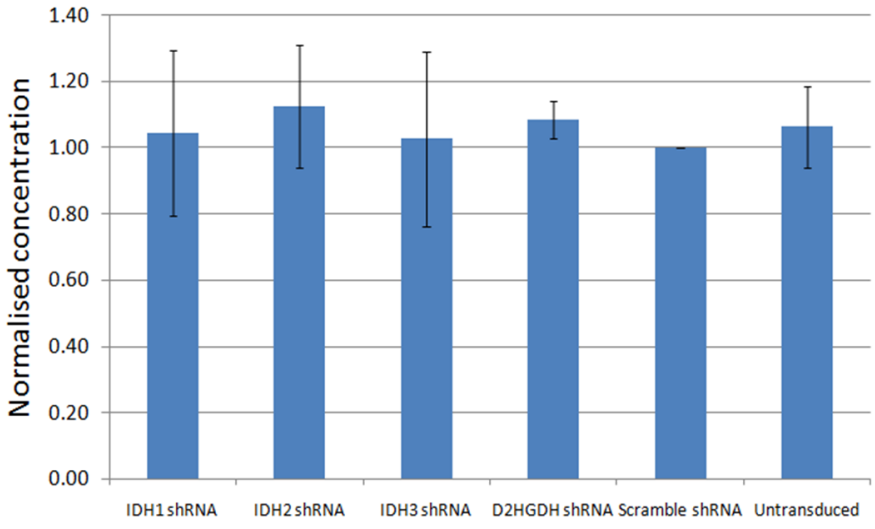


Given that αKG levels were not reduced in IDH1, IDH2 or IDH3 knockdown LN18 cell lines, I hypothesised that knockdown of one IDH enzyme leads to upregulation of another, and hence overall, cellular αKG levels remain unchanged. Consequently the effect of knockdown of one *IDH* gene on the expression of other *IDH* genes was assessed by qRT-PCR.

Knockdown of *IDH1* resulted in a statistically significant 1.53-fold increase in *IDH3* expression (p=0.0073) **(*Figure 4-16*).** A 1.22-fold increase in *IDH2* expression (p=0.1431)

was also seen in IDH1 knockdown cells but this change was not statistically significant. Knockdown of *IDH2* resulted in a 1.26-fold increase in *IDH1* expression (p=0.0183) and a 1.5-fold increase in *IDH3* expression (p=0.0247), both of which were statistically significant findings. Knockdown of *IDH3* resulted in a 2.21-fold increase in *IDH1* expression (p=0.0062), but no increase in *IDH2* expression was observed. It is important to note that although upregulation of *IDH1* and *IDH3* expression was observed at an mRNA level in IDH knockdown cell lines, these findings were not reproduced at a protein level ***(Figure 4-2; Figure 4-4; Figure 4-8)***.

**Figure 4-16: Effects of IDH1, IDH2, and IDH3 shRNA knockdown on the expression of *IDH1*, *IDH2* and *IDH3*.**

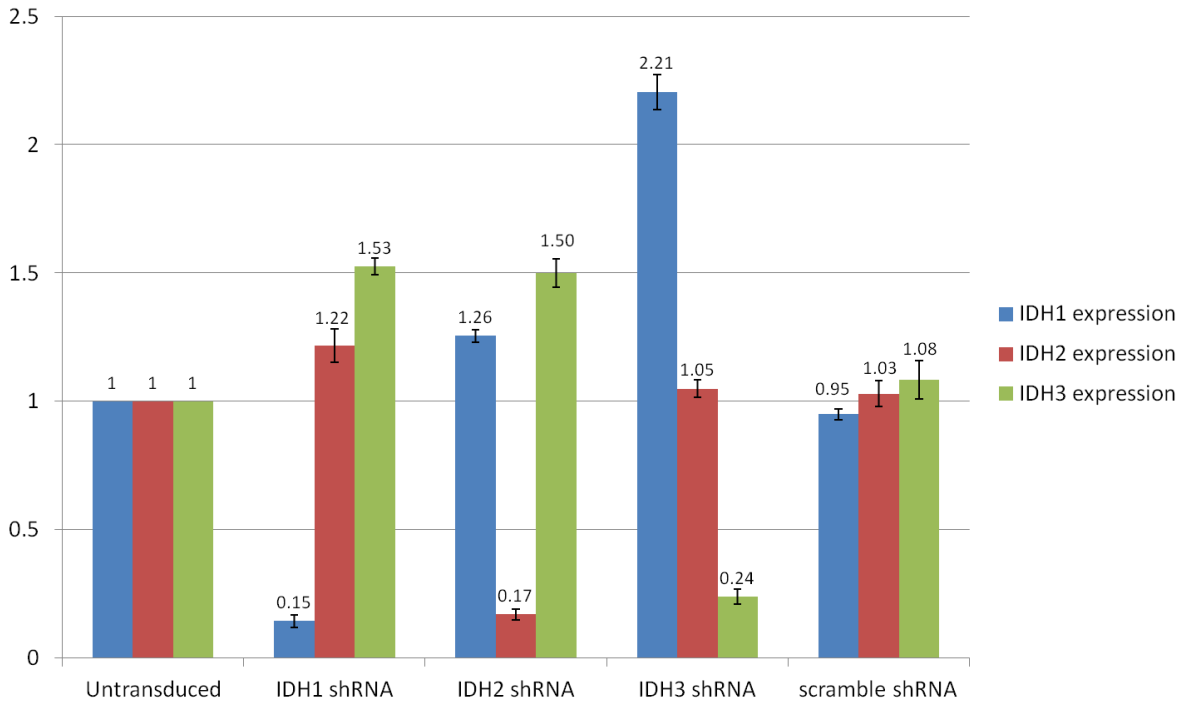


αKG levels were reduced by 57% (p<0.001) and 60% (p<0.001) in IDH1 R132H and IDH1 R132C mutant LN18 cell lines respectively, and were also reduced by 50% (p<0.001) and 54% (p<0.001) in IDH2 R172K and IDH2 R172M mutant LN18 cell lines respectively ***(Figure 4-17)***. Furthermore, 2-HG levels were increased by 12-fold in IDH1 R132H mutant LN18 cells (p<0.001) and by 11-fold in IDH1 R132C (p<0.001), IDH2 R172K (p=0.013),

and IDH2 R172M (p=0.038) mutant cell lines when compared to untransduced control samples ***(Figure 4-18)***. The levels of all other TCA cycle metabolites measured were however unchanged.

**Figure 4-17: α-KG levels in IDH1 and IDH2 mutant LN18 cell lines**

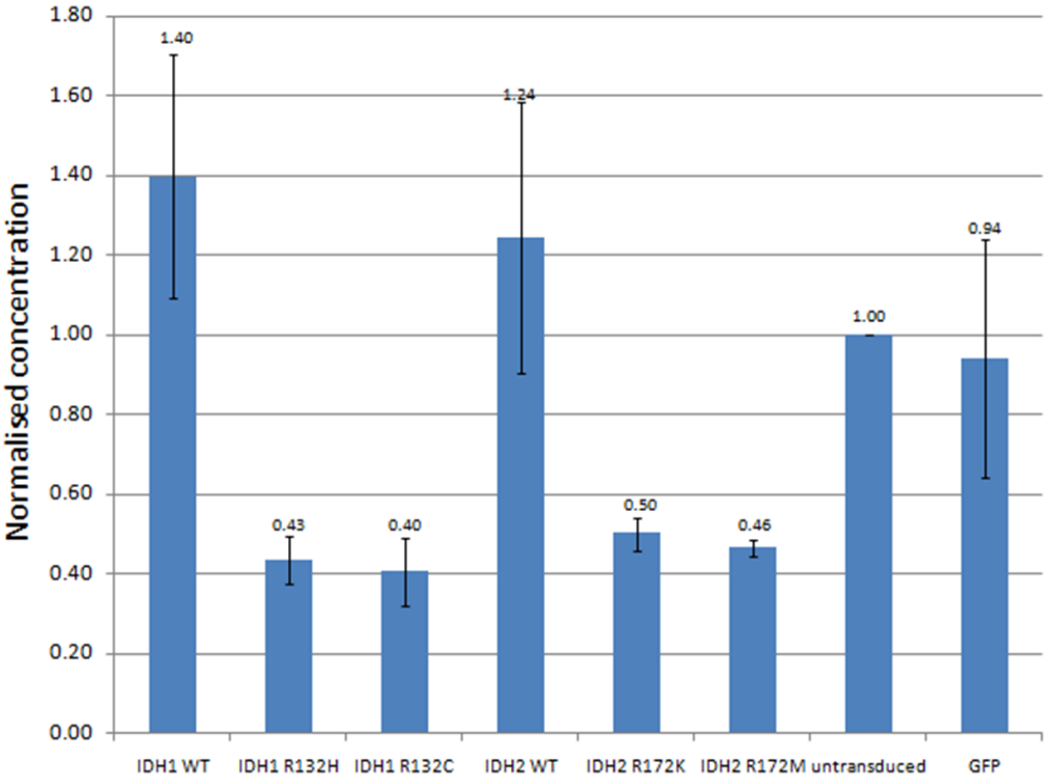

**Figure 4-18: 2-HG levels in IDH1 and IDH2 mutant LN18 cell lines**

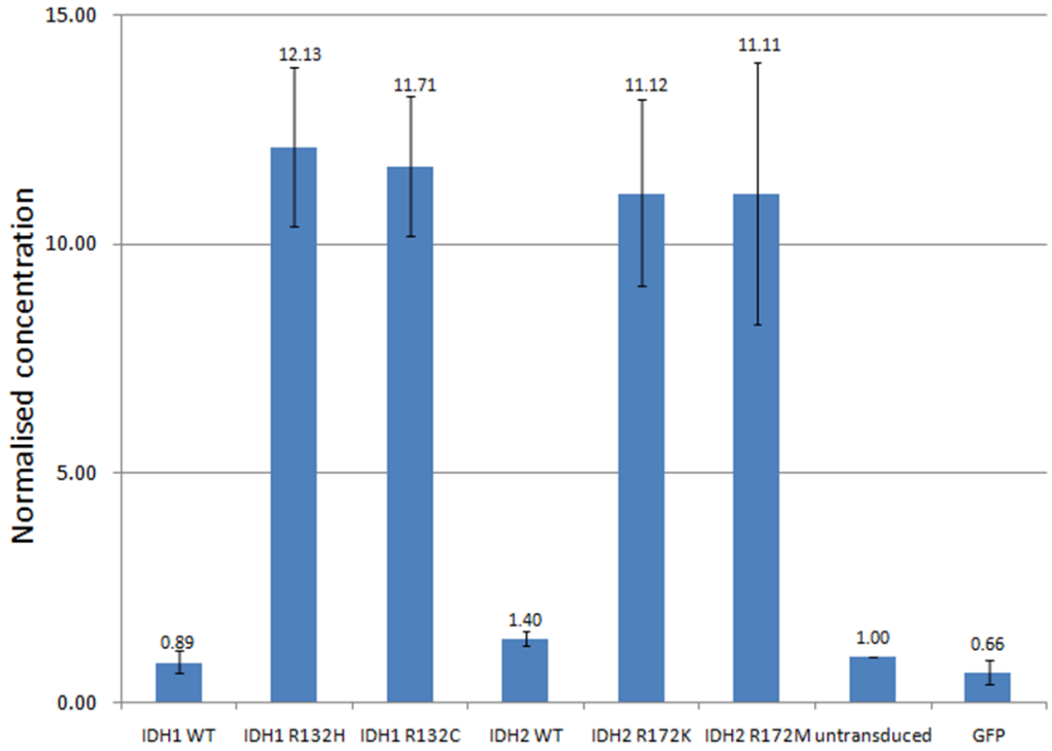


A 4-fold (p=0.106), 7-fold (p=0.192), and 10-fold (p=0.234) increase in 2-HG was seen in Idh1 R132H a11, c11 and h12 mutant ES cell clones respectively ***(Figure 4-19)*** but these changes were not statistically significant. Furthermore a 25-fold (p=0.325), 26-fold (p=0.08), and 26-fold (p=0.06) increase in 2-HG was observed in Idh2 R172K a1,c3 and d6 mutant ES cell clones respectively, but again these changes did not reach statistical significance ***(Figure 4-19)***. Additionally α-KG levels were not significantly reduced in any of the Idh1 or Idh2 mutant ES cell clones ***(Figure 4-20)***, and the levels of all other TCA cycle metabolites measured were also unchanged in these models.

**Figure 4-19: 2-HG levels in Idh1 and Idh2 mutant ES cell lines**

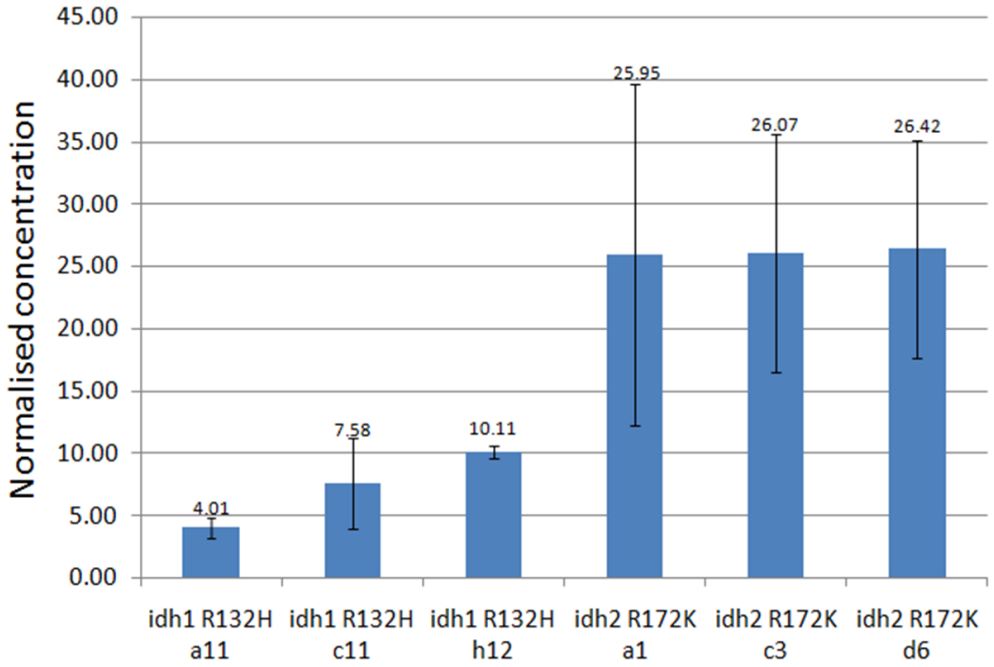


**Figure 4-20: α-KG levels in Idh1 and Idh2 mutant ES cell lines**

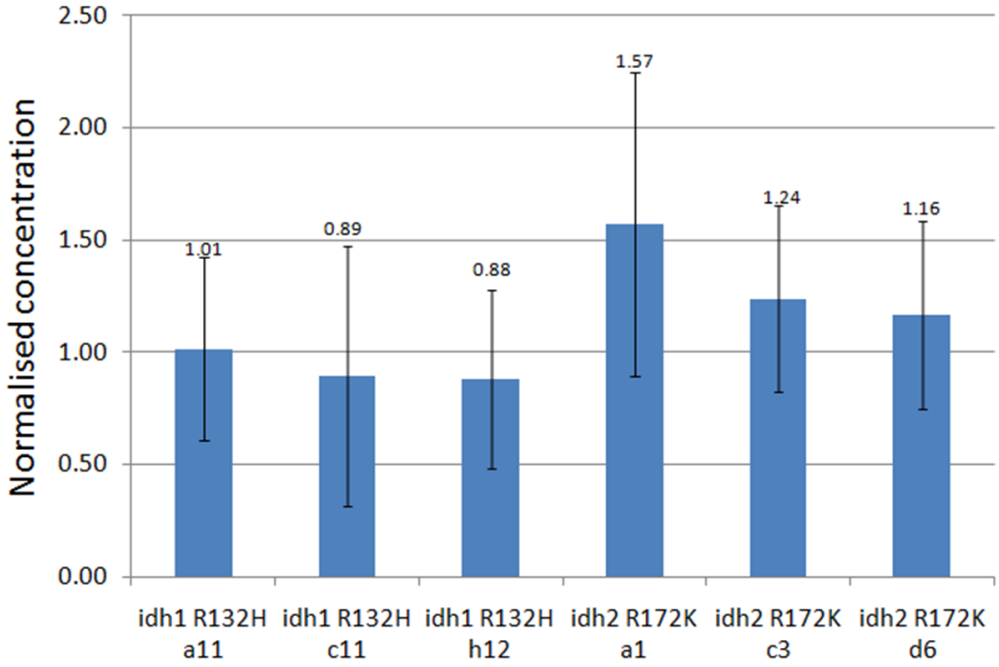

## 4.4.6 Analysis of HIF1α expression

### 4.4.6.1 HIF1α expression in knockdown cell lines

The knockdown of IDH1 and IDH2 in U87MG cells with siRNA resulted in an increase in HIF1α protein expression ***(Figure 4-21).***

**Figure 4-21: HIF1α protein expression in U87MG cells 72 hours after transduction with siRNA targeting IDH1/IDH2**

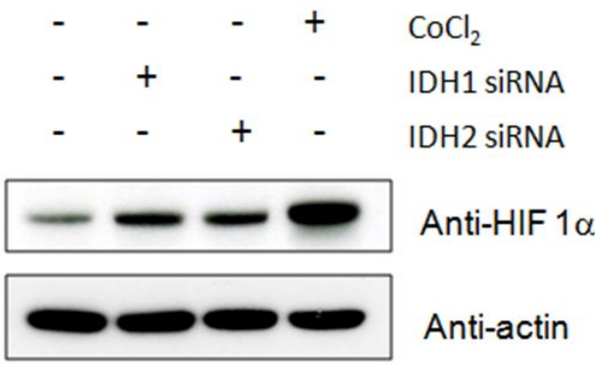


In LN18 cells, shRNA knockdown of IDH1 resulted in a 2.0-fold (p=0.0184) increase in *GLUT1* expression and a 1.6-fold (p=0.0023) increase in *VEGF* expression ***(Figure 4-22)***, and a 1.89-fold (p=0.0005) increase in HIF1α protein expression was also observed ***(Figure 4-22 and Figure 4-23)***. Knockdown of IDH2 resulted in a 1.9-fold (p=0.254) increase in *GLUT1* expression and 1.75-fold (p=0.165) increase in *VEGF* expression but these changes were not statistically significant ***(Figure 4-22)*** and no increase in HIF1α protein expression was seen ***(Figure 4-22 and Figure 4-23)***. *PGK1* expression was not increased by knockdown of either IDH1 or IDH2. Knockdown of IDH3 resulted in a 1.4-fold (p=0.117) in *GLUT1* expression but this was not statistically significant and *VEGF* and *PGK1* expression were also not increased. Furthermore, although a 1.25-fold (p=0.064) increase in HIF1α protein expression was seen in IDH3 knockdown cells, this change was not statistically significant ***(Figure 4-22 and Figure 4-23)***. Knockdown of D2HGDH resulted in a 1.5-fold (p=0.0063) increase in *GLUT1* expression and a 1.2-fold (p=0.656) increase in *VEGF* expression,

although the latter result was not statistically significant. A 1.3-fold (p=0.368) increase in *GLUT1* expression and a 1.5-fold (p=0.246) increase in *VEGF* expression were also seen in scramble shRNA controls, but these changes were not statistically significant and furthermore, HIF1α protein expression was not increased in these cells ***(Figure 4-22 and Figure 4-23)***.

**Figure 4-22: HIF target gene expression and HIF1α protein expression in LN18 cells transduced with shRNA.**

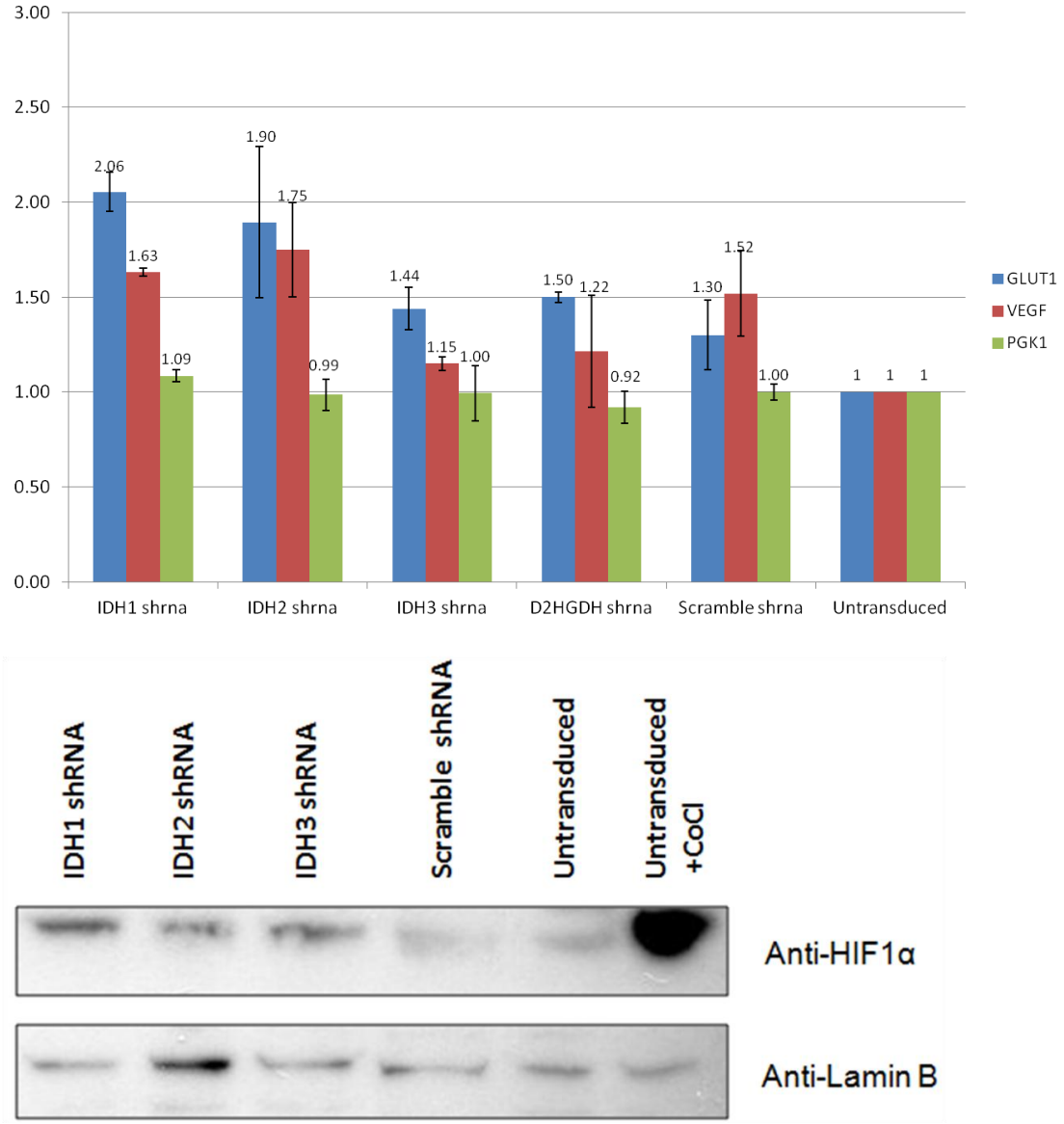

**Figure 4-23: HIF1α protein expression in LN18 cells transduced with shRNA. Analysis of western blot using ImageJ to measure grey scale values.**

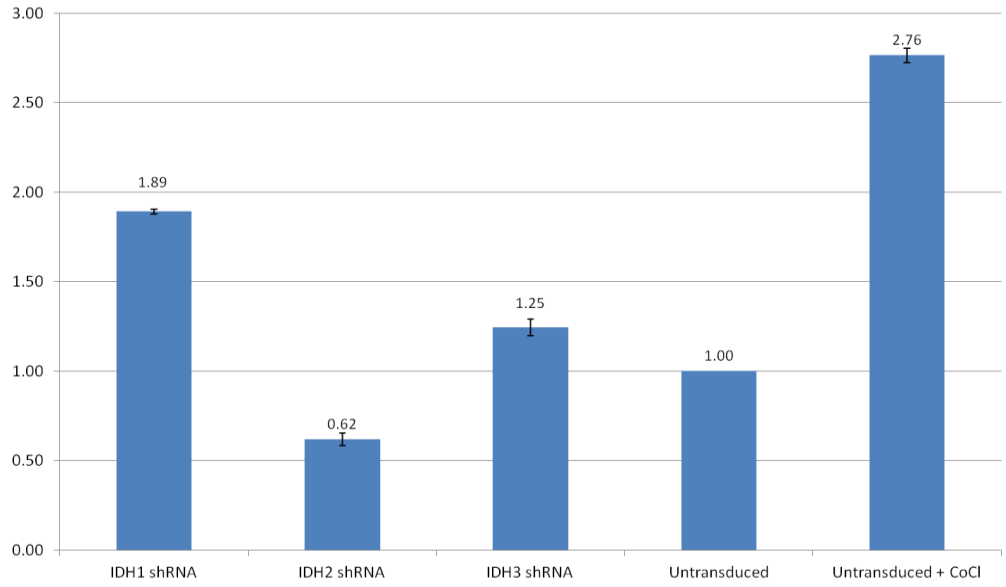


Values given as a ratio of HIF:Lamin grey scale ratios, standardised against untransduced controls.

### 4.4.6.2 HIF1α expression in IDH mutant cell lines

#### 4.4.6.2.1 IDH mutant LN18 cells

In IDH1 R132H mutant LN18 cells the expression of *GLUT1*, *VEGF* and *PGK1* were increased by 1.9-fold (p=0.0135), 1.9-fold (p=0.04), and 1.8-fold (p=0.05) respectively. In IDH1 R132C mutant cells the expression of *GLUT1*, *VEGF* and *PGK1* were also increased by 3.7-fold (p<0.01), 4.3-fold (p<0.01), and 2.2-fold (p=0.023) respectively. These increases were lost when mutant expression was 'switched off' with doxycycline ***(Figure 4-24)***.

In IDH2 R172K mutant LN18 cells the expression of *VEGF* and *PGK1* were increased by 1.6-fold (p=0.023) and 1.8-fold (p=0.002) respectively. A 1.3-fold (p=0.12) increase in *GLUT1* expression was also observed, but this was not statistically significant. In IDH2 R172M mutant cells the expression of *PGK1* was increased by 1.6-fold (p=<0.01) but the 1.2-fold (p=0.103) and 1.6-fold (p=0.154) increase observed in *GLUT1* and *VEGF* expression

respectively were not statistically significant ***(Figure 4-25)***. Again, these increases were negated when mutant expression was 'switched off' with doxycycline.

Additionally, HIF1α protein expression was markedly increased in both IDH1 and IDH2 mutant cell lines ***(Figure 4-26)***.

**Figure 4-24: Expression of HIF target genes in mutant IDH1 expressing LN18 cells.**

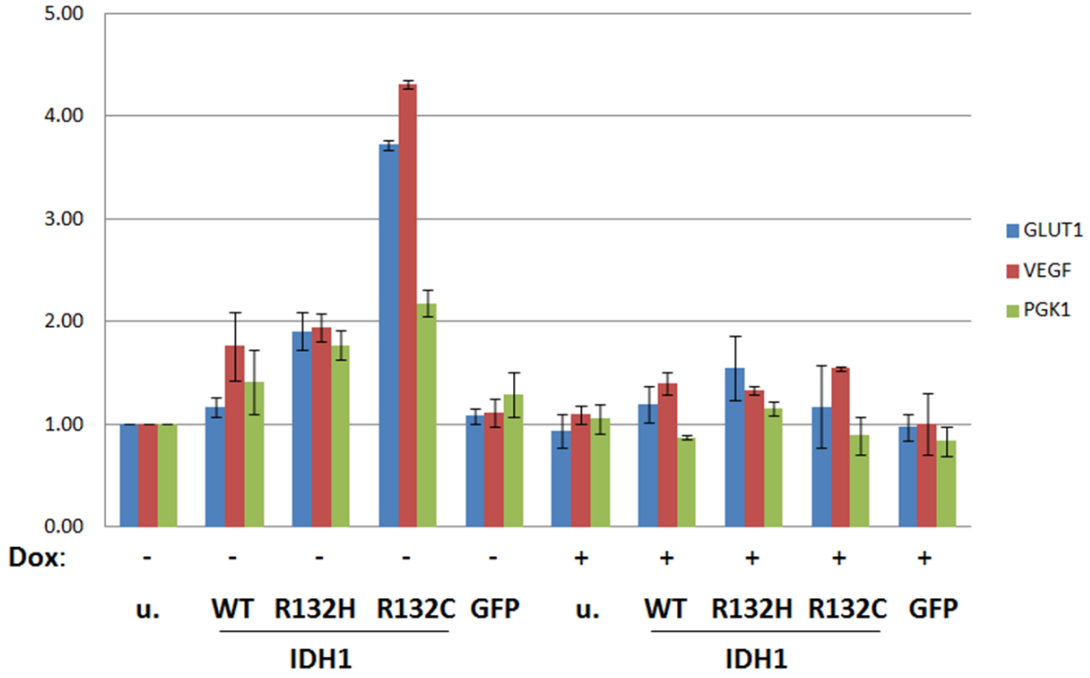


**Figure 4-25: Expression of HIF target genes in mutant IDH2 expressing LN18 cells.**

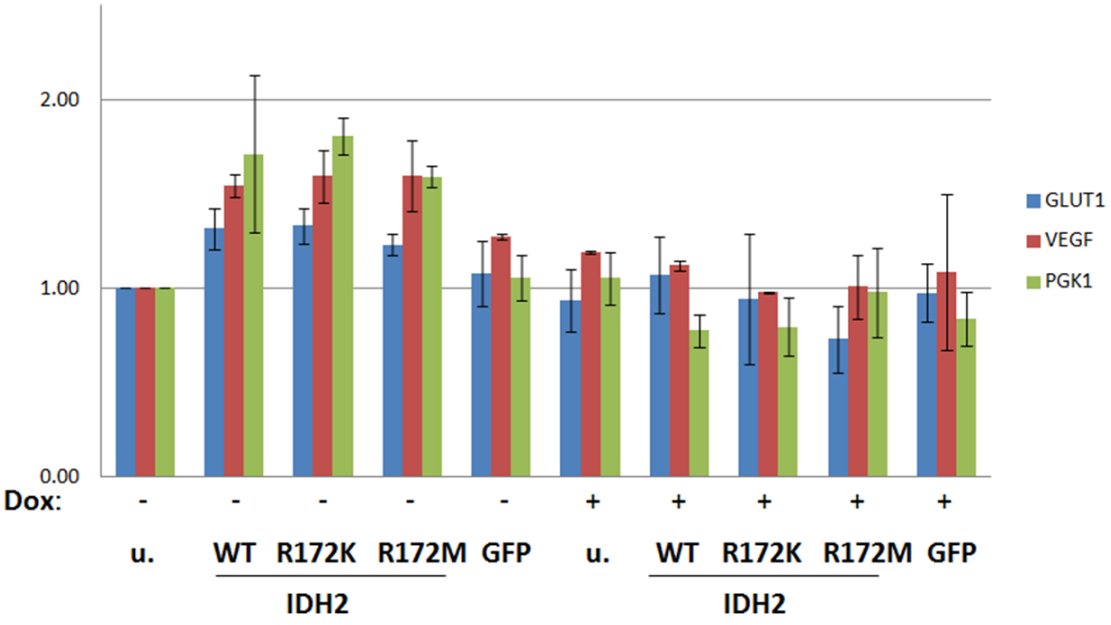

**Figure 4-26: HIF1α protein expression in mutant IDH1 and mutant IDH2 expressing LN18 cells**

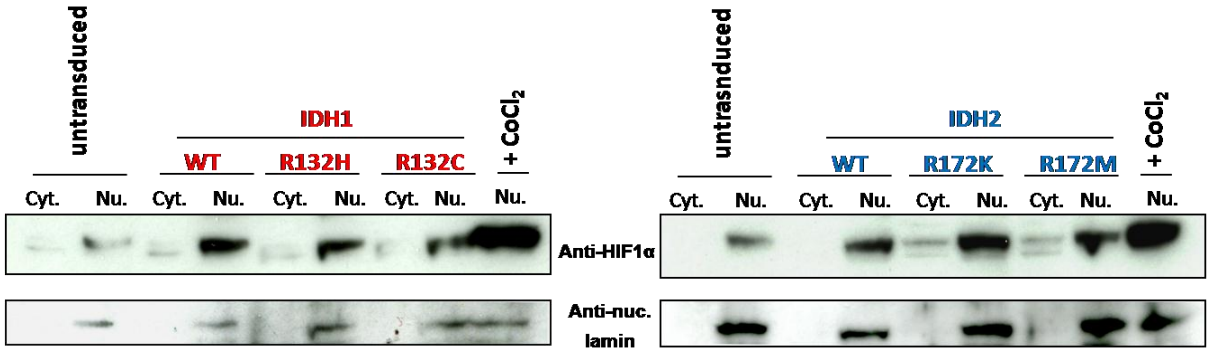


Nu.=Nuclear; Cyt.=Cytosolic

Interestingly, over expression of wild-type IDH1 resulted in a 1.8-fold (p=0.118) and 1.4-fold (p=0.318) increase in *VEGF* and *PGK1* expression respectively ***(Figure 4-24)***, but these changes were not statistically significant. However, over expression of wild-type IDH2 resulted in a 1.3-fold (p=0.04), 1.5-fold (p=0.001) and 1.7-fold (p=0.21) increase in *GLUT1*, *VEGF* and *PGK1* expression respectively ***(Figure 4-25)***, with the changes in the expression of *GLUT1* and *VEGF* being statistically significant. Furthermore, HIF1α protein expression was increased in cells in which wild-type IDH1 and IDH2 was overexpressed ***(Figure 4-26)***. These findings perhaps suggest that LV transduction itself may result in an increase in HIF1α expression, perhaps due to an increase in oxidative stress. Alternatively it is possible that changes in α-KG levels occurring as a result of increased wild-type IDH1/2 activity may itself exert an effect on HIF-PHD, although in this model, an increase rather than a decrease in α-KG production would be expected.

#### 4.4.6.2.2 Idh1/2 mutant ES cells

The expression of VEGF was increased by 1.8-fold (p=0.01) in Idh1 mutant ES cell lines ***(Figure 4-27)***. PGK1 expression was also increased by 2.2-fold (p=0.179) but this was not statistically significant.

In Idh2 mutant ES cells GLUT1, VEGF and PGK1 expression were increased by 2.0-fold ($p<0.01$), 1.3-fold ($p=0.04$) and 1.8-fold ($p=0.03$) respectively ***(Figure 4-27)***. Furthermore HIF1α protein expression was increased in 2 out of 3 Idh1 R132H mutant ES cell clones (c11 and h12) , and in all 3 Idh2 R172K mutant clones ***(Figure 4-28).***

**Figure 4-27: Expression of HIF target genes Idh1 and Idh2 mutant ES cells**

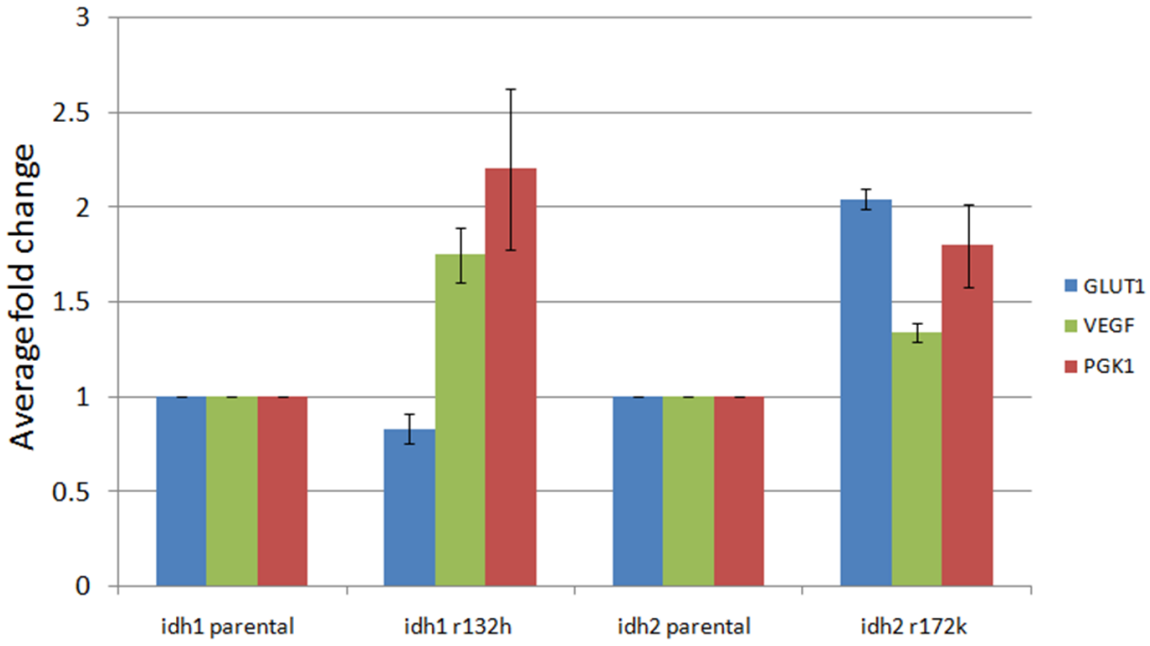


**Figure 4-28: HIF1α protein expression in Idh1 and Idh2 mutant ES cell clones**

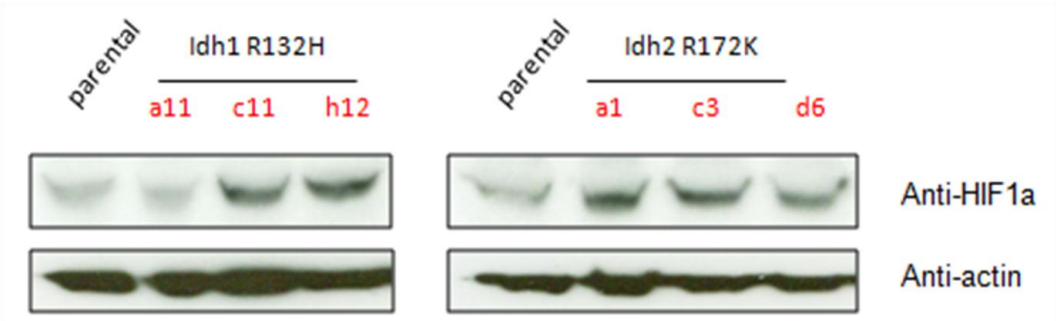

### 4.4.7 Assessment of TET function in Idh1/2 mutant ES cells

The level of 5hmC was reduced by 70.31% ($p<0.01$) and 51.86% ($p=0.04$) in Idh1 mutant ES cell clones C11 and H12 respectively ***(Figure 4-29).*** 5hmC content was also reduced by 37.47% ($p=0.029$) in Idh2 R172K C3 ***(Figure 4-30)***. These findings suggest that the expression of mutant IDH1/2 resulted in an inhibition of TET function, and hence a reduction in the conversion of 5mC to 5hmC. 5hmC content was also reduced by 12.87% ($p=0.39$) in Idh1 R132H A1, and by 13.2% ($p=0.17$) and 44.71% ($p=0.17$) Idh2 R172K A11 and D6 respectively, but these changes were not statistically significant. The level of 2-HG accumulation seen in Idh1 R132H C11 and H12 was higher than that observed in Idh1 R132H A11, and the level of α-KG was also lower in the former 2 clones which may explain the discrepancy in hmC content observed in the Idh1 R132H clones. There was however no correlation between 2-HG or α-KG levels and 5hmC content in Idh2 R172K clones.

**Figure 4-29: 5hmC content in Idh1 R132H mutant ES cell clones**

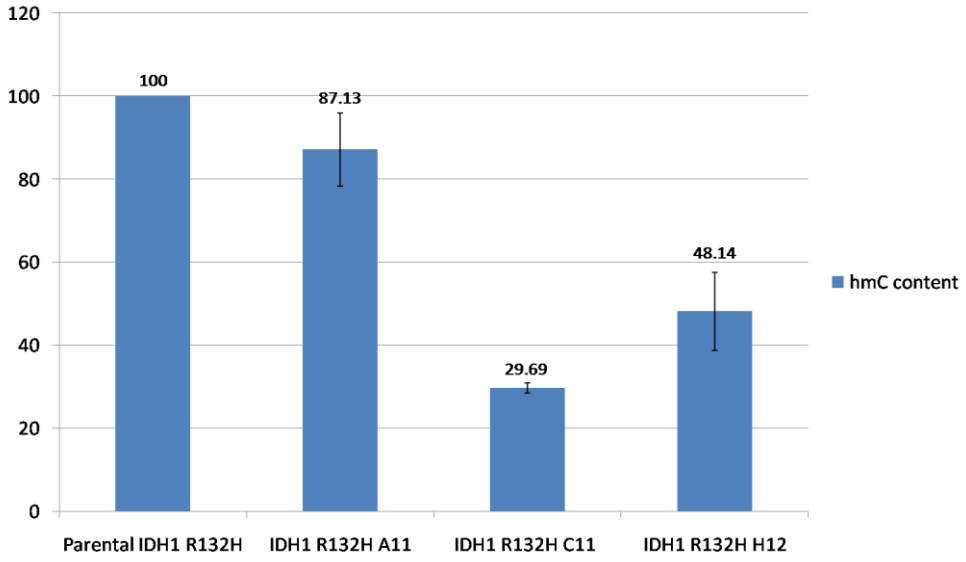

**Figure 4-30: 5hmC content in Idh2 R172K mutant ES cell clones**

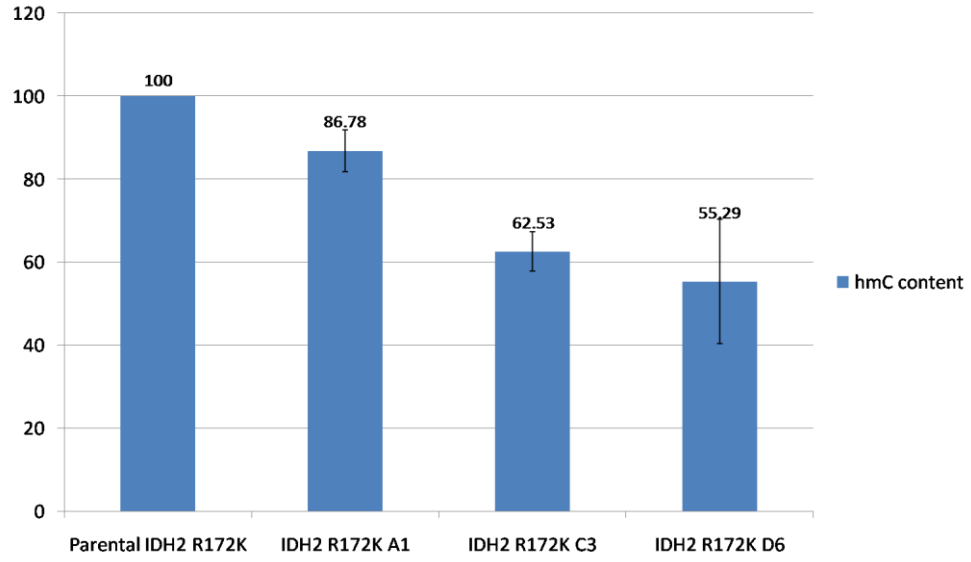


## 4.4.8 Assessment of markers of histone methylation in Idh1/2 mutant ES cells

A small increase in the histone methylation marker H3K4me3 was seen in Idh2 R172K a1 and d6 mutant ES cell clones ***(Figure 4-31)***, however no increase in H3K9me2 was seen. Furthermore the levels of H3K4me3 and H3K9me2 were not increased in Idh1 R132H mutant clones ***(Figure 4-31)***. The inhibition of JHDM in Idh1/2 mutant ES cells could therefore not be convincingly demonstrated in this model.

**Figure 4-31: H3K4me3 and H3K9me2 levels in IDH2 R172K mutant ES cells**

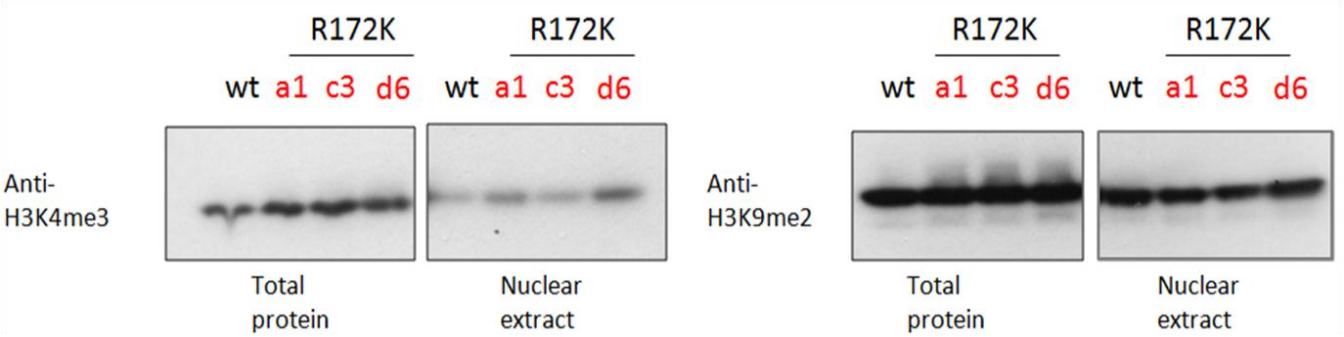

## 4.4.9 Assessment of oxidation state and oxidative stress

### 4.4.9.1 NADPH

NADPH was reduced by 36% (p=0.09), 52% (p=0.026), and 61% (p=0.019) in IDH1, IDH2 and IDH3 shRNA knockdown LN18 cells respectively ***(Figure 4-32)***. A reduction in NADPH of 37% (p<0.01), 10% (p=0.61), 19% (p=0.36), and 47% (p=0.22) was also seen in IDH1 R132H, IDH1 R132C, IDH2 R172K, and IDH2 172M mutant LN18 cell lines respectively ***(Figure 4-33)***.

**Figure 4-32: NADPH quantification in IDH shRNA knockdown LN18 cells**

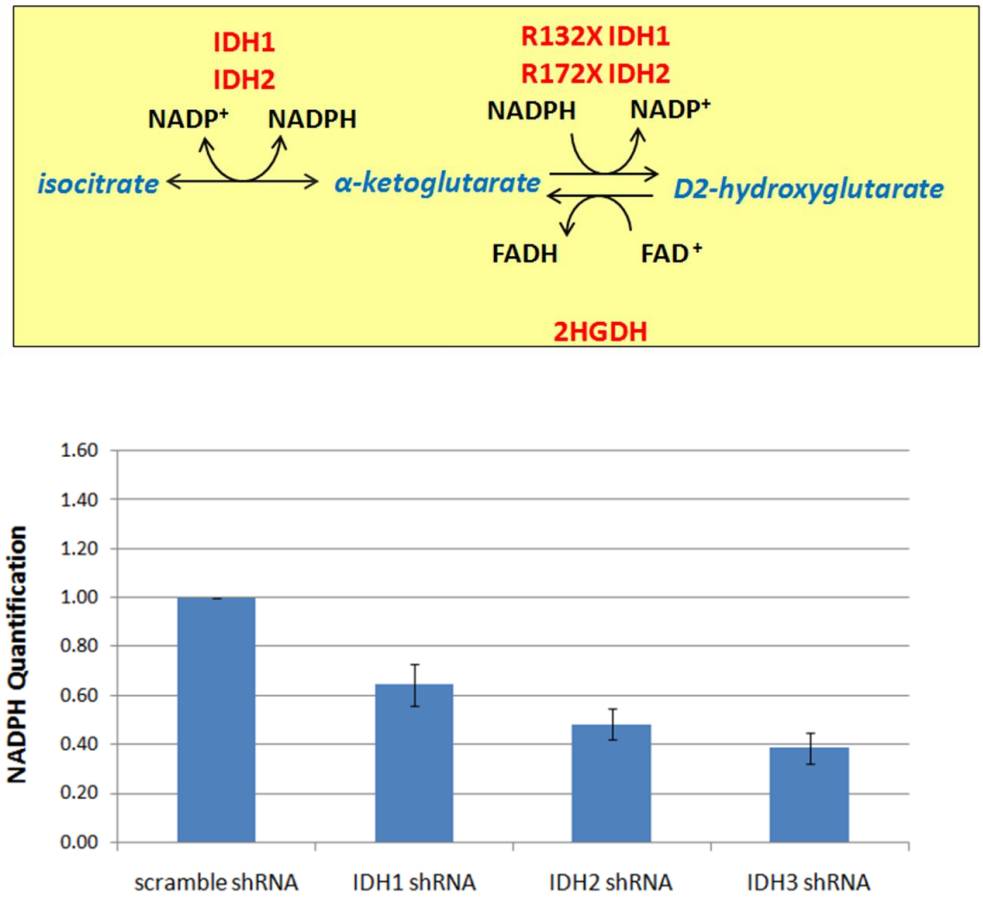

**Figure 4-33: NADPH quantification in IDH mutant LN18 cells**

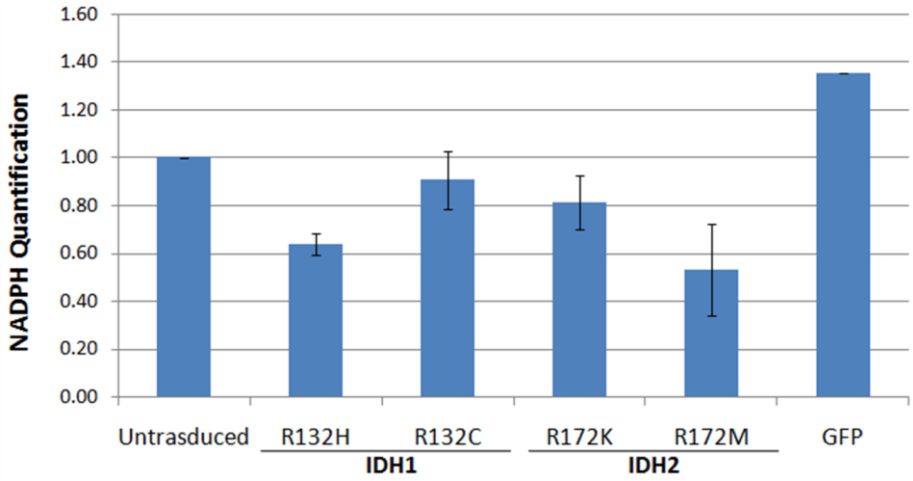


In Idh1 R132H mutant ES cells the $NADP^+$/NADPH ratio was increased by 2.6 (p=0.24), 1.5 (p<0.01) and 2.2-fold (p=0.17) in a11, c11 and h12 clones respectively ***(Figure 4-34)***, whilst in Idh2 R172K cells a 2.7 (p=0.06), 2.2 (p<0.01) and 2.3-fold (p<0.01) increase in the $NADP^+$/NADPH ratio was seen in a1, c3, and d6 clones respectively ***(Figure 4-34)***.

**Figure 4-34: $NADP^+$/NADPH ratio in Idh mutant ES cells**

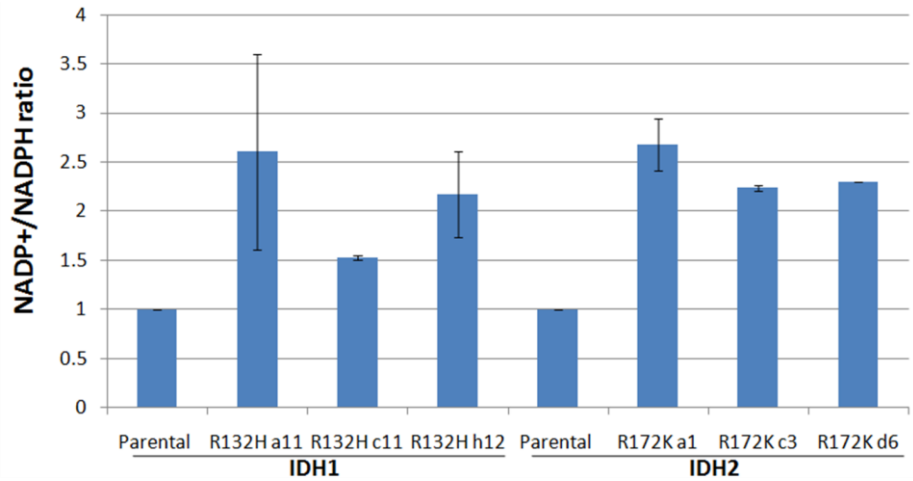


### 4.4.9.2 ROS

ROS levels were increased by 5% (p=0.38), 10% (p=0.20), and 12% (p=0.36) in IDH1, IDH2 and IDH3 siRNA knockdown U87MG cells respectively ***(Figure 4-35)***. This increase became more apparent when oxidative stress was induced by $H_2O_2$, with ROS levels increasing by

12% (p=0.15), 20% (p=0.037), and 29% (p=0.04) in IDH1, IDH2 and IDH3 siRNA knockdown cells respectively in the presence of 1mM $H_2O_2$, and by 15% (p=0.23), 35% (p=0.028), and 41% (p=0.01) in the presence of 2.5mM $H_2O_2$. An increase in ROS of 12% (p=0.59), 29% (p=0.075) and 40% (p=0.053) was also seen in scramble siRNA controls under basal conditions and in the presence of 1mM and 2.5mM of $H_2O_2$ respectively, but these changes were not statistically significant.

**Figure 4-35: Percentage of ROS positive cells in IDH siRNA knockdown U87MG cell lines**

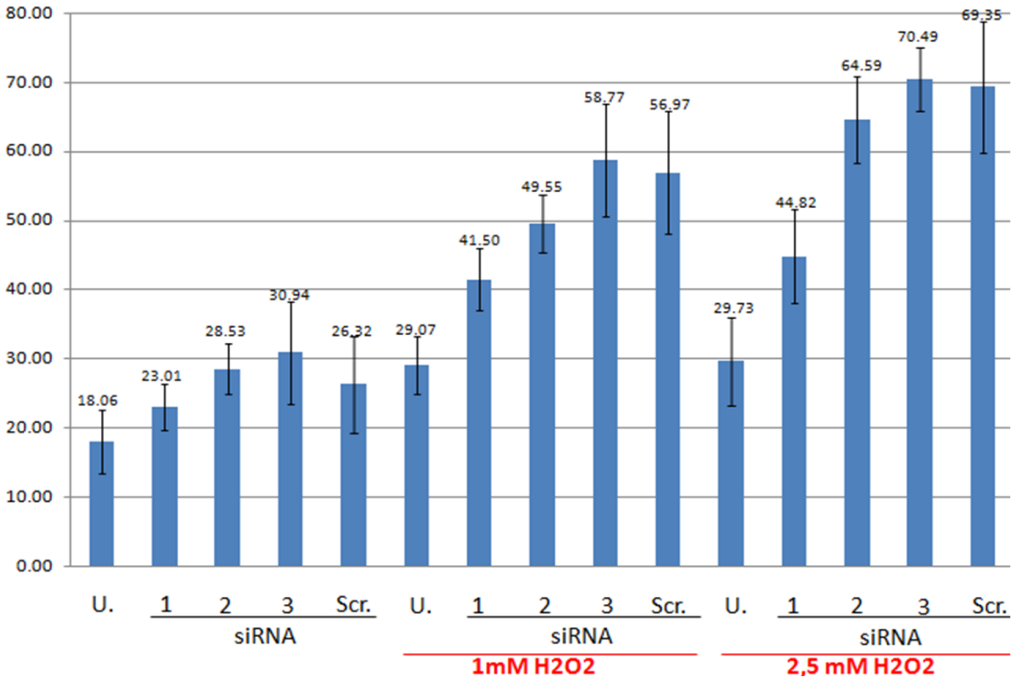


ROS levels were also increased by 23% (p<0.01), and 19% (p<0.01) in IDH1 and IDH3 shRNA knockdown cells respectively, but no increase was seen in association with IDH2 shRNA knockdown ***(Figure 4-36)***. The absence of an increase in ROS in IDH2 shRNA knockdown cells may have occurred as a result of a loss of IDH2 knockdown in the cells used in this experiment, however IDH2 expression was not re-checked immediately prior to ROS measurement.

When oxidative stress was induced by $H_2O_2$, the relative increase in ROS was nullified in IDH1 knockdown cells, and significantly reduced in IDH3 knockdown cells, when compared to untransduced controls ***(Figure 4-36)***, perhaps because ROS levels had already reached their peak levels under basal conditions in IDH1/3 knockdown cells. It is also important to note that ROS levels were also increased by 9% ($p<0.01$) in D2HGDH knockdown cells and by 25% ($p<0.01$) in scramble shRNA controls perhaps suggesting that off target effects resulted in an increase in oxidative stress in these cells.

**Figure 4-36: Percentage of ROS positive cells in IDH shRNA knockdown LN18 cell lines**

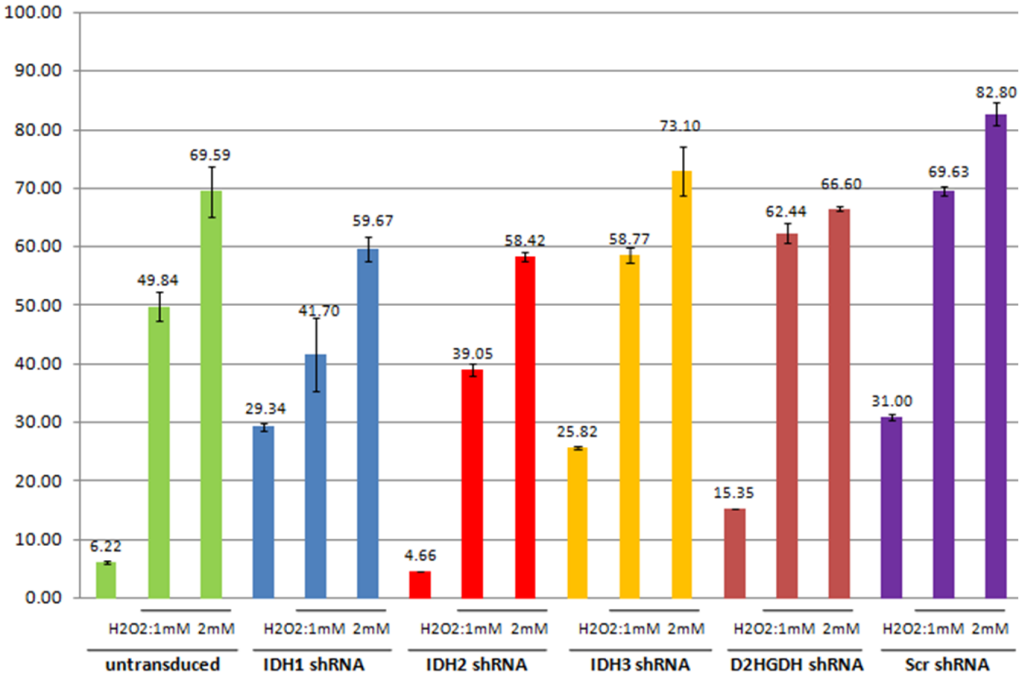


An increase in ROS was also seen in association with IDH1 mutant expression in LN18 cells. Indeed a 16% ($p=0.09$) and 26% ($p=0.04$) increase in ROS was observed in IDH1 R132H and R132C mutant cell lines following incubation in 2mM $H_2O_2$ and a 17% ($p=0.09$) increase was seen in R132C cells incubated in 1mM $H_2O_2$ ***(Figure 4-37)***. These increases were nullified when IDH1 mutant expression was inhibited by doxycycline. No increase in ROS was seen in association with IDH1 mutant expression in LN18 cells under basal conditions.

**Figure 4-37: Percentage of ROS positive cells in IDH1 mutant LN18 cell lines**

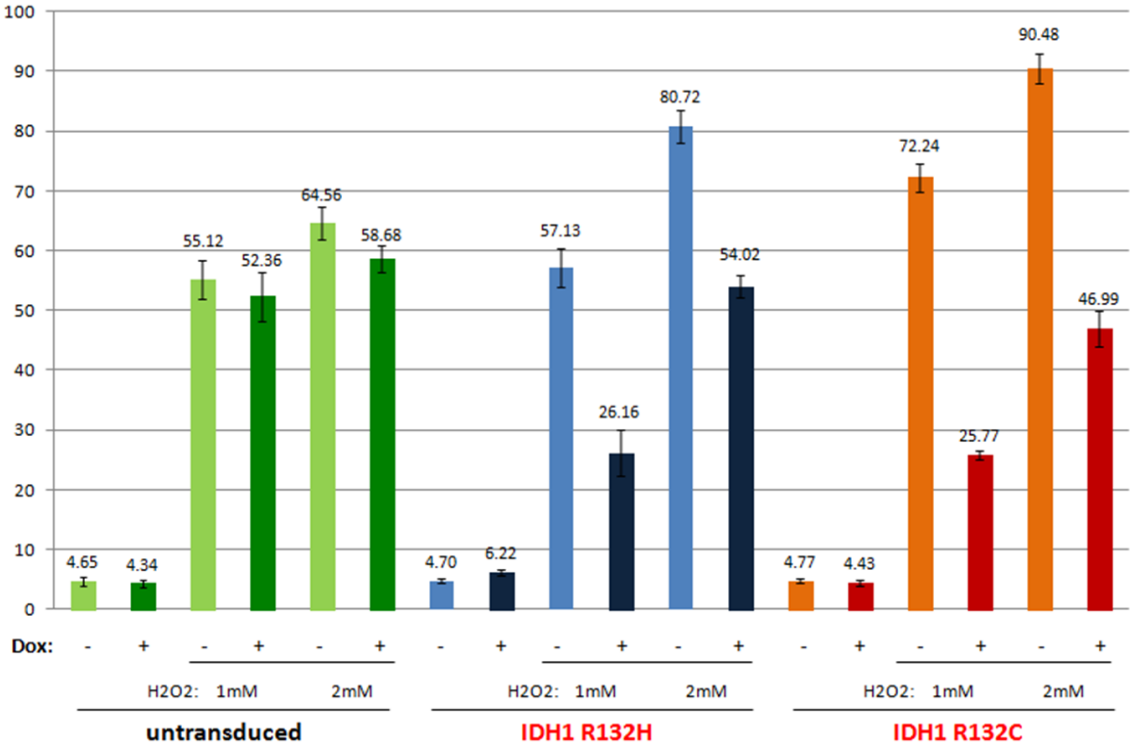


In Idh1 R132H mutant ES cells ROS levels were increased by 4% (p=0.79) and 9% (p=0.21) following incubation with 1mM and 2.5mM of $H_2O_2$ respectively ***(Figure 4-38)***, but these changes were not statistically significant. Expression of Idh2 R172K in ES cells resulted in an increase in ROS levels of 14% (p=0.08) under basal conditions, and 11% (p=0.10) and 15% (p=0.11) following incubation with 1mM and 2.5mM of $H_2O_2$ respectively, although again these changes were not statistically significant ***(Figure 4-38)***.

**Figure 4-38: Percentage of ROS positive cells in Idh1 and Idh2 mutant ES cells**

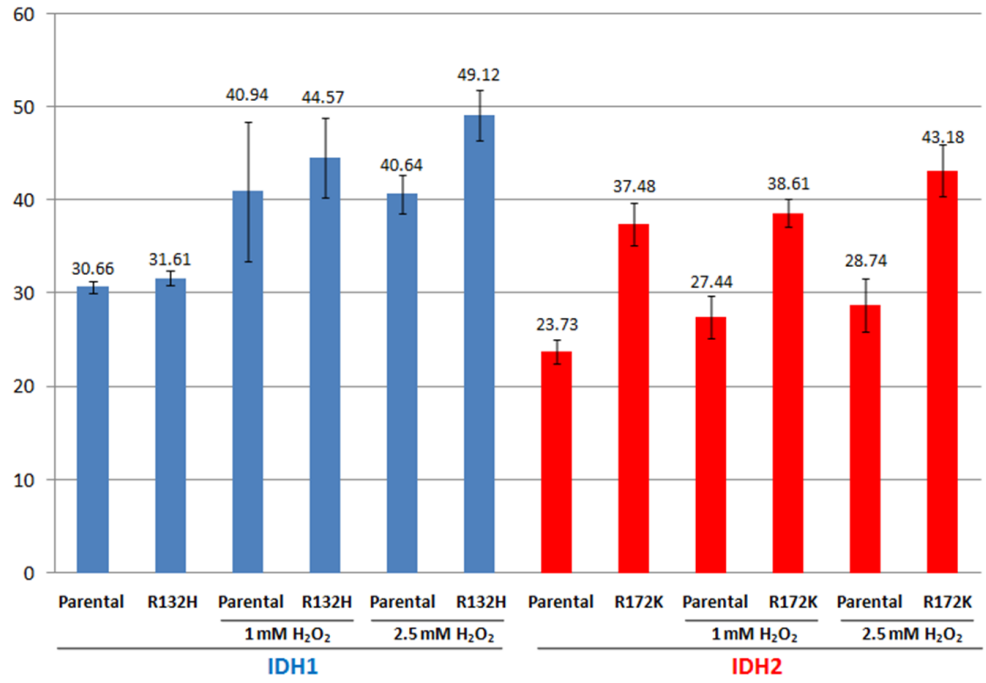


## 4.4.10 Assessment of cellular proliferation rate

Cellular proliferation was assessed in IDH1/2/3 knockdown LN18 cell lines over a 120 hour period. Cell lines with reduced wild-type IDH1/2/3 function demonstrated a lower proliferation rate than both untransduced and scramble controls ***(Figure 4-39)***. Indeed, whilst at 120 hours the growth rate of untransduced and scramble control cells appeared to increase, in IDH1/2/3 knockdown cells growth rate was considerably reduced.

Cellular proliferation was assessed in IDH1/2 mutant LN18 cells over a 96 hour period. Cellular proliferation rate was reduced in both IDH1 and IDH2 mutant cell lines when compared to untransduced and gfp controls ***(Figure 4-40 and Figure 4-41)***, although this reduction was less marked than that observed in association with IDH1/2 knockdown.

**Figure 4-39: Cellular proliferation in IDH knockdown LN18 cells**

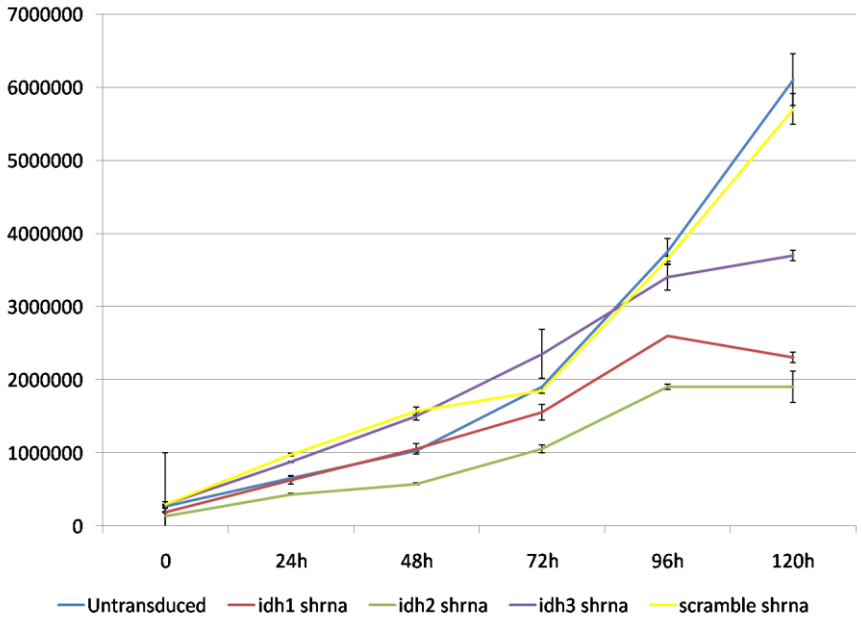


**Figure 4-40: Cell proliferation in IDH1 mutant LN18 cells**

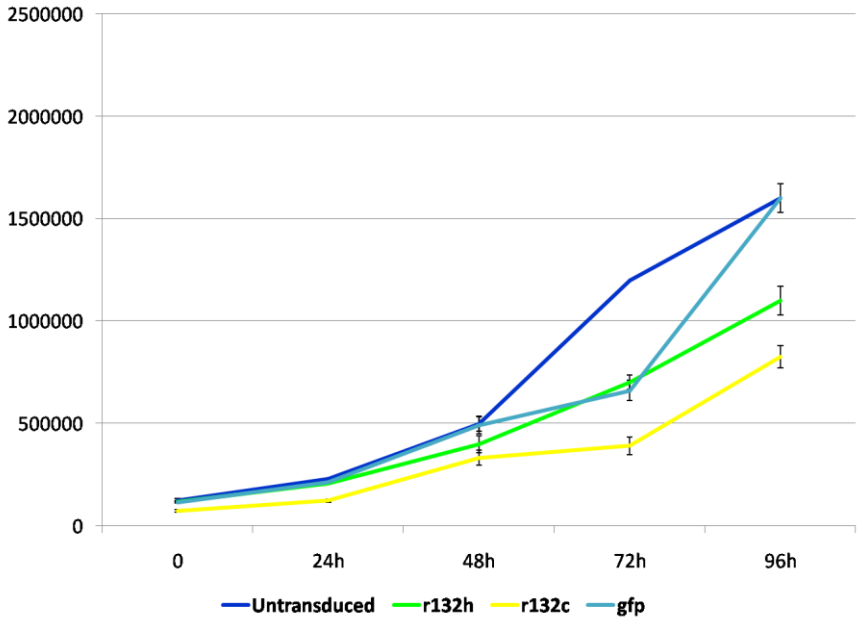

**Figure 4-41: Cell proliferation in IDH2 mutant LN18 cells**

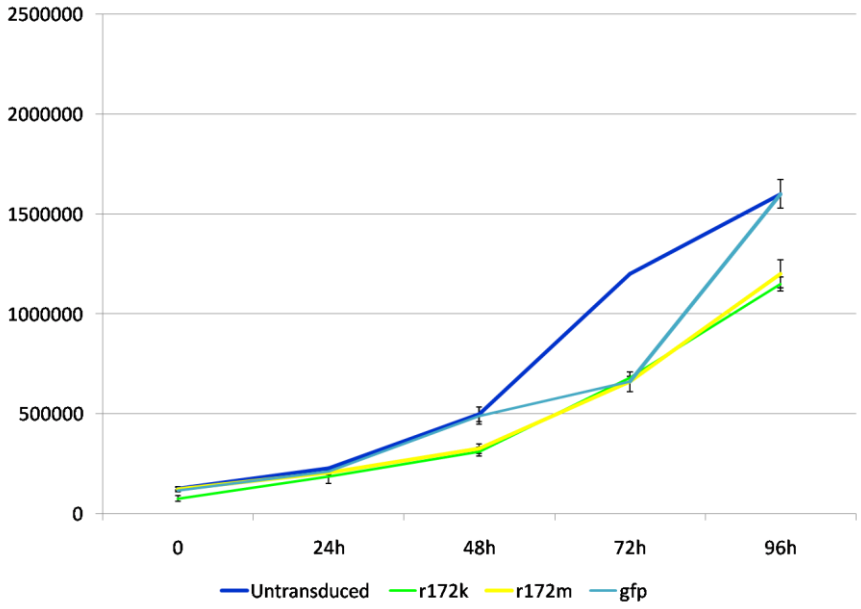

## 4.5 Discussion

### 4.5.1 shRNA knockdown of a single IDH enzyme does not reduce cellular α-KG levels in vitro

Lentiviral transduction of LN18 cells with shRNA targeting IDH1/2/3 was an effective means of reducing *IDH1/2/3* gene expression, although there was variability in the level of knockdown achieved between the different IDHs, and cell viability was compromised when cells were exposed to higher concentrations of LV.

However, despite effectively reducing IDH gene expression, cellular α-KG levels were not reduced in either IDH1, IDH2, or IDH3 knockdown cells. Given that α-KG levels have been shown to be reduced in association with mutant IDH expression (Zhao S 2009, Xu W 2011), my IDH1/2/3 shRNA knockdown cell lines do not serve as optimal models to investigate IDH1/2 loss of function as a pathogenic mechanism in IDH1/2 driven tumourigenesis, as conclusions cannot be drawn on the role of α-KG depletion in this process. However, as will be discussed later, knockdown of IDH function did result in other cellular effects, namely a reduction in NADPH levels and cellular proliferation rate, and an alteration in HIF1α expression. This suggests that whilst the level of IDH knockdown was not sufficient to result in a reduction in cellular α-KG production, it was sufficient to alter other aspects of cellular metabolism. Alternatively, it is possible that IDH knockdown cells were able to adapt to the decrease in α-KG production resulting from IDH down-modulation and were able to overcome this depletion using other sources of α-KG such as via an increase in glutamine/glutamate flux. Furthermore, one might hypothesise that inhibition of one IDH enzyme resulted in upregulation in the expression of either one or two of the other IDHs, hence negating any knockdown effect, and maintaining α-KG at basal levels overall. Indeed I have demonstrated that knockdown of IDH1 led to an increase in IDH3 expression at an mRNA level, and vice versa, whilst knockdown of IDH2 resulted in an up regulation of IDH3

and potentially, to a lesser extent, IDH1. It is important to note that these findings were not reproducible at a protein level, however, other groups have also demonstrated that the activity of one IDH enzyme can increase to compensate for the loss of another (MacDonald MJ 2013). Furthermore, given that there is rapid transport of citrate, isocitrate and α-KG between the cytosol and mitochondria, any precursor, substrate or product of one IDH reaction can be imported between cellular compartments, and hence replace any losses that may occur with inhibition of another. In fact it has been demonstrated that when the activities of both mitochondrial IDH enzymes are significantly inhibited, the transport of substrate and product to the mitochondria from the reaction of cytosolic IDH1 can support normal cell growth and survival, but is insufficient to support processes that require rapid fuel consumption, such as insulin secretion (MacDonald MJ 2013).

In addition to a possible functional compensation amongst the three IDH enzymes, it is possible that redundancy of function also exists between IDH and non-IDH enzymes. For example the transport of TCA cycle intermediates between the mitochondria and cytosol has been proposed to contribute to NADPH-producing reactions in the cytosol and to participate in insulin secretion in pancreatic cells (Farfari S 2000, MacDonald MJ 2005, Ronnebaum SM 2006). These reactions occur in cycles in which the exported metabolite is oxidized by $NADP^+$ to produce NADPH in the cytosol, with the oxidized metabolite then being re-imported into the mitochondria for reduction and re-exportation to the cytosol. In fact, an isocitrate cycle involving either or both of the mitochondrial IDHs and cytosolic IDH1 has been proposed as one such NADPH cycle (MacDonald MJ 2005, Ronnebaum SM 2006). In view of this, it may be necessary to inhibit the function of either two or all three IDH enzymes in order to cause a reduction in cellular α-KG levels. Indeed Macdonald *et al.* demonstrated that glucose stimulated α-KG levels were lowered by 90% in pancreatic beta-cells (INS-1 832/13) with shRNA induced knockdown of both IDH2 and IDH3a (MacDonald

MJ 2013), although a 70% reduction in α-KG was also seen with knockdown of IDH3a alone. Interestingly, knockdown of IDH2 alone did not result in a reduction in α-KG in this study. Furthermore, Zhao *et al*. demonstrated that in U87MG cells, shRNA knockdown of *IDH1* by more than 75% at an mRNA level, reduced cellular α-KG levels by up to 50% (Zhao S 2009), whilst Xu *et al.* showed that shRNA knockdown of *IDH1* in the same cell line was sufficient to increase H3K79 dimethylation induced expression of several *HOXA* genes, although data on cellular α-KG levels was not published (Xu W 2011). Conversely however in Macdonald's study, knockdown of *IDH1* by greater than 50% in pancreatic beta-cells was not compatible with cell line viability, whilst knockdown of less than 50% did not result in inhibition of IDH1 enzyme function (MacDonald MJ 2013).

In conclusion, it appears that the effects and viability of shRNA knockdown of IDH1/2/3 are variable between different cell lines. In my LN18 cells, it was not possible to demonstrate a reduction in α-KG levels despite a reduction in mRNA expression of *IDH1*, *IDH2*, and *IDH3* of 87%, 77%, and 68% respectively, and a reduction in corresponding protein levels. The reduction in IDH1/2/3 expression that I achieved at an mRNA level, are lower than the 90% knockdown in IDH3a expression, and the 75% and 90% knockdown in dual IDH2/IDH3a expression achieved by Macdonald *et al.* that did result in an α-KG reduction (MacDonald MJ 2013), but are comparable with those achieved by Zhao *et al.* (Zhao S 2009). It is possible that by knocking down two or more IDH enzymes in a single cell line, I would have been able to demonstrate a reduction in α-KG. Alternatively I could have used a different mechanism to inhibit IDH enzyme function, such as that used by Xu *et al.* who treated IDH1/2 wild-type cells with the competitive IDH1 and IDH2 inhibitor, oxalomalate. Oxalomalate treatment significantly inhibited JHDM function, suggesting a reduction in cellular α-KG had been achieved with this method, although corresponding data on α-KG levels was not published (Xu W 2011). Nevertheless, this study by Xu et al. demonstrates that

loss of wild-type IDH1/2 function exerts interesting effects on cellular function and that IDH1/2 loss of function may indeed serve as a pathogenic mechanism in IDH1/2 driven tumourigenesis.

### 4.5.2 shRNA knockdown of D2HGDH does not lead to an accumulation of 2-HG

2-HG did not accumulate in D2HGDH knockdown cells despite an 82% reduction in D2HGDH mRNA expression. It is possible D2HGDH protein is very stable, and hence despite a significant reduction in *D2HGDH* gene expression at an mRNA level, corresponding protein expression, and hence enzyme function remained unaffected. However, due to a lack of specificity of the two D2HGDH antibodies used, I was unable to successfully prove this theory by western blotting. Dual knockdown of both D- and L2HDGH function did not result in 2-HG accumulation either. Consequently these models do not serve as a meaningful positive control in this study. Treatment of cells with exogenous cell permeable D-2HG has been shown to lead to its intracellular accumulation (Xu W 2011), and this method would have provided an alternative positive control model to that which I attempted to develop. *In vitro* studies using this technique have successfully demonstrated the inhibition by exogenous D-2HG of TET, HIF PHD, C-P4H, and histone demethylase (Xu W 2011), and have illustrated the effects of D-2HG accumulation on the cellular metabolome (Reitman ZJ 2011), although they have not directly demonstrated the effects of D-2HG on tumourigenesis. Concentrations of between 7.5mM and 30mM of D-2HG were added to tissue culture media in these studies, and treatment with the latter concentration achieved intracellular levels of D-2HG similar to those observed with mutant IDH1/2 expression (Reitman ZJ 2011).

It is interesting to note that ROS levels were increased in D2HGDH knockdown cells. The D2HGDH enzyme reaction is $FAD^+$-dependent and produces FADH, as well as α-KG. It is possible that although knockdown of D2HGDH function with shRNA was not sufficient to promote 2-HG accumulation, it may have resulted in a reduction in FADH and increase in $FAD^+$, resulting in an increase in cellular oxidative stress, thus explaining the increased ROS levels observed. Alternatively, and given that increased ROS levels were also seen in scramble shRNA controls, it is possible that off target effects of the specific shRNAs used resulted in increased oxidative stress in these cells. It is unlikely that LV transduction itself resulted in an increase in oxidative stress as if this were the case then one would also have expected to see an increase in ROS in IDH1/2 mutant expressing LN18 cells treated with doxycycline, and this was not the case.

Also of note is the observation that *IDH2* expression was reduced in association with *D2HGDH* gene silencing. Furthermore, this effect appeared to be dependent on the efficiency of D2HGDH knockdown, with lower levels of *IDH2* expression seen with increased efficiency of D2HGDH knockdown. The mechanism by which a reduction in *D2HGDH* expression would result in down-regulation of *IDH2* gene expression is not immediately clear, although it is worth noting that cases of patients with hereditary D-2HGA with mutations in *IDH2* but wild-type *D2HGDH* have been described (Kranendijk M 2010) suggesting a possible link between the expression of these two genes. An alternative explanation would be that the reduction in *IDH2* expression occurred as a result of off target effects of the D2HGDH shRNA clone used, although if this was the case, one may also have expected a reduction in *IDH1* expression, which shows high sequence homology with *IDH2* to have occurred in D2HGDH knockdown cells. Furthermore the reduction in *IDH2* expression was reproduced in cells transduced with a second D2HGDH shRNA clone, whilst

the expression of two non-IDH related genes, *FOXA3* and *KLF5*, were unaltered, making the suggestion of off target effects less credible.

The possible association between *D2HGDH* and *IDH2* gene expression is interesting, and was further investigated in a *D2hgdh* knock-out mouse model, the results of which are given and discussed in chapter 5.

### 4.5.3 Expression of mutant IDH1 and IDH2 in LN18 cells results in an accumulation of 2-HG and a reduction in α-KG

The expression of mutant IDH1 or IDH2 in LN18 cells resulted in an 11-12 fold increase in 2-HG production, and a 50-60% decrease in α-KG production. These findings are consistent with those of other studies that have also demonstrated an increase in D-2HG, and/or a reduction in α-KG in association with expression of either IDH1 R132H or IDH2 R172K in various cell lines ***(Table 4-1)*** and also mirrors the accumulation of D-2HG observed in IDH1/2 mutant tumours *in vivo* (Dang L 2009, Gross S 2010, Ward PS 2010). Consequently the IDH1/2 mutant LN18 cell lines generated in this study serve as a reliable *in vitro* model of mutant IDH1/2.

**Table 4-1: Changes in D-2HG and α-KG in mutant IDH1 and IDH2 expressing *in vitro* models.**

| Author | IDH mutation expressed | Cell line | D-2HG increase (fold change) | α-KG reduction (%) |
|---|---|---|---|---|
| Zhao *et al*. 2009 | IDH1 R132H | U87MG | N/A | 50 |
| Dang *et al.* 2009 | IDH1 R132H | U87MG | 90 | N/A |
| | IDH1 R132H | LN18 | 200 | N/A |
| Ward *et al.* 2010 | IDH1 R132H | 293T | 100 | N/A |
| | IDH2 R172K | 293T | 100 | N/A |
| Xu *et al.* 2011 | IDH1 R132H | U87MG | 20 | 60 |
| Lu *et al.* 2012 | IDH2 R172K | 3T3-L1 | >80 | N/A |
| Koivunen *et al.* 2012 | IDH1 R132H | Immortalised human astrocytes | 13 | N/A |

### 4.5.4 Expression of mutant Idh1 and Idh2 in ES cells does not result in a significant accumulation of 2-HG or a reduction in α-KG production

The expression of mutant Idh1 or Idh2 in ES cells resulted in a 4-10 fold and 25-26 fold increase in 2-HG levels respectively, when compared to parental controls, but these changes were not statistically significant. Furthermore, in contrast to IDH1/2 mutant LN18 cells, no reduction in α-KG production was seen in Idh1/2 mutant ES cells. It is possible that this discrepancy occurred due to the fact that IDH1/2 mutations were over-expressed in LN18 cell

models but not in ES cell models. Alternatively, it is possible that these results demonstrate that the effect of mutant IDH1/2 expression differs in human and murine cell models. Additionally, given the large degree of error seen between duplicate experiments, it is possible that these results reflect a degree of inaccuracy which could be improved upon by repeating the experiment again. Nevertheless, in view of the fact that both 2-HG accumulation and reduced α-KG production have been shown to occur in association with mutant IDH1/2 activity (Dang L 2009, Zhao S 2009, Ward PS 2010, Xu W 2011, Koivunen P 2012, Lu C 2012), the mutant ES cells developed in this study may not serve as an optimal *in vitro* model of mutant IDH1/2.

### 4.5.5 Levels of TCA cycle metabolites are not altered by shRNA knockdown of IDH1/2 function or expression of mutant IDH1/2

Inhibition of IDH enzyme activity, through shRNA knockdown of *IDH1*, *IDH2* or *IDH3* gene expression did not alter cellular levels of TCA cycle metabolites. In the case of IDH1 knockdown, these findings may be expected, because IDH1 functions in the cytosol and although its enzyme substrates and products flux into the mitochondria, it plays a less obvious role in TCA cycle activity. However given the major function of IDH3 in the TCA cycle, and the contribution that IDH2 plays in regulating this process, it is perhaps surprising that down-regulation of this system was not seen in association with down-modulation of either *IDH2* or *IDH3*. Nevertheless, Macdonald *et al.* have also demonstrated, through assessment of concentrations of malate, that TCA cycle function remains unaltered in cell lines with knockdown of only one mitochondrial IDH. However, malate levels were lowered by 60% in glucose-stimulated cell lines with dual *IDH2* and *IDH3* knock down (MacDonald MJ 2013). This finding, which was seen only in the presence of knockdown of both mitochondrial IDHs and with glucose stimulation, suggests decreased flux through the TCA cycle, and demonstrates an inhibition of its normal function. Furthermore it illustrates that

although IDH3 is the primary catalyser of the conversion of isocitrate to α-KG in the TCA cycle under normal conditions, IDH2 can compensate when IDH3 activity is decreased. This supports the theory discussed in 4.5.1, that IDH enzymes can perform redundant functions with respect to α-KG formation and TCA cycle function, and gives an explanation as to why TCA cycle function remained intact in my IDH2 and IDH3 knockdown cells.

Additionally, given that TCA cycle metabolites are present in both the cytosol and mitochondria, and can flux between the two compartments, it may be necessary to measure mitochondrial and cytosolic levels separately in order to more accurately assess the effects of inhibiting the function of each enzyme independently. In my study however, no discrepancy was made between mitochondrial and cytosolic levels.

The levels of TCA cycle metabolites were also unchanged in IDH1/2 mutant LN18 and ES cell lines, with the exception of α-KG which was reduced in the former model as discussed in section 4.5.3. These findings conflict with those of Rietman *et al*., who demonstrated a significant depletion of TCA cycle metabolites, particularly fumarate (3.0- and 1.8-fold in IDH1 and IDH2 mutants respectively) and malate (5.6- and 2.2-fold in IDH1 and IDH2 mutants respectively), as well as citrate, *cis*-aconitate and α-KG, together with an accumulation of biosynthetic precursors, in human oligodendroglioma cell lines that expressed IDH1 R132H and IDH2 R172K (Reitman ZJ 2011). However my results are in keeping with the findings of both Dang *et al.* and Ward *et al.*, who also failed to demonstrate significant changes in TCA cycle metabolites in IDH1 mutant U87MG/LN18 cells and 293T cell lines respectively (Dang L 2009, Ward PS 2010). This discrepancy may suggest that the effect of mutant IDH1/2 expression on TCA cycle function varies between different cell lines, or it may be explained by the fact that in Rietman's study single clones of IDH mutant cells were selected for analysis, whilst in my study the unselected bulk cell population and

not single clones were used. Nevertheless, I could not prove a direct effect of mutant IDH1/2 activity on TCA cycle function. Consequently, and in contrast to observations described in *SDH* and *FH* mutant tumours, in which an accumulation of succinate and fumarate respectively support tumour formation (Pollard PJ 2005, Bardella C 2011, Frezza C 2011), I could not show the pathogenic effect of mutant IDH1/2 to result from an accumulation of TCA cycle metabolites, or to be due to metabolic dysregulation. It is still feasible however that IDH1/2 mutations may exert an effect on mitochondrial function through other mechanisms such as the inhibition by accumulated D-2HG of cytochrome *c* oxidase and ATP synthase, or due to alterations in cellular NADP+ and NADPH levels, or indeed as a result of reduced α-KG production.

### 4.5.6 HIF1α expression is increased in association with siRNA knockdown of *IDH1* and *IDH2* and shRNA knockdown of *IDH1*

Knockdown of *IDH1* and *IDH2* with siRNA resulted in an increase in HIF1α protein expression. Knockdown of *IDH1* with shRNA also resulted in an increase in both HIF1α target gene expression and HIF1α protein expression. However, shRNA knockdown of *IDH2* did not result in an increase in HIF1α expression either at an mRNA or protein level. This may be due to the fact that shRNA silencing of *IDH2* expression was less marked, and consequently IDH2 function was not reduced to a sufficient degree to alter HIF1α levels.

The association between IDH1 loss of function and HIF1α upregulation which I have demonstrated is consistent with findings published by Zhao et al. who showed that HIF1α protein levels were elevated in U87MG cells in response to shRNA-mediated knockdown of *IDH1* and that the expression of *GLUT1*, *PGK1* and *VEGF* was increased by between 2-5 fold through inhibition of IDH1 activity by oxalomalate (Zhao S 2009). Given that α-KG levels were reduced by IDH1 inhibition in this study, the authors concluded that HIF1α

upregulation resulted from the inhibition of HIF-PHD. In view of the fact that α-KG production was not reduced in my IDH1 knockdown cells it is unlikely that the inhibition of HIF-PHD was responsible for the upregulation of HIF1α expression demonstrated in my study, although an alternative mechanism such as an increase in oxidative stress, resulting from increased ROS and reduced NADPH may have been responsible. Indeed it has been well documented that HIF is stabilised by increased oxidative stress (Gerald D 2004, Jung SN 2008, Diebold I 2010, Reuter S 2010).

In view of the fact that α-KG levels were not reduced in my IDH knockdown cell lines, and 2-HG did not accumulate in D2HGDH knockdown cells, it is not possible to draw conclusions as to the role played by changes in the levels of these two metabolites in inhibiting HIF-PHD in IDH1/2 mutant tumours, using these cell lines.

### 4.5.7 HIF1α expression is increased in association mutant IDH1/2 expression in LN18 and ES cell lines

The expression of mutant IDH1/2 in my LN18 and ES cell lines resulted in HIF1α target gene up-regulation and an increase in HIF1α protein expression. Given that 2-HG was increased in both models, but a reduction in α-KG production could only be convincingly demonstrated in IDH mutant LN18 cells it is plausible that the upregulation of HIF1α occurred as a result of the inhibition of HIF-PHD by 2-HG. However it has been demonstrated that both exogenous D-2HG (Xu W 2011) and reduced levels of α-KG (Zhao S 2009) can inhibit HIF-PHD *in vitro*. I could have investigated these mechanisms further by treating IDH1/2 mutant cells, which had reduced α-KG levels, with exogenous α-KG and then re-measuring HIF1α expression, but whilst this method would serve to increase α-KG back to basal levels it may also simply counteract the competitive inhibitory effect of D-2HG on HIF-PHD. Alternatively I could have measured HIF1α expression in untransduced LN18 cells that had

been treated with exogenous 2-HG. Performing cell-free assays of HIF-PHD enzyme activity in the presence of varying levels of 2-HG and α-KG would also be beneficial. The potential roles of 2-HG accumulation and reduced α-KG production on HIF1α levels are further investigated in Idh1 mutant and D2hgdh knockout mouse models and discussed in Chapter 5.

Overall results from my IDH1/2 mutant cells lines support the theory proposed by others that the over-expression of HIF1α maybe a pathogenic mechanism in IDH1/2 mutant tumours (Zhao S 2009, Xu W 2011, Sasaki M 2012b). However, my findings conflict with evidence presented in other studies which suggests that D-2HG in fact exerts an agonistic effect on HIF-PHD, and that HIF1α levels are actually reduced by mutant IDH1 expression (Koivunen P 2012, Losman J 2013).

### 4.5.8 Mutant Idh1/2 expression in ES cells reduces 5hmC production suggesting an inhibition of TET function

The reduction in 5hmC content observed in ES cells expressing mutant Idh1 and Idh2 demonstrates that TET function may be inhibited in these cells. The variability in 5hmC content seen between each clone may reflect experimental variability or may be due to the presence of a variable number of non-recombinant cells present in the cell population of each cell clone.

These findings are consistent with those described by others, who also demonstrate a reduction in 5hmC content in both *in vitro* and *in vivo* models of IDH1 mutant glioma (Xu W 2011, Koivunen P 2012), and provide a plausible mechanism for the extensive DNA hypermethylation observed in IDH1/2 mutant tumours. Furthermore, the degree of reduction in 5hmC content observed in my IDH1/2 mutant ES cells is comparable with the 40-60% reduction in 5hmC observed in studies of TET1 deficient ES cells (Dawlaty MM 2013).

Given that I was unable to demonstrate a statistically significant accumulation of 2-HG or reduction in α-KG in my Idh1/2 mutant ES cells lines, I am unable to conclude whether TET activity was inhibited by changes in the levels of either of these metabolites. However, in view of the fact that TET has been shown to be inhibited *in vitro* by both exogenous D-2HG (Xu W 2011) and by over expression of wild-type IDH1 (Turcan S 2012), it is feasible that alterations in the level of either metabolite may affect TET function. These mechanisms were further investigated using *in vivo* models and are discussed in Chapter 5.

### 4.5.9 Mutant Idh1/2 expression in ES cells does not increase markers of histone methylation

I did not observe an increase in the histone methylation markers H3K4me3 and H3K9me2 in Idh1/2 mutant ES cells, and therefore cannot demonstrate an inhibition of JHDMs in these models. Although both H3K4, H3K9 and other histone methylation markers have been shown to be elevated in association with IDH1/2 mutant expression *in vitro* and in cell cultures treated with exogenous D-2HG (Chowdhury R 2011, Xu W 2011, Lu C 2012), global histone methylation was shown to be unchanged in the brains of brain-specific Idh1 mutant mice (Sasaki M 2012b), and H3K9 hypermethylation is found in both IDH1 mutant (Duncan CG 2012) and IDH1 wild-type gliomas (Venneti S 2013). Consequently the role played by the inhibition of JHDM function, and increased histone methylation in the pathogenesis of IDH1/2 mutant tumours remains unclear.

### 4.5.10 Mutant IDH expression and down-modulation of wild-type IDH expression reduces NADPH levels but does not consistently increase ROS levels

NADPH plays an important role in detoxification processes and in the scavenging of oxygen radicals, and NADPH levels have been shown to be reduced in human IDH1 mutant GBM

(Bleeker FE 2010). I have shown that levels of NADPH are reduced in association with both knockdown of IDH1/2 expression and with expression of mutant IDH1/2. Furthermore, down-modulation of IDH1/2/3 expression with siRNA increased ROS levels in U87MG cells, and knockdown of IDH1/3 with shRNA increased ROS levels in LN18 cells. Additionally, expression of IDH1 R132C in LN18 cells also resulted in an increase in ROS levels, although no increase was seen in IDH1 R132H mutant LN18 cells or in Idh1 or Idh2 mutant ES cells.

Oxidative stress has been shown to activate a variety of transcription factors (Reuter S 2010), and sustained oxidative stress can damage cell structure and functions and induce somatic mutations and neoplastic transformation (Khandrika L 2009) and has been linked to both cancer initiation and progression (Visconti R 2009). However, conflicting data exists as to the role of oxidative stress in the pathogenesis of IDH1/2 mutant tumours (Koivunen P 2012, Sasaki M 2012a, Sasaki M 2012b). My data supports the theory that both gain and loss of IDH1/2 function can affect intracellular oxidative state, in this case through changes in NADPH, and it is feasible that these changes may result in oxidative DNA damage and tumourigenesis in IDH1/2 mutant tumours. Furthermore, I was able to demonstrate that loss of wild-type IDH1/2 function results in an increase in intracellular ROS levels, although I was unable to demonstrate a consistent correlation between mutant IDH1/2 expression and increased ROS levels in this study.

### 4.5.11 Cellular proliferation rate is reduced by shRNA knockdown of IDH function and IDH mutant expression

shRNA induced knockdown of IDH1/2/3 activity led to a reduction in cellular proliferation rate. In the case of IDH2 and IDH3, this suggests that disruption of mitochondrial IDH enzyme function may reduce the efficiency of cellular metabolism and hence cell growth. Furthermore, given that substrates and products formed by the activity of cytoplasmic IDH1

can be imported into the mitochondria and used in the TCA cycle and other mitochondrial pathways, a reduction in IDH1 activity may also reduce cellular proliferation in the same way.

Expression of IDH1 R132H and R132C, and IDH2 R172K and R172M also resulted in a reduction in cellular proliferation, and this finding may provide an explanation as to why IDH1/2 mutant gliomas exhibit a relatively less aggressive phenotype, and are associated with a better prognosis than IDH1/2 wild-type tumours (Hartmann C 2009, Yan H 2009).

Given that flux through the TCA cycle remained unchanged in my IDH1/2/3 knockdown and IDH1/2 mutant cell lines, the disruption to cellular metabolism presumed to be responsible for the reduced growth rates observed, must have occurred due to another mechanism such as those discussed in section 4.5.4.

## 4.6 Conclusions

I have shown that the down-modulation of IDH function results in a reduction in NADPH levels, together with an increase in HIF1α expression and ROS levels, in the absence of changes in cellular α-KG or 2-HG levels.

Furthermore, I have demonstrated that a reduction in 5hmC and NADPH levels occurs, together with an increase in HIF1α expression and ROS levels, in association with the expression of mutant IDH1/2, in conjunction with 2-HG accumulation and a reduction in α-KG production.

It seems plausible therefore, that an increase in DNA methylation, HIF1α expression and oxidative stress may indeed play a role in the pathogenesis of IDH1/2 mutant tumours. In IDH1/2 mutant cells, the changes in 5hmC and HIF1α observed may occur through the

inhibition of the α-KG dependent enzymes TET and HIF-PHD, as a result of accumulated 2-HG or reduced levels of α-KG. However in IDH knockdown cell lines, in which α-KG and 2-HG remain at basal levels, the increase in HIF1α seen is likely to have occurred via a different mechanism, such as an increase in oxidative stress.

Changes in histone methylation or TCA cycle flux were not shown to occur as a consequence of IDH1/2 mutant expression and therefore the role of these mechanisms in the pathogenesis of IDH1/2 mutant tumours remain a matter for debate.

In view of the fact that I was unable to generate a cell model of IDH1/2 loss of function using shRNA mediated knockdown of IDH1/2, in which cellular α-KG levels were also reduced, I was unable to compare the effects of reduced α-KG production with those of 2-HG accumulation. Consequently I am unable to conclude, using cell models, whether gain or loss of IDH1/2 function is the dominant pathogenic mechanism promoting cellular transformation in IDH1/2 mutant tumours. However these mechanisms will be investigated further, using mouse models, as described in Chapter 5.

# 5. Chapter Five

## Development of an *Idh1* mutant mouse model of glioma

### 5.1 Introduction

Our understanding of the molecular mechanisms involved in glioma initiation and its progression from grade II to grade IV disease have in the past been hampered as a result of a lack of suitable experimental models. This is due in part to the fact that cell lines developed from human CNS tumours are difficult to establish in long-term cultures (Westphal M 1998, Westphal M 1998, Shiras A 2003) and frequently demonstrate a lack of growth after 10 to 15 passages (Westphal M 1998, Shiras A 2003). Furthermore, cell culture experiments have inherent limitations and are less reliable methods in the investigation of tumourigenic mechanisms such as invasion, angiogenesis and metastasis, or in the analysis of the tumour microenvironment (Hambardzumyan D 2011).

Genetically engineered mouse models of glioma, based on specific genetic alterations that are observed in human tumours, have been developed that recapitulate the histopathology and biology of gliomas and provide an experimental system to design and test novel therapeutic agents (Hambardzumyan D 2011). Indeed, genetically engineered models developed around key glioma signature mutations in *PDGFR* (Holland EC 1998, Uhrbom L 1998, Hede SM 2009, Becher OJ 2010), *EGFR* (Weiss WA 2003, Wei Q 2006, Zhu H 2009) and *NF1* (Reilly KM 2004, Zhu Y 2005, Alcantara Llaguno S 2009) genes and pathways have provided insights into many fundamental and mechanistic aspects of tumour initiation, maintenance and response to therapy, and have highlighted the role played by both oncogenes and tumour suppressor genes in these processes. A noteworthy finding in several of these studies was the importance of the subventricular zone (SVZ), the major stem and progenitor niche of adult

brains, in glioma initiation and maintenance. In the human brain, the SVZ is known to consists of three main cells: types A, B and C. Type B cells represent the adult neural stem cell (NSC) and express the astroglial marker GFAP and the NSC marker, nestin (Doetsch F 1999). B cells give rise to highly proliferative progenitor cells, type C cells, which retain multipotency. Type B and C cells can be defined by the expression of nestin, and nestin expression is lost following NSC differentiation, being retained postnatally only in neurogenic zones. Type C cells give rise to the more mature, transiently dividing progenitors or neuroblasts, type A cells (Alvarez-Buylla A 2004), which migrate in bundles through the RMS to the olfactory bulb, where they integrate in the cortical layers as new interneurons (Pincus DW 1997, Kukekov VG 1999, Curtis MA 2007). A similar hierarchical NSC system in the SVZ, and migratory pattern through the RMS to the olfactory bulb, has also been observed in the murine brain (Seri B 2004, Quiñones-Hinojosa A 2006). A growing body of evidence suggests that human GBMs originate from NSCs which have accumulated tumourigenic mutations over a period of time (Ignatova T 2002, Singh SK 2003, Tabatabai G 2011). These so called glioma-initiating cells (GICs) are thought in some cases to originate in the SVZ and several studies using murine glioma models have supported this theory (Zhu Y 2005, Alcantara Llaguno S 2009). Indeed the accumulation of cooperative oncogenic glioma-driving mutations occurring in type B and type C cells of the SVZ, have been shown to lead to tumour initiation in the early stages of gliomagenesis in *p53* mutant mouse models (Wang Y 2009). Furthermore, prospective histopathological analysis of pre-tumourigenic brains in genetically engineered mice carrying germline null mutations in both *p53* and *Nf1* also revealed that early abnormalities seen in mice genetically destined to develop glioma were found in cells residing in the SVZ. These early tumour cells were found to be highly infiltrative, were strongly Ki-67 positive, and expressed the stem cell markers nestin and GFAP, but did not express myelin basic protein (MBP), a marker of differentiation (Zhu Y

2005). Additionally, in studies of *Pten* haploinsufficient mice that developed high grade astrocytoma, pulse chase experiments with DNA synthesis-labelling agents such as bromodeoxyuridine, permitted visualization of stem-like cells migrating away from the SVZ, through the RMS to the olfactory bulb, and into surrounding regions such as the striatum and corpus callosum (Kwon CH 2008). It was subsequently shown that targeting inactivating mutations in *Nf1, p53* and/or *Pten* to NSCs/progenitors within the SVZ of mice using either the tamoxifen-inducible *nestin-creER*$^{T2}$ transgene or by stereotactic viral-mediated cre recombinase delivery to the SVZ, resulted in the development of grade III glioma or GBM in all adult mice subjected to SVZ targeting (Alcantara Llaguno S 2009), demonstrating that mutation of these glioma-relevant tumour suppressor genes in the SVZ is sufficient to induce tumour formation *in vivo*. Additionally, in mice with *Pdgfr*-induced gliomas, the microenvironment of the SVZ was shown to provide important signalling stimuli to cancer stem cells in this region. Indeed nitric oxide released from tumour endothelial cells is able to activate notch signalling in the stem cells of the SVZ, a mechanism shown also to occur in human *PDGFR*-amplified human gliomas (Charles N 2010).

At the time of starting this project, and still to date, no genetically engineered mouse model of *Idh1* mutant glioma has been developed. It was therefore desirable to develop such a model that reflected human disease, in order to study the pathogenesis of tumours harbouring these mutations from their earliest stage. Once developed, this model could also be used to determine the impact of therapeutic interventions such as mutant IDH1 inhibitors and conventional chemotherapy agents on resulting tumours.

Since starting this project an orthotopic xenograft mouse model of *Idh1* mutant glioma has been developed, by the injection of human grade III glioma cells in to the brains of non-obese diabetic/severe combined immune deficiency (NOD SCID) mice (Luchman HA 2012). Endogenous 2-HG accumulation was detectable in the xenograft serum, however this was not

a genetically engineered model, and the method of tumour initiation in xenograft mice differs considerably from spontaneous tumour development, and may not accurately represent many aspects of tumour biology. Furthermore, cancer formation and progression involve immune surveillance evading paradigms which select for cancer developmental processes that are not represented in an immunocompromised xenograft system. Additionally, DNA repair defects in immunocompromised mice have been shown to limit their capacity to tolerate therapeutic interventions (Biedermann KA 1991).

More recently, Sasaki *et al.* have developed and characterised the phenotype of conditional Idh1 R132H knock-in (KI) mouse models which expressed mutant Idh1 in either the brain (Sasaki M 2012b) or the hematopoietic system of mice (Sasaki M 2012a). Brain-specific expression of Idh1 R132H during embryogenesis using the *Nestin-Cre* transgene, resulted in cerebral haemorrhage as early as E15.5 and subsequent perinatal lethality of the mice, without any evidence of underlying malignancy. A reduction in α-kg production and an accumulation of 2-HG was however seen in *Idh1-KI* cells in this study, in conjunction with an increase in HIF1α target gene expression (most notably in *Vegf*), impaired collagen maturation and aberrant basement membrane formation, and the authors concluded that cerebral haemorrhage had most likely occurred as a direct result of 2-HG induced inhibition of collagen prolyl-hydroxylation (Sasaki M 2012b). Although it is possible that these brain-specific Idh1 R132H KI mice may have developed brain tumours if they had survived longer, the hematopoietic-specific Idh1 R132H KI mice had a normal life span, but similarly did not develop malignant disease. Furthermore, although the brain-specific expression of Idh1 R132H using *Gfap-cre* (G*fap-KI*) also resulted in cerebral haemorrhage and embryonic lethality in the majority of embryos, a proportion (8.3%) of *Gfap-KI* mice survived until adulthood, but also did not develop brain tumours (Sasaki M 2012b).

Two brain specific Idh1 R132H mutant mouse models were developed as part of this thesis, in work undertaken by myself and Dr C. Bardella in collaboration. The first model was developed by crossing *Idh1*$^{+/fl(R132H)}$ (*Idh1-KI)* mice with *Nestin-Cre* animals to generate *Nes-Cre*;*Idh1*$^{+/fl(R132H)}$ animals (*Nes-KI)*. Under the control of the *Nestin* promoter, Cre recombinase was expected to be expressed as early as E10.5 in NSCs, and to lead to near-complete recombination throughout the brain and spinal cord by E12.5 (Graus-Porta D 2001). However, as both we and Sasaki *et al.* subsequently demonstrated, the brain specific expression of mutant Idh1 in utero results in perinatal death, without the development of brain tumours. A second model was therefore developed, by crossing *Idh1-KI* mice with inducible *nestin-creER*$^{T2}$ mice to generate *nes-creER*$^{T2}$;*Idh1*$^{+/fl(R132H)}$ animals (*nesER*$^{T2}$*-KI*). *nes-creER*$^{T2}$ mice express a Cre/ERT2 fusion protein under the control of the rat *Nestin* promoter and following induction with tamoxifen, the *nes-creER*$^{T2}$ transgene directs *Cre* expression in *Nestin*-expressing cells. It was hypothesised that by delaying the expression of mutant Idh1 until after birth, we would be able to overcome the lack of embryonic viability observed in the non-inducible model.

Furthermore, in order to investigate the effect of constitutive expression of Idh1 R132H *in vivo*, we attempted to develop *Sox2-cre*;*Idh1*$^{+/fl(R132H)}$ (*Sox-KI*) mice, by crossing *Idh1-KI* mice with *Sox2-Cre* animals. *Sox-2* is expressed in pluripotent embryonic stem cells, and is a key transcription factor required for the maintenance of pluripotency in embryonic cells and morphogenesis of several epithelia (Driessens G 2011). *Sox2-Cre* mice express Cre recombinase under the control of the mouse SRY-box containing gene 2 promoter. Under the control of this promoter, Cre recombinase activity is expected to be expressed in epiblast cells at E6.5 (Driessens G 2011). In adult mice, *Sox2* is expressed in stem cells in a broad range of tissues including stratified and glandular epithelia of ectodermal and endodermal origin such as the glandular stomach, the oesophagus, the tongue, the brain, the trachea, and

the bronchiolar epithelium, as well as in sensory cells (Merkel and taste bud cells) and spermatogonial stem cells (Driessens G 2011).

A constitutive *D2hgdh*$^{fl/fl}$ knockout mouse (*D2hgdh* KO), predicted to accumulate 2-HG, was also used in this study in order to better evaluate the possible phenotypic effects given by 2-HG accumulation and to allow a comparison of these effects to be made with those seen in *Idh1-KI* mice, in which reduced levels of α-KG in addition to 2-HG accumulation were predicted to occur.

Germ line mutations in *FH* and *SDH*, which like *IDH1* encode key metabolic enzymes of the TCA cycle, have been implicated in the development hereditary renal cell carcinoma (Tomlinson IP 2002, Ricketts C 2008). It was hypothesised that mice expressing mutant Idh1 in kidney cells may develop renal tumours by mechanisms similar to those seen in *FH/SDH* mutant disease. Consequently we developed a kidney-specific *Ksp-Cre*;*Idh1*$^{+/fl(R132H)}$ mouse (*Ksp-KI*) by crossing *Idh1-KI* mice with *Ksp-Cre* animals.

Mutations in *IDH1* at R132 have also been described in a few cases of colon cancer (Sjöblom T 2006). Consequently we sought to develop a colon-specific, *Villin-Cre*;*Idh1*$^{+/fl(R132H)}$ mouse (*Vil-KI*) by crossing *Idh1-KI* mice with *Villin-Cre* animals, with the expectation that genetic recombination would occur in the entire intestinal epithelium by E12.5 (el Marjou F 2004) and could lead to the development of intestinal tumours.

## 5.2 Aims

The aim of this work was to develop a faithful mouse model of *Idh1* mutant glioma in order to study the effects of mutant Idh1 function in gliomagenesis from its earliest stages. It was also hoped that, should tumours develop in brain specific *Idh1-KI* mice, they could be used as a test system for anti-glioma directed therapies. Other tissue-specific models were also developed in order to investigate the possible role of mutant Idh1 in the development of both renal and colonic tumours.

A *D2hgdh* KO mouse was developed, with the aim that it would allow us to establish whether 2-HG accumulation alone can result in tumourigenesis, and also to allow a comparison of the phenotypic effects of 2-HG accumulation to be made with those seen in *Idh1-KI* mice, in which reduced levels of α-KG in addition to 2-HG accumulation were predicted to occur.

## 5.3 Methods

All animals were bred, housed and experiments carried out in accordance with the United Kingdom Animal Procedures act 1986. Animals were housed in the animal unit at The Wellcome Trust Centre for Human Genetics, Oxford.

### 5.3.1 Mouse breeding

Constructs to generate the *Idh1-KI* mouse were designed by Professor I. Tomlinson ***(Figure 5-1)***. *Idh1-KI* mice were then made using this construct by Caliper (Hopkinton, Ma), using cre-lox and Flp-frt technology.

**Figure 5-1: Construct design used to develop the *Idh1-KI* mice (16897 bp)**

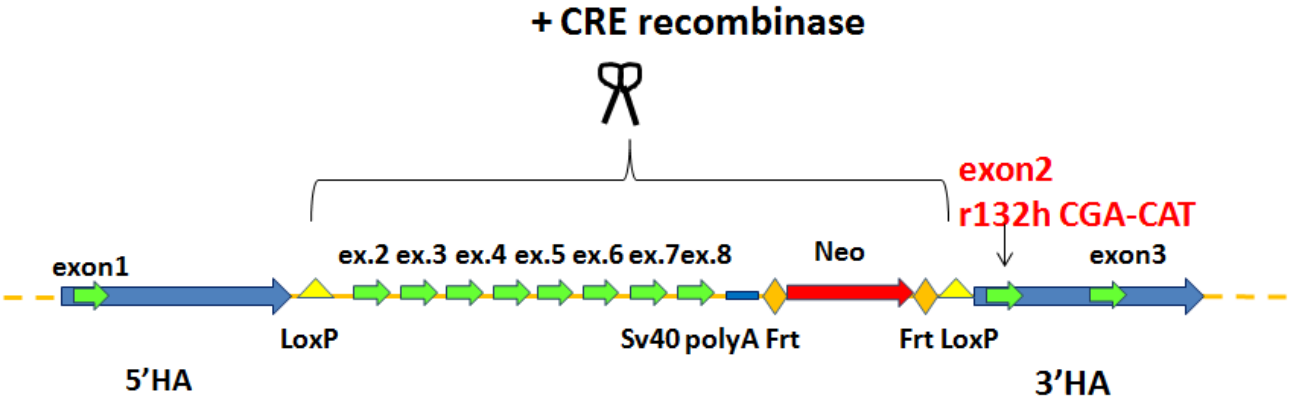


The expression of CRE recombinase led to the excision of the loxP-flanked WT exons 2-8, and subsequent recombination with the mutant Idh1 construct on exon 2, resulting in the expression of mutant Idh1 in relevant tissues.

In order to produce the initial, non-inducible *Nes-KI* mice on a C57BL/6J (BL6) background, male and female *Idh1-KI* mice were first backcrossed in order to obtain mice that were heterozygous *Idh1*$^{+/fl(R132H)}$ (*Idh1-KI*$^{+/fl}$) or homozygous *Idh1*$^{fl(R132H)/fl(R132H)}$ (*Idh1-KI*$^{fl/fl}$) mutant carriers. Attempts were then made to excise the loxP-flanked, Frt-flanked neomycin-resistance (Neo R) cassette of mutant mice, by inter-crossing *Idh1-KI* mice with a Flpo deleter mouse. *Idh1-KI* mice were then also inter-crossed with *Tp53*$^{fl/fl}$ (T*p53* KO) mice as it was hoped that by generating *Nes-KI;Tp53*$^{fl/fl}$ mice, this would further promote

tumourigenesis given that mutations in *Tp53* are over-represented in human gliomas with *IDH1/2* mutations. *Idh1-KI* and *Idh1-KI;Tp53*$^{+/fl}$ mice were then intercrossed with *Nestin-cre* animals to produce both *Nes-KI* and *Nes-KI;Tp53*$^{+/fl}$ mice.

*Idh1-KI* mice were also inter-crossed with *Sox2-cre* animals in order to produce simple KI (*Sox-KI*) mutants.

Inducible, *nesER*$^{T2}$*-KI* mice were subsequently developed by inter-crossing *Idh1-KI* and *Idh1-KI*;*Tp53*$^{+/fl}$ mice with *nestin-creER*$^{T2}$ animals. The expression of Cre recombinase was induced 6 weeks post partum by injecting mice intraperitoneally with 1mg of tamoxifen daily for 5 consecutive days, as outlined in Methods 2.16.1. *Idh1* wild-type (*Idh1*-WT) litter mates were also injected with tamoxifen in order to provide a control.

*Idh1-KI* mice were also crossed with *Ksp-Cre* and *Villin-Cre* animals in order to produce *Ksp-KI* and *Vil-KI* mice respectively.

The *D2hgdh* KO mouse was obtained from Dr. P. Pollard (Cancer Biology and Metabolism Group, Edinburgh Cancer Research UK Centre, Edinburgh, UK). In order to obtain the ablation of *D2hgdh*, the *LacZ* gene was inserted after the second exon of the *D2hgdh* sequence using conventional gene targeting, in order to replace exons 3,4,5 of *D2hgdh* leading to the expression of a shorter *D2hgdh* mRNA, which was predicted to be unstable and to produce a non-functional, truncated D2hgdh protein product in all murine tissues ***(Figure 5-2)***. This was demonstrated using PCR and qRT-PCR analysis.

**Figure 5-2: Construct design used to develop the *D2hgdh* KO mice (22314 bp)**

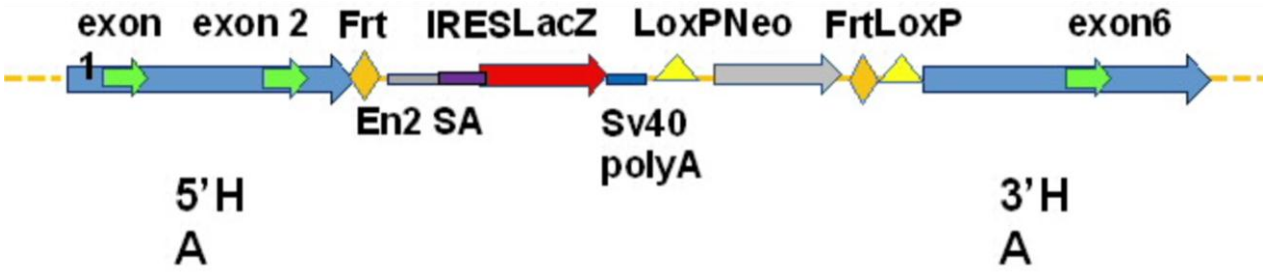


The targeting of the *D2hgdh* gene led to the replacement of exons 3-5 of *D2hgdh* (with respect to the ENSMUST00000112881 *D2hgdh* transcript; ENSMUSE00000659760, ENSMUSE00000659759 and ENSMUSE00000659758) with an FRT flanked IRES-lacZ-pA cassette which is linked to a strong splice acceptor signal.
This deletion allele provides a putative loss of function through the removal of a significant proportion of the coding region. Furthermore, the mutant transcript may be subject to nonsense mediated decay, however it is also possible that a truncated protein product corresponding to the upstream exons could continue to be expressed.
Mice heterozygous for this deletion allele have the potential to facilitate expression analysis of the *D2hgdh* transcript via the lacZ Knock-in. The complete reporter/selection cassette can be removed by Flp recombinase mediated deletion. The selection cassette component of the reporter/selection cassette can be removed by Cre mediated deletion.

The mice used in this study, their abbreviated name, and their intended purpose are summarised in the table below ***(Table 5-1)***

## 5.3.2 Genotyping

In the case of live or culled adult mice, DNA was extracted from earsnips as described in Methods 2.1.3. In the case of embryos, DNA was extracted from embryonic tail snips as described in 2.1.4. Genotyping was then performed appropriately for wild-type or mutant *Idh1*, *Tp53*, or *D2hgdh*, and for the presence or absence of Flp recombinase, and relevant Cre recombinases using PCR (primer sequences and appropriate conditions are illustrated in Appendix 1), followed by agarose gel electrophoresis, as outlined in Methods 2.4 and 2.5 respectively.

**Table 5-1: Genotype, abbreviated name and intended purpose of mice developed in this study**

| Genotype | Abbreviated name | Purpose |
|---|---|---|
| *Idh1*$^{+/fl(R132H)}$ | *Idh1-KI*<br><br>(heterozygous-*Idh1-KI*$^{+/fl}$ homozygous- *Idh1-KI*$^{fl/fl}$) | *Idh1* mutant mouse. To cross with specific Cre in order to develop tissue-specific *Idh1* mutant mice. |
| *Tp53*$^{fl/fl}$ | *Tp53* KO | To cross with *Idh1-KI* mice to further promote tumourigenesis |
| *Flp* | *Flp* | To excise the loxP-flanked, Frt-flanked Neo R cassette of mutant mice |
| *Idh1*$^{+/fl(R132H)}$;*Neo*$^{R+/fl}$ | *NeoR* | *Idh1* mutant mouse with NeoR cassette present |
| *Idh1*$^{+/fl(R132H)}$;*Neo*$^{R+/+}$ | *Neo-* | *Idh1* mutant mouse with NeoR cassette removed |
| *Nes-Cre*; *Idh1*$^{+/fl(R132H)}$ | *Nes-KI* | A non-inducible brain-specific *Idh1* mutant mouse to model *IDH1* mutant glioma |
| *nes-creER*$^{T2}$; *Idh1*$^{+/fl(R132H)}$ | *nesER*$^{T2}$*-KI* | An inducible brain-specific *Idh1* mutant mouse to model *IDH1* mutant glioma |
| *Sox-Cre*;*Idh1*$^{+/fl(R132H)}$ | *Sox-KI* | A simple KI *Idh1* mutant mouse to investigate the effect of constitutive expression of mutant Idh1. |
| *Villin-Cre*;*Idh1*$^{+/fl(R132H)}$ | *Vil-KI* | To investigate the effect of mutant Idh1 expression in the intestine. |
| *Ksp-Cre*;*Idh1*$^{+/fl(R132H)}$ | *Ksp-KI* | To investigate the effect of mutant Idh1 expression in the kidney. |
| *D2hgdh*$^{fl/fl}$ | *D2hgdh* KO | To investigate whether 2-HG accumulation alone can result in tumourigenesis and to compare the phenotypic effects of 2-HG accumulation with those seen in *Idh1-KI* mice. |

### 5.3.3 Analysis of embryos

Embryos generated from crosses between *Idh1-KI* mice and either *Flp* deleter mice, *Sox2-Cre* mice, or *Nestin-Cre* mice, were analysed for phenotype (size and gross morphological defects) and genotype. Pregnant females were sacrificed and embryos were removed at between E12.5 and E17. Phenotype was assessed, and DNA was extracted and genotyping was performed for *Idh1, Sox2-Cre, Flp, and Nestin-Cre*. In the case of embryos resulting from *Idh1-KI* x *Nestin-Cre* crosses, the head of each embryo was dissected from the body and photographed. Entire brains were then removed, frozen in liquid nitrogen and stored at -80ºC. Samples were subsequently prepared for UPLC-MS analysis as described in Methods 2.14.2, and analysed for α-KG and 2-HG levels as described in Methods 2.14.3.

### 5.3.4 Analysis of *nesER$^{T2}$-KI* mice

*nesER$^{T2}$-KI* mice were aged and sacrificed by cervical dislocation at 112 days (4 months), 194-228 days (6-7 months), and 228-245 days (7-8 months), or at the time that they became unwell. Genotyping was repeated from the earsnips of sacrificed animals as described in Methods 2.1.3, 2.4, and 2.5. The brain was removed and if grossly abnormal, was photographed. The brain was then either kept in its entirety for FFPE as outlined in Methods 2.16.2; dissected longitudinally into two segments one being kept for FFPE and the other half being frozen in liquid nitrogen; or dissected into 4 segments that were frozen in liquid nitrogen. Samples frozen in liquid nitrogen were stored at-80ºC prior to future use.

#### 5.3.4.1 Assessment of Idh1 R132H expression by direct sequencing

DNA and RNA were extracted from tissue taken from random areas of the brains of 4 month old *nes-creER$^{T2}$;Idh1-KI* mice and *nes-creER$^{T2}$;Idh1*-WT controls as described in Methods 2.1.4.2 and 2.2.2 respectively. RNA was reverse transcribed to cDNA as outlined in Methods

2.7. Direct sequencing of both cDNA and DNA was carried out, using primers designed to recognise codon 132 of *Idh1* as outlined in Methods 2.6.

This method was also undertaken using samples taken from the frontal, temporal and occipital areas of the brains of 8 month old animals, to confirm whether mutant Idh1 was expressed throughout the brain.

#### 5.3.4.2 Assessment of 2-HG, α-KG and other TCA cycle metabolites by UPLC-MS

Tissue metabolites were extracted from frozen samples as described in Methods 2.14.2, and analysed by UPLC-MS using the technique outlined in Methods 2.14.3.

#### 5.3.4.3 Assessment of the expression Hif1α target genes, neural stem cell markers and markers of differentiation

RNA was extracted from the brains of *nesER$^{T2}$-KI* mice that had been sacrificed at 4 or 8 months, and reverse transcribed to cDNA as outlined in Methods 2.2.2 and 2.7 respectively. The expression of the gene of interest was assessed by qRT-PCR as described in Methods 1.8. RNA was extracted from the brains of *Idh1*-WT mice of a similar age to be use as a control.

The expression of the Hif1α target genes *Glut1, Pgk1, Vegf,* and *Egln1* were assessed by qRT-PCR using TaqMan probes. *β-actin* was used as an endogenous control, because although *GAPDH* has been shown to be a reliable choice of housekeeping gene to determine the expression of hypoxia induced gene expression, its expression is regulated in part by HIF-1α (Said HM 2007).

The expression of neural stem cell gene markers *Nes, Smarca4, Sox2, Msi1, and Prom1* was assessed in 8 month old mice, whilst *Nes* expression was also assessed in 5 and 7 month old animals.

The expression of neural differentiation gene markers *Cnp, Gfap, Aqp4,* and *Cspg4* was assessed in 4 and 8 month old mice.

The expression of Hif1α, Phd2 and Nestin proteins were assessed using western blotting. Protein was extracted from the brains of *nesER$^{T2}$-KI* and *Idh1*-WT mice as described in Methods 2.10.3, and western blotting carried out as outlined in Methods 2.10.4.

#### 5.3.4.4 Assessment of TET function and *Rbp1* expression

DNA was extracted from the brains of 4, 7, and 8 month old *nesER$^{T2}$-KI* mice and *Idh1*-WT controls of similar age as outlined in Methods 2.1.4.2. Assessment of 5hmC and 5mC levels in the DNA samples was then carried out as outlined in Methods 2.15.

Given that hypermethylation of various different genes involved in RAR activation are known to be independently targeted in several IDH mutant tumour types (Semenza GL 2003) and that more specifically the promoter region of *RBP1* is hypermethylated in the vast majority of IDH mutant gliomas (Guilhamon P 2013), *Rbp1* expression was assessed in 4 and 8 month old *nesER$^{T2}$-KI* mice using the method outlined in section 5.3.4.3.

#### 5.3.4.5 Assessment of histone methylation

Histone methylation was assessed by measuring the expression of H3K9me3 and total H3 in protein extract from the brains of 8 month old *nesER$^{T2}$-KI* mice. Protein extraction and western blotting was carried out using the same method as outlined in section 5.3.4.3.

#### 5.3.4.6 Immunohistochemistry

Tissue samples were fixed in formalin and embedded in paraffin as outline in Methods 2.16.2. IHC was carried out on 4µm sections for Nestin, Caspase-3 and Phospho-histone H3 (PHH3) as described in Methods 2.9. 2.16.2

#### 5.3.4.7 Assessment of behaviour using the Open Field Test

The behaviour of *nesER$^{T2}$-KI* mice was assessed using an OFT as outlined in Methods 2.16.5. 4 *nesER$^{T2}$-KI* mice aged 4 months and 4 *Idh1*-WT controls of similar age were placed individually into the OF for 5 minutes. The following measurements were made: number of squares crossed; number of rears made; time spent in the centre square (seconds); number of faecal boli produced; frequency of urination.

#### 5.3.4.8 MRI imaging of the brain

MRI imaging was performed on 2 *nesER$^{T2}$-KI* and 2 *Idh1*-WT mice as outlined in Methods 2.16.6.

### 5.3.5 Analysis of *D2hgdh* KO mice

*D2hgdh* KO mice were sacrificed at 70 days old (2.5 months), and between 252-287 days old (9-10 months) by cervical dislocation. The following organs were harvested: brain; heart liver; kidney; spleen; lung; and skeletal muscle. Brain tissue was processed using the same methods as for *nesER$^{T2}$-KI* mouse brains. Other organs were dissected into 4 segments that were frozen in liquid nitrogen and then stored at -80ºC prior to future use.

The absence or otherwise of *D2hgdh* expression in the brain of these mice was assessed through PCR and qRT-PCR analysis of extracted RNA, following reverse transcription to cDNA as outlined in Methods 2.2.2, 2.4, 2.5 and 2.7 and 2.8, and using primers designed to span the deleted exons 2,3, and 4 of *D2hgdh*.

Tissue metabolites were extracted from various organs taken from 2.5 month old mice as described in Methods 2.14.2, and analysed by UPLC-MS using the technique outlined in Methods 2.14.3.

The expression of Hif1α target genes *Egln1*, *Egln3*, *Glut1*, *Pfk*, and *Pgk1* was assessed in all tissues harvested from 10 month old mice, as outlined in section 5.3.4.3. The expression of Hif1α and Phd2 protein in the brain was assessed by western blot as outlined in section 5.3.4.3.

The level of 5hmC and 5mC in the brains of 10 month old mice was assessed by HPLC as outlined in section 5.3.5.4.

In view of the fact that *IDH2* expression appeared to be affected by shRNA knockdown of *D2HGDH in vitro*, the expression levels of both *Idh1* and *Idh2* were measured by qRT-PCR in the brains of *D2hgdh* KO mice as outlined in section 5.3.4.3.

### 5.3.6 Histological assessment

4µm sections were made from FFPE brain tissue from *nesER$^{T2}$-KI*, *Idh1*-WT, and *D2hgdh* KO mice. Slides were stained with H&E out as outlined in Methods 2.16.3. Both H&E stained and unstained slides were examined by a pathologist (O. Ansorge) blinded to the genotype of the mice as outlined in Methods 2.16.4.

## 5.4 Results

### 5.4.1 Removal of the Neo R cassette of *Idh1-KI* mice

In order to excise the loxP flanked, Frt-flanked Neo R cassette of *Idh1-KI* mice, they were crossed with *Flp* deleter mice. In total 16 *Idh1-KI*$^{+/fl}$ x *Flp* crosses, and 1 *Idh1-KI*$^{fl/fl}$ x *Flp* cross were made. 74 live offspring resulted from these crosses (litter sizes ranged from 1 to 9), but none of the offspring were *Neo*-, including all 9 offspring resulting from the *Idh1-KI*$^{fl/fl}$ x *Flp* cross ***(Table 5-2)***.

**Table 5-2: Genotype of live-born mice from *Idh1-KI* x *Flp* crosses**

| Genotype | | | Total (mean) litter size |
|---|---|---|---|
| *Idh1*$^{+/+}$ | *Idh1*$^{+/fl(R132H)}$;*Neo*$^{R+/fl}$ | *Idh1*$^{+/fl(R132H)}$;*Neo*$^{R+/+}$ | |
| 40 (54%) | 34 (46.0%) | 0 (0%) | 74 (4.35) |

To investigate whether *Neo*- embryos developed lethal defects *in utero*, embryos from *Idh1-KI* x *Flp* crosses were analysed for both phenotype (size and gross morphological defects) and genotype. A male *Idh1-KI*$^{fl/fl}$ mouse and a female *Flp* mouse were crossed. The pregnant female was sacrificed at E12.5 and 8 embryos were removed. Additionally, a female *Idh1-KI*$^{+/fl}$ mouse and a male *Flp* mouse were crossed and the pregnant female was sacrificed at E14.5 and 9 embryos were removed. Each embryo was assessed for gross morphological defects, and the size of each embryo was assessed and labelled as small or normal based on the expected size for gestational age. DNA was extracted from embryonic tail snips and genotyping was performed for *IDH1* and Flp recombinase. 2 out of 8 embryos removed at E12.5 and 5 out of 9 embryos removed at E14.5 were considered to be small for their respective gestational age. However no correlation was found between the size of each embryo and their respective genotype. It is important to note however that contamination of

extracted embryonic DNA from the yolk sac, containing maternal DNA may have occurred thus making the genotyping results uninterpretable.

### 5.4.2 Analysis of the constitutive expression of mutant Idh1

In order to develop a simple KI *Idh1* mutant mouse and to investigate the effect of constitutive expression of mutant Idh1, *Idh1-KI* mice were crossed with *Sox2-Cre* mice. It was expected that Cre-mediated recombination would result in deletion of the floxed sequences, including the NeoR cassette, in *Sox2*-expressing tissues and would result in expression of mutant Idh1 in a broad range of tissues. In total 4 crosses were made between *Idh1-KI*$^{+/fl}$ and *Sox2-Cre* crosses. 22 live offspring resulted from these crosses (litter sizes ranged from 5 to 7) but no *Sox2-Cre;Idh1-KI* (*Sox-KI*) mice were generated ***(Table 5-3)***.

**Table 5-3: Genotype of live-born mice from *Idh1-KI* x *Sox2-Cre* crosses**

| Genotype | | | | Total (mean) litter size |
|---|---|---|---|---|
| *Idh1*$^{+/+}$ | *Sox2-Cre*;*Idh1*$^{+/+}$ | *Idh1*$^{+/fl(R132H)}$ | *Sox2-Cre*;*Idh1*$^{+/fl(R132H)}$ | |
| 12 (54.5%) | 10 (45.5%) | 0 (0%) | 0 (0%) | 22 (5.5) |

In order to understand if *Sox-KI* mice were not viable due to developmental or lethal defects occurring *in utero*, embryos resulting from crosses between *Idh1-KI* x *Sox2-Cre* mice were analysed at E13.5 and E16.5. All 9 embryos resulting from a cross between an *Idh1-KI*$^{+/fl}$ and a *Sox2-Cre* mouse were either *Idh1*$^{+/+}$ or *Sox2-Cre*;*Idh1*$^{+/+}$ and appeared to be of normal size for gestational age. Conversely 8 out of 9 embryos resulting from a cross between an *Idh1-KI*$^{fl/fl}$ and a *Sox2-Cre* mouse were *Sox2-Cre*;*Idh1*$^{+/fl(R132H)}$ and were small for gestational age, whilst 1 out of 9 embryos was found dead and genotyping was not performed because the DNA extracted from this embryo was degredated.

### 5.4.3 Analysis of non-inducible brain-specific expression of mutant Idh1in mice

In order to investigate the effects of the brain-specific expression of mutant Idh1, *Idh1-KI* mice were crossed with *Nestin-Cre* mice. In total, 6 crosses were made between *Idh1-KI*$^{+/fl}$;*Tp53*$^{+/fl}$ and homozygous *Nestin-Cre* mice. 15 live offspring resulted (litter sizes ranged from 1 to 4), but no *Nes-KI* mice were generated ***(Table 5-4)***. Of the live *Nes-Cre*;*Idh1*$^{+/+}$ offspring resulting from these crosses, there was a preponderance of *Nes-Cre*;*Idh1*$^{+/+}$;*Tp53*$^{+/+}$ (60%) mice compared to *Nes-Cre*;*Idh1*$^{+/+}$;*Tp53*$^{+/fl}$ (40%) mice.

**Table 5-4: Genotype of live-born mice from *Idh1-KI*$^{+/fl}$;*Tp53*$^{+/fl}$ x *Nestin-Cre* crosses**

| Genotype | | | | Total (mean) litter size |
|---|---|---|---|---|
| *Nes-Cre*; *Idh1*$^{+/+}$;*Tp53*$^{+/+}$ | *Nes-Cre*; *Idh1*$^{+/+}$;*Tp53*$^{+/fl}$ | *Nes-Cre*; *Idh1*$^{+/fl(R132H)}$;*Tp53*$^{+/+}$ | *Nes-Cre*; *Idh1*$^{+/fl(R132H)}$;*Tp53*$^{+/fl}$ | |
| 9 (60%) | 6 (40%) | 0 (0%) | 0 (0%) | 15 (2.5) |

An additional 3 litters were born from matings between *Idh1-KI*$^{fl/fl}$;*Tp53*$^{+/+}$ and homozygous *Nestin-Cre* mice but in each case the entire litter, all *Nes-Cre*;*Idh1-KI*$^{fl/fl}$;*Tp53*$^{+/+}$, were found to be dead at P0.

Consequently, to summarise the above results, no live born *Neo*$^{-}$, *Sox-KI,* or *Nes-KI* offspring were generated from *Flp* x *Idh1*$^{+/fl(R132H)}$;*Neo*$^{R+/fl}$, *Sox2-Cre* x *Idh1*$^{+/fl(R132H)}$;*Neo*$^{R+/fl}$, *Nes-Cre* x *Idh1*$^{+/fl(R132H)}$;*Neo*$^{R+/fl}$, or *Nes-Cre* x *Idh1*$^{+/fl(R132H)}$;*Neo*$^{R+/fl}$;*Tp53*$^{+/fl}$ crosses respectively, and it was not possible to remove the NeoR cassette by *Flp* or to activate mutant Idh1 by *Sox2*- or *Nestin-Cre* without causing embryonic or neonatal lethality.

In order investigate why live *Nes-KI* mice could not be generated, an analysis was performed of embryos resulting from *Idh1-KI* x *Nestin-Cre* crosses. 2 crosses were made between a male *Idh1-KI*$^{fl/fl}$ mouse and a female homozygous *Nestin-Cre* mouse. The pregnant female

from the first mating was sacrificed at E17 and 8 embryos were removed. The pregnant female from the second mating was sacrificed at E16.5 and again 8 embryos were removed. The resulting genotype of all 16 embryos was *Nes-Cre*;*Idh1*$^{+/fl(R132H)}$ (*Nes-KI*).

Macroscopically, 10 out of 16 *Nes-KI* embryos removed at E16 and E17.5 appeared to have grossly haemorrhagic areas within their brain parenchyma, an example of which is illustrated in ***Figure 5-3***.

**Figure 5-3: Haemorrhagic area compared in the brain of a *Nes-KI* embryo (E14.5) (left panel) versus *Idh1-WT* control (right panel).**

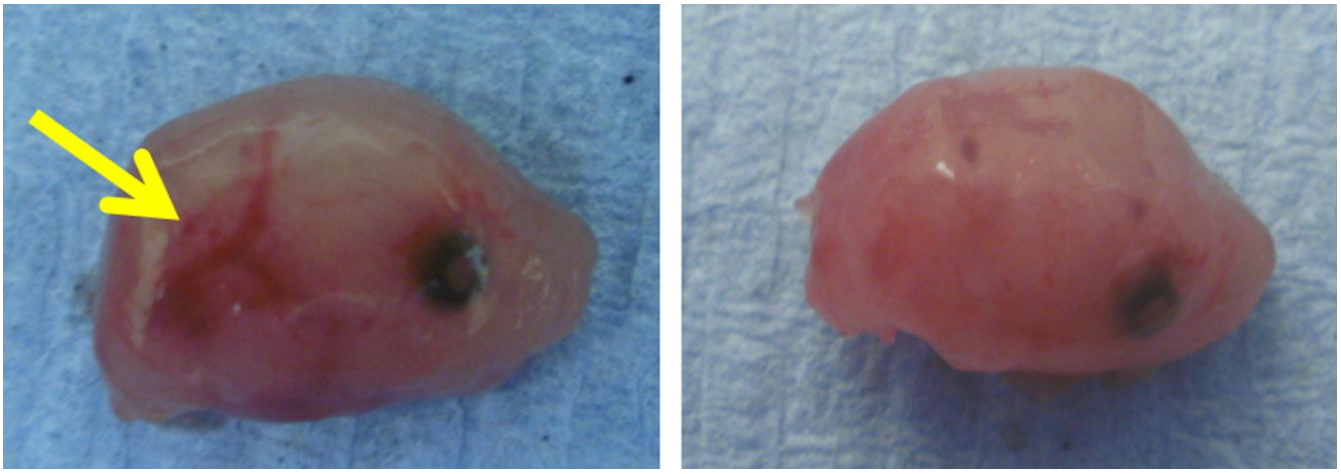

Haemorrhagic areas were noted in the brain parencyhma of 10 of 16 of the *Nes-KI* embryos

Furthermore, both 2-HG and α-KG levels were altered in the whole brains of *Nes-KI* embryos ***(Figure 5-4)***. 2-HG levels of between 1963 nmol/g and 260872 nmol/g (average 72612 [+/-71208] nmol/g, p=0.026), and α-KG levels of between 13.86 nmol/g and 107.73 nmol/g (average=59.5 [+/-26.5] nmol/g, p<0.01) were demonstrated. These results represent an average increase in 2-HG levels of 44-fold, and an average reduction in α-KG levels of 5.5-fold when compared to wild-type controls ***(Figure 5-5)***.

**Figure 5-4: α-KG and 2-HG levels in the brains of *Nes-KI* embryos by UPLC-MS**

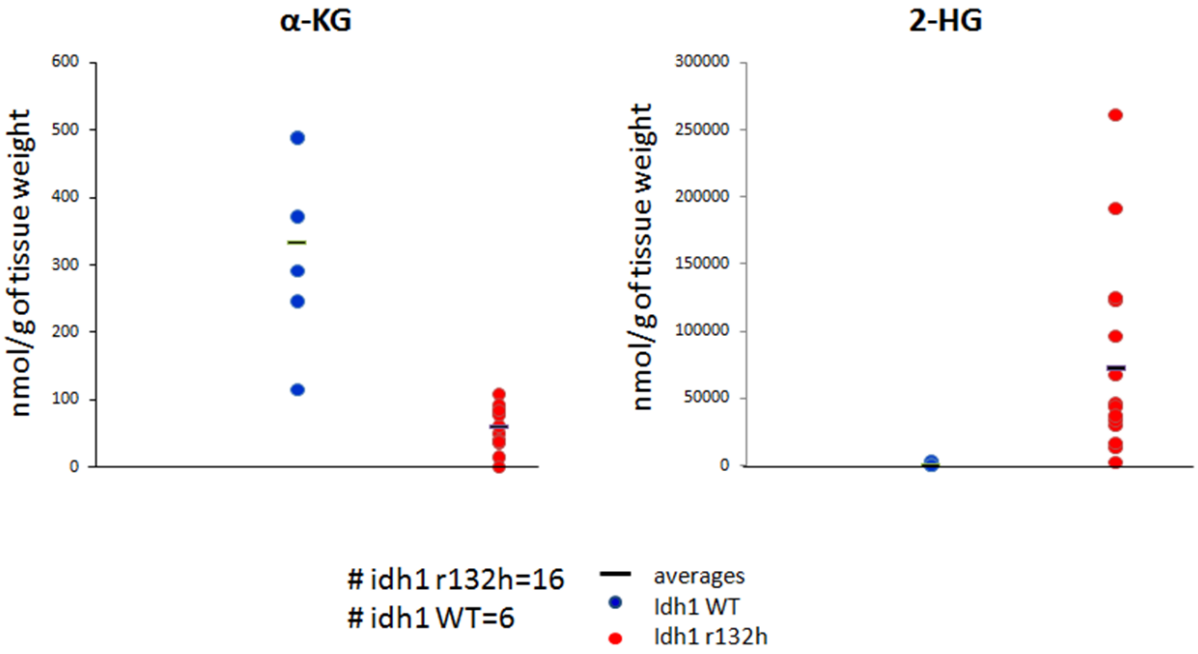


**Figure 5-5: Ratio of α-KG and 2-HG levels in the brains of *Nes-KI* embryos compared to *Idh1-WT* controls**

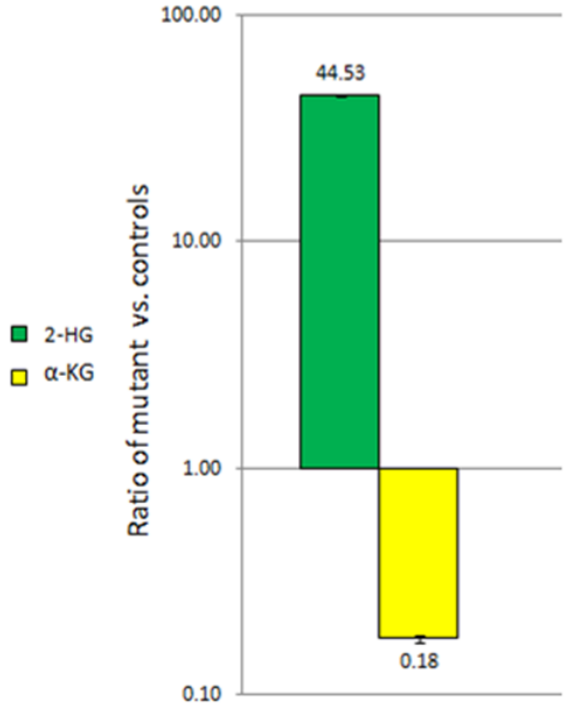


In addition to the reduction in α-KG seen, the levels of other TCA cycle metabolites, namely fumarate, succinate and malate were also found to be significantly reduced in the brains of *Nes-KI* embryos ***(Figure 5-6)***, possibly suggesting reduced TCA cycle function, and levels of

both glutamine and glutamate were also reduced ***(Figure 5-7)***. These results were found to be statistically significant using a two-tailed, unpaired *t*-test ***(Table 5-5)***.

**Figure 5-6: Levels of fumarate, succinate and malate in brains of *Nes-KI* embryos**

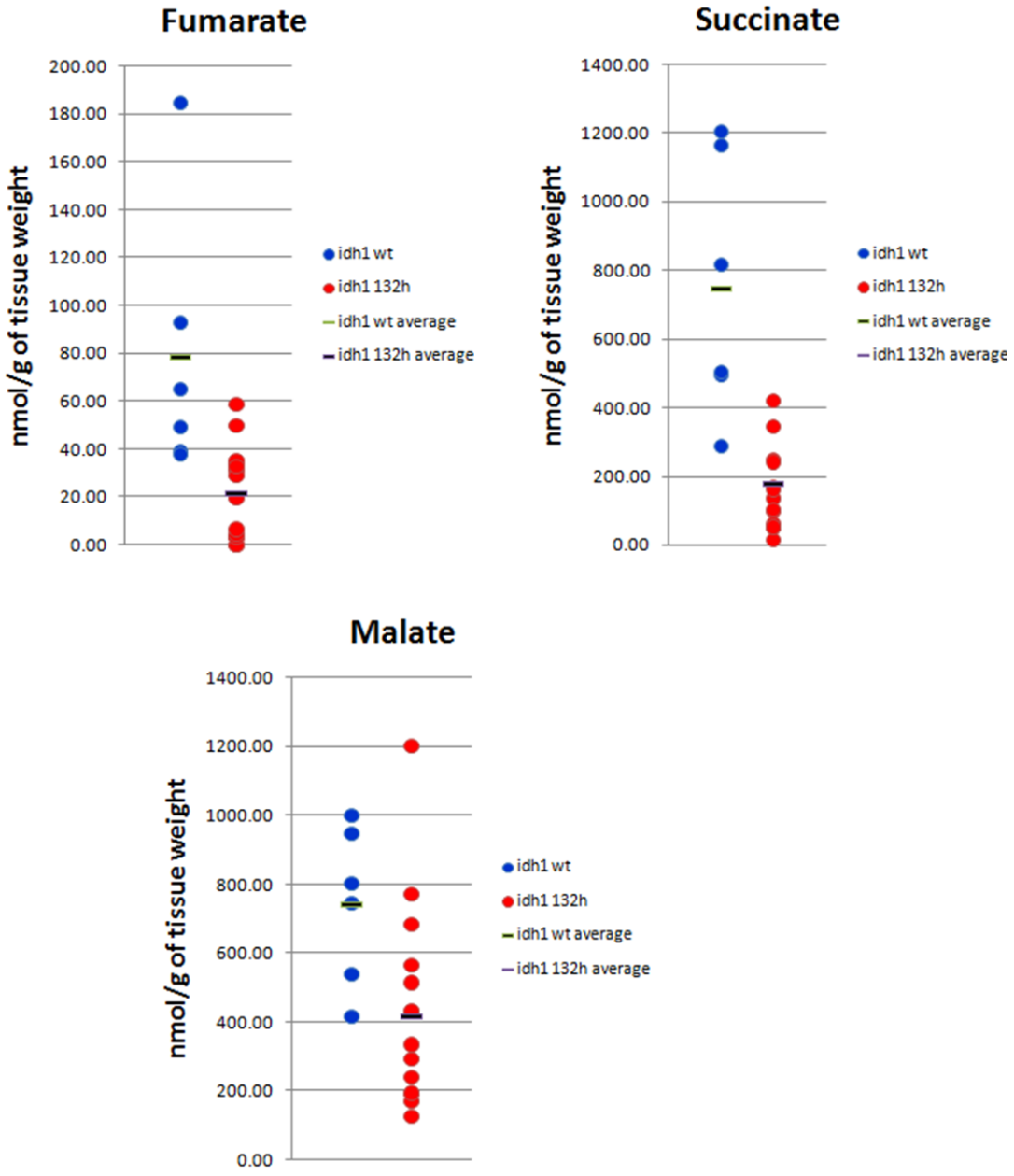

**Figure 5-7: Levels of glutamine and glutamate in brains of *Nes-KI* embryos**

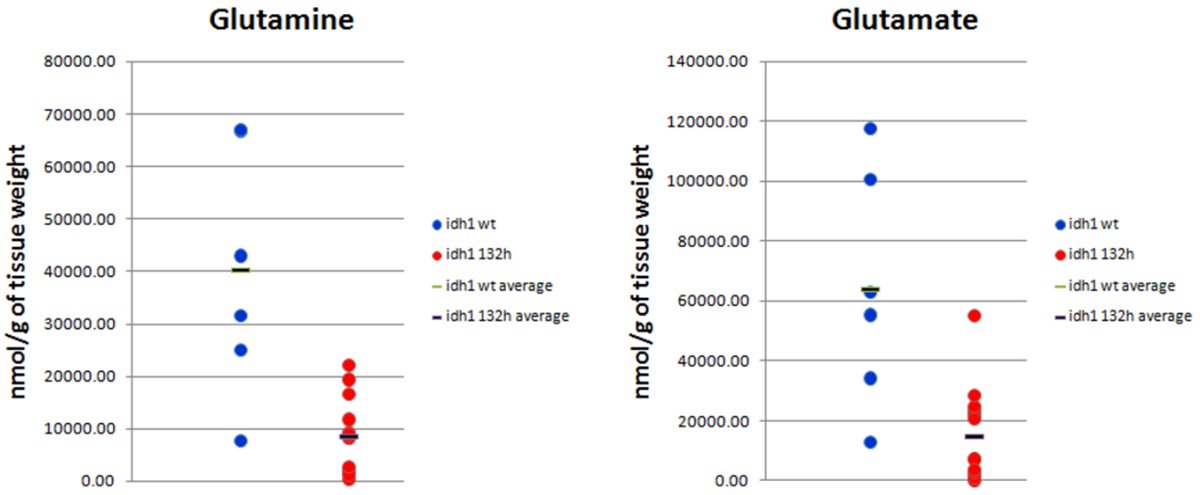


**Table 5-5: Levels of fumarate, succinate, malate, glutamine and glutamate in *Nes-KI* embryos compared to *Idh1-WT* controls**

| Metabolite | Average level in *Nes-KI* (nmol/g) | Average level in *Idh1-WT* (nmol/g) | Average difference (nmol/g) | p-value |
|---|---|---|---|---|
| **Fumarate** | 21.20 +/- 18.80 | 78.12 +/- 55.84 | -56.92 | <0.01 |
| **Succinate** | 175.6 +/- 156.32 | 745.24 +/- 379.56 | -569.64 | <0.01 |
| **Malate** | 414.33 +/- 283.29 | 739.82 +/- 227.38 | -325.49 | 0.02 |
| **Glutamine** | 8485.12 +/- 6673.10 | 40094.93 +/- 23644.65 | -31,609.81 | <0.01 |
| **Glutamate** | 14723.72 +/- 14585.55 | 63676.16 +/- 39401.97 | -48,952.44 | <0.01 |

### 5.4.4 Analysis of inducible brain-specific expression of mutant Idh1 in mice

Given that activation of mutant Idh1 in the brain using non-inducible *Nestin-Cre* was found to be lethal, a second brain-specific *Idh1* mutant mouse was developed, by crossing *Idh1-KI* mice with inducible *nestin-creER*$^{T2}$ mice to generate *nes-creER*$^{T2}$;*Idh1*$^{+/fl(R132H)}$ animals (*nesER*$^{T2}$*-KI*). It was hypothesised that delaying the expression of mutant Idh1 until after birth would enable viable adult *nesER*$^{T2}$*-KI* mice to be generated.

### 5.4.4.1 Expression of Idh1 R132H in the brain of *nesER$^{T2}$-KI* mice

In total, the ratio of live born *nes-creER$^{T2}$;Idh1$^{+/fl(R132H)}$* and *nes-creER$^{T2}$;Idh1$^{+/+}$* mice was 1:1. Expression of Idh1 R132H was demonstrated in the brains of *nesER$^{T2}$-KI* mice, but was not identified in *Idh1*-WT controls ***(Figure 5-8).*** Furthermore, mutant expression was seen throughout the entire brain ***(Figure 5-9)***.

**Figure 5-8: Expression of mutant Idh1 compared in the brains of 4 month old *Idh1*-WT and *nesER$^{T2}$-KI* mice (cDNA)**

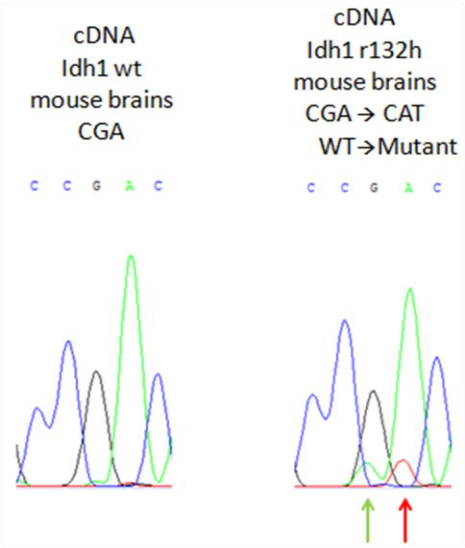


**Figure 5-9: Expression of mutant Idh1 in the frontal (A) temporal (B) and occipital (C) lobes of 9 month old *nesER$^{T2}$-KI* mice (cDNA)**

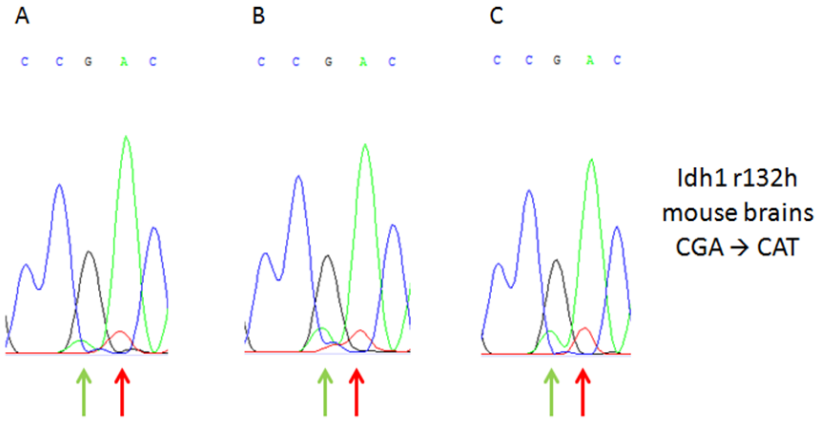


Sequencing analysis was repeated in 4 *nesER$^{T2}$-KI* and 4 Idh1-WT, and in several sites throughout the brain in order to verify these findings. I could have attempted to verify the

finding further using restriction study techniques or by sequencing of sub clones or by using deep sequencing techniques which would have added more reliability to the result. I was unable to use IHC to confirm expression of mutant Idh1 in the brain due to the lack of an available murine antibody directed against mutant Idh1. The advantages of using Sanger sequencing in this situation is that it is cost effective and relatively quick to perform. The disadvantages, as discussed above are that this technique lacks sensitivity and contamination of wild type samples with mutant tissue and vice-versa can lead to false positive results and false negative results respectively.

#### 5.4.4.2 Assessment of *nesER$^{T2}$-KI* mice behaviour using the open field test

It was expected that *nesER$^{T2}$-KI* mice may demonstrate increased signs of stress and anxiety, if they were becoming unwell as a result of mutant Idh1 activity. However, whilst there appeared to be differences in certain behavioural characteristics between *Idh1*-WT and *nesER$^{T2}$-KI* mice, *nesER$^{T2}$-KI* mice were actually demonstrated to be hyperactive with increased rapid exploratory behaviour showed by an increase in locomotion, with *nesER$^{T2}$-KI* mice crossing an average of 140.25 squares and *Idh1*-WT controls crossing 76.5 squares ($p<0.001$) and *nesER$^{T2}$-KI* mice performing an increased number or rears compared to *Idh1*-WT controls (38.5 vs 28.25, $p=0.08$) ***(Figure 5-10)***. N*esER$^{T2}$-KI* mice also appeared to demonstrate an increased level of thigmotaxis, an anxiety behaviour represented by the number of seconds spent in the centre square of the open field, but this result did not reach statistical significance (11.5 vs 20.75, $p=0.365$). The level of autonomic nervous system activity, characterised by the frequency of urination and defecation was not significantly different in mutant and control mice.

**Figure 5-10: Open field test results showing the average number of events observed in *NesER$^{T2}$-KI* mice compared to *Idh1*-WT controls**

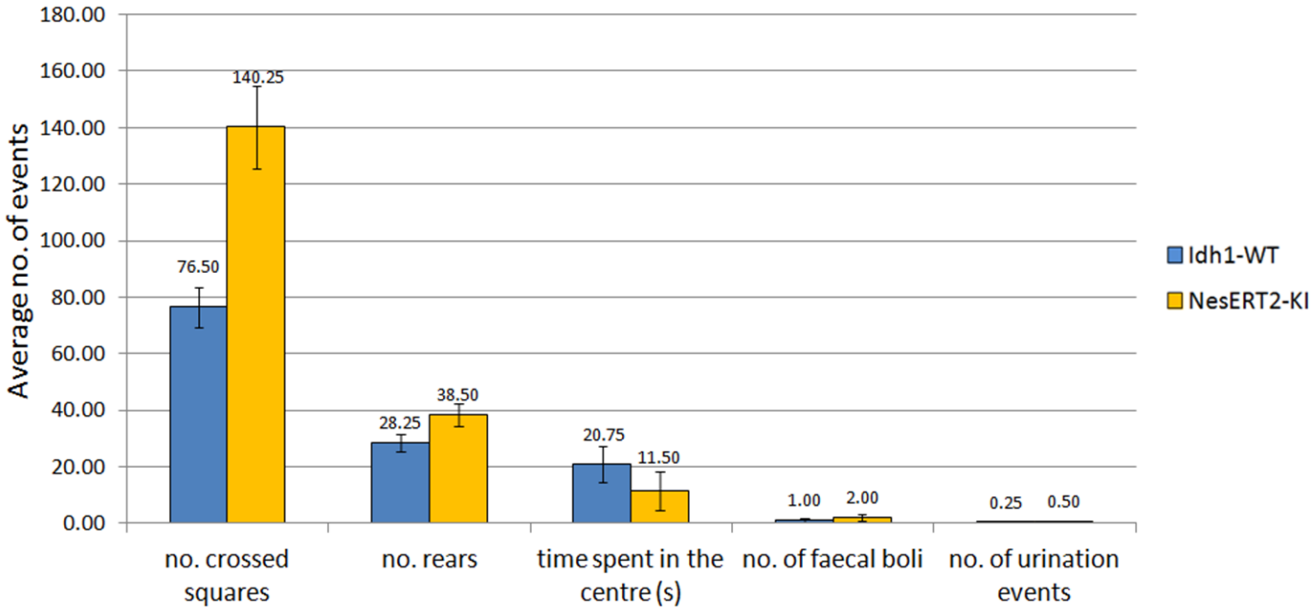


### 5.4.4.3 Hunching and weight loss observed in *nesER$^{T2}$-KI* mice

Hunching and weight loss were seen in 6/56 (11%) of the *Idh1-KI* mice generated in this study ***(Table 5-6)***, which necessitated them to be culled at between 108 and 620 days old ***(Table 5-7)***. 4/6 of these mice were *nes-creER$^{T2}$;Idh1$^{+/fl(R132H)}$* and resulted from crosses between *Idh-KI* and *nes-creER$^{T2}$* animals. The remaining 2/6 were *Idh1$^{+/fl(R132H)}$;Neo$^{R+/fl}$* and *Idh1$^{fl(R132H)/fl(R132H)}$;Neo$^{R+/fl}$* respectively, and resulted from inter-crosses between *Idh1-KI* mice, that had not been yet crossed with *nes-creER$^{T2}$* animals and in whom mutant Idh1 expression should therefore not yet have been activated. This phenotype had not been observed previously in other *Neo$^{R}$* mice perhaps because it occurs less frequently or takes longer to develop in these animals compared to *nesER$^{T2}$-KI* mice.

Indeed, although hunching an weight loss were seen in both *nesER$^{T2}$-KI* and *Neo$^{R}$* mice, overall it was more commonly observed in animals of the former genotype (4/19 [21%]) than the latter (2/19 [11%]). Furthermore, it took on average 328 days longer (p=0.017) for the

Neo$^{R}$ mice to demonstrate this phenotype (422-620 days, Mean=521 [+/-140]), than it did in *nesER$^{T2}$-KI* animals (108-279 days, mean=193 [+/-75]) ***(Table 5-7)***. Weight loss and hunching were not observed in any of 18 *Idh1*-WT mice resulting from *Idh1-KI* x *nes-creER$^{T}$* crosses, regardless of their *nes-creER$^{T}$* status.

Furthermore, in order to confirm weight loss in, both Idh1-WT and *nesER$^{T2}$-KI* mice were weighed. The weight of *nesER$^{T2}$-KI* mice (25-33g, mean=28 [+/-3.83]) was on average 6.25g (18.25%) less than that of *Idh1*-WT mice (31-37g, mean=34.25g [+/-3.20]), of the equivalent sex and age (p=0.046) ***(Figure 5-11)***.

**Table 5-6: Hunching and weight loss *nesER$^{T2}$-KI* and *Neo$^{R}$* mice**

| Genotype | No. mice hunched/weight loss | Total no. mice with this genotype | % with phenotype |
|---|---|---|---|
| *Idh1$^{+/+}$* | 0 | 7 | 0 |
| *nes-creER$^{T2}$; Idh1$^{+/+}$* | 0 | 11 | 0 |
| *Idh1$^{fl(R132H)/fl(R132H)}$; Neo$^{Rfl/fl}$* | 1 | 2 | 50 |
| *nes-creER$^{T2}$; Idh1$^{fl(R132H)/fl(R132H)}$* | 0 | 0 | 0 |
| *Idh1$^{+/fl(R132H)}$; Neo$^{R+/fl}$* | 1 | 17 | 6 |
| *nes-creER$^{T2}$; Idh1$^{+/fl(R132H)}$* | 4 | 19 | 21 |
| **Total** | 6 | 56 | |

**Table 5-7: Characteristics of mice that developed weight loss and hunching**

| Genotype | Litter no. | Sex | Age at tamoxifen injection (days) | Age at cull (days) |
|---|---|---|---|---|
| *Idh1$^{+/fl(R132H)}$; Neo$^{R+/fl}$* | 36A n.9 | m | n/a | 422 |
| *Idh1$^{fl(R132H)/fl(R132H)}$; Neo$^{Rfl/fl}$* | 4B n.6 | m | n/a | 620 |
| *nes-creER$^{T2}$; Idh1$^{+/fl(R132H)}$* | 57A n. 1 | f | 48 | 108 |
| *nes-creER$^{T2}$; Idh1$^{+/fl(R132H)}$* | 50A n.3 | f | 45 | 228 |
| *nes-creER$^{T2}$; Idh1$^{+/fl(R132H)}$* | 50B n.9 | m | 46 | 279 |
| *nes-creER$^{T2}$; Idh1$^{+/fl(R132H)}$* | 63B n.10 | f | 72 | 160 |

Figure 5-11: Average weight of *NesER$^{T2}$-KI* and *Idh1*-WT mice

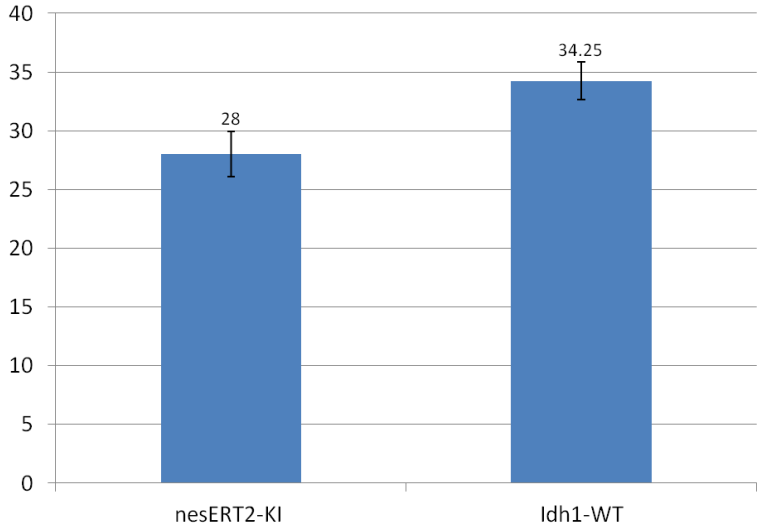


### 5.4.4.4 Hydrocephalus and ventriculomegaly observed in *nesER$^{T2}$-KI* mice

Macroscopic and microscopic abnormalities were observed in the brains of 6/19 (32%) *nesER$^{T2}$-KI* mice at post mortem. These abnormalities were also seen in 5/17 (30%) *NeoR* mice ***(Table 5-8)***.

**Table 5-8: Ventriculomegaly in *nesER$^{T2}$-KI* and NeoR mice**

| Genotype | No. mice with ventriculomegaly | Total no. mice with this genotype | % with phenotype |
|---|---|---|---|
| *Idh1$^{+/+}$; Neo$^{R+/fl}$* | 0 | 7 | 0 |
| *nes-creER$^{T2}$; Idh1$^{+/+}$* | 0 | 11 | 0 |
| *Idh1$^{fl(R132H)/fl(R132H)}$; Neo$^{Rfl/fl}$* | 0 | 2 | 0 |
| *Idh1$^{+/fl(R132H)}$; Neo$^{R+/fl}$* | 5* | 17 | 30 |
| *nes-creER$^{T2}$;Idh1$^{+/fl(R132H)}$* | 6** | 19 | 32 |
| **Total** | 11 | 56 | |

* 3 mice had not been injected with tamoxifen
** one mouse was also hunched/had weight loss

Macroscopically, these brains appeared larger than those of *Idh1*-WT controls, and were hydrocephalic in appearance, with both right and left frontal and parietal lobes appearing enlarged. Furthermore, these brains had a less rigid consistency, and the interhemispheric fissure appeared less well demarcated ***(Figure 5-12)***. In addition to being larger in

appearance, the weight of *nesER$^{T2}$-KI* brains (mean=0.6g [+/-0.014]) were found to be on average 0.1g (20%) more than those of *Idh1*-WT brains (mean=0.5g [+/-0.014]) when matched for age and sex (p=0.02) ***(Figure 5-13)***.

Microscopically, ventriculomegaly, defined by enlargement of the lateral ventricle, was also seen in these animals, but no gross tumour foci were seen in the surrounding brain tissue. Ventriculomegaly was also seen on MRI brain scans performed on 2 *nesER$^{T2}$-KI* mice but not in *Idh1*-WT mice ***(Figure 5-14)***. Further analysis of this MRI imaging is required to ascertain the cause of the hydrocephalus seen and to ascertain whether the hydrocephalus is restricted to the lateral ventricles or if indeed it occurs in other areas of the ventricular system. MRI analysis of the rostral migratory system would also be desirable to identify if macroscopic alterations occur in this region. Assessment of intracranial pressure would also help to identify the cause of the hydrocephalus seen.

**Figure 5-12: Abnormal appearance of the brain in *nesER$^{T2}$-KI* mice**

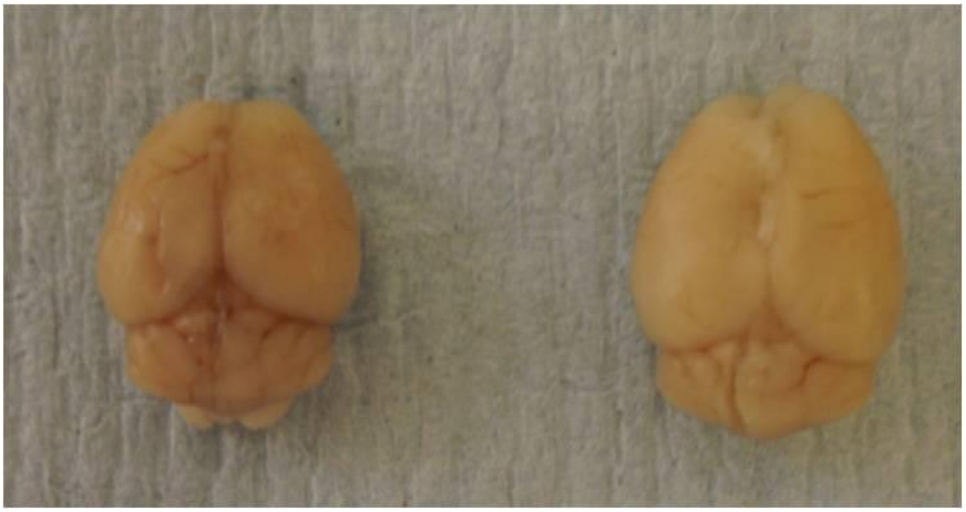

***Idh1*-WT** ***nesER$^{T2}$-KI***

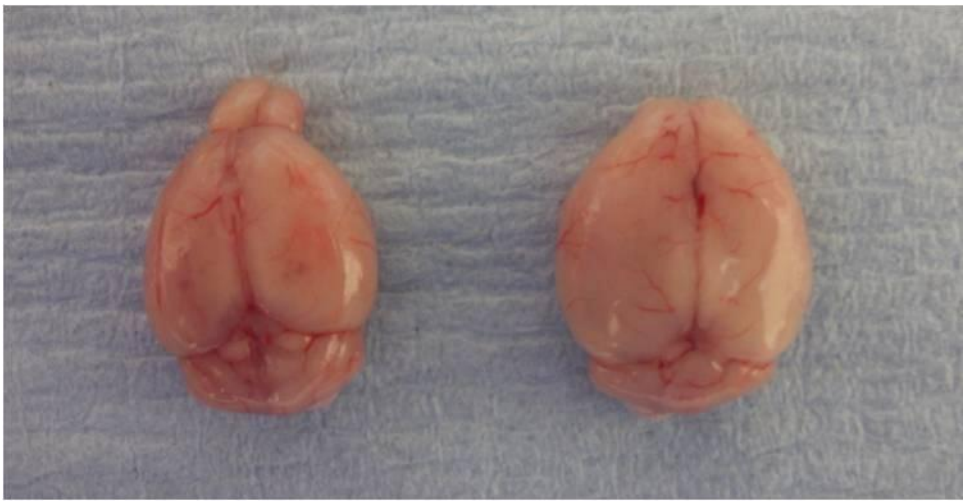

***Idh1*-WT** ***nesER$^{T2}$-KI***

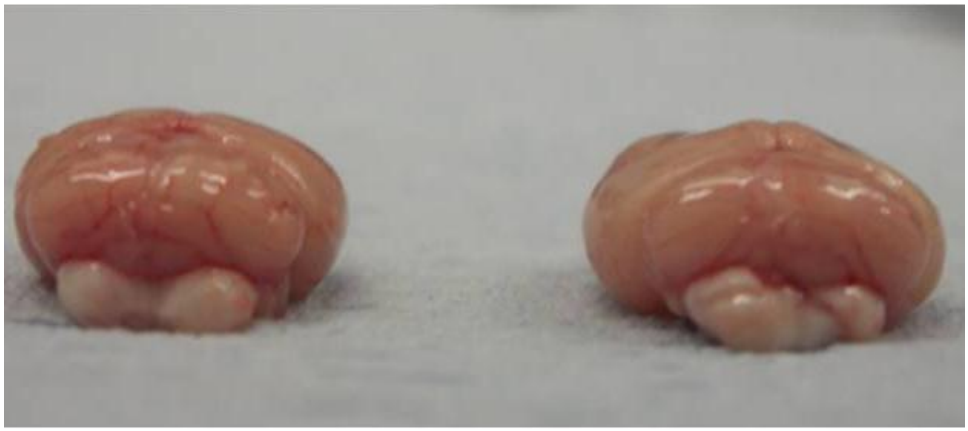

***Idh1*-WT** ***nesER$^{T2}$-KI***

**Figure 5-13: Weight of *nesER$^{T2}$-KI* brain compared to *Idh1*-WT brain**

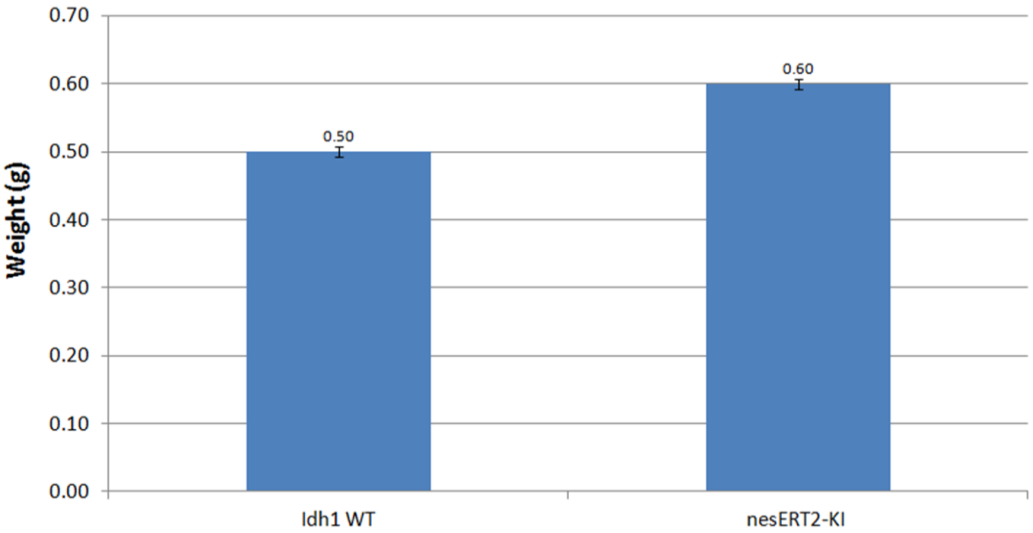


**Figure 5-14: MRI brain image showing ventriculomegaly in a *nesER$^{T2}$-KI* mouse (bottom left) compared to age matched *Idh1*-WT control (top right)**

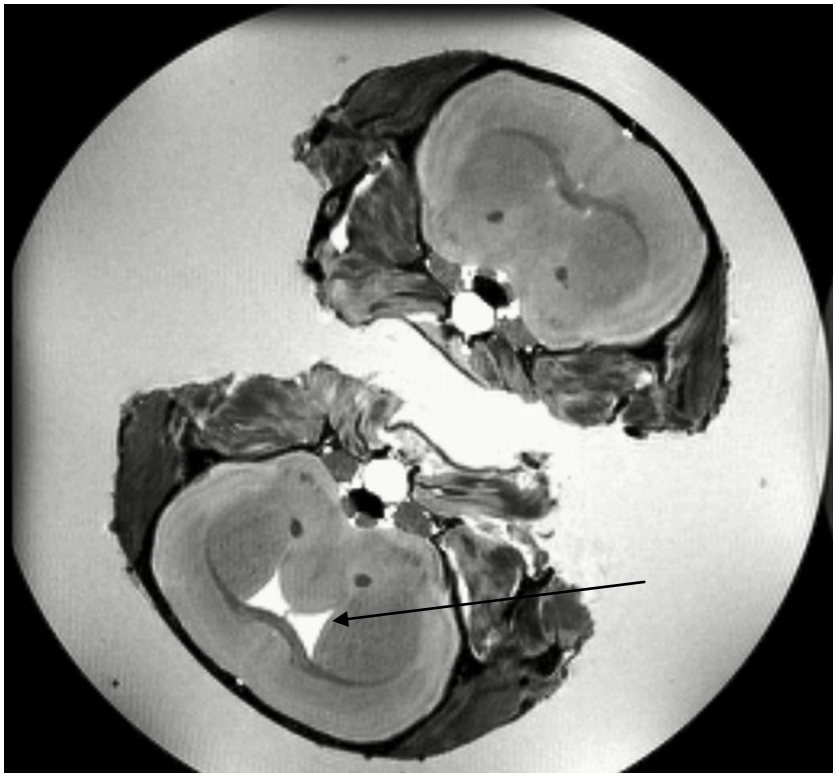

Images of coronal sections through the brain at the level of the lateral ventricles. The lateral ventricles appear white due to the presence of paraformaldehyde and are enlarged in the *nesER$^{T2}$-KI* mouse. This imaging was performed in 2 *nesER$^{T2}$-KI* and 2 *Idh1-WT* mice.

Hydrocephalus and ventriculomegaly were observed in both male and female *nesER$^{T2}$-KI* mice sacrificed at between 111 and 245 days old (mean 185), and in both male and female *NeoR* mice sacrificed at between 114 and 521 days old (mean 361), 3 of which had not

received tamoxifen injections. These features were not seen in *Idh1*-WT mice irrespective of their *nes-creER*$^{T2}$ status ***(Table 5-9)***.

**Table 5-9: Characteristics of *nesER$^{T2}$-KI* and NeoR mice that developed ventriculomegaly**

| Genotype | Litter no. | Sex | No. mice with ventricumegaly | Total no. of mice with this genotype | % with this phenotype | Age at tamoxifen injection (days) | Age at cull (days) |
|---|---|---|---|---|---|---|---|
| *Idh1*$^{+/fl(R132H)}$; *Neo*$^{R+/fl}$ * | 33a n.6 | f | 3 | 11 | 27 | n/a | 521 |
| *Idh1*$^{+/fl(R132H)}$; *Neo*$^{R+/fl}$ * | 37c n.3 | m | | | | n/a | 404 |
| *Idh1*$^{+/fl(R132H)}$; *Neo*$^{R+/fl}$ * | 33a n.12 | m | | | | n/a | 521 |
| *Idh1*$^{+/fl(R132H)}$; *Neo*$^{R+/fl}$ | 50b n.3 | f | 2 | 6 | 33 | 46 | 245 |
| *Idh1*$^{+/fl(R132H)}$; *Neo*$^{R+/fl}$ | 63c n.14 | m | | | | 48 | 114 |
| *nes-creER$^{T2}$;Idh1*$^{+/fl(R132H)}$ | 50b n.6 | f | 6 | 19 | 32 | 56 | 119 |
| *nes-creER$^{T2}$;Idh1*$^{+/fl(R132H)}$ | 50a n.3 | f | | | | 45 | 228 |
| *nes-creER$^{T2}$;Idh1*$^{+/fl(R132H)}$ | 50b n.5 | f | | | | 46 | 245 |
| *nes-creER$^{T2}$;Idh1*$^{+/fl(R132H)}$ | 63c n.13 | m | | | | 48 | 111 |
| *nes-creER$^{T2}$;Idh1*$^{+/fl(R132H)}$ | 49b n.13 | f | | | | 42 | 204 |
| *nes-creER$^{T2}$;Idh1*$^{+/fl(R132H)}$ | 49b n.5 | m | | | | 42 | 204 |

* not injected with tamoxifen

### 5.4.4.5 *Idh1*$^{fl(R132H)}$;*Neo*$^{R}$ is a leaky allele

Given that hydrocephalus and ventriculomegaly were observed in both *nesER*$^{T2}$*-KI* mice and *NeoR* mice, albeit at a much older age in the latter, this raised the possibility that the expression of Idh1 R132H in the brain was possible without the need for Cre-lox recombination to have occurred. In order to investigate this theory further both DNA and RNA were extracted from the brains of *NeoR* mice. RNA was retrotranscribed to cDNA, which together with extracted DNA was then sequenced in order to identify codon 132 of *Idh1*. RNA primers were designed so that they would not amplify DNA, and DNA primers were designed so they would not amplify RNA. Idh1 R132H expression was demonstrated in both DNA and cDNA sequences ***(Figure 5-15)***, indicating that *Idh1*$^{fl(R132H)}$;*NeoR* is a leaky allele. In view of this, only *Idh1*-WT mice and not *NeoR* mice were used as controls in subsequent experiments.

**Figure 5-15: Sequencing analysis showing expression of Idh1 R132H in DNA and cDNA extracted from brains of *NeoR* (left) and *NesER*$^{T2}$*-KI* mice (right)**

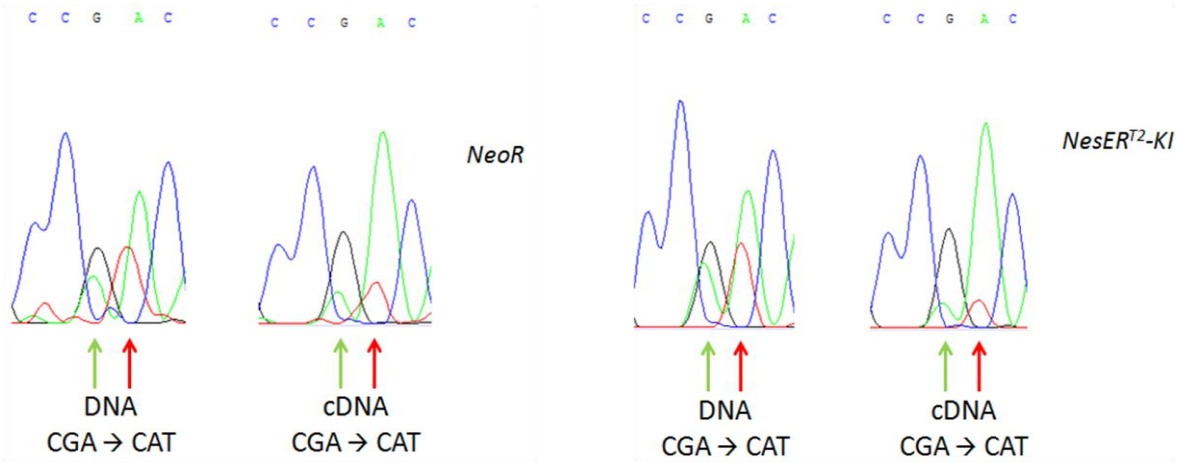


Given that *Idh1*$^{fl(R132H)}$;*NeoR* was found to be a leaky allele, this raised the possibility that Idh1 R132H could also have been expressed in other tissues without Cre-lox recombination having occurred. Consequently a full post-mortem examination was performed on *NesER*$^{T2}$*-KI* mice to investigate whether any changes were apparent in organs other than the brain as a

result of leaky expression of mutant Idh1. No gross macroscopic changes, or differences in weight were however seen in the liver, spleen, kidney, lung, or heart removed from *NesER$^{T2}$-KI* mice when compared to *Idh1*-WT controls ***(Figure 5-16)***.

**Figure 5-16: Images of the spleen, heart and kidney from *NesER$^{T2}$-KI* mice (left) compared to *Idh1*-WT control (right)**

**Spleen** **Heart** **Kidney**

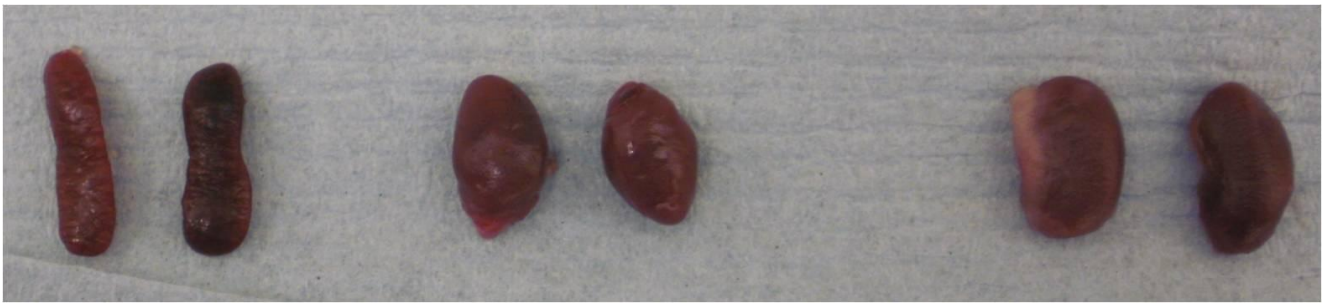

#### 5.4.4.6 Analysis of α-KG, 2-HG, and TCA cycle metabolites in *NesER$^{T2}$-KI* and NeoR mice

2-HG accumulated in the brains of *NesER$^{T2}$-KI* mice, whilst α-KG levels were reduced ***(Figure 5-17)***. In 4 month old *NesER$^{T2}$-KI* mice, 2-HG levels were increased by 38.15 nmol/g (range=43.86-96.38, mean=78.65 nmol/g [+/-19.5], p<0.01) when compared to *Idh1*-WT animals (range=31.0-51.13, mean=40.5 [+/-8.3]), whilst in 8 month old *NesER$^{T2}$-KI* mice, 2-HG levels were increased by 72.24 nmol/g (range=136.5-165.8, mean=147.69 [+/-12.78], p<0.01) compared to *Idh1*-WT controls (range=61.96-89.25, mean=75.45 nmol/g [+/-13.65]).

α-KG levels were reduced by 2.8 nmol/g (range=4.81-19.75, mean=12.67 [+/-5.53], p=0.45) in 4 month old *NesER$^{T2}$-KI* mice when compared to *Idh1*-WT mice (range=12.14-19.38, mean=15.47 [+/-3.66]), whilst in 8 month old *NesER$^{T2}$-KI* mice a 2.08 nmol/g reduction in α-KG (range=3.32-6.05, mean=4.37 [+/-1.47], p=0.12) was seen when compared *Idh1*-WT controls (range=5.18-7.25, mean=6.45 [+/-1.11]).

These results represent an average increase in 2-HG of 1.94-fold and 1.96-fold, and an average reduction in α-KG of 1.2-fold and 1.5-fold, in 4 and 8 month old mice respectively. The differences observed were not as considerable as the 44-fold increase in 2-HG or the 5.5-fold decrease in α-KG seen in the brains of non-inducible *Nes-KI* embryos ***(Figure 5-18)***. Furthermore, unlike in *Nes-KI* embryos, the reduction in α-KG seen in the brains of *NesER$^{T2}$-KI* mice did not reach statistical significance, possibly due to the fact that mutant Idh1 expression was less marked in *NesER$^{T2}$-KI* mice, or due to the fact that there are likely to be a lower proportion of nestin expressing cells in the brain of these mice.

**Figure 5-17: α-KG and 2-HG levels in 4 and 8 month old *NesER$^{T2}$-KI* mice compared to Idh1-WT controls**

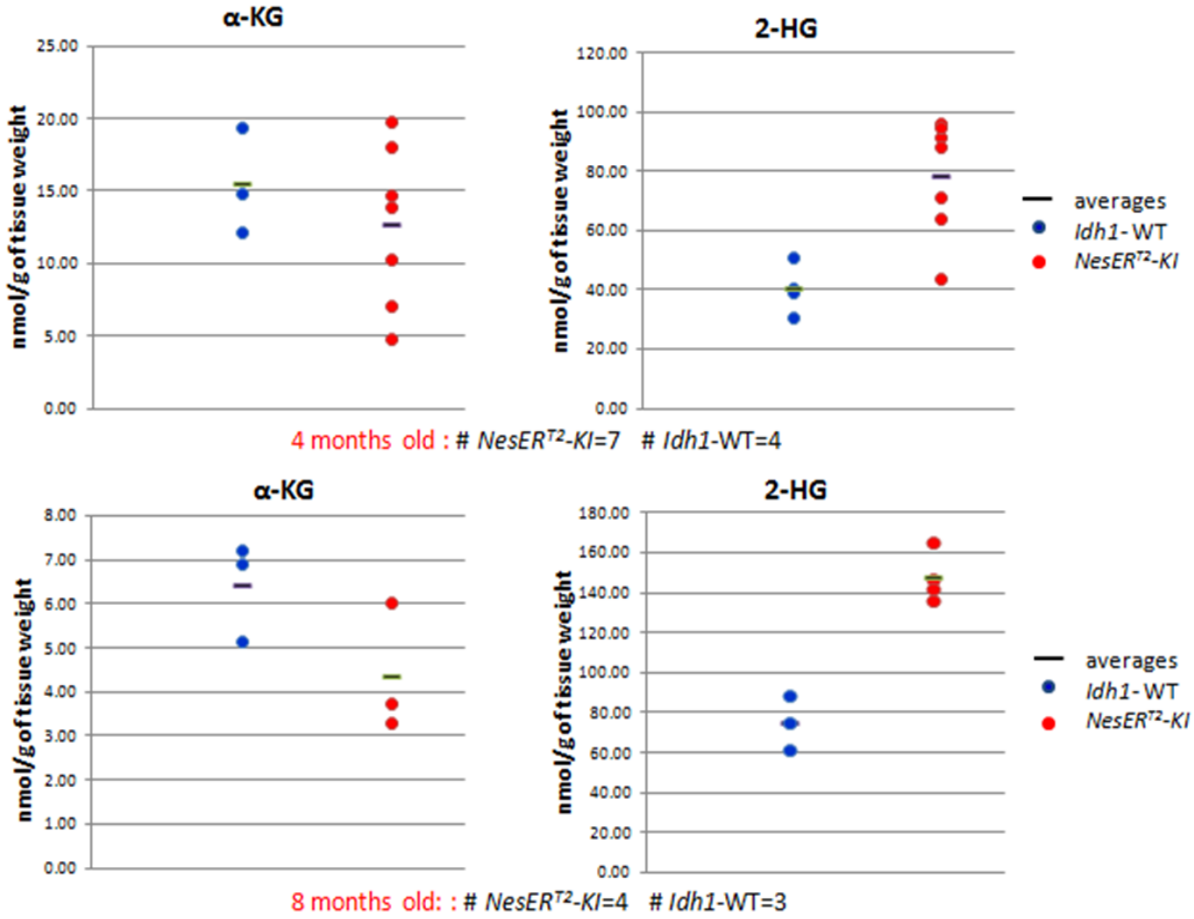

**Figure 5-18: Relative levels of 2-HG and α-KG in the brains of non-inducible *Nes-KI* and inducible *NesER$^{T2}$-KI* mice**

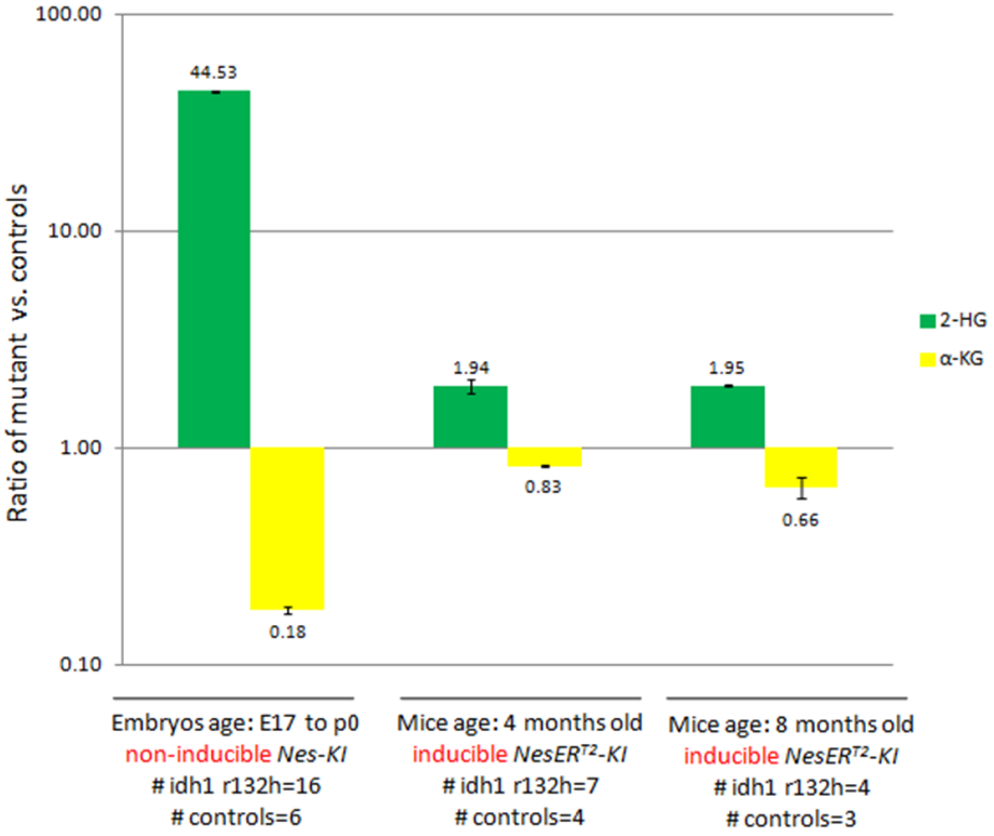


Additionally, although a small reduction in fumarate was detected in the brains of both 4 and 8 month old *NesER$^{T2}$-KI* mice ***(Figure 5-19)***, this did not reach statistical significant ***(Table 5-10)***, and levels of other TCA cycle metabolites were not reduced. Consequently, in contrast to *Nes-KI* mice, the levels of TCA cycle metabolites were not markedly reduced in *NesER$^{T2}$-KI* animals. Furthermore glutamine and glutamate levels were also unchanged.

**Figure 5-19: Fumarate levels in the brains of 4 and 8 month old *NesER$^{T2}$-KI* mice compared to *Idh1*-WT controls**

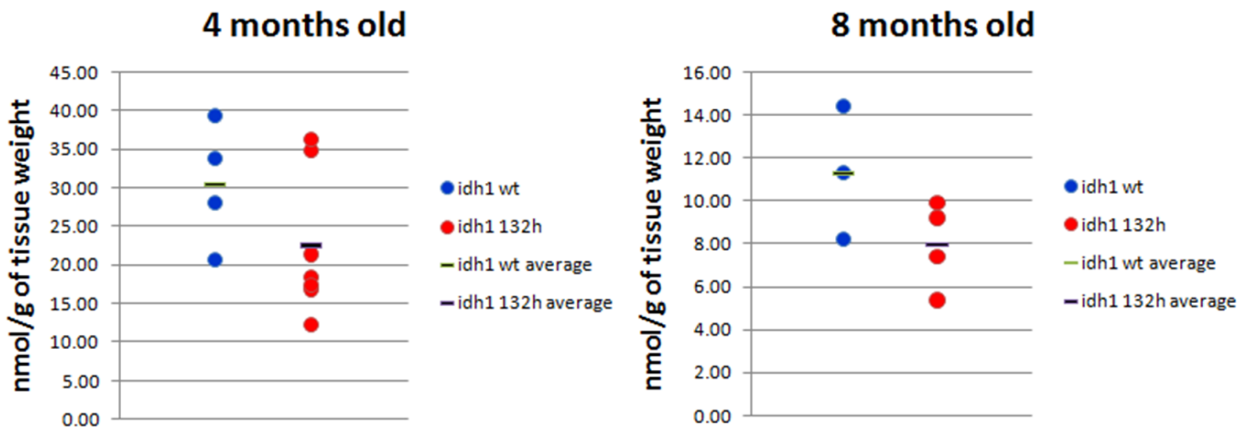


**Table 5-10: Unpaired t-test analysis of fumarate data**

| age (mths) | P value | significant | t-score | df | standard error of difference |
|---|---|---|---|---|---|
| 4 | 0.19 | no | 1.414 | 9 | 0.648 |
| 8 | 0.1456 | no | 1.73 | 5 | 0.223 |

In view of the fact that Idh1 R132H expression was also demonstrated in the brains of *NeoR* mice, the level of 2-HG and α-KG in the brain of these animals was also measured ***(Figure 5-20)***. 2-HG was found to accumulate in both 8 month old (mean=193.19 nmol/g [+/-86.4], p=0.025) and 17 month (mean=177.46 nmol/g [+/-39.9], p<0.01) old *NeoR* mice when compared to *Idh1*-WT controls (mean=94 nmol/g [+/-22.89]), and the level of 2-HG accumulation was comparable to that seen in 8 month old *NesER$^{T2}$-KI* mice (2.0-fold vs 1.9-fold vs 1.96-fold respectively). α-KG levels were also reduced by an average of 1.38 nmol/g in 17 month old *NeoR* mice (mean=3.45 nmol/g [+/-1.17], p=0.39) compared to *Idh1*-WT controls (mean=4.83 nmol/g [+/-1.95]) this reduction was not statistically significant, and no reduction in α-KG was seen in 8 month old *NeoR* mice. Although the sample number included in this analysis were small, these findings suggest that whilst 2-HG may accumulate at a similar rate in the brains of both *NesER$^{T2}$-KI* and *NeoR* mice, it takes longer for a detectable reduction in α-KG production to occur in the latter. This may explain why it

generally took longer for a phenotype to be observed in *NeoR* mice compared to *NesER$^{T2}$-KI* mice; however an analysis of a greater number of *NeoR* mice would be required in order to confirm this theory.

**Figure 5-20: 2-HG and α-KG levels in the brain of *NeoR* mice compared to *Idh1*-WT controls**

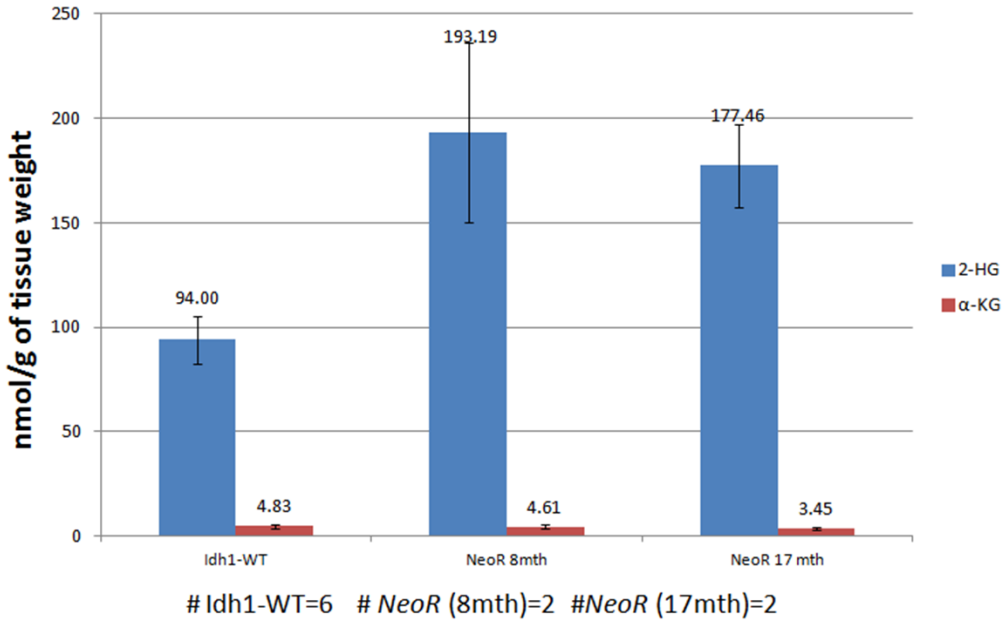


### 5.4.4.7 Hif1α target gene expression in *NesER$^{T2}$-KI* mice

The mRNA expression levels of the Hif1α target genes *Glut1*, *Pgk1*, and *Vegf* were unchanged in 8 month old *NesER$^{T2}$-KI* mice by qRT-PCR analysis ***(Figure 5-21)***. Furthermore no reduction in Hif1α protein expression was seen by western blot ***(Figure 5-22)***. However, the expression level of *Egln1* was reduced by 71% ($p<0.001$). *Egln1* encodes for Phd2, and is itself a Hif1α target gene that is upregulated in hypoxia. Given that a reduction in *Egln1* expression could lead to a reduction in Phd2 protein expression and subsequent stabilisation of Hif1α, Phd2 protein expression was measured by western blot but no reduction in Phd2 protein expression was seen ***(Figure 5-23).***

**Figure 5-21: Fold change in mRNA expression of Hif1α target genes in the brain of *NesER$^{T2}$-KI* mice by qRT-PCR**

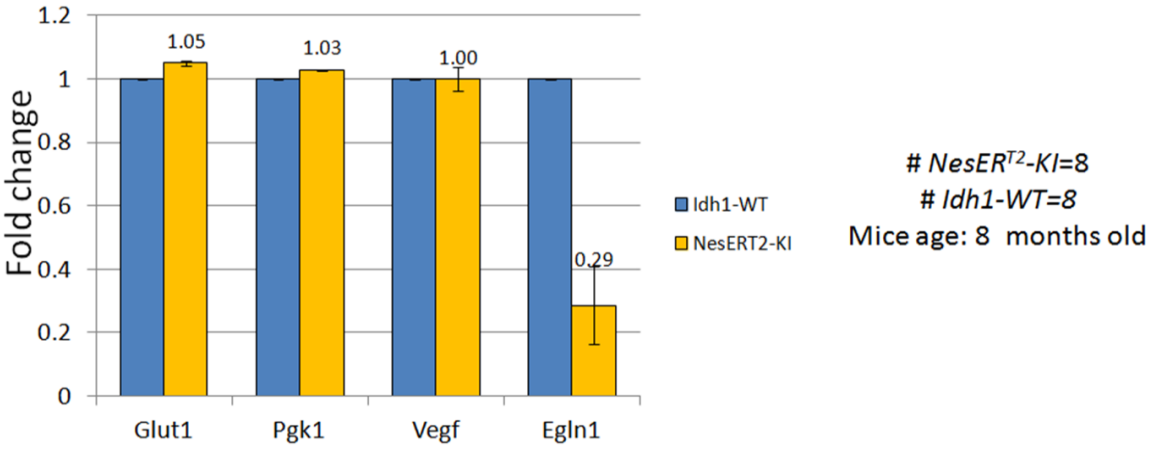


**Figure 5- 22: Western blot showing Hif1α protein expression in the brain of *NesER$^{T2}$-KI* mice**

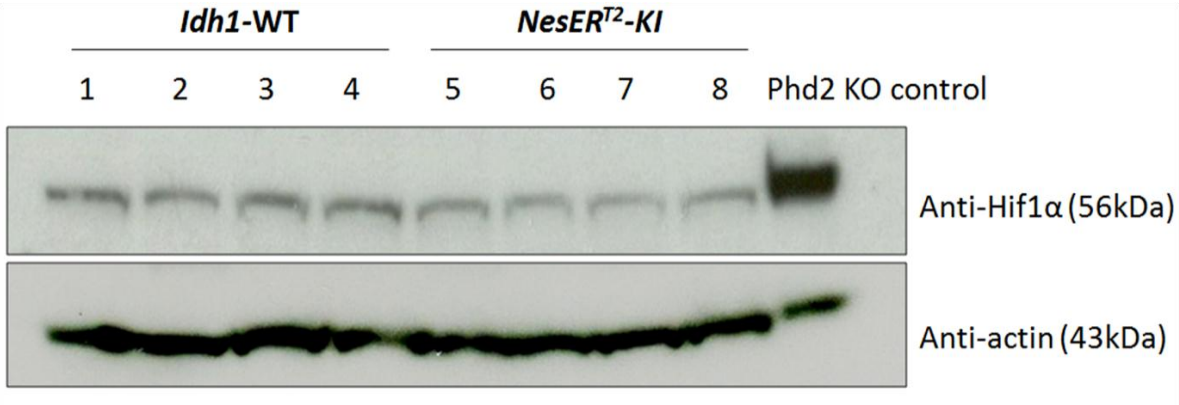


**Figure 5-23: Western blot showing Phd2 protein expression in the brain of *NesER$^{T2}$-KI* mice**

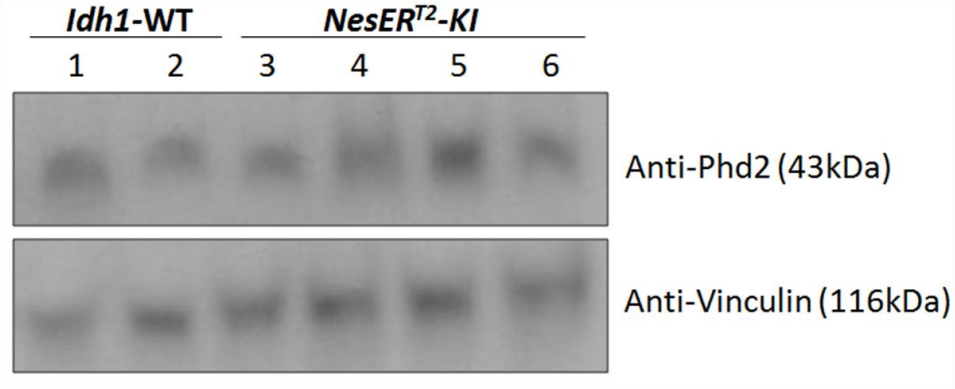

### 5.4.4.8 Expression of neural stem cell markers in *NesER$^{T2}$-KI* mice

The mRNA expression level of the stem cell marker gene *Nes* was increased by 24-fold (p=0.001) in the whole brains of *NesER$^{T2}$-KI* mice by qRT-PCR analysis ***(Figure 5-24)***. The mRNA expression levels of *Smarca4*, *Sox2*, *Msi1*, and *Prom1* were not demonstrably altered. Given that mutant Idh1 expression had been demonstrated in frontal, temporal and occipital lobes of the brain, the mRNA expression level of *Nes* was also measured in these three areas separately using qRT-PCR. *Nes* expression was increased by 152-fold (p<0.001), 36-fold (p<0.001, and 46-fold (p=0.025) in the frontal, temporal and occipital lobes respectively ***(Figure 5-25)***.

**Figure 5- 24: Fold change in mRNA expression of stem cell markers in the brain of *NesER$^{T2}$-KI* mice by qRT-PCR**

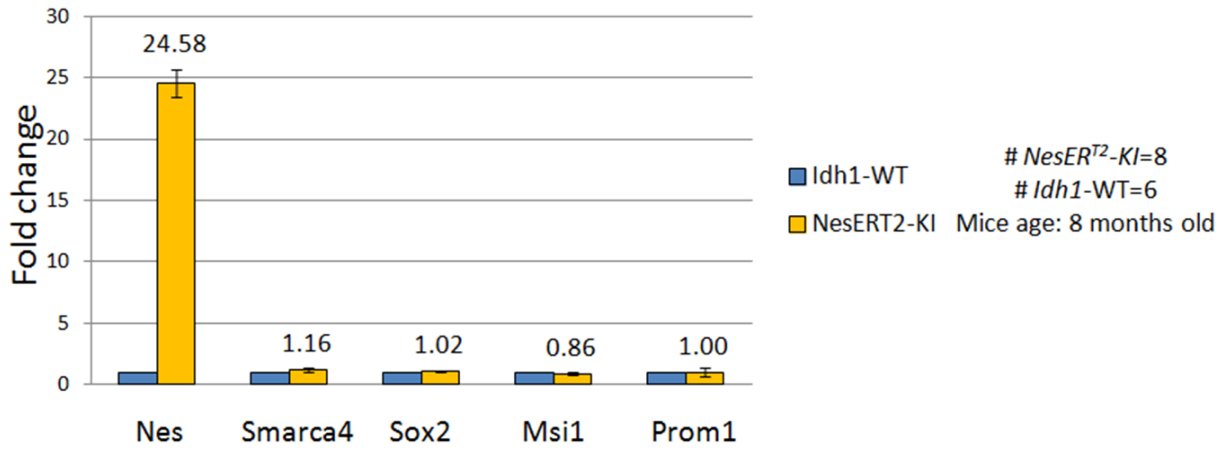


In order to investigate whether the increase in *Nes* expression observed in the brains of *NesER$^{T2}$- KI* mice could in fact have resulted not from mutant Idh1 expression, but due in some way to the expression of nestin cre recombinase, the mRNA expression level of *Nes* was assessed by qRT-PCR in *nes-creER$^{T2}$;Idh1$^{+/+}$* mice, and compared that in to both *Idh1$^{+/+}$* mice and *NesER$^{T2}$-KI* mice. *Nes* expression was found not to be increased in *nes-creER$^{T2}$;Idh1$^{+/+}$* mice and was in fact 114-fold lower (p<0.001) than that seen in *NesER$^{T2}$-KI* mice ***(Figure 5-26)***, suggesting that the increase in *Nes* expression observed in *NesER$^{T2}$-KI*

mice occurred as a result of Idh1 R132H expression rather than the expression of nestin cre recombinase.

**Figure 5-25: Fold change in mRNA expression of *Nes* in the frontal, temporal and occipital lobes of NesERT2-KI mice brains compared to *Idh1*-WT controls by qRT-PCR**

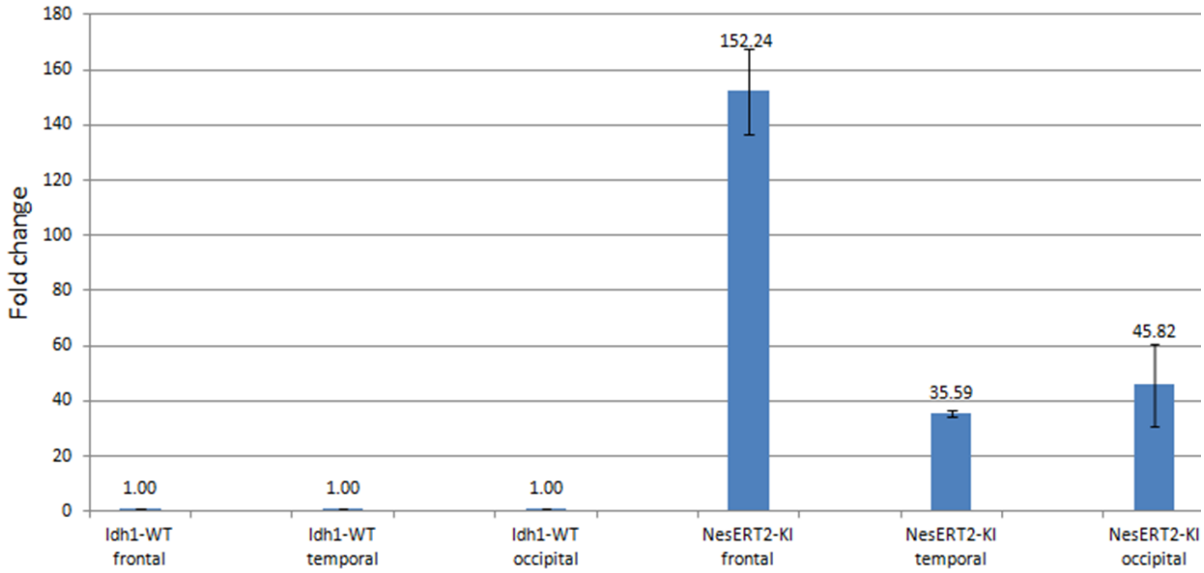


**Figure 5-26: Relative mRNA expression level of *Nes* in *nes-creER$^{T2}$;Idh1$^{+/+}$*, *Idh1$^{+/+}$ NesER$^{T2}$-KI* mice by qRT-PCR**

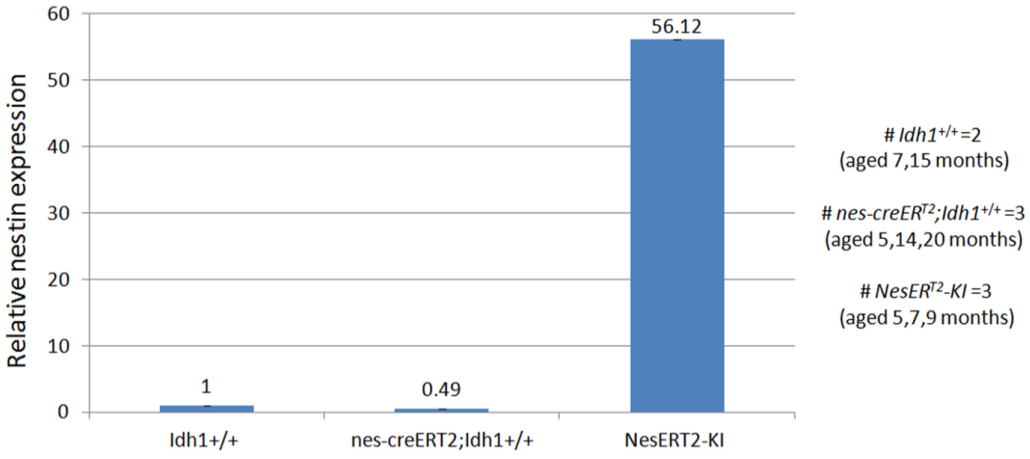


I was unable to demonstrate an increase in nestin protein expression by western blot due to a lack of sensitivity of the nestin primary antibody used. The protein bands observed in both the *Idh1*-WT and *NesER$^{T2}$-KI* samples were very faint, despite repeating the western blot

several times and increasing the amount of protein loaded, and the concentration of both primary and secondary antibody used.

However, nestin expression was found to be increased by IHC in cells within the SVZ of the brain of *NesER$^{T2}$-KI* mice ***(Figure 5-27)***, and an increase in nestin expression was also seen in the region of the RMS. The SVZ is of particular interest because this region, located between the lateral ventricle and the parenchyma of the striatum, functions as a source of both NSCs and progenitor cells in mice and retains the ability to produce neurons and glia throughout adult life. Nestin expression is lost in the adult mouse brain following differentiation of NSCs, but its expression is retained within the SVZ. Consequently mutant Idh1 expression would be expected to be activated by nestin cre recombinase in cells in this region. Furthermore, the SVZ has been shown to play an important role in glioma initiation and maintenance, and mutations expressed in NSCs and progenitor cells in the SVZ have been shown to lead to tumour initiation in the early stages of gliomagenesis in other mouse models.

It would be important to identify if an increase in Nestin expression was seen only in cells which expressed mutant Idh1. This could be achieved by performing IHC for mutant Idh1 expression in the SVZ of *NesER$^{T2}$-KI* mice to identify whether the same cells which expressed nestin in SVZ also expressed mutant Idh1. However I was able to demonstrate this due to the fact that no commercially available mouse-specific Idh1 r132h antibody is currently available.

**Figure 5-27: IHC analysis showing an increase in nestin expression in the SVZ of *NesERT2-KI* mice compared to *Idh1*-WT controls**

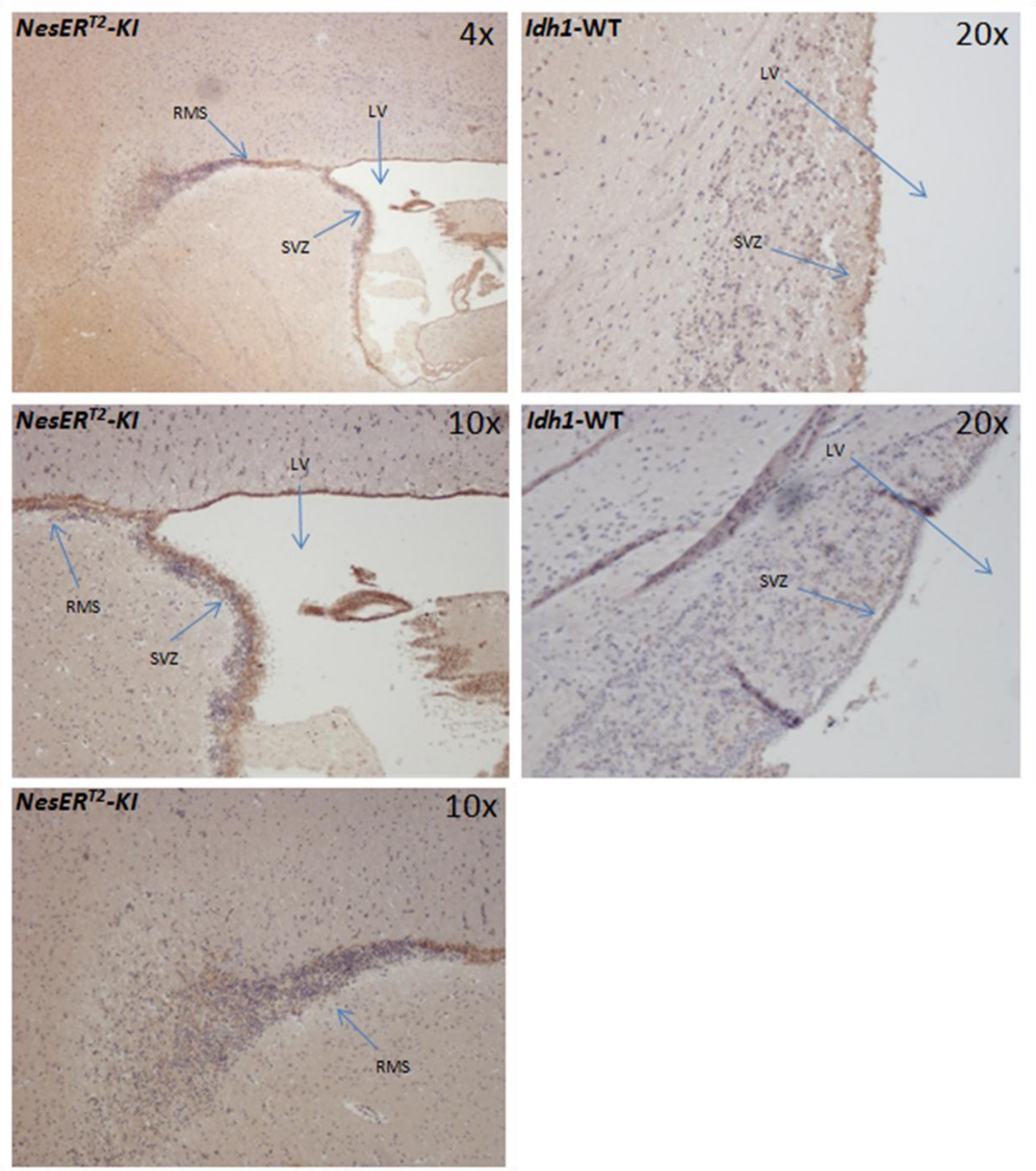


LV: lateral ventricle; RMS: rostral migratory system; SVZ: subventricular zone

### 5.4.4.9 Assessment of proliferation and apoptosis in the SVZ of *NesER$^{T2}$-KI* mice

In view of the fact that an increase in nestin expression was seen in cells within the SVZ of *NesER$^{T2}$-KI* mice, analysis of other characteristics of cells in this region was performed using

IHC. Specifically, cellular proliferation rate and apoptosis were assessed by IHC using antibodies directed against phospho-histone H3 (PHH3) and caspase-3 respectively.

PHH3 detects endogenous histone H3 when histone H3 is phosphorylated at serine 10. Phosphorylation of histone H3 at serine 10 is tightly correlated with chromosome condensation during mitosis and is therefore used as a marker of cellular proliferation activity. An increase in PHH3 expression was seen by IHC, in cells within the SVZ of *NesER$^{T2}$-KI* mice and in the region of the RMS, suggesting that an increase in proliferative activity occurred in these areas ***(Figure 5-28)***. Conversely, no observable change in caspase-3 expression was seen in the SVZ of *NesER$^{T2}$-KI* mice when compared to *Idh1*-WT controls.

**Figure 5-28: IHC showing an increase in PHH3 expression in the SVZ of *NesERT2-KI* mice compared to *Idh1*-WT controls**

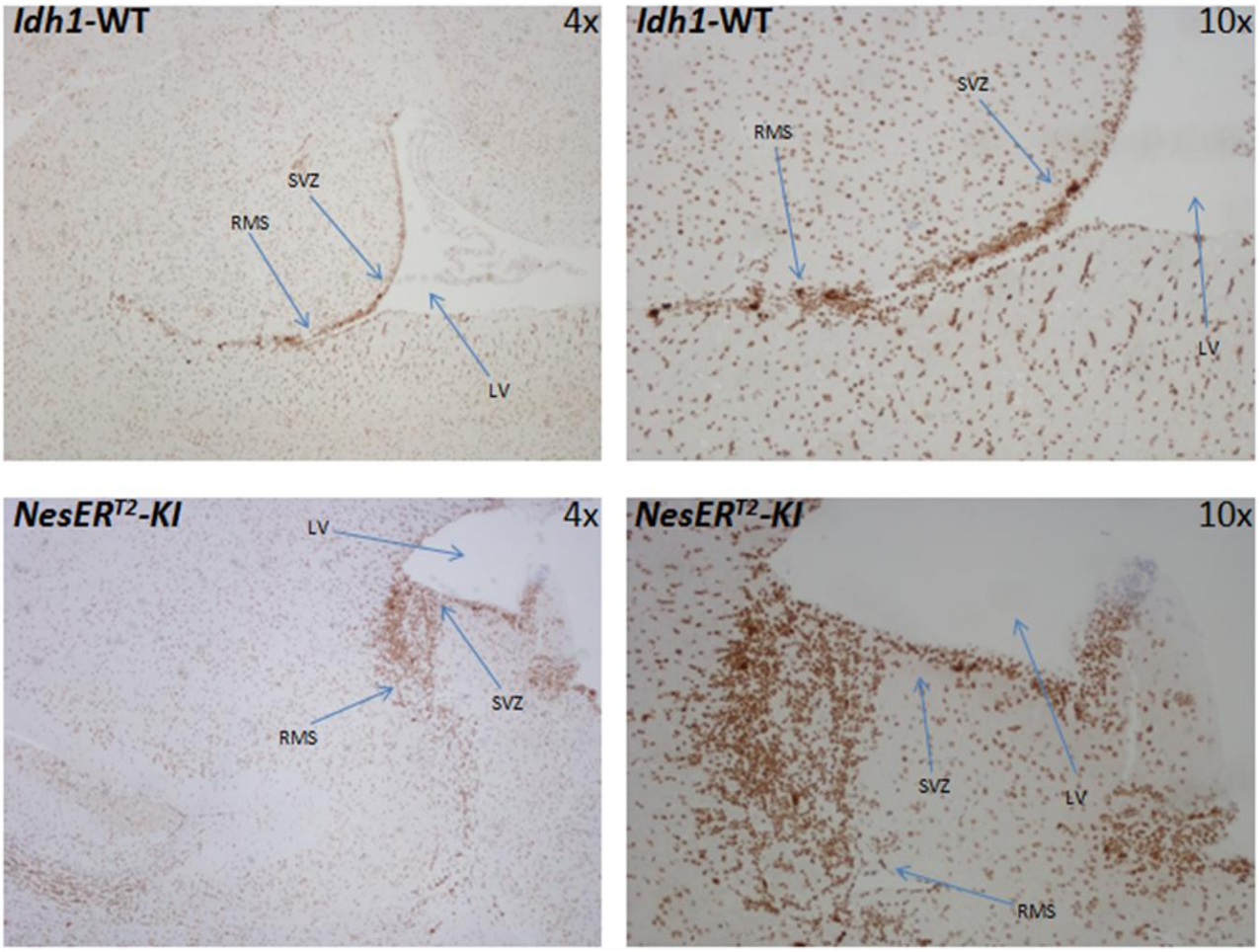


LV: lateral ventricle; RMS: rostral migratory system; SVZ: subventricular zone

It is apparent from this IHC analysis that the Nestin expressing cells and the proliferating cells are not congruent. Indeed there are a greater number of proliferating cells seen that Nestin expression cells and the proliferating cells distributed more diffusely than the Nestin expressing cells. This raises the possibility that mutant Idh1 expressing cells may exert a paracrine effect on neighbouring cells. More specifically, it is possible that D2HG accumulating as a result of mutant Idh1 activity in nestin expressing cells leaks out of these cells and exerts a 'field' effect on neighbouring cells which do not express mutant Idh1. Indeed the theory that mutant IDH activity within a cell, can exert a paracrine effect on neighbouring cells has been suggested to occur in patient with OD and MS (Amary M 2011),

and is strengthened by the finding that D2HG accumulates in tissue culture media aspirated from cultured IDH1 mutant cells lines at a level 100-fold greater than that seen in media aspirated from IDH1-WT cells (Duncan C 2012). This theory could have important clinical implications. In particular it may reduce the reliability of using antibodies directed against IDH1R132H to delineate tumours at surgery or in histopathological analysis, given that the tumourigenic effects may also occur in neighbouring IDH1-WT cells.

#### 5.4.4.10 Expression of markers of neural differentiation in *NesER$^{T2}$-KI* mice

The mRNA expression of gene markers of neural differentiation was assessed by qRT-PCR. The mRNA expression level of genes associated with astrocytic differentiation, *Gfap* and *Aqp4*, were found to be comparable in the brains of 8 month old *NesER$^{T2}$-KI* and *Idh1*-WT mice. However the mRNA expression level of genes associated with oligodendrocytic differentiation, *Cnp* and *Cspg4*, were reduced by 16% (p=0.05) and 14% (p<0.001) respectively in the brains 8 month old *NesER$^{T2}$-KI* mice ***(Figure 5-29)***, and by 25% (p=0.026) and 10% (p=0.38) respectively in the brains of 4 month old *NesER$^{T2}$-KI* mice ***(Figure 5-30)***.

**Figure 5-29: Fold change in mRNA expression of markers of neural differentiation in the brain of 8 month old *NesER$^{T2}$-KI* mice compared to *Idh1*-WT controls**

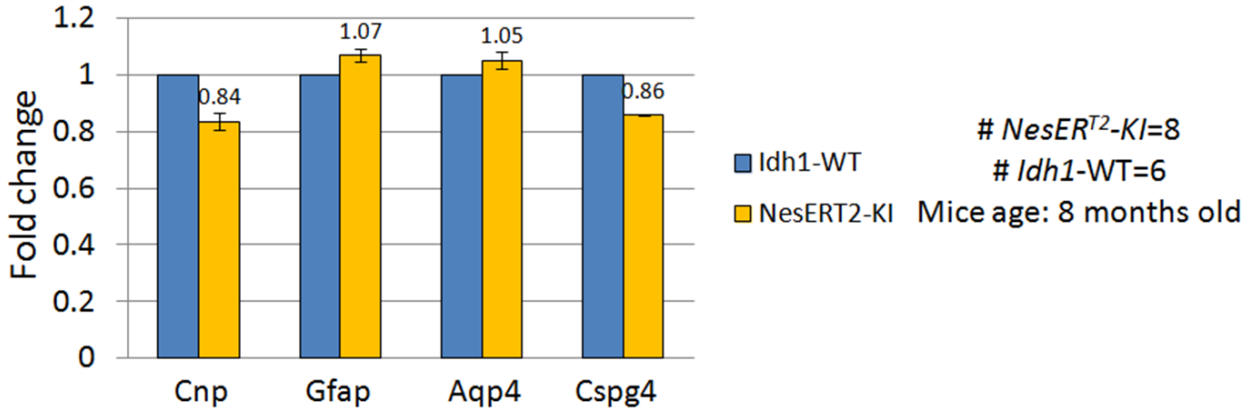

**Figure 5-30: Fold change in mRNA expression of markers of oligodendrocytic differentiation in the brains of 4 month old *NesER$^{T2}$-KI* mice compared to Idh1-WT controls**

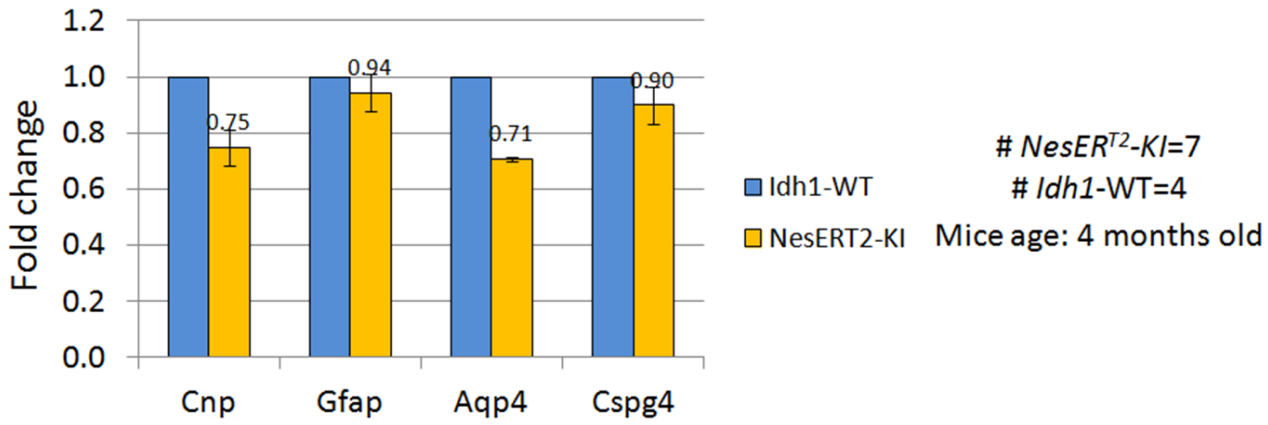


### 5.4.4.11 Assessment of markers of TET function and *Rbp1* expression in *NesER$^{T2}$-KI* mice

The α-KG-dependent, DNA-modifying, TET enzymes hydroxylate 5mC to generate 5hmC. TET enzymes function as epigenetic regulators of gene expression by mediating the demethylation of DNA. The inhibition of TET has been implicated in the pathogenesis of IDH1/2 mutant tumours and IDH1 mutant gliomas accumulate significantly lower levels of 5hmC and higher levels of 5mC than wild-type tumours. Consequently levels of 5hmC and 5mC were measured in the brains of *NesER$^{T2}$-KI* mice, as a marker of TET function. Levels of 5hmC were significantly reduced, by 24% (p=0.001), in the brains of *NesER$^{T2}$-KI* mice. A 3.3% increase in 5mC levels was also seen but this increase did not reach statistical significance (p=0.6156) ***(Figure 5-31)***. The 5mC:5hmC ratio in the brains of *NesER$^{T2}$-KI* mice was 6.7:1 (p<0.001), compared to a ratio of 5:1 (p<0.001) in *Idh1*-WT controls, further demonstrating a change in the relative levels of these DNA methylation variants in association with mutant Idh1 expression.

**Figure 5-31: Relative levels of 5-hmC and 5-mC levels in *NesER$^{T2}$-KI* mice**

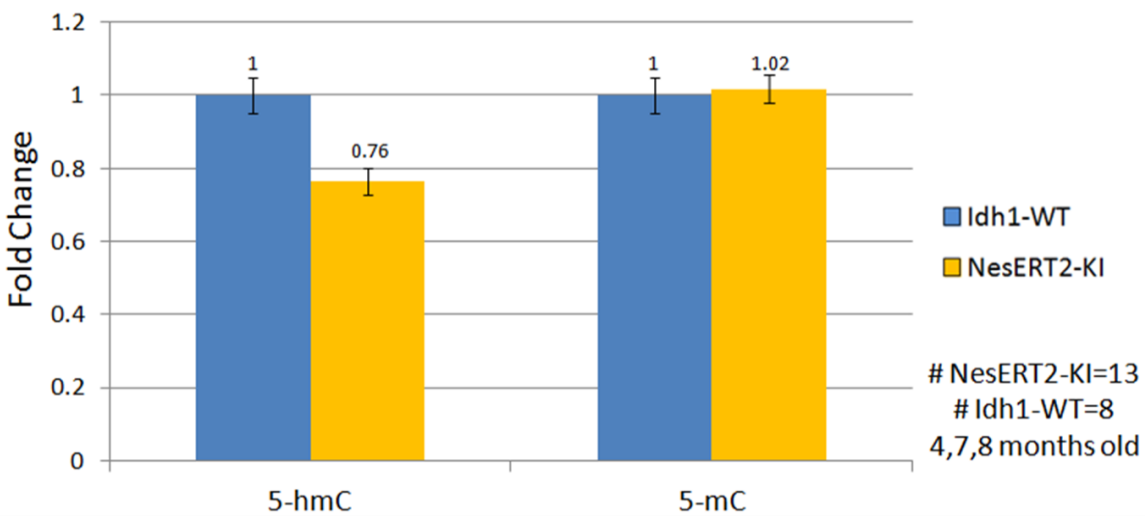


The expression of *Rbp1*, whose promoter region is hypermethylated in the vast majority of IDH1 mutant gliomas, was also analysed to be used as a more sensitive marker of DNA methylation and because *RBP1* expression has been shown to be reduced in IDH1 mutant tumours. The mRNA expression level of *Rbp1*, measured by qRT-PCR, was found to be reduced by 25% (p=0.01) and 30% (p=0.04) in the brains of 4 month and 8 month old *NesER$^{T2}$-KI* mice, respectively ***(Figure 5-32)***.

**Figure 5-32: qRT-PCR analysis of mRNA expression levels of *Rbp1* in the brain of *NesER$^{T2}$-KI* mice compared to *Idh1*-WT controls**

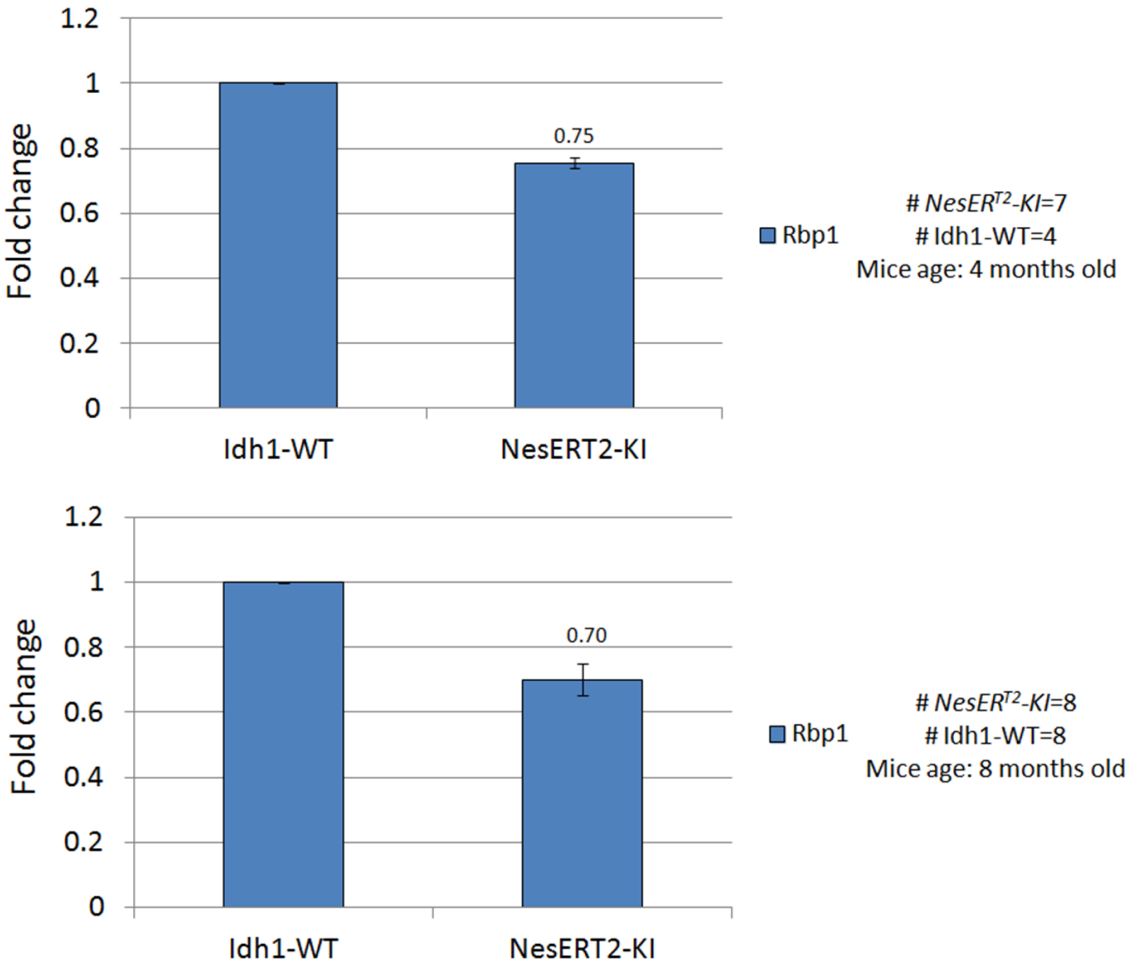


### 5.4.4.12 Assessment of markers of JHDM function in the brain of *NesER$^{T2}$-KI* mice

JHDM's function as epigenetic regulators of gene expression by binding to and removing methyl groups from specific histone lysine residues. The methylation of histone residues can be used as a marker of JHDM function and changes in the levels of histone methylation markers such as H3K4, H3K9, H3K27, H3K36, and H3K79 have been shown to be elevated in association with mutant IDH1/2 expression both *in vitro* and *in vivo*. The level of H3K9 trimethylation (H3K9me3) in the brain of *NesER$^{T2}$-KI* mice was therefore assessed by western blot, in order to act as a marker of JHDM function. However, an increase in H3K9me3 could not be consistently demonstrated in the brains of *NesER$^{T2}$-KI* mice, when

compared to levels in *Idh1*-WT controls, suggesting that JHDM function was not inhibited in mutant animals ***(Figure 5-33)***.

**Figure 5-33: Western blot showing H3K9me3 and total H3 levels in the brain of *NesER$^{T2}$-KI* mice compared to *Idh1*-WT controls**

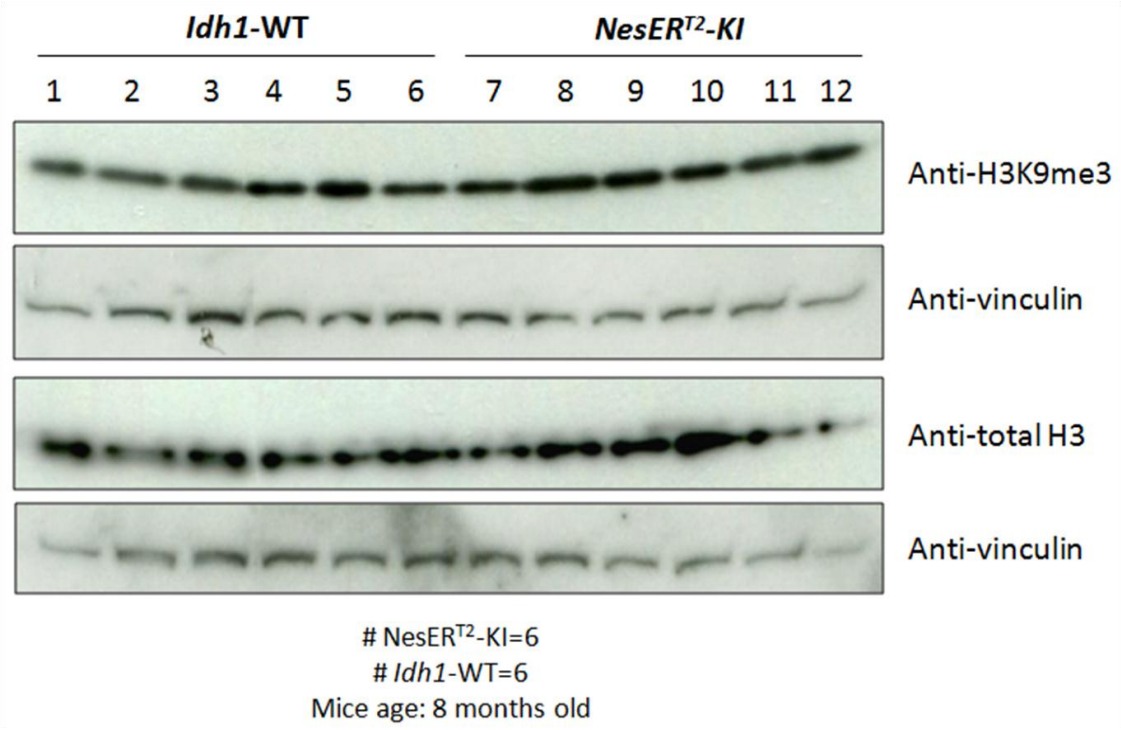


## 5.4.5 Analysis of *D2hgdh* KO mice

We bred constitutive *D2hgdh* KO mice and aged them until between 2.5 and 10 months prior to sacrifice. No gross phenotype was observed by that time. Specifically, and in contrast to both *NesER$^{T2}$-KI* and *NeoR* mice, hunching and weight loss were not observed in *D2hgdh* KO mice. Furthermore, none of the 15 brains removed from *D2hgdh* KO animals appeared hydrocephalic, and ventriculomegaly was not observed macro- or microscopically.

In order to establish whether *D2hgdh* was expressed in *D2hgdh* KO mice, mRNA was extracted from the brains of 4 *D2hgdh* KO mice and retrotranscribed to cDNA before being analysed by PCR and qRT-PCR. Both PCR and qRT-PCR analysis of cDNA, demonstrated an absence of *D2hgdh* expression ***(Figure 5-34 and Figure 5-35)*.**

**Figure 5-34: PCR analysis of *D2hgdh* expression in the brains of *D2hgdh* KO mice**

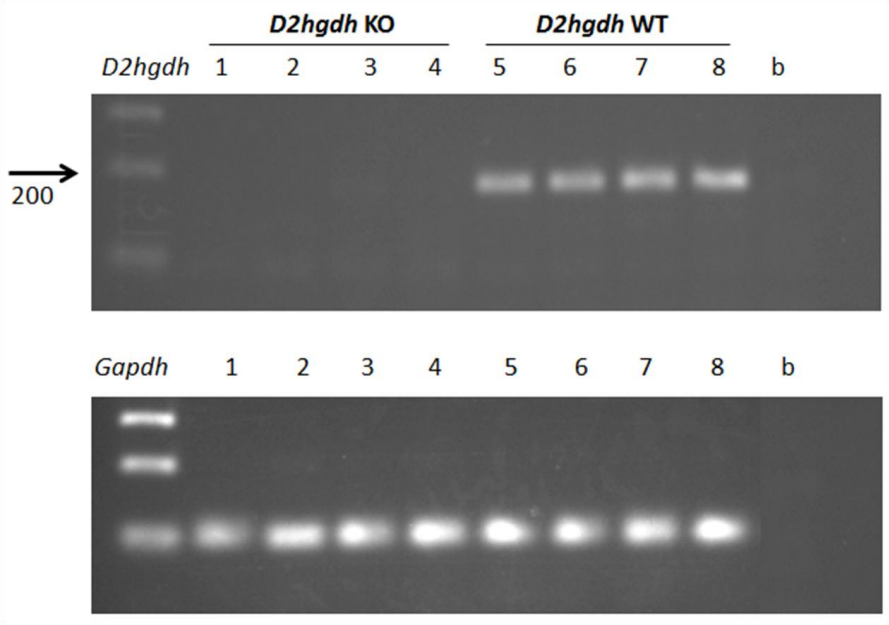


Fw primers recognise exon 1 of *D2hgdh*; Rv primers recognise exon 3 of *D2hgdh*

**Figure 5-35: qRT-PCR analysis of *D2hgdh* expression in the brains of *D2hgdh* KO mice**

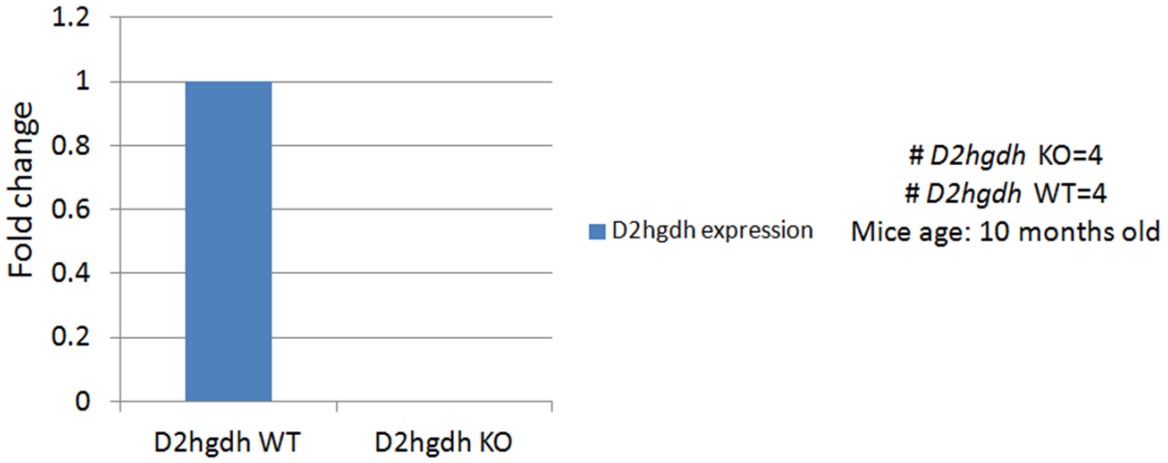


Levels of 2-HG and α-KG were measured in the brain, liver, kidney and spleen of 2.5 month old *D2hgdh* KO mice. In the brain, a 6.4-fold increase ($p<0.01$) in 2-HG was observed, but α-KG levels were not reduced. In fact, a 1.2-fold increase ($p=0.08$) in α-KG was seen but this was not statistically significant ***(Figure 5-36)***. 2-HG was also found to be increased by 13.6-fold ($p<0.01$), 9.6-fold ($p<0.01$) and 7-fold ($p<0.01$) in the liver, kidney and spleen**.** A 0.7-

fold (p=0.08) and 0.9-fold (p=0.23) decrease in α-KG was seen in the kidney and spleen respectively, but these changes were not statistically significant.

**Figure 5-36: Relative levels of 2-HG and α-KG levels in the brain, liver, kidney and spleen of 10 week old *D2hgdh* KO mice compared to *D2hgdh* WT controls.**

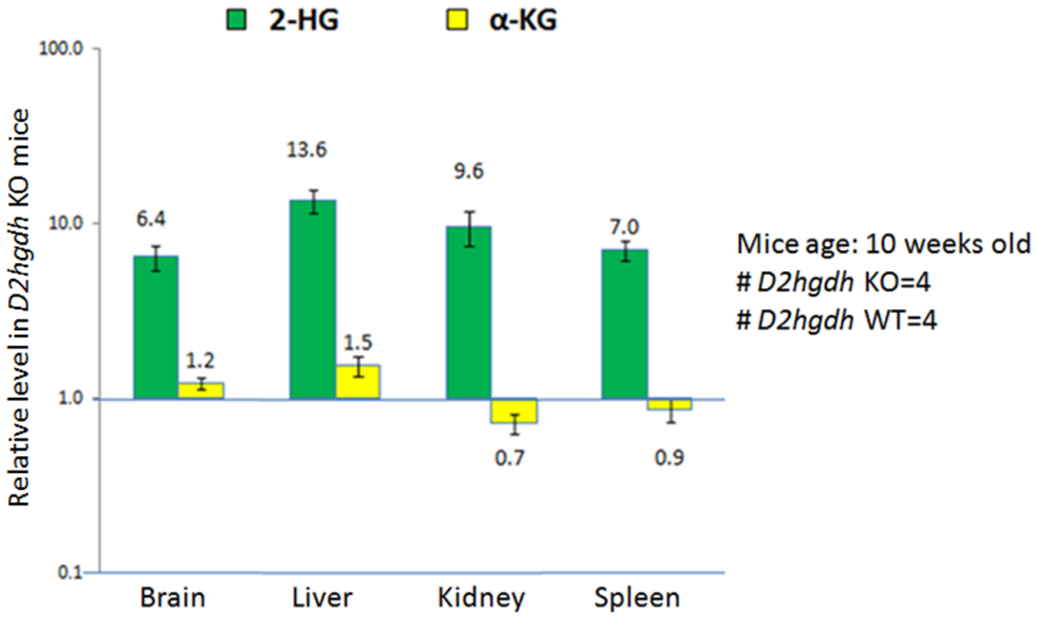


In contrast to *NesER$^{T2}$-KI* mice where a reduction in 5hmC together with an increase in the 5mC:5hmC ratio was seen in the brain, levels of 5mC and 5hmC were unchanged in the brains of *D2hgdh* KO mice when compared to *D2hgdh* WT controls ***(Figure 5-37)*** and the 5-mC:5hmC ratio was not increased (0.9:1).

Additionally and again in contrast *NesER$^{T2}$-KI* mice, the mRNA expression level of *Nes*, assessed by qRT-PCR, was not increased in the brain of *D2hgdh* KO mice when compared to *D2hgdh* WT controls ***(Figure 5-38)***.

**Figure 5-37: Relative levels of 5mC and 5hmC in the brain of *D2hgdh* KO mice compared to D2hgdh WT controls**

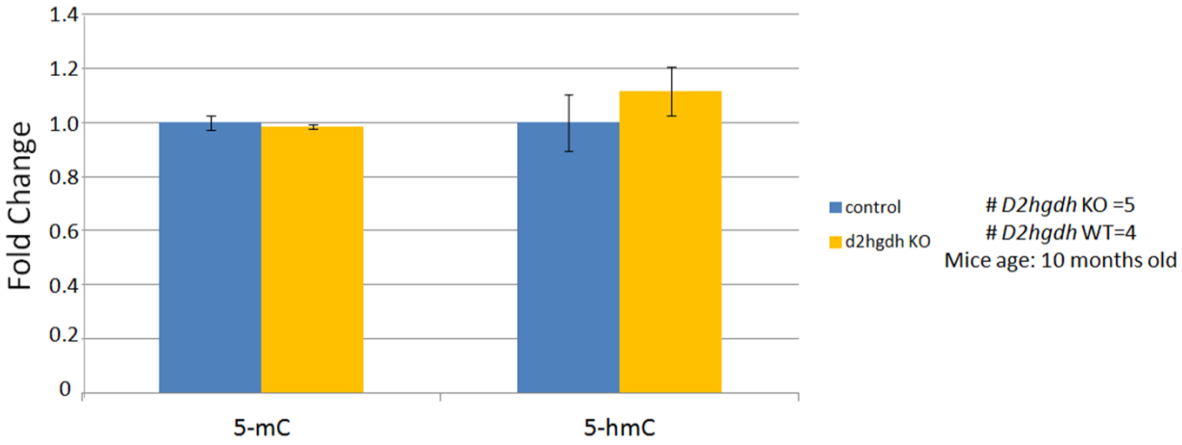


**Figure 5-38: Relative mRNA expression level of *Nes* in the brain of *D2hgdh* KO mice compared to *D2hgdh* WT controls**

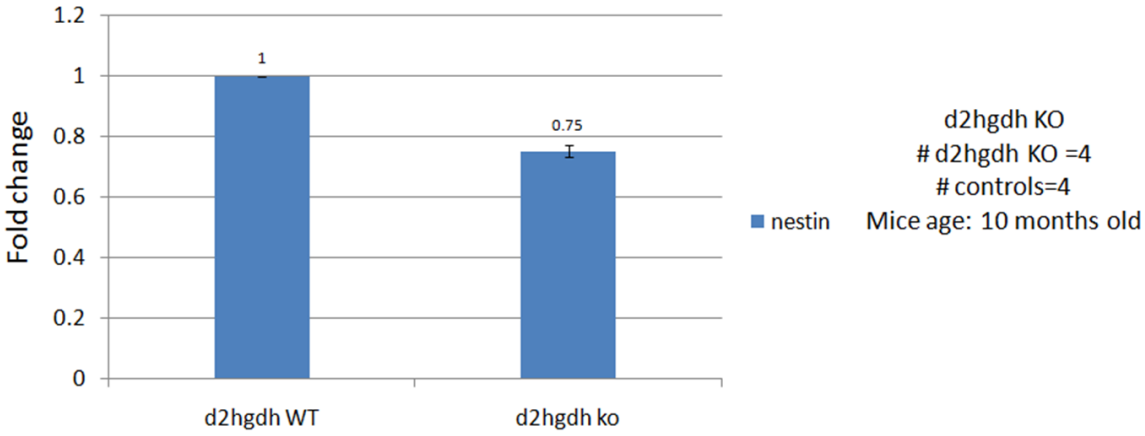


The mRNA expression level of various Hif1α target genes was assessed in the brains of *D2hgdh* KO by qRT-PCR ***(Figure 5-39)***. *Egln1* expression was found to be reduced by 21% (p=0.02), however, as in *NesER$^{T2}$-KI* mice, corresponding Phd2 protein expression was not reduced on western blotting (***Figure 5-40)***. *Egln3* expression was also reduced by 19% (p=0.11), and *Glut1* expression was increased by 27% (p=0.59), but these changes were not statistically significant. Furthermore, the expression levels *Pfk* and *Pgk1* were unchanged, and Hif1α protein expression was not increased on western blotting.

**Figure 5-39: Hif1α target gene expression in the brain of *D2hgdh* KO mice**

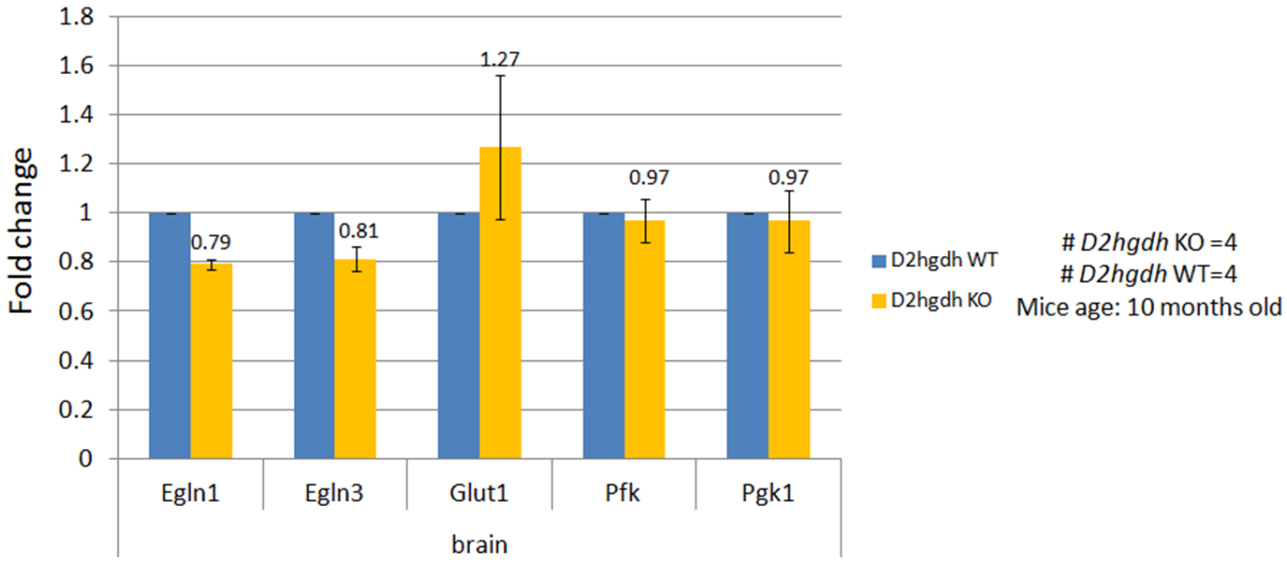


**Figure 5-40: Western blot showing Phd2 protein expression in the brain of *D2hgdh* KO mice and *D2hgdh* WT controls**

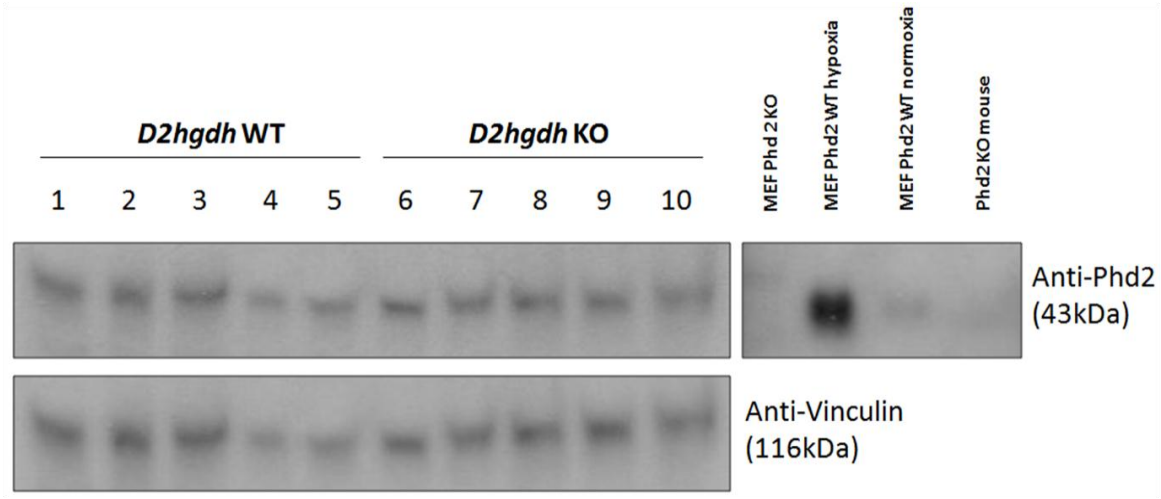


Interestingly the expression level of *Egln1* was also reduced by 19% ($p<0.01$) and 11% ($p<0.01$) respectively, in the liver and kidney of *D2hgdh* KO mice by qRT-PCR ***(Figure 5-41* and *Figure 5-42)***. Furthermore, in the liver, the expression levels of *Egln3, Glut1, Pfk, and Pgk1* were increased by 99% ($p<0.01$), 76% ($p<0.01$), 98% ($p<0.01$) and 40% ($p=0.02$) respectively, whilst in the kidney, a 13% ($p=0.21$), 42% ($p=0.01$) and 51% ($p=0.03$) increase was seen in the expression of *Egln3, Glut1 and Pfk* respectively. 2-HG was found to accumulate to a greater extent in the liver and kidney than in the brain, and this may explain

why an increase in Hif1α target gene expression was seen in the former two tissues, but not in the latter. Alternatively these findings may demonstrate that the effect of 2-HG accumulation on Hif phd activity differs between tissues. It is also plausible that the reduction in *Egln1* expression seen in the liver and kidney, led to a reduction in Phd2 protein levels in these tissues, stabilising Hif1α and resulting in the increase in the expression of the other Hif1α target genes analysed.

**Figure 5-41: Hif1α target gene expression in the liver of *D2hgdh* KO mice compared to *D2hgdh* WT controls**

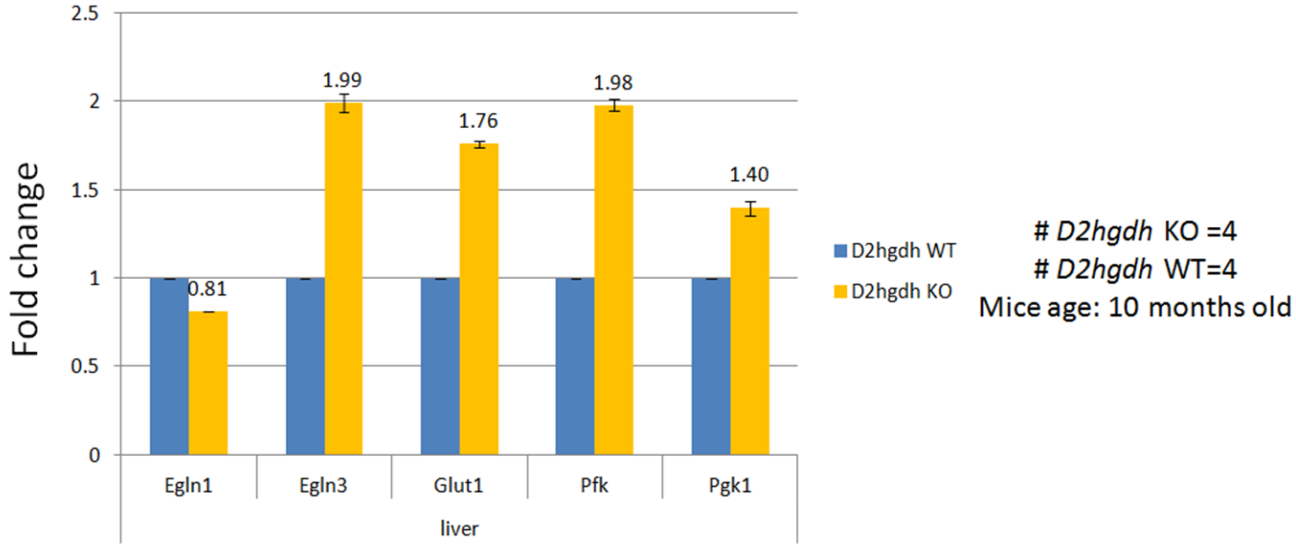


**Figure 5-42: Hif1α target gene expression in the kidney of *D2hgdh* KO mice compared to *D2hgdh* WT controls**

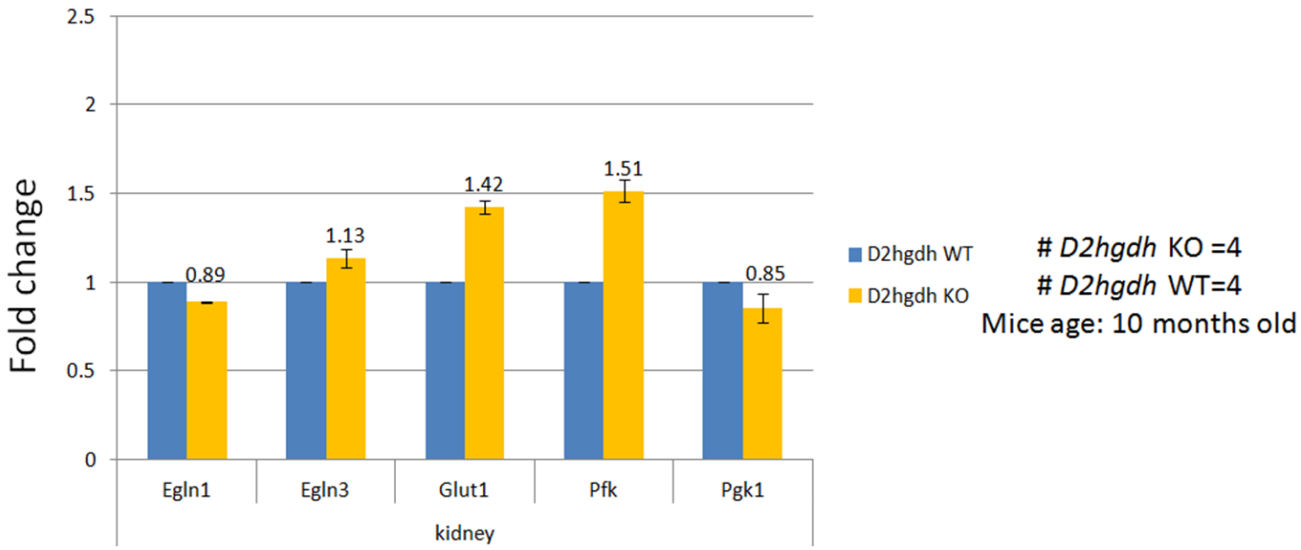

In view of the fact that IDH2 expression was reduced by both qRT-PCR and western blot in cell lines with shRNA induced knockdown of *D2HGDH*, *Idh2* expression levels were also assessed in the brains of *D2hgdh* KO mice by qRT-PCR. No reduction in *Idh2* expression was demonstrated, in fact, an 11% (p=0.15) increase was seen but this was not statistically significant ***(Figure 5-43)***. Consequently, it appears that knockdown of D2*hgdh* does not affect *Idh2* expression levels *in vivo*.

**Figure 5-43: *Idh2* expression in the brain of *D2hgdh* KO mice compared to *D2hgdh* WT controls**

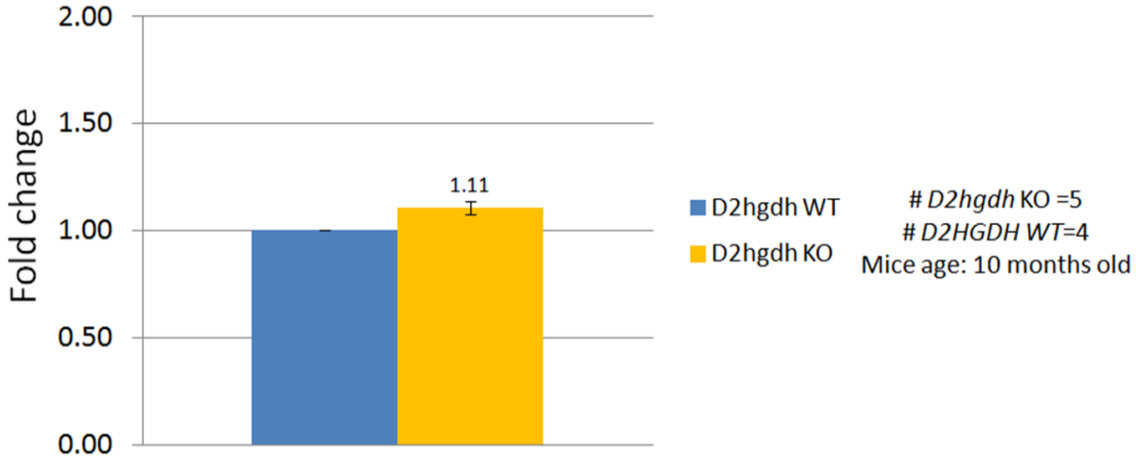


## 5.4.6 Analysis of *Ksp-KI* and *Vil-KI* mice

Mutations in *IDH1* at R132 have been described in a few cases of colon cancer, and mutations in other TCA cycle enzymes, namely *SDH* and *FH* have been implicated in the development hereditary renal cell carcinoma. Therefore, *Idh1-KI* mice were crossed with both *Ksp-Cre* and *Villin-Cre* mice in order to assess the effects of mutant Idh1 expression in the kidney and intestine respectively.

In total 26 live mice were generated by *Idh1-KI* x *Ksp-Cre* crosses. 4 of these mice developed the same hunched posture and weight loss that were observed in *NesER$^{T2}$-KI* and *NeoR* mice, necessitating them to be culled at between 257-380 days old ***(Table 5-11)***. Similarly this

phenotype was seen in both *Ksp-KI* and *NeoR* mice but not in *Idh1*-WT animals, further demonstrating that *Idh1*$^{fl(R132H)}$;*Neo*$^{R}$ is a leaky allele.

**Table 5-11: Hunching and weight loss in offspring from *Idh1-KI* x *Ksp-Cre* crosses**

| Genotype | No. mice hunched/weight loss | Total no. mice with this genotype | % with phenotype |
|---|---|---|---|
| *Idh1*$^{+/+}$ | 0 | 1 | 0 |
| *Ksp-Cre*;*Idh1*$^{+/+}$ | 0 | 8 | 0 |
| *Ksp-Cre*;*Idh1*$^{fl(R132H/fl(R132H)}$ | 1 | 1 | 100 |
| *Idh1*$^{+/fl(R132H)}$;*Neo*$^{R+/fl}$ | 2 | 7 | 29 |
| *Ksp-Cre*;*Idh1*$^{+/fl(R132H)}$ | 1 | 9 | 11 |
| **Total** | 4 | 26 | |

A total of 14 mice were generated from *Idh1-KI* x *Villin-Cre* crosses. 2 of these mice, both *Villin-Cre*;*Idh1*$^{+/fl(R132H)}$, developed a hunched posture and weight loss, necessitating them to be culled at 292 and 337 days old respectively ***(Table 5-12)***.

**Table 5-12: Hunching and weight loss in offspring from *Idh1-KI* x *Villin-Cre* crosses**

| Genotype | No. mice hunched/weight loss | Total no. mice with this genotype | % with phenotype |
|---|---|---|---|
| *Idh1*$^{+/+}$ | 0 | 1 | 0 |
| *Villin-Cre*;*Idh1*$^{+/+}$ | 0 | 3 | 0 |
| *Idh1*$^{+/fl(R132H)}$;*Neo*$^{R+/fl}$ | 0 | 5 | 0 |
| *Villin-Cre;Idh1*$^{+/fl(R132H)}$ | 2 | 5 | 40 |
| **Total** | 2 | 14 | |

It is possible that leakiness of the *Idh1*$^{fl(R132H)}$;*Neo*$^{R}$ allele in the brain of *Ksp-KI* and *Vil-KI* mice results in hunching and weight loss in the same way that mutant Idh1 expression in the brain is assumed to cause this phenotype in *NesER*$^{T2}$*-KI* mice. Alternatively the tissue specific effects of mutant Idh1 expression in the kidney or intestine may be responsible. Further analysis of the brain, kidney and intestine, in addition to the assessment of 2-HG and α-KG levels in these tissues in *Ksp-KI* and *Vil-KI* mice is therefore required.

## 5.5 Discussion

No live born *Neo-KI*, *Sox-KI,* or *Nes-KI* offspring were generated from *Flp* x *Idh1*$^{+/fl(R132H)}$;*Neo*$^{R+/fl}$, *Sox2-Cre* x *Idh1*$^{+/fl(R132H)}$;*Neo*$^{R+/fl}$, *Nes-Cre* x *Idh1*$^{+/fl(R132H)}$;*Neo*$^{R+/fl}$, or *Nes-Cre* x *Idh1*$^{+/fl(R132H)}$;*Neo*$^{R+/fl}$;*Tp53*$^{+/fl}$ crosses respectively, and it was not possible to remove the NeoR cassette by *Flp* or to activate mutant Idh1 by *Sox2*- or *Nestin-Cre* without causing embryonic or neonatal lethality. *Nes-KI* embryos do however develop cerebral haemorrhage *in utero* and accumulate an increased level of 2-HG and reduced levels of α-KG, fumarate, succinate, malate, glutamine and glutamate in the brain. In view of the fact that we were unable to generate live born *Nes-KI* mice, and due to the discovery by Sasaki et al. at a similar time that this was a non-viable model, due to the development of cerebral haemorrhage *in utero*, we abandoned this approach in order to focus our efforts on developing a brain-specific *Idh1-KI* using an inducible Nestin-Cre in the hope that this model would produce live born *NesER*$^{T2}$*-KI* for analysis.

Viable, adult *NesER*$^{T2}$*-KI* mice are generated by activating mutant Idh1 expression six weeks post partum by intraperitoneal injection of tamoxifen and these mice become unwell at between 108-279 days developing a hunched posture and weight loss. Hydrocephalus and ventriculomegally are observed in the brains of *NesER*$^{T2}$*-KI* mice, together with an accumulation of 2-HG and a reduction in α-KG production, but changes in the levels of these metabolites are less marked than in the brains of *Nes-KI* embryos and levels of other TCA cycle metabolites are not significantly altered. Hunching, weight loss, hydrocephalus and ventriculomegally also develop in *NeoR* mice, albeit at an older age than in *NesER*$^{T2}$*-KI* mice, and 2-HG accumulates in the brain, demonstrating that *Idh1*$^{(R132H)}$;*Neo*$^{R}$ is a leaky allele.

Nestin expression levels are significantly increased throughout the brain of *NesER*$^{T2}$*-KI* mice, whilst the expression levels of markers of oligodendrocytic differentiation are reduced. An

increase in nestin expression is also seen, in conjunction with an increase in proliferative activity, in the SVZ of *NesER$^{T2}$-KI* by IHC. A decrease in 5hmc levels and an increase in the 5mC:5hmC ratio is seen in the brain of *NesER$^{T2}$-KI* mice, together with a reduction in *RBP1* expression levels, possibly signifying that a change in global DNA methylation occurs in association with mutant Idh1 expression in the brain. The expression of Hif1α was not increased at an mRNA or protein level in the brain of *NesER$^{T2}$-KI* mice and nor were markers of histone methylation.

2-HG also accumulates at various levels in the brain, liver, kidney, and spleen of *D2hgdh* KO mice. However hunching, weight loss, hydrocephalus and ventriculomegally are not seen in mice with this genotype. *Egln1* expression levels are reduced and the expression levels of other Hif1α target genes are increased in the liver and spleen of *D2hgdh* KO mice, but no increase in Hif1α target gene expression is seen in the brain, where 2-HG accumulation is also less marked. Furthermore, unlike in *NesER$^{T2}$-KI* mice, 5hmc levels are not reduced, and neither the 5mC:5hmC ratio nor the level of nestin expression are increased in the brains of *D2hgdh* KO mice.

Hunching and weight loss also occur in *Ksp-KI* and *Vil-KI* mice, most likely due to either leaky expression of the *Idh1$^{(R132H)}$;Neo$^{R}$* allele in the brain, or due to the effects of mutant Idh1 expression in the kidney or intestine. Further analysis of the kidney, intestine and brain of these mice is however required.

### 5.5.1 No live-born *Neo-KI* mice were generated from *Idh1-KI* x *Flp* crosses

No live-born *Neo-KI* mice were obtained, and hence the NeoR cassette could not be removed from the target gene of interest in the germline using *Flp* deleter mice. It is likely that removal of the NeoR cassette by *Flp* caused embryonic lethality in *Neo-KI* mice, although

analysis of *Neo-KI* embryos did not reveal any gross morphological abnormalities when compared to *Idh1*$^{+/fl(R132H)}$;*Neo*$^{R+/fl}$ embryos.

### 5.5.2 No live-born *Sox-KI* mice were generated from *Idh1-KI* x *Sox-Cre* crosses

No live-born *Sox-KI* mice were generated, and consequently it was not possible to produce a mouse model in which mutant Idh1 was expressed ubiquitously. This finding most likely reflects the possibility that the ubiquitous expression of mutant Idh1 results in developmental or lethal defects in utero. Indeed *Sox-KI* embryos were found to be small in size for their gestational age when compared to *Neo*$^{R}$ embryos, although no other gross morphological abnormalities were seen.

### 5.5.3 Expression of Idh1 R132H in the murine brain in utero results in 2-HG accumulation, reduced α-KG production and embryonic lethality

No live-born *Nes-KI* mice were generated from *Idh1-KI* x *Nestin-Cre* crosses, most likely reflecting the possibility that brain specific expression of mutant Idh1 results in developmental or lethal defects in utero. 2-HG was found to accumulate at a high level (1963 nmol/g to 260872 nmol/g [average 72612 nmol/g]) in the brains of *Nes-KI* embryos, and α-KG levels were reduced (13.86 nmol/g to 107.73 nmol/g [average 59.5 nmol/g]). 2-HG has been shown to accumulate at levels of between 5000 nmol/g and 35000 mmol/g in human glioma tumour samples (Chou A 2012). The level of 2-HG accumulation seen in the brains of *Nes-KI* embryos was on average twice as high as this, and although one must be cautious in comparing these two different models, it is possible that whilst levels of 2-HG seen in human gliomas are sufficient to cause tumourigenesis, the higher levels seen in the brains of *Nes-KI* embryos are not compatible with life.

Macroscopically, the brains of *Nes-KI* embryos appeared to demonstrate haemorrhagic areas within the parenchyma. Sasaki *et al*. also described a haemorrhagic phenotype in their brain specific Idh1 R132H conditional KI mice developed using both *Nestin-Cre* and *Gfap-Cre*, which occurred in association with a significant accumulation of 2-HG (2000 vs. 5 ng/mg of tissue [*Nes-KI*], $p<0.01$) in brain cells, as well as a modest reduction in α-KG (0.45 vs. 0.55 fmol/cell [*Nes-KI*], $p=0.02$), when compared to wild-type controls (Dang L 2009). Most significantly in that study, 2-HG levels were found to correlate closely with the haemorrhagic phenotype observed, and in the case of *Gfap-KI* mice, haemorrhage only occurred in brains which also accumulated high levels of 2-HG, and not in those without it. The authors proposed that brain haemorrhage occurred due to Vegf overproduction and increased basement membrane fragility resulting from 2-HG-induced inhibition of HIF-PHD, C-P4H and procollagen-lysine 2-oxoglutarate 5-dioxygenases 1, 2, and 3 (Plod1–3). It seems highly plausible therefore that the haemorrhagic phenotype observed in our mice also occurred through the same mechanisms, and most likely explains why we did not generate any live-born *Nes-Cre* mice in our study.

### 5.5.4 *NesER$^{T2}$-KI* mice do not demonstrate behaviour associated with stress or anxiety during an open field test

It was proposed that *NesER$^{T2}$-KI* mice would demonstrate behavioural characteristics attributed to increased stress and anxiety such as thigmotaxis. However during the OFT, *NesER$^{T2}$-KI* mice actually elicited behaviour attributed to reduced anxiety, namely an increase in locomotion and rearing, but thigmotaxis was not observed. Autonomic nervous system activity, characterised by the frequency of urination and defecation was also not increased.

### 5.5.5 2-HG accumulates and α-KG levels are reduced in *NesER$^{T2}$-KI* mice

An accumulation of 2-HG and a reduction in α-KG production is seen in the brains of *NesER$^{T2}$-KI* adults. Interestingly these changes are less marked than those seen in *Nes-KI* embryos. Several factors may account for these findings. Firstly, because neurogenesis in mice decreases with age; starting at E10, increasing until birth and then declining post-natally, the pre-natal brain has more NSCs per area, and these cells proliferate at a greater rate in embryos than in adult mice. Furthermore, only a small proportion of these NSCs remain in the adult, as many differentiate post-natally into ependymal cells, astrocytes and oligodendrocytes, and those that do remain are limited to the SVZ and SGZ. Consequently, nestin expressing cells are found more diffusely and in greater numbers in the embryonic brain than in the adult brain, and since the *Nes-Cre* transgene directs Cre expression in nestin expressing cells, mutant Idh1 expression would have occurred in a higher proportion of brain cells in embryonic mice.

Secondly, in adult mice, metabolomic analysis was performed on a single tissue section that had been dissected from a random piece of the brain, whilst the whole brain was analysed from embryos. Given that in adult mice, the majority of nestin expressing cells are found in the SVZ and SGZ, this area may not have been incorporated in the section used for analysis, and therefore a relatively large number of cells that did not express nestin or mutant Idh1 will have been included in sample analysis. Consequently, the actual changes in 2-HG and α-KG levels, in cells in which Idh1 R132H expression was activated, may have been diluted as a result.

Thirdly, it is possible that tamoxifen induced activation of mutant Idh1 expression with *nes-creER$^{T2}$* was less efficient than with standard *Nes-Cre*. Indeed, although CreER$^{T2}$ recombinase, is currently considered to be the best model of inducible mutagenesis in mice

(Feil R 1997, Indra AK 1999 , Sasaki M 2012b) and has proven to be useful in several studies (Kuhbandner S 2000, Imai T 2001, Kim JE 2004, Mori T 2006), tamoxifen-induced gene activation in a given tissue is often incomplete, and induced mice are usually mosaics with varying fractions of co-existing wild-type and mutant cells (Leone DP 2003). In view of this, we aim to investigate the tissue specificity and recombination efficiency of *nestin-creER*$^{T2}$ further using ROSA26-Enhanced Yellow Fluorescent Protein (EYFP) reporter mice and have recently crossed *NesER*$^{T2}$*-KI* mice with these animals. The results of these studies would be considered in future work.

### 5.5.6 Hunching and weight loss are observed in *NesER*$^{T2}$*-KI, Ksp-KI, Vil-KI* and *NeoR* mice

Hunching and weight loss are observed in *NesER*$^{T2}$*-KI* mice. This phenotype is also seen in *Ksp-KI, Vil-KI* and *NeoR* mice, albeit with a higher latency ***(Table 5-13)***, but is not in seen *Idh1*-WT or *D2hgdh* KO mice.

**Table 5-13: Age at which mice developed hunching and weight loss**

| Genotype | Age range (days) | Mean (days) |
|---|---|---|
| *NesER*$^{T2}$*-KI* | 108-279 | 193.74 |
| *Ksp-KI* | 257-380 | 318.5 |
| *Vil-KI* | 292-337 | 314.5 |
| *NeoR* | 422-620 | 531 |

It appears feasible that this phenotype occurs in *NesER*$^{T2}$*-KI* mice as a result of the brain-specific expression of Idh1 R132H. The occurrence of this phenotype in *NeoR* mice most likely illustrates that the cre-lox system used is leaky, whilst its occurrence in *Ksp-Cre* and *Vil-Cre* mice is likely to be due to either leaky expression of the *Idh1*$^{(R132H)}$;*Neo*$^{R}$ allele in the brain, or due to the effects of mutant Idh1 expression in the kidney or intestine. Gross

morphological and histological analysis of the kidney, intestine and brain of *Ksp-KI* and *Vil-KI* mice, as well as the analysis of Idh1 R132H expression, and 2-HG and α-KG levels in these tissues is required, in order to draw a more definitive conclusion about the mechanism causing this phenotype, in kidney and intestine-specific mutant mice.

It is also important to note that 2-HG has been shown to accumulate in the tissue culture media of IDH1 R132H overexpressing LN18 cells (Feil S 2009), and although this is a different model, it raises the possibility that 2-HG may also be excreted from cells and act in a paracrine fashion in *Idh1-KI* mice.

### 5.5.7 Hydrocephalus and ventriculomegaly are observed in *NesER$^{T2}$-KI* and *NeoR* mice

Hydrocephalus and ventriculomegaly are observed at comparable frequencies in both *NesER$^{T2}$-KI* and *NeoR* mice (32% vs. 29%), but are not seen in *Idh1*-WT or *D2hgdh* KO mice. This provides evidence that mutant Idh1 activity is likely to be responsible for the development of this brain-specific phenotype**.** The fact that this phenotype was seen in both *NesER$^{T2}$-KI* mice and *NeoR* mice, together with the demonstration that mutant Idh1 is also expressed in *NeoR* animals, undoubtedly highlights that the *Idh1*$^{(R132H)}$;*Neo*$^{R}$ allele is leaky (discussed subsequently in more detail).

Clinical signs of hydrocephalus are readily apparent in young mice because their cranial sutures have not yet closed. The classic manifestation in this age group is an enlarged domed head, accompanied by ataxia and depression. Pressure necrosis of the surrounding brain and ventriculomegaly ensue, resulting in death. However, hydrocephalic adults do not exhibit a domed skull, and consequently the only finding may be enlargement of the lateral ventricles at necroscopy. It is possible therefore that hydrocephalus is present in a greater proportion of

our adult *NesER$^{T2}$-KI* mice than has been documented, but that these mice have not yet become unwell.

The expression of mutant Idh1 in the brain of *NesER$^{T2}$-KI* and *NeoR* mice may result in hydrocephalus and ventriculomegaly by several potential mechanisms. Given that we have shown an increase in nestin expression and proliferation in the SVZ of *NesER$^{T2}$-KI* mice, the most likely explanation is that an increase in the proliferation of NSCs and progenitors in the SVZ results in the occlusion of the Foramen of Monro, which connects the paired-lateral and third ventricles in the midline of the brain, thus blocking the flow of CSF. Alternatively overproduction of CSF, degeneration of the cortex, or improper functioning of the cilia on the surface of ependymal cells lining the ventricles may be responsible. These potential mechanisms require further investigation.

It is considerably less likely that the hydrocephalus and ventriculomegaly seen in *NesER$^{T2}$-KI* and *NeoR* resulted from mechanisms unrelated to mutant Idh1 expression. However, congenital hydrocephalus has been reported to occur in mice as a result of spontaneous mutations (Dang L 2009) especially those relating to structural morphology (Robinson ML 2002), or resulting in defects in the arachnoid villi (Lyon MF 1996). Furthermore, hydrocephalus is seen as a background lesion in several strains of inbred mice, although at considerably lower levels than those observed in this study ***(Table 5-14)***. In these cases defective development of the mesencephalic aqueduct or subarachnoid space is sometimes observed (Ibanez-Tallon I. 2002), although in other cases the cause is unknown. Hydrocephalus may also be acquired in association with infections such as polyoma virus, reovirus and Theiler's murine encephalomyelitis virus but there was no clinical evidence of such infections in our mice.

**Table 5-14: Commonly used mouse strains and corresponding percentage of mice culled at weaning age due to hydrocephalus**

| Strain | Percent hydrocephalus (%) |
|---|---|
| C57BL/6J | 0.02900 |
| B6.V-*Lepob* | 0.03200 |
| BKS.Cg-m+/+*Leprdb* | 0.02800 |
| C57BLKS/J | 0.36000 |
| BALB/cJ | 0.00023 |
| NOD.CB17-*Prkdcscid*/J | 0.00440 |
| NOD/LtJ | 0.00140 |
| BALB/cByJ | 0.00075 |
| C3H/HeJ | 0.00000 |
| SJL/J | 0.00000 |
| DBA/2J | 0.00330 |

Data taken from The Jackson Laboratory data- JAX® NOTES Issue 490, Summer 2003.

A form of communicating hydrocephalus has also been demonstrated to occur in mice as a direct result of nestin-cre expression in the nucleus of neuronal progenitors (Bruni JE 1988). However, in this case, reduced neuronal proliferation and increased cell death were seen within the SVZ, together with defects in the ependymal lining and lamination of the cortex, resulting in microencephaly and communicating hydrocephalus (Forni PE 2006), features which differ significantly from those that we have shown in our *NesER$^{T2}$-KI* mice. Furthermore many other groups have used *Nes-Cre* mice for various purposes and have not reported this phenotype (Forni PE 2006).

### 5.5.8 Leaky expression of Idh1 R132H occurred in *Idh1-KI* mice

The control of gene expression using the cre-lox system is widely considered to be the best model to allow genetic analysis in mice (Karaca M 2014). However this system does have its limitations (Ryding AD 2001). Firstly, expression of Cre within a particular cell type or tissue is rarely uniform, which can lead to mosaic recombination. Secondly transcriptional interference by vector-derived sequences, such as the NeoR cassette, or even the loxP sites

can occur, whilst Cre expression itself may also cause unwanted effects on the genome (Thyagarajan B 2000, Ryding AD 2001). Thirdly, leaky expression of the gene of interest can occur in unexpected tissues or in an unrestricted temporal manner in some cases due to its insertion into the vicinity of an endogenous enhancer or promoter (Schmidt EE 2000).

Indeed, the *Idh1*$^{fl(R132H)}$;*Neo*$^{R}$ allele in our *Idh1-KI* mice is leaky, and mutant Idh1 expression, hydrocephalus and ventriculomegaly are observed in the brains of both *NesER*$^{T2}$*-KI* and *NeoR* animals. However hydrocephalus and ventriculomegaly occur at a younger age in *NesER*$^{T2}$*-KI* mice than in *NeoR* mice (185 days vs 361 days), most likely demonstrating that Cre recombination increases the level of mutant expression above that of the leaky background level.

Given that the activation of Idh1 R132H expression in *NesER*$^{T2}$*-KI* mice is not entirely under the control of Cre recombinase, it is possible that mutant Idh1 expression may also have occurred in tissues other than the brain, resulting in unexpected biological effects. However, we did not observe any gross morphological abnormalities in other organs in our *NesER*$^{T2}$*-KI* mice at post mortem. Interestingly, non-brain specific effects, namely splenomegaly, liver tumours, neutrophilia, reticulocytosis and anaemia were observed by Sasaki *et al.* in their brain-specific Idh1 R132H *Gfap-KI* mice (Sasaki M 2012b). To determine the cause of these changes, the authors verified the expression pattern of *Gfap-Cre* using Rosa26-LSL-TdTomato reporter mice. Expression of TdTomato protein was observed not only in the brain, but also in a wide variety of other tissues, but in their model it was *Gfap-cre* rather than the Idh1 construct that was leaky.

### 5.5.9 2-HG accumulates in *D2hgdh* KO mice but there is no gross phenotype or brain related defect and α-KG levels are unchanged

2-HG also accumulated in the brain of *D2hgdh* KO mice. Indeed higher levels of 2-HG were seen in 2.5 month old *D2hgdh* KO mice (6-fold increase) than in 4 and 8 month *NesER$^{T2}$-KI* animals (1.94-fold and 2.04-fold increase). However, this may be explained by the fact that knockout of *D2hgdh* in the brain was constitutive, where as expression of mutant Idh1, and hence 2-HG accumulation, should have occurred only in nestin expressing cells of adult mice.

In contrast to both *Nes-KI* and *NesER$^{T2}$-KI* mice, α-KG production was not reduced in *D2hgdh* KO animals. Given that the phenotype and other changes seen in both *Nes-KI* and *NesER$^{T2}$-KI* mice were not observed in *D2hgdh* KO animals, this suggests that 2-HG accumulation alone was not sufficient to cause these effect, and implies that they occurred as a result of a reduction in α-KG alone, or in conjunction with 2-HG accumulation, or through other mechanisms specific to mutant Idh1 activity.

### 5.5.10 Brain-specific expression of Idh1 R132H results in an upregulation of nestin

Nestin is a cytoplasmic intermediate filament protein that was originally described in 1990 as an embryonic NSC marker (Sasaki M 2012b). It is selectively expressed in both NSCs and neural progenitors during foetal development of the CNS, but expression is lost following their differentiation into neurons and glial cells (Lendahl U 1990). In the postnatal brain, nestin expression is only retained in cells found in the neurogenic zones, which function as a cellular reserve capable of proliferation, differentiation, and migration (Tohyama T 1992). More recently, nestin has also been recognised to serve as a cancer stem cell marker (Singh SK 2004, Wiese C 2004, Takakuwa O 2013, Narita K 2014).

Brain specific expression of Idh1 R132H resulted in an increase in nestin expression throughout the brain. Furthermore, increased nestin expression was demonstrated in the SVZ cells of *NesER$^{T2}$-KI* mice, in conjunction with an increase in proliferative activity. Nestin expression was not however upregulated in *nes-creER$^{T2}$*; *Idh1$^{+/+}$* or *D2hgdh* KO mice, which suggests that this finding is likely to have occurred as a direct result of mutant Idh1 activity. Indeed, increased nestin expression has in fact been demonstrated to occur in conjunction with 2HG accumulation in a human IDH1 mutant anaplastic astrocytoma cell line *in vitro* (Liu J 2010).

It is most plausible that the upregulation in nestin seen in *NesER$^{T2}$-KI* mice occurs due to a generalised increase in NSC/neural progenitor cell numbers within the SVZ, as a result of their increased proliferation, in a process driven by mutant Idh1 activity. The mechanism driving the increased proliferation of these cells is not yet clear, but it may result from global changes in DNA methylation and gene expression associated with mutant Idh1 activity. Indeed, it has been hypothesised that the hypermethylation phenotype associated with IDH1/2 mutant glioma can result in aberrant gene expression which blocks cellular differentiation and results in the malignant expansion of NSCs (Turcan S 2012, Jin G 2013). In fact mutant IDH1 expression has been shown to block the differentiation of progenitor cells *in vitro* (Duncan CG 2012), and IDH1 mutant gliomas have been shown to exhibit a gene expression profile enriched for genes expressed in undifferentiated neural progenitor cells (Lu C 2012).

The possibility that glioma may develop from transformed NSCs has long been considered (Lu C 2012), and it has been proposed that glioma may actually originate from NSCs within the SVZ, which then infiltrate into surrounding areas, differentiate and form tumours (Singh SK 2003). Indeed it has been demonstrated that the accumulation of mutations in NSCs is an important mechanism in gliomagenesis in mouse xenograft models (Sanai N 2005), whilst in other mouse studies, brain cells expressing neural progenitor markers have been shown to be

more receptive to oncogenic transformation than differentiated brain cells (Holland E 2000, Holland E 2001, Singh K 2004).

We have demonstrated reduced levels of 5hmC in the brains of our *NesERT2-KI* mice, and 5hmC is known play a role in DNA demethylation and transcriptional regulation (Fults D 2002). Furthermore, we have demonstrated a reduction in markers of oligodendrocytic differentiation in these animals. One could speculate therefore that the increase in nestin expression seen in conjunction with an increase in proliferative activity in the SVZ of our mutant mice represents the expansion of undifferentiated, nestin expressing NSCs, which occurs due to DNA hypermethylation and aberrant gene expression, and that this may represent an early malignant process. Further analysis of DNA methylation and gene expression profiles in the brains of our mice, as well as the isolation and analysis of NSC and progenitor cells from the SVZ would however be required to investigate this theory in more detail.

An alternative theory is that mutant Idh1 activity increases *Nes* gene expression directly, by altering its transcriptional regulation or epigenetic control and that nestin upregulation itself then results in the increased proliferative activity seen in the SVZ. A tissue-specific enhancer located in the second intron of the *Nes* gene is crucial to the regulation of nestin expression in NSCs (Guo J 2011), as is the binding of transcription factors to an enhancer element located in the 3′ region of this intron (Zimmerman L 1994, Josephson R 1998). The epigenetic regulation of nestin expression is less well understood (Tanaka S 2004), although current data suggest that histone modifications rather than changes in DNA methylation are of primary importance in this process (Han DW 2009). Nestin expression is increased in glioma when compared to normal brain tissue (Han DW 2009, Arai H 2012), particularly in GBM, where its expression correlates with increased tumour migration, invasion and aggressiveness, and a poorer prognosis (Ma YH 2008, Zhang M 2008). An increase in nestin expression has also

been shown to occur in GBM patients with proneural phenotype (Lei L 2011). The injection of GBM cell clones exhibiting high levels of nestin expression into nude mice results in the formation of larger tumours than those resulting from clones with low nestin expression (Strojnik T 2007). Conversely blocking nestin expression in these xenograft models, via intratumoral injection of shRNA, significantly slows tumour growth (Lu WJ 2011). Furthermore, the downregulation of nestin in GBM cell lines *in vitro* induces cell cycle arrest at the G1/S transition (Lu WJ 2011).

Consequently, it seems plausible that nestin expression may be directly involved in the development and/or progression of GBM, and several functions attributed to nestin may be responsible for this. Indeed, nestin is able to maintain neural progenitor cells in an undifferentiated state throughout adulthood (Reimer R 2009) and is able to promote a high rate of proliferation in these cells (Lendahl U 1990), which it achieves in part by sequestering the glucocorticoid receptor (GR) within the cell cytoplasm, and blocking GR-induced growth arrest (Wiese C 2004). Furthermore, nestin expression promotes cell survival in neural progenitor cells and inhibits apoptosis, in part through the regulation of cyclin-dependent kinase 5 (Cdk5) signalling pathways (Reimer R 2009) (Sahlgren CM 2003, Chen HL 2010). Changes in DNA demethylation are known to occur as a result of mutant IDH1/2 activity (Sahlgren CM 2006, Xu W 2011, Koivunen P 2012, Lu C 2012) and given that we have demonstrated a decrease in 5hmC in our *NesER$^{T2}$-KI* mice, it is possible that alterations in epigenetic control resulted in the upregulation in nestin expression seen in these mice. Furthermore, given that nestin itself can maintain progenitor cells in an undifferentiated, proliferative state, this theory could explain the increase in both nestin expression and proliferative activity seen in the SVZ of *NesER$^{T2}$-KI* mice. More speculatively, if the upregulation of nestin is in fact an early malignant mechanism in gliomagenesis, then the inhibition of nestin expression may serve as a potential target for treatment.

It is also conceivable, given that mutant Idh1 should only have been expressed in nestin expressing cells, that an initial increase in nestin expression in these mutant cells, further stimulated mutant Idh1 expression under the control of the nestin-cre promoter and hence further increased nestin expression in a 'forward loop' type system. However it seems more likely that the increase in nestin expression seen was in fact due to an increase in proliferation of nestin expressing cells.

### 5.5.11 Markers of oligodendrocytic differentiation are reduced in the brain of *NesER$^{T2}$-KI* mice

The expression of the oligodendrocytic markers Cnp and Cspg4 are reduced in the brains of *NesER$^{T2}$-KI* mice, suggesting that mutant Idh1 expression may block cellular differentiation. Indeed others have shown that mutant IDH1 expression can result in a reduction in cellular differentiation both *in vitro* and *in vivo* (Koivunen P 2012, Lu C 2012, Turcan S 2012), whilst the treatment of IDH1 mutant glioma cells with the mutant IDH1 inhibitor AGI-5198 induces the expression of genes associated with gliogenic differentiation (Sasaki M 2012a). Furthermore, it has also been hypothesised that DNA hypermethylation seen in human G-CIMP$^{+}$ tumours blocks the differentiation of glioma cells and allows the malignant expansion of GICs to occur, thus driving tumourigenesis (Turcan S 2012, Rohle D 2013). As will be discussed below, the reduction in both Tet function and Rbp1 expression observed in *NesER$^{T2}$-KI* mice may be responsible for the reduced expression of markers of oligodendrocytic differentiation seen in these animals.

### 5.5.12 Idh1 R132H reduces 5hmC production in the brain of *NesER$^{T2}$-KI* mice suggesting an inhibition of Tet function

5hmC levels were reduced by 24% in the brains of *NesER$^{T2}$-KI* mice. These findings are consistent with those of Sasaki *et al.* who also demonstrated a reduction in 5hmC in their brain-specific *Nes-KI* mice (Sasaki M 2012b).

Expression of mutant IDH1/2 has been shown to reduce 5hmC production *in vitro* and *in vivo* through the inhibition of TET1/2 enzyme function (Xu W 2011, Sasaki M 2012b). The depletion of TET1/2 in murine ES cells results in a reduction in 5hmC of between 35-60% (Koivunen P 2012, Dawlaty MM 2013 ), whilst 5hmC is also significantly reduced in the brain of Tet1/2-deficient mice (Dawlaty MM 2011) and in the haematopoietic tissues of Tet2-deficient mice (Ko M 2011, Li Z 2011, Dawlaty MM 2013 ). TET enzymes are proposed to function as epigenetic regulators of gene expression by mediating the demethylation of DNA. Indeed an increase in DNA methylation and/or aberrant gene expression are seen in association with both depleted TET function (Figueroa ME 2010, Dawlaty MM 2011, Quivoron C 2011), and mutant IDH1/2 expression (Christensen BC 2011, Laffaire J 2011, Turcan S 2012, Dawlaty MM 2013 ). Furthermore the depletion of TET function induces potentially oncogenic changes such as growth factor independence and a cessation of cellular differentiation (Figueroa ME 2010, Ko M 2011, Quivoron C 2011, Losman J 2013), which mirror those changes seen with mutant IDH1/2 expression (Figueroa ME 2010, Moran-Crusio K 2011, Koivunen P 2012). Taken together, these findings suggest a common mechanism linking gain of function in IDH1/2 enzymes with reduced demethylation and oncogenic transformation, and implicate the inhibition of TET enzyme function as pivotal in this process. It seems likely therefore that the decrease in 5hmC see in the brains of our *NesER$^{T2}$-KI* mice also occurs through the inhibition of Tet activity. More speculatively, this

mechanism may also explain the increased proliferative activity and enhanced expression of the stem cell gene marker *Nes* seen in the brains of these animals.

Given that 5hmC production is unaltered in *D2hgdh* KO, in whom a greater relative increase in 2-HG is observed, it appears that 2-HG accumulation alone is insufficient, or perhaps not required, to inhibit Tet function in this model. In fact, one could hypothesise that a reduction in α-KG production is required, either alone, or in combination with 2-HG accumulation, in order to inhibit Tet function. Indeed, D-2HG has been shown to be only a weak inhibitor of TET in vitro, and its effects on TET function are reversed by the addition of exogenous α-KG (Sasaki M 2012a). Conversely the complete omission of α-KG from in vitro enzymatic assays entirely abolishes the activity of TET (Xu W 2011), suggesting that TET activity is indeed dependent upon the availability of α-KG.

### 5.5.13 Idh1 R132H reduces Rbp1 expression in the brain of *NesER$^{T2}$-KI* mice

Rbp1 expression was reduced in the brains of *NesER$^{T2}$-KI* mice. These findings correspond with those of Chou *et al.* who demonstrated a decrease in RBP1 expression to occur in the majority of IDH1/2 mutant gliomas as a result of RBP1 promoter hypermethylation (Chou A 2012). Analysis of Rbp1 promoter methylation in our *NesER$^{T2}$-KI* mice is warranted, to investigate whether Rbp1 promoter hypermethylation is also responsible for the reduction in Rbp1 expression seen in these animals.

RBP1 is involved in RAR activation, and several other genes involved in this pathway are known to be hypermethylated in IDH1/2 mutant tumours (Chou A 2012). RBP1 functions in the synthesis of AtrA (Guilhamon P 2013), which itself serves as a regulator of transcription (Blomhoff R 2006), and it is feasible that decreased RBP1 activity may lead to aberrant transcription and malignant transformation in association with mutant IDH1/2 activity.

Chromosomal translocations involving the *RAR-α* gene are involved in the pathogenesis of acute promyelocytic leukemia (Tang 2011), and this condition is sensitive to treatment with AtrA (Pandolfi PP. 2001). Furthermore AtrA has been shown to induce differentiation in glioma stem and progenitor cells *in vitro* (Tallman MS 2002, Shi Z 2013), and also inhibits proliferation in mature glioma cell lines (Karsy M 2010). If alterations in RAR signalling are truly involved in the pathogenesis of IDH1/2 mutant glioma, then AtrA may represent an attractive treatment option for patients with these tumours.

### 5.5.14 Idh1 R132H does not increase the methylation of H3K9 in the brain of *NesER$^{T2}$-KI* mice

Methylation of H3K9 is not increased in the brains of *NesER$^{T2}$-KI* mice. Consequently, I could not demonstrate an inhibition of histone demethylation in this model, and it is unlikely that the inhibition of JHDMs played a role in the development of the phenotype observed in these mice.

These findings are consistent with those of Sasaki *et al.* who also found no difference in histone 3 methylation in their brain-specific *Nes-KI* mice, although the phenotype that they observed was very different to that seen in our model (Lu J 2013). The levels of histone 3 methylation markers, including H3K9, have however have been shown to be elevated in mutant IDH1/2 expressing cells (Chowdhury R 2011, Xu W 2011, Sasaki M 2012b). This increase was shown to precede a rise in DNA methylation and resulted in a block in cellular differentiation (Lu C 2012). Furthermore the treatment of IDH1 mutant glioma cells with the mutant IDH1 inhibitor AGI-5198 induced both the demethylation of H3K9me3 and the expression of genes associated with gliogenic differentiation (Lu C 2012). Additionally histone methylation was found to be increased in IDH1/2 mutant gliomas (Duncan CG 2012, Rohle D 2013), although histone hypermethylation is also seen in IDH1/2 wild-type tumours

(Lu C 2012) and therefore may occur independently of IDH1/2 mutation status. Hence, whilst it remains unclear whether inhibition of histone demethylases contributes to malignant transformation in IDH1/2 mutant tumours, results from our *in vitro* and *in vivo* studies do not support this theory.

### 5.5.15 Idh1 R132H expression in utero results in reduced levels of TCA cycle metabolites and reduced glutamine and glutamate concentrations in the brain

The levels of fumarate, succinate and malate were significantly reduced in the brains of *Nes-KI* embryos, suggesting that downregulation of TCA cycle function occurs as a result of mutant Idh1 expression in this model, most plausibly due to a reduction in α-KG production. These findings are consistent with those of Reitman *et al.*, who demonstrated a depletion of TCA cycle metabolites in conjunction with an accumulation of biosynthetic precursors, in cell lines that expressed IDH1 mutations (Reitman ZJ 2011), but conflict those seen in our IDH1 mutant cell lines and with other *in vitro* studies (Dang L 2009).

Both glutamine and glutamate levels were also reduced in the brains of *Nes-KI* embryos and these results are consistent with those of Reitman *et al.* who also reported a depletion of glutamate to occur in IDH1 mutant cell lines (Reitman ZJ 2011). It is possible this reduction occurred as a result of increased glutamine flux, which was initiated in order to compensate for decreased α-KG production, and these findings are interesting given that the glutaminergic pathway has been linked to the promotion and progression of glioma (Piao Y 2009, Luksch H 2011, Reitman ZJ 2011). Furthermore, in view of the fact that increased glutamine flux has been observed in glioma cell lines (Lyons S 2007) and inhibition of the glutamine-glutamate cycle reduces the growth rate of IDH1 mutant glioma cells (Dang L 2009), our data may add support to the theory that IDH1 mutant tumour cells rely on

glutamine flux to maintain their viability in the presence of reduced cellular α-KG concentrations.

The levels of fumarate, succinate, malate, glutamine and glutamate were not however significantly reduced in the brains of *NesER$^{T2}$-KI* mice. As discussed in section 5.5.5 this may have occurred as a result there being a lower number of nestin expressing cells and hence Idh1 R132H expressing cells in the brains of adult *NesER$^{T2}$-KI* mice compared to *Nes-KI* embryos, thus diluting the effect of any changes in TCA-cycle metabolites in the adult brain. Alternatively, as discussed above, it is possible that tamoxifen induced activation of mutant Idh1 expression with *nes-creER$^{T2}$* was less efficient than with standard *Nes-Cre*.

Additionally, it is possible that the 1.2-fold and 1.5-fold reduction in α-KG production detected in the brain of 4 and 8 month old *NesER$^{T2}$-KI* mice were not low enough to exert an effect on the level of other TCA cycle metabolites, or to stimulate an increase in glutamine flux in these animals. If this is the case, then the phenotype observed in *NesER$^{T2}$-KI* mice could not be attributed to changes in TCA cycle function or glutamine flux.

Overall, one would have to conclude from my results that it is unclear whether changes in TCA cycle metabolites and glutamine flux are pathologically relevant in IDH1/2 mutant tumours. Nevertheless, if an increase in glutamine flux does truly occur as a result of mutant IDH1 activity then inhibition of this pathway could represent an interesting target for treatment in IDH1/2 mutant tumours.

### 5.5.16 Stabilisation of HIF1α does not occur in *NesER$^{T2}$-KI* or *D2hgdh* KO mice

Hif1α target gene expression was not upregulated in the brains of our *NesER$^{T2}$-KI* mice and no increase in Hif1α protein expression was seen. These findings conflict with results

obtained from our IDH1 mutant cell lines and from other *in vitro* and *in vivo* studies in which an increase in HIF1α target gene expression was observed in association with mutant IDH1 expression (Zhao S 2009, Seltzer MJ 2010, Xu W 2011). Indeed Sasaki *et al.* demonstrated an upregulation of Vegf, Pgk1 and Glut1 expression in their brain-specific *Nes-KI* mice, but this was seen in conjunction with a 400-fold increase in 2-HG levels (in conjunction with a 1.2-fold reduction in α-KG). Furthermore, in *in vitro* studies, HIF1α target gene expression was increased in association with a 20 to 200-fold increased in 2-HG (and a 1.6- to 2.0-fold reduction in α-KG) (Xu W 2011, Sasaki M 2012b). In view of the fact that D-2HG has been shown to be a relatively weak inhibitor of HIF PHD (Zhao S 2009) it is likely that the near 2-fold increase in 2-HG seen in the brains of our *NesER$^{T2}$-KI* mice was simply insufficient to inhibit Hif Phd function. More speculatively, it is also possible that the increase in Hif1α observed in the brains of *Nes-KI* embryos in Sasaki's study did not in fact occur as a result of the inhibition of Hif Phd by 2-HG, but due to an alternative mechanism such as hypoxia, or an increase in ROS, resulting from brain haemorrhage, which was not seen in our *NesER$^{T2}$-KI* mice.

Nevertheless, although the upregulation of HIF1α has been proposed, by some authors, to cause malignant transformation in IDH1 mutant tumours (Zhao S 2009, Chowdhury R 2011, Xu W 2011), this mechanism was not demonstrated in our *NesER$^{T2}$-KI* mice, and therefore cannot be attributed to the increase in proliferative activity and nestin expression seen in the brain of these animals.

Similarly, Hif1α was not upregulated in the brains of *D2hgdh* KO mice. Again, this may reflect the fact that the 6-fold increase in 2-HG levels observed in the brains of these mice was insufficient to inhibit Hif phd function. Indeed an increase in Hif1α target gene expression was seen in the liver and to a lesser extent in the kidney in association with a 13-

and 9-fold increase in 2-HG levels respectively, suggesting that Hif Phd activity is indeed inhibited by higher concentrations of 2-HG. Additionally, these findings may demonstrate that the inhibitory effect of 2-HG on Hif Phd activity differs between specific tissues.

The expression of Egln1, which encodes for Phd2, was reduced in *NesER$^{T2}$-KI* mice. Phd2 is the primary regulator of Hif1α steady state levels during normoxia, and RNA interference directed against Phd2, is sufficient to stabilise Hif1α in normoxia, resulting in increased Hif1α nuclear accumulation and Hif-dependent transcription (Metzen E 2005). It is possible that the reduction seen in Egln1 expression occurred as a result of changes in its epigenetic regulation and if this theory could be proved through DNA methylation analysis, then this finding would provide an alternative explanation for the upregulation of Hif1α seen with mutant IDH expression. However, the significance of the reduction in Egln1 gene expression seen in our mutant mice, in the absence of a proven reduction in corresponding Phd2 or indeed Hif1α protein expression, remains unclear.

### 5.5.17 *NesER$^{T2}$-KI* mice do not develop glioma

None of our *NesER$^{T2}$-KI* mice developed glioma, suggesting that perhaps mutations in other genes, in addition to *Idh1*,are required for tumour initiation to occur *in vivo*. We did attempt to enhance the chance of glioma formation by crossing *NesER$^{T2}$-KI* mice with *Tp53* KO mice, in order to generate *nes-creER$^{T2}$;Idh1$^{+/fl(R132H)}$;Tp53$^{fl/fl}$* offspring. These mice are currently being analysed and are not included in this thesis.

It is also possible that gliomas may have formed in *NesER$^{T2}$-KI* mice at a later time point, but due to the development of hydrocephalus, these animals became unwell and died before tumours could develop. It is important to note however, that hematopoietic-specific Idh1 R132H KI mice have a normal life span and similarly do not develop malignancy, but do

show increased numbers of early haematopoietic progenitors and develop splenomegaly and anaemia, and also demonstrate increases in both histone and DNA methylation similar to those observed in human IDH1/2 mutant AML (Sasaki M 2012a).

I have however demonstrated an increase in nestin expression and cellular proliferation in the SVZ of *NesER$^{T2}$-KI* mice, together with a reduction in 5hmC levels and markers of oligodendrocytic differentiation, and it is conceivable that the increase in proliferative activity and upregulation in nestin expression seen in the SVZ of these mice represents a pre-malignant process occurring in NSCs and progenitors, most plausibly as a result of changes in epigenetic control. In fact these observations mirror those seen in the bone marrow cells of haematopoietic-specific Idh R132HI KI mice which also show a selective expansion of their haematopoietic stem and early progenitor compartments, in conjunction with altered epigenetic control (Sasaki M 2012a).

## 5.6 Conclusions

2-HG accumulates in the brains of *Nes-KI* embryos and α-KG production is reduced. However the activation of Idh1 R132H expression in utero by *Nestin-Cre* is embryonic lethal in *Nes-KI* embryos, most likely due to the development of brain haemorrhage. The activation of mutant Idh1 expression by *Sox2-Cre* is also embryonic lethal, as is the removal of *NeoR* from the genome of *Idh1-KI* mice by Flp.

Expression of Idh1 R132H in the brain of adult mice, using tamoxifen-inducible *nestin-creER$^{T2}$*, results in the development of hydrocephalus and ventriculomegaly, as well as the accumulation of 2-HG and a reduction in α-KG production in the brain. An increase in nestin expression and cellular proliferation is seen in the SVZ of *NesER$^{T2}$-KI* mice, together with a reduction in 5hmC levels and markers of oligodendrocytic differentiation throughout the brain. Although glioma did not develop in *NesER$^{T2}$-KI* mice, it is conceivable that the increase in proliferative activity and upregulation in nestin expression seen in the SVZ of these mice represents a pre-malignant process, occurring in NSCs and progenitor cells, most plausibly as a result of changes in epigenetic control. These findings are the first demonstration of a potentially tumour-associated, brain-specific phenotype for Idh1 R132H in a mouse model, and appear to implicate the alteration of epigenetic modification as an important tumourigenic aspect of mutant Idh1 activity, although further analysis of NSCs and progenitors from the SVZ is required to investigate this theory in more detail.

The above mentioned observations were not seen in *D2hgdh* KO mice, despite the fact that 2-HG accumulated to a greater extent in these animals. Consequently, although the current weight of evidence supports the theory that accumulated 2-HG is responsible for the tumourigenic affect of mutant IDH1 activity (Dang L 2009, Gross S 2010, Chowdhury R 2011, Reitman ZJ 2011, Xu W 2011, Koivunen P 2012, Lu C 2012, Sasaki M 2012a, Losman

J 2013), our data provides evidence that a reduction in α-KG production may also be required, alone, or in combination with 2-HG accumulation, in order for this to occur.

I did not demonstrate an inhibition of Hif-Phd or Jhdm activity as a consequence of Idh1 R132H expression, although this may reflect the fact that 2-HG accumulation did not occur at an adequate level to exert an effect on these enzymes, rather than refute the results of previous studies which demonstrate that these mechanisms play a role in tumourigenesis in IDH1/2 mutant glioma. Furthermore, although we have demonstrated a reduction in TCA cycle metabolite and glutamine/glutamate levels to occur in the brains of our *Nes-KI* embryos, these findings were not reproduced in the brains of adult *NesER$^{T2}$-KI* mice, and it remains unclear whether TCA cycle dysfunction or increased glutamine flux represent pathological mechanisms in IDH1/2 mutant glioma.

# 6. Chapter Six

## Summary, Implication of Findings and Future Perspectives

### 6.1 Summary and implication of findings

Gliomas account for 80% of all primary malignant brain tumours (Sasaki M 2012b). GBM, the most common and aggressive form of glioma, is associated with a very poor prognosis and the median overall survival is generally less than one year (Puzzilli F 1998, Scott JN 1998, Buckner JC 2003, Stark AM 2005, Goodenberger ML 2012). In fact, even with optimal combination therapy incorporating surgery, radiotherapy and TMZ chemotherapy, median OS is only 14.6 months, and observed 2- and 5-year survival rates are 26.5% and 9.8% respectively (Curran WJ Jr 1993, Stupp R 2009).

Following Stupps's pivotal trial in 2005, the addition of concurrent and adjuvant TMZ chemotherapy to surgery and radiotherapy, as first line therapy in GBM, represented the first treatment to improve prognosis in a population in whom survival outcomes had not improved for over thirty years (Stupp R 2005). The median time to recurrence after optimal surgery and TMZ chemoradiotherapy is however only 6.9 months (Stupp R 2009) and at this stage repeat surgical resection and re-irradiation are often not feasible. Furthermore, treatment with nitrosourea-based chemotherapy, currently considered to be the most active therapeutic option in this setting, is associated with an objective tumour response rate of less than 10% (Stupp R 2005) and does not offer a significant OS benefit (Wong ET 1999), whilst alternative chemotherapeutic agents offer lower response rates and additional toxicity (Grossman SA 2004). Consequently, patients with relapsed GBM have limited treatment options.

Our understanding of the molecular mechanisms and signalling pathways involved in gliomagenesis has improved over the last decade, as a result of genome-wide molecular characterisation and profiling analyses (Friedman HS 1999), and subsequent research efforts have focused on developing molecularly targeted therapies directed against such aberrations, with the hope of improving treatment outcomes in patients with GBM (McLendon R 2008). However such therapies, used alone or in combination, have to date proved largely disappointing, and have failed to improve OS in patients with newly diagnosed or relapsed disease. This contrasts with the situation seen in other tumour types such as breast, lung, renal, and colon cancer, and in melanoma, in which the development of drugs that directly target the overexpression or mutation of genes involved in key tumourigenic signalling pathways, such as *HER2* (Marty M 2005, Collins VP 2007, Perez EA 2011, Verma S 2012), *EGFR* (Maemondo M 2010, Rosell R 2012, Sequist LV 2013, Swain SM 2013), *VEGF* (Giantonio BJ 2007, Motzer RJ 2009, Sternberg CN 2010, Van Cutsem E 2012, Ye LC 2013), *BRAF* (Bennouna J 2013) and *MEK* (Chapman PB 2011), has improved the treatment landscape and increased survival in patients with these cancers. A fuller understanding of the complex genetic changes that occur in GBM, as well as the identification of novel therapeutic targets, is therefore required, in order for molecularly targeted agents to also offer the potential to improve treatment and survival in patients with GBM.

Somatic mutations at R132 of IDH1 and R172 of IDH2 have recently been shown to occur in 80-90% of adult grade II/III glioma and secondary GBM and in 5-10% of primary GBM (Balss J 2008, Bleeker FE 2009, Yan H 2009, Flaherty KT 2012), raising the possibility that mutant IDH1/2 may represent an attractive therapeutic target in these tumours. Consequently, research efforts have focused on investigating the tumourigenic effects of mutant IDH1/2 in the hope that a greater understanding of these processes may allow such therapies to be developed.

It has been widely proposed that mutant IDH1/2 exerts its tumourigenic effect by catalysing the conversion of α-KG to D-2HG, which accumulates in IDH1/2 mutant cells and is thought to act as an oncometabolite through the inhibition of α-KG dependent enzymes (Chowdhury R 2011, Kloosterhof NK 2011, Xu W 2011, Lu C 2012). Indeed, both the expression of mutant IDH1/2 and D-2HG accumulation have been shown to inhibit the activity of HIF-PHD (Zhao S 2009, Xu W 2011, Koivunen P 2012), TET (Xu W 2011, Sasaki M 2012b), and JHDMs (Chowdhury R 2011, Xu W 2011, Koivunen P 2012), and to affect changes in HIF1α target gene expression (Zhao S 2009, Lu C 2012), DNA methylation (Figueroa ME 2010, Lu C 2012, Turcan S 2012, Sasaki M 2012b, Losman J 2013) and histone methylation (Chowdhury R 2011, Xu W 2011, Lu C 2012, Sasaki M 2012a) respectively. It has also been postulated that mutant IDH1/2 activity may promote cellular transformation by changing the redox state of cells, or by altering normal TCA cycle function and shifting cellular energy production from oxidative phosphorylation towards glycolysis, stimulating the so called 'Warburg effect'. I have attempted to investigate the importance of these potential mechanisms in the development of IDH1/2 mutant tumours, using cell and mouse models. The results from these studies in summarised in Table 6-1.

**Table 6-1: Summary of results from cell and mouse models discussed in this thesis**

| | **IDH1 Knockdown LN18 cell** | **IDH2 Knockdown LN18 cell** | **IDH1 mutant LN18 cell** | **IDH2 mutant LN18 cell** | **IDH1 mutant ES cell line** | **IDH2 mutant ES cell** | ***Nes-KI* embryos** | ***NesER$^{T2}$-KI* mice** | ***D2hgdh-KO* mice** |
|---|---|---|---|---|---|---|---|---|---|
| **Cerebral haemorrhage** | N/A | N/A | N/A | N/A | N/A | N/A | Yes | No | No |
| **Hydrocephalus** | N/A | N/A | N/A | N/A | N/A | N/A | N/A | Yes | No |
| **Ventriculomegaly** | N/A | N/A | N/A | N/A | N/A | N/A | N/A | Yes | No |
| **α-KG level** | ↔ | ↔ | ↓ | ↓ | ↔ | ↔ | ↓ | ↓ | ↔ |
| **2-HG level** | ↔ | ↔ | ↑ | ↑ | ↔ | ↔ | ↑ | ↑ | ↑ |
| **Levels of other TCA metabolites** | ↔ | ↔ | ↔ | ↔ | ↔ | ↔ | ↓ | ↔ | N/A |
| **Glutamine/Glutamate** | N/A | N/A | N/A | N/A | N/A | N/A | ↓ | ↔ | N/A |
| **HIF1α expression** | ↑ | ↔ | ↑ | ↑ | ↑ | ↑ | N/A | ↔ | ↔ |
| **5hmC levels** | N/A | N/A | N/A | N/A | ↓ | ↓ | N/A | ↓ | ↔ |
| **Rbp1 expression** | N/A | N/A | N/A | N/A | N/A | N/A | N/A | ↓ | N/A |
| **Histone methylation** | N/A | N/A | N/A | N/A | ↔ | ↔ | N/A | ↔ | N/A |
| **Nestin expression** | N/A | N/A | ↔ | ↔ | N/A | N/A | N/A | ↑ | ↔ |
| **Markers of differentiation** | N/A | N/A | N/A | N/A | N/A | N/A | N/A | ↓ | N/A |
| **Proliferation rate** | ↓ | ↓ | ↓ | ↓ | N/A | N/A | N/A | ↑ | N/A |
| **NADPH** | ↓ | ↓ | ↓ | ↓ | ↓ | ↓ | N/A | N/A | N/A |
| **ROS levels** | ↑ | ↔ | ↑ | ↔ | ↔ | ↔ | N/A | N/A | N/A |

I have demonstrated that a reduction in 5hmC levels and an increase in HIF1α expression occur in association with the expression of mutant IDH1/2 *in vitro*. 2-HG accumulation and a reduction in α-KG production are also seen in these mutant cells and it is plausible that the changes in 5hmC levels and HIF1α expression observed occurred through the inhibition of TET and HIF-PHD, by accumulated 2-HG and/or reduced levels of α-KG. However, in view of the fact that I was unable to generate IDH1/2 knockdown cell lines in which cellular α-KG levels were reduced, I was unable to conclude whether 2-HG accumulation or reduced α-KG were most likely to be responsible for the decrease in 5hmC and increase in HIF1α expression observed in IDH1/2 mutant cell lines. Changes in cellular redox state, as evidenced by a reduction in cellular NADPH levels and an increase in levels of ROS, were also observed in IDH1/2 mutant cell lines, however, changes in histone methylation and TCA cycle flux were not shown to occur.

I have demonstrated that 5hmC levels are also reduced in the brains of adult, brain-specific, Idh1 R132H KI (*NesER$^{T2}$-KI*) mice. 2-HG accumulation and a reduction in α-KG production are also seen in the brain of these animals, and together, these findings provide further evidence that Tet function is likely to be inhibited by mutant Idh1 activity.

An increase in nestin expression and cellular proliferation are also seen in the SVZ of *NesER$^{T2}$-KI* mice, and markers of oligodendrocytic differentiation are reduced throughout the brain. Although *NesER$^{T2}$-KI* mice did not develop glioma, it is conceivable that the increase in proliferative activity and upregulation in nestin expression seen in the SVZ of these animals represents a pre-malignant process occurring in NSCs and progenitor cells, and given that 5hmC levels are also reduced in the brains of these mice, it is most plausible that this occurs as a result of changes in epigenetic control. These findings are the first demonstration of a potentially tumour-associated, brain-specific phenotype for Idh1 R132H in a mouse

model, and appear to implicate the alteration of epigenetic modification as an important tumourigenic aspect of mutant Idh1 activity.

In view of the fact that changes in 5hmC levels, nestin expression and proliferation were not seen in the brains of *D2hgdh* KO mice, despite the fact that 2-HG accumulated to a greater extent in these animals, it seems plausible that a reduction in α-KG production may also be required, alone, or in combination with 2-HG accumulation, in order for these changes to occur. This finding conflicts with previous evidence and consensus in the literature, which support the theory that accumulated 2-HG is responsible for the tumourigenic affect of mutant IDH1 activity (Dang L 2009, Gross S 2010, Chowdhury R 2011, Reitman ZJ 2011, Xu W 2011, Duncan CG 2012, Koivunen P 2012, Lu C 2012, Losman J 2013). However, the possibility that 2-HG accumulation alone may be insufficient to cause tumourigenesis, is further supported by the fact that mutations in other genes, also theoretically capable of causing increased 2-HG production, namely *HOT, L2HGDH* and *D2HGDH* were found not to occur in the panel of IDH1/2 wild-type GBMs analysed as part of this thesis.

In contrast to my IDH1/2 mutant cell lines, I could not demonstrate any evidence of Hif-Phd inhibition in the brains of *NesER$^{T2}$-KI* mice. Furthermore, Jhdm function did not appear to be inhibited in these animals. Although these findings may reflect the fact that 2-HG accumulation, or the reduction in α-KG production, did not occur at an adequate level to exert an effect on Jhdm or Hif-Phd activity in *NesER$^{T2}$-KI* mice, they do appear to refute the results of previous studies which suggest that these mechanisms play a role in tumourigenesis in IDH1/2 mutant glioma (Zhao S 2009, Chowdhury R 2011, Xu W 2011, Sasaki M 2012b).

A reduction in TCA cycle metabolite and glutamine/glutamate levels were demonstrated in the brains of our *Nes-KI* embryos, however these findings were not reproduced in adult *NesER$^{T2}$-KI* mice, or indeed in IDH1/2 mutant cell lines, and therefore it remains unclear

whether TCA cycle dysfunction or increased glutamine flux represent pathological mechanisms in IDH1/2 mutant glioma.

Overall my findings, substantiate those of other studies (Figueroa ME 2010, Xu W 2011, Koivunen P 2012, Lu C 2012, Turcan S 2012, Losman J 2013), by demonstrating that the inhibition of TET function may plausibly contribute to the pathogenesis of IDH1/2 mutant glioma, most likely as a result of changes in epigenetic control. I have however additionally demonstrated that both 2-HG accumulation and a reduction in α-KG production may be required in order for these changes to occur. Changes in cellular redox state may also play a role in the pathogenesis of IDH1/2 mutant glioma and I have demonstrated a decrease in NADPH and an increase in ROS to occur in IDH1/2 mutant cell lines, but have yet to confirm these findings *in vivo*. It remains unclear from my results whether the inhibition of HIF-PHD, or changes in TCA cycle function or glutamine flux represent pathological mechanisms in IDH1/2 mutant glioma. Finally, I did not demonstrate an increase in histone methylation to occur as a result of mutant IDH1/2 expression *in vitro* or *in vivo*, although evidence from other studies have suggested that this does occur (Chowdhury R 2011, Xu W 2011, Duncan CG 2012, Lu C 2012, Sasaki M 2012a).

The above findings are clinically relevant, as each of the mechanisms discussed represent a potential target in the treatment of IDH1/2 mutant glioma.

Indeed, two compounds directly targeting mutant IDH1 R132H (AGI 5198) (Rohle D 2013) and IDH2 R140Q (AGI 6780) (Popovici-Muller J 2012) have recently been developed, and although the potential clinical benefit of such inhibitors is not yet clear, they have shown early promise in pre-clinical trials (Wang F 2013) (Losman J 2013) (Rohle D 2013), and their emergence raises new hope for the treatment of IDH1/2 mutant glioma. However, given that IDH1/2 mutant glioma are associated with a relatively favourable prognosis compared to

IDH1/2-WT tumours, it remains to be seen whether blockade of neomorphic enzyme activity and subsequent removal of the block to cellular differentiation associated with this is beneficial or in fact harmful to patients.

In addition to inhibiting the activity of mutant IDH1/2, it may also be possible to directly target mutations in *IDH1/2* with antisense oligonucleotides, or to pharmacologically revert the epigenetic changes associated with such mutations using histone deacetylase inhibitors (HDAC) or DNA methyltransferase (DNMT) inhibitors (Rohle D 2013). Early clinical studies have shown the HDAC inhibitor vorinostat to be active in GBM (Malzkorn B 2011) and to be well tolerated as a single agent (Galanis E 2009), and when combined with TMZ (Galanis E 2009). Furthermore, valproic acid, which has HDAC inhibitory activity, has been shown to prolong survival in some glioma patients (Lee EQ 2012) and to increase the sensitivity of glioma cells to radiation (Weller M 2011). HDAC inhibitors have also shown promise in early clinical trials in AML (Garcia-Manero 2012, Van Nifterik KA 2012). It is important to note however that these studies were not stratified on the basis of IDH1/2 mutational status, so direct conclusions as to the efficacy of HDAC inhibitors in IDH1/2 mutant versus wild-type disease cannot be drawn. The DNMT inhibitor, decitabine, has however shown promise in early pre-clinical trials as a treatment in IDH1 mutant tumours. Treatment with decitabine reversed mutant IDH1 induced hypermethylation and block in differentiation, and resulted in a dramatic loss of stem-like properties, in IDH1 mutant but not IDH1 wild-type GICs, and also decreased tumour growth and replicative potential *in vivo*. Furthermore it did so in a more efficient manner than was seen with the mutant IDH1 enzyme inhibitor AGI 5198 (Mims A 2012).

Directly targeting 2-HG production by inhibiting the conversion of glutamine to α-KG may also represent an attractive treatment strategy. Indeed, the inhibition of glutamine to α-KG conversion using siRNA and the small molecule inhibitor bis-2-(5-phenyl-acetamido1,2,4-

thiadiazol-2-yl)ethyl sulfide (BPTES), has been shown to slow the growth rate of IDH1 mutant glioma cells, suggesting that 'starving' mutant IDH1/2 cells of α-KG may have therapeutic benefit (Turcan S 2013). However, conversely, it is possible that treatment with exogenous α-KG may also be beneficial, in order to reverse the competitive inhibitory effect of 2-HG on α-KG dependent enzymes, and to reverse the reduction in α-KG production seen in association with mutant IDH1/2 expression.

Targeting other aspects of the glutamate system may also hold promise. Indeed, the efficacy of Talampanel, an antagonist of the α-Amino-3-hydroxy-5-methyl-4-isoxazolepropionic Acid (AMPA) glutamate receptor was studied in a phase II trial, in combination with radiotherapy and TMZ in patients with newly diagnosed GBM (Seltzer MJ 2010). A 5.7-month improvement in median OS was observed when compared to historical controls that had received radiotherapy and TMZ alone (Grossman S 2009). Although, again, this study did not stratify patients based on IDH1/2 mutation status, and therefore conclusions specific to IDH1/2 mutant disease cannot be drawn. It should also be noted that in a phase II trial of single agent Talampanel in patients with recurrent GBM and anaplastic glioma, no significant anti-tumour effect was observed and the trial was terminated early due to treatment futility (Grossman S 2009).

More controversially, given the uncertainty regarding its role in IDH1/2 mutant malignant transformation, it may also be beneficial to explore the potential of HIF-PHD inhibitors in the treatment of IDH1/2 mutant tumours. Such compounds have been investigated in early stage trials in non malignant disease (Iwamoto F 2010), but not as of yet in GBM.

Even more speculatively, if an increase in nestin expression is directly involved in an early malignant process in GBM, then the direct inhibition of nestin expression may serve as a potential target for treatment. Indeed, it is noteworthy that in pancreatic cancer cells

downregulation of nestin has been shown to inhibit the growth of liver metastasis *in vivo* (Robinson A 2008). Furthermore, in lung cancer cell lines, Akt inhibitors have been shown to effectively decrease nestin expression through the downregulation of Sox2, and to inhibit nestin induced tumour sphere formation *in vitro* (Matsuda Y 2012).

As well as representing a potential target for treatment, IDH1/2 mutations also undoubtedly have a role to play as prognostic and predictive biomarkers in GBM (Narita K 2014) and as new treatments options emerge in this disease, a greater understanding of the predictive value of IDH1/2 mutation status may enable therapies to be tailored more appropriately to patients in the future.

## 6.2 Future Perspectives

The fact that abnormal DNA methylation patterns are a common feature of IDH1/2 mutant tumours suggests that the inhibition of TET by 2-HG accumulation or reduced α-KG production are likely to be responsible for tumourigenesis, rather than TCA cycle dysregulation per se. The development of a 'pseudohypoxic state' resulting from the stabilization of HIF1α may also play a role, although activation of this pathway may not be the primary tumour initiating event. The absolute effects of these phenomena however remain unknown and further research, perhaps using genetically engineered mouse models, is required to characterize the 'downstream' genetic effects and pathways that give IDH1/2 mutant cells their pro-tumourigenic potential. To date, no tumour-forming genetically engineered Idh1/2-mutant model has been established. It is hoped that the development of such a model, perhaps through the use of the *NesER$^{T2}$-KI* mouse developed in this thesis, will benefit patients with IDH1/2 mutant tumours by enabling us to better understand the relationship between IDH1/2 mutations and tumourigenesis, and to develop and test effective therapies directed against these tumours in the future. Indeed, such therapies are now

emerging in pre-clinical trials, but they have not yet been tested in clinical practice and their potential benefit to patients with GBM remains to be determined. The potential clinical application of IDH1/2 mutations as diagnostic, prognostic, and predictive tools also requires further evaluation and this may be achieved in the future through clinical trials stratified specifically by IDH1/2 mutation status.

# 7. Chapter Seven

## Future Work

The main aims of future work related to this thesis are to:

1) Confirm and further investigate the changes seen in the brains and other organs of *NesER$^{T2}$-KI* mice, and

2) To attempt to generate brain tumours in *NesER$^{T2}$-KI* mice by crossing these mice with *Tp53 KO* mice and with *D2hgdh KO* mice.

It is known that tamoxifen-induced gene activation in a given tissue is often incomplete, and induced mice are usually mosaics with varying fractions of wild-type and mutant cells (Choi C 2012). We aim to investigate the tissue specificity and recombination efficiency of *nestin-creER$^{T2}$* further using ROSA26-Enhanced Yellow Fluorescent Protein (EYFP) reporter mice and have recently crossed *NesER$^{T2}$-KI* mice with these animals. We hope to be able to confirm the efficient recombination of *nestin-creER$^{T2}$* specifically in the brain of these animals.

We aim to further investigate the DNA methylation profile of *NesER$^{T2}$-KI* mice brains using methylated DNA immunoprecipitation high output sequencing (MeDIP-seq) techniques. It is hoped that this will allow us to identify which genes are hypermethylated in association with mutant Idh1 expression. In particular, we would like to confirm whether hypermethylation of the Rbp1 promoter region, or hypermethylation of other genes involved in RAR activation are seen.

Measurement of NADPH and ROS levels will also be performed in the brains of *NesER$^{T2}$-KI* mice, in order to confirm that changes in cellular redox state also occur as a result of mutant IDH1/2 expression *in vivo*.

We aim to analyse 5hmC, HIF1α, and H3K9me3 levels in cells within the SVZ of *NesER$^{T2}$-KI* mice using IHC to a) confirm that 5hmC levels are reduced in the hyperproliferating cells seen in this region; and b) to assess whether changes in HIF1α and H3K9me3 levels can be detected specifically in these cells, in view of the fact that their levels were not seen to be altered in the whole brain using western blotting. We also aim to confirm the increase in proliferative activity of cells, seen by IHC, with in the SVZ of *NesER$^{T2}$-KI* mice (and potentially also in the RMS and OB), using 5-bromo-2-deoxyuridine (BrdU), flourescently-labelled BrdU antibodies and immunoflourescence techniques.

It would also be desirable to specifically isolate cells from the SVZ of *NesER$^{T2}$-KI* mice and culture them ex vivo in order to assess characteristics of these cells such as their 2-HG and α-KG content, DNA hypermethylation and gene expression profiles, proliferation rate, stem cell-like features, and features associated with malignant transformation such as anchorage independent growth.

Further analysis of MRI imaging of the brains of *NesER$^{T2}$-KI* mice is required to ascertain the cause of the hydrocephalus observed in these animals and to ascertain whether hydrocephalus is limited to the lateral ventricles or if indeed it occurs in other areas of the ventricular system. MRI analysis of the rostral migratory system would also be desirable to identify if macroscopic alterations occur in this region. Assessment of intracranial pressure would also help to identify the cause of the hydrocephalus seen.

Given the fact that the metabolic effects of mutant Idh1 expression may pertubate to other areas of the brain where nestin is not expressed such as the cerebellum, or indeed to other organs, we would also propose to perform the above analyses on tissue taken from the cerebellum and other organs of *NesER$^{T2}$-KI* mice to identify if mutant Idh1 expression can in fact exert a paracrine effect on surrounding tissues.

In view of the fact that mutations in *Idh1* alone may be insufficient to promote tumourigenesis, and in order to increase the likelihood of brain tumours developing in *NesER$^{T2}$-KI* mice, Tp53 KO mice were crossed with *NesER$^{T2}$-KI* animals. *NesER$^{T2}$-KI;Tp53$^{fl/fl}$* offspring are currently being aged, and will be analysed at a time at which they become unwell. *NesER$^{T2}$-KI* mice have also been crossed with *D2hgdh KO* mice, as it is predicted that *NesER$^{T2}$-KI;D2hgdh$^{fl/fl}$* offspring will accumulate higher levels of 2-HG in the brain than *NesER$^{T2}$-KI;D2hgdh$^{+/+}$* mice, and that this may in turn increase the likelihood of glioma developing in these animals. *NesER$^{T2}$-KI;D2hgdh$^{fl/fl}$* mice are currently being aged and will also be analysed at a time at which they become unwell.

# References.


Abdel-Wahab O, Mullally A, Hedvat C, Garcia-Manero G, Patel J, Wadleigh M, Malinge S, Yao J, Kilpivaara O, Bhat R, Huberman K, Thomas S, Dolgalev I, Heguy A, Paietta E, Le Beau MM, Beran M, Tallman MS, Ebert BL, Kantarjian HM, Stone RM, Gilliland DG, Crispino JD, Levine RL. (2009). "Genetic characterization of TET1, TET2, and TET3 alterations in myeloid malignancies." Blood. **114**(1): 144-147.

Abdel-Wahab O, Patel J, Levine RL. (2011). "Clinical implications of novel mutations in epigenetic modifiers in AML." Hematol Oncol Clin North Am **25**: 1119–1133.

Achouri Y, Noel G, Vertommen D, Rider MH, Veiga-da-Cunha M, Schaftingen E. (2004). "Identification of a dehydrogenase acting on D-2-hydroxyglutarate." Biochem J **381**: 35-42.

Acker T, Diez-Juan A, Aragones J, Tjwa M, Brusselmans K, Moons L, Fukumura D, Moreno-Murciano MP, Herbert JM, Burger A, Riedel J, Elvert G, Flamme I, Maxwell PH, Collen D, Dewerchin M, Jain RK, Plate KH, Carmeliet P. (2005). "Genetic evidence for a tumour suppressor role of HIF2α." Cancer cell **8**: 131-141.

Agarwal S, Sharma M, Jha P, Pathak P, Suri V, Sarkar C, Chosdol K, Suri A, Kale SS, Mahapatra AK, Jha P. (2013). "Comparative study of IDH1 mutations in gliomas by immunohistochemistry and DNA sequencing." Neuro Oncol. **15** (6): 718-726.

Aghili M, Zahedi Z, Rafiee E. (2009). "Hydroxyglutaric aciduria and malignant brain tumour: a case report and literature review." J Neurooncol **91**: 233-236.

Al Aqeel A, Rashed M, Ozand PT, Gascon GG, Rahbeeni Z, al Gstseo S, al Odaib A, Brismar J. (1994). "A new patient with alpha-ketoglutaric aciduria and progressive extrapyramidal tract disease." Brain Dev **16(Suppl)**: 33–37.

Alcantara Llaguno S, Chen J, Kwon CH, Jackson EL, Li Y, Burns DK, Alvarez-Buylla A, Parada LF (2009). "Malignant astrocytomas originate from neural stem/progenitor cells in a somatic tumor suppressor mouse model." Cancer cell **15**(1): 45-56.

Alvarez-Buylla A, Lim D (2004). "For the long run: Maintaining germinal niches in the adult brain." Neuron **41**: 683–686.

Amary MF, Bacsi K, Maggiani F, Damato S, Halai D, Berisha F, Pollock R, O'Donnell P, Grigoriadis A, Diss T, Eskandarpour M, Presneau N, Hogendoorn PC, Futreal A, Tirabosco R, Flanagan AM. (2011a). "IDH1 and IDH2 mutations are frequent events in central chondrosarcoma and central and periosteal chondromas but not in other mesenchymal tumours." The journal of Pathology **224(3)**(3): 334-343.

Amary MF, Damato S, Halai D, Eskandarpour M, Berisha F, Bonar F, McCarthy S, Fantin VR, Straley KS, Lobo S, Aston W, Green CL, Gale RE, Tirabosco R, Futreal A, Campbell P, Presneau N, Flanagan AM. (2011b). "Ollier disease and Maffucci syndrome are caused by somatic mosaic mutations of IDH1 and IDH2." Nat Genet. **43**(12): 1262-1265.

Arai H, Ikota H, Sugawara K, Nobusawa S, Hirato J, Nakazato Y (2012). "Nestin expression in brain tumors: its utility for pathological diagnosis and correlation with the prognosis of high-grade gliomas." Brain Tumor Pathol **29**: 160-167.

Attenello FJ, Mukherjee D, Datoo G, McGirt MJ, Bohan E, Weingart JD, Olivi A, Quinones-Hinojosa A, Brem H. (2008). "Use of Gliadel (BCNU) wafer in the surgical treatment of malignant glioma: a 10-year institutional experience." Ann Surg Oncol. **15**(10): 2887-2893.

Bach F. (2011). "Current status of a phase III trial of nimotuzumab (ti-EGF-R) in newly diagnosed glioblastoma" Journal of Clinical Oncology **29, supplement, 2011, Abstract no. 2059**.

Bachoo RM, Maher EA, Ligon KL, Sharpless NE, Chan SS, You MJ, Tang Y, DeFrances J, Stover E, Weissleder R, Rowitch DH, Louis DN, DePinho RA (2002). "Epidermal growth factor receptor and Ink4a/Arf: convergent mechanisms governing terminal differentiation and transformation along the neural stem cell to astrocyte axis." Cancer Cell. **1**(3): 269-277.

Baglietto L, Giles GG, English DR, Karahalios A, Hopper JL, Severi G. (2011). "Alcohol consumption and risk of glioblastoma; evidence from the Melbourne Collaborative Cohort Study." Int J Cancer. **128**(8): 1929-1934.

Bähr O, Hattingen E, Rieger J, Steinbach JP. (2011). "Bevacizumab-induced tumor calcifications as a surrogate marker of outcome in patients with glioblastoma." Neuro Oncol. **13**(9): 1020-1029.

Balss J, Meyer J, Mueller W, Korshunov A, Hartmann C, von Deimling A. (2008). "Analysis of the IDH1 codon 132 mutation in brain tumors." Acta Neuropathol. **116** (6): 597-602.

Bao S, Wu Q, McLendon RE. (2006). "Glioma stem cells promote radioresistance by preferential activation of the DNA damage response." Nature **444**: 756–760. .

Bardella C, Pollard PJ, Tomlinson I. (2011). "SDH mutations in cancer." Biochimica et biophysica acta, **1807** (11): 1432-1443

Bardelli A, Longati P, Gramaglia D, Basilico C, Tamagnone L, Giordano S, Ballinari D, Michieli P, Comoglio PM. (1998). "Uncoupling signal transducers from oncogenic MET mutants abrogates cell transformation and inhibits invasive growth." Proc. Natl. Acad. Sci. USA, **95** 14379-14383.

Barker FG 2nd, Davis RL, Chang SM, Prados MD. (1996). "Necrosis as a prognostic factor in glioblastoma multiforme." Cancer **77**: 1161-1166.

Barnes LD, Kuehn GD, Atkinson DE. (1971). "Yeast diphosphopyridine nucleotide specific isocitrate dehydrogenase. Purification and some properties." Biochemistry. **10**(21): 3939-3944.

Batchelor TT, Betensky RA, Esposito JM, Pham LD, Dorfman MV, Piscatelli N, Jhung S, Rhee D, Louis DN. (2004). "Age-dependent prognostic effects of genetic alterations in glioblastoma." Clin Cancer Res. **10**: 228-233.

Batchelor TT, Mulholland P, Neyns B, Nabors LB, Campone M, Wick A, Mason W, Mikkelsen T, Phuphanich S, Ashby LS, Degroot J, Gattamaneni R, Cher L, Rosenthal M, Payer F, Jürgensmeier JM, Jain RK, Sorensen AG, Xu J, Liu Q, van den Bent M. (2013). "Phase III randomized trial comparing the efficacy of cediranib as monotherapy, and in combination with lomustine, versus lomustine alone in patients with recurrent glioblastoma." J Clin Oncol. **31** (26): 3212-3218.

Becher OJ, Hambardzumyan D, Walker TR, Helmy K, Nazarian J, Albrecht S, Hiner RL, Gall S, Huse JT, Jabado N, MacDonald TJ, Holland EC. (2010). "Preclinical evaluation of radiation and perifosine in a genetically and histologically accurate model of brainstem glioma." Cancer Res. **70**(6): 2548-2557.

Beier D, Wischhusen J, Dietmaier W, Hau P, Proescholdt M, Brawanski A, Bogdahn U, Beier CP. (2008). "CD133 expression and cancer stem cells predict prognosis in high-grade oligodendroglial tumors." Brain Pathol **18**: 370–377.

Bennouna J, Sastre J, Arnold D, Österlund P, Greil R, Van Cutsem E, von Moos R, Viéitez JM, Bouché O, Borg C, Steffens CC, Alonso-Orduña V, Schlichting C, Reyes-Rivera I, Bendahmane B, André T, Kubicka S; ML18147 Study Investigators. (2013). "Continuation of bevacizumab after first progression in metastatic colorectal cancer (ML18147): a randomised phase 3 trial." Lancet Oncol. **14** (1): 29-37.

Bent MJ, Afra D, Witte O, Ben Hassel M, Schraub S, Hoang-Xuan K, Malmström PO, Collette L, Piérart M, Mirimanoff R, Karim AB; EORTC Radiotherapy and Brain Tumor Groups and the UK Medical Research Council. (2005). "Long-term efficacy of early versus delayed radiotherapy for low-grade astrocytoma and oligodendroglioma in adults: the EORTC 22845 randomised trial." Lancet **366**: 985–990.

Berra E, Benizri E, Ginouvès A, Volmat V, Roux D, Pouysségur J. (2003). "HIF prolyl-hydroxylase 2 is the key oxygen sensor setting low steady-state levels of HIF-1alpha in normoxia." EMBO J. **22** (16): 4082-4090.

Biedermann KA, Sun JR, Giaccia AJ, Tosto LM, Brown JM (1991). "scid mutation in mice confers hypersensitivity to ionizing radiation and a deficiency in DNA double-strand break repair." Proc Natl Acad Sci U S A. **88** (4): 1394-1397.

Binello E, Germano IM. (2011). "Targeting glioma stem cells a novel framework for brain tumors. ." Cancer sci. **102** (11): 1958-1966.

Biswas A, Hutchins R. (2007). "Embryonic stem cells." Stem Cells and Development **16**(2): 213-222. .

Bleeker FE, Atai NA, Lamba S, Jonker A, Rijkeboer D, Bosch KS, Tigchelaar W, Troost D, Vandertop WP, Bardelli A, Van Noorden CJ. (2010). "The prognostic IDH1( R132 ) mutation is associated with reduced NADP+-dependent IDH activity in glioblastoma." Acta Neuropathol. **119** (4): 487-494. .

Bleeker FE, Lamba S, Leenstra S, Troost D, Hulsebos T, Vandertop WP, Frattini M, Molinari F, Knowles M, Cerrato A, Rodolfo M, Scarpa A, Felicioni L, Buttitta F, Malatesta S, Marchetti A, Bardelli A. (2009). "IDH1 mutations at residue p.R132 (IDH1(R132)) occur frequently in high-grade gliomas but not in other solid tumors." Hum Mutat. **30**(1): 7-11.

Block K, Gorin Y. (2012). "Aiding and abetting roles of NOX oxidases in cellular transformation." Nat Rev Cancer. **12**(9): 627-637.

Blomhoff R, Blomhoff HK. (2006). "Overview of retinoid metabolism and function." J Neurobiol 606–630. **66**(7): 606–630.

Blouw B, Song H, Tihan T, Bosze J, Ferrara N, Gerber HP, Johnson RS, Bergers G. (2003). "The hypoxic response of tumors is dependent on their microenvironment." Cancer cell **4**(2): 133-146.

Borger DR, Tanabe KK, Fan KC, Lopez HU, Fantin VR, Straley KS, Schenkein DP, Hezel AF, Ancukiewicz M, Liebman HM, Kwak EL, Clark JW, Ryan DP, Deshpande V, Dias-Santagata D, Ellisen LW, Zhu AX, Iafrate AJ. (2012). "Frequent mutation of isocitrate dehydrogenase (IDH)1 and IDH2 in cholangiocarcinoma identified through broad-based tumour genotyping." The oncologist **17**(1): 72-79.

Bralten LB, Kloosterhof NK, Balvers R, Sacchetti A, Lapre L, Lamfers M, Leenstra S, de Jonge H, Kros JM, Jansen EE, Struys EA, Jakobs C, Salomons GS, Diks SH, Peppelenbosch M, Kremer A, Hoogenraad CC, Smitt PA, French PJ. (2011). "IDH1 R132H decreases proliferation of glioma cell lines in vitro and in vivo." Ann Neurol. **69** (3): 455-463.

Bruni JE, Del Bigio MR, Cardoso ER, Persaud TV. (1988). "Hereditary hydrocephalus in laboratory animals and humans." Exp Pathol. **35**(4): 239-246.

Buckner JC. (2003). "Factors influencing survival in high-grade gliomas." Semin Oncol **30**(Suppl 19): 10-14.

Burger PC, Green SB. (1987). "Patient age, histologic features, and length of survival in patients with glioblastoma multiforme." Cancer **59**(9): 1617-1625.

Butowski N, Chang SM, Lamborn KR, Polley MY, Pieper R, Costello JF, Vandenberg S, Parvataneni R, Nicole A, Sneed PK, Clarke J, Hsieh E, Costa BM, Reis RM, Hristova-Kazmierski M, Nicol SJ, Thornton

DE, Prados MD. (2011). "Phase II and pharmacogenomics study of enzastaurin plus temozolomide during and following radiation therapy in patients with newly diagnosed glioblastoma multiforme and gliosarcoma." Neuro Oncol. **13** (12): 1331-1338.

Cairncross G, Berkey B, Shaw E. (2006). "Phase III trial of chemotherapy plus radiotherapy compared with radiotherapy alone for pure and mixed anaplastic oligodendroglioma: Intergroup Radiation Therapy Oncology Group Trial 9402." J Clin Oncol **24**: 2707-2714.

Cairns RA, Iqbal J, Lemonnier F, Kucuk C, de Leval L, Jais JP, Parrens M, Martin A, Xerri L, Brousset P, Chan LC, Chan WC, Gaulard P, Mak TW. (2012). "IDH2 mutations are frequent in angioimmunoblastic T-cell lymphoma." Blood **119**(8): 1901-1903.

Capper D, Reuss D, Schittenhelm J, Hartmann C, Bremer J, Sahm F, Harter PN, Jeibmann A, von Deimling A. (2011). "Mutation-specific IDH1 antibody differentiates oligodendrogliomas and oligoastrocytomas from other brain tumours with oligodendroglioma-like morphology." Acta neuropathologica **121**(2): 241-252.

Capper D, Sahm F, Hartmann C, Meyermann R, von Deimling A, Schittenhelm J. (2010). "Application of mutant IDH1 antibody to differentiate diffuse glioma from nonneoplastic central nervous system lesions and therapy-induced changes." Am J Surg Pathol **34** (8): 1199-1204.

Capper D, Simon M, Langhans CD, Okun JG, Tonn JC, Weller M, von Deimling A, Hartmann C; German Glioma Network. (2012). " 2-Hydroxyglutarate concentration in serum from patients with gliomas does not correlate with IDH1/2 mutation status or tumour size." International journal of cancer **131** (3): 766-768

Capper D, Weissert S, Balss J, Habel A, Meyer J, Jäger D, Ackermann U, Tessmer C, Korshunov A, Zentgraf H, Hartmann C, von Deimling A. (2010). "Characterization of R132H mutation-specific IDH1 antibody binding in brain tumours." Brain Pathol **20**: 245-254

Capper D, Zentgraf H, Balss J, Hartmann C, von Deimling A. (2009). "Monoclonal antibody specific for IDH1 for R132H mutation." Acta Neuropathol **118**: 599-601.

Cea V, Sala C, Verpelli C (2012). "Antiangiogenic therapy for glioma." J Signal Transduct. **2012**: 483040.

Cerrato JA, Yung WK, Liu TJ. (2001). "Introduction of mutant p53 into a wild-type p53-expressing glioma cell line confers sensitivity to Ad-p53-induced apoptosis." Neuro Oncol. **3**(2): 113-122.

Cha S (2006). "Update on brain tumor imaging: from anatomy to physiology." AJNR Am J Neuroradiol. **27**(3): 475-487.

Chakravarti A, Wang M, Robins HI, Lautenschlaeger T, Curran WJ, Brachman DG, Schultz CJ, Choucair A, Dolled-Filhart M, Christiansen J, Gustavson M, Molinaro A, Mischel P, Dicker AP, Bredel M, Mehta M. RTOG 0211. (2013). "A Phase 1/2 Study of Radiation Therapy With Concurrent Gefitinib for Newly Diagnosed Glioblastoma Patients." Int. J. Radiat. Oncol. Biol. Phys . **85**(5): 1206-1211.

Chalmers R, Lawson A, Watts R, Tavill AS, Kamerling JP, Hey E, Ogilvie D. (1980). "D-2-hydroxyglutaric aciduria: case report and biochemical studies. " J inherit Metab Dis **3** 11-15.

Chang SM, Kuhn J, Lamborn K, T Cloughesy, Robins I, Lieberman F, Yung A, Dancey J, Prados M, Wen P. (2009). "Phase I/II study of erlotinib and temsirolimus for patients with recurrent malignant gliomas (MG) (NABTC 04-02) " J. Clin. Oncol. **27**(15s). 2004

Chapman PB, Hauschild A, Robert C, Haanen JB, Ascierto P, Larkin J, Dummer R, Garbe C, Testori A, Maio M, Hogg D, Lorigan P, Lebbe C, Jouary T, Schadendorf D, Ribas A, O'Day SJ, Sosman JA, Kirkwood JM, Eggermont AM, Dreno B, Nolop K, Li J, Nelson B, Hou J, Lee RJ, Flaherty KT, McArthur GA; BRIM-3 Study Group. (2011). "Improved survival with vemurafenib in melanoma with BRAF V600E mutation." N Engl J Med. **364** (26): 2507-2516.

Chaponis D, Barnes JW, Dellagatta JL, Kesari S, Fast E, Sauvageot C, Panagrahy D, Greene ER, Ramakrishna N, Wen PY, Kung AL, Stiles C, Kieran MW. (2011). "Lonafarnib (SCH66336) improves the activity of temozolomide and radiation for orthotopic malignant gliomas." J Neurooncol. **104** (1): 179-189.

Charles N, Ozawa T, Squatrito M, Bleau AM, Brennan CW, Hambardzumyan D, Holland EC. (2010). "Perivascular nitric oxide activates notch signaling and promotes stem-like character in PDGF-induced glioma cells." Cell Stem Cell. **6**(2): 141-152.

Chen HL, Yuh CH, Wu KK. (2010). "Nestin is essential for zebrafish brain and eye development through control of progenitor cell apoptosis." Plos One **5** (2): e9318. .

Chernova OB, Somerville RP, Cowell JK. (1998). "A novel gene, LGI1, from 10q24 is rearranged and downregulated in malignant brain tumors." Oncogene. **17**(22): 2873-2881.

Chesnelong C, Chaumeil MM, Blough MD, Al-Najjar M, Stechishin OD, Chan JA, Pieper RO, Ronen SM, Weiss S, Luchman HA, Cairncross JG. (2013). "Lactate dehydrogenase A silencing in IDH mutant gliomas." Neuro Oncol. **16**(5):686-95.

Chi AS, Wen PY. (2007). "Inhibiting Kinases in malignant gliomas." Expert opinion on therapeutic targets **11**(4): 473-496.

Chi J, Gu B, Zhang C, Peng G, Zhou F, Chen Y, Zhang G, Guo Y, Guo D, Qin J, Wang J, Li L, Wang F, Liu G, Xie F, Feng D, Zhou H, Huang X, Lu S, Liu Y, Hu W, Yao K. (2012). "Human herpesvirus 6 latent infection in patients with glioma." J Infect Dis. **206**(9): 1394-1398.

Chinnaiyan P, Won M, Wen PY, Rojiani AM, Wendland M, Dipetrillo TA, Corn BW, Mehta MP. (2013). "RTOG 0913: a phase 1 study of daily everolimus (RAD001) in combination with radiation therapy and temozolomide in patients with newly diagnosed glioblastoma." Int J Radiat Oncol Biol Phys. **86**(5): 880-884.

Chinot O, Wick W, Mason W. (2012). "Phase III trial of bevacizumab added to standard radiotherapy and temozolomide for newly diagnosed glioblastoma: mature progression-free survival and preliminary overall survival results in AVAGlio." Neuro-oncology **14**(Suppl 6): vi101-vi105.

Choi C, Ganji SK, DeBerardinis RJ, Hatanpaa KJ, Rakheja D, Kovacs Z, Yang XL, Mashimo T, Raisanen JM, Marin-Valencia I, Pascual JM, Madden CJ, Mickey BE, Malloy CR, Bachoo RM, Maher EA. (2012). "2-hydroxyglutarate detection by magnetic resonance spectroscopy in IDH-mutated patients with gliomas." Nature medicine **18**(4): 624-629.

Chou A, Chowdhury R, Li S, Chen W, Kim AJ, Piccioni DE, Selfridge JM, Mody RR, Chang S, Lalezari S, Lin J, Sanchez DE, Wilson RW, Garrett MC, Harry B, Mottahedeh J, Nghiemphu PL, Kornblum HI, Mischel PS, Prins RM, Yong WH, Cloughesy T, Nelson SF, Liau LM, Lai A. (2012). "Identification of retinol Binding Protein 1 Promoter Hypermethylation in isocitrate Dehydrogenase 1 and 2 Mutant Gliomas." J Natl Cancer Inst. **104**(19): 1458-1469.

Chou WC, Lei WC, Ko BS. (2011). "The prognostic impact and stability of Isocitrate dehydrogenase 2 mutation in adult patients with acute myeloid leukemia." Leukemia : official journal of the Leukemia Society of America, Leukemia Research Fund, U.K. **25** (2): 246-253

Chowdhury R, Yeoh KK, Tian YM, Hillringhaus L, Bagg EA, Rose NR, Leung IK, Li XS, Woon EC, Yang M, McDonough MA, King ON, Clifton IJ, Klose RJ, Claridge TD, Ratcliffe PJ, Schofield CJ, Kawamura A. (2011). "The oncometabolite 2-hydroxyglutarate inhibits histone lysine demethylases." EMBO reports **12**(5): 463-469.

Christensen BC, Smith AA, Zheng S, Koestler DC, Houseman EA, Marsit CJ, Wiemels JL, Nelson HH, Karagas MR, Wrensch MR, Kelsey KT, Wiencke JK. (2011). "DNA methylation, isocitrate dehydrogenase mutation, and survival in glioma." Journal of the National Cancer Institute **103**(2): 143-153

Cleary JM, Shapiro GI. (2010). "Development of phosphoinositide-3 kinase pathway inhibitors for advanced cancer." Curr. Oncol. Rep. **12**(2): 87–94.

Cloos PA, Christensen J, Agger K, Helin K. (2008). "Erasing the methyl mark: Histone demethylases at the center of cellular differentiation and disease." Genes Dev **22**: 1115-1140.

Cloughesy TF, Prados MD, Wen PY, Mikkelsen T, Abrey LE, Schiff D, Yung WK, Maoxia Z, Dimery I, Friedman HS. (2008). "A Phase II, randomized, non-comparative clinical trial of the effect of bevacizumab (BV) alone or in combination with irinotecan (CPT) on 6-month progression free

survival (PFS6) in recurrent, treatment-refractory glioblastoma (GBM)." J. Clin. Oncol. (Meeting Abstracts) **26**: 2010b.

Cloughesy TF, Wen PY, Robins HI, Chang SM, Groves MD, Fink KL, Junck L, Schiff D, Abrey L, Gilbert MR, Lieberman F, Kuhn J, DeAngelis LM, Mehta M, Raizer JJ, Yung WK, Aldape K, Wright J, Lamborn KR, Prados MD (2006). "Phase II trial of tipifarnib in patients with recurrent malignant glioma either receiving or not receiving enzyme-inducing antiepileptic drugs: a North American Brain Tumor Consortium Study." J Clin Oncol. **24**(22): 3651-3656.

Collins VP. (2007). "Mechanisms of disease: genetic predictors of response to treatment in brain tumors." Nat Clin Pract Oncol. **4**(6): 62-74.

Combs SE, Schulz-Ertner D, Roth W, Herold-Mende C, Debus J, Weber KJ. (2007). "In vitro responsiveness of glioma cell lines to multimodality treatment with radiotherapy, temozolomide, and epidermal growth factor receptor inhibition with cetuximab." Int J Radiat Oncol Biol Phys. **68** (3): 873-882.

Comte B, Vincent G, Bouchard B, Benderdour M, Des Rosiers C. (2002). "Reverse flux through cardiac NADP(+)-isocitrate dehydrogenase under normoxia and ischemia." Am J Physiol Heart Circ Physiol. **283**(4): 1505-1514.

Conrad C, Friedman H, Reardon D. (2004). "A Phase I/II trial of PTK787/ZK222584 (PTK/ZK), a novel, oral angiogenesis inhibitor, in combination with either temozolomide or lomustine for patients with recurrent glioblastoma multiforme (GBM)." J. Clin. Oncol. **22**: 1512.

Craigen WJ, Jakobs C, Sekul EA, Levy ML, Gibson KM, Butler IJ, Herman GE. (1994). "D-2-Hydroxyglutaric aciduria in a neonate with seizures and CNS dysfunction." Pediatr Neurol **10**: 49-53.

Creelan BC (2014). Update on immune checkpoint inhibitors in lung cancer. Cancer Control. **21**(1):80-9.

Curran WJ Jr, Scott CB, Horton J, Nelson JS, Weinstein AS, Fischbach AJ, Chang CH, Rotman M, Asbell SO, Krisch RE. (1993). "Recursive partitioning analysis of prognostic factors in three Radiation Therapy Oncology Group malignant glioma trials." J Natl Cancer Inst. **85**(9): 704-710.

Curtis MA, Kam M, Nannmark U, Anderson MF, Axell MZ, Wikkelso C, Holtås S, van Roon-Mom WM, Björk-Eriksson T, Nordborg C, Frisén J, Dragunow M, Faull RL, Eriksson PS (2007). "Human neuroblasts migrate to the olfactory bulb via a lateral ventricular extension." Science. **315**(5816 ): 1243-1249.

Dahlstrand J, Lardellli M, Lendahl U. (1995). Nestin mRNA expression correlates with the central nervous system progenitor state in many but not all regions of the developing central nervous system. Brain Res Dev Brain Res. **84**:109-29.

D'Atri S, Tentori L, Lacal P.M, Graziani G, Pagani, E Benincasa E, Zambruno G, Bonmassar E, Jiricny J. (1998). "Involvement of the mismatch repair system in temozolomide- induced apoptosis ." Mol. Pharmacol. **54** (2): 334-341.

Dalziel K. (1980). "Isocitrate dehydrogenase and related oxidative decarboxylases." FEBS Lett. **117**: Suppl:K45-55.

Dang L, White DW, Gross S, Bennett BD, Bittinger MA, Driggers EM, Fantin VR, Jang HG, Jin S, Keenan MC, Marks KM, Prins RM, Ward PS, Yen KE, Liau LM, Rabinowitz JD, Cantley LC, Thompson CB, Vander Heiden MG, Su SM. (2009). "Cancer-associated IDH1 mutations produce 2-hydroxyglutarate." Nature **462** (7274): 739-744.

Dawlaty MM, Breiling A, Le T, Raddatz G, Barrasa MI, Cheng AW, Gao Q, Powell BE, Li Z, Xu M, Faull KF, Lyko F, Jaenisch R. (2013 ). "Combined deficiency of Tet1 and Tet2 causes epigenetic abnormalities but is compatible with postnatal development." Dev Cell. **24** (3): 310-323.

Dawlaty MM, Ganz K, Powell BE, Hu YC, Markoulaki S, Cheng AW, Gao Q, Kim J, Choi SW, Page DC, Jaenisch R. (2011). "Tet1 is dispensable for maintaining pluripotency and its loss is compatible with embryonic and postnatal development." Cell Stem Cell. **9** (2): 166-175. .

de Groot JF, Lamborn KR, Chang SM, Gilbert MR, Cloughesy TF, Aldape K, Yao J, Jackson EF, Lieberman F, Robins HI, Mehta MP, Lassman AB, Deangelis LM, Yung WK, Chen A, Prados MD, Wen PY. (2011). "Phase II study of aflibercept in recurrent malignant glioma: a North American Brain Tumor Consortium study." J Clin Oncol. **29**(19).

De Witt Hamer PC (2010). "Small molecule kinase inhibitors in glioblastoma: a systematic review of clinical studies." Neuro-oncology **12**(3): 304–316.

DeBerardinis RJ, Lum JJ, Hatzivassiliou G, Thompson CB. (2008). "The biology of cancer: metabolic reprogramming fuels cell growth and proliferation." Cell metabolism **7**(1): 11-20.

Diebold I, Flügel D, Becht S, Belaiba RS, Bonello S, Hess J, Kietzmann T, Görlach A. (2010). "The hypoxia-inducible factor-2alpha is stabilized by oxidative stress involving NOX4." Antioxid Redox Signal. **13** (4): 425-436.

Dietrich PY, Dutoit V, Walker PR. (2014). Immunotherapy for glioma: from illusion to realistic prospects? Am Soc Clin Oncol Educ Book. **2014**:51-9.

Dinardo C, Propert K, Loren A, Paietta E, Sun Z, Levine RL, Straley KS, Yen K, Patel JP, Agresta S, Abdel-Wahab O, Perl AE, Litzow MR, Rowe JM, Lazarus HM, Fernandez HF, Margolis DJ, Tallman MS, Luger SM, Carroll M. (2013). "Serum 2-hydroxyglutarate levels predict isocitrate dehydrogenase mutations and clinical outcome in acute myeloid leukaemia." Blood **121** (24): 4917-4924.

Diserens AC, de Tribolet N, Martin-Achard A, Gaide AC, Schnegg JF, Carrel S. (1981). "Characterization of an established human malignant glioma cell line: LN-18." Acta Neuropathol. **53** (1): 21-28.

do Carmo A, Balça-Silva J, Matias D, Lopes MC. (2013). "PKC signaling in glioblastoma." Cancer Biol Ther. **14**(4): 287-294.

Doetsch F, Caille I, Lim DA, Garcia-Verdugo JM, Alvarez-Buylla A. (1999). "Subventricular zone astrocytes are neural stem cells in the adult mammalian brain." Cell **97**: 703–716.

Doherty L, Gigas DC, Kesari S, Drappatz J, Kim R, Zimmerman J, Ostrowsky L, Wen PY. (2006). "Pilot study of the combination of EGFR and mTOR inhibitors in recurrent malignant gliomas." Neurology. **67**: 156–158.

Drappatz J, Wong ET, Schiff D, Kesari S, Batchelor TT, Doherty L, Lafrankie DC, Ramakrishna N, Weiss S, Smith ST, Ciampa A, Zimmerman J, Ostrowsky L, David K, Norden A, Barron L, Sceppa C, Black PM, Wen PY. (2009). "A pilot safety study of lenalidomide and radiotherapy for patients with newly diagnosed glioblastoma multiforme." Int J Radiat Oncol Biol Phys. **73**(1): 222-227.

Driessens G, Blanpain C. (2011). "Long live sox2: sox2 lasts a lifetime." Cell Stem Cell. **9**(4): 283-284. .

Dubrow R, Darefsky AS, Freedman ND, Hollenbeck AR, Sinha R. (2012). "Coffee, tea, soda, and caffeine intake in relation to risk of adult glioma in the NIH-AARP Diet and Health Study." Cancer Causes Control. **23**(5): 757-768.

Duncan CG, Barwick BG, Jin G, Rago C, Kapoor-Vazirani P, Powell DR, Chi JT, Bigner DD, Vertino PM, Yan H. (2012). "A heterozygous IDH1R132H/WT mutation induces genome-wide alterations in DNA methylation." Genome Res. **22**(12): 2339-2355. .

Eagle LR, Yin X, Brothman AR, Williams BJ, Atkin NB, Prochownik EV (1995). "Mutation of the MXI1 gene in prostate cancer." Nat Genet. **9**(3): 249-255.

Eisenstat DD (2011). "A phase II study of daily afatinib (BIBW 2992) with or without temozolomide (21/28 days) in the treatment of patients with recurrent glioblastoma." Journal of Clinical Oncology, **29, supplement, 2011, Abstract no. 2010.** .

el Marjou F, Janssen KP, Chang BH, Li M, Hindie V, Chan L, Louvard D, Chambon P, Metzger D, Robine S. (2004). "Tissue-specific and inducible Cre-mediated recombination in the gut epithelium." Genesis. **39**(3): 186-193.

Eller JL, Longo SL, Kyle MM, Bassano D, Hicklin DJ, Canute GW (2005). "Anti-epidermal growth factor receptor monoclonal antibody cetuximab augments radiation effects in glioblastoma multiforme in vitro and in vivo." Neurosurgery. **56**(1): 155-162.

Engqvist M, Drincovich MF, Flugge UI, Maurino VG. (2009). "Two D-2-hydroxy-acid dehydrogenases in Arabidopsis thaliana with catalytic capacities to participate in the last reactions of the methylglyoxal and β-oxidation pathways." J Biol Chem **284** 25026–25037.

Eriksson P, Perfilieva E, Björk-Eriksson T, Alborn AM, Nordborg C, Peterson DA, Gage FH. (1998). "Neurogenesis in the adult human hippocampus." Nature Med. **4**: 1313-1317.

Esteller M, Garcia-Foncillas J, Andion E, Goodman SN, Hidalgo OF, Vanaclocha V, Baylin SB, Herman JG. (2000). "Inactivation of the DNA-repair gene MGMT and the clinical response of gliomas to alkylating agents." N Engl J Med. **343**(19): 1350-1354.

Esteller M, Hamilton SR, Burger PC et al. (1999). "Inactivation of the DNA repair gene O6-methylguanine-DNA methyltransferase by promoter hypermethylation is a common event in primary human neoplasia." Cancer Res. **59**: 793–797.

Evans JM, Donnelly LA, Emslie-Smith AM, Alessi DR, Morris AD. (2005). "Metformin and reduced risk of cancer in diabetic patients." BMJ **330**(7503 ): 1304-1305

Farfari S, Schulz V, Corkey B, Prentki M. (2000). "Glucose-regulated anaplerosis and cataplerosis in pancreatic beta-cells: possible implication of a pyruvate/citrate shuttle in insulin secretion." Diabetes care **49**: 718–726.

Fathi AT, Sadrzadeh H, Borger DR, Ballen KK, Amrein PC, Attar EC, Foster J, Burke M, Lopez HU, Matulis CR, Edmonds KM, Iafrate AJ, Straley KS, Yen KE, Agresta S, Schenkein DP, Hill C, Emadi A, Neuberg DS, Stone RM, Chen YB. (2012). "Prospective serial evaluation of 2-hydroxyglutarate, during treatment of newly diagnosed acute myeloid leukemia, to assess disease activity and therapeutic response." Blood **120**(23): 4649-4652.

Feil R, Wagner J, Metzger D, Chambon P. (1997). "Regulation of Cre recombinase activity by mutated estrogen receptor ligand-binding domains." Biochem Biophys Res Commun. **237** 752-757.

Feil S, Valtcheva N, Feil R. (2009). "Inducible Cre mice." Methods Mol Biol. **530** 343-363.

Feldkamp MM, Lala P, Lau N, Roncari L, Guha A. (1999). "Expression of activated epidermal growth factor receptors, Ras-guanosine triphosphate, and mitogen-activated protein kinase in human glioblastoma multiforme specimens." Neurosurgery. **45**(6): 1442-1453.

Feldkamp MM, Lau N, Guha A (1999). "Growth inhibition of astrocytoma cells by farnesyl transferase inhibitors is mediated by a combination of anti-proliferative, pro-apoptotic and anti-angiogenic effects." Oncogene. **18**(52): 7514-7526.

Figueroa ME, Abdel-Wahab O, Lu C et al. (2010). "Leukemic IDH1 and IDH2 mutations result in a hypermethylation phenotype, disrupt TET2 function, and impair hematopoietic differentiation." Cancer cell **18**(6): 553-567.

Filipp FV, Scott DA, Ronai ZA, Osterman AL, Smith JW. (2012). "Reverse TCA cycle flux through isocitrate dehydrogenases 1 and 2 is required for lipogenesis in hypoxic melanoma cells." Pigment Cell Melanoma Res. **25**(3): 375-383. .

Fine HA, Figg WD, Jaeckle K, Wen PY, Kyritsis AP, Loeffler JS, Levin VA, Black PM, Kaplan R, Pluda JM, Yung WK (2000). "Phase II trial of the antiangiogenic agent thalidomide in patients with recurrent high-grade gliomas." J Clin Oncol. **18** (4): 708-715.

Fisher JL, Schwartzbaum JA, Wrensch M, Wiemels JL. (2007). "Epidemiology of brain tumors." Neurol Clin. **25**(4): 867-890.

Flaherty KT, Robert C, Hersey P, Nathan P, Garbe C, Milhem M, Demidov LV, Hassel JC, Rutkowski P, Mohr P, Dummer R, Trefzer U, Larkin JM, Utikal J, Dreno B, Nyakas M, Middleton MR, Becker JC, Casey M, Sherman LJ, Wu FS, Ouellet D, Martin AM, Patel K, Schadendorf D; METRIC Study Group. (2012). "Improved survival with MEK inhibition in BRAF-mutated melanoma." N Engl J Med. **367** (2): 107-114.

Forni PE, Scuoppo C, Imayoshi I, Taulli R, Dastrù W, Sala V, Betz UA, Muzzi P, Martinuzzi D, Vercelli AE, Kageyama R, Ponzetto C. (2006). "High levels of Cre expression in neuronal progenitors cause defects in brain development leading to microencephaly and hydrocephaly." J Neurosci. **26** (37): 9593-9602.

Frederick L, Wang XY, Eley G, James CD. (2000). "Diversity and frequency of epidermal growth factor receptor mutations in human glioblastomas." Cancer Res . **60** (5): 1383–1387.

Frezza C, Pollard PJ, Gottlieb E. (2011). "Inborn and acquired metabolic defects in cancer." J Mol Med (Berl) **89**(3): 213-220.

Friedman HS, Petros WP, Friedman AH. (1999). "Irinotecan therapy in adults with recurrent or progressive malignant glioma." J Clin Oncol **17**: 1516–1525.

Fujisawa H, Kurrer M, Reis RM, Yonekawa Y, Kleihues P, Ohgaki H. (1999). "Acquisition of the glioblastoma phenotype during astrocytoma progression is associated with loss of heterozygosity on 10q25-qter." Am J Pathol. **155**(2): 387-394.

Fujisawa H, Reis RM, Nakamura M, Colella S, Yonekawa Y, Kleihues P, Ohgaki H. (2000). "Loss of heterozygosity on chromosome 10 is more extensive in primary (de novo) than in secondary glioblastomas." Lab Invest. **80**(1): 65-72.

Fulci G, Labuhn M, Maier D, Lachat Y, Hausmann O, Hegi ME, Janzer RC, Merlo A, Van Meir EG (2000). "p53 gene mutation and ink4a-arf deletion appear to be two mutually exclusive events in human glioblastoma." Oncogene **19**(33): 3816-3822.

Fults D, Pedone C, Dai C, Holland EC. (2002). "MYC expression promotes the proliferation of neural progenitor cells in culture and in vivo." Neoplasia **4** 32-39.

Fults D, Pedone CA, Thompson GE, Uchiyama CM, Gumpper KL, Iliev D, Vinson VL, Tavtigian SV, Perry WL 3rd (1998). "Microsatellite deletion mapping on chromosome 10q and mutation analysis of MMAC1, FAS, and MXI1 in human glioblastoma multiforme." Int J Oncol. **12**(4): 905-910.

Furnari FB, Fenton T, Bachoo RM, Mukasa A, Stommel JM, Stegh A, Hahn WC, Ligon KL, Louis DN, Brennan C, et al. (2007). "Malignant astrocytic glioma: genetics, biology, and paths to treatment. ." Genes Dev **21**: 2683–2710.

Gaal J, Burnichon N, Korpershoek E, Roncelin I, Bertherat J, Plouin PF, de Krijger RR, Gimenez-Roqueplo AP, Dinjens WN. (2010). "Isocitrate dehydrogenase mutations are rare in pheochromocytomas and paragangliomas." J Clin Endocrinol Metab **95**: 1274–1278.

Gabriel JL, Zervos PR, Plaut GW. (1986). "Activity of purified NAD-specific isocitrate dehydrogenase at modulator and substrate concentrations approximating conditions in mitochondria." Metabolism. **35**(7): 661-667.

Gaidzik VI, Paschka P, Späth D, Habdank M, Köhne CH, Germing U, von Lilienfeld-Toal M, Held G, Horst HA, Haase D, Bentz M, Götze K, Döhner H, Schlenk RF, Bullinger L, Döhner K. (2012). "TET2 mutations in acute myeloid leukemia (AML): results from a comprehensive genetic and clinical analysis of the AML study group." J Clin Oncol. **30**(12): 1350-1357.

Galanis E, Buckner JC, Maurer MJ, Kreisberg JI, Ballman K, Boni J, Peralba JM, Jenkins RB, Dakhil SR, Morton RF, Jaeckle KA, Scheithauer BW, Dancey J, Hidalgo M, Walsh DJ; North Central Cancer Treatment Group. (2005). "Phase II trial of temsirolimus (CCI-779) in recurrent glioblastoma multiforme: a North Central Cancer Treatment Group Study." J Clin Oncol. **23**(23): 5294-5304.

Galanis E, Jaeckle KA, Maurer MJ. (2009). "Phase II trial of vorinostat in recurrent glioblastoma multiforme: a north central cancer treatment group study. " Journal of clinical oncology : official journal of the American Society of Clinical Oncology **27** (12): 2052-2058.

Galeone C, Malerba S, Rota M, Bagnardi V, Negri E, Scotti L, Bellocco R, Corrao G, Boffetta P, La Vecchia C, Pelucchi C. (2013). "A meta-analysis of alcohol consumption and the risk of brain tumours." Ann Oncol. **24**(2): 514-523.

Galli R, Binda E, Orfanelli U, Cipelletti B, Gritti A, De Vitis S, Fiocco R, Foroni C, Dimeco F, Vescovi A. (2004). "Isolation and characterization of tumorigenic, stem-like neural precursors from human glioblastoma." Cancer Res. **64**(19): 7011-7021.

Garcia-Manero G. (2012). "Can we improve outcomes in patients with acute myelogenous leukemia? Incorporating HDAC inhibitors into front-line therapy. ." Best practice & research. Clinical haematology **25** (4): 427-435

Gerald D, Berra E, Frapart YM, Chan DA, Giaccia AJ, Mansuy D, Pouysségur J, Yaniv M, Mechta-Grigoriou F. (2004). "JunD reduces tumor angiogenesis by protecting cells from oxidative stress." Cell. **118** (6): 781-794.

Ghiam AF, Cairns RA, Thoms J, Dal Pra A, Ahmed O, Meng A, Mak TW, Bristow RG. (2012). "IDH mutation status in prostate cancer." Oncogene **31**(33): 3826.

Giantonio BJ, Catalano PJ, Meropol NJ, O'Dwyer PJ, Mitchell EP, Alberts SR, Schwartz MA, Benson AB 3rd; Eastern Cooperative Oncology Group Study E3200. (2007). "Bevacizumab in combination with oxaliplatin, fluorouracil, and leucovorin (FOLFOX4) for previously treated metastatic colorectal cancer: results from the Eastern Cooperative Oncology Group Study E3200." J Clin Oncol. **25** (12): 1539-1544.

Gibson KM, Craigen W, Herman GE, Jakobs C. (1993). "D-2-Hydroxyglutaric aciduria in a newborn with neurological abnormalities: a new neurometabolic disorder?" J inherit Metab Dis **16**: 497-500.

Giese A, Westphal M (1996). "Glioma invasion in the central nervous system." Neurosurgery **39**: 235-250.

Gilbert MR, Dignam J, Won M. (2013). "RTOG 0825: Phase III double-blind placebo-controlled trial evaluating bevacizumab (Bev) in patients (Pts) with newly diagnosed glioblastoma (GBM)." J Clin Oncol **31**(Suppl(abstr 1).

Gilbert MR, Wang M, Aldape KD. (2011). "RTOG 0525: a randomized phase III trial comparing standard adjuvant temozolomide (TMZ) with a dose-dense (dd) schedule in newly diagnosed glioblastoma (GBM)." J Clin Oncol **29: suppl;** abstr 2006.

Glass TL, Liu TJ, Yung WK (2000). "Inhibition of cell growth in human glioblastoma cell lines by farnesyltransferase inhibitor SCH66336." Neuro Oncol. **2**(3): 151-158.

Goodenberger ML, Jenkins RB. (2012). "Genetics of adult glioma." Cancer Genet **205**(12): 613-621.

Gottlieb E, Tomlinson IP. (2005). "Mitochondrial tumour suppressors: a genetic and biochemical update." Nature reviews. Cancer **5** (11): 857-866

Graus-Porta D, Blaess S, Senften M, Littlewood-Evans A, Damsky C, Huang Z, Orban P, Klein R, Schittny JC, Müller U. (2001). "Beta1-class integrins regulate the development of laminae and folia in the cerebral and cerebellar cortex." Neuron. **31** (3): 367-379.

Gross S, Cairns RA, Minden MD, Driggers EM, Bittinger MA, Jang HG, Sasaki M, Jin S, Schenkein DP, Su SM, Dang L, Fantin VR, Mak TW. (2010). "Cancer-associated metabolite 2-hydroxyglutarate accumulates in acute myelogenous leukemia with isocitrate dehydrogenase 1 and 2 mutations." The Journal of experimental medicine **207**(2): 339-344

Grossman S, Ye X, Chamberlain M, Mikkelsen T, Batchelor T, Desideri S, Piantadosi S, Fisher J, Fine HA. (2009). "Talampanel with standard radiation and temozolomide in patients with newly diagnosed glioblastoma: a multicentre phase II trial." J Clin Oncol **27**(25): 4155-4161.

Grossman SA, Batara JF. (2004). "Current management of glioblastoma multiforme." Seminars in oncology **31**(5): 635-644.

Guha A, Feldkamp M, Lau N, Boss G, Pawson A. (1997). "Proliferation of human malignant astrocytomas is dependent on Ras activation." Oncogene **15**: 2755–2765.

Guilhamon P, Eskandarpour M, Halai D, Wilson GA, Feber A, Teschendorff AE, Gomez V, Hergovich A, Tirabosco R, Fernanda Amary M, Baumhoer D, Jundt G, Ross MT, Flanagan AM, Beck S. (2013). "Meta-analysis of IDH-mutant cancers identifies EBF1 as an interaction partner for TET2." Nature Communications **4**: 2166.

Guo J, Su Y, Zhong C, Ming GL, Song H. (2011). "Emerging roles of TET proteins and 5-Hydroxymethylcytosines in active DNA demethylation and beyond." Cell Cycle **10**(16): 2662-2668.

Gupta R, Flanagan S, Li CC, Lee M, Shivalingham B, Maleki S, Wheeler HR, Buckland ME. (2013). "Expanding the spectrum of IDH1 mutations in gliomas." Mod Pathol. **26**(5):619-25.

Gurney J, van Wijngaarden E. (1999). "Extremely low frequency EMF and brain cancer in adults and children: review and comment." Neuro Oncol **1**(3): 212-220.

Gurney JG, Kadan-Lottick N. (2001). "Brain and other central nervous system tumors: rates, trends, and epidemiology." Curr Opin Oncol. **13**(3): 160-166.

Haas-Kogan DA, Prados MD, Tihan T, Eberhard DA, Jelluma N, Arvold ND, Baumber R, Lamborn KR, Kapadia A, Malec M, Berger MS, Stokoe D. (2005). "Epidermal growth factor receptor, protein kinase B/Akt, and glioma response to erlotinib." J. Natl Cancer Inst. **97**: 880–887.

Hainsworth JD, Shih KC, Shepard GC, Tillinghast GW, Brinker BT, Spigel DR. (2012). "Phase II study of concurrent radiation therapy, temozolomide, and bevacizumab followed by bevacizumab/everolimus as first-line treatment for patients with glioblastoma." Clin Adv Hematol Oncol. **10**(4): 240-246.

Haliloglu G, Jobard F, Oguz K et al. (2008). "L-2-Hydroxyglutaric aciduria and brain tumours in children with mutations in the L2HGDH gene: neuroimaging findings." Neuropediatrics **39**: 119-122.

Hambardzumyan D, Parada LF, Holland EC, Charest A. (2011). "Genetic modeling of gliomas in mice: new tools to tackle old problems." Glia **59**(8): 1155-1168.

Han DW, Do JT, Araúzo-Bravo MJ, Lee SH, Meissner A, Lee HT, Jaenisch R, Schöler HR. (2009). "Epigenetic hierarchy governing Nestin expression." Stem Cells **27** 1088-1097.

Hanahan D, Weinberg R. (2011). "Hallmarks of cancer: the next generation." Cell **144** (5): 646-674.

Hardell L, Carlberg M, Söderqvist F, Mild KH. (2013). "Case-control study of the association between malignant brain tumours diagnosed between 2007 and 2009 and mobile and cordless phone use." Int J Oncol **43** (6): 1833-1845.

Hartmann C, Meyer J, Balss J, Capper D, Mueller W, Christians A, Felsberg J, Wolter M, Mawrin C, Wick W, Weller M, Herold-Mende C, Unterberg A, Jeuken JW, Wesseling P, Reifenberger G, von Deimling A. (2009). "Type and frequency of IDH1 and IDH2 mutations are related to astrocytic and oligodendroglial differentiation and age: a study of 1,010 diffuse gliomas." Acta neuropathologica **118**(4): 469-474.

Hartong D, McGee T, Berson E, Dryia T, Colman R. (2008). "Insights from retinitis pigmentosa into the roles of isocitrate dehydrogenases in the Krebs cycle." Nat Genet **40**(10): 1230-1234.

Haruyama N, Cho A, Kulkarni AB. (2009). "Overview: engineering transgenic constructs and mice." Curr Protoc Cell Biol. **Chapter 19**: Unit 19.10.

Haselback RJ, McAlister-Henn L. (1993). "Function and expression of yeast mitochondrial NAD and NADP-specific isocitrate dehydrogenases." The Journal of biological chemistry **268**(16): 12116-12122.

Hasselbalch B, Lassen U, Hansen S, Holmberg M, Sorensen M, Kosteljanetz M, Broholm H, Stockhausen MT, Poulsen HS. (2010). "Cetuximab, bevacizumab, and irinotecan for patients with primary glioblastoma and progression after radiation therapy and temozolomide: a phase II trial." Neuro. Oncol. **12** (5): 508–516.

Hatanpaa KJ, Burma S, Zhao D, Habib AA. (2010). "Epidermal growth factor receptor in glioma: signal transduction, neuropathology, imaging, and radioresistance." Neoplasia. **12**(9): 675-684.

Hatzimichael E, Lo Nigro C, Lattanzio L, Syed N, Shah R, Dasoula A, Janczar K, Vivenza D, Monteverde M, Merlano M, Papoudou-Bai A, Bai M, Schmid P, Stebbing J, Bower M, Dyer MJ, Karran LE, ElguetaKarstegl C, Farrell PJ, Thompson A, Briasoulis E, Crook T. (2012). "The collagen prolyl

hydroxylases are novel transcriptionally silenced genes in lymphoma." Br J Cancer. **107**(8): 1423-1432.

Hausinger RP. (2004). "FeII/alpha-ketoglutarate-dependent hydroxylases and related enzymes." Crit Rev Biochem Mol Biol. **39**(1): 21-68.

He J, Mokhtari K, Sanson M, Marie Y, Kujas M, Huguet S, Leuraud P, Capelle L, Delattre JY, Poirier J, Hoang-Xuan K. (2001). "Glioblastomas with an oligodendroglial component: a pathological and molecular study." J Neuropathol Exp Neurol. **60**(9): 863-871.

Hede SM, Hansson I, Afink GB, Eriksson A, Nazarenko I, Andrae J, Genove G, Westermark B, Nistér M. (2009). "GFAP promoter driven transgenic expression of PDGFB in the mouse brain leads to glioblastoma in a Trp53 null background." Glia. **57** (11): 1143-1153.

Hegi ME, Diserens AC, Gorlia T, Hamou MF, de Tribolet N, Weller M, Kros JM, Hainfellner JA, Mason W, Mariani L, Bromberg JE, Hau P, Mirimanoff RO, Cairncross JG, Janzer RC, Stupp R. (2005). "MGMT gene silencing and benefit from temozolomide in glioblastoma." N Engl J Med. **352**(10): 997-1003.

Hilton DA, Penney M, Pobereskin L, Sanders H, Love S. (2004). "Histological indicators of prognosis in glioblastomas: Retinoblastoma protein expression and oligodendroglial differentiation indicate improved survival." Histopathology **44**(44): 555-560

Hlavaty J, Jandl G, Liszt M, Petznek H, König-Schuster M, Sedlak J, Egerbacher M, Weissenberger J, Salmons B, Günzburg WH, Renner M. (2011). "Comparative evaluation of preclinical in vivo models for the assessment of replicating retroviral vectors for the treatment of glioblastoma." J Neurooncol. **102** (1): 59-69.

Hockfield S, McKay R. (1985). "Identification of major cell classes in the developing mammalian nervous system." The Journal of neuroscience **5**(12): 3310.

Hoelzinger DB, Mariani L, Weis J, Woyke T, Berens TJ, McDonough WS, Sloan A, Coons SW, Berens ME. (2005). "Gene expression profile of glioblastoma multiforme invasive phenotype points to new therapeutic targets." Neoplasia. **7**(1): 7-16.

Holick CN, Giovannucci EL, Rosner B, Stampfer MJ, Michaud DS. (2007a). "Prospective study of intake of fruit, vegetables, and carotenoids and the risk of adult glioma." Am J Clin Nutr. **85**(3): 877-886.

Holick CN, Giovannucci EL, Rosner B, Stampfer MJ, Michaud DS. (2007b). "Prospective study of cigarette smoking and adult glioma: dosage, duration, and latency." Neuro Oncol. **9**(3): 326-334.

Holland E. (2001). "Gliomagenesis: genetic alterations and mouse models." Nat Rev Genet. **2**(2): 120-129.

Holland E, Celestino J, Dai C, Schaefer L, Sawaya R, Fuller G. (2000). "Combined activation of Ras and Akt in neural progenitors induces glioblastoma formation in mice." Nat Genet. **25**: 55-57.

Holland EC, Varmus HE. (1998). "Basic fibroblast growth factor induces cell migration and proliferation after glia-specific gene transfer in mice." Proc Natl Acad Sci U S A. **95** (3): 1218-1223.

Holmberg J, He X, Peredo I, Orrego A, Hesselager G, Ericsson C, Hovatta O, Oba-Shinjo SM, Marie SK, Nistér M, Muhr J. (2011). "Activation of neural and pluripotent stem cell signatures correlates with increased malignancy in human glioma." Plos One **6**: e18454.

Homma T, Fukushima T, Vaccarella S, Yonekawa Y, Di Patre PL, Franceschi S. (2006). "Correlation among pathology, genotype and patient outcomes in glioblastoma." J Neuropathol Exp Neurol **65**: 846-854.

Horbinski C, Kofler J, Kelly LM, Murdoch GH, Nikiforova MN. (2009). "Diagnostic use of IDH1/2 mutation analysis in routine clinical testing of formalin-fixed, paraffin-embedded glioma tissues." Journal of neuropathology and experimental neurology **68** (12): 1319-1325.

Horton JK, Wilson SH. (2007). "Hypersensitivity phenotypes associated with genetic and synthetic inhibitor-induced base excision repair deficiency." DNA Repair **6** (4): 530-543.

Hossain M, Banik NL, Ray SK. (2012). "Synergistic anti-cancer mechanisms of curcumin and paclitaxel for growth inhibition of human brain tumor stem cells and LN18 and U138MG cells." Neurochem Int. **61**(7): 1102-1113.

Humphrey PA, Wong AJ, Vogelstein B, Zalutsky MR, Fuller GN, Archer GE, Friedman HS, Kwatra MM, Bigner SH, Bigner DD. (1990). "Anti-synthetic peptide antibody reacting at the fusion junction of deletion-mutant epidermal growth factor receptors in human glioblastoma." Proc Natl Acad Sci U S A. **87**: 4207-4211.

Huncharek M, Kupelnick B. (2000). "Epidermal growth factor receptor gene amplification as a prognostic marker in glioblastoma multiforme: results of a meta-analysis." Oncol Res **12**: 107-112.

Hurley SF, McNeil JJ, Donnan GA, Forbes A, Salzberg M, Giles GG. (1996). "Tobacco smoking and alcohol consumption as risk factors for glioma: a case-control study in Melbourne, Australia." J Epidemiol Community Health. **50**(4): 442-446.

Ibanez-Tallon I., Gorokhova S, Heintz N. (2002). "Loss of function of axonemal dynein Mdnah5 causes primary ciliary dyskinesia and hydrocephalus." Hum Mol Genet **11**: 715-721.

Ichimura K, Schmidt EE, Miyakawa A, Goike HM, Collins VP. (1998). "Distinct patterns of deletion on 10p and 10q suggest involvement of multiple tumor suppressor genes in the development of astrocytic gliomas of different malignancy grades." Genes Chromosomes Cancer. **22**(1): 9-15.

Ignatova T, Kukekov V, Laywell E, Suslov O, Vrionis F, Steindler D. (2002). "Human cortical glial tumors contain neural stemlike cells expressing astroglial and neuronal markers in vitro. Glia." Glia **39**: 193–206.

Il'yasova D, McCarthy B, Marcello J, Schildkraut JM, Moorman PG, Krishnamachari B, Ali-Osman F, Bigner DD, Davis F. (2009). "Association between glioma and history of allergies, asthma, and eczema: a case-control study with three groups of controls." Cancer Epidemiol Biomarkers Prev. **18**(4): 1232-1238.

Imai T, Jiang M, Chambon P, Metzger D. (2001). "Impaired adipogenesis and lipolysis in the mouse upon selective ablation of the retinoid X receptor alpha mediated by a tamoxifen-inducible chimeric Cre recombinase (Cre-ERT2) in adipocytes." Proc Natl Acad Sci USA **98**: 224-228.

Indra AK, Warot X, Brocard J, Bornert JM, Xiao JH, Chambon P, Metzger D. (1999 ). "Temporally-controlled site-specific mutagenesis in the basal layer of the epidermis: comparison of the recombinase activity of the tamoxifen-inducible Cre-ER(T) and Cre-ER(T2) recombinases." Nucleic Acids Res. **27** (22): 4324-4327.

Ishii N, Maier D, Merlo A, Tada M, Sawamura Y, Diserens AC, Van Meir EG. (1999). "Frequent co-alterations of TP53, p16/CDKN2A, p14ARF, PTEN tumor suppressor genes in human glioma cell lines." Brain Pathol. **9**(3): 469-479.

Ito S, D'Alessio AC, Taranova OV, Hong K, Sowers LC, Zhang Y. (2010). "Role of Tet proteins in 5mC to 5hmC conversion, ES-cell self-renewal and inner cell mass specification." Nature **466**(7310 ): 1129-1133.

Iwamoto F, Kreisl T, Kim L, Duic JP, Butman JA, Albert PS, Fine HA. (2010). "Phase 2 trial of talampanel, a glutamate receptor inhibitor for adults with recurrent malignant gliomas " Cancer **116**(7): 1776-1782.

Jin G, Reitman Z, Duncan C, Spasojevic I, Gooden DM, Rasheed BA, Yang R, Lopez GY, He Y, McLendon RE, Bigner DD, Yan H. (2013). "Disruption of wild type IDH1 suppresses D-2-hydroxyglutarate production in IDH1-mutated gliomas." Cancer Res. **73** 496.

Jin G, Reitman ZJ, Spasojevic I, Batinic-Haberle I, Yang J, Schmidt-Kittler O, Bigner DD, Yan H. (2011). "2-hydroxyglutarate production, but not dominant negative function, is conferred by glioma-derived NADP-dependent isocitrate dehydrogenase mutations." PLoS One. **6**(2): e16812.

Jin Q, Zhang W, Qiu XG, Yan W, You G, Liu YW, Jiang T, Wang L. (2011 ). "Gene expression profiling reveals Ki-67 associated proliferation signature in human glioblastoma." Chin Med J (Engl). **124**(17): 2584-2588.

Jin SG, Jiang Y, Qiu R, Rauch TA, Wang Y, Schackert G, Krex D, Lu Q, Pfeifer GP. (2011). " 5-Hydroxymethylcytosine is strongly depleted in human cancers but its levels do not correlate with IDH1 mutations." Cancer Research **71** (24): 7360-7365.

Johannessen TC, Wang J, Skaftnesmo KO, Sakariassen PØ, Enger PØ, Petersen K, Øyan AM, Kalland KH, Bjerkvig R, Tysnes BB (2009). "Highly infiltrative brain tumours show reduced chemosensitivity associated with a stem cell-like phenotype." Neuropathol Appl Neurobiol. **35**(4): 380-393.

Joseph JW, Jensen MV, Ilkayeva O, Palmieri F, Alárcon C, Rhodes CJ, Newgard CB. (2006). "The mitochondrial citrate/isocitrate carrier plays a regulatory role in glucose-stimulated insulin secretion." The Journal of biological chemistry **281**(47): 35624-35632.

Josephson R, Müller T, Pickel J, Okabe S, Reynolds K, Turner PA, Zimmer A, McKay RD. (1998). "POU transcription factors control expression of CNS stem cell-specific genes." Development. **125** (16): 3087-3100.

Josset E, Burckel H, Noël G, Bischoff P. (2013). "The mTOR inhibitor RAD001 potentiates autophagic cell death induced by temozolomide in a glioblastoma cell line." Anticancer Res. **33**(5): 1845-1851.

Jung SN, Yang WK, Kim J, Kim HS, Kim EJ, Yun H, Park H, Kim SS, Choe W, Kang I, Ha J. (2008). "Reactive oxygen species stabilize hypoxia-inducible factor-1 alpha protein and stimulate transcriptional activity via AMP-activated protein kinase in DU145 human prostate cancer cells." Carcinogenesis. **29** (4): 713-721.

Kaelin WG, Jr. (2009). "SDH5 mutations and familial paraganglioma: somewhere Warburg is smiling." Cancer cell **16**(3): 180-182.

Karaca M, Maechler P. (2014). "Development of mice with brain-specific deletion of floxed glud1 (glutamate dehydrogenase 1) using cre recombinase driven by the nestin promoter." Neurochem Res. **39** (3): 456-459.

Karsy M, Albert L, Tobias ME, Murali R, Jhanwar-Uniyal M. (2010). "All-trans retinoic acid modulates cancer stem cells of glioblastoma multiforme in an MAPK-dependent manner." Anticancer Res. **30** (12): 4915-4920.

Kato Y, Jin G, Kuan C, McLendon RE, Yan H, Bigner DD. (2009). "A monoclonal antibody IMab-1 specifically recognizes IDH1R132H, the most common glioma-derived mutation." Biochem Biophys Commun **390**: 547-551.

Kaufman E, Nelson T, Fales H, Levin D. (1988). "Isolation and characterization of a hydroxyacid-oxoacid transhydrogenase from rat kidney mitochondria." J Biol Chem **263** 16872–16879.

Kelly JJ, Blough MD, Stechishin OD, Chan JA, Beauchamp D, Perizzolo M, Demetrick DJ, Steele L, Auer RN, Hader WJ, Westgate M, Parney IF, Jenkins R, Cairncross JG, Weiss S. (2010). "Oligodendroglioma cell lines containing t(1;19)(q10;p10)." Neuro Oncol. **12**(7): 745-755.

Khandrika L, Kumar B, Koul S, Maroni P, Koul HK. (2009). "Oxidative stress in prostate cancer." Cancer Lett. **282** (2): 125-136.

Khurana VG, Teo C, Kundi M, Hardell L, Carlberg M. (2009). "Cell phones and brain tumors: a review including the long-term epidemiologic data." Surg Neurol. **72**(3): 205-214.

Kil IS, Chung KH, Park JW. (2010). "Silencing of mitochondrial NADP+-dependent isocitrate dehydrogenase gene enhances selenite-induced apoptosis. ." Free Radical Research **44** (3): 332-339

Kil IS, Kim SY, Lee SJ, Park JW. (2007). "Small interfering RNA-mediated silencing of mitochondrial NADP+-dependent isocitrate dehydrogenase enhances the sensitivity of HeLa cells toward tumour necrosis factor-alpha and anticancer drugs." Free radical biology & medicine **42**(8): 1197-1207.

Kim JE, Nakashima K, de Crombrugghe B. (2004). "Transgenic mice expressing a ligand-inducible cre recombinase in osteoblasts and odontoblasts: a new tool to examine physiology and disease of postnatal bone and tooth." Am J Pathol **165** 1875–1882.

Kim SY, Lee SM, Tak JK, Choi KS, Kwon TK, Park JW. (2007). "Regulation of singlet oxygen-induced apoptosis by cytosolic NADP+-dependent isocitrate dehydrogenase." Mol Cell Biochem. **302** (1-2): 27-34.

Kim SY, Yoo YH, Park JW. (2013). "Silencing of mitochondrial NADP(+)-dependent isocitrate dehydrogenase gene enhances glioma radiosensitivity." Biochem Biophys Res Commun. **433** (2): 260-265. .

Kim YH, Pierscianek D, Mittelbronn M, Vital A, Mariani L, Hasselblatt M, Ohgaki H. (2011). "TET2 promoter methylation in low-grade diffuse gliomas lacking IDH1/2 mutations ." J. Clin. Pathol. **64**: 850–852.

Kim YS, Kim SH, Cho J, Kim JW, Chang JH, Kim DS, Lee KS, Suh CO. (2012). "MGMT gene promoter methylation as a potent prognostic factor in glioblastoma treated with temozolomide-based chemoradiotherapy: a single-institution study." Int J Radiat Oncol Biol Phys. **84** (3): 661-667.

Kleiheus P, Nakazato Y, Burger P, Plate K, Aldape K. (2007). "Glioblastoma." WHO Classification of Tumours of the Central Nervous System. Lyon IARC Press.: 33-49.

Kloosterhof NK, Bralten LB, Dubbink HJ, French PJ, van den Bent MJ. (2011). "Isocitrate dehydrogenase-1 mutations: a fundamentally new understanding of diffuse glioma?" The lancet oncology **12**(1): 83-91.

Klose RJ, Kallin EM, Zhang Y. (2006). "JmjC-domain-containing proteins and histone demethylation." Nat Rev Genet **7** 715-727.

Ko M, Bandukwala HS, An J, Lamperti ED, Thompson EC, Hastie R, Tsangaratou A, Rajewsky K, Koralov SB, Rao A. (2011). "Ten-Eleven-Translocation 2 (TET2) negatively regulates homeostasis and differentiation of hematopoietic stem cells in mice." Proc Natl Acad Sci U S A. **108**(35): 14566-14571.

Kohlschutter A, Behbehani A, Langenbeck U, Albani M, Heidemann P, Hoffmann G, Kleineke J, Lehnert W, Wendel U. (1982). "A familial progressive neurodegenerative disease with 2-oxoglutaric aciduria." Eur J Pediatr. **138** 32–37.

Koivunen P, Lee S, Duncan CG, Lopez G, Lu G, Ramkissoon S, Losman JA, Joensuu P, Bergmann U, Gross S, Travins J, Weiss S, Looper R, Ligon KL, Verhaak RG, Yan H, Kaelin WG Jr. (2012). "Transformation by the (R)-enantiomer of 2-hydroxyglutarate linked to EGLN activation. " Nature **483**(7390): 484-488.

Kolker S, Pawlak V, Ahlemeyer B, Okun JG, Hörster F, Mayatepek E, Krieglstein J, Hoffmann GF, Köhr G. (2002). "NMDA receptor activation and respiratory chain complex V inhibition contribute to neurodegeneration in d-2-hydroxyglutaric aciduria." The European journal of neuroscience **16** (1): 21-28.

Korshunov A, Sycheva R, Golanov A. (2005). "The prognostic relevance of molecular alterations in glioblastomas for patients age < 50 years." Cancer. **104** (4): 825–832.

Kosmider O, Gelsi-Boyer V, Slama L, Dreyfus F, Beyne-Rauzy O, Quesnel B, Hunault-Berger M, Slama B, Vey N, Lacombe C, Solary E, Birnbaum D, Bernard OA, Fontenay M. (2010). "Mutations of IDH1 and IDH2 genes in early and accelerated phases of myelodysplastic syndromes and MDS/myeloproliferative neoplasms." Leukemia. **24**(5): 1094-1096.

Kranendijk M, Struys E, Gibson K, Wickenhagen WV, Abdenur JE, Buechner J, Christensen E, de Kremer RD, Errami A, Gissen P, Gradowska W, Hobson E, Islam L, Korman SH, Kurczynski T, Maranda B, Meli C, Rizzo C, Sansaricq C, Trefz FK, Webster R, Jakobs C, Salomons GS. (2010). "Evidence for genetic heterogenicity in D-2-hydroxyglutaric aciduria." Hum Mutat **31** 279-283.

Kranendijk M, Struys E, Salomons G, Van der Knaap MS, Jakobs C. (2012). "Progress in understanding 2-hydroxyglutaric acidurias." J Inherit Metab Dis **35** 571–587.

Kranendijk M, Struys E, van Schafting E, Gibson KM, Kanhai WA, van der Knaap MS, Amiel J, Buist NR, Das AM, de Klerk JB, Feigenbaum AS, Grange DK, Hofstede FC, Holme E, Kirk EP, Korman SH, Morava E, Morris A, Smeitink J, Sukhai RN, Vallance H, Jakobs C, Salomons GS. (2010). "IDH2 mutations in patients with D-2-hydroxyglutaric aciduria." Science **330**(6002): 336.

Kraus JA, Lamszus K, Glesmann N, Beck M, Wolter M, Sabel M, Krex D, Klockgether T, Reifenberger G, Schlegel U. (2001). "Molecular genetic alterations in glioblastomas with oligodendroglial component." Acta Neuropathol. **101**(4): 311-320.

Kreisl TN, Smith P, Sul J, Salgado C, Iwamoto FM, Shih JH, Fine HA. (2013). "Continuous daily sunitinib for recurrent glioblastoma." J Neurooncol. **111**(1): 41-48.

Krell D, Assoku M, Galloway M, Mulholland P, Tomlinson I, Bardella C. (2011). "Screen for IDH1, IDH2, IDH3, D2HGDH and L2HGDH Mutations in Glioblastoma." Plos One **6**(5): Article ID e19868.

Kreth FW, Berlis A, Spiropoulou V et al. (1999). "The role of tumor resection in the treatment of glioblastoma multiforme in adults." Cancer **86**: 2117–2123.

Krex D, Klink B, Hartmann C, von Deimling A, Pietsch T, Simon M, Sabel M, Steinbach JP, Heese O, Reifenberger G, Weller M, Schackert G; German Glioma Network (2007). "Long-term survival with glioblastoma multiforme." Brain. **130**: 2596-2606.

Kroonen J, Nassen J, Boulanger YG, Provenzano F, Capraro V, Bours V, Martin D, Deprez M, Robe P, Rogister B. (2011). "Human glioblastoma-initiating cells invade specifically the subventricular zones and olfactory bulbs of mice after striatal injection." Int J Cancer. **129**(3): 574-585.

Kuhbandner S, Brummer S, Metzger D, Chambon P, Hofmann F, Feil R. (2000). "Temporally controlled somatic mutagenesis in smooth muscle." Genesis. **28.**(15-22).

Kuhn J, Robins HI, Mehta M, Fine H, Cloughesy T, Wen PY, Chang S, DeAngelis LM, Lieberman F, Reardon D, Abrey LE, Lassman AB, Aldape K, Yung WK, Dancey J, Lamborn K, Prados M. (2008). "ET-05. Tumor sequestration of lapatinib." Neuro Oncol. **10**: 783.

Kukekov VG, Laywell ED, Suslov O, Davies K, Scheffler B, Thomas LB, O'Brien TF, Kusakabe M, Steindler DA (1999). "Multipotent stem/progenitor cells with similar properties arise from two neurogenic regions of adult human brain." Exp Neurol. **156**(2): 333-344.

Kwon CH, Zhao D, Chen J, Alcantara S, Li Y, Burns DK, Mason RP, Lee EY, Wu H, Parada LF. (2008). "Pten haploinsufficiency accelerates formation of high-grade astrocytomas." Cancer Res. **68**(9): 3286-3294.

Kyrtopoulos SA, Anderson LM, Chhabra SK, Souliotis VL, Pletsa V, Valavanis C, Georgiadis P. (1997). "DNA adducts and the mechanism of carcinogenesis and cytotoxicity of methylating agents of environmental and clinical significance." Cancer Detect. Prev. **21** (5): 391-405.

Laffaire J, Everhard S, Idbaih A, Crinière E, Marie Y, de Reyniès A, Schiappa R, Mokhtari K, Hoang-Xuan K, Sanson M, Delattre JY, Thillet J, Ducray F. (2011). "Methylation profiling identifies 2 groups of gliomas according to their tumourigenesis." Neuro-oncology **13**(1): 84-98.

Lai RK, Chen Y, Guan X, Nousome D, Sharma C, Canoll P, Bruce J, Sloan AE, Cortes E, Vonsattel JP, Su T, Delgado-Cruzata L, Gurvich I, Santella RM, Ostrom Q, Lee A, Gregersen P, Barnholtz-Sloan J. (2014). "Genome-wide methylation analyses in glioblastoma multiforme." PLoS One. **9** (2): e89376.

Lamborn KR, Chang SM, Prados MD. (2004). "Prognostic factors for survival of patients with glioblastoma: recursive partitioning analysis." Neuro Oncol. **6** (3): 227-235.

Lassen U, Sorensen M, Gaziel TB, Hasselbalch B, Poulsen HS. (2013). "Phase II study of bevacizumab and temsirolimus combination therapy for recurrent glioblastoma multiforme." Anticancer Res. **33**(4): 1657-1660.

Latini A, da Silva CG, Ferreira GC, Schuck PF, Scussiato K, Sarkis JJ, Dutra Filho CS, Wyse AT, Wannmacher CM, Wajner M. (2005). "Mitochondrial energy metabolism is markedly impaired by D-2-hydroxyglutaric acid in rat tissues." Molecular genetics and metabolism **86** 188-199.

Lee EQ, Puduvalli VK, Reid JM et al. (2012). "Phase I study of vorinostat in combination with temozolomide in patients with high-grade gliomas: North American Brain Tumour Consortium Study 04-03." Clinical cancer research : an official journal of the American Association for Cancer Research **18**(21): 6032-6039.

Lee JC, Vivanco I, Beroukhim R, Huang JH, Feng WL, DeBiasi RM, Yoshimoto K, King JC, Nghiemphu P, Yuza Y, Xu Q, Greulich H, Thomas RK, Paez JG, Peck TC, Linhart DJ, Glatt KA, Getz G, Onofrio R, Ziaugra L, Levine RL, Gabriel S, Kawaguchi T, O'Neill K, Khan H, Liau LM, Nelson SF, Rao PN, Mischel P, Pieper RO, Cloughesy T, Leahy DJ, Sellers WR, Sawyers CL, Meyerson M, Mellinghoff IK. (2006). "Epidermal growth factor receptor activation in glioblastoma through novel missense mutations in the extracellular domain." PLoS Med. **3**(12): e485.

Lee P, Eppinga W, Lagerwaard F, Cloughesy T, Slotman B, Nghiemphu PL, Wang PC, Kupelian P, Agazaryan N, Demarco J, Selch MT, Steinberg M, Kang JJ (2013). "Evaluation of high ipsilateral subventricular zone radiation therapy dose in glioblastoma: a pooled analysis." Int J Radiat Oncol Biol Phys. **86**(4): 609-615.

Lee SH, Jo SH, Lee SM, Koh HJ, Song H, Park JW, Lee WH, Huh TL. (2004). "Role of NADP+-dependent isocitrate dehydrogenase on cellular defence against oxidative injury by gamma-rays" International journal of radiation biology **80**(9): 635-642.

Lee SM, Park SY, Shin SW, Kil IS, Yang ES, Park JW. (2009). "Silencing of cytosolic NADP(+)-dependent isocitrate dehydrogenase by small interfering RNA enhances the sensitivity of HeLa cells toward staurosporine." Free Radical Research **43**(2): 165-173.

Lei L, Sonabend AM, Guarnieri P, Soderquist C, Ludwig T, Rosenfeld S, Canoll P. (2011). Glioblastoma models reveal the connection between adult glial progenitors and the proneural phenotype. PLoS ONE. **6**:e20041

Lemons JM, Feng XJ, Bennett BD, Legesse-Miller A, Johnson EL, Raitman I, Pollina EA, Rabitz HA, Rabinowitz JD, Coller HA. (2010). "Quiescent fibroblasts exhibit high metabolic activity." PLoS Biol. **8**(10): e1000514.

Lendahl U, Zimmerman LB, McKay RD. (1990). "CNS stem cells express a new class of intermediate filament protein. ." Cell **60** 585-595.

Leone DP, Genoud S, Atanasoski S, Grausenburger R, Berger P, Metzger D, Macklin WB, Chambon P, Suter U. (2003). "Tamoxifen-inducible glia-specific Cre mice for somatic mutagenesis in oligodendrocytes and Schwann cells." Mol Cell Neurosci **22** 430–440.

Li D, Ambrogio L, Shimamura T, Kubo S, Takahashi M, Chirieac LR, Padera RF, Shapiro GI, Baum A, Himmelsbach F, Rettig WJ, Meyerson M, Solca F, Greulich H, Wong KK. (2008). "BIBW2992, an irreversible EGFR/HER2 inhibitor highly effective in preclinical lung cancer models." Oncogene. **27**(34): 4702-4711.

Li Z, Cai X, Cai CL, Wang J, Zhang W, Petersen BE, Yang FC, Xu M. (2011). "Deletion of Tet2 in mice leads to dysregulated hematopoietic stem cells and subsequent development of myeloid malignancies." Blood **118** (17): 4509-4518.

Libby G, Donnelly LA, Donnan PT, Alessi DR, Morris AD, Evans JM. (2009). "New users of metformin are at low risk of incident cancer: a cohort study among people with type 2 diabetes." Diabetes care **32** (9): 1620-1625.

Lie DC, Song H, Colamarino SA, Ming GL, Gage FH. (2004). "Neurogenesis in the adult brain: new strategies for central nervous system diseases." Annu Rev Pharmacol Toxicol. **44**: 399-421.

Lieberman FS, Cloughesy T, Fine H, Kuhn J, Lamborn K, Malkin M, Robbins HI, Yung WA, Wen P, Prados M. (2004). "NABTC Phase I/II trial of ZD-1839 for recurrent malignant gliomas and unresectable meningiomas." J. Clin. Oncol. **22**: 1510.

Lim DA, Cha S, Mayo MC, Chen MH, Keles E, VandenBerg S, Berger MS. (2007). "Relationship of glioblastoma multiforme to neural stem cell regions predicts invasive and multifocal tumor phenotype." Neuro Oncol. **9**(4): 424-429.

Lindahl G, Lindstedt G, Lindstedt S. (1967). "Metabolism of 2-amino-5-hydroxyadipic acid in the rat." Arch Biochem Biophys **119** 347-352.

Linos E, Raine T, Alonso A, Michaud D. (2007). "Atopy and risk of brain tumors." Journal of the National Cancer Institute **99**(20): 1544-1550.

Liu G, Yuan X, Zeng Z, et al. (2006). "Analysis of gene expression and chemoresistance of CD133+ cancer stem cells in glioblastoma." Mol Cancer **5**: 67.

Liu J, Brown RE. (2010). "Immunohistochemical detection of epithelialmesenchymal transition associated with stemness phenotype in anaplastic thyroid carcinoma." Int J Clin Exp Pathol. **3** (8): 755-762.

Liu X, Kato Y, Kaneko MK, Sugawara M, Ogasawara S, Tsujimoto Y, Naganuma Y, Yamakawa M, Tsuchiya T, Takagi M. (2013). "Isocitrate dehydrogenase 2 mutation is a frequent event in osteosarcoma detected by a multi-specific monoclonal antibody MsMab-1." Cancer Med. **2** (6): 803-814.

Loenarz C, Schofield C. (2008). "Expanding chemical biology of 2-oxoglutarate oxygenases." Nat. Chem. Biol **4**(152–156).

Loilome W, Joshi AD, ap Rhys CM, Piccirillo S, Vescovi AL, Gallia GL, Riggins GJ. (2009). "Glioblastoma cell growth is suppressed by disruption of Fibroblast Growth Factor pathway signaling." J Neurooncol. **94**: 359-366.

Lonardi S, Tosoni A, Brandes AA. (2005). "Adjuvant chemotherapy in the treatment of high grade gliomas." Cancer Treat Rev **31**(2): 79-89.

Losman J, Looper R, Koivunen P. (2013). "(R)-2-hydroxyglutarate is sufficient to promote leukemogenesis and its effects are reversible." Science **339**(6127): 1621-1625.

Losman JA, Kaelin WG Jr. (2013). "What a difference a hydroxyl makes: mutant IDH, (R)-2-hydroxyglutarate, and cancer." Genes Dev. **27** (8): 836-852.

Loussouarn D, Le Loupp A, Frenel J, Leclair F, Von Deimling A, Aumont M, Martin S, Campone M, Denis MG. (2012). "Comparison of immunohistochemistry DNA sequencing and allele-specific PCR for the detection of IDH1 mutations in gliomas." Int J Oncol **40**(6): 2058-2062.

Lu-Emerson C, Norden AD, Drappatz J, Quant EC, Beroukhim R, Ciampa AS, Doherty LM, Lafrankie DC, Ruland S, Wen PY. (2011). "Retrospective study of dasatinib for recurrent glioblastoma after bevacizumab failure." J Neurooncol. **104**(1): 287-291.

Lu C, Ward PS, Kapoor GS, Rohle D, Turcan S, Abdel-Wahab O, Edwards CR, Khanin R, Figueroa ME, Melnick A, Wellen KE, O'Rourke DM, Berger SL, Chan TA, Levine RL, Mellinghoff IK, Thompson CB. (2012). " IDH mutation impairs histone demethylation and results in a block to cell differentiation " Nature **483** 474-478.

Lu J, Zhang F, Yuan Y, Ding C, Zhang L, Li Q. (2013). "All-trans retinoic acid upregulates the expression of p53 via Axin and inhibits the proliferation of glioma cells." Oncol Rep. **29** (6): 2269-2274.

Lu WJ, Lan F, He Q, Lee A, Tang CZ, Dong L, Lan B, Ma X, Wu JC, Shen L. (2011). "Inducible expression of stem cell associated intermediate filament nestin reveals an important role in glioblastoma carcinogenesis." Int J Cancer **128** 343-351.

Luchman HA, Stechishin OD, Dang NH, Blough MD, Chesnelong C, Kelly JJ, Nguyen SA, Chan JA, Weljie AM, Cairncross JG, Weiss S. (2012). "An in vivo patient-derived model of endogenous IDH1-mutant glioma." Neuro-oncology **14**(2): 184-191.

Luksch H, Uckermann O, Stepulak A, Hendruschk S, Marzahn J, Bastian S, Staufner C, Temme A, Ikonomidou C. (2011). "Silencing of selected glutamate receptor subunits modulates cancer growth." Anticancer Res **31**(10): 3181-3192.

Luskin MB. (1993). "Restricted proliferation and migration of postnatally generated neurons derived from the forebrain subventricular zone." Neuron **11**(1): 173-189.

Lustig R, Mikkelsen T, Lesser G, Grossman S, Ye X, Desideri S, Fisher J, Wright J, New Approaches to Brain Tumor Therapy CNS Consortium (2008). "Phase II preradiation R115777 (tipifarnib) in newly diagnosed GBM with residual enhancing disease." Neuro Oncol. **10** (6): 1004-1009.

Lv S, Teugels E, Sadones J, De Brakeleer S, Duerinck J, Du Four S, Michotte A, De Grève J, Neyns B. (2012). "Correlation of EGFR, IDH1 and PTEN status with the outcome of patients with recurrent glioblastoma treated in a phase II clinical trial with the EGFR-blocking monoclonal antibody cetuximab." Int J Oncol. **41**(3): 1029-1035.

Lyon MF, Quinney R, Glenister PH, Kerscher S, Guillot P, Boyd Y. (1996). "Doublefoot: a new mouse mutant affecting development of limbs and head." Genet Res. **68** (3): 221-231.

Lyons S, Chung W, Weaver A, Ogunrinu T, Sontheimer H. (2007). "Autocrine glutamate signaling promotes glioma cell invasion. Cancer Res." Cancer Res. **67** (19): 9463-9471.

Ma YH, Mentlein R, Knerlich F, Kruse ML, Mehdorn HM, Held-Feindt J. (2008). "Expression of stem cell markers in human as- trocytomas of different WHO grades." J Neurooncol **86** 31-45.

MacDonald MJ, Brown LJ, Longacre MJ, Stoker SW, Kendrick MA. (2013). "Knockdown of both mitochondrial isocitrate dehydrogenase enzymes in pancreatic beta cells inhibits insulin secretion." Biochim Biophys Acta. **1830** (11): 5104-5111.

MacDonald MJ, Fahien LA, Brown LJ, Hasan NM, Buss JD, Kendrick MA. (2005). "Perspective: emerging evidence for signaling roles of mitochondrial anaplerotic products in insulin secretion." Am. J. Physiol. Endocrinol. Metab. **288** E1–E15.

MacKenzie ED, Selak MA, Tennant DA, Payne LJ, Crosby S, Frederiksen CM, Watson DG, Gottlieb E. (2007). "Cell-permeating alpha-ketoglutarate derivatives alleviate pseudohypoxia in succinate dehydrogenase-deficient cells." Molecular and cellular biology **27** (9): 3282-3289.

Maemondo M, Inoue A, Kobayashi K, Sugawara S, Oizumi S, Isobe H, Gemma A, Harada M, Yoshizawa H, Kinoshita I, Fujita Y, Okinaga S, Hirano H, Yoshimori K, Harada T, Ogura T, Ando M, Miyazawa H, Tanaka T, Saijo Y, Hagiwara K, Morita S, Nukiwa T; North-East Japan Study Group. (2010). "Gefitinib or chemotherapy for non-small-cell lung cancer with mutated EGFR." N Engl J Med. **362** (25): 2380-2388.

Mahadevan D, Chiorean EG, Harris WB, VonHoff DD, Stejskal-Barnett A, Qi W, Anthony SP, Younger AE, Rensvold DM, Cordova F, Shelton CF, Becker MD, Garlich JR, Durden DL, Ramanathan RK. (2012). " Phase I pharmacokinetic and pharmacodynamic study of the pan-PI3K/mTORC vascular targeted pro-drug SF1126 in patients with advanced solid tumours and B-cell malignancies." Eur. J. Cancer. **48**(18): 3319-3327.

Maher EA, Furnari FB, Bachoo RM, Rowitch DH, Louis DN, Cavenee WK, DePinho RA. (2001). "Malignant glioma: genetics and biology of a grave matter." Genes Dev **15**(11): 1311-1333.

Majmundar AJ, Wong WJ, Simon MC. (2010). "Hypoxia-inducible factors and the response to hypoxic stress." Molecular cell **40**(2): 294-309.

Malmer B, Iselius L, Holmberg E, Collins A, Henriksson R, Grönberg H. (2001). "Genetic epidemiology of glioma." Br J Cancer. **84**(3): 429-434.

Malmström A, Grønberg BH, Marosi C, Stupp R, Frappaz D, Schultz H, Abacioglu U, Tavelin B, Lhermitte B, Hegi ME, Rosell J, Henriksson R, Nordic Clinical Brain Tumour Study Group (NCBTSG). (2012). "Temozolomide versus standard 6-week radiotherapy versus hypofractionated radiotherapy in patients older than 60 years with glioblastoma: the Nordic randomised, phase 3 trial." Lancet Oncol. **13** (9): 916-926.

Malzkorn B, Wolter M, Reimenschneider M, Reifenberger G. (2011). "Unraveling the glioma epigenome: from molecular mechanisms to novel biomarkers and therapeutic targets." Brain Pathol **21**(6): 619-632.

Mardis ER, Ding L, Dooling DJ, Larson DE, McLellan MD, Chen K, Koboldt DC, Fulton RS, Delehaunty KD, McGrath SD, Fulton LA, Locke DP, Magrini VJ, Abbott RM, Vickery TL, Reed JS, Robinson JS, Wylie T, Smith SM, Carmichael L, Eldred JM, Harris CC, Walker J, Peck JB, Du F, Dukes AF, Sanderson GE, Brummett AM, Clark E, McMichael JF, Meyer RJ, Schindler JK, Pohl CS, Wallis JW, Shi X, Lin L, Schmidt H, Tang Y, Haipek C, Wiechert ME, Ivy JV, Kalicki J, Elliott G, Ries RE, Payton JE, Westervelt P, Tomasson MH, Watson MA, Baty J, Heath S, Shannon WD, Nagarajan R, Link DC, Walter MJ, Graubert TA, DiPersio JF, Wilson RK, Ley TJ. (2009). "Recurring mutations found by sequencing an acute myeloid leukemia genome." The New England journal of medicine **361**(11): 1058-1066

Margison GP, Santibanez-Koref MF. (2002). "O-6-alkylguanine-DNA alkyltransferase: role in carcinogenesis and chemotherapy. ." Bioessays. **24** (3): 255-266. .

Marosi C, Vedadinejad M, Haberler C. (2006). "Imatinib mesylate in the treatment of patients with recurrent high grade gliomas expressing PDGF-R." J. Clin. Oncol. **24**: 1526.

Marty M, Cognetti F, Maraninchi D, Snyder R, Mauriac L, Tubiana-Hulin M, Chan S, Grimes D, Antón A, Lluch A, Kennedy J, O'Byrne K, Conte P, Green M, Ward C, Mayne K, Extra JM. (2005). "Randomized phase II trial of the efficacy and safety of trastuzumab combined with docetaxel in patients with human epidermal growth factor receptor 2-positive metastatic breast cancer administered as first-line treatment: the M77001 study group." J Clin Oncol. **23**(19): 4265-4274.

Maslov A, Barone T,Plunkett R, Pruitt S. (2004). Neural stem cell detection, characterization, and age-related changes in the subventricular zone of Mice. J Neuroscience. **24**(7):1726-1733.

Matsuda Y, Kure S, Ishiwata T. (2012). "Nestin and other putative cancer stem cell markers in pancreatic cancer." Med Mol Morphol. **45** (2): 59-65.

McCubrey JA, Steelman LS, Chappell WH, Abrams SL, Wong EW, Chang F, Lehmann B, Terrian DM, Milella M, Tafuri A, Stivala F, Libra M, Basecke J, Evangelisti C, Martelli AM, Franklin RA. (2007). "Roles of the Raf/MEK/ERK pathway in cell growth, malignant transformation and drug resistance." Biochim Biophys Acta. **1773**(8): 1263-1284.

McDonald KL, McDonnell J, Muntoni A, Henson JD, Hegi ME, von Deimling A, Wheeler HR, Cook RJ, Biggs MT, Little NS, Robinson BG, Reddel RR, Royds JA. (2010). "Presence of alternative lengthening of telomeres mechanism in patients with glioblastoma identifies a less aggressive tumour type with longer survival." Journal of neuropathology and experimental neurology **69**(7): 729-736.

McDonough M, Loenarz C, Chowdhury R, Clifton I, Schofield C. (2010). "Structural studies on human 2-oxoglutarate dependent oxygenases." Curr. Opin. Struct. Biol **20**: 659.

McDowell KA, Riggins GJ, Gallia GL. (2011). "Targeting the AKT pathway in glioblastoma. ." Curr. Pharm. Des . **17**(23): 2411–2420.

McFarland MS, Cripps R. (2010). "Diabetes mellitus and increased risk of cancer: focus on metformin and the insulin analogs." Pharmacotherapy **30**(11): 1159-1178.

McKay R. (1997). "Stem cells in the central nervous system." Science **276**: 66-71.

McLendon R, Friedman A, Bigner D, Cancer Genome Atlas Research Network. (2008). "Comprehensive genomic characterization defines human glioblastoma genes and core pathways." Nature **455**: 1061–1068.

Medical Research Council Brain Tumor Working Party (2001). "Randomised trial of procarbazine, lomustine, and vincristine in the adjuvant treatment of high grade astrocytoma: A Medical Research Council Trial." J. Clin. Oncol. **19**(2): 509-518.

Mellinghoff IK, Wang MY, Vivanco I, Haas-Kogan DA, Zhu S, Dia EQ, Lu KV, Yoshimoto K, Huang JH, Chute DJ, Riggs BL, Horvath S, Liau LM, Cavenee WK, Rao PN, Beroukhim R, Peck TC, Lee JC, Sellers WR, Stokoe D, Prados M, Cloughesy TF, Sawyers CL, Mischel PS. (2005). "Molecular determinants of the response of glioblastomas to EGFR kinase inhibitors." N. Engl. J. Med. **353**: 2012–2024.

Metallo CM, Gameiro PA, Bell EL, Mattaini KR, Yang J, Hiller K, Jewell CM, Johnson ZR, Irvine DJ, Guarente L, Kelleher JK, Vander Heiden MG, Iliopoulos O, Stephanopoulos G. (2012). "Reductive glutamine metabolism by IDH1 mediates lipogenesis under hypoxia." Nature **481**(7381): 380-384.

Metellus P, Colin C, Taieb D et al. (2011). "IDH mutation status impact on in vivo hypoxia biomarkers expression: new insights from a clinical, nuclear imaging and immunohistochemical study in 33 glioma patients." Journal of neuro-oncology **105** (3): 591-600

Metro G, Foglietta J, Russillo M, Stocchi L, Vidiri A, Giannarelli D, Crinò L, Papaldo P, Mottolese M, Cognetti F, Fabi A, Gori S. (2011). "Clinical outcome of patients with brain metastases from HER2-positive breast cancer treated with lapatinib and capecitabine." Ann Oncol. **22**(3): 625-630.

Metzen E, Stiehl DP, Doege K, Marxsen JH, Hellwig-Bürgel T, Jelkmann W. (2005). "Regulation of the prolyl hydroxylase domain protein 2 (phd2/egln-1) gene: identification of a functional hypoxia-responsive element." Biochem J. **387**: 711-717.

Mims A, Walker AR, Huang X et al. (2012). "Increased anti-leukemic activity of decitabine via AR-42-induced upregulation of miR-29b: a novel epigenetic-targeting approach in acute myeloid leukemia." Leukemia **27**(4): 871-878.

Minniti G, De Sanctis V, Muni R, Filippone F, Bozzao A, Valeriani M, Osti MF, De Paula U, Lanzetta G, Tombolini V, Maurizi Enrici R (2008). "Radiotherapy plus concomitant and adjuvant temozolomide for glioblastoma in elderly patients." J Neurooncol. **88** (1): 97-103.

Mojas N, Lopes M, Jiricny J. (2007). "Mismatch repair-dependent processing of methylation damage gives rise to persistent single-stranded gaps in newly replicated DNA." Genes Dev. **21** (24): 3342-3355.

Momota H, Nerio E, Holland EC. (2005). "Perifosine inhibits multiple signaling pathways in glial progenitors and cooperates with temozolomide to arrest cell proliferation in gliomas in vivo." Cancer Res. **65**(16): 7429-7435.

Monni E, Cusulin C, Cavallaro M, Lindvall O, Kokaia Z1. (2014). "Human Fetal Striatum-Derived Neural Stem (NS) Cells Differentiate to Mature Neurons in Vitro and in Vivo." Curr Stem Cell Res Ther.

Montine TJ, Vandersteenhoven JJ, Aguzzi A, Boyko OB, Dodge RK, Kerns BJ, Burger PC. (1994). "Prognostic significance of Ki-67 proliferation index in supratentorial fibrillary astrocytic neoplasms." Neurosurgery. **34**(4): 674-678.

Moore CB, Guthrie EH, Huang MT, Taxman DJ. (2010). "Short hairpin RNA (shRNA): design, delivery, and assessment of gene knockdown." Methods Mol Biol. **629** 141-158.

Moran-Crusio K, Reavie L, Shih A, Abdel-Wahab O, Ndiaye-Lobry D, Lobry C, Figueroa ME, Vasanthakumar A, Patel J, Zhao X, Perna F, Pandey S, Madzo J, Song C, Dai Q, He C, Ibrahim S, Beran M, Zavadil J, Nimer SD, Melnick A, Godley LA, Aifantis I, Levine RL. (2011). "Tet2 loss leads to increased hematopoietic stem cell self-renewal and myeloid transformation." Cancer Cell. **20** (1): 11-24.

Mori T, Tanaka K, Buffo A, Wurst W, Kuhn R, Gotz M. (2006). "Inducible gene deletion in astroglia and radial glia – a valuable tool for functional and lineage analysis." Glia **54** 21–34.

Moroni I, Bugiani M, D'Incerti L, Maccagnano C, Rimoldi M, Bissola L, Pollo B, Finocchiaro G, Uziel G. (2004). "L-2Hydroxyglutaric aciduria and malignant brain tumours: a predisposing condition?" Neurology **62**: 1882-1884.

Motzer RJ, Escudier B, Oudard S, Hutson TE, Porta C, Bracarda S (2008). Efficacy of everolimus in advanced renal cell carcinoma: a double-blind, randomised, placebo-controlled phase III trial. Lancet. **372**(9637):449-56.

Motzer RJ, Hutson TE, Tomczak P, Michaelson MD, Bukowski RM, Oudard S, Negrier S, Szczylik C, Pili R, Bjarnason GA, Garcia-del-Muro X, Sosman JA, Solska E, Wilding G, Thompson JA, Kim ST, Chen I, Huang X, Figlin RA. (2009). "Overall survival and updated results for sunitinib compared with interferon alfa in patients with metastatic renal cell carcinoma." J Clin Oncol. **27**(22): 3584-3590.

Murat A, Migliavacca E, Gorlia T, Lambiv WL, Shay T, Hamou MF, de Tribolet N, Regli L, Wick W, Kouwenhoven MC, Hainfellner JA, Heppner FL, Dietrich PY, Zimmer Y, Cairncross JG, Janzer RC, Domany E, Delorenzi M, Stupp R, Hegi ME. (2008). "Stem cell-related "self-renewal" signature and high epidermal growth factor receptor expression associated with resistance to concomitant chemoradiotherapy in glioblastoma." J Clin Oncol **26**(18): 3015-3024.

Myung SK, Ju W, McDonnell DD, Lee YJ, Kazinets G, Cheng CT, Moskowitz JM. (2009). "Mobile phone use and risk of tumors: a meta-analysis." J Clin Oncol. **27**(33): 5565-5572.

Nakamura H, Yoshida M, Tsuiki H, Ito K, Ueno M, Nakao M, Oka K, Tada M, Kochi M, Kuratsu J, Ushio Y, Saya H (1998). "Identification of a human homolog of the Drosophila neuralized gene within the 10q25.1 malignant astrocytoma deletion region." Oncogene. **16**(8): 1009-1019.

Nakamura M, Ishida E, Shimada K, Kishi M, Nakase H, Sakaki T, Konishi N (2005). "Frequent LOH on 22q12.3 and TIMP-3 inactivation occur in the progression to secondary glioblastomas." Lab Invest. **85**(2): 165-175.

Nakamura M, Watanabe T, Klangby U, Asker C, Wiman K, Yonekawa Y, Kleihues P, Ohgaki H (2001a). "p14ARF deletion and methylation in genetic pathways to glioblastomas." Brain Pathol. **11**(2): 159-168.

Nakamura M, Yang F, Fujisawa H, Yonekawa Y, Kleihues P, Ohgaki H (2000). "Loss of heterozygosity on chromosome 19 in secondary glioblastomas." J Neuropathol Exp Neurol. **59**(6): 539-543.

Nakamura M, Yonekawa Y, Kleihues P, Ohgaki H (2001b). "Promoter hypermethylation of the RB1 gene in glioblastomas." Lab Invest. **81**(1): 77-82.

Narita K, Matsuda Y, Seike M, Naito Z, Gemma A, Ishiwata T. (2014). "Nestin regulates proliferation, migration, invasion and stemness of lung adenocarcinoma." Int J Oncol. **44** (4): 1118-1130.

Naumov GN, Nilsson MB, Cascone T, Briggs A, Straume O, Akslen LA, Lifshits E, Byers LA, Xu L, Wu HK, Jänne P, Kobayashi S, Halmos B, Tenen D, Tang XM, Engelman J, Yeap B, Folkman J, Johnson BE, Heymach JV. (2009). "Combined vascular endothelial growth factor receptor and epidermal growth factor receptor (EGFR) blockade inhibits tumor growth in xenograft models of EGFR inhibitor resistance." Clin Cancer Res. **15**(10): 3484-3494.

Nguyen TD, Lassman AB, Lis E, Rosen N, Shaffer DR, Scher HI, Deangelis LM and Abrey LE. (2006). "A pilot study to assess the tolerability and efficacy of RAD-001 (everolimus) with gefitinib in patients with recurrent glioblastoma multiforme (GBM)." J. Clin. Oncol. **24**: 1507.

Nobusawa S, Watanabe T, Kleihues P, Ohgaki H. (2009). "IDH1 mutations as molecular signature and predictive factor of secondary glioblastomas." Clin Cancer Res. **15** (19): 6002-6007.

Noch E, Khalili K. (2009). "Molecular mechanisms of necrosis in glioblastoma: the role of glutamate excitotoxicity." Cancer Biol Ther. **8**(19): 1791-1797.

Noch E, Sariyer IK, Gordon J, Khalili K. (2012). "JC virus T-antigen regulates glucose metabolic pathways in brain tumor cells." PLoS One. **7**(4).

Noushmehr H, Weisenberger DJ, Diefes K, Phillips HS, Pujara K, Berman BP, Pan F, Pelloski CE, Sulman EP, Bhat KP, Verhaak RG, Hoadley KA, Hayes DN, Perou CM, Schmidt HK, Ding L, Wilson RK, Van Den Berg D, Shen H, Bengtsson H, Neuvial P, Cope LM, Buckley J, Herman JG, Baylin SB, Laird PW, Aldape K; Cancer Genome Atlas Research Network. (2010). "Identification of a CpG island methylator phenotype that defines a distinct subgroup of glioma." Cancer cell **17**(5): 510-522.

O'Reilly MS, Boehm T, Shing Y, Fukai N, Vasios G, Lane WS, Flynn E, Birkhead JR, Olsen BR, Folkman J. (1997). "Endostatin: an endogenous inhibitor of angiogenesis and tumour growth." Cell **88**(2): 277-285.

Ohgaki H. (2005b). "Genetic pathways to glioblastomas." Neuropathology. **25**(1): 1-7.

Ohgaki H, Dessen P, Jourde B, Horstmann S, Nishikawa T, Di Patre PL, Burkhard C, Schuler D, Probst-Hensch NM, Maiorka PC, Baeza N, Pisani P, Yonekawa Y, Yasargil MG, Lutolf UM, Kleihues P. (2004). "Genetic pathways to glioblastoma: a population-based study." Cancer Res. **64**: 6892–6899.

Ohgaki H, Kleihues P. (2005a). "Population-based studies on incidence, survival rates, and genetic alterations in astrocytic and oligodendroglial gliomas." J Neuropathol Exp Neurol. **64** (6): 479-489.

Ohgaki H, Kleihues P. (2007). "Genetic Pathways to Primary and Secondary Glioblastoma." Am J Pathol. **170**(5): 1445-1453.

Ohgaki H, Kleihues P. (2011). "Genetic profile of astrocytic and oligodendroglial gliomas. ." Brain Tumor Pathol. **28**: 177–183.

Ohka F, Natsume A, Wakabayashi T. (2012). "Current trends in targeted therapies for glioblastoma multiforme." Neurol Res Int. **2012:878425.**

Osborne RH, Houben MP, Tijssen CC, Coebergh JW, van Duijn CM. (2001). "The genetic epidemiology of glioma." Neurology. **57**(10): 1751-1755.

Pandolfi PP. (2001). "Oncogenes and tumor suppressors in the molecular pathogenesis of acute promyelocytic leukemia." Hum Mol Genet. **7** 769-775.

Pansuriya T, Kroon HM, Bovee JV. (2010) Enchondromatosis:insights on the different subtypes. Int. J. Clin. Exp. Pathol. **3**, 557–569.

Pansuriya TC, van Eijk R, d'Adamo P, van Ruler MA, Kuijjer ML, Oosting J, Cleton-Jansen AM, van Oosterwijk JG, Verbeke SL, Meijer D, van Wezel T, Nord KH, Sangiorgi L, Toker B, Liegl-Atzwanger B, San-Julian M, Sciot R, Limaye N, Kindblom LG, Daugaard S, Godfraind C, Boon LM, Vikkula M, Kurek KC, Szuhai K, French PJ, Bovée JV. (2011). "Somatic mosaic IDH1 and IDH2 mutations are associated with enchondroma and spindle cell hemangioma in Ollier disease and Maffucci syndrome." Nat Genet. **43**(12): 1256-1261.

Pardanani A, Lasho TL, Finke CM, Mai M, McClure RF, Tefferi A. (2010). "IDH1 and IDH2 mutation analysis in chronic- and blast-phase myeloproliferative neoplasms." Leukemia. **24**(6): 1146-1151.

Park CK, Lee SH, Kim TM, Choi SH, Park SH, Heo DS, Kim IH, Jung HW. (2013). "The value of temozolomide in combination with radiotherapy during standard treatment for newly diagnosed glioblastoma." J Neurooncol. **112** (2): 277-283.

Parsons DW, Jones S, Zhang X, Lin JC, Leary RJ, Angenendt P, Mankoo P, Carter H, Siu IM, Gallia GL, Olivi A, McLendon R, Rasheed BA, Keir S, Nikolskaya T, Nikolsky Y, Busam DA, Tekleab H, Diaz LA Jr, Hartigan J, Smith DR, Strausberg RL, Marie SK, Shinjo SM, Yan H, Riggins GJ, Bigner DD, Karchin R, Papadopoulos N, Parmigiani G, Vogelstein B, Velculescu VE, Kinzler KW. (2008). "An integrated genomic analysis of human glioblastoma multiforme." Science **321**(5897): 1807-1812

Paschka P, Schlenk RF, Gaidzik VI, Habdank M, Krönke J, Bullinger L, Späth D, Kayser S, Zucknick M, Götze K, Horst HA, Germing U, Döhner H, Döhner K. (2010). "IDH1 and IDH2 mutations are frequent genetic alterations in acute myeloid leukemia and confer adverse prognosis in cytogenetically normal acute myeloid leukemia with NPM1 mutation without FLT3 internal tandem duplication." J Clin Oncol. **28** (22): 3636-3643.

Patnaik MM, Hanson CA, Hodnefield JM, Lasho TL, Finke CM, Knudson RA, Ketterling RP, Pardanani A, Tefferi A. (2012). "Differential prognostic effect of IDH1 versus IDH2 mutations in myelodysplastic syndromes: A Mayo Clinic study of 277 patients." Leukemia **26**: 101–105.

Peereboom DM, Ahluwalia MS, Ye X, Supko JG, Hilderbrand SL, Phuphanich S, Nabors LB, Rosenfeld MR, Mikkelsen T, Grossman SA; New Approaches to Brain Tumor Therapy Consortium. (2013). "NABTT 0502: a phase II and pharmacokinetic study of erlotinib and sorafenib for patients with progressive or recurrent glioblastoma multiforme." Neuro Oncol. **15**(4): 490-496.

Peereboom DM, Shepard DR, Ahluwalia MS, Brewer CJ, Agarwal N, Stevens GH, Suh JH, Toms SA, Vogelbaum MA, Weil RJ, Elson P, Barnett GH. (2010). "Phase II trial of erlotinib with temozolomide and radiation in patients with newly diagnosed glioblastoma multiforme." J Neurooncol. **98**(1): 93-99.

Perez EA, Romond EH, Suman VJ, Jeong JH, Davidson NE, Geyer CE Jr, Martino S, Mamounas EP, Kaufman PA, Wolmark N. (2011). "Four-year follow-up of trastuzumab plus adjuvant chemotherapy for operable human epidermal growth factor receptor 2-positive breast cancer: joint analysis of data from NCCTG N9831 and NSABP B-31." J Clin Oncol. **29** (25): 3366-3373.

Piao Y, Lu L, de Groot J. (2009). "AMPA receptors promote perivascular glioma invasion via beta integrin-dependent adhesion to the extracellular matrix." Neuro Oncol **11** (3): 260-273

Piaskowski S, Bienkowski M, Stoczynska-Fidelus E, Stawski R, Sieruta M, Szybka M, Papierz W, Wolanczyk M, Jaskolski DJ, Liberski PP, Rieske P. (2011). "Glioma cells showing IDH1 mutation cannot be propagated in standard cell culture conditions." Br J Cancer. **104**(6): 968-970. .

Pietrak B, Zhao H, Qi H et al. (2011). "A tale of two subunits: how the neomorphic R132H IDH1 mutation enhances production of alphaHG." Biochemistry **50(21)** (21): 4804-4812.

Pincus DW, Harrison-Restelli C, Barry J, Goodman RR, Fraser RA, Nedergaard M, Goldman SA (1997). "In vitro neurogenesis by adult human epileptic temporal neocortex." Clin Neurosurg. **44**: 17-25.

Pitter KL, Galbán CJ, Galbán S, Tehrani OS, Li F, Charles N, Bradbury MS, Becher OJ, Chenevert TL, Rehemtulla A, Ross BD, Holland EC, Hambardzumyan D. (2011). "Perifosine and CCI 779 co-operate to induce cell death and decrease proliferation in PTEN-intact and PTEN-deficient PDGF-driven murine glioblastoma." PLoS One. **6**(1): e14545.

Pollard P, Wortham N, Barclay E, Alam A, Elia G, Manek S, Poulsom R, Tomlinson I. (2005). "Evidence of increased microvessel density and activation of the hypoxia pathway in tumours from the hereditary leiomyomatosis and renal cell cancer syndrome." The journal of Pathology **205**(1): 41-49.

Pollard PJ, Briere JJ, Alam NA, Barwell J, Barclay E, Wortham NC, Hunt T, Mitchell M, Olpin S, Moat SJ, Hargreaves IP, Heales SJ, Chung YL, Griffiths JR, Dalgleish A, McGrath JA, Gleeson MJ, Hodgson SV, Poulsom R, Rustin P, Tomlinson IP. (2005). "Accumulation of Krebs cycle intermediates and over-expression of HIF1alpha in tumours which result from germline FH and SDH mutations. ." Human molecular genetics **14**(15): 2231-2239

Pope WB, Prins RM, Albert Thomas M, Nagarajan R, Yen KE, Bittinger MA, Salamon N, Chou AP, Yong WH, Soto H, Wilson N, Driggers E, Jang HG, Su SM, Schenkein DP, Lai A, Cloughesy TF, Kornblum HI, Wu H, Fantin VR, Liau LM. (2012). "Non-invasive detection of 2-hydroxyglutarate and other metabolites in IDH1 mutant glioma patients using magnetic resonance spectroscopy." Journal of neuro-oncology **107**(1): 197-205.

Popovici-Muller J, Saunders J, Salituro F, Travins JM, Yan S, Zhao F, Gross S, Dang L, Yen KE, Yang H, Straley KS, Jin S, Kunii K, Fantin VR, Zhang S, Pan Q, Shi D, Biller SA, Su SM. (2012). "Discovery of the first potent inhibitors of mutant IDH1 that lower tumor 2-HG in vivo." ACS Med. Chem. Lett. **3**: 850.

Pore N, Liu S, Haas-Kogan DA, O'Rourke DM, Maity A. (2003). "PTEN mutation and epidermal growth factor receptor activation regulate vascular endothelial growth factor (VEGF) mRNA expression in human glioblastoma cells by transactivating the proximal VEGF promoter." Cancer Res . **63**: 236-241.

Prados M, Gilbert M, Kuhn J , Lamborn K, Cloughesy T, Lieberman S, Puduvalli V, Robins HI, Lassman A, Wen PY (2009). "Phase I/II study of sorefenib and erlotinib for patients with recurrent glioblastoma (GBM) (NABTC 05-02) " J. Clin. Oncol. (Meeting Abstracts) **27**(15s): 2005.

Prasad G, Sottero T, Yang X, Mueller S, James CD, Weiss WA, Polley MY, Ozawa T, Berger MS, Aftab DT, Prados MD, Haas-Kogan DA. (2011). "Inhibition of PI3K/mTOR pathways in glioblastoma and implications for combination therapy with temozolomide." Neuro Oncol. **13**(4): 384-392.

Preusser M, Wohrer A, Stary S et al. (2011). "Value and limitations of immunohistochemistry and gene sequencing for detection of the IDH1-R132H mutation in diffuse glioma biopsy specimens." J Neuropathol Exp Neurol **70**(8): 715-723.

Price RL, Song J, Bingmer K, Kim TH, Yi JY, Nowicki MO, Mo X, Hollon T, Murnan E, Alvarez-Breckenridge C, Fernandez S, Kaur B, Rivera A, Oglesbee M, Cook C, Chiocca EA, Kwon CH. (2013).

"Cytomegalovirus contributes to glioblastoma in the context of tumor suppressor mutations." Cancer Res. **73** (11): 3441-3450.

Pusch S, Sahm F, Meyer J, Mittelbronn M, Hartmann C, von Deimling A. (2011). "Glioma IDH1 mutation patterns off the beaten track." Neuropathol Appl Neurobiol **37**: 428–430.

Puzzilli F, Ruggeri A, Mastronardi L, Di Stephano D, Lunardi P. (1998). "Long-term survival in cerebral glioblastoma. Case report and critical review of the literature." Tumori **84** (1): 69-74.

Querings S, Altmuller J, Ansen S. (2011). Benchmarking of mutation diagnostics in clinical lung cancer specimens. PLoS One. **6**:e19601.

Quinlivan EP, Gregory JF 3rd. (2008). "DNA digestion to deoxyribonucleoside: a simplified one-step procedure." Anal Biochem. **373** (2): 383-385.

Quiñones-Hinojosa A, Sanai N, Soriano-Navarro M, Gonzalez-Perez O, Mirzadeh Z, Gil-Perotin S, Romero-Rodriguez R, Berger MS, Garcia-Verdugo JM, Alvarez-Buylla A. (2006). "Cellular composition and cytoarchitecture of the adult human subventricular zone: a niche of neural stem cells." J Comp Neurol. **494**(3): 415-434.

Quivoron C, Couronné L, Della Valle V, Lopez CK, Plo I, Wagner-Ballon O, Do Cruzeiro M, Delhommeau F, Arnulf B, Stern MH, Godley L, Opolon P, Tilly H, Solary E, Duffourd Y, Dessen P, Merle-Beral H, Nguyen-Khac F, Fontenay M, Vainchenker W, Bastard C, Mercher T, Bernard OA. (2011). "TET2 inactivation results in pleiotropic hematopoietic abnormalities in mouse and is a recurrent event during human lymphomagenesis." Cancer Cell. **20**(1): 25-38.

Radke J, Bortolussi G, Pagenstecher A. (2013). "Akt and c-Myc induce stem-cell markers in mature primary $p53^{-/-}$ astrocytes and render these cells gliomagenic in the brain of immunocompetent mice." PLoS One. **8**(2): e56691.

Raimundo N, Baysal BE, Shadel GS. (2011). "Revisiting the TCA cycle: signaling to tumour formation." Trends in molecular medicine **17**(11): 641-649.

Rakheja D, Konoplev S, Medeiros LJ, Chen W. (2012). "IDH mutations in acute myeloid leukemia." Hum Pathol. **43**(10): 1541-1551.

Rasheed BK, McLendon RE, Friedman HS, Friedman AH, Fuchs HE, Bigner DD, Bigner SH (1995). "Chromosome 10 deletion mapping in human gliomas: a common deletion region in 10q25." Oncogene. **10**(11): 2243-2246.

Raymond E, Brandes AA, Dittrich C, Fumoleau P, Coudert B, Clement PM, Frenay M, Rampling R, Stupp R, Kros JM, Heinrich MC, Gorlia T, Lacombe D, van den Bent MJ, European Organisation for Research and Treatment of Cancer Brain Tumor Group Study (2008). "Phase II study of imatinib in

patients with recurrent gliomas of various histologies: a European Organisation for Research and Treatment of Cancer Brain Tumor Group Study." J Clin Oncol. **26**(28): 4659-4665.

Reardon DA, Conrad CA, Cloughesy T, Prados MD, Friedman HS, Aldape KD, Mischel P, Xia J, DiLea C, Huang J, Mietlowski W, Dugan M, Chen W, Yung WK. (2012). "Phase I study of AEE788, a novel multitarget inhibitor of ErbB- and VEGF-receptor-family tyrosine kinases, in recurrent glioblastoma patients." Cancer Chemother Pharmacol. **69**(6): 1507-1518.

Reardon DA, Desjardins A, Vredenburgh JJ et al., (2010). "Phase 2 trial of erlotinib plus sirolimus in adults with recurrent glioblastoma." Journal of neuro-oncology **96 219–230.**(2): 219–230.

Reardon DA, Fink KL, Mikkelsen T, Cloughesy TF, O'Neill A, Plotkin S, Glantz M, Ravin P, Raizer JJ, Rich KM, Schiff D, Shapiro WR, Burdette-Radoux S, Dropcho EJ, Wittemer SM, Nippgen J, Picard M, Nabors LB (2008). "Randomized phase II study of cilengitide, an integrin-targeting arginine-glycine-aspartic acid peptide, in recurrent glioblastoma multiforme." J Clin Oncol. **26**(34): 5610-5617.

Reardon DA, Groves MD, Wen PY, Nabors L, Mikkelsen T, Rosenfeld S, Raizer J, Barriuso J, McLendon RE, Suttle AB, Ma B, Curtis CM, Dar MM, de Bono J. (2013). "A phase I/II trial of pazopanib in combination with lapatinib in adult patients with relapsed malignant glioma." Clin Cancer Res. **19**(4): 900-908.

Reardon DA, Quinn JA, Vredenburgh JJ, Gururangan S, Friedman AH, Desjardins A, Sathornsumetee S, Herndon JE 2nd, Dowell JM, McLendon RE, Provenzale JM, Sampson JH, Smith RP, Swaisland AJ, Ochs JS, Lyons P, Tourt-Uhlig S, Bigner DD, Friedman HS, Rich JN. (2006). "Phase 1 trial of gefitinib plus sirolimus in adults with recurrent malignant glioma." Clin. Cancer Res. **12**: 860–868.

Reifenberger G, Liu L, Ichimura K, Schmidt EE, Collins VP. (1993). "Amplification and overexpression of the MDM2 gene in a subset of human malignant gliomas without p53 mutations." Cancer Res. **53**: 2736–2739.

Reilly KM, Tuskan RG, Christy E, Loisel DA, Ledger J, Bronson RT, Smith CD, Tsang S, Munroe DJ, Jacks T. (2004). "Susceptibility to astrocytoma in mice mutant for Nf1 and Trp53 is linked to chromosome 11 and subject to epigenetic effects." Proc Natl Acad Sci U S A. **101**(35): 13008-13013.

Reimer R, Helmbold H, Szalay B, Hagel C, Hohenberg H, Deppert W, Bohn W. (2009). "Nestin modulates glucocorticoid receptor function by cytoplasmic anchoring. " PLoS One. **4**(6): e6084.

Reitman ZJ, Jin G, Karoly ED, Spasojevic I, Yang J, Kinzler KW, He Y, Bigner DD, Vogelstein B, Yan H. (2011). "Profiling the effects of isocitrate dehydrogenase 1 and 2 mutations on the cellular metabolome." Proceedings of the National Academy of Sciences of the United States of America **108**(8): 3270-3275.

Reitman ZJ, Yan H (2010). "Isocitrate dehydrogenase 1 and 2 mutations in cancer: alterations at a crossroads of cellular metabolism." Journal of the National Cancer Institute **102**(13): 932-941.

Reuter S, Gupta SC, Chaturvedi MM, Aggarwal BB. (2010). "Oxidative stress, inflammation, and cancer: how are they linked?" Free Radic Biol Med. **49**(11): 1603-1616.

Rich JN, Reardon DA, Peery T, Dowell JM, Quinn JA, Penne KL, Wikstrand CJ, Van Duyn LB, Dancey JE, McLendon RE, Kao JC, Stenzel TT, Ahmed Rasheed BK, Tourt-Uhlig SE, Herndon JE 2nd, Vredenburgh JJ, Sampson JH, Friedman AH, Bigner DD, Friedman HS (2004). "Phase II trial of gefitinib in recurrent glioblastoma." Journal of Clinical Oncology, **22**(1): 133-142.

Ricketts C, Woodward ER, Killick P, Morris MR, Astuti D, Latif F, Maher ER. (2008). "Germline SDHB mutations and familial renal cell carcinoma." J Natl Cancer Inst. **100** (17): 1260-1262.

Robinson A, Keely S, Karhausen J, Gerich ME, Furuta GT, Colgan SP. (2008). "Mucosal protection by hypoxia-inducible factor prolyl hydroxylase inhibition." Gastroenterology. **134**(1): 145-155.

Robinson ML, Allen CE, Davy BE, Durfee WJ, Elder FF, Elliott CS, Harrison WR. (2002). "Genetic mapping of an insertional hydrocephalus-inducing mutation allelic to hy3." Mamm Genome. **13** (11): 625-632.

Rohle D, Popovici-Muller J, Palaskas N et al. (2013). "An inhibitor of mutant IDH1 delays growth and promotes differentiation of glioma cells." Science **340** 626-630.

Ronnebaum SM, Ilkayeva O, Burgess SC, Joseph JW, Lu D, Stevens RD, Becker TC, Sherry AD, Newgard CB, Jensen MV. (2006). "A pyruvate cycling pathway involving cytosolic NADP-dependent isocitrate dehydrogenase regulates glucose-stimulated insulin secretion." The Journal of biological chemistry **281**(41): 30593-30602.

Roos W, Baumgartner M, Kaina B. (2004). "Apoptosis triggered by DNA damage O-6-methylguanine in human lymphocytes requires DNA replication and is mediated by p53 and Fas/CD95/Apo-1." Oncogene **23**(2): 359-367.

Rosell R, Carcereny E, Gervais R, Vergnenegre A, Massuti B, Felip E, Palmero R, Garcia-Gomez R, Pallares C, Sanchez JM, Porta R, Cobo M, Garrido P, Longo F, Moran T, Insa A, De Marinis F, Corre R, Bover I, Illiano A, Dansin E, de Castro J, Milella M, Reguart N, Altavilla G, Jimenez U, Provencio M, Moreno MA, Terrasa J, Muñoz-Langa J, Valdivia J, Isla D, Domine M, Molinier O, Mazieres J, Baize N, Garcia-Campelo R, Robinet G, Rodriguez-Abreu D, Lopez-Vivanco G, Gebbia V, Ferrera-Delgado L, Bombaron P, Bernabe R, Bearz A, Artal A, Cortesi E, Rolfo C, Sanchez-Ronco M, Drozdowskyj A, Queralt C, de Aguirre I, Ramirez JL, Sanchez JJ, Molina MA, Taron M, Paz-Ares L; Spanish Lung Cancer Group in collaboration with Groupe Français de Pneumo-Cancérologie and Associazione Italiana Oncologia Toracica. (2012). "Erlotinib versus standard chemotherapy as first-line treatment for European patients with advanced EGFR mutation-positive non-small-cell lung cancer (EURTAC): a multicentre, open-label, randomised phase 3 trial." Lancet Oncol. **13** (3): 239-246.

Roy Choudhury S, Karmakar S, Banik NL, Ray SK. (2011). "Valproic acid induced differentiation and potentiated efficacy of taxol and nanotaxol for controlling growth of human glioblastoma LN18 and T98G cells." Neurochem Res. **36** (12): 2292-2305.

Ruano Y, Ribalta T, de Lope AR, Campos-Martín Y, Fiaño C, Pérez-Magán E, Hernández-Moneo JL, Mollejo M, Meléndez B. (2009). "Worse outcome in primary glioblastoma multiforme with concurrent epidermal growth factor receptor and p53 alteration." Am J Clin Pathol. **131**(2): 257-263.

Ryding AD, Sharp MG, Mullins JJ. (2001). "Conditional transgenic technologies." J Endocrinol. **171** (1): 1-14.

Rzem R, Van Schaftingen E, Veiga-da-Cunha M. (2005). "The gene mutated in l-2-hydroxyglutaric aciduria encodes l-2-hydroxyglutarate dehydrogenase". *Biochimie* **88** (1): 113–6.

Rzem R, Vincent MF, Van Schaftingen E, Veiga-da-Cunha M. (2007). "L-2-hydroxyglutaric aciduria, a defect of metabolite repair." J Inherit Metab Dis **30**: 681–689.

Sahlgren CM, Mikhailov A, Vaittinen S, Pallari HM, Kalimo H, Pant HC, Eriksson JE. (2003). "Cdk5 regulates the organization of nestin and its association with p35." Mol Cell Biol **23**: 5090-5106.

Sahlgren CM, Pallari HM, He T, Chou YH, Goldman RD, Eriksson JE. (2006). "A nestin scaffold links Cdk5/p35 signaling to oxidant-induced cell death." EMBO J **25** 4808-4819.

Said HM, Hagemann C, Stojic J, Schoemig B, Vince GH, Flentje M, Roosen K, Vordermark D. (2007). "GAPDH is not regulated in human glioblastoma under hypoxic conditions." BMC Mol Biol. **8**: 55.

Salmaggi A, Boiardi A, Gelati M, Russo A, Calatozzolo C, Ciusani E, Sciacca FL, Ottolina A, Parati EA, La Porta C, Alessandri G, Marras C, Croci D, De Rossi M. (2006). "Glioblastoma-derived tumorospheres identify a population of tumor stem-like cells with angiogenic potential and enhanced multidrug resistance phenotype." Glia **54**(8): 850-860.

Sanai N, Alvarez-Buylla A, Berger M. (2005). "Neural stem cells and the origin of gliomas." N. Engl. J. Med. **353**: 811–822.

Sano T, Lin H, Chen X, Langford LA, Koul D, Bondy ML, Hess KR, Myers JN, Hong YK, Yung WK, Steck PA. (1999). "Differential expression of MMAC/PTEN in glioblastoma multiforme: relationship to localization and prognosis." Cancer Res. **59**(8): 1820-1824.

Sanson M, Hosking FJ, Shete S, Zelenika D, Dobbins SE, Ma Y, Enciso-Mora V, Idbaih A, Delattre JY, Hoang-Xuan K, Marie Y, Boisselier B, Carpentier C, Wang XW, Di Stefano AL, Labussière M, Gousias K, Schramm J, Boland A, Lechner D, Gut I, Armstrong G, Liu Y, Yu R, Lau C, Di Bernardo MC, Robertson LB, Muir K, Hepworth S, Swerdlow A, Schoemaker MJ, Wichmann HE, Müller M, Schreiber S, Franke A, Moebus S, Eisele L, Försti A, Hemminki K, Lathrop M, Bondy M, Houlston RS, Simon M. (2011). "Chromosome 7p11.2 (EGFR) variation influences glioma risk." Hum Mol Genet. **20**(14): 2897-2904.

Sanson M, Marie Y, Paris S, Idbaih A, Laffaire J, Ducray F, El Hallani S, Boisselier B, Mokhtari K, Hoang-Xuan K, Delattre JY. (2009). "Isocitrate dehydrogenase 1 codon 132 mutation is an important prognostic biomarker in gliomas." Journal of clinical oncology : official journal of the American Society of Clinical Oncology **27** (25): 4150-4154.

Sasaki M, Knobbe CB, Itsumi M, Elia AJ, Harris IS, Chio II, Cairns RA, McCracken S, Wakeham A, Haight J, Ten AY, Snow B, Ueda T, Inoue S, Yamamoto K, Ko M, Rao A, Yen KE, Su SM, Mak TW. (2012b). "D-2-hydroxyglutarate produced by mutant IDH1 perturbs collagen maturation and basement membrane function." Genes & development **26**(18): 2038-2049.

Sasaki M, Knobbe CB, Munger JC, Lind EF, Brenner D, Brüstle A, Harris IS, Holmes R, Wakeham A, Haight J, You-Ten A, Li WY, Schalm S, Su SM, Virtanen C, Reifenberger G, Ohashi PS, Barber DL, Figueroa ME, Melnick A, Zúñiga-Pflücker JC, Mak TW. (2012a). "IDH1(R132H) mutation increases murine haematopoietic progenitors and alters epigenetics." Nature **488** (7413): 656-659.

Sathornsumetee S, Desjardins A, Vredenburgh JJ, McLendon RE, Marcello J, Herndon JE, Mathe A, Hamilton M, Rich JN, Norfleet JA, Gururangan S, Friedman HS, Reardon DA. (2010). "Phase II trial of bevacizumab and erlotinib in patients with recurrent malignant glioma." Neuro Oncol. **12**(12): 1300-1310.

Schiff D, Brown PD, Giannini C. (2007). "Outcome in adult low-grade glioma: the impact of prognostic factors and treatment." Neurology **69**: 1366–1373.

Schiff D, Shaffrey ME. (2003). "Role of resection for newly diagnosed malignant gliomas." Expert Rev Anticancer Ther. **3** (5): 621-630.

Schmidt EE, Taylor DS, Prigge JR, Barnett S, Capecchi MR. (2000). "lllegitimate Cre-dependent chromosome rearrangements in transgenic mouse spermatids." PNAS **97**: 13702-13707.

Schmidt MC, Antweiler S, Urban N, Mueller W, Kuklik A, Meyer-Puttlitz B, Wiestler OD, Louis DN, Fimmers R, von Deimling A. (2002). "Impact of genotype and morphology on the prognosis of glioblastoma." J Neuropathol Exp Neurol. **61**(4): 321-328.

Schwartzbaum JA, Fisher JL, Aldape KD, Wrensch M. (2006). "Epidemiology and molecular pathology of glioma." Nat Clin Pract Neurol. **2**(9): 494-503.

Scott JN, Rewcastle NB, Brasher PM, Fulton D, Hagen NA, MacKinnon JA, Sutherland G, Cairncross JG, Forsyth P. (1998). "Long-term glioblastoma multiforme survivors: a population-based study." Can J Neurol Sci. **25**(3): 197-201.

Sehgal A. (1998). "Molecular changes during the genesis of human gliomas." Semin Surg Oncol. **14**(1): 3-12.

Seltzer MJ, Bennett BD, Joshi AD, Gao P, Thomas AG, Ferraris DV, Tsukamoto T, Rojas CJ, Slusher BS, Rabinowitz JD, Dang CV, Riggins GJ. (2010). "Inhibition of glutaminase preferentially slows growth of glioma cells with mutant IDH1." Cancer Research **70**(22): 8981-8987.

Semenza GL. (2003). "Targeting HIF-1 for cancer therapy." Nat Rev Cancer. **3** (10): 721-732.

Semenza GL. (2012). "Hypoxia-inducible factors in physiology and medicine." Cell. **148** (3): 399-408.

Sequist LV, Heist RS, Shaw AT, Fidias P, Rosovsky R, Temel JS, Lennes IT, Digumarthy S, Waltman BA, Bast E, Tammireddy S, Morrissey L, Muzikansky A, Goldberg SB, Gainor J, Channick CL, Wain JC, Gaissert H, Donahue DM, Muniappan A, Wright C, Willers H, Mathisen DJ, Choi NC, Baselga J, Lynch TJ, Ellisen LW, Mino-Kenudson M, Lanuti M, Borger DR, Iafrate AJ, Engelman JA, Dias-Santagata D. (2011). "Implementing multiplexed genotyping of non-small-cell lung cancers into routine clinical practice." Ann Oncol. **22** (12): 2616-2624.

Sequist LV, Yang JC, Yamamoto N, O'Byrne K, Hirsh V, Mok T, Geater SL, Orlov S, Tsai CM, Boyer M, Su WC, Bennouna J, Kato T, Gorbunova V, Lee KH, Shah R, Massey D, Zazulina V, Shahidi M, Schuler M. (2013). "Phase III study of afatinib or cisplatin plus pemetrexed in patients with metastatic lung adenocarcinoma with EGFR mutations." J Clin Oncol. **31**(27): 3327-3334.

Seri B, Garcia-Verdugo JM, Collado-Morente L, McEwen BS, Alvarez-Buylla A. (2004). "Cell types, lineage, and architecture of the germinal zone in the adult dentate gyrus." J. Comp. Neurol. **478**: 359–378.

Seshacharyulu P, Ponnusamy MP, Haridas D, Jain M, Ganti AK, Batra SK. (2012). "Targeting the EGFR signaling pathway in cancer therapy. ." Expert Opin. Ther. Targets . **16**(1): 15–31.

Shaw E, Berkey B, Coons S, et al (2006). "Initial report of Radiation Therapy Oncology Group (RTOG) 9802: Prospective studies in adult low-grade glioma (LGG)." J Clin Oncol **24**: 58s.

Sherr CJ, Roberts JM. (1999). "CDK inhibitors: positive and negative regulators of G1-phase progression." Genes Dev. **13**: 1501–1512.

Shete S, Hosking FJ, Robertson LB, Dobbins SE, Sanson M, Malmer B, Simon M, Marie Y, Boisselier B, Delattre JY, Hoang-Xuan K, El Hallani S, Idbaih A, Zelenika D, Andersson U, Henriksson R, Bergenheim AT, Feychting M, Lönn S, Ahlbom A, Schramm J, Linnebank M, Hemminki K, Kumar R, Hepworth SJ, Price A, Armstrong G, Liu Y, Gu X, Yu R, Lau C, Schoemaker M, Muir K, Swerdlow A, Lathrop M, Bondy M, Houlston RS. (2009). "Genome-wide association study identifies five susceptibility loci for glioma." Nat Genet. **41** (8): 899-904. .

Shi Z, Lou M, Zhao Y, Zhang Q, Cui D, Wang K. (2013). "Effect of all-trans retinoic acid on the differentiation of U87 glioma stem/progenitor cells." Cell Mol Neurobiol. **33** (7): 943-951.

Shibata T, Kokubu A, Miyamoto M, Sasajima Y, Yamazaki N. (2011). "Mutant IDH1 confers an in vivo growth in a melanoma cell line with BRAF mutation." The American journal of pathology **178**(3): 1395-1402.

Shinojima N, Tada K, Shiraishi S, Kamiryo T, Kochi M, Nakamura H, Makino K, Saya H, Hirano H, Kuratsu J, Oka K, Ishimaru Y, Ushio Y. (2003). "Prognostic value of epidermal growth factor receptor in patients with glioblastoma multiforme." Cancer Res. **63**(20): 6962-6970.

Shirai K, Siedow MR, Chakravarti A. (2012). "Antiangiogenic therapy for patients with recurrent and newly diagnosed malignant gliomas." J Oncol. **2012**: e193436.

Shiras A, Bhosale A, Shepal V, Shukla R, Baburao VS, Prabhakara K, Shastry P. (2003). "A unique model system for tumor progression in GBM comprising two developed human neuro-epithelial cell lines with differential transforming potential and coexpressing neuronal and glial markers." Neoplasia **5**(6): 520-532.

Sibtain NA, Howe F, Saunders DE. (2007). "The clinical value of proton magnetic resonance spectroscopy in adult brain tumours." Clin Radiol. **62** (2): 109-119.

Silva-Vargas V, Crouch EE, Doetsch F. (2013). "Adult neural stem cells and their niche: a dynamic duo during homeostasis, regeneration, and aging." Curr Opin Neurobiol. **23**(6): 935-942.

Simmons ML, Lamborn KR, Takahashi M, Chen P, Israel MA, Berger MS, Godfrey T, Nigro J, Prados M, Chang S, Barker FG 2nd, Aldape K. (2001). "Analysis of complex relationships between age, p53, epidermal growth factor receptor, and survival in glioblastoma patients." Cancer Res. **61**(3): 1122-1128.

Singh K, Hawkins C, Clarke ID, Squire JA, Bayani J, Hide T, Henkelman RM, Cusimano MD, Dirks PB. (2004). "Identification of human brain tumour initiating cells." Nature **432**(7015): 396-401.

Singh SK, Clarke ID, Hide T, Dirks PB. (2004). "Cancer stem cells in nervous system tumors." Oncogene **23** 7267-7273.

Singh SK, Clarke ID, Terasaki M, Bonn VE, Hawkins C, Squire J, Dirks PB (2003). "Identification of a cancer stem cell in human brain tumors." Cancer Res. **63**(18): 5821-5828.

Sjöblom T, Jones S, Wood LD, Parsons DW, Lin J, Barber TD, Mandelker D, Leary RJ, Ptak J, Silliman N, Szabo S, Buckhaults P, Farrell C, Meeh P, Markowitz SD, Willis J, Dawson D, Willson JK, Gazdar AF, Hartigan J, Wu L, Liu C, Parmigiani G, Park BH, Bachman KE, Papadopoulos N, Vogelstein B, Kinzler KW, Velculescu VE. (2006). "The consensus coding sequences of human breast and colorectal cancers." Science **314**: 268-274.

Smith JS, Tachibana I, Passe SM, Huntley BK, Borell TJ, Iturria N, O'Fallon JR, Schaefer PL, Scheithauer BW, James CD, Buckner JC, Jenkins RB. (2001). "PTEN mutation, EGFR amplification, and outcome in patients with anaplastic astrocytoma and glioblastoma multiforme." J Natl Cancer Inst. **93**(16): 1246-1256.

Solomón MT, Selva JC, Figueredo J, Vaquer J, Toledo C, Quintanal N, Salva S, Domíngez R, Alert J, Marinello JJ, Catalá M, Griego MG, Martell JA, Luaces PL, Ballesteros J, de-Castro N, Bach F, Crombet T. (2013). "Radiotherapy plus nimotuzumab or placebo in the treatment of high grade glioma patients: results from a randomized, double blind trial." BMC Cancer. **19** (13): 299.

SongTao Q, Lei Y, Si G, YanQing D, HuiXia H, XueLin Z, LanXiao W, Fei Y. (2012). "IDH mutations predict longer survival and response to temozolomide in secondary glioblastoma. " Cancer science **103** (2): 269-273.

Stark AM, Nabavi A, Mehdorn HM, Blomer U. (2005). "Glioblastoma multiforme: report of 267 cases treated at a single institution." Surg Neurol. **63** (2): 162-169

Steenweg M, Jakobs C, Errami A, van Dooren SJ, Adeva Bartolomé MT, Aerssens P, Augoustides-Savvapoulou P, Baric I, Baumann M, Bonafé L, Chabrol B, Clarke JT, Clayton P, Coker M, Cooper S, Falik-Zaccai T, Gorman M, Hahn A, Hasanoglu A, King MD, de Klerk HB, Korman SH, Lee C, Meldgaard Lund A, Mejaski-Bosnjak V, Pascual-Castroviejo I, Raadhyaksha A, Rootwelt T, Roubertie A, Ruiz-Falco ML, Scalais E, Schimmel U, Seijo-Martinez M, Suri M, Sykut-Cegielska J, Trefz FK, Uziel G, Valayannopoulos V, Vianey-Saban C, Vlaho S, Vodopiutz J, Wajner M, Walter J, Walter-Derbort C, Yapici Z, Zafeiriou DI, Spreeuwenberg MD, Celli J, den Dunnen JT, van der Knaap MS, Salomons GS. (2010). "An overview of L-2-hydroxyglutarate dehydrogenase gene (L2HGDH) variants: a genotype-phenotype study." Human Mutat **31** (4): 380-390.

Sternberg CN, Davis ID, Mardiak J, Szczylik C, Lee E, Wagstaff J, Barrios CH, Salman P, Gladkov OA, Kavina A, Zarbá JJ, Chen M, McCann L, Pandite L, Roychowdhury DF, Hawkins RE. (2010). "Pazopanib in locally advanced or metastatic renal cell carcinoma: results of a randomized phase III trial." J Clin Oncol. **28** (6): 1061-1068.

Stiles BL. (2009). "PI-3-K and AKT: Onto the mitochondria." Adv Drug Deliv Rev. **61**(14): 1276-1282.

Stiles CD, Rowitch DH. (2008). "Review Glioma stem cells: a midterm exam." Neuron. **58**(6): 832-846.

Stojic L, Brun R, Jiricny J. (2004). "Mismatch repair and DNA damage signalling. ." DNA Repair (Amst) **3** (8-9): 1091-1101.

Stommel JM, Kimmelman AC, Ying H, Nabioullin R, Ponugoti AH, Wiedemeyer R, Stegh AH, Bradner JE, Ligon KL, Brennan C, Chin L, DePinho RA. (2007). "Coactivation of receptor tyrosine kinases affects the response of tumor cells to targeted therapies." Science. **318** (5848): 287-290.

Strojnik T, Røsland GV, Sakariassen PO, Kavalar R, Lah T. (2007). "Neural stem cell markers, nestin and musashi proteins, in the progression of human glioma: correlation of nestin with prognosis of patient survival." Surg Neurol. **68**: 133–143.

Struys EA. (2006). " D-2-Hydroxyglutaric aciduria: unravelling the biochemical pathway and the genetic defect." J Inherit Dis **29** (1): 21-29.

Struys EA, Salomons GS, Achouri Y, et al. (2005). "Mutations in the D-2-hydroxyglutarate dehydrogenase gene cause D-2-hydroxyglutaric aciduria." Am J Hum Genet **76** 358 –360.

Struys EA, Verhoeven NM, Brink HJ, Wickenhagen WV, Gibson KM, Jakobs C (2005). "Kinetic characterisation of human hydroxyacid-oxoacid transhydrogenase: relevance to D-2-hydroxyglutaric and gamma-hydroxybrutyric acidurias." J inherit Metab Dis **28**: 921-930.

Struys EA, Verhoeven NM, Jansen EEW, ten Brink HJ, Gupta M, Burlingame TG, Quang LS, Maher T, Rinaldo P, Snead OC, Goodwin AK, Weerts EM, Brown PR, Murphy TC, and Picklo MJ, Jakobs C, Gibson KM (2006). "Metabolism of γ-hydroxybutyrate to D-2-hydroxyglutarate in mammals: further evidence for D-2-hydroxyglutarate transhydrogenase." Metabolism **55**(3): 353-358.

Struys EA, Verhoeven NM, Salomons GS, Berthelot J, Vianay-Saban C, Chabrier S, Thomas JA, Tsai AC, Gibson KM, Jakobs C. (2006). "D-2-hydroxyglutaric aciduria in three patients with proven SSADH deficiency: genetic coincidence or a related biochemical epiphenomenon." Mol Genet Metab **88**: 53-57.

Stupp R, Hegi M, Gorlia T, Erridge S, Grujicic D, Steinbach J, Wick W, Tarnawski R, Nam D, Weyerbrock A, Hau P, Taphoorn M, Nabors L, Reardon D, Van Den Bent M, Perry J, Hong Y, Hicking C, Picard M, Welle M. (2013). "Cilengitide combined with standard treatment for patients with newly diagnosed glioblastoma and methylated O6-methylguanine-DNA methyltransferase (MGMT) gene promoter: Key results of the multicenter, randomized, open-label, controlled, phase III CENTRIC study." J Clin Oncol **31 (suppl; abstr LBA2009)**.

Stupp R, Hegi ME, Gilbert MR, Chakravarti A. (2007). "Chemoradiotherapy in malignant glioma: standard of care and future directions." J Clin Oncol. **25**(26): 4127-4136.

Stupp R, Hegi ME, Mason WP, van den Bent MJ, Taphoorn MJ, Janzer RC, Ludwin SK, Allgeier A, Fisher B, Belanger K, Hau P, Brandes AA, Gijtenbeek J, Marosi C, Vecht CJ, Mokhtari K, Wesseling P, Villa S, Eisenhauer E, Gorlia T, Weller M, Lacombe D, Cairncross JG, Mirimanoff RO; European Organisation for Research and Treatment of Cancer Brain Tumour and Radiation Oncology Groups; National Cancer Institute of Canada Clinical Trials Group. (2009). "Effects of radiotherapy with concomitant and adjuvant temozolomide versus radiotherapy alone on survival in glioblastoma in a randomised phase III study: 5-year analysis of the EORTC-NCIC trial." Lancet Oncol. **10**(5): 459-466.

Stupp R, Mason WP, vandenBent MJ, Weller M, Fisher B, Taphoorn MJ, Belanger K, Brandes AA, Marosi C, Bogdahn U, Curschmann J, Janzer RC, Ludwin SK, Gorlia T, Allgeier A, Lacombe D,

Cairncross JG, Eisenhauer E, Mirimanoff RO. (2005). "Radiotherapy plus concomitant and adjuvant temozolomide for glioblastoma." N. Engl. J. Med. **352**(10): 987–996.

Stupp R, Tonn JC, Brada M, Pentheroudakis G. (2010). "High-grade malignant glioma: ESMO Clinical Practice Guidelines for diagnosis, treatment and follow-up." Ann Onco **21 Suppl 5**: 190-193.

Surawicz TS, McCarthy BJ, Kupelian V, Jukich PJ, Bruner JM, Davis FG. (1999). "Descriptive epidemiology of primary brain and CNS tumors: results from the Central Brain Tumor Registry of the United States, 1990-1994." Neuro Oncol. **1**(1): 14-25.

Swain SM, Kim SB, Cortés J, Ro J, Semiglazov V, Campone M, Ciruelos E, Ferrero JM, Schneeweiss A, Knott A, Clark E, Ross G, Benyunes MC, Baselga J. (2013). "Pertuzumab, trastuzumab, and docetaxel for HER2-positive metastatic breast cancer (CLEOPATRA study): overall survival results from a randomised, double-blind, placebo-controlled, phase 3 study." Lancet Oncol. **14** (6): 461-471.

Tabatabai G, Weller M. (2011). "Glioblastoma stem cells." Cell Tissue Res **34**(3): 459–465.

Tahiliani M, Koh K, Shen Y, Pastor WA, Bandukwala H, Brudno Y, Agarwal S, Iyer LM, Liu DR, Aravind L, Rao A. (2009). "Conversion of 5-Methylcytosine to 5-Hydroxymethylcytosine in Mammalian DNA by MLL Partner TET1." Science **324**(5929 ): 930-935.

Takakuwa O, Maeno K, Kunii E, Ozasa H, Hijikata H, Uemura T, Kasai D, Ohkubo H, Miyazaki M, Oguri T, Niimi A. (2013). " Involvement of intermediate filament nestin in cell growth of small-cell lung cancer." Lung Cancer. **81** (2): 174-179.

Takano S, Tian W, Matsuda M, Yamamoto T, Ishikawa E, Kaneko MK, Yamazaki K, Kato Y, Matsumura A. (2011). "Detection of IDH1 mutation in human gliomas: comparison of immunohistochemistry and sequencing." Brain tumour pathology **28**(2): 115-123.

Tallman MS, Andersen JW, Schiffer CA, Appelbaum FR, Feusner JH, Woods WG, Ogden A, Weinstein H, Shepherd L, Willman C, Bloomfield CD, Rowe JM, Wiernik PH. (2002). "All-trans retinoic acid in acute promyelocytic leukemia: long-term outcome and prognostic factor analysis from the North American Intergroup protocol." Blood. **100** (13): 4298-4302.

Tanaka S, Kamachi Y, Tanouchi A, Hamada H, Jing N, Kondoh H. (2004). "Interplay of SOX and POU factors in regulation of the Nestin gene in neural primordial cells." Mol Cell Biol. **24** (20): 8834-8846.

Tang XH, Gudas L J. (2011). "Retinoids, retinoic acid receptors, and cancer. " Annu. Rev. Pathol. **6**: 345-364.

Tefferi A, Lasho TL, Abdel-Wahab O, Guglielmelli P, Patel J, Caramazza D, Pieri L, Finke CM, Kilpivaara O, Wadleigh M, Mai M, McClure RF, Gilliland DG, Levine RL, Pardanani A, Vannucchi AM. (2010).

"IDH1 and IDH2 mutation studies in 1473 patients with chronic-, fibrotic- or blast-phase essential thrombocythemia, polycythemia vera or myelofibrosis." Leukemia. **24**(7): 1302-1309.

Terada K, Tamiya T, Daido S, Kambara H, Tanaka H, Ono Y, Matsumoto K, Ito S, Ouchida M, Ohmoto T, Shimizu K. (2002). "Prognostic value of loss of heterozygosity around three candidate tumor suppressor genes on chromosome 10q in astrocytomas." J Neurooncol **58** (2): 107-114.

Thaker NG, Pollack IF. (2009). "Molecularly targeted therapies for malignant glioma: rationale for combinatorial strategies." Expert Rev Neurother. **9**(12): 1815-1836.

The Cancer Genome Atlas Research Network (2008). "Comprehensive genomic characterization defines human glioblastoma genes and core pathways." Nature **455** 1061-1068.

Thiessen B, Stewart C, Tsao M, Kamel-Reid S, Schaiquevich P, Mason W, Easaw J, Belanger K, Forsyth P, McIntosh L, Eisenhauer E. (2010). "A phase I/II trial of GW572016 (lapatinib) in recurrent glioblastoma multiforme: clinical outcomes, pharmacokinetics and molecular correlation." Cancer Chemother Pharmacol. **353-61**(65): 2.

Thol F, Weissinger EM, Krauter J, Wagner K, Damm F, Wichmann M, Göhring G, Schumann C, Bug G, Ottmann O, Hofmann WK, Schlegelberger B, Ganser A, Heuser M. (2010). "IDH1 mutations in patients with myelodysplastic syndromes are associated with an unfavorable prognosis." Haematologica. **95** (10): 1668-1674.

Thyagarajan B, Guimaraes MJ, Groth AC, Calos MP. (2000). "Mammalian genomes contain active recombinase recognition sites." Gene **244** 47-54.

Tohyama T, Lee VM-Y, Rorke LB, Marvin M, McKay EDG, Trojanowski JQ. (1992). "Nestin expression in embryonic human neuroepithelium and in human neuroepithelial tumor cells." Lab Invest. **66** 303–313.

Tomlinson IP, Alam NA, Rowan AJ, Barclay E, Jaeger EE, Kelsell D, Leigh I, Gorman P, Lamlum H, Rahman S, Roylance RR, Olpin S, Bevan S, Barker K, Hearle N, Houlston RS, Kiuru M, Lehtonen R, Karhu A, Vilkki S, Laiho P, Eklund C, Vierimaa O, Aittomäki K, Hietala M, Sistonen P, Paetau A, Salovaara R, Herva R, Launonen V, Aaltonen LA; Multiple Leiomyoma Consortium. (2002). "Germline mutations in FH predispose to dominantly inherited uterine fibroids, skin leiomyomata and papillary renal cell cancer." Nat Genet. **30** (4): 406-410.

Toth J, Egervari K, Klekner A, Bognar L, Szanto J, Nemes Z, Szollosi Z. (2009). "Analysis of EGFR gene amplification, protein over-expression and tyrosine kinase domain mutation in recurrent glioblastoma." Pathol. Oncol. Res **15**(2): 225–229.

Tsiatis AC, Norris-Kirby A, Rich RG. (2010). Comparison of Sanger sequencing, pyrosequencing, and melting curve analysis for the detection of KRAS mutations. J Mol Diagn. **12**:425–432.

Turcan S, Fabius AW, Borodovsky A, Pedraza A, Brennan C, Huse J, Viale A, Riggins GJ, Chan TA. (2013). "Efficient induction of differentiation and growth inhibition in IDH1 mutant glioma cells by the DNMT Inhibitor Decitabine." Oncotarget. **4** (10): 1729-1736.

Turcan S, Rohle D, Goenka A, Walsh LA, Fang F, Yilmaz E, Campos C, Fabius AW, Lu C, Ward PS, Thompson CB, Kaufman A, Guryanova O, Levine R, Heguy A, Viale A, Morris LG, Huse JT, Mellinghoff IK, Chan TA. IDH1 mutation is sufficient to establish the glioma hypermethylator phenotype. Nature, 483, 479-483 (2012) (2012). "IDH1 mutation is sufficient to establish the glioma hypermethylator phenotype." Nature **48** 479-483.

Uchida N, Buck DW, He D, Reitsma MJ, Masek M, Phan TV, Tsukamoto AS, Gage FH, Weissman IL. (2000). "Direct isolation of human central nervous system stem cells." Proc Natl Acad Sci U S A. **97**(26): 14720-14725.

Uhm JH, Ballman KV, Wu W, Giannini C, Krauss JC, Buckner JC, James CD, Scheithauer BW, Behrens RJ, Flynn PJ, Schaefer PL, Dakhill SR, Jaeckle KA. (2004). "Phase II study of ZD1839 in patients with newly diagnosed grade 4 astrocytoma." J. Clin. Oncol. **22**: 1505.

Uhrbom L, Dai C, Celestino JC, Rosenblum MK, Fuller GN, Holland EC (2002). "Ink4a-Arf loss cooperates with KRas activation in astrocytes and neural progenitors to generate glioblastomas of various morphologies depending on activated Akt." Cancer Res. **62**(19): 5551-5558.

Uhrbom L, Hesselager G, Nistér M, Westermark B. (1998). "Induction of brain tumors in mice using a recombinant platelet-derived growth factor B-chain retrovirus." Cancer Res. **58**(23): 5275-5279.

Valko M, Rhodes CJ, Moncol J, Izakovic M, Mazur M. (2006). "Free radicals, metals and antioxidants in oxidative stress-induced cancer." Chem Biol Interact **160**: 1-40.

Van Cutsem E, Tabernero J, Lakomy R, Prenen H, Prausová J, Macarulla T, Ruff P, van Hazel GA, Moiseyenko V, Ferry D, McKendrick J, Polikoff J, Tellier A, Castan R, Allegra C. (2012). "Addition of aflibercept to fluorouracil, leucovorin, and irinotecan improves survival in a phase III randomized trial in patients with metastatic colorectal cancer previously treated with an oxaliplatin-based regimen." J Clin Oncol. **30** (28): 3499-3506. .

Van den Bent M, Carpentier A, Brandes A, et al. (2006). "Adjuvant procarbazine, lomustine, and vincristine improves progression-free survival but not overall survival in newly diagnosed anaplastic oligodendrogliomas and oligoastrocytomas: A randomized European Organisation for Research and Treatment of Cancer phase III trial." J Clin Oncol **24**: 2715-2722.

Van den Bent M, Hartmann C, Preusser M et al. (2013). "Interlaboratory comparison of IDH mutation detection." J Neurooncol **112**: 173-178.

Van den Bent MJ, Brandes AA, Rampling R et al., (2009). "Randomized phase II trial of erlotinib versus temozolomide or carmustine in recurrent glioblastoma: EORTC brain tumor group study 26034." Journal of Clinical Oncology **27** (8): 1268-1274.

Van den Bent MJ, Dubbink HJ, Marie Y et al. (2010). "IDH1 and IDH2 mutations are prognostic but not predictive for outcome in anaplastic oligodendroglial tumours: a report of the European Organization for Research and Treatment of Cancer Brain Tumour Group." Clinical cancer research : an official journal of the American Association for Cancer Research **16** (5): 1597-1604.

Van Nifterik KA, Van den Berg J, Slotman BJ, Lafleur MV, Sminia P, Stalpers LJ. (2012). "Valproic acid sensitizes human glioma cells for temozolomide and gamma-radiation." Journal of neuro-oncology **107**(1): 61-67.

Varier RA, Timmers HT. (2011). "Histone lysine methylation and demethylation pathways in cancer." Biochim Biophys Acta. **1815** 75-89.

Vecht C, Wagner G, Wilms E (2003). "Treating seizures in patients with brain tumours: drug interactions between antiepileptic and chemotherapeutic agents." Semin Oncol **30**(6): 49-52.

Veninga T, Langendijk HA, Slotman BJ et al. (2001). "Reirradiation of primary brain tumourssurvival, clinical response and prognostic factors." Radiother Oncol **59**: 127–137.

Venneti S, Felicella MM, Coyne T, Phillips JJ, Gorovets D, Huse JT, Kofler J, Lu C, Tihan T, Sullivan LM, Santi M, Judkins AR, Perry A, Thompson CB. (2013). "Histone 3 lysine 9 trimethylation is differentially associated with isocitrate dehydrogenase mutations in oligodendrogliomas and high-grade astrocytomas." J Neuropathol Exp Neurol. **72** (4): 298-306. .

Verhaak RG, Hoadley KA, Purdom E, Wang V, Qi Y, Wilkerson MD, Miller CR, Ding L, Golub T, Mesirov JP, Alexe G, Lawrence M, O'Kelly M, Tamayo P, Weir BA, Gabriel S, Winckler W, Gupta S, Jakkula L, Feiler HS, Hodgson JG, James CD, Sarkaria JN, Brennan C, Kahn A, Spellman PT, Wilson RK, Speed TP, Gray JW, Meyerson M, Getz G, Perou CM, Hayes DN. (2010). "Integrated genomic analysis identifies clinically relevant subtypes of glioblastoma characterized by abnormalities in PDGFRA, IDH1, EGFR, and NF1." Cancer Cell. **17**(1): 98-110.

Verma S, Miles D, Gianni L, Krop IE, Welslau M, Baselga J, Pegram M, Oh DY, Diéras V, Guardino E, Fang L, Lu MW, Olsen S, Blackwell K; EMILIA Study Group. (2012). "Trastuzumab emtansine for HER2-positive advanced breast cancer." N Engl J Med. **367** (19): 1783-1791. .

Viana-Pereira M, Lopes JM, Little S, Milanezi F, Basto D, Pardal F, Jones C, Reis RM. (2008). "Analysis of EGFR overexpression, EGFR gene amplification and the EGFRvIII mutation in Portuguese high-grade gliomas." Anticancer Res. **28** (2A): 913-920.

Viel T, Monfared P, Schelhaas S, Fricke IB, Kuhlmann MT, Fraefel C, Jacobs AH. (2013). "Optimizing glioblastoma temozolomide chemotherapy employing lentiviral-based anti-MGMT shRNA technology." Mol Ther. **21**(3): 570-579.

Vigna E, Amendola M, Benedicenti F, Simmons AD, Follenzi A, Naldini L. (2005). "Efficient Tet-dependent expression of human factor IX in vivo by a new self-regulating lentiviral vector." Mol Ther. **11**(5): 763-775.

Visconti R, Grieco D. (2009). "New insights on oxidative stress in cancer." Curr Opin Drug Discov Devel. **12** (2): 240-245.

Vogelbaum MA, Peereboom D, Stevens G, Barnett G, Brewer C, et al. (2004). "Phase II trial of the EGFR tyrosine kinase inhibitor erlotinib for single agent therapy of recurrent glioblastoma multiforme: interim results." J. Clin. Oncol. **22**: 1558.

Vredenburgh JJ, Desjardins A, Herndon JE, Dowell JM, Reardon DA, Quinn JA, Rich JN, Sathornsumetee S, Gururangan S, Wagner M, Bigner DD, Friedman AH, Friedman HS. (2007). "Phase II trial of bevacizumab and irinotecan in recurrent malignant glioma. " Clin. Cancer Res. **13**: 1253–1259.

Wang F, Travins J, DeLaBarre B. (2013). "Targeted inhibition of mutant IDH2 in leukemia cells induces cellular differentiation." Science **340**(6132): 622-626.

Wang P, Dong Q, Zhang C, Kuan PF, Liu Y, Jeck WR, Andersen JB, Jiang W, Savich GL, Tan TX, Auman JT, Hoskins JM, Misher AD, Moser CD, Yourstone SM, Kim JW, Cibulskis K, Getz G, Hunt HV, Thorgeirsson SS, Roberts LR, Ye D, Guan KL, Xiong Y, Qin LX, Chiang DY. (2013). "Mutations in isocitrate dehydrogenase 1 and 2 occur frequently in intrahepatic cholangiocarcinomas and share hypermethylation targets with glioblastomas." Oncogene **32** (25): 3091-3100.

Wang Y, Yang J, Zheng H, Tomasek GJ, Zhang P, McKeever PE, Lee EY, Zhu Y (2009). "Expression of mutant p53 proteins implicates a lineage relationship between neural stem cells and malignant astrocytic glioma in a murine model." Cancer Cell. **15**(6): 514-526.

Ward PS, Cross JR, Lu C, Weigert O, Abel-Wahab O, Levine RL, Weinstock DM, Sharp KA, Thompson CB. (2012). "Identification of additional IDH mutations associated with oncometabolite R(-)-2-hydroxyglutarate production." Oncogene **31**(19): 2491-2498.

Ward PS, Lu C, Cross JR, Abdel-Wahab O, Levine RL, Schwartz GK, Thompson CB. (2013). "The potential for isocitrate dehydrogenase mutations to produce 2-hydroxyglutarate depends on allele specificity and subcellular compartmentalization." J Biol Chem **288**: 3804–3815.

Ward PS, Patel J, Wise DR et al. (2010). "The common feature of leukemia-associated IDH1 and IDH2 mutations is a neomorphic enzyme activity converting alpha-ketoglutarate to 2-hydroxyglutarate." Cancer cell **17**(3): 225-234.

Watanabe T, Nobusawa S, Kleihues P, Ohgaki H. (2009). "IDH1 mutations are early events in the development of astrocytomas and oligodendrogliomas." The American journal of pathology **174**(4): 1149-1153

Wei Q, Clarke L, Scheidenhelm DK, Qian B, Tong A, Sabha N, Karim Z, Bock NA, Reti R, Swoboda R, Purev E, Lavoie JF, Bajenaru ML, Shannon P, Herlyn D, Kaplan D, Henkelman RM, Gutmann DH, Guha A. (2006). "High-grade glioma formation results from postnatal pten loss or mutant epidermal growth factor receptor expression in a transgenic mouse glioma model." Cancer Res. **66** (15): 7429-7437.

Weiss WA, Burns MJ, Hackett C, Aldape K, Hill JR, Kuriyama H, Kuriyama N, Milshteyn N, Roberts T, Wendland MF, DePinho R, Israel MA. (2003). "Genetic determinants of malignancy in a mouse model for oligodendroglioma." Cancer Res. **63** (7): 1589-1595.

Weljie AM, Bondareva A, Zang P, Jirik FR. (2011). "(1)H NMR metabolomics identification of markers of hypoxia-induced metabolic shifts in a breast cancer model system." Journal of biomolecular NMR **49** 185-193

Wellen KE, Hatzivassiliou G, Sachdeva UM, Bui TV, Cross JR, Thompson CB. (2009). "ATP-citrate lyase links cellular metabolism to histone acetylation." Science **324** (5930 ): 1076-1080.

Weller M, Gorlia T, Cairncross JG et al. (2011). "Prolonged survival with valproic acid use in the EORTC/NCIC temozolomide trial for glioblastoma." Neurology **77**(12): 1156-1164

Wen PY, Yung WK, Lamborn KR, Dahia PL, Wang Y, Peng B, Abrey LE, Raizer J, Cloughesy TF, Fink K, Gilbert M, Chang S, Junck L, Schiff D, Lieberman F, Fine HA, Mehta M, Robins HI, DeAngelis LM, Groves MD, Puduvalli VK, Levin V, Conrad C, Maher EA, Aldape K, Hayes M, Letvak L, Egorin MJ, Capdeville R, Kaplan R, Murgo AJ, Stiles C, Prados MD (2006). "Phase I/II study of imatinib mesylate for recurrent malignant gliomas: North American Brain Tumor Consortium Study 99-08." Clin Cancer Res. **12**(16): 4899-4907.

Westphal M, Bach F. (2012). "Final results of a randomized phase III trial of nimotuzumab for the treatment of newly diagnosed glioblastoma in addition to standard radiation and chemotherapy with temozolomide versus standard radiation and temoziolamide." J Clin Oncol. **13(suppl; abstr 2033)**.

Westphal M, Meissner H. (1998). "Establishing human glioma derived cell-lines." Methods in Cell Biology. **57**: 147–165.

Westphal M, Ram Z, Riddle V, Hilt D, Bortey E; Executive Committee of the Gliadel Study Group. (2006). "Gliadel wafer in initial surgery for malignant glioma: long-term follow-up of a multicenter controlled trial." Acta Neurochir (Wien). **148**(3): 269-275.

Wick W, Hartmann C, Engel C, Stoffels M, Felsberg J, Stockhammer F, Sabel MC, Koeppen S, Ketter R, Meyermann R, Rapp M, Meisner C, Kortmann RD, Pietsch T, Wiestler OD, Ernemann U, Bamberg M, Reifenberger G, von Deimling A, Weller M. (2009). "NOA-04 randomized phase III trial of sequential radiochemotherapy of anaplastic glioma with procarbazine, lomustine, and vincristine or temozolomide." J Clin Oncol. **27** (35): 5874-5880.

Wick W, Platten M, Meisner C, Felsberg J, Tabatabai G, Simon M, Nikkhah G, Papsdorf K, Steinbach JP, Sabel M, Combs SE, Vesper J, Braun C, Meixensberger J, Ketter R, Mayer-Steinacker R, Reifenberger G, Weller M, NOA-08 Study Group of Neuro-oncology Working Group (NOA) of German Cancer Society (2012). "Temozolomide chemotherapy alone versus radiotherapy alone for malignant astrocytoma in the elderly: the NOA-08 randomised, phase 3 trial." Lancet Oncol. **13** (7): 707-715.

Wick W, Puduvalli VK, Chamberlain MC, van den Bent MJ, Carpentier AF, Cher LM, Mason W, Weller M, Hong S, Musib L, Liepa AM, Thornton DE, Fine HA. (2010). "Phase III study of enzastaurin compared with lomustine in the treatment of recurrent intracranial glioblastoma." J Clin Oncol. **28**(7): 1168-1174.

Wiese C, Rolletschek A, Kania G, Blyszczuk P, Tarasov KV, Tarasova Y, Wersto RP, Boheler KR, Wobus AM. (2004). "Nestin expression--a property of multi-lineage progenitor cells?" Cell Mol Life Sci. **61**: 2510-2522.

Willers IM, Cuezva JM. (2011). "Post-transcriptional regulation of the mitochondrial H+-ATP synthase: A key regulator of the metabolic phenotype in cancer." Biochim Biophys Acta **1807**: 543-551.

Williams SC, Karajannis MA, Chiriboga L, Golfinos JG, von Deimling A, Zagzag D. (2011). "R132H-mutation of isocitrate dehydrogenase-1 is not sufficient for HIF-1alpha upregulation in adult glioma." Acta neuropathologica **121**(2): 279-281

Wise DR, Ward PS, Shay JE *et al.* (2011). "Hypoxia promotes isocitrate dehydrogenase-dependent carboxylation of alpha-ketoglutarate to citrate to support cell growth and viability." Proceedings of the National Academy of Sciences of the United States of America **108**(49): 19611-19616.

Wong ET, Hess KR, Gleason MJ, Jaeckle KA, Kyritsis AP, Prados MD, Levin VA, and Yung WK. (1999). "Outcomes and prognostic factors in recurrent glioma patients enrolled onto phase II clinical trials." J Clin Oncol **17**: 2572-2578.

Wrensch M, Bondy ML, Wiencke J, Yost M (1993). "Environmental risk factors for primary malignant brain tumors: a review." J Neurooncol. **17**(1): 47-64.

Wrensch M, Jenkins RB, Chang JS, Yeh RF, Xiao Y, Decker PA, Ballman KV, Berger M, Buckner JC, Chang S, Giannini C, Halder C, Kollmeyer TM, Kosel ML, LaChance DH, McCoy L, O'Neill BP, Patoka J, Pico AR, Prados M, Quesenberry C, Rice T, Rynearson AL, Smirnov I, Tihan T, Wiemels J, Yang P,

Wiencke JK. (2009). "Variants in the CDKN2B and RTEL1 regions are associated with high-grade glioma susceptibility." Nat Genet. **41** (8): 905-908.

Wrensch M, Minn Y, Chew T, Bondy M, Berger MS (2002). "Epidemiology of primary brain tumors: current concepts and review of the literature." Neuro Oncol. **4**(4): 278-299.

Wrensch M, Yost M, Miike R, Lee G, Touchstone J. (1999). "Adult glioma in relation to residential power frequency electromagnetic field exposures in the San Francisco Bay area." Epidemiology. **10**(5): 523-527.

Xu W, Yang H, Liu Y, Yang Y, Wang P, Kim SH, Ito S, Yang C, Wang P, Xiao MT, Liu LX, Jiang WQ, Liu J, Zhang JY, Wang B, Frye S, Zhang Y, Xu YH, Lei QY, Guan KL, Zhao SM, Xiong Y. (2011). "Oncometabolite 2-hydroxyglutarate is a competitive inhibitor of alpha-ketoglutarate-dependent dioxygenases." Cancer cell **19**(1): 17-30.

Xu X, Zhao J, Xu Z, Peng B, Huang Q, Arnold E, Ding J. (2004). "Structures of human cytosolic NADP-dependent isocitrate dehydrogenase reveal a novel self-regulatory mechanism of activity." The Journal of biological chemistry **279**(32): 33946-33957.

Yan H, Parsons DW, Jin G, McLendon R, Rasheed BA, Yuan W, Kos I, Batinic-Haberle I, Jones S, Riggins GJ, Friedman H, Friedman A, Reardon D, Herndon J, Kinzler KW, Velculescu VE, Vogelstein B, Bigner DD. (2009). "IDH1 and IDH2 mutations in gliomas." The New England journal of medicine **360**(8): 765-773.

Yang C, Sudderth J, Dang T, Bachoo RM, McDonald JG, DeBerardinis RJ. (2009). "Glioblastoma cells require glutamate dehydrogenase to survive impairments of glucose metabolism or Akt signaling." Cancer Research **69**(20): 7986-7993.

Yang ES, Park JW. (2011). "Knockdown of cytosolic NADP(+) -dependent isocitrate dehydrogenase enhances MPP(+) -induced oxidative injury in PC12 cells." BMB reports **44**(5): 312-316.

Ye LC, Liu TS, Ren L, Wei Y, Zhu DX, Zai SY, Ye QH, Yu Y, Xu B, Qin XY, Xu J. (2013). "Randomized controlled trial of cetuximab plus chemotherapy for patients with KRAS wild-type unresectable colorectal liver-limited metastases." J Clin Oncol. **31** (16): 1931-1938.

Yen KE, Bittinger MA, Su SM, Fantin VR. Cancer-associated IDH mutations: biomarker and therapeutic opportunities. Oncogene, 29(49), 6409-6417 (2010). (2010). "Cancer-associated IDH mutations: biomarker and therapeutic opportunities. ." Oncogene **29** (49): 6409-6417.

Young GS, Macklin EA, Setayesh K, Lawson JD, Wen PY, Norden AD, Drappatz J, Kesari S (2011). "Longitudinal MRI evidence for decreased survival among periventricular glioblastoma." J Neurooncol. **104**(1): 261-269.

Yust-Katz S, Liu D, Yuan Y, Liu V, Kang S, Groves M, Puduvalli V, Levin V, Conrad C, Colman H, Hsu S, Yung WK, Gilbert MR. (2013). "Phase 1/1b study of lonafarnib and temozolomide in patients with recurrent or temozolomide refractory glioblastoma." Cancer. **119**(15): 2747-2753.

Zhang M, Song T, Yang L, Chen R, Wu L, Yang Z, Fang J. (2008). "Nestin and CD133 valuable stem cell-specific markers for determining clinical outcome of glioma patients." J Exp Clin Cancer Res **27**: 85.

Zhang R, Banik NL, Ray SK. (2008). "Differential sensitivity of human glioblastoma LN18 (PTEN-positive) and A172 (PTEN-negative) cells to Taxol for apoptosis." Brain Res **1239**: 216-225.

Zhao S, Lin Y, Xu W et al. (2009). "Glioma-derived mutations in IDH1 dominantly inhibit IDH1 catalytic activity and induce HIF-1alpha." Science **324** (5924): 261-265

Zheng H, Ying H, Yan H, Kimmelman AC, Hiller DJ, Chen AJ, Perry SR, Tonon G, Chu GC, Ding Z, Stommel JM, Dunn KL, Wiedemeyer R, You MJ, Brennan C, Wang YA, Ligon KL, Wong WH, Chin L, DePinho RA. (2008). "p53 and Pten control neural and glioma stem/progenitor cell renewal and differentiation." Nature. **455**: 1129–1133.

Zhou KG, Jiang LJ, Shang Z, Wang J, Huang L, Zhou JF. ( 2012.). "Potential application of IDH1 and IDH2 mutations as prognostic indicators in non-promyelocytic acute myeloid leukemia: A meta-analysis." Leuk Lymphoma **53**: 2423–2429.

Zhu H, Acquaviva J, Ramachandran P, Boskovitz A, Woolfenden S, Pfannl R, Bronson RT, Chen JW, Weissleder R, Housman DE, Charest A. (2009). "Oncogenic EGFR signaling cooperates with loss of tumor suppressor gene functions in gliomagenesis." Proc Natl Acad Sci U S A. **106** (8): 2712-2716. .

Zhu Y, Guignard F, Zhao D, Liu L, Burns DK, Mason RP, Messing A, Parada LF (2005). "Early inactivation of p53 tumor suppressor gene cooperating with NF1 loss induces malignant astrocytoma." Cancer Cell. **8**(2): 119-130.

Zimmerman L, Parr B, Lendahl U, Cunningham M, McKay R, Gavin B, Mann J, Vassileva G, McMahon A. (1994). "Independent regulatory elements in the nestin gene direct transgene expression to neural stem cells or muscle precursors." Neuron **12**: 11-24

Zustovich F, Landi L, Lombardi G, Porta C, Galli L, Fontana A, Amoroso D, Galli C, Andreuccetti M, Falcone A, Zagonel V. (2013). "Sorafenib plus daily low-dose temozolomide for relapsed glioblastoma: a phase II study." Anticancer Res. **33**(8): 3487-3494.

# Appendix

**Appendix 1. Primers and conditions**

| Gene Name | Forward Primer Sequence | Reverse Primer Sequence | Amplicon Size, bp | Q soln. (Qiagen) Y or N | Annealing Temp °C | No. Cycles |
|---|---|---|---|---|---|---|
| ***D2HGDH*** | | | | | | |
| **Exon 1a** | CCCCCACCAAGGAGGA | TGCTTAGACACCGTGGAGAA | | N | 60 | 35 |
| **Exon 1b** | CCTGGCCCGCAGAGG | TTGTTCTCAGCCCGCTTTG | | N | 60 | 35 |
| **Exon 2** | GAGGGAGAGGTTGCAGTGAG | CACAGGCTCCATGAGGAAAT | | N | 60 | 35 |
| **Exon 3** | CGTAGGGGTGGGGACAG | ACGCTGGCAAGGAAGAACT | | N | 60 | 35 |
| **Exon 4** | CCACTGGAAGCCAAGTGC | ACCCCGTGGCGACCT | | N | 60 | 35 |
| **Exon 5** | TCAGGAGGCTGGCAGGT | ACAGTGGCACCATCAGAGC | | N | 60 | 35 |
| **Exon 6** | ATGAGTCGGGCTGATGTTG | ATGTGTCCAGACGTGCAGAA | | N | 60 | 35 |
| **Exon 7** | CGGAGCCTCTGCTCACTCT | TGTCTAGGCTGCACCAATGA | | N | 60 | 35 |
| **Exon 8** | CGGGTGTCGTTCCCATAG | ACCACCCAGCACACACAG | | N | 60 | 35 |
| **Exon 9a** | GGGAGGAGTGGGGTCCT | CGTCTTGTAGGGGTTGAGGA | | N | 60 | 35 |
| **Exon 9b** | CACGGAGTGGGCTTCAG | CAGTCCCTTCAACCAGGTG | | N | 60 | 35 |
| ***IDH1*** | | | | | | |
| **Exon 4** | CGGTCTTCAGAGAAGCCATT | TGCTTAATGGGTGTAGATACCAAA | | N | 55 | 35 |
| ***IDH2*** | | | | | | |
| **Exon 4** | AGCCCATCATCTGCAAAAAC | TGTGGCCTTGTACTGCAGAG | | N | 55 | 35 |
| ***IDH3A*** | | | | | | |
| **Exon 1** | AGGCCAGTCACAGAGAGACG | CCAGCGCTCACCTTAGAGAGAT | | N | 55 | 35 |
| **Exon 2** | CAGGACTTCCTCGCTCTTGT | TCCCAAATTCTAAATGAATGGA | | N | 55 | 35 |
| **Exon 3** | TCTCATAAAGTGGATTTCTCTGTCA | TTCACAGAATCCAACTGGCTAA | | N | 55 | 35 |
| **Exon 4** | CATTGCAGTATGAATGCCAGTT | AACCCCTGTAGCGGAAATCT | | N | 55 | 35 |
| **Exon 5** | CACGTGAGACCAGAATTCCTT | GATGCACAGAAAGCAGTCCA | | N | 55 | 35 |
| **Exon 6** | CCACCCTCTGTCTCCCACT | TCCCACAACAAAGCAAGATG | | N | 55 | 35 |

| | | | | | | |
|---|---|---|---|---|---|---|
| **Exon 7** | TGGCTTCTGGAACTTAAATGTCT | TCAATTGAAAATGTTAAGCCATAAT | | N | 55 | 35 |
| **Exon 8** | TCTGGGTGCTAGGTGAGATG | CCTGAGTTCACACGCTGTTC | | N | 55 | 35 |
| **Exon 9** | TGAATTGCACGCAGTAGCTT | GGCCCGCCTGAGAACTATTA | | N | 55 | 35 |
| **Exon 10** | GGCTTTAAAATCTCCTTGGTTT | CAAGCAAACCAATGCATACATAC | | N | 55 | 35 |
| ***IDH3B*** | | | | | | |
| **Exon 1+2** | CTCAGTACAGGCCGGAAGTC | GGGAGTAGAGAAGTAGGGAGACC | | N | 55 | 35 |
| **Exon 3+4** | CTACTCCCAGGATCCGTGCT | CATAGCATGTGGGGAGAAGG | | N | 55 | 35 |
| **Exon 5+6** | ACTGGTCTGAGTTCCCTTGG | AAGGAGCTCCACCTCTCTCC | | N | 55 | 35 |
| **Exon 7** | GCAAGGATGAAGATGGGAGA | GGGACAGAATCAGCCAAGAA | | N | 55 | 35 |
| **Exon 8** | ATGGGTTCCTGGGAAGGTAG | GCAGGCATGAAGTAAATTCCA | | N | 55 | 35 |
| **Exon 9** | AGGAGGAGGGTGGGGAGT | GAATGGCGGACTTGAGGT | | N | 55 | 35 |
| **Exon 10** | CCCCTCCCATAATGTCCTTT | TAATTTCCCCACCTGCTCCT | | N | 55 | 35 |
| **Exon 11** | AGGTGTCTTGGGGGAGTCAC | AGGTTCCCCAGAGGGTAGTG | | N | 55 | 35 |
| **Exon 12** | CAGACTGTTGGGTGGTGATG | GGTTCATGTTCTTTATTGAACACCT | | N | 55 | 35 |
| ***IDH3G*** | | | | | | |
| **Exon 1** | GAGAGCGGTATCTGCGTGTC | CCCCTAGCCAATCGGACTC | | N | 60 | 35 |
| **Exon 2** | GGTCCGTTTTTCCTTCCAAC | CAGAAGAGGGGTGGGTAGC | | N | 60 | 35 |
| **Exon 3** | GGAACCTTGGCTGATTGTGT | CCCCCACCTGGAATTTAGTT | | N | 60 | 35 |
| **Exon 4** | AGTGGGAAGAAGGGAATTGG | CCCCTGGCTGAGGACAA | | N | 60 | 35 |
| **Exon 5** | GCAACAGGAGAGAGGTAGCC | GTAAGCAAGAAACGAAGGAAGA | | N | 60 | 35 |
| **Exon 6** | CATTTTTGCTCCCCAAGTCT | ACTGGCTCACCCCACCTTAG | | N | 60 | 35 |
| **Exon 7** | CTCCAGTCAGCCACCTGTC | GCTCTCCCCTTAATCTTGACG | | N | 60 | 35 |
| **Exon 8** | GTCGCGCCAGCTTGTTT | GGACCACAAATCCCTCAGA | | N | 60 | 35 |
| **Exon 9** | TGGCTGACTGTTGCGATG | GCTGGCTGAGGAGCAGATT | | N | 60 | 35 |
| **Exon 10** | GCTTCTCTCACCCATGCTTC | GAACGGGCTAACCGGATG | | N | 60 | 35 |

| | | | | | | |
|---|---|---|---|---|---|---|
| **Exon 11** | CATCCTTCTGCCCTCCAC | GACAGCCAGCCTTCAGTCC | | N | 60 | 35 |
| **Exon 12** | CAAGTGAGTGGCTCCCAGTG | CCAGCTAAGGGCCAGAAGAT | | N | 60 | 35 |
| **Exon 13** | CTGCACGTCACAGGAGACAG | CTGGAGTGGGAAGGGGAAT | | N | 60 | 35 |
| ***L2HGDH*** | | | | | | |
| **Exon 1** | GGGTCAAGTGGCTTCTTCTG | GGGACAGGGAAATACGAACA | | N | 60 | 35 |
| **Exon 2** | ATGTGAAGTTTGGCGAGGTC | GAGCAGATGCCCAAGTAAGC | | N | 60 | 35 |
| **Exon 3** | ACAAGCAGTGTGGCAAGGTA | AAAGGGCGAATTGTATGGTG | | N | 60 | 35 |
| **Exon 4** | CTGATGATACATTCACCTCTATCCA | ACCCTCAGCCTCCATGTCT | | N | 60 | 35 |
| **Exon 5a** | GGCAAAATCAACTCCTCT | GGCTTACCATCTATACTTCTTG | | N | 54 | 35 |
| **Exon 5b** | ATTGATTGTCCACATACTGG | CATCCTCAGTTGGTTAAAAC | | N | 54 | 35 |
| **Exon 6** | GAACTGTAAGGTGCAATCATAG | CAGCCCTGTGGGTTAA | | N | 54 | 35 |
| **Exon 7** | TTCCCCTCTTGACCTATT | GAGAAGTAGGAAGCATCATTAC | | N | 54 | 35 |
| **Exon 8** | TGGAATGTGAAATGAGGCTGT | CAAGAAAGACAAAACTTCCCACAT | | N | 60 | 35 |
| **Exon 9** | GCCTAGATTTTTGTGATGAC | CACATAGGTCAGGACTGTATT | | N | 54 | 35 |
| **Exon 10a** | CTTTTTGGAAACGCTGACT | GAAGAAGTAGCAGCAGGAGAA | | N | 54 | 35 |
| **Exon 10b** | CCTGGATAGAGATGGAAATC | CTTGTTGCTGACATGAAGAT | | N | 54 | 35 |
| ***HOT*** | | | | | | |
| **Exon 1** | TGGCTTGAGGCTTAGACAGG | AAGACTGCGCAGGATCTGA | | N | 60 | 35 |
| **Exon 2** | TGCCAAGAACTACCAATTTGA | GCCAAATGCAGAAACCAAAA | | N | 60 | 35 |
| **Exon 3** | TGTTCACTGCTGGATTTTACTATCA | TGGTCTGATCAAATAGAGATTATGGA | | N | 60 | 35 |
| **Exon 4** | ATGGACTGGCCAACTCTCAA | CTTCTGGCAAACTCACGTTG | | N | 60 | 35 |
| **Exon 5** | GCAGTTCTAGTGGAGTTGAACCTA | GCTTCTGCTTAAAGTAAAGAAACAA | | N | 60 | 35 |
| **Exon 6** | GGCATGGCAATTTATTTCTGA | CTCATTGCAAAATAAAACAAACA | | N | 60 | 35 |
| **Exon 7** | TTTCCTTCTCTAATTTTGTTCCTCA | TGGAGTTGAAAGGTAAGGGAGA | | N | 60 | 35 |
| **Exon 8** | AATGATGCCCATGGCTTTAG | TGTGCGTTGAGCAACAAAAT | | N | 60 | 35 |
| **Exon 9** | GAGGAAGATGACGCTTTCCA | TGTGGGCCTCCTGTTCTATT | | N | 60 | 35 |
| **Exon 10** | AGGAATTGCCAATGTTGATG | AAATTTTACCACCTGTCCTGAA | | N | 60 | 35 |
| **Exon 11** | GCATCCCCATAAGAGTATCTTTC | TCTAAGCAGGCGAGAATTGG | | N | 60 | 35 |
| **Exon 12** | CAGGGAAGAACAGCTTTGTCA | CTCCCAAAATGCTGGGATTA | | N | 60 | 35 |
| **Exon 13** | AGAGCCCGTTTCTTCCTCTC | CTCCTTCGCAGGGAGTGA | | N | 60 | 35 |
| **Exon 14** | CTTTTCAAAGCCCTGGGTAA | TCAGCTCTTGCTCTCAGCAC | | N | 60 | 35 |

**Mouse Primer Sequences**

| **Gene name** | **Forward Primer Sequence** | **Reverse Primer Sequence** | **Amplicon Size, bp** | **Q soln. (Qiagen) Y** | **Annealing Temp °C** | **No. Cycles** |
|---|---|---|---|---|---|---|

| | | | | or N | | |
|---|---|---|---|---|---|---|
| **D2HGDH** | TCCGCCACTGTACTACTTGGT | 1. GTCTGGGGTCTCAGCAAAAC<br>2. CCAACCCCTTCCTCCTACAT | **Wt-474<br>KOhet-474 and 231<br>KO hom-231** | N | 60 | 35 |
| **FLP** | ACGGAACAGCAATCAAGAGAGCCA | TCGATCCTACCCCTTGCGCTAAA | **Present-450** | Y | 57 | 35 |
| **Gen-Cre** | TTACCGGTCGATGCAACGAG | CCACCGTCAGTACGTGAGAT | **Present-500** | Y | 60 | 35 |
| **IDH1 r132h** | GGTTGGACTTGGCTTTAATTTG | ATTGGTGGCATCACGATTCT | **Wt -393<br>r132h-551** | N | 60 | 35 |
| **KSP-Cre** | GCAGATCTGGCTCTCCAAAG | AGGCAAATTTTGGTGTACGG | **Present-400** | N | 60 | 35 |
| **NeoR** | AGGATCTCCTGTCATCTCACCTTGCTCCTG | AAGAACTCGTCAAGAAGGCGATAGAAGGCG | **Present 492<br>Absent- nil** | N | 60 | 30 |
| **P53** | AAGGGGTATGAGGGACAAGG | GAAGACAGAAAAGGGGAGGG | **Wt- 400<br>Floxed-600** | Y | 57 | 35 |
| **SOX2-Cre** | AAAGCGTTAATTTGGATGGG | ACAAGAGAATTGGGAGGGGT | **Present-360** | Y | 58 | 35 |

**Primers for qRT-PCR**

| Gene name | Forward Primer Sequence | Reverse Primer Sequence |
|---|---|---|
| **AQP4** | GCGAGGACAGCTCCTATGAT | ACTGGTGCCAGCATGAATC |
| **CNP** | AGCCTTCCCGTAGTCACAAA | CAAGAAGGAGCTGCGACAAT |
| **CSPG4** | TGCAGGTCTATGTCGGTCAG | TATGTTGGCCAGACTTGCAT |
| **D2HGDH** | CATTGAGGTGCAGGTTACCA | GGAGCGGCTCTACGACATC |
| **EGLN1** | TACCTTGGCATCCCAGTCTT | AGCTACAAAATCAATGGCCG |
| **EGLN3** | CTGTTCCATTTCCCGGATAG | TCGACAGGCTGGTCCTCTAC |
| **GFAP** | CACCACGATGTTCCTCTTGA | GTGCAGACCTTCTCCAACCT |
| **GLUT1** | AGAGGTGTCACCTACAGCTC | AACAGGATACACTGTAGCAG |
| **HK2** | AGCCCTTTCTCCATCTCCTT | AACCATGACCAAGTGCAGAA |
| **IDH1** | CTTTTGGGTTCCGTCACTTG | GTCGTCATGCTTATGGGGAT |
| **IDH2** | TACGGGTCATCTCATCACCA | ACCTCGCAAGAGCAGCC |
| **IDH3A** | CCTCTGGTCACCTGTTTTGG | CAGGAGGGGAAGCGATG |
| **L2HGDH** | GCCTGGGCTCTTACTCCAG | AGCATGTTTTCTTGGTGCAA |
| **MSI1** | TTGTCAAACATCAGCATGGC | GAAGAAGATCTTTGTGGGGG |
| **Nestin** | GGTCCTAGGGAATTGCAGC | CTCAAGATGTCCCTCAGCCT |

| | | |
|---|---|---|
| **PFK** | TGGAGACACTCTCCCAGTCG | GGGCCAAGGTGTACTTCATC |
| **PGK1** | CAAATTTGATGAGAATGCCAAGACT | TTCTTGCTGCTCTCAGTACCACA |
| **PROM1** | TTTGGATTCATATGCCTTCTGT | CCATTGGCATTCTCTTTGAA |
| **RBP1** | CTCATCACCCTCGATCCACT | GAGGAGGATCTGACAGGCAT |
| **SMARCA4** | AGTGGACATCTTCACGGGAG | GTGAAGAGAAGCGAGACGCC |
| **SOX2** | GCTTAGCCTCGTCGATGAAC | AACCCCAAGATGCACAACTC |
| **VEGF** | TACTGCCGTCCGATTGAGAC | TGATCTGCATGGTGATGTTG |